

IMPROVING THE PROCESS SYNTHESIS, POTENCY, AND PHARMACOKINETICS OF
THE ANTICANCER COMPOUND PAC-1

BY

HOWARD STEVEN ROTH

DISSERTATION

Submitted in partial fulfillment of the requirements
for the degree of Doctor of Philosophy in Chemistry
in the Graduate College of the
University of Illinois at Urbana-Champaign, 2015

Urbana, Illinois

Doctoral Committee:

Professor Paul J. Hergenrother, Chair
Professor John A. Katzenellenbogen
Professor Douglas A. Mitchell
Professor Timothy M. Fan

ABSTRACT

PAC-1 is an *ortho*-hydroxy-*N*-acylhydrazone that induces apoptosis by chelation of antiapoptotic labile zinc, relieving zinc-mediated inhibition of procaspase-3. Favorable results from cell culture and *in vivo* experiments with **PAC-1** and its derivative **S-PAC-1** have indicated the potential for translation to the clinic. However, several challenges exist in using **PAC-1** in these experiments. This report describes the attempts to improve upon the process synthesis, potency, pharmacokinetics, and safety of **PAC-1**.

The synthetic route to access **PAC-1** was successful for the generation of batches of approximately 25 grams, but adaptation to multi-kilogram scale, as would be necessary for a human clinical trial, was not feasible using the existing route. In particular, the route included three chromatographic purification steps, as well as the use of anhydrous hydrazine. Optimization studies indicated that the active pharmaceutical ingredient could be synthesized without purification of any intermediates, and hydrazine monohydrate could be used in place of the anhydrous reagent. A batch of 155 grams of **PAC-1** was synthesized using the improved route, and the route was scaled up to produce a batch of greater than 10 kilograms by a contract research organization. The lessons learned through this optimization effort were general and should be applicable if an alternative **PAC-1** derivative is identified.

In an effort to discover **PAC-1** derivatives with improved potency, a combinatorial library of 837 compounds was synthesized. Each of 31 hydrazides was condensed with each of 27 aldehydes. Because standard techniques for isolation and purification of products are impractical for libraries of this size, a solid-phase purification strategy was employed that yielded the library members with an average purity of 91%. Compounds were screened in cell culture, and six potent hits were identified. One of these compounds, **B-PAC-1**, was studied further in primary isolates from leukemia patients, and animal experiments are currently in progress.

An additional challenge is the relatively rapid clearance of **PAC-1** from circulation. Many sites of metabolism exist, giving metabolites that arise from oxidative *N*-dealkylation, olefin oxidation, and arene oxidation. Several derivatives were synthesized containing modifications that prevent the formation of these metabolites. The compounds were evaluated in cell culture, liver microsomes, and mice, and four lead compounds were identified.

Pharmacokinetic analysis indicated that each of these four compounds displayed extended elimination half-lives compared to **PAC-1** and **S-PAC-1**, making these compounds viable candidates as next-generation **PAC-1** derivatives.

One of the most significant challenges in working with **PAC-1** *in vivo* is the neuroexcitation observed upon treatment with elevated doses of compound. Preliminary experiments suggested that the neurotoxicity was not related to the ability of the compound to bind zinc. In order to confirm these results and attempt to determine the portion of the molecule responsible for neurotoxicity, a series of compounds was designed and synthesized containing systematic modifications to **PAC-1**. Evaluation in cell culture and *in vitro* further defined the essential nature of the *ortho*-hydroxy-*N*-acylhydrazone for activity. Evaluation of the compounds in mice confirmed previous experiments that the neurotoxicity is most likely not a result of metal chelation, but no further conclusions could be drawn from these experiments, and further study will be necessary to fully define the observed neurotoxicity.

ACKNOWLEDGMENTS

The completion of my degree would not have been possible without the contributions of several individuals, whose efforts I greatly appreciate. First, I thank my advisor, Prof. Paul Hergenrother, for accepting me into his research group, continuing to believe in my abilities, and encouraging me to reach my full potential. I also thank Profs. John Katzenellenbogen and Doug Mitchell for taking the time to serve on my committee. I am also grateful to the efforts of Prof. Tim Fan for performing and helping to interpret many of the animal experiments, in addition to serving as a member of my committee. In addition, I thank the American Chemical Society Division of Medicinal Chemistry for awarding me a predoctoral fellowship during my fourth year of graduate study, and Prof. Richard Silverman (Northwestern University) for generously sponsoring the fellowship, in addition to making me excited to pursue medicinal chemistry during my time at Northwestern. I also thank my undergraduate research advisors, Profs. Karl Scheidt and Thomas O'Halloran, for giving me the first opportunities to pursue my passion. I am also greatly appreciative of Dr. Paul Richardson and Dr. Michael Hillier of AbbVie, Inc., for giving me the opportunity to participate in summer internships. These were very valuable experiences, and I enjoyed having this exposure to drug discovery and development in the industrial setting.

Since my first day in the Hergenrother group, I have worked directly with many talented individuals on the procaspase activation project, who have helped me by performing experiments related to my projects, as well as providing help and guidance. I thank Danny Hsu, Quinn Peterson, Diana West, Isak Im, Rachel Botham, and Jessie Peh for their contributions; my achievements would not have been possible without their help. Evaluation was also performed by Profs. Levent Dirikolu, Gregory Riggins, and Varsha Gandhi, enabling us to gain important knowledge beyond what was learned from our own experiments. I am also grateful to my two undergraduate assistants, Steve Schmid and Matt Frost, for their efforts in large-scale synthesis of our two lead compounds. In addition, I appreciate the time taken by other members of the Hergenrother group, especially Matt Brichacek, Ryan Rafferty, Rob Huigens, Joe Bair, Rob Hicklin, Betsy Parkinson, and Claire Knezevic, to engage in helpful discussions.

Finally, I thank my family for their constant support during my journey. I have been fortunate to have a wonderful support system throughout my life, and without their guidance, my achievements would not have been possible.

TABLE OF CONTENTS

| | |
|---|----|
| Chapter 1. Anticancer Activity of PAC-1 and Derivatives | 1 |
| 1.1. Introduction: Procaspase-3 activation as an anticancer strategy..... | 1 |
| 1.2. PAC-1 | 3 |
| 1.2.1. Initial discovery of PAC-1 | 3 |
| 1.2.2. PAC-1 mechanism of action..... | 5 |
| 1.2.3. Structure-activity relationships | 6 |
| 1.2.4. Relationship to other metal-binding compounds in medicine | 10 |
| 1.3. Diaryl urea conjugates | 12 |
| 1.4. Benzothiazole PAC-1 derivatives..... | 17 |
| 1.5. Oxadiazole PAC-1 derivatives | 20 |
| 1.6. Replacement of benzylidene | 22 |
| 1.7. Study of matrix metalloproteinase inhibition | 24 |
| 1.8. Modification of piperazine..... | 25 |
| 1.9. S-PAC-1 | 27 |
| 1.9.1. Discovery and initial evaluation | 27 |
| 1.9.2. Safety and pharmacokinetics | 29 |
| 1.9.3. Evaluation in canine lymphoma patients | 30 |
| 1.9.4. Comparison to PAC-1 | 32 |
| 1.10. WF-210 and WF-208 | 35 |
| 1.10.1. Discovery and initial evaluation | 35 |
| 1.10.2. Caspase-dependent cell death | 37 |
| 1.10.3. Antitumor efficacy <i>in vivo</i> | 39 |
| 1.11. B-PAC-1 | 40 |
| 1.11.1. Discovery and cell death induction..... | 40 |
| 1.11.2. Role of zinc in B-PAC-1 activity | 41 |
| 1.11.3. Role of apoptotic proteins in B-PAC-1 activity | 42 |
| 1.11.4. Combination of B-PAC-1 with Smac mimetic..... | 43 |
| 1.12. Summary and outlook | 43 |
| 1.13. References..... | 45 |

| | |
|--|-----|
| Chapter 2. Synthetic and Spectroscopic Studies of PAC-1 , and Synthesis of S-PAC-1 | 52 |
| 2.1. Introduction..... | 52 |
| 2.2. Improved large-scale synthesis of PAC-1 | 52 |
| 2.2.1. First-generation synthesis of PAC-1 | 52 |
| 2.2.2. Second-generation synthesis of PAC-1 | 53 |
| 2.3. Determination of <i>N</i> -acylhydrazone isomers by NMR spectroscopy | 57 |
| 2.3.1. Assignment of NMR spectral resonances | 57 |
| 2.3.1.1. ¹ H-NMR and ¹³ C-NMR spectroscopy | 57 |
| 2.3.1.2. Two-dimensional heteronuclear spectroscopy..... | 59 |
| 2.3.2. Interconversion of species by exchange spectroscopy..... | 62 |
| 2.3.3. Assignment of isomers by chemical shifts..... | 63 |
| 2.3.4. Diphenylmethylene hydrazone | 65 |
| 2.4. Improved large-scale synthesis of S-PAC-1 | 67 |
| 2.4.1. First-generation synthesis of S-PAC-1 | 67 |
| 2.4.2. Second-generation synthesis of S-PAC-1 | 68 |
| 2.5. Materials and methods | 69 |
| 2.5.1. Chemical information | 69 |
| 2.5.2. Spectra..... | 76 |
| 2.6. References..... | 87 |
| Chapter 3. Parallel Synthesis and Biological Evaluation of 837 Analogues of PAC-1 | 88 |
| 3.1. Combinatorial library design and synthesis..... | 88 |
| 3.1.1. Library design | 88 |
| 3.1.2. Synthesis of library building blocks | 90 |
| 3.1.3. Synthesis of library members..... | 92 |
| 3.2. Cell culture evaluation of library | 95 |
| 3.3. Cell culture, <i>in vitro</i> , and <i>in silico</i> evaluation of hit compounds..... | 97 |
| 3.4. Evaluation of B-PAC-1 | 101 |
| 3.5. Discussion | 103 |
| 3.6. Materials and methods | 105 |
| 3.6.1. Chemical information | 105 |
| 3.6.2. Biological evaluation | 109 |

| | |
|--|-----|
| 3.6.3. Spectra..... | 112 |
| 3.7. References..... | 118 |
| Chapter 4. Removal of metabolic liabilities enables development of PAC-1 derivatives with improved pharmacokinetics..... | 120 |
| 4.1. Introduction..... | 120 |
| 4.2. First-generation library for enhancement of metabolic stability..... | 121 |
| 4.2.1. Compound design and synthesis..... | 121 |
| 4.2.2. Evaluation of library..... | 125 |
| 4.3. Second-generation library for enhancement of metabolic stability..... | 127 |
| 4.3.1. Compound design and synthesis..... | 127 |
| 4.3.2. Evaluation of library <i>in silico</i> , in cell culture, and <i>in vitro</i> | 131 |
| 4.3.3. Compound tolerability in mice..... | 135 |
| 4.4. Evaluation of compound 4.12 | 136 |
| 4.5. Blood-brain barrier permeability of selected derivatives..... | 137 |
| 4.6. Secondary biological assays..... | 139 |
| 4.7. Pharmacokinetics..... | 144 |
| 4.8. Discussion..... | 145 |
| 4.9. Materials and methods..... | 147 |
| 4.9.1. Chemical information..... | 147 |
| 4.9.2. Biological evaluation..... | 158 |
| 4.9.3. Spectra..... | 164 |
| 4.10. References..... | 186 |
| Chapter 5. Investigation of Neurotoxicity Induced by PAC-1 | 188 |
| 5.1. PAC-1 neurotoxicity is most likely not mechanism-based..... | 188 |
| 5.2. Compound design and synthesis..... | 190 |
| 5.3. Evaluation of PAC-1 derivatives..... | 194 |
| 5.3.1. Predicted blood-brain barrier permeability..... | 194 |
| 5.3.2. Cell culture evaluation..... | 195 |
| 5.3.3. Zinc binding determination..... | 197 |
| 5.3.4. Summary of structure-activity relationships..... | 198 |
| 5.4. Evaluation of PAC-1 derivatives in mice..... | 199 |

| | |
|--|-----|
| 5.5. Comparison of PAC-1 derivatives..... | 202 |
| 5.6. Summary and future directions | 206 |
| 5.7. Materials and methods | 207 |
| 5.7.1. Chemical information | 207 |
| 5.7.2. Biological evaluation | 218 |
| 5.7.3. Spectra..... | 222 |
| 5.8. References..... | 237 |

Chapter 1. Anticancer Activity of PAC-1 and Derivatives

Portions of the text of this chapter are adapted with permission from literature (Hsu, D. C.; Roth, H. S.; West, D. C.; Botham, R. C.; Novotny, C. J.; Schmid, S. C.; Hergenrother, P. J. Parallel synthesis and biological evaluation of 837 analogues of Procaspase-Activating Compound 1 (PAC-1). *ACS Comb. Sci.* **2012**, 14, 44-50.¹ Roth, H. S.; Botham, R. C.; Schmid, S. C.; Fan, T. M.; Dirikolu, L.; Hergenrother, P. J. Removal of metabolic liabilities enables development of derivatives of Procaspase-Activating Compound 1 (PAC-1) with improved pharmacokinetics. *J. Med. Chem.* **2015**, 58(9), 4046-4065.²)

1.1. Introduction: Procaspase-3 activation as an anticancer strategy

Apoptosis is a process used by higher organisms to maintain homeostasis by removing cells that are in excess, damaged, or potentially dangerous. Critical to apoptosis is the activation of caspase enzymes, a class of cysteine proteases that cleave cellular substrates after recognition sequences with C-terminal aspartate residues.³ There are two canonical apoptotic pathways, differing in that the apoptosis-initiating stimulus is intracellular (intrinsic pathway) or extracellular (extrinsic pathway).⁴ These pathways converge at the cleavage of procaspase-3 to form the active caspase-3, the key “executioner” caspase that catalyzes the hydrolysis of hundreds of protein substrates,⁵⁻⁸ leading to cell death. As one of the hallmarks of cancer is the ability to evade apoptosis,^{9, 10} many recent efforts to develop new anticancer drugs have focused on inhibition of antiapoptotic proteins, including MDM2,^{11, 12} Bcl-2,^{13, 14} and XIAP^{15, 16} (Figure 1.1). The mutation and upregulation of these proteins provides targets that exist at much higher concentrations in cancer cells, reducing the potential for induction of apoptosis in healthy cells, which could lead to undesired toxicity. Similarly, small molecules capable of enhancing the activity of proapoptotic proteins hold promise for the treatment of cancer. One target that has received considerable attention is procaspase-3.¹⁷⁻²⁰ The low frequency of procaspase-3 mutations in cancer,²¹ its downstream location relative to apoptotic proteins that are frequently mutated,⁴ and the overexpression of procaspase-3 in a number of cancer types, including lymphoma,^{22, 23} leukemia,^{24, 25} melanoma,^{26, 27} glioblastoma,^{28, 29} pancreatic cancer,³⁰ liver cancer,³¹ lung cancer,³²⁻³⁴ breast cancer,³⁵⁻³⁸ esophageal cancer,³⁹ and colon cancer,^{17, 40-42} have

made the small molecule-mediated activation of procaspase-3 an attractive strategy for personalized medicine.¹⁷⁻²⁰

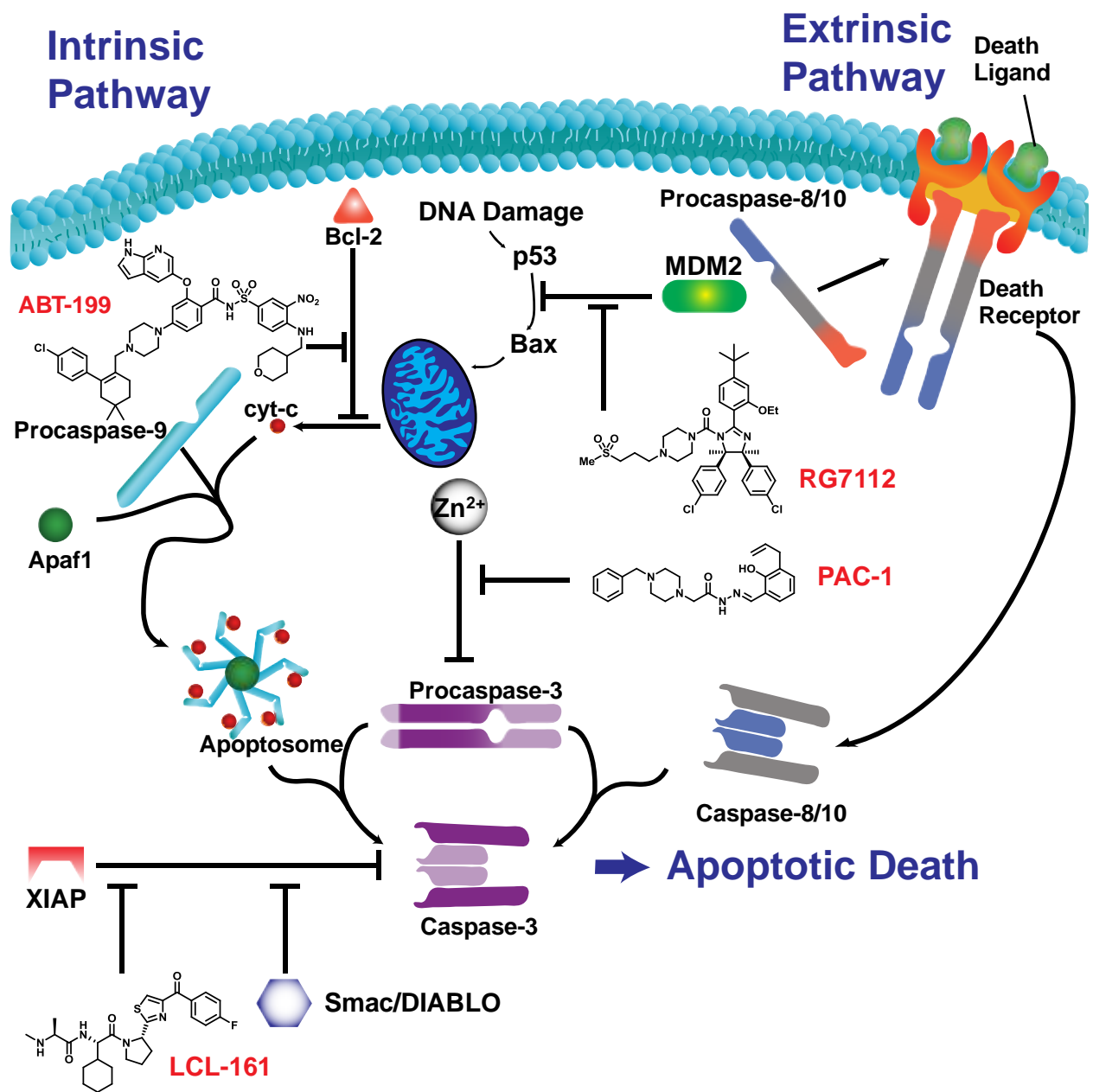


Figure 1.1. Representative small-molecule modulators of apoptotic regulators.

1.2. PAC-1

1.2.1 Initial discovery of PAC-1

Procaspase Activating Compound 1 (**PAC-1**, **1.1**, Figure 1.2) was discovered in the Hergenrother laboratory via a high-throughput screen of over 20,000 small molecules as a compound that could enhance the enzymatic activity of procaspase-3 *in vitro*, with an EC₅₀ of 0.22 μM for procaspase-3 activation. **PAC-1** induced apoptosis in cancer cells in culture, with a 72-hour IC₅₀ of 0.92 μM against HL-60 (human leukemia) cells. **PAC-1** is cytotoxic against a diverse array of cancer cells in culture, including cell lines derived from hematopoietic tumors (lymphoma,^{1, 2, 17, 43-49} leukemia,^{2, 17, 45, 48-53} and multiple myeloma⁵³), carcinomas of diverse origin (breast,^{17, 45, 48-52, 54-56} renal,¹⁷ adrenal,^{17, 57} colon,^{17, 48, 53, 55, 56, 58} lung,^{17, 48-56, 58-61} cervical,^{45, 53} gastric,^{48, 49, 53, 55, 56, 58} ovarian,⁵³ liver,^{48, 49, 53} prostate,^{48, 49} and gallbladder^{48, 49}), and other solid tumor histologies (melanoma,^{17, 45, 48, 49} osteosarcoma,⁵³ neuroblastoma,^{17, 53, 55, 56} and glioblastoma^{48, 49}). **PAC-1** and derivatives also induce apoptosis in patient-derived samples from colon cancer,¹⁷ and chronic lymphocytic leukemia,²⁵ and anticancer efficacy has been observed in multiple murine tumor models^{17, 48, 49, 54, 60-62} and in pet dogs with cancer.⁴⁵ In addition, **PAC-1** displayed potent synergy with the antitumor agent paclitaxel,⁶⁰⁻⁶² as well as the second reported procaspase-3 activator, **1541B**,⁵⁴ in various cell culture and *in vivo* models of cancer; a derivative of **PAC-1** showed synergy with an investigational Smac mimetic in cell culture.²⁵ The remainder of this chapter details studies of the structure-activity relationships (SAR) and the mechanism of action of **PAC-1** performed by other members of the Hergenrother laboratory and by outside research groups.

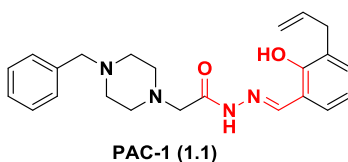


Figure 1.2. Structure of **PAC-1** (**1.1**), with *ortho*-hydroxy-*N*-acylhydrazone highlighted in red.¹⁷

An initial evaluation of SAR was undertaken with a small number of closely related compounds and synthetic intermediates (Table 1.1). **PAC-1** was the most potent compound evaluated, while removal of the allyl group (**1.2**) led to a slight loss in potency. However, each of

the other compounds studied (1.3-1.10) was inactive in both procaspase-3 activation and cytotoxicity assays.¹⁷

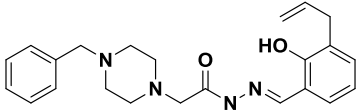
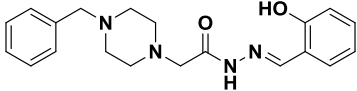
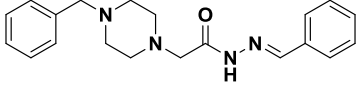
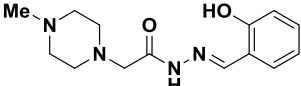
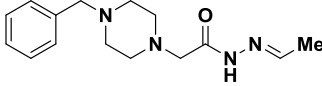
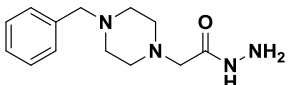
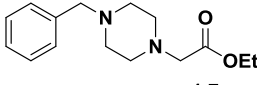
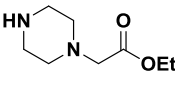
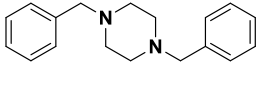
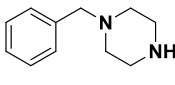
| Compound | Procaspase-3 EC ₅₀ (μM) | HL-60 72-hour IC ₅₀ (μM) |
|---|---------------------------------------|--|
|  PAC-1 (1.1) | 0.22 | 0.92 |
|  1.2 | 0.43 | 1.74 |
|  PAC-1a (1.3) | >50 | >100 |
|  1.4 | >50 | >100 |
|  1.5 | >50 | >100 |
|  1.6 | >50 | >100 |
|  1.7 | >50 | >100 |
|  1.8 | >50 | >100 |
|  1.9 | >50 | >100 |
|  1.10 | >50 | >100 |

Table 1.1. Preliminary SAR studies of PAC-1.¹⁷

1.2.2. PAC-1 mechanism of action

One of the most informative results from the initial report on **PAC-1** was that removal of the hydroxyl group (compound **1.3**, also known as **PAC-1a**) abolished activity. This suggested the essential nature of the *ortho*-hydroxy-*N*-acylhydrazone moiety for anticancer activity of **PAC-1**. The *ortho*-hydroxy-*N*-acylhydrazone is known to chelate metals, including iron,⁶³ copper,⁶⁴ and zinc,⁶⁵ and many divalent metal cations are also known to inhibit procaspase⁴³ and caspase⁶⁶⁻⁶⁹ enzymes. In particular, zinc from the labile zinc pool, which is bound loosely to certain proteins, has been shown to co-localize with procaspase-3⁷⁰ and inhibit the enzymatic activity of both procaspase-3⁴³ and caspase-3,⁶⁷ as illustrated in Figure 1.1. In addition, a putative binding site on procaspase-3/caspase-3 for labile zinc ions has been identified.⁷¹ Based on this, the role of zinc in the mechanism of action of **PAC-1** was investigated.⁴³ **PAC-1** was shown to bind zinc in a 1:1 ratio with a K_d of 52 ± 2 nM.^{43, 44} **PAC-1** showed no activity toward procaspase-3 in a metal-free buffer; however, the addition of zinc inhibited procaspase-3 activity, and **PAC-1** was able to restore this activity in a dose-dependent manner (Figure 1.3A). In addition, **PAC-1** was shown to induce apoptosis in U-937 (human lymphoma) cells, but the addition of zinc to the cell culture medium abolished the ability of **PAC-1** to induce apoptosis. Finally, **PAC-1a** displayed no affinity toward zinc and was unable to induce procaspase-3 activation. Based on these results, a mechanism of action has been proposed for **PAC-1** activity (Figure 1.3B). Zinc binds loosely to procaspase-3, inhibiting its activity and its ability to be cleaved to the active caspase-3. **PAC-1** chelates the zinc from the labile pool, allowing for cleavage of procaspase-3 to caspase-3 and the initiation of the execution pathway of apoptosis.⁴³ The affinity of **PAC-1** for zinc is not strong enough to disrupt proteins containing essential zinc ions; **PAC-1** and several derivatives showed no inhibitory activity toward matrix metalloproteinases-9 and -14,⁷² as well as carboxypeptidase A and histone deacetylase,²⁵ enzymes containing active site zinc ions.

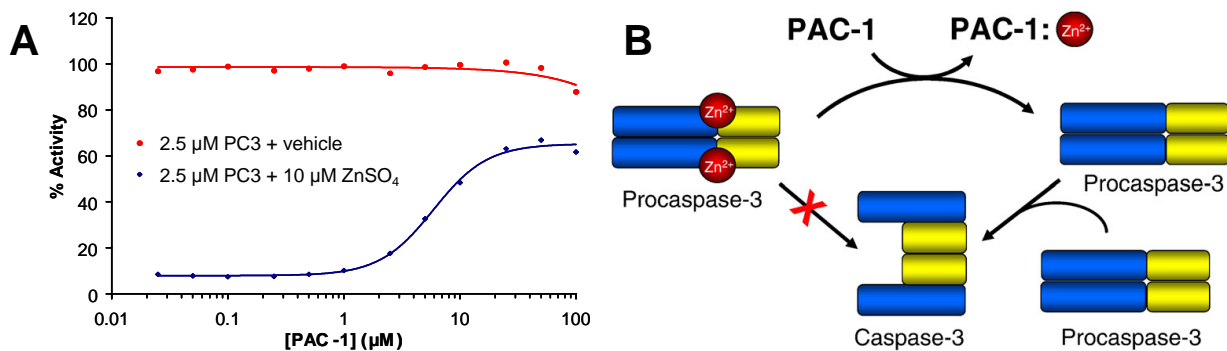


Figure 1.3. A. PAC-1 has no effect on procaspase-3 in a metal-free buffer but relieves zinc-mediated inhibition of procaspase-3 in a dose-dependent manner. **B.** Proposed mechanism of action of PAC-1. PAC-1 chelates labile zinc from procaspase-3, facilitating activation to caspase-3. Figures adapted with permission from literature.⁴³

1.2.3. Structure-activity relationships

With a preliminary understanding of the mechanism of action of PAC-1, the SAR studies of the compound were initiated by members of the Hergenrother group.⁴⁴ In order to investigate the SAR, four classes of PAC-1 derivatives were designed (Figure 1.4). Class I derivatives (**1.2**, **1.3**, **1.11a-h**, and **1.12**) contained modifications to the benzylidene group, Class II derivatives (**1.13a-c** and **1.14a-d**) contained modifications to the benzyl group, and the single Class III derivative (**1.15**) contained modifications to both aromatic rings. Class IV derivatives (**1.16a-b**, **1.17a-b**, **1.18**, **1.19**, and **1.20**) contained modifications to the four nitrogen atoms present in PAC-1. In total, 26 derivatives were synthesized and compared to PAC-1 in a series of experiments.⁴⁴

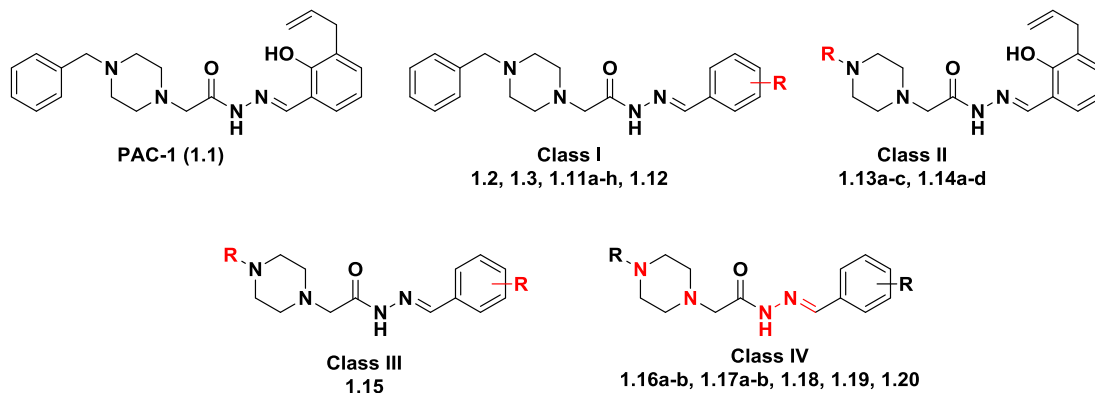
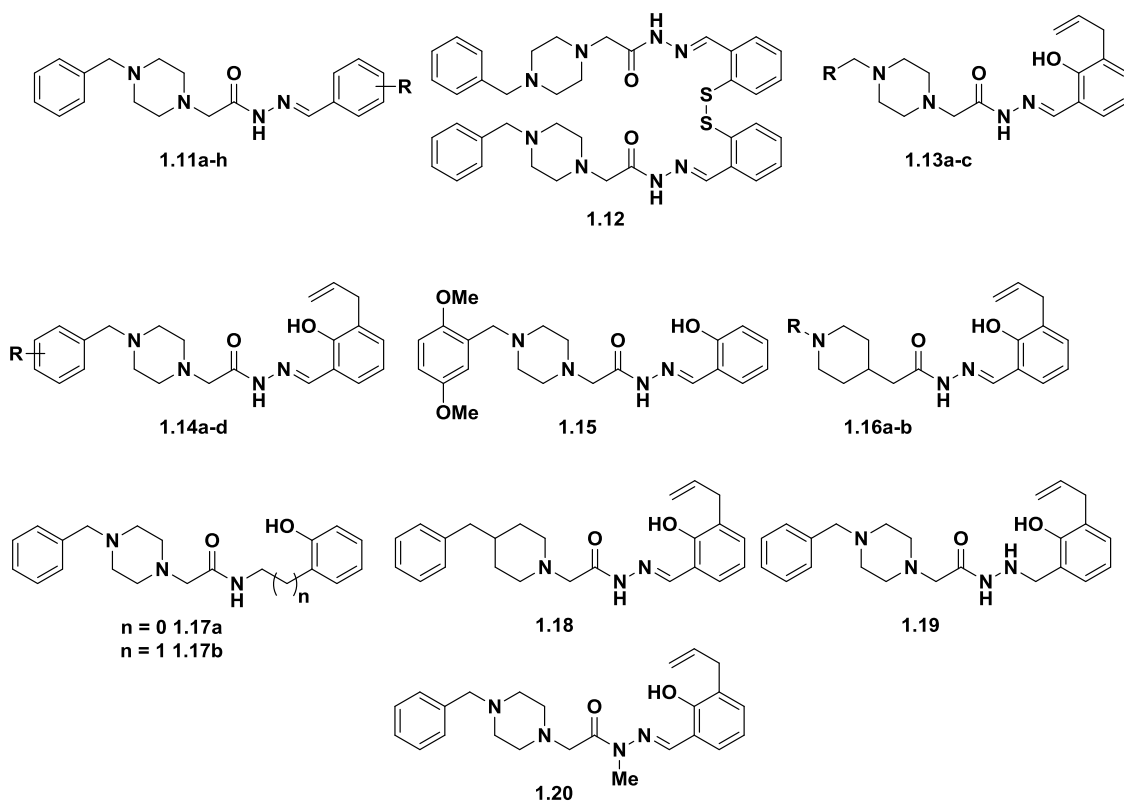


Figure 1.4. Four classes of PAC-1 derivatives synthesized for SAR determination.⁴⁴

The evaluation of the compounds is shown in Table 1.2. Compounds were evaluated for their ability to chelate zinc, relieve zinc-mediated inhibition of caspase-3, and induce cell death in U-937 cells. These experiments confirmed the essential nature of the *ortho*-hydroxy-*N*-acylhydrazone for activity. Class I derivatives lacking the phenol showed significantly reduced activity compared to **PAC-1** in these experiments, while the two Class I derivatives containing the phenol (**1.2** and **1.11h**) retained activity. However, modification of the benzyl group was tolerated, as Class II derivatives showed similar activity to **PAC-1**. The Class III derivative (**1.15**) was also active, suggesting that substitution of both aromatic rings could be tolerated, as long as the *ortho*-hydroxy-*N*-acylhydrazone remained intact. Class IV derivatives that contained the *ortho*-hydroxy-*N*-acylhydrazone (**1.16a-b** and **1.18**) were capable of binding zinc and inducing cell death, although compounds **1.16a-b** showed inhibitory activity toward caspase-3. Class IV derivatives containing modifications to the hydrazone (**1.17a-b**, **1.19**, and **1.20**) showed diminished activity relative to **PAC-1**. In order to further investigate the cellular effects of **PAC-1** and derivatives, U-937 cells were treated with **PAC-1**, **1.14a**, or **1.18** at 50 μ M for 12 hours, and cell death was assessed by flow cytometry with Annexin V-FITC/propidium iodide staining. Large populations of Annexin V-FITC positive, propidium iodide negative cells were present for each compound treatment, indicating that cell death proceeds through apoptosis.⁴⁴



| compound | R | Zn ²⁺ K _d (nM) | % Caspase-3 Activation at 10 μM | U-937 72-hour IC ₅₀ (μM) |
|----------|---------------------------|---|---------------------------------------|---|
| PAC-1 | - | 52 ± 2 | 45.8 ± 4.8 | 4.8 ± 1.0 |
| 1.2 | - | 77 ± 2 | 30 ± 2 | 15.3 ± 2.0 |
| 1.3 | - | >10 ⁴ | 0 | >100 |
| 1.11a | 2-SMe | >10 ⁴ | 0 | >100 |
| 1.11b | 2-NH ₂ | >10 ⁴ | 0 | >100 |
| 1.11c | 2-CO ₂ H | >10 ⁴ | 0 | >100 |
| 1.11d | 2-CO ₂ Me | >10 ⁴ | 0 | >100 |
| 1.11e | 2-Cl | >10 ⁴ | 0 | 57 ± 5 |
| 1.11f | 2-SH | >10 ⁴ | 0 | >100 |
| 1.11g | 2-OH-3,5-All ₂ | 43 ± 9 | 59 ± 5 | 1.8 ± 0.4 |
| 1.11h | 2-OMe-3-All | >10 ⁴ | 0 | 32 ± 12 |
| 1.12 | - | >10 ⁴ | 0 | >100 |
| 1.13a | 2-Py | 68 ± 10 | 48 ± 3 | 9.5 ± 1.8 |
| 1.13b | 3-Py | 62 ± 9 | 20.6 ± 1.6 | 14 ± 2 |
| 1.13c | 4-Py | 80 ± 14 | 26.3 ± 0.1 | 21 ± 6 |
| 1.14a | 4-F | 48 ± 3 | 24.2 ± 1.7 | 2.0 ± 0.2 |
| 1.14b | 2,5-(OMe) ₂ | 39 ± 3 | 31 ± 3.6 | 1.0 ± 0.1 |
| 1.14c | 4-OMe | 47 ± 5 | 24 ± 3.4 | 2.7 ± 0.8 |
| 1.14d | 3-NO ₂ | 45 ± 13 | 19.5 ± 1.8 | 4.6 ± 1.0 |
| 1.15 | - | 65 ± 4 | 30.7 ± 1.2 | 12 ± 2 |
| 1.16a | Bn | 44 ± 2 | 0 ^a | 2.8 ± 1.1 |
| 1.16b | Boc | 48 ± 7 | 0 ^a | 6.5 ± 3.6 |
| 1.17a | - | >10 ⁴ | 4.4 ± 0.9 | >100 |
| 1.17b | - | >10 ⁴ | 4.1 ± 1.0 | >100 |
| 1.18 | - | 49 ± 2 | 36 ± 3 | 2.7 ± 1.1 |
| 1.19 | - | >10 ⁴ | 17.1 ± 1.2 | 59 ± 14 |
| 1.20 | - | >10 ⁴ | 0 | 22 ± 3 |

Table 1.2. Zinc chelation, *in vitro* caspase-3 activation, and cytotoxicity of PAC-1 and derivatives. ^a – These derivatives slightly inhibited caspase-3, masking any activation.⁴⁴

An additional derivative of **PAC-1** was synthesized containing a fluorophore conjugated to the benzyl ring through a triazole linker. This compound (**AF350-PAC-1**, **1.21**, Figure 1.5) was found to bind zinc, activate caspase-3 *in vitro*, and induce cell death in culture. As shown in Figure 1.6, SK-MEL-5 cells were treated with **1.21** and FAM-DEVD-fmk, a covalent inhibitor for caspases-3 and -7 that covalently modifies the enzyme with a fluorophore. FAM-DEVD-fmk therefore represents a marker for sites of caspase-3/-7 activity within cells. Cells were treated for one hour, washed in phenol red-free medium, and incubated for an additional two hours. The cells were then visualized at emission wavelengths of 400 nm (**1.21**, pseudo-colored green) and 520 nm (FAM-DEVD-fmk, pseudo-colored red). Treatment of cells with vehicle (Figure 1.6A, B, C) showed minimal fluorescence in either channel. Minimal increases in fluorescence were observed upon treatment with FAM-DEVD-fmk alone (Figure 1.6D, E, F). Treatment with **1.21** alone (Figure 1.6G, H, I) showed punctate staining in the cytoplasm at 400 nm. Finally, cells treated with both **1.21** and FAM-DEVD-fmk (Figure 1.6J, K, L) showed punctate staining at both 400 nm and 520 nm, and the merged image (Figure 1.6L) shows overlap for the majority of these sites of fluorescence. This confirms that **1.21** induces activation of executioner caspases in cells and co-localizes with sites of caspase-3/-7 activity.⁴⁴

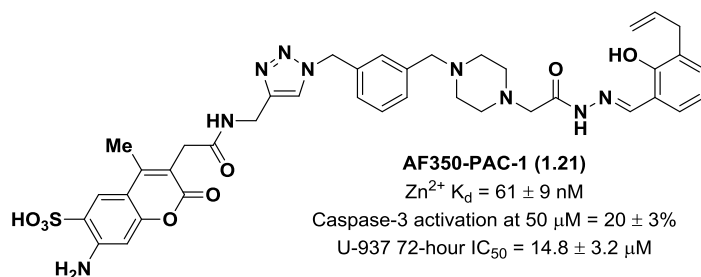


Figure 1.5. Structure of fluorescent **PAC-1** derivative **1.21**.⁴⁴

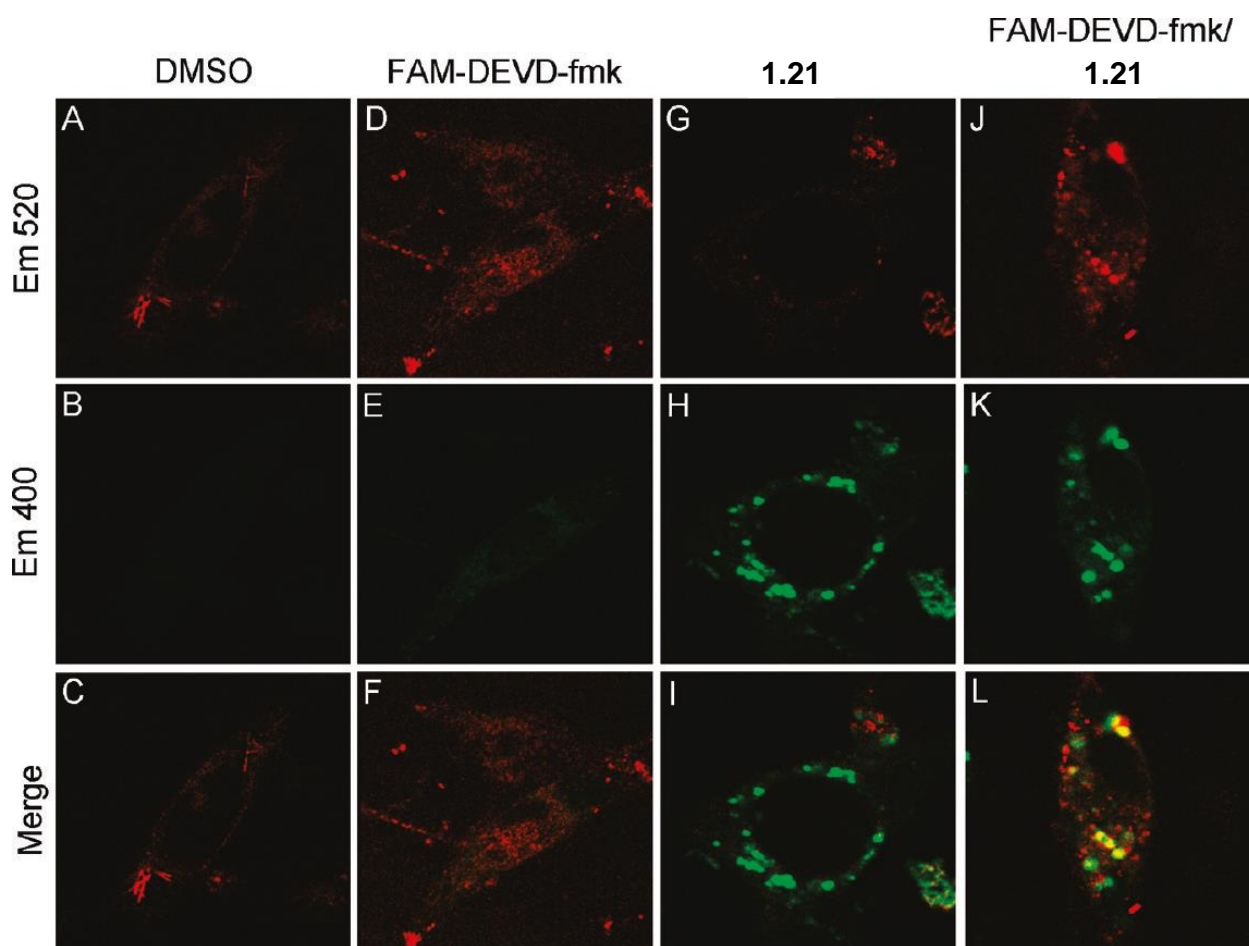


Figure 1.6. Fluorescent PAC-1 derivative **1.21** co-localizes with sites of caspase-3/-7 activity in SK-MEL-5 cells. **A-C.** Background levels of fluorescence in cells treated with DMSO alone. **D-F.** Minimal fluorescence over background in cells treated with FAM-DEVD-fmk alone. **G-I.** Cells treated with **1.21** show punctate staining in cytoplasm. **J-L.** Cells treated with FAM-DEVD-fmk and **1.21** show sites of caspase activity, which co-localize with punctate staining of **1.21**. Figures adapted with permission from literature.⁴⁴

1.2.4 Relationship to other metal-binding compounds in medicine

Given the increased attention paid to so-called “PAINS” (pan-assay interference compounds),⁷³ a further discussion of **PAC-1** and derivatives in relationship to PAINS compounds is warranted. The metal-binding ability of *ortho*-hydroxy-*N*-acylhydrazones can cause members of this class of compounds to appear as hits in screening assays due to interference with the assay screening system, rather than via specific interactions with biological targets.⁷³ In these cases, attempts to validate such hits will fail because the apparent activity of

the screening hit is unrelated to the target. However, rather than interfering with the *in vitro* procaspase-3 enzymatic assay, the chelation of zinc from procaspase-3 *in vitro* by **PAC-1** is highly biologically relevant; **PAC-1** is directly modulating zinc, an endogenous inhibitor of procaspase-3, and a putative binding site on procaspase-3/caspase-3 for this inhibitory zinc has been identified.⁷¹ Through this “inhibiting the inhibitor” mechanism, **PAC-1** is similar to compounds that bind to other endogenous apoptotic inhibitors and induce apoptosis, such as those binding MDM2¹¹ and XIAP.¹⁵ **PAC-1** shows minimal inhibitory activity towards zinc-dependent enzymes, including matrix metalloproteinases-9 and -14,⁷² and a derivative of **PAC-1** showed minimal inhibition toward carboxypeptidase A and histone deacetylases.²⁵ These results are consistent with the known modest affinity of **PAC-1** for zinc,⁴³ allowing for a high degree of selectivity for chelation of zinc ions from the labile pool over essential zinc ions in canonical zinc binding sites within metalloproteins. In addition, **PAC-1** is stable in aqueous solution; degradation of **PAC-1** is observed only when the compound is subjected to extremes in temperature and pH outside of relevant physiological ranges.⁷⁴

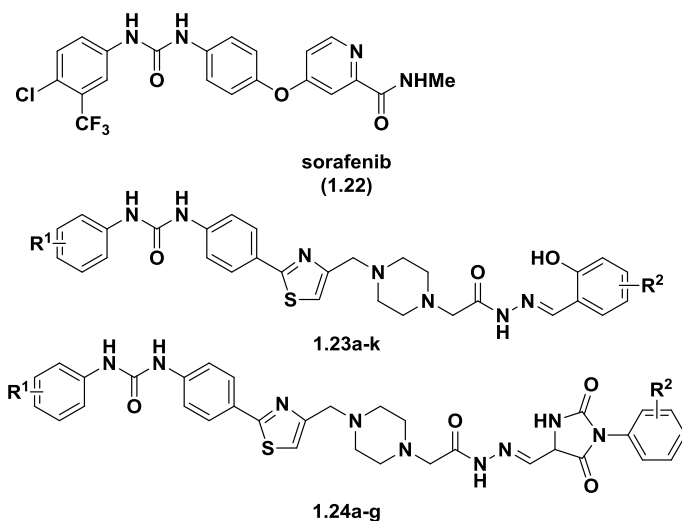
PAC-1 also chelates labile zinc in cancer cells in culture, as determined by detailed experiments with genetically encoded fluorescent sensors specific for zinc.⁴⁷ This removal of zinc leads to the observed anticancer effect in cell culture. **PAC-1** shows no activity toward several other enzymes as assessed by *in vitro* assays,⁷⁵ **PAC-1** and derivatives do not affect the activity of proteins that rely on tightly-bound zinc,^{25, 72} and **PAC-1** derivatives that do not bind zinc *in vitro* are inactive in cells.⁴⁴ As shown by multiple investigators, treatment of cells with **PAC-1** or a derivative results in the cleavage of procaspase-3 prior to the cleavage of initiator procaspases-8 and -9,^{48, 49} and co-treatment of **PAC-1** with a covalent inhibitor of caspase-9 does not prevent cleavage of procaspase-3,⁷⁶ further supporting the hypothesis that the proapoptotic activity of **PAC-1** is due to chelation of labile inhibitory zinc from procaspase-3, leading to the activation of procaspase-3 without the intermediacy of caspase-9, and subsequent apoptotic cell death.

While many metal chelators will interfere with *in vitro* enzyme assays, it would be inappropriate to disregard all metal chelators from consideration as drug candidates due to this *in vitro* artifact. Indeed, metal chelators have a rich history in drug discovery and have made a positive impact on many diseases through a diverse range of mechanisms and targets.⁷⁷ The marketed drugs vorinostat (Zn^{2+}),⁷⁸ penicillamine (Cu^{2+}),⁷⁷ and the entire class of

bisphosphonates (Ca^{2+}),⁷⁹ as well as the experimental therapeutics elesclomol (Cu^{2+}),⁷⁷ ML-133/Apto-253 (Zn^{2+}),⁸⁰ and triapine ($\text{Fe}^{3+}/\text{Fe}^{2+}$),⁸¹ among other small molecules, all rely on metal chelation *in vivo* for their mechanism of action. It is safe to say that many of these compounds would interfere with certain *in vitro* assays that are contingent upon metal-bound proteins. While it is reasonable for metal chelators and metal-chelating motifs to be structural alerts when examining screening hits, if the desired biological activity is metal chelation, then metal chelation is the precise trait to look for in a screening hit.

1.3. Diaryl urea conjugates

With the goal of improving upon **PAC-1**, several classes of derivatives were synthesized and evaluated. One approach toward improving the potency of **PAC-1** explored by Gong and coworkers involved the conjugation of fragments derived from sorafenib (**1.22**), a diaryl urea that inhibits several kinases, including VEGFR, PDGFR, and B-Raf, to **PAC-1**.⁵⁰⁻⁵² Initially, two series of compounds were synthesized (Table 1.3).⁵⁰ In the first series (**1.23a-k**), diaryl ureas were conjugated via a thiazole to the piperazine/*ortho*-hydroxy-*N*-acylhydrazone portion of **PAC-1**, and substituents on each terminal arene were varied. In the second series (**1.24a-g**), the phenol ring was replaced with a hydantoin. The cytotoxicity of the 18 compounds was evaluated in A549 (human lung), HL-60 (human leukemia), and MDA-MB-231 (human breast) cancer cell lines in culture and compared to **PAC-1** and sorafenib. In general, the compounds of series **1.23** were much more potent than the compounds of series **1.24**, confirming the essential nature of the *ortho*-hydroxy-*N*-acylhydrazone for activity of **PAC-1** derivatives. Many of the **1.23** compounds were even more potent than **PAC-1** or sorafenib, suggesting the potential for improved potency via dual pharmacophores. Compound **1.24g** displayed comparable potency to the parent compounds, and because it lacks the hydroxyl group, it likely acts via a different mechanism than **PAC-1**.

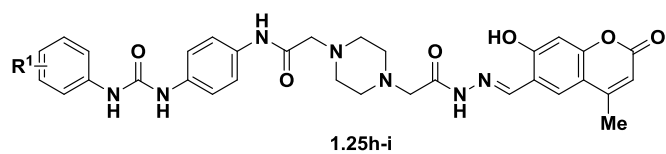
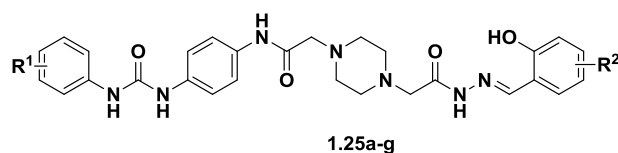
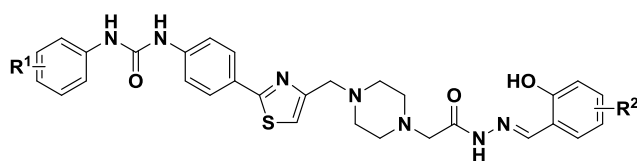


| compound | R ¹ | R ² | IC ₅₀ (μM) | | |
|-----------|-------------------------------------|----------------------------------|-----------------------|-------|------------|
| | | | A549 | HL-60 | MDA-MB-231 |
| 1.23a | 3-F | 5-Br | 2.3 | 7.1 | 1.4 |
| 1.23b | 3-F | 3,4-F ₂ | 1.9 | 6.2 | 1.1 |
| 1.23c | 3-F | 3,5-(<i>t</i> -Bu) ₂ | >100 | 1.1 | 23 |
| 1.23d | 2-Cl-4-CF ₃ | - | 2.0 | 9.9 | 1.4 |
| 1.23e | 3-Cl | 5-Cl | 4.4 | 6 | 1.6 |
| 1.23f | 3-Cl | 3,5-(<i>t</i> -Bu) ₂ | 0.7 | 2.7 | 1.0 |
| 1.23g | 3-Cl | 4-Me | >100 | 1.2 | >100 |
| 1.23h | 3-F | 4-OBn | 1.1 | 1.1 | 1.0 |
| 1.23i | 3-F | 4-O(4-Cl-Bn) | 0.8 | 2.8 | 0.8 |
| 1.23j | 3-F | 4-O(2,4-Cl ₂ -Bn) | 0.7 | 0.13 | 0.5 |
| 1.23k | 3-F | 4-O(3-F-Bn) | 0.9 | 1.6 | 0.7 |
| 1.24a | 3-F | 4-Me | 18 | 32 | 93 |
| 1.24b | 3-F | 4-Cl | 12 | 22 | 31 |
| 1.24c | 3-Cl | 4-Me | 73 | 24 | 14 |
| 1.24d | 3-OMe | 4-CF ₃ | >100 | >100 | >100 |
| 1.24e | 2-Cl-4-CF ₃ | 4-CF ₃ | >100 | 30 | >100 |
| 1.24f | 3,5-(CF ₃) ₂ | 4-CF ₃ | 12 | 12 | 31 |
| 1.24g | 3,4-F ₂ | 4-CF ₃ | 3.5 | 6.2 | 3.0 |
| sorafenib | | | 2.6 | N.D. | 5.4 |
| PAC-1 | | | 5.6 | 9.1 | 4.1 |

Table 1.3. Structure and cytotoxicity of hybrid **PAC-1**/sorafenib derivatives. N.D. = not determined.⁵⁰

In order to build upon these results, a second set of 18 diaryl urea/**PAC-1** conjugates was synthesized (Table 1.4).⁵¹ Because the hydantoin derivatives were significantly less active, synthesis of derivatives was limited to those containing the *ortho*-hydroxy-*N*-acylhydrazone moiety. Nine additional derivatives of the **1.23** series (**1.23l-t**) were synthesized. In addition, nine derivatives (**1.25a-i**) were synthesized that contained an amide linkage instead of the thiazole. These compounds were also evaluated in A549, HL-60, and MDA-MB-231 cells in culture and compared to **PAC-1** and sorafenib. Most of the compounds displayed comparable potency to both of the parent compounds in the cell lines tested. In general, the compounds of the **1.23**

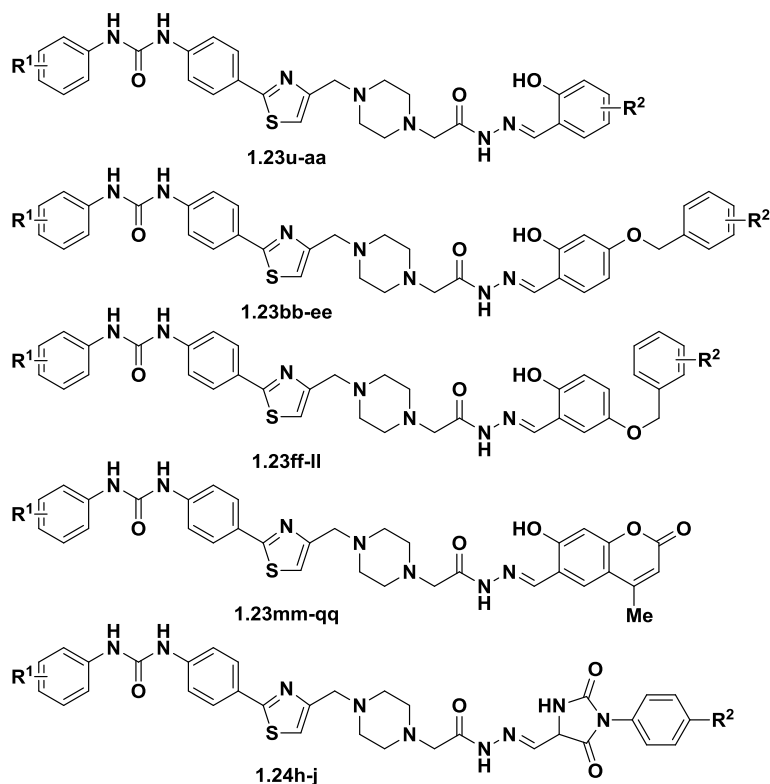
series were somewhat more potent than the compounds of the **1.25** series. The addition of a benzyloxy substituent to the benzylidene ring increased potency for compounds of the **1.23** series. Three of the derivatives (**1.23l**, **1.23q**, and **1.23s**), as well as **PAC-1** and sorafenib, were evaluated in a human embryonic lung fibroblast-derived cell line (WI-38) in culture. The compounds exhibited slightly reduced potency in this cell line compared to the cancer cell lines, suggesting a degree of selectivity for toxicity to cancer cells over normal cells.⁵¹



| compound | R ¹ | R ² | 72-hour IC ₅₀ (μM) | | | |
|--------------|-------------------------|----------------------------------|-------------------------------|-------|------------|-------|
| | | | A549 | HL-60 | MDA-MB-231 | WI-38 |
| 1.23l | 2-CF ₃ | - | 3.88 | 2.40 | 4.65 | 11.67 |
| 1.23m | 2,4-Cl ₂ | - | 2.40 | 0.33 | 1.27 | N.D. |
| 1.23n | 3-OCF ₃ | 3,5-(<i>t</i> -Bu) ₂ | 1.49 | 2.11 | 0.90 | N.D. |
| 1.23o | - | 5-OBn | 1.67 | 0.55 | 0.74 | N.D. |
| 1.23p | 2-Cl-4-CF ₃ | 5-OBn | 2.30 | 1.03 | 0.59 | N.D. |
| 1.23q | 2-OCF ₃ | 5-OBn | 0.41 | 0.23 | 0.24 | 4.53 |
| 1.23r | 2-OCF ₃ | 5-OBn | 0.45 | 0.35 | 0.30 | N.D. |
| 1.23s | 3-Cl | 4-OBn | 0.83 | 1.18 | 0.52 | 6.91 |
| 1.23t | 3,4-Cl ₂ | 4-OBn | 0.78 | 0.80 | 0.47 | N.D. |
| 1.25a | 3-CF ₃ | - | 8.97 | 4.24 | 2.39 | N.D. |
| 1.25b | 3-CF ₃ | 3,5-(<i>t</i> -Bu) ₂ | 1.34 | 1.29 | 0.49 | N.D. |
| 1.25c | 3-Cl | - | 52.0 | 2.44 | 1.18 | N.D. |
| 1.25d | 3-CF ₃ -4-Cl | - | 10.7 | 4.42 | 1.07 | N.D. |
| 1.25e | 3-CF ₃ | 5-OBn | 3.16 | 2.66 | 1.48 | N.D. |
| 1.25f | 3-Cl | 5-OBn | >100 | 1.70 | >100 | N.D. |
| 1.25g | 3-CF ₃ -4-Cl | 5-OBn | 4.02 | 1.82 | 1.92 | N.D. |
| 1.25h | 3-CF ₃ | - | 18.0 | 5.54 | >100 | N.D. |
| 1.25i | 3-Cl-4-CF ₃ | - | >100 | 3.08 | 8.92 | N.D. |
| sorafenib | | | 1.30 | N.D. | 2.70 | 10.8 |
| PAC-1 | | | 2.81 | 4.56 | 2.04 | 6.63 |

Table 1.4. Structure and cytotoxicity of hybrid **PAC-1**/sorafenib derivatives. N.D. = not determined.⁵¹

The final set of 26 diaryl urea/**PAC-1** conjugates is shown in Table 1.5. This set of compounds included 23 phenol derivatives (**1.23u-qq**) and three hydantoin derivatives (**1.24h-j**), conjugated to the diaryl urea moiety via a thiazole linker.⁵² The compounds were evaluated in A549, HL-60, and MDA-MB-231 cells in a 72-hour cytotoxicity assay and compared to **PAC-1** and sorafenib. The compounds of the hydantoin series were again observed to be less potent than the compounds of the phenol series. Within the phenol series, the coumarin derivatives (**1.23mm-qq**) were less potent than the other derivatives. Many of the substituted phenol derivatives had sub-micromolar potency in the cell lines, improving upon the activity of either parent compound alone, and the benzyloxy derivatives were among the most potent compounds in this library. This provides additional validation that the conjugation of other cytotoxic agents to **PAC-1** can help to increase the potency of either agent alone.⁵²

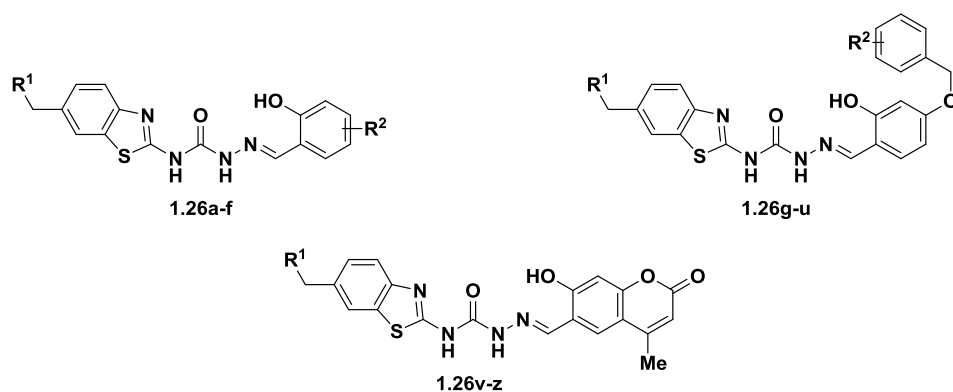


| compound | R ¹ | R ² | 72-hour IC ₅₀ (μM) | | |
|-----------|-------------------------------------|--|-------------------------------|--------------|--------------|
| | | | A549 | HL-60 | MDA-MB-231 |
| 1.23u | 3-F | 4-Me | 0.64 ± 0.12 | N.D. | 1.9 ± 0.16 |
| 1.23v | 3,5-Cl ₂ | 4-CH ₂ C(=CH ₂)Me | 0.78 ± 0.02 | 0.56 ± 0.04 | 0.48 ± 0.02 |
| 1.23w | 3-Cl-4-F | 3,5-(<i>t</i> -Bu) ₂ | 0.48 ± 0.06 | 13.0 ± 0.37 | 0.26 ± 0.01 |
| 1.23x | 4-CF ₃ | 3-Me-6- <i>i</i> -Pr | 5.1 ± 0.25 | 8.8 ± 0.31 | 8.5 ± 0.44 |
| 1.23y | 4-CF ₃ | 5- <i>t</i> -Bu | 1.6 ± 0.41 | 0.82 ± 0.08 | 0.92 ± 0.24 |
| 1.23z | 4-CF ₃ | 5-OMe | 1.3 ± 0.16 | 0.63 ± 0.17 | 0.82 ± 0.05 |
| 1.23aa | 3-CF ₃ | - | 0.50 ± 0.04 | 6.0 ± 0.09 | 0.58 ± 0.03 |
| 1.23bb | 3-F | 4-Cl | 0.59 ± 0.02 | 2.6 ± 0.11 | 0.71 ± 0.01 |
| 1.23cc | 3-Cl | 2,4-Cl ₂ | 1.7 ± 0.12 | 3.8 ± 0.13 | 0.53 ± 0.02 |
| 1.23dd | 3-Cl | 3-F | 0.49 ± 0.05 | 2.3 ± 0.11 | 0.35 ± 0.02 |
| 1.23ee | 3-Cl | 4-Cl | 2.8 ± 0.21 | 4.7 ± 0.19 | 0.48 ± 0.05 |
| 1.23ff | 3,4-Cl ₂ | - | 1.6 ± 0.14 | 0.55 ± 0.09 | 0.73 ± 0.06 |
| 1.23gg | 3,4-Cl ₂ | - | 1.2 ± 0.05 | 0.51 ± 0.01 | 0.73 ± 0.02 |
| 1.23hh | 3-OCF ₃ | 2-F | 0.34 ± 0.01 | 0.22 ± 0.01 | 0.41 ± 0.3 |
| 1.23ii | - | 2-F | 1.8 ± 0.04 | 0.50 ± 0.004 | 0.90 ± 0.006 |
| 1.23jj | 2-CF ₃ | 4-Cl | 0.54 ± 0.06 | 0.38 ± 0.01 | 0.44 ± 0.4 |
| 1.23kk | 3-CF ₃ -4-Cl | 2-F | 0.96 ± 0.20 | 0.31 ± 0.14 | 2.0 ± 0.12 |
| 1.23ll | 3-Cl-4-F | 3-Cl | 2.3 ± 0.08 | 2.0 ± 0.11 | 0.22 ± 0.04 |
| 1.23mm | - | - | 17.0 ± 0.52 | 15.2 ± 0.22 | 5.6 ± 0.36 |
| 1.23nn | 3-CF ₃ | - | >50 | 3.6 ± 0.12 | 3.8 ± 0.28 |
| 1.23oo | 3-OMe | - | 6.4 ± 0.42 | 3.3 ± 0.25 | 3.6 ± 0.28 |
| 1.23pp | 3,5-(CF ₃) ₂ | - | 1.7 ± 0.15 | 4.0 ± 0.33 | 1.8 ± 0.07 |
| 1.23qq | 3,4-Me ₂ | - | 19.0 ± 0.57 | 4.5 ± 0.13 | 8.9 ± 0.41 |
| 1.24h | 3-Cl-4-CF ₃ | CF ₃ | 37.2 ± 0.46 | 12.0 ± 0.32 | 7.0 ± 0.18 |
| 1.24i | 3-CF ₃ | CF ₃ | 3.4 ± 0.10 | 25.5 ± 0.29 | 13.3 ± 0.32 |
| 1.24j | 3-CF ₃ | F | 7.8 ± 0.20 | >50 | 13.1 ± 0.37 |
| sorafenib | - | - | 1.3 ± 0.06 | N.D. | 2.7 ± 0.11 |
| PAC-1 | - | - | 2.8 ± 0.10 | 4.5 ± 0.03 | 2.0 ± 0.05 |

Table 1.5. Structure and cytotoxicity of hybrid PAC-1/sorafenib derivatives. N.D. = not determined.⁵²

1.4 Benzothiazole PAC-1 derivatives

Building on the promising results from the phenylthiazole-containing **PAC-1** derivatives, two series of benzothiazole-conjugated semicarbazone **PAC-1** derivatives were synthesized by Gong and coworkers.^{55, 56} The benzothiazole derivatives were substituted at the 6-position to block metabolism. Positively-charged substituents were chosen in order to mimic the piperazine nitrogen atoms present in **PAC-1**.^{55, 56} The first series (Table 1.6) contained 26 derivatives (**1.26a-z**).⁵⁵ Cytotoxicity of the compounds was evaluated over 72 hours in HT-29 (human colon cancer), MDA-MB-231 (human breast cancer), MKN-45 (human gastric cancer), NCI-H226 (human lung cancer), and SK-N-SH (human neuroblastoma) cell lines in culture. Many of the compounds were found to display equal or greater potency compared to **PAC-1**. As with the diaryl urea conjugates, the benzyloxy substituent increased potency, while the coumarin-derived compounds were less potent. Importantly, the semicarbazone proved to be an acceptable replacement for the hydrazone of **PAC-1**, as compounds retained potency in the cell lines tested.⁵⁵



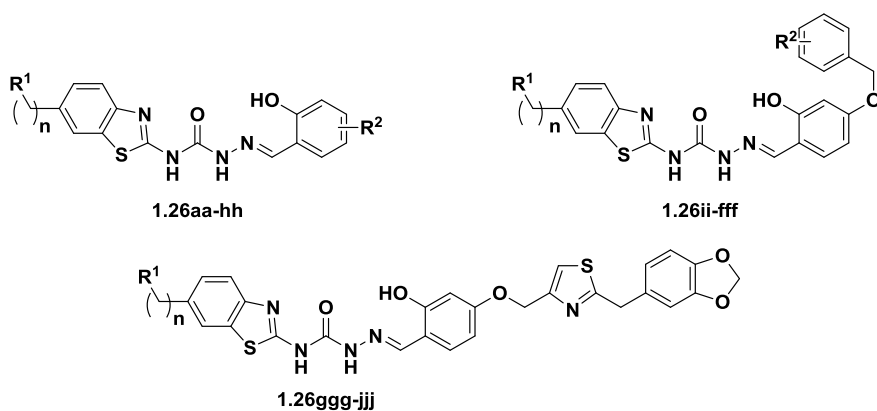
| compound | R ¹ | R ² | 72-hour IC ₅₀ (μM) | | | | |
|----------|------------------|----------------------------------|-------------------------------|--------------|-------------|-------------|-------------|
| | | | HT-29 | MDA-MB-231 | MKN-45 | NCI-H226 | SK-N-SH |
| 1.26a | NMe ₂ | 3-All | N.D. | 3.55 ± 0.17 | 1.01 ± 0.15 | N.D. | 1.68 ± 0.11 |
| 1.26b | NMe ₂ | 3,5-(<i>t</i> -Bu) ₂ | N.D. | 13.9 ± 0.24 | 2.48 ± 0.08 | N.D. | 2.28 ± 0.04 |
| 1.26c | NEt ₂ | 3-All | N.D. | 5.25 ± 0.19 | 1.80 ± 0.12 | N.D. | 2.10 ± 0.09 |
| 1.26d | NEt ₂ | 3,5-(<i>t</i> -Bu) ₂ | N.D. | 7.23 ± 1.01 | 4.06 ± 1.26 | N.D. | 2.46 ± 0.21 |
| 1.26e | 4-Me-1-Pip | 3-All | N.D. | 3.11 ± 0.31 | 1.31 ± 0.22 | N.D. | 2.58 ± 0.12 |
| 1.26f | 4-Me-1-Pip | 3,5-(<i>t</i> -Bu) ₂ | N.D. | 12.1 ± 0.15 | 9.70 ± 0.26 | N.D. | 2.79 ± 0.13 |
| 1.26g | NMe ₂ | - | 2.19 ± 0.17 | 1.34 ± 0.11 | 1.06 ± 0.10 | 0.91 ± 0.03 | 1.14 ± 0.11 |
| 1.26h | NMe ₂ | 4-F | 1.32 ± 0.07 | 2.02 ± 0.01 | 1.72 ± 0.04 | 0.42 ± 0.05 | 0.88 ± 0.03 |
| 1.26i | NMe ₂ | 3-F | 1.03 ± 0.12 | 2.02 ± 0.12 | 1.35 ± 0.04 | 0.51 ± 0.03 | 1.29 ± 0.08 |
| 1.26j | NMe ₂ | 2-F | 1.51 ± 0.04 | 0.66 ± 0.02 | 0.35 ± 0.03 | 0.59 ± 0.01 | 1.94 ± 0.15 |
| 1.26k | NMe ₂ | 4-CF ₃ | 0.92 ± 0.08 | 0.63 ± 0.03 | 0.29 ± 0.01 | 0.24 ± 0.02 | 0.60 ± 0.02 |
| 1.26l | NMe ₂ | 2,4-Cl ₂ | N.D. | 2.02 ± 0.13 | 1.38 ± 0.05 | 0.50 ± 0.04 | 0.59 ± 0.01 |
| 1.26m | NMe ₂ | 2,3-Cl ₂ | N.D. | 2.94 ± 0.08 | 1.45 ± 0.03 | 0.81 ± 0.01 | 0.87 ± 0.02 |
| 1.26n | NEt ₂ | 4-F | 1.47 ± 0.03 | 0.97 ± 0.08 | 0.31 ± 0.07 | 0.57 ± 0.07 | 0.71 ± 0.06 |
| 1.26o | NEt ₂ | 3-F | 0.76 ± 0.02 | 1.12 ± 0.11 | 0.63 ± 0.10 | 1.05 ± 0.03 | 1.34 ± 0.05 |
| 1.26p | NEt ₂ | 2-F | 1.06 ± 0.12 | 0.88 ± 0.02 | 0.55 ± 0.02 | 0.62 ± 0.06 | 0.91 ± 0.15 |
| 1.26q | NEt ₂ | 4-CF ₃ | 1.59 ± 0.14 | 1.06 ± 0.05 | 0.57 ± 0.01 | 0.54 ± 0.04 | 0.85 ± 0.02 |
| 1.26r | NEt ₂ | 2,3-Cl ₂ | 4.01 ± 0.27 | 1.74 ± 0.02 | 0.71 ± 0.05 | 0.95 ± 0.02 | 1.41 ± 0.13 |
| 1.26s | 4-Me-1-Pip | 4-F | 4.01 ± 0.18 | 2.37 ± 0.04 | 0.79 ± 0.12 | 0.31 ± 0.03 | 0.40 ± 0.01 |
| 1.26t | 4-Me-1-Pip | 3-F | 1.02 ± 0.11 | 0.83 ± 0.05 | 0.38 ± 0.01 | 0.36 ± 0.04 | 0.56 ± 0.09 |
| 1.26u | 4-Me-1-Pip | 2-F | 1.65 ± 0.13 | 0.42 ± 0.01 | 0.40 ± 0.02 | 0.45 ± 0.05 | 1.38 ± 0.11 |
| 1.26v | 4-Me-1-Pip | 4-CF ₃ | 1.12 ± 0.06 | 0.58 ± 0.03 | 0.31 ± 0.02 | 0.65 ± 0.11 | 0.75 ± 0.08 |
| 1.26w | 4-Me-1-Pip | 2,3-Cl ₂ | 3.34 ± 0.18 | 1.00 ± 0.11 | 0.45 ± 0.07 | 0.33 ± 0.05 | 0.55 ± 0.09 |
| 1.26x | NMe ₂ | - | N.D. | 16.18 ± 0.55 | 5.32 ± 0.12 | N.D. | 6.12 ± 1.12 |
| 1.26y | NEt ₂ | - | N.D. | 12.7 ± 0.36 | 5.83 ± 0.48 | N.D. | 4.37 ± 0.69 |
| 1.26z | 4-Me-1-Pip | - | N.D. | 10.49 ± 1.05 | 4.35 ± 1.08 | N.D. | 2.72 ± 0.15 |
| PAC-1 | | | 1.36 ± 0.02 | 4.58 ± 0.05 | 3.56 ± 0.05 | 1.02 ± 0.08 | 3.06 ± 0.16 |

Table 1.6. Structure, procaspase-3 activity, and cytotoxicity of benzothiazole **PAC-1** derivatives.

Pip = piperidinyl; N.D. = not determined.⁵⁵

Based on these results, a second set of benzothiazole **PAC-1** derivatives was designed (Table 1.7).⁵⁶ These 36 compounds (**1.26aa-jjj**) were also linked via the semicarbazone and contained basic substituents at the 6 position of the benzothiazole. Several of the compounds (**1.26ii-fff**) contained the benzyloxy group that helped to improve potency for the first series of benzothiazole derivatives. In four derivatives (**1.26ggg-jjj**) the phenyl of the benzyloxy was modified to a piperonylthiazole moiety, a motif present in the **PAC-1** derivatives **WF-210** and **WF-208**^{48, 49} (discussed in Section 1.10). The compounds were evaluated in a 72-hour cell

culture assay against the five cell lines previously discussed. All compounds were potent in the cytotoxicity assays, with many exhibiting sub-micromolar IC₅₀ values. As previously, the compounds containing the benzyloxy substituents were among the most potent compounds in the library, and the piperonylthiazole derivatives were also potent in cell culture. Compounds containing the morpholino substituent were somewhat less potent than other derivatives. In addition, there was a general correlation between potency and intracellular procaspase-3 concentration; NCI-H226 cells express procaspase-3 to a much greater degree than SK-N-SH cells, and the compounds were more potent in the NCI-H226 cells than the SK-N-SH cells. This provides further support to the proposed mechanism of action of **PAC-1**.⁵⁶



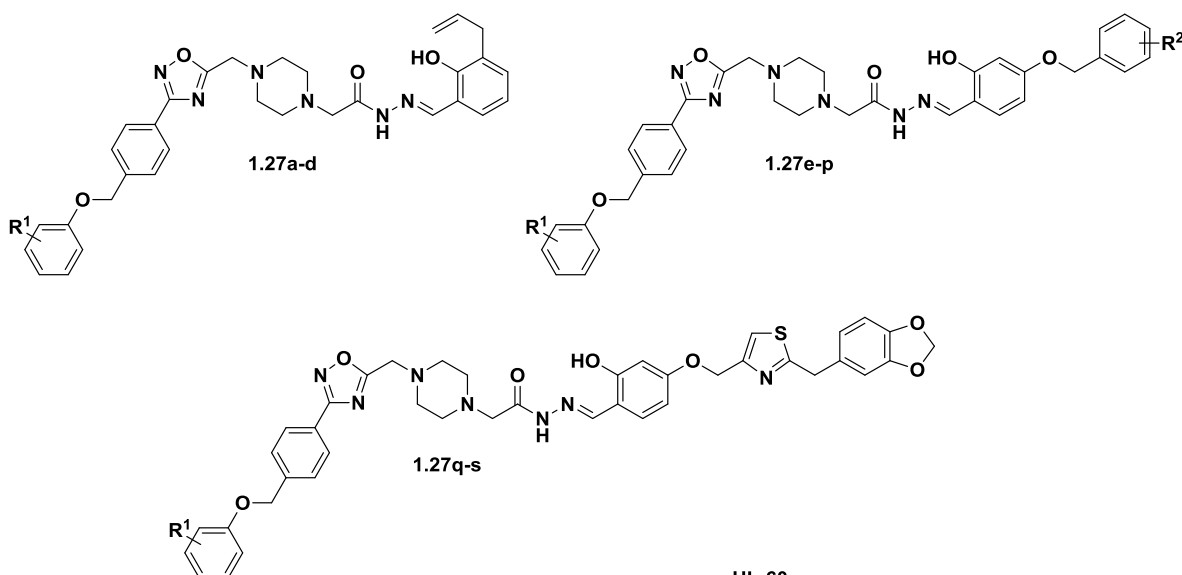
| compound | n | R ¹ | R ² | 72-hour IC ₅₀ (μM) | | | | |
|----------|---|------------------|---------------------|-------------------------------|--------------|-------------|-------------|--------------|
| | | | | HT-29 | MDA-MB-231 | MKN-45 | NCI-H226 | SK-N-SH |
| 1.26aa | 1 | NMe ₂ | - | 5.96 ± 0.52 | 5.95 ± 0.21 | 1.54 ± 1.01 | 2.03 ± 0.38 | 5.14 ± 1.02 |
| 1.26bb | 1 | NMe ₂ | 4-OH | 77.92 ± 5.40 | >100 | 2.85 ± 0.13 | 2.98 ± 0.34 | 14.31 ± 1.35 |
| 1.26cc | 1 | NEt ₂ | - | 4.03 ± 0.54 | 11.33 ± 0.23 | 1.71 ± 0.08 | 1.81 ± 0.11 | 5.79 ± 1.01 |
| 1.26dd | 1 | NEt ₂ | 4-OH | 23.73 ± 1.67 | 4.11 ± 0.16 | 1.74 ± 0.26 | 5.16 ± 0.19 | 6.05 ± 0.17 |
| 1.26ee | 1 | 4-Me-1-Pip | - | 10.40 ± 2.62 | 12.29 ± 0.03 | 0.68 ± 0.06 | 2.96 ± 0.28 | 4.36 ± 1.52 |
| 1.26ff | 1 | 4-Me-1-Pip | 4-OH | 2.73 ± 0.05 | 1.66 ± 0.31 | 4.09 ± 0.16 | 4.61 ± 0.15 | 7.74 ± 1.26 |
| 1.26gg | 1 | 4-Morph | - | 10.32 ± 1.06 | 12.04 ± 1.21 | 2.34 ± 0.32 | 2.71 ± 0.18 | 7.05 ± 0.76 |
| 1.26hh | 0 | 4-Morph | - | 67.93 ± 2.11 | >100 | 9.31 ± 0.51 | 4.26 ± 0.11 | 11.68 ± 0.78 |
| 1.26ii | 1 | NMe ₂ | 4-Me | 2.13 ± 0.04 | 2.65 ± 0.02 | 1.27 ± 0.02 | 1.08 ± 0.05 | 2.58 ± 0.11 |
| 1.26jj | 1 | NMe ₂ | 4- <i>t</i> -Bu | 1.51 ± 0.11 | 1.14 ± 0.01 | 1.04 ± 0.01 | 0.83 ± 0.17 | 1.66 ± 0.15 |
| 1.26kk | 1 | NMe ₂ | 4-Cl | 2.15 ± 0.18 | 0.60 ± 0.05 | 0.70 ± 0.09 | 1.17 ± 0.10 | 2.74 ± 0.12 |
| 1.26ll | 1 | NMe ₂ | 3-Cl | 2.94 ± 0.11 | 0.54 ± 0.04 | 0.19 ± 0.01 | 0.36 ± 0.07 | 1.19 ± 0.18 |
| 1.26mm | 1 | NMe ₂ | 2-Cl | 1.61 ± 0.25 | 0.68 ± 0.12 | 0.33 ± 0.01 | 0.58 ± 0.01 | 2.94 ± 0.15 |
| 1.26nn | 1 | NEt ₂ | 4-Me | 1.33 ± 0.13 | 0.71 ± 0.03 | 0.58 ± 0.01 | 1.01 ± 0.02 | 1.43 ± 0.09 |
| 1.26oo | 1 | NEt ₂ | 4- <i>t</i> -Bu | 0.77 ± 0.01 | 0.98 ± 0.03 | 0.50 ± 0.02 | 0.16 ± 0.01 | 0.48 ± 0.02 |
| 1.26pp | 1 | NEt ₂ | 4-Cl | 1.02 ± 0.02 | 0.61 ± 0.01 | 0.54 ± 0.08 | 0.43 ± 0.01 | 0.74 ± 0.05 |
| 1.26qq | 1 | NEt ₂ | 3-Cl | 1.88 ± 0.01 | 0.57 ± 0.02 | 0.42 ± 0.02 | 1.30 ± 0.14 | 1.83 ± 0.13 |
| 1.26rr | 1 | NEt ₂ | 2-Cl | 2.23 ± 0.16 | 0.74 ± 0.03 | 0.42 ± 0.01 | 0.56 ± 0.10 | 2.01 ± 0.01 |
| 1.26ss | 1 | NEt ₂ | 2,4-Cl ₂ | 2.43 ± 0.03 | 1.52 ± 0.03 | 0.52 ± 0.03 | 0.70 ± 0.02 | 1.04 ± 0.05 |
| 1.26tt | 1 | NEt ₂ | - | 1.44 ± 0.23 | N.D. | N.D. | 0.88 ± 0.01 | 1.67 ± 0.07 |
| 1.26uu | 1 | 4-Me-1-Pip | 4-Me | 1.04 ± 0.03 | 1.51 ± 0.02 | 0.31 ± 0.02 | 1.06 ± 0.05 | 1.56 ± 0.02 |
| 1.26vv | 1 | 4-Me-1-Pip | 4- <i>t</i> -Bu | 0.87 ± 0.03 | 0.56 ± 0.01 | 0.17 ± 0.02 | 0.18 ± 0.02 | 0.27 ± 0.03 |
| 1.26ww | 1 | 4-Me-1-Pip | 4-Cl | 0.95 ± 0.10 | 0.88 ± 0.03 | 0.21 ± 0.01 | 0.41 ± 0.06 | 1.06 ± 0.07 |
| 1.26xx | 1 | 4-Me-1-Pip | 3-Cl | 1.72 ± 0.04 | 1.12 ± 0.02 | 0.67 ± 0.09 | 0.36 ± 0.03 | 0.34 ± 0.01 |
| 1.26yy | 1 | 4-Me-1-Pip | 2-Cl | 1.03 ± 0.14 | 2.3 ± 0.05 | 0.76 ± 0.06 | 0.79 ± 0.06 | 0.85 ± 0.07 |
| 1.26zz | 1 | 4-Me-1-Pip | 2,4-Cl ₂ | 1.00 ± 0.09 | 0.30 ± 0.03 | 0.28 ± 0.03 | 0.39 ± 0.06 | 1.03 ± 0.19 |
| 1.26aaa | 1 | 4-Me-1-Pip | - | 1.57 ± 0.02 | N.D. | N.D. | 0.61 ± 0.11 | 1.32 ± 0.05 |
| 1.26bbb | 0 | 4-Morph | 4-Me | 1.58 ± 0.17 | 19.34 ± 0.31 | 0.75 ± 0.03 | 0.53 ± 0.05 | 2.51 ± 0.15 |
| 1.26ccc | 0 | 4-Morph | 4- <i>t</i> -Bu | 0.92 ± 0.15 | 1.04 ± 0.05 | 0.46 ± 0.04 | 0.24 ± 0.03 | 0.92 ± 0.33 |
| 1.26ddd | 0 | 4-Morph | 4-Cl | 0.0018 ± 0.0002 | 4.46 ± 0.03 | 0.29 ± 0.01 | 0.26 ± 0.01 | 1.37 ± 0.03 |
| 1.26eee | 0 | 4-Morph | 3-Cl | 0.59 ± 0.04 | 1.18 ± 0.01 | 0.28 ± 0.02 | 0.79 ± 0.11 | 1.48 ± 0.13 |
| 1.26fff | 0 | 4-Morph | 2,4-Cl ₂ | 4.72 ± 0.13 | 15.06 ± 1.01 | 1.75 ± 0.10 | 1.22 ± 0.23 | 3.14 ± 0.08 |
| 1.26ggg | 1 | NMe ₂ | - | 1.88 ± 0.03 | 1.04 ± 0.11 | 0.62 ± 0.01 | 0.72 ± 0.03 | 0.79 ± 0.01 |
| 1.26hhh | 1 | NEt ₂ | - | 0.72 ± 0.02 | 0.55 ± 0.01 | 0.51 ± 0.01 | 0.14 ± 0.01 | 0.48 ± 0.03 |
| 1.26iii | 1 | 4-Me-1-Pip | - | 1.12 ± 0.15 | 0.88 ± 0.02 | 0.55 ± 0.03 | 0.81 ± 0.02 | 1.25 ± 0.01 |
| 1.26jjj | 0 | 4-Morph | - | 2.31 ± 0.16 | 4.03 ± 0.04 | 1.01 ± 0.01 | 2.14 ± 0.11 | 6.21 ± 0.23 |
| PAC-1 | | | | 1.36 ± 0.02 | 4.8 ± 0.02 | 2.61 ± 0.05 | 1.02 ± 0.01 | 3.06 ± 0.04 |

Table 1.7. Structure and cytotoxicity of benzothiazole PAC-1 derivatives. Pip = piperidinyl; Morph = morpholino; N.D. = not determined.⁵⁶

1.5. Oxadiazole PAC-1 derivatives

In addition to the benzothiazole-containing compounds, several PAC-1 derivatives (1.27a-s) were synthesized by Gong, Wu, and coworkers, containing an oxadiazole with a

substituted (phenoxyethyl)phenyl linked to the piperazine ring (Table 1.8).^{48, 49} The *ortho*-hydroxy-*N*-acylhydrazone remained intact, while substitution varied on the benzylidene ring. Four derivatives (**1.27a-d**) contained the 3-allyl substituent characteristic of **PAC-1**. An additional 12 derivatives (**1.27e-p**) contained a substituted benzyloxy group at the 4-position of the benzylidene ring. Finally, three derivatives (**1.27q-s**) contained a piperonyl substituent attached via a thiazole linker. The cytotoxicity of the compounds to HL-60 cells was evaluated in a 72-hour experiment. **PAC-1** had an IC₅₀ value of 2.10 μM under these conditions, and most of the derivatives were more potent than **PAC-1** in the HL-60 cell line, although compound **1.27p** was inactive in this experiment. In general, the compounds containing the allyl and the piperonylthiazole substituents were more potent than those containing the benzyloxy substituents. Compounds **1.27r-s** showed high potency in cell culture, with 80 nM IC₅₀ values, and further experiments were performed with these two derivatives.^{48, 49} These efforts will be discussed in Section 1.10.



| compound | R ¹ | R ² | HL-60 72-hour IC ₅₀ (μM) |
|----------------|--------------------|---------------------|---|
| 1.27a | 4-Cl | - | 0.25 |
| 1.27b | 4-F | - | 0.39 |
| 1.27c | 3-Cl | - | 0.40 |
| 1.27d | 2-CF ₃ | - | 0.35 |
| 1.27e | 4-Cl | - | 1.26 |
| 1.27f | 4-F | 2,4-Cl ₂ | 1.02 |
| 1.27g | 4-F | 3-CF ₃ | 0.98 |
| 1.27h | 4-Cl | 4- <i>t</i> -Bu | 0.67 |
| 1.27i | 4-Cl | 2,4-Cl ₂ | 1.07 |
| 1.27j | 4-F | 4- <i>t</i> -Bu | 0.60 |
| 1.27k | 3,4-F ₂ | - | 0.34 |
| 1.27l | 3,4-F ₂ | 4-Cl | 0.30 |
| 1.27m | 3,4-F ₂ | 2,4-Cl ₂ | 0.41 |
| 1.27n | 2-CF ₃ | 4- <i>t</i> -Bu | 0.40 |
| 1.27o | 2-CF ₃ | 3-F | 1.93 |
| 1.27p | 4-Cl | 3-Cl | >20 |
| 1.27q | 2-CF ₃ | - | 1.08 |
| 1.27r (WF-208) | 4-Cl | - | 0.08 |
| 1.27s (WF-210) | 4-F | - | 0.08 |
| PAC-1 | | | 2.10 |

Table 1.8. Structure and cytotoxicity of oxadiazole-containing **PAC-1** derivatives.^{48, 49}

1.6. Replacement of benzylidene

PAC-1 chelates zinc with affinity in the low nanomolar range,^{43, 44} which is strong enough to remove the labile pool of zinc, but not strong enough to disrupt essential zinc ions.^{25, 72} In contrast, **TPEN** (**1.28**, Figure 1.7), which binds zinc with 0.26 fM affinity,⁸² inhibits the activity of certain metalloenzymes via chelation of the essential metal ion.⁸³ It is likely that the relatively modest affinity of **PAC-1** for zinc is responsible for its selectivity for chelation of labile zinc over essential zinc ions. However, in an effort to slightly increase the affinity of **PAC-1** for zinc, two new **PAC-1** derivatives were synthesized by Rongved and coworkers.⁵⁷ For **ZnA-**

DPA (1.29), the benzylidene was replaced by a dipicolylamine (DPA) moiety, which is present in **TPEN**. For **ZnA-Pyr (1.30)**, the phenol was replaced by a 4-pyridoxyl group, which also contains the *ortho*-hydroxyl substituent necessary for **PAC-1** activity.⁵⁷

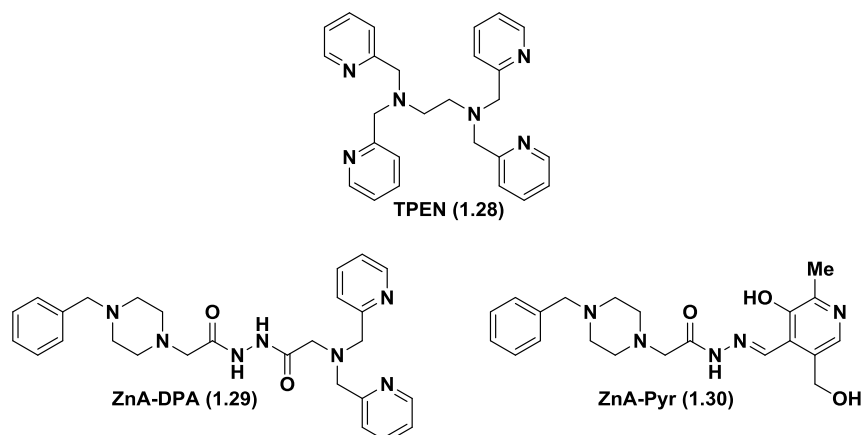


Figure 1.7. Structures of **TPEN (1.28)** and **PAC-1** derivatives **ZnA-DPA (1.29)** and **ZnA-Pyr (1.30)**.⁵⁷

ZnA-Pyr was found to bind zinc in a dose-dependent manner, although a K_d value was not calculated. The binding of **ZnA-DPA** to zinc could not be assessed due to the lack of a chromophore. Dissociation constants for compounds analogous to **ZnA-DPA** and **ZnA-Pyr** were in the low nanomolar⁸⁴ and high femtomolar⁸⁵ ranges, respectively. **PAC-1**, **TPEN**, **ZnA-DPA**, and **ZnA-Pyr** were evaluated in PC-12 cells in a 24-hour experiment (Figure 1.8). **TPEN** (Figure 1.8A) was the most potent compound in inducing cell death, followed by **PAC-1** (Figure 1.8B). Neither **ZnA-DPA** (Figure 1.8C) nor **ZnA-Pyr** (Figure 1.8D) induced greater than 40% cell death at concentrations up to 200 μ M. All four compounds induced activation of caspases-3/-7 in whole cells, as measured by cleavage of the fluorogenic substrate (DEVD)₂-Rhodamine 110. The activity of **PAC-1** and **TPEN** in this experiment was slightly higher than **ZnA-DPA** and **ZnA-Pyr**. The addition of zinc or the caspase-3/-7 inhibitor Ac-DEVD-cmk reduced the amount of cell death induced by each agent, although zinc-mediated protection of cell death induced by **ZnA-DPA** was not statistically significant.⁵⁷ While it remains possible that an alternative zinc-binding motif could lead to an improved **PAC-1** derivative, this study shows that the DPA and pyridoxyl substituents are most likely not appropriate for this purpose.

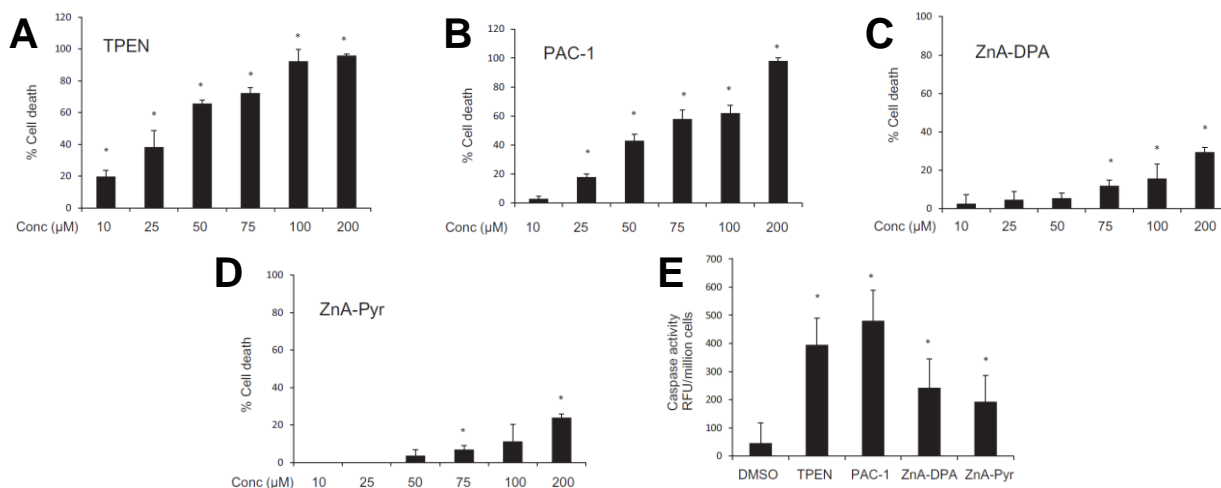


Figure 1.8. A. TPEN, B. PAC-1, C. ZnA-DPA, and D. ZnA-Pyr induce dose-dependent cell death. PC-12 cells were treated with compounds for 24 hours. **E.** The four derivatives induce activation of executioner caspases in PC-12 cells over a 24-hour treatment. Figures adapted with permission from literature.⁵⁷

1.7 Study of matrix metalloproteinase inhibition

In an effort to evaluate potential off-target effects of **PAC-1**, a series of derivatives (**1.31a-f**, Figure 1.9) was synthesized, and the ability of the compounds to inhibit zinc-dependent matrix metalloproteinases-9 and -14 was evaluated by Winberg and coworkers.⁷² The compounds do not inhibit the enzymes at 5 μM. Slight inhibition is observed at the high concentration of 100 μM, which is outside of physiologically relevant ranges. IC₅₀ values for **1.31a** and **1.31b** were calculated at >100 μM.⁷² This relatively weak level of inhibition of the metalloenzymes provides further support that **PAC-1** and derivatives selectively chelate the labile pool of zinc over essential metal ions.

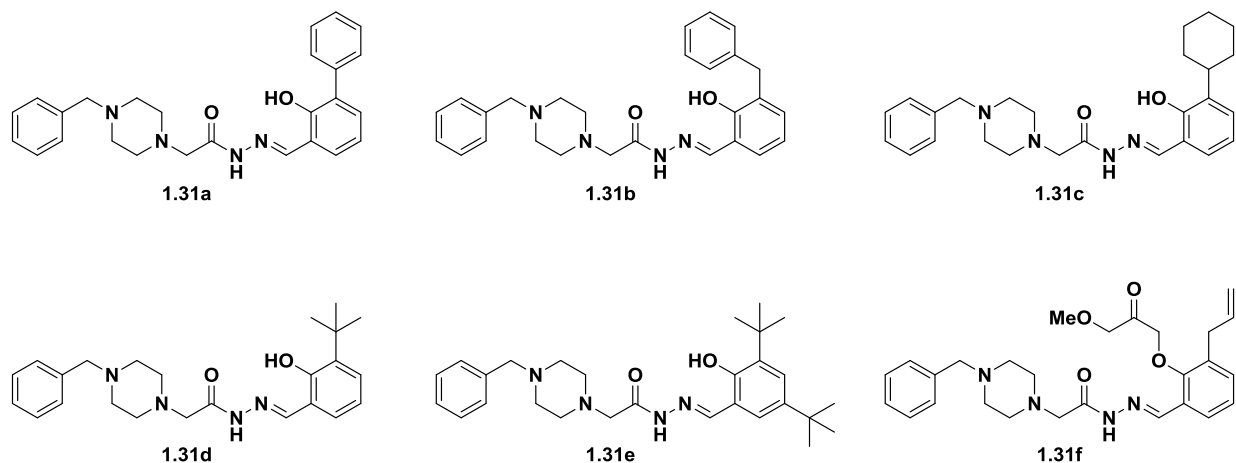
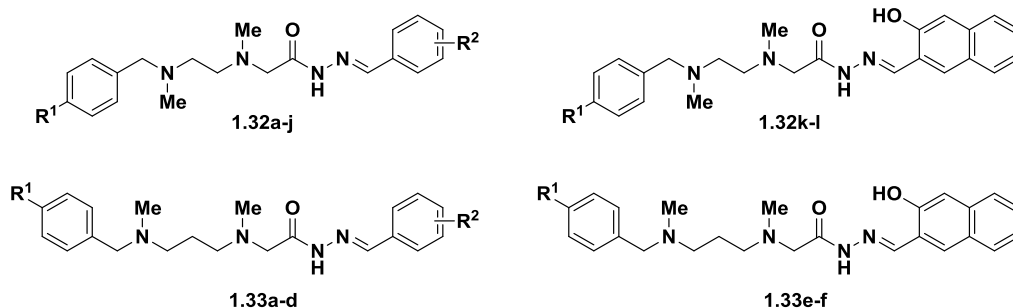


Figure 1.9. Structures of compounds (**1.31a-f**) used to study matrix metalloproteinase inhibition.⁷²

1.8. Modification of piperazine

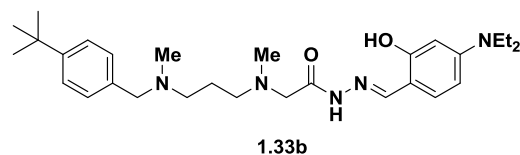
An additional strategy to improve the potency of **PAC-1** involved modification of the piperazine to acyclic 1,2-ethylenediamine and 1,3-propylenediamine linkers (Table 1.9), as performed by Jun-hai, Xiao-hong, and coworkers.⁵⁹ These derivatives (**1.32a-l**, **1.33a-f**) retained the benzyl substituent, and all but two (**1.32d** and **1.32h**) of the 18 derivatives synthesized contained the *ortho*-hydroxy-*N*-acylhydrazone; substituents on both aromatic rings were varied to assess structure-activity relationships. The compounds were evaluated in HL-60 (human leukemia) and HLF (human embryonic lung fibroblast) cells over 72 hours and compared to **PAC-1**. Many of the compounds were highly potent against the HL-60 cells, with IC₅₀ values below 1 μM, compared to **PAC-1** at 1.90 ± 0.01 μM. Notably, the two derivatives lacking the *ortho*-hydroxyl group were significantly less potent, confirming the previously determined structure-activity relationships. Unfortunately, many of the compounds displayed comparable potency in the non-cancerous HLF cell line, suggesting that there may be a narrow therapeutic window for these compounds.



| compound | R ¹ | R ² | 72-hour IC ₅₀ (μM) | |
|--------------|----------------|---------------------------------------|-------------------------------|---------------|
| | | | HL-60 | HLF |
| 1.32a | H | 2-OH | 3.63 ± 0.32 | 3.02 ± 0.58 |
| 1.32b | H | 2-OH-3-All | 2.32 ± 0.41 | 3.36 |
| 1.32c | H | 2-OH-4-NEt ₂ | 0.27 ± 0.12 | 0.17 ± 0.13 |
| 1.32d | H | 3-OH | 183.51 ± 5.52 | N.D. |
| 1.32e | <i>t</i> -Bu | 2-OH-3-All | 0.73 ± 0.57 | 0.9 ± 0.01 |
| 1.32f | <i>t</i> -Bu | 2-OH-3,5-(<i>t</i> -Bu) ₂ | 0.82 ± 0.22 | 0.98 ± 0.12 |
| 1.32g | <i>t</i> -Bu | 2-OH-4-NEt ₂ | 0.25 ± 0.15 | 0.86 ± 0.04 |
| 1.32h | <i>t</i> -Bu | 3-OH | 11.65 ± 3.42 | 111.37 ± 0.45 |
| 1.32i | OMe | 2-OH-3,5-(<i>t</i> -Bu) ₂ | 0.91 ± 0.17 | 1.07 ± 0.31 |
| 1.32j | OMe | 2-OH-4-NEt ₂ | 0.30 ± 0.08 | 1.80 ± 0.95 |
| 1.32k | <i>t</i> -Bu | - | 0.28 ± 0.03 | 1.86 ± 0.04 |
| 1.32l | OMe | - | 0.56 ± 0.36 | 1.39 ± 0.30 |
| 1.33a | H | 2-OH-3,5-(<i>t</i> -Bu) ₂ | 0.85 ± 0.02 | 0.87 ± 0.03 |
| 1.33b | <i>t</i> -Bu | 2-OH-4-NEt ₂ | 0.26 ± 0.06 | 25.13 ± 3.01 |
| 1.33c | OMe | 2-OH-3,5-(<i>t</i> -Bu) ₂ | 0.54 ± 0.13 | 1.15 ± 0.18 |
| 1.33d | OMe | 2-OH-4-NEt ₂ | 0.46 ± 0.22 | 0.37 |
| 1.33e | <i>t</i> -Bu | - | 0.28 ± 0.07 | 0.29 ± 0.06 |
| 1.33f | OMe | - | 0.71 ± 0.31 | N.D. |
| PAC-1 | | | 1.90 ± 0.01 | 5.82 ± 0.58 |

Table 1.9 Structure and cytotoxicity of ethylenediamine and propylenediamine **PAC-1** derivatives.⁵⁹

Compound **1.33b** was ten-fold less potent in the HLF cell line than the HL-60 cell line. For this reason, compound **1.33b** was selected for further study in a panel of 14 additional human cancer cell lines (Table 1.10). Compound **1.33b** was more potent than **PAC-1** in all of the cancerous cell lines evaluated, suggesting that modification of the piperazine may be a useful strategy for the development of improved **PAC-1** derivatives. In this experiment, three cell lines (A-498, DU145, and MCF7) were insensitive to **PAC-1**, as IC₅₀ values were higher than 300 μM.⁵⁹ The reason for this insensitivity is unclear; **PAC-1** was cytotoxic to DU145 and MCF7 cells in other reports^{48, 49} (this is the only reported evaluation of **PAC-1** in A-498 cells). However, it is possible that slight differences in experimental design and execution led to this observed difference in cytotoxicity.



| Cell Line | Origin | 72-hour IC ₅₀ (μM) | |
|-----------|------------------|-------------------------------|--------------|
| | | PAC-1 | 1.33b |
| A-498 | renal | >300 | 7.26 ± 1.56 |
| A2780 | ovarian | 56.02 ± 3.46 | 20.37 ± 4.13 |
| BGC-823 | gastric | 3.02 ± 1.01 | 0.35 ± 0.03 |
| Caco-2 | colon | 6.49 ± 1.35 | 1.35 ± 0.32 |
| DU145 | prostate | >300 | 25.29 ± 4.58 |
| HCT-8 | colon | 1.48 ± 0.24 | 0.18 ± 0.04 |
| HeLa | cervical | 7.25 ± 2.31 | 1.50 ± 0.28 |
| Hep G2 | liver | 7.26 ± 1.43 | 1.05 ± 0.04 |
| HL-60 | leukemia | 1.90 ± 0.01 | 0.26 ± 0.06 |
| HOS | osteosarcoma | 2.82 ± 0.05 | 0.79 ± 0.06 |
| IM-9 | multiple myeloma | 1.87 ± 0.05 | 0.15 ± 0.01 |
| K562 | leukemia | 45.87 ± 3.65 | 3.00 ± 1.21 |
| MCF7 | breast | >300 | 14.76 ± 2.67 |
| NCI-H460 | lung | 4.16 ± 0.33 | 1.21 ± 0.42 |
| SH-SY5Y | neuroblastoma | 13.93 ± 2.21 | 1.20 ± 0.01 |
| HLF | lung fibroblast | 5.82 ± 0.58 | 25.13 ± 3.01 |

Table 1.10. Cytotoxicity of **PAC-1** and derivative **1.33b** against a panel of human cell lines.⁵⁹

1.9 S-PAC-1

1.9.1 Discovery and initial evaluation

In addition to its procaspase-3 activating properties, **PAC-1** can also induce significant neuroexcitation *in vivo*. Seizures are observed after administration of high doses via IV or IP injection in animals, and elevated doses are lethal.⁴⁵ It was hypothesized that in order to induce this neuroexcitation, **PAC-1** must cross the blood-brain barrier (BBB), although the specific interactions leading to this phenotype are not well understood. Therefore, in order to develop a compound with improved safety, the design of a **PAC-1** derivative that would not cross the BBB was explored. Compounds that cross the BBB tend to be small, rigid, and lipophilic;⁸⁶ therefore, the introduction of a polar substituent would help to prevent passage of the compound across the BBB. With the knowledge that substituents on the aromatic rings of **PAC-1** could be modified while still maintaining anticancer activity,⁴⁴ a derivative containing a highly polar sulfonamide group, **S-PAC-1** (**1.34**, Figure 1.10), was designed and developed by researchers in the Hergenrother group.⁴⁵ **S-PAC-1** bound zinc with a K_d of 46 ± 5 nM, comparable to the value for **PAC-1**,⁴⁴ and it was able to relieve zinc-mediated inhibition of procaspase-3 *in vitro*, although it was not as potent as **PAC-1** in this assay.⁴⁵

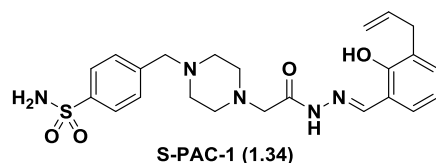


Figure 1.10. Structure of **S-PAC-1 (1.34)**.⁴⁵

After confirmation that **S-PAC-1** was active *in vitro*, **S-PAC-1** and **PAC-1** were evaluated in cell culture against a panel of cell lines over 72 hours (Table 1.11). In preparation for an animal model of lymphoma, five lymphoma cell lines were evaluated, including U-937 (human), EL4 (mouse), 17-71 (dog), GL-1 (dog), and OSW (dog). **PAC-1** and **S-PAC-1** both displayed IC₅₀ values in the low micromolar range for all five cell lines evaluated. The compounds were also evaluated in four additional human cell lines, including Jurkat (leukemia), SK-MEL-5 (melanoma), HeLa (cervical), and MDA-MB-231 (breast), and comparable potency was observed across these cell lines as well. Investigation of the mode of cell death induced by **S-PAC-1** was performed by treatment of U-937 cells with **S-PAC-1** and staining with Annexin V-FITC/propidium iodide. Flow cytometry analysis indicated that **S-PAC-1** induces cell death via apoptosis.⁴⁵

| Cell Line | Species | Origin | 72-hour IC ₅₀ (μM) | |
|-------------------|---------|----------|-------------------------------|------------|
| | | | PAC-1 | S-PAC-1 |
| U-937 | Human | Lymphoma | 9.3 ± 0.5 | 6.4 ± 0.8 |
| EL4 | Mouse | Lymphoma | 3.8 ± 0.9 | 7.1 ± 1.3 |
| 17-71 | Dog | Lymphoma | 2.5 ± 0.9 | 2.7 ± 0.8 |
| GL-1 | Dog | Lymphoma | 4.9 ± 0.3 | 7.1 ± 0.3 |
| OSW | Dog | Lymphoma | 8.6 ± 1.3 | 11.0 ± 0.9 |
| Jurkat | Human | Leukemia | 5.7 ± 2.8 | 4.5 ± 1.1 |
| SK-MEL-5 | Human | Melanoma | 11.5 ± 3.6 | 8.6 ± 1.3 |
| HeLa | Human | Cervical | 15.5 ± 3.8 | 28.4 ± 7.7 |
| MDA-MB-231 | Human | Breast | 9.9 ± 1.0 | 11.7 ± 5.3 |

Table 1.11. Comparison of cytotoxicity of **PAC-1** and **S-PAC-1**. Values shown are mean ± s.e.m. (n = 3).⁴⁵

In order to determine an effective *in vivo* dosing regimen, the cytotoxicity of **S-PAC-1** was evaluated after varying treatment times (Table 1.12). U-937 cells were treated with **S-PAC-1** for times ranging from 1-72 hours. The compound was then washed out, and cells were allowed to grow until 72 hours after the initiation of treatment. The compound induces minimal cell death at time points up to 6 hours, and the first toxicity is observed at 9 hours. The potency

increases until 24 hours and does not change significantly between 24-72 hours. These results indicated that in order to observe anticancer efficacy *in vivo*, serum concentrations of 10 μM for at least 24 hours would be most effective.⁴⁵

| Exposure Time (h) | U-937 S-PAC-1 |
|----------------------|---|
| | 72-hour IC ₅₀ (μM) |
| 1 | >100 |
| 3 | >100 |
| 6 | >100 |
| 9 | 20 \pm 12 |
| 12 | 9.7 \pm 1.1 |
| 24 | 5.9 \pm 1.0 |
| 48 | 5.6 \pm 0.8 |
| 72 | 6.4 \pm 0.8 |

Table 1.12. Time-dependence of cytotoxicity of **S-PAC-1** in U-937 cells. Cells were treated with **S-PAC-1** for the indicated time, compound was washed out, and cell death was assessed 72 hours after initiation of treatment. Values shown are mean \pm s.e.m. (n = 3).⁴⁵

1.9.2. Safety and pharmacokinetics

S-PAC-1 was advanced to *in vivo* experiments based on its promising activity *in vitro* and in cell culture. **S-PAC-1** was administered to mice via IV injection, and no adverse effects were observed at doses up to 350 mg/kg. In contrast, **PAC-1** induces mild neurological symptoms at doses as low as 20 mg/kg when administered via IV injection. The pharmacokinetic profiles of **PAC-1** and **S-PAC-1** were evaluated, and the peak plasma concentration was compared between **S-PAC-1** at 350 mg/kg and **PAC-1** at 20 mg/kg, the lowest dose to induce neurological symptoms, and 50 mg/kg, a dose at which neurotoxicity is severe. The maximum serum concentration of **PAC-1** at 20 mg/kg was approximately 50 μM , and the maximum concentration at 50 mg/kg was approximately 100 μM . However, the 350 mg/kg dose of **S-PAC-1** resulted in serum concentration of approximately 3500 μM , a 70-fold increase over the threshold for induction of neurotoxicity for **PAC-1**.⁴⁵

Despite the improved safety profile of **S-PAC-1**, evaluation in murine tumor models was not feasible due to the rapid clearance of the compound from circulation; the half-life was approximately 1 hour following IP administration of compound to mice (Figure 1.11A). Therefore, further *in vivo* evaluation of **S-PAC-1** was performed in dogs. A 25 mg/kg intravenous dose of **S-PAC-1** administered over 10 minutes (Figure 1.11B) was well tolerated

and gave a peak plasma concentration of approximately 150 μM . However, the compound was cleared rapidly from dogs as well, with an elimination half-life of 1.09 ± 0.02 hours. In order to achieve serum concentrations of 10 μM for 24 hours, a continuous-rate infusion strategy was investigated, with an initial loading dose administered over 10 minutes, followed by a maintenance dose over 24 hours (Figure 1.11C). Healthy research dogs tolerated the continuous administration of **S-PAC-1** well, and a loading dose of 7 mg/kg followed by a constant-rate infusion of 3 mg/kg/h was chosen to achieve a serum concentration of 10 μM during the course of the treatment.⁴⁵

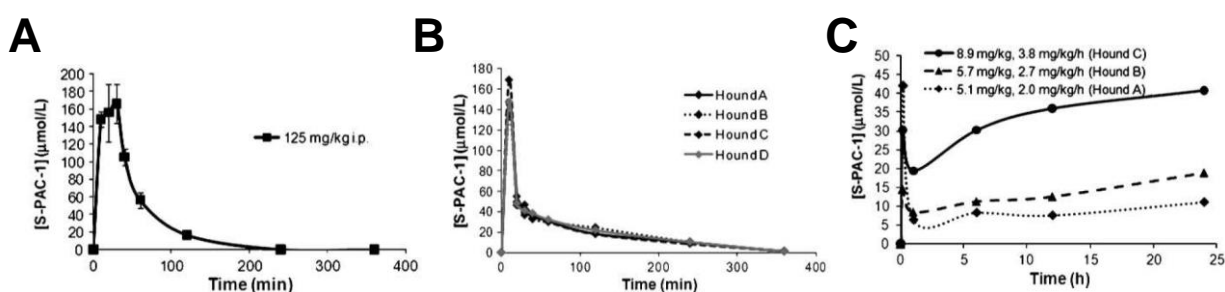


Figure 1.11. Pharmacokinetics of **S-PAC-1** following **A.** 125 mg/kg i.p. injection in mice, **B.** 25 mg/kg i.v. injection in dogs administered over 10 minutes, and **C.** initial loading dose followed by 24-hour continuous rate infusion in dogs administered by i.v. injection. Figures adapted with permission from literature.⁴⁵

1.9.3. Evaluation in canine lymphoma patients

With an initial understanding of the pharmacokinetics of **S-PAC-1** upon continuous-rate infusion, a clinical trial of six canine lymphoma patients was initiated. Three patients received four doses via 24-hour continuous infusions once weekly, while three additional patients received two 72-hour continuous infusions two weeks apart. In general, the 7 mg/kg loading dose followed by the 3 mg/kg/h continuous infusion was successful in maintaining the desired 10 μM serum concentration during the administration. No hematologic or nonhematologic toxicity was observed in any of the six patients, and only minor adverse events were reported, including mild gastrointestinal symptoms and localized irritation at the site of injection. Encouragingly, one of the six patients showed a partial response to **S-PAC-1** therapy (Figure 1.12). A 30% reduction in the tumor size was observed both by caliper RECIST score (Figure 1.12A) and CT scan of the

lymph nodes (Figure 1.12B). Three of the patients showed stable disease, while two showed disease progression. Flow cytometry analysis of lymph node aspirates from two patients demonstrated the presence of procaspase-3 prior to treatment, as well as an increase in cleaved caspase-3 seven days after initiation of treatment. A rapid increase in the tumor volume in all six patients was observed immediately after therapy ceased. These results provide the first validation for procaspase-3 activation as an anticancer strategy.⁴⁵

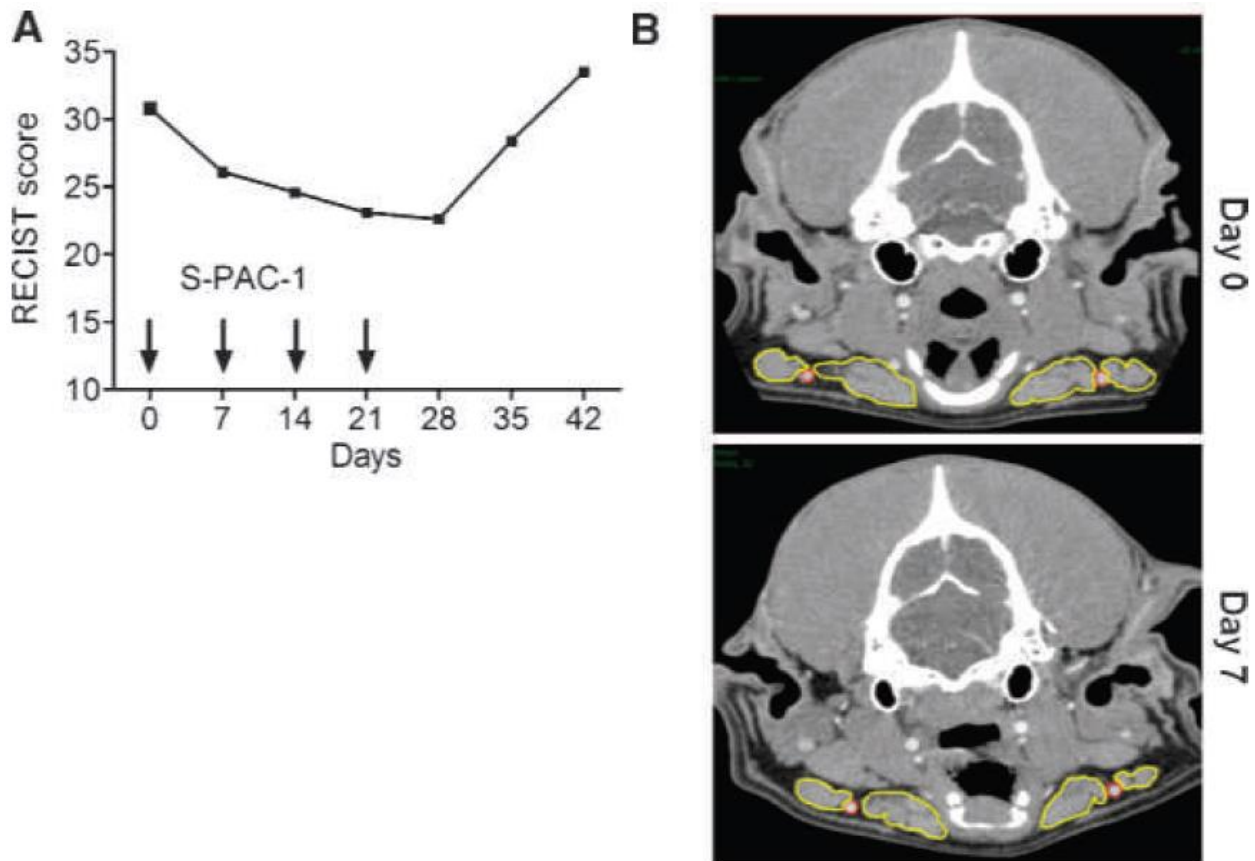


Figure 1.12. Partial response to **S-PAC-1** therapy in canine patient. **A.** RECIST scores for patient administered **S-PAC-1** on days 0, 7, 14, and 21. Tumor size decreased upon each dose and rapidly increased upon cessation of treatment. **B.** CT scans of lymph nodes on days 0 and 7 show decreased tumor size after a single dose of **S-PAC-1**. Figures adapted with permission from literature.⁴⁵

1.9.4. Comparison to PAC-1

Efforts were undertaken to further elucidate the mechanism of action of **PAC-1** and **S-PAC-1** in order to further understand the significant difference in tolerability.⁴⁷ An initial experiment involved treatment of HeLa cells containing the genetically encoded fluorescent zinc sensor ZapCY2. This sensor contains a zinc finger conjugated to cyan fluorescent protein (CFP) and yellow fluorescent protein (YFP). The sensor undergoes a conformational change upon binding to zinc, allowing for fluorescence resonance energy transfer (FRET) to occur between CFP and YFP, and the YFP fluorescence is observed. Release of zinc prevents FRET, and CFP fluorescence is observed. Therefore, the cellular zinc concentration is proportional to the FRET ratio (FRET/CFP).⁸⁷ Both **PAC-1** and **S-PAC-1** reduced intracellular zinc concentrations within seconds after addition of compound, and the rate and amount of zinc sequestration were similar for both compounds (Figure 1.13).⁴⁷

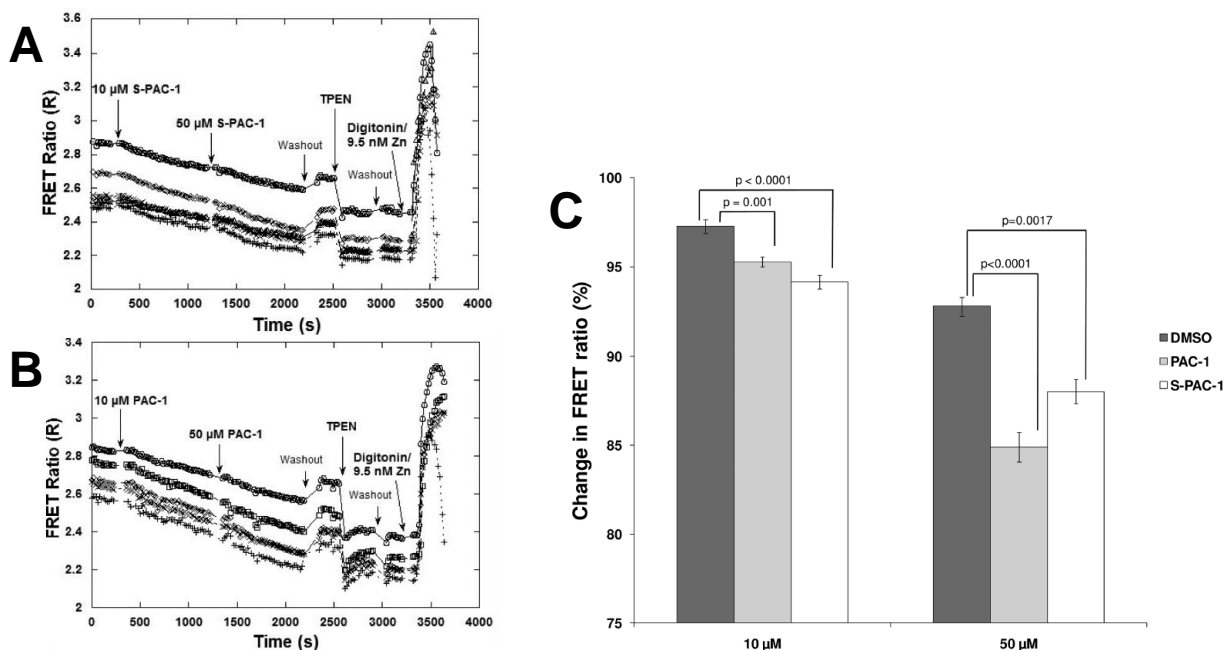


Figure 1.13. Changes in intracellular zinc concentration upon treatment with **A. PAC-1** or **B. S-PAC-1**. **C.** Both **PAC-1** and **S-PAC-1** cause significant decreases in intracellular zinc concentration compared to untreated controls. Figures adapted with permission from literature.⁴⁷

To confirm that the compounds act similarly in cells, a transcript profiling experiment was performed to assess differences in global gene expression upon treatment with compounds.

In this experiment, HL-60 cells were treated with either **PAC-1** or **S-PAC-1** at 25 μM , mRNA was collected after six hours, and the transcript levels were compared to a vehicle-treated control. In general, there was a high correlation between the two different treatment groups; many of the most upregulated transcripts for **PAC-1** were also highly upregulated in **S-PAC-1**, while expression of many of the most downregulated transcripts for **PAC-1** was also suppressed for **S-PAC-1** treatment. The degree of similarity was measured by calculating the Spearman rank correlation value for the two treatment groups. The value was calculated at 0.928, very close to a perfect correlation of 1.0, demonstrating that **PAC-1** and **S-PAC-1** induce a similar transcriptional response and likely act similarly within cells at the 25 μM concentration.⁴⁷

In order to further understand the difference in the observed neurological phenotypes for **PAC-1** and **S-PAC-1**, experiments were performed to determine the ability of the compounds to penetrate relevant physiological barriers (Figure 1.14). It was proposed that **PAC-1** enters the brain to induce the neuroexcitation by a mechanism that is not yet well understood, while the polar sulfonamide group prevents **S-PAC-1** from crossing the BBB.⁴⁵ An initial experiment demonstrated that equal concentrations of **PAC-1** and **S-PAC-1** enter Neuro-2a (murine neuroblastoma) cells after incubation with either compound at 50 μM for 30 minutes (Figure 1.14A), suggesting that the difference in toxicity is not related to a difference in cell permeability. Following this, an experiment was performed to determine the BBB permeability of the compounds *in vivo* (Figure 1.14B-C). C57BL/6 mice were administered **PAC-1** or **S-PAC-1** at 75 mg/kg via i.v. injection. Mice were sacrificed after five minutes, samples from blood and brains were collected, and concentrations were analyzed by HPLC. **PAC-1** displayed approximately 30:70 distribution between brain and blood, consistent with the observed neurological phenotype. In contrast, less than 1% of **S-PAC-1** entered the brain.⁴⁷ This difference in BBB permeability is most likely sufficient to explain the difference in neurotoxicity, although further experiments on the mechanism of neuroexcitation are necessary to determine whether other factors may be partially responsible.

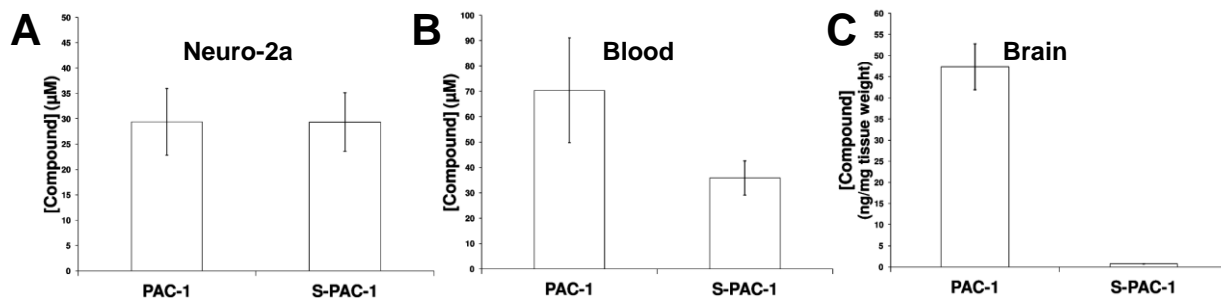


Figure 1.14. Penetration of physiological barriers by **PAC-1** and **S-PAC-1**. **A.** Concentrations of **PAC-1** and **S-PAC-1** in Neuro-2a cells following treatment with 50 μM for 30 minutes. **B.** Concentrations of **PAC-1** and **S-PAC-1** in serum, and **C.** concentrations of **PAC-1** and **S-PAC-1** in brains of mice. C57BL/6 mice received **PAC-1** or **S-PAC-1** at 75 mg/kg via lateral tail vein injection and sacrificed 5 minutes post-injection. Values shown are mean \pm standard deviation (n = 4). Figures adapted with permission from literature.⁴⁷

Finally, the effect of treatment time on cell death induced by **PAC-1** and **S-PAC-1** was assessed in order to determine effective dosing strategies for *in vivo* studies. U-937 cells were treated with compounds at 100 μM for 4, 8, 12, or 24 hours. The cells were then washed, and fresh growth medium was added. Cell death was assessed 24 hours after the initiation of treatment via Annexin V-FITC/propidium iodide staining. The results are shown in Figure 1.15. **PAC-1** induced greater than 50% cell death after only 4 hours, and greater than 90% of cells were no longer viable after an 8-hour treatment. In contrast, **S-PAC-1** induced apoptosis much more slowly; the 50% cell death threshold was reached between 8-12 hours of treatment.⁴⁷ This is consistent with the previous study on the rate of apoptosis induced by **S-PAC-1**.⁴⁵ Taken together, these results suggest that achieving a high serum concentration for a short time period may represent an effective dosing strategy for **PAC-1**, while serum concentrations of **S-PAC-1** should be higher for sustained periods of time in order to achieve efficacy.

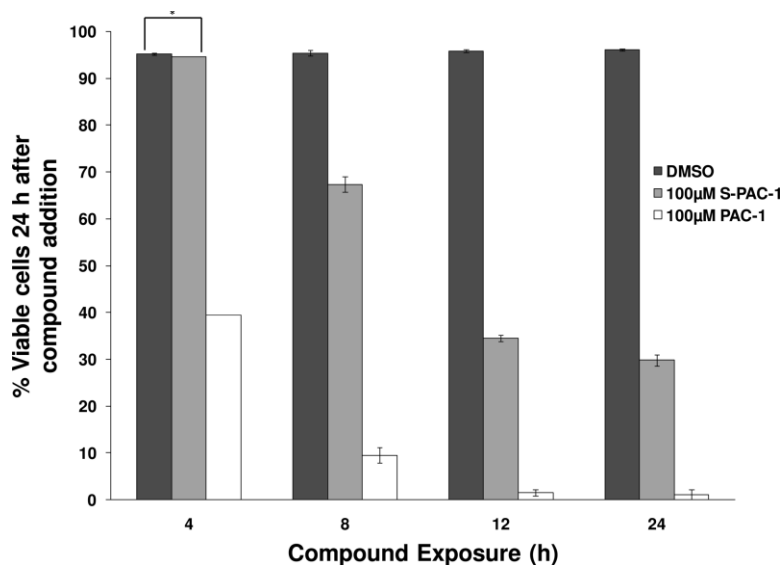


Figure 1.15. High concentrations of **PAC-1**, but not **S-PAC-1**, induce apoptosis upon short treatment times. U-937 cells were treated with DMSO or compound (100 μ M) for various exposure times, and cell viability was assessed by flow cytometry of the cells double stained with Annexin V-FITC/propidium iodide. Values shown are mean \pm s.e.m. ($n = 3$). Figure adapted with permission from literature.⁴⁷

1.10 WF-210 and WF-208

1.10.1 Discovery and initial evaluation

As discussed in Section 1.5, a series of oxadiazole-containing **PAC-1** derivatives were synthesized and evaluated in HL-60 cells by Gong, Wu, and coworkers.^{48, 49} The two most potent compounds identified from this assay (Figure 1.16) were **WF-208 (1.27r)** and **WF-210 (1.27s)**, each of which contains a piperonylthiazole attached to the benzylidene ring and a halogen-substituted (phoxymethyl)phenyl group attached to the oxadiazole. Each compound was highly potent against HL-60 cells in culture, with 72-hour IC_{50} values of 80 nM.^{48, 49}

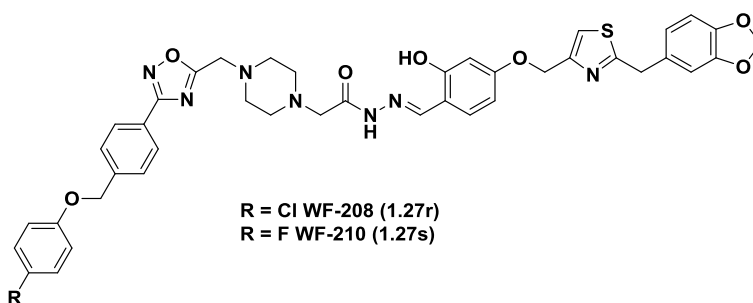


Figure 1.16. Structure of **WF-208 (1.27r)** and **WF-210 (1.27s)**.^{48, 49}

PAC-1 and the two new derivatives were then evaluated in a panel of 15 cancer cell lines in culture for their ability to induce cell death (Table 1.13). The cell lines represented a wide range of tumor types, including leukemia, lung cancer, liver cancer, gastric cancer, breast cancer, glioma, prostate cancer, colon cancer, and gallbladder cancer. In general, **WF-208** and **WF-210** were highly potent in the cell lines evaluated, with 72-hour IC_{50} values in the mid-nanomolar to low micromolar range, and potency was greater than that of **PAC-1** in all cell lines evaluated. In addition, all three compounds were evaluated in four non-cancerous cell lines. Less than 50% cell death was observed at concentrations up to 100 μ M, suggesting the potential for selectivity of cancer cell death over healthy tissue toxicity *in vivo*.^{48, 49}

| Cell Line | Origin | 72-hour IC_{50} (μ M) | | |
|--------------------|--------------|------------------------------|---------------|---------------|
| | | PAC-1 | WF-208 | WF-210 |
| A549 | Lung | 25.48 | 0.42 | 1.78 |
| COLO205 | Colon | 11.46 | 12.85 | 1.1 |
| DU145 | Prostate | 26.03 | 0.08 | 0.08 |
| GBC-SD | Gallbladder | 53.44 | 0.08 | 0.08 |
| Hep 3B | Liver | 25.48 | 0.98 | 0.86 |
| Hep G2 | Liver | 16.35 | 0.73 | 0.22 |
| HGC-27 | Gastric | 13.18 | 0.52 | 0.99 |
| HL-60 | Leukemia | 4.03 | 0.08 | 0.08 |
| K-562 | Leukemia | 14.55 | 0.20 | 0.22 |
| MCF7 | Breast | 12.65 | 0.32 | 2.8 |
| MDA-MB-435S | Melanoma | 14.49 | 0.76 | 1.24 |
| NCI-H226 | Lung | 28.74 | 4.59 | 2.58 |
| U-87 MG | Glioblastoma | 8.82 | 1.67 | 1.05 |
| PC-3 | Prostate | 20.13 | 1.28 | 0.08 |
| U-937 | Lymphoma | 16.42 | 0.08 | 0.08 |

Table 1.13. Potency of **PAC-1**, **WF-208**, and **WF-210** against a diverse array of cancer cell lines in culture.^{48, 49}

1.10.2. Caspase-dependent cell death

The dependence of caspase activity on cell death induced by **PAC-1**, **WF-208**, and **WF-210** was evaluated in a series of assays. The first set of experiments demonstrated the ability of the compounds to activate caspase enzymes in cells. Treatment of HL-60 or U-937 cells with **PAC-1**, **WF-208**, or **WF-210** for time periods between 0 and 24 hours, followed by immunofluorescence staining for cleaved caspase-3, indicated that each compound led to the activation of caspase-3 in a dose- and time-dependent manner. The cells were then treated with **PAC-1** (50 μ M), **WF-208** (10 μ M), or **WF-210** (10 μ M), and western blotting was used to analyze procaspases-3, -8, and -9, as well as poly (ADP-ribose) polymerase (PARP), a canonical caspase-3 substrate. Western blots from HL-60 cells are shown in Figure 1.17. For each compound in both cell lines, cleavage of procaspase-3 and PARP were the earliest events, followed by cleavage of procaspases-8 and -9. These results were further supported by analysis of fluorogenic substrates for each of these three caspase enzymes. In HL-60 cells treated with **PAC-1** or **WF-210**, caspase-3 activity was detected as early as 1 hour after the initiation of treatment, followed by caspase-8 and -9 activities at 4 hours (boxes in Figure 1.17). In contrast, cells treated with the DNA topoisomerase II inhibitor etoposide, which induces apoptosis via the intrinsic pathway, showed caspase-3 and -9 activities simultaneously at 4 hours, followed by caspase-8 at 6 hours. These results suggest that **PAC-1** and derivatives induce apoptosis via a different mechanism than the canonical intrinsic or extrinsic pathways.^{48, 49}

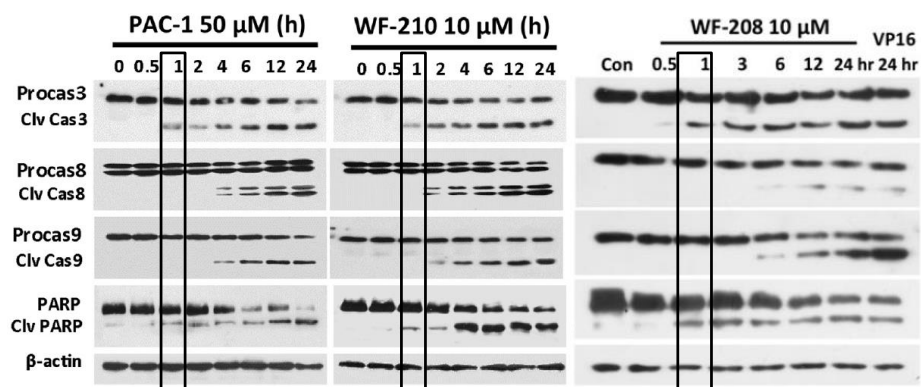


Figure 1.17. Activation of caspases in HL-60 cells by **PAC-1**, **WF-210**, and **WF-208**. Cells were treated with compounds for 24 hours. Cleavage of caspase-3 and PARP were detected first, followed by caspases-8 and -9 (boxes). Figures adapted with permission from literature.^{48, 49}

Following this experiment, HL-60 and U-937 cells were treated with compound for 12 hours (**WF-208**) or 24 hours (**PAC-1** and **WF-210**). Flow cytometry analysis with Annexin V-FITC/propidium iodide staining indicated significant portions of apoptotic cells. **WF-210** was more potent than **PAC-1** in this assay, while both compounds induced apoptosis to a greater degree after 24 hours than did **WF-208** at 12 hours.^{48,49}

The ability of caspase inhibitors to protect against apoptosis induced by **PAC-1** and derivatives was then evaluated. HL-60 and U-937 cells were treated for 24 hours with **PAC-1** (50 μ M), **WF-208** (10 μ M), or **WF-210** (10 μ M) alone or in combination with a pan-caspase inhibitor (Z-VAD-fmk), a caspase-3/-7 inhibitor (Z-DEVD-fmk), a caspase-8 inhibitor (Z-IETD-fmk), or a caspase-9 inhibitor (Z-LEHD-fmk). Cell death was assessed by Annexin V-FITC/propidium iodide staining. Results for HL-60 cells are shown in Figure 1.18. Apoptosis induced by all three compounds was significantly reduced by either the pan-caspase inhibitor or the caspase-3/-7 inhibitor, but not by the inhibitors of the initiator caspases.^{48,49} In addition, co-treatment of **WF-208** with zinc led to a decrease in cell death;⁴⁹ although this experiment was not performed with **WF-210**, previous experiments have shown the protective effects of zinc on **PAC-1**-induced apoptosis.⁴³

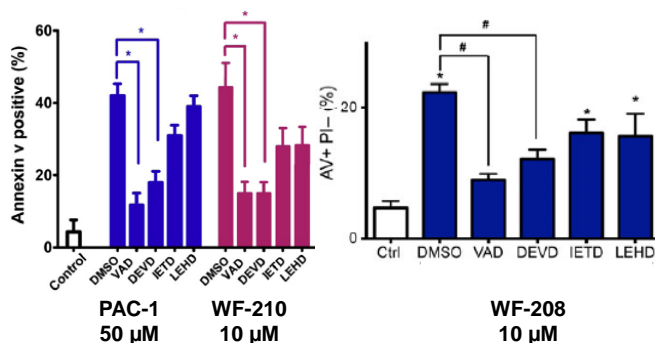


Figure 1.18. Pan-caspase and caspase-3/-7 inhibitors, but not inhibitors of caspases-8 and -9, protect against apoptosis induced by **PAC-1**, **WF-210**, and **WF-208**. HL-60 cells were treated with compound and caspase inhibitor for 24 hours, and cell death was assessed via Annexin V-FITC/propidium iodide staining ($p < 0.05$). Figures adapted with permission from literature.^{48,49}

Finally, the dependence on procaspase-3 for the cytotoxic activity of **PAC-1** and derivatives was studied using HL-60 cells, which overexpress procaspase-3, and MCF7 (human

breast cancer) cells, which do not express procaspase-3. Knockdown of caspase-3 in HL-60 cells with siRNA resulted in a loss of potency for all three compounds compared to a control siRNA. Further, the addition of a plasmid encoding for procaspase-3 increased susceptibility of MCF7 cells to the **PAC-1** derivatives compared to the control plasmid. Western blots for caspase-3 and PARP demonstrated decreased procaspase-3 activation in knockdown HL-60 cells, as well as increased caspase-3 activity in transfected MCF7 cells. In contrast, knockdown or overexpression of procaspase-3 showed no effect on the cytotoxicity of the pan-kinase inhibitor staurosporine or etoposide. These results support the importance of caspase-3 activity for the cytotoxicity of **PAC-1** and derivatives.^{48, 49}

1.10.3. Antitumor efficacy *in vivo*

Based on favorable results from cell culture experiments, **PAC-1**, **WF-208**, and **WF-210** were evaluated in a series of murine xenograft tumor models. **PAC-1** and **WF-210** were first evaluated in Hep 3B (human hepatocellular carcinoma) and MDA-MB-435S (human melanoma) models. Mice received **PAC-1** (5 mg/kg) or **WF-210** (2.5 mg/kg) daily for two weeks via i.v. injection. Both compounds reduced tumor volume significantly compared to control in both models, although **WF-210** showed a greater effect than **PAC-1**, especially in the Hep 3B model (Figure 1.19A). These results correlate with the increased cell culture potency of **WF-210** as compared with **PAC-1**. Western blots of samples derived from the tumors showed increased cleavage of caspase-3 and PARP in both treatment groups compared to control. In addition, **WF-210** was evaluated in a GBC-SD (human gallbladder carcinoma) xenograft and a second MDA-MB-435S xenograft, with oral administration of compound (100 mg/kg). **WF-210** significantly reduced tumor volume compared to control in these models as well. Finally, **PAC-1** and **WF-210** were evaluated in an MCF7 xenograft model. Since this cell line lacks functional procaspase-3, any efficacy in this model would suggest that factors other than procaspase-3 activation are important in **PAC-1** activity. Neither **PAC-1** (5 mg/kg i.v.) nor **WF-210** (2.5 mg/kg i.v.) demonstrated anticancer efficacy in the MCF7 model (Figure 1.19B), and western blots showed minimal PARP cleavage in all treatment groups, demonstrating the importance of procaspase-3 for the mechanism of action of **PAC-1** and derivatives.⁴⁸

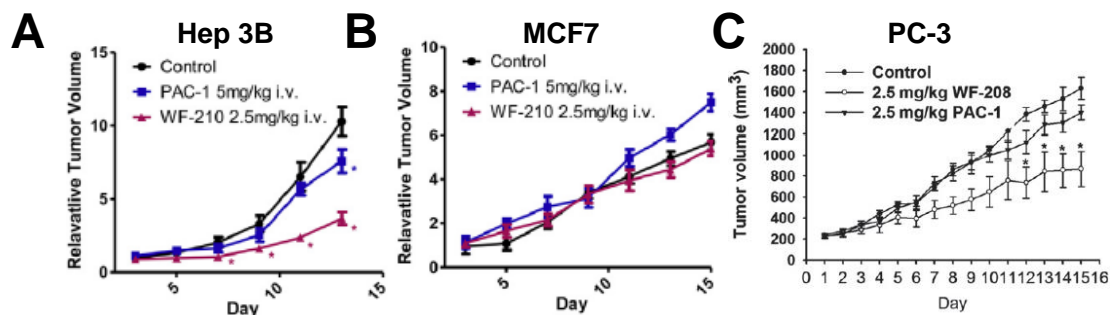


Figure 1.19. **A.** WF-210 slows tumor growth in Hep 3B xenograft model compared to PAC-1 and untreated control (* $p < 0.05$ compared to control). **B.** Neither PAC-1 nor WF-210 slow tumor growth in MCF7 xenograft model. **C.** WF-208 slows tumor growth in PC-3 xenograft model compared to PAC-1 and untreated control (* $p < 0.05$ compared to control). Figures adapted with permission from literature.^{48, 49}

PAC-1 and WF-208 were evaluated in a PC-3 (human prostate cancer) model (Figure 1.19C). Both compounds were given at 2.5 mg/kg via i.v. injection daily for 15 days. WF-208 showed significant tumor reduction compared to control, while PAC-1 showed no significant tumor reduction. Western blots of samples derived from the tumors demonstrated increased caspase-3 cleavage in samples from mice treated with WF-208 or PAC-1, as well as increased PARP cleavage in WF-208-treated animals, further demonstrating the importance of procaspase-3 for PAC-1 and WF-208 activity.⁴⁹

1.11. B-PAC-1

1.11.1. Discovery and cell death induction

In an effort to discover more potent derivatives of PAC-1, a combinatorial library of 837 PAC-1 derivatives was synthesized and evaluated by members of the Hergenrother group. Six highly potent compounds were discovered to induce apoptosis in U-937 cells.¹ These efforts will be discussed further in Chapter 3. One compound discovered from this library, named B-PAC-1 (1.35, Figure 1.20) for the benzyloxy and butyl substituents, was evaluated by Gandhi and coworkers in patient-derived samples from chronic lymphocytic leukemia (CLL).²⁵

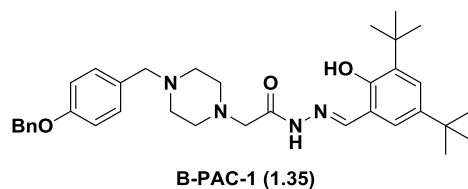


Figure 1.20. Structure of **B-PAC-1**.^{1, 25}

B-PAC-1 induced apoptosis in CLL cells in a dose-dependent manner. Apoptosis was rapid; at 10 μM **B-PAC-1**, cells began to die as early as 6 hours post-treatment, and cell death was significant at 10 hours. Treatment of CLL lymphocytes across 38 samples with 10 μM **B-PAC-1** led to a median of 60% cell death. This was significantly greater than cytotoxicity to noncancerous peripheral blood mononuclear cells (median 21%, $n = 6$) or normal B lymphocytes (median 31%, $n = 6$), demonstrating potential selectivity for apoptosis induction by **B-PAC-1** in cancer cells over healthy cells.²⁵

1.11.2. Role of zinc in **B-PAC-1** activity

Because the proposed mechanism of action of **PAC-1** involves chelation of labile zinc,⁴³ experiments were performed to assess the role of zinc in **B-PAC-1** cytotoxicity. CLL cells were treated for 24 hours with the Bcl-2 inhibitor **ABT-199** (1 nM), staurosporine (100 nM), **B-PAC-1** (10 μM), or the negative control compound **PAC-1a** (10 μM), in the presence or absence of ZnSO_4 (100 μM). **ABT-199** and staurosporine induce apoptosis via the intrinsic pathway through mechanisms independent of zinc, while **PAC-1a** does not bind zinc. The addition of zinc fully inhibited cell death induced by **B-PAC-1**, consistent with the proposed mechanism of action, while having no effect on the cytotoxicity of **ABT-199** or staurosporine. Treatment with **PAC-1a** or ZnSO_4 alone did not induce apoptosis. Similar results were observed whether zinc was added at the same time as **B-PAC-1** or five hours later, and zinc protected against **B-PAC-1** cytotoxicity in a dose-dependent manner.²⁵

For the development of any therapeutic metal-chelating compound, it is important to ensure that chelation will be selective for the metal ion of interest, in order to minimize off-target effects. For this reason, **B-PAC-1** was evaluated against carboxypeptidase A and histone deacetylase, two zinc-dependent enzymes, *in vitro*. **B-PAC-1** showed no inhibition of either

enzyme, confirming the selectivity of **PAC-1** derivatives for sequestration of labile zinc over essential metal ions.²⁵

1.11.3. Role of apoptotic proteins in **B-PAC-1** activity

Several experiments were performed in order to assess the role of caspase activity in **B-PAC-1**-mediated apoptosis. After 24 hours of treatment with **B-PAC-1** (10 μ M), increased cleavage of initiator caspases-8 and -9, as well as executioner caspases-3 and -7 was observed by western blot; executioner caspase-6 was not activated in response to **B-PAC-1** treatment. In addition, the caspase-3 substrate PARP was cleaved in the treated samples, but not in untreated samples, demonstrating that **B-PAC-1** induces caspase-3 activation in CLL cells.²⁵

Following this experiment, the effect of genetic knockdown of key apoptotic proteins on **B-PAC-1** activity was evaluated. The extent of apoptosis induced by **B-PAC-1** (5 μ M) or staurosporine (100 nM) in wild-type Jurkat cells was identical to the cell death in caspase-8 double knockout Jurkat cells (Casp8 (-/-)) in a 24-hour treatment. In contrast, the Fas ligand (100 ng/mL), which induces apoptosis via the extrinsic pathway, was cytotoxic in wild-type Jurkat cells but showed minimal cytotoxicity in Casp8 (-/-) cells. These results suggest that the extrinsic pathway is not important in **B-PAC-1** cytotoxicity, and that caspase-8 is most likely cleaved after the activation of caspase-3 or -7.²⁵

The role of caspases-3 and -7 in **B-PAC-1** activity was then evaluated, using mouse embryonic fibroblasts (MEFs) with a single knockout of both genes (Casp3/7 (+/-)) or a double knockout of both genes (Casp3/7 (-/-)), and cells were treated with compounds for 24 hours. Both staurosporine (100 nM) and **B-PAC-1** (5 μ M) were equally potent in the wild-type and Casp3/7 (+/-) MEFs, but a significant decrease in cell death was observed for each compound in the Casp3/7 (-/-) MEFs. These results demonstrate the importance of the executioner caspases in **B-PAC-1** activity.²⁵

In addition, the role of proapoptotic Bcl-2 family proteins Bax and Bak in **B-PAC-1**-mediated apoptosis was evaluated. Both proteins were doubly knocked down in MEFs (Bax/Bak (-/-)), and the cells were treated with staurosporine (100 nM) or **B-PAC-1** (2 or 5 μ M) for 24 hours. **B-PAC-1** was not cytotoxic at 2 μ M, but approximately 50% cell death was observed in both the wild-type and Bax/Bak (-/-) MEFs. In contrast, staurosporine induced nearly 100% cell death in wild-type MEFs, but minimal cell death was observed in Bax/Bak (-/-) MEFs. These

results indicate that **B-PAC-1** can induce apoptosis independent of certain upstream apoptotic effector proteins.²⁵

Finally, the ability of pan-caspase inhibitors Z-VAD-fmk and Q-VD-OPh to inhibit **B-PAC-1**-induced apoptosis was assessed. In a 24-hour experiment, Z-VAD-fmk and Q-VD-OPh (50 μ M each) partially but significantly reduced the extent of apoptosis induced by **B-PAC-1** (10 μ M); both fully inhibited apoptosis induced by staurosporine (100 nM). In addition, the effect of these inhibitors on PARP cleavage was assessed by western blot. Co-treatment of **B-PAC-1** (10 μ M) or **ABT-199** (5 nM) with Q-VD-OPh (50 μ M) fully inhibited cleavage of PARP, while co-treatment with Z-VAD-fmk (50 μ M) partially reduced the amount of cleaved PARP detected.²⁵

1.11.4. Combination of **B-PAC-1** with Smac mimetic

Smac, a proapoptotic protein, binds to the antiapoptotic IAPs and inhibits their interaction with procaspase-3. This relief of inhibition allows for procaspase-3 to be cleaved to caspase-3, and cells undergo apoptosis.³ Many small-molecule mimics of Smac, including **SM-164**,¹⁵ **LCL-161**,¹⁶ and **Smac066**,⁸⁸ are currently under development as anticancer agents. Treatment of CLL cells with **B-PAC-1** led to an elevation in Smac protein levels. Because this effect was observed, it was proposed that a small molecule with Smac-like activity could synergize with **B-PAC-1** to induce apoptosis. Cells were treated with **B-PAC-1**, **Smac066**, or a combination at 5, 7.5, or 10 μ M. Combinations were synergistic for the majority of samples evaluated, as measured by combination indices of less than 1.0, demonstrating the potential for induction of apoptosis via combination therapy with **B-PAC-1** and additional proapoptotic agents.²⁵

1.12. Summary and outlook

Previous work by the Hergenrother group and others has identified the activation of procaspase-3 by small molecules as a promising anticancer strategy. Because labile zinc pools exist throughout the body, induction of apoptosis via the removal of labile zinc has the potential to treat a diverse array of tumors. The efficacy of **PAC-1** and related derivatives in cell culture and *in vivo* cancer models reinforce the hypotheses formed from *in vitro* data and has led to the initiation of a Phase 1 clinical trial in human cancer patients. As further studies are performed, the potential therapeutic effect of procaspase-3 activation will be fully elucidated. Described herein are chemical studies on **PAC-1**, efforts to further understand the structure-activity

relationships of **PAC-1** and derivatives, and the development of novel **PAC-1** derivatives with the goal of improving potency, metabolic stability, and safety.

1.13. References

1. Hsu, D. C.; Roth, H. S.; West, D. C.; Botham, R. C.; Novotny, C. J.; Schmid, S. C.; Hergenrother, P. J. Parallel synthesis and biological evaluation of 837 analogues of Procaspase-Activating Compound 1 (PAC-1). *ACS Comb. Sci.* **2012**, *14*, 44-50.
2. Roth, H. S.; Botham, R. C.; Schmid, S. C.; Fan, T. M.; Dirikolu, L.; Hergenrother, P. J. Removal of metabolic liabilities enables development of derivatives of Procaspase-Activating Compound 1 (PAC-1) with improved pharmacokinetics. *J. Med. Chem.* **2015**, *58*, 4046-4065.
3. Hengartner, M. O. The biochemistry of apoptosis. *Nature* **2000**, *407*, 770-776.
4. Elmore, S. Apoptosis: A review of programmed cell death. *Toxicol. Pathol.* **2007**, *35*, 495-516.
5. Nicholson, D. W. Caspase structure, proteolytic substrates, and function during apoptotic cell death. *Cell Death Differ.* **1999**, *6*, 1028-1042.
6. Earnshaw, W. C.; Martins, L. M.; Kaufmann, S. H. Mammalian caspases: Structure, activation, substrates, and functions during apoptosis. *Annual Review of Biochemistry* **1999**, *68*, 383-424.
7. Slee, E. A.; Adrain, C.; Martin, S. J. Executioner caspase-3, -6, and -7 perform distinct, non-redundant roles during the demolition phase of apoptosis. *J. Biol. Chem.* **2001**, *276*, 7320-7326.
8. Sakahira, H.; Enari, M.; Nagata, S. Cleavage of CAD inhibitor in CAD activation and DNA degradation during apoptosis. *Nature* **1998**, *391*, 96-99.
9. Hanahan, D.; Weinberg, R. A. The hallmarks of cancer. *Cell* **2000**, *100*, 57-70.
10. Hanahan, D.; Weinberg, R. A. Hallmarks of cancer: the next generation. *Cell* **2011**, *144*, 646-674.
11. Vassilev, L. T.; Vu, B. T.; Graves, B.; Carvajal, D.; Podlaski, F.; Filipovic, Z.; Kong, N.; Kammlott, U.; Lukacs, C.; Klein, C.; Fotouhi, N.; Liu, E. A. In vivo activation of the p53 pathway by small-molecule antagonists of MDM2. *Science* **2004**, *303*, 844-848.
12. Vu, B.; Wovkulich, P.; Pizzolato, G.; Lovey, A.; Ding, Q.; Jiang, N.; Liu, J. J.; Zhao, C.; Glenn, K.; Wen, Y.; Tovar, C.; Packman, K.; Vassilev, L.; Graves, B. Discovery of RG7112: A small-molecule MDM2 inhibitor in clinical development. *ACS Med. Chem. Lett.* **2013**, *4*, 466-469.
13. Oltsersdorf, T.; Elmore, S. W.; Shoemaker, A. R.; Armstrong, R. C.; Augeri, D. J.; Belli, B. A.; Bruncko, M.; Deckwerth, T. L.; Dinges, J.; Hajduk, P. J.; Joseph, M. K.; Kitada, S.; Korsmeyer, S. J.; Kunzer, A. R.; Letai, A.; Li, C.; Mitten, M. J.; Nettlesheim, D. G.; Ng, S.; Nimmer, P. M.; O'Connor, J. M.; Oleksijew, A.; Petros, A. M.; Reed, J. C.; Shen, W.; Tahir, S. K.; Thompson, C. B.; Tomaselli, K. J.; Wang, B. L.; Wendt, M. D.; Zhang, H. C.; Fesik, S. W.; Rosenberg, S. H. An inhibitor of Bcl-2 family proteins induces regression of solid tumours. *Nature* **2005**, *435*, 677-681.
14. Souers, A. J.; Levenson, J. D.; Boghaert, E. R.; Ackler, S. L.; Catron, N. D.; Chen, J.; Dayton, B. D.; Ding, H.; Enschede, S. H.; Fairbrother, W. J.; Huang, D. C.; Hymowitz, S. G.; Jin, S.; Khaw, S. L.; Kovar, P. J.; Lam, L. T.; Lee, J.; Maecker, H. L.; Marsh, K. C.; Mason, K. D.; Mitten, M. J.; Nimmer, P. M.; Oleksijew, A.; Park, C. H.; Park, C. M.; Phillips, D. C.; Roberts, A. W.; Sampath, D.; Seymour, J. F.; Smith, M. L.; Sullivan, G. M.; Tahir, S. K.; Tse, C.; Wendt, M. D.; Xiao, Y.; Xue, J. C.; Zhang, H.; Humerickhouse, R. A.; Rosenberg, S. H.; Elmore, S. W. ABT-199, a potent and selective BCL-2 inhibitor, achieves antitumor activity while sparing platelets. *Nat. Med.* **2013**, *19*, 202-208.

15. Lu, J.; Bai, L.; Sun, H.; Nikolovska-Coleska, Z.; McEachern, D.; Qiu, S.; Miller, R. S.; Yi, H.; Shangary, S.; Sun, Y.; Meagher, J. L.; Stuckey, J. A.; Wang, S. SM-164: a novel, bivalent Smac mimetic that induces apoptosis and tumor regression by concurrent removal of the blockade of cIAP-1/2 and XIAP. *Cancer Res.* **2008**, *68*, 9384-9393.
16. Houghton, P. J.; Kang, M. H.; Reynolds, C. P.; Morton, C. L.; Kolb, E. A.; Gorlick, R.; Keir, S. T.; Carol, H.; Lock, R.; Maris, J. M.; Billups, C. A.; Smith, M. A. Initial testing (stage 1) of LCL161, a SMAC mimetic, by the pediatric preclinical testing program. *Pediatr. Blood Cancer* **2012**, *58*, 636-639.
17. Putt, K. S.; Chen, G. W.; Pearson, J. M.; Sandhorst, J. S.; Hoagland, M. S.; Kwon, J. T.; Hwang, S. K.; Jin, H.; Churchwell, M. I.; Cho, M. H.; Doerge, D. R.; Helferich, W. G.; Hergenrother, P. J. Small-molecule activation of procaspase-3 to caspase-3 as a personalized anticancer strategy. *Nat. Chem. Biol.* **2006**, *2*, 543-550.
18. Wolan, D. W.; Zorn, J. A.; Gray, D. C.; Wells, J. A. Small-molecule activators of a proenzyme. *Science* **2009**, *326*, 853-858.
19. Schipper, J. L.; MacKenzie, S. H.; Sharma, A.; Clark, A. C. A bifunctional allosteric site in the dimer interface of procaspase-3. *Biophys. Chem.* **2011**, *159*, 100-109.
20. Vickers, C. J.; Gonzalez-Paez, G. E.; Umotoy, J. C.; Cayan-Garrett, C.; Brown, S. J.; Wolan, D. W. Small-molecule procaspase activators identified using fluorescence polarization. *ChemBioChem* **2013**, *14*, 1419-1422.
21. Ghavami, S.; Hashemi, M.; Ande, S. R.; Yeganeh, B.; Xiao, W.; Eshraghi, M.; Bus, C. J.; Kadkhoda, K.; Wiechec, E.; Halayko, A. J.; Los, M. Apoptosis and cancer: mutations within caspase genes. *J. Med. Genet.* **2009**, *46*, 497-510.
22. Soini, Y.; Paakko, P. Apoptosis and expression of caspases 3, 6 and 8 in malignant non-Hodgkin's lymphomas. *APMIS* **1999**, *107*, 1043-1050.
23. Wrobel, G.; Maldyk, J.; Kazanowska, B.; Rapala, M.; Maciejka-Kapuscinska, L.; Chaber, R. Immunohistochemical expression of procaspase-3 and its clinical significance in childhood non-Hodgkin lymphomas. *Pediatr. Dev. Pathol.* **2011**, *14*, 173-179.
24. Estrov, Z.; Thall, P. F.; Talpaz, M.; Estey, E. H.; Kantarjian, H. M.; Andreeff, M.; Harris, D.; Van, Q.; Walterscheid, M.; Kornblau, S. M. Caspase 2 and caspase 3 protein levels as predictors of survival in acute myelogenous leukemia. *Blood* **1998**, *92*, 3090-3097.
25. Patel, V.; Balakrishnan, K.; Keating, M. J.; Wierda, W. G.; Gandhi, V. Expression of executioner procaspases and their activation by a procaspase activating compound in chronic lymphocytic leukemia cells. *Blood* **2015**, *125*, 1126-1136.
26. Fink, D.; Schlagbauer-Wadl, H.; Selzer, E.; Lucas, T.; Wolff, K.; Pehamberger, H.; Eichler, H. G.; Jansen, B. Elevated procaspase levels in human melanoma. *Melanoma Res.* **2001**, *11*, 385-393.
27. Chen, N.; Gong, J.; Chen, X.; Meng, W.; Huang, Y.; Zhao, F.; Wang, L.; Zhou, Q. Caspases and inhibitor of apoptosis proteins in cutaneous and mucosal melanoma: expression profile and clinicopathologic significance. *Hum. Pathol* **2009**, *40*, 950-956.
28. Gdynia, G.; Grund, K.; Eckert, A.; Bock, B. C.; Funke, B.; Macher-Goeppinger, S.; Sieber, S.; Herold-Mende, C.; Wiestler, B.; Wiestler, O. D.; Roth, W. Basal caspase activity promotes migration and invasiveness in glioblastoma cells. *Mol. Cancer Res.* **2007**, *5*, 1232-1240.
29. Murphy, A. C.; Weyhenmeyer, B.; Schmid, J.; Kilbride, S. M.; Rehm, M.; Huber, H. J.; Senft, C.; Weissenberger, J.; Seifert, V.; Dunst, M.; Mittelbronn, M.; Kogel, D.; Prehn, J. H.;

- Murphy, B. M. Activation of executioner caspases is a predictor of progression-free survival in glioblastoma patients: a systems medicine approach. *Cell Death Dis.* **2013**, *4*, e629.
30. Virkajarvi, N.; Paakko, P.; Soini, Y. Apoptotic index and apoptosis influencing proteins bcl-2, mcl-1, bax and caspases 3, 6 and 8 in pancreatic carcinoma. *Histopathology* **1998**, *33*, 432-439.
 31. Persad, R.; Liu, C.; Wu, T. T.; Houlihan, P. S.; Hamilton, S. R.; Diehl, A. M.; Rashid, A. Overexpression of caspase-3 in hepatocellular carcinomas. *Mod. Pathol.* **2004**, *17*, 861-867.
 32. Tormanen-Napankangas, U.; Soini, Y.; Kahlos, K.; Kinnula, V.; Paakko, P. Expression of caspases-3, -6 and -8 and their relation to apoptosis in non-small cell lung carcinoma. *Int. J. Cancer* **2001**, *93*, 192-198.
 33. Krepela, E.; Prochazka, J.; Liul, X.; Fiala, P.; Kinkor, Z. Increased expression of Apaf-1 and procaspase-3 and the functionality of intrinsic apoptosis apparatus in non-small cell lung carcinoma. *Biol. Chem.* **2004**, *385*, 153-168.
 34. Krepela, E.; Prochazka, J.; Fiala, P.; Zatloukal, P.; Selinger, P. Expression of apoptosome pathway-related transcripts in non-small cell lung cancer. *J. Cancer Res. Clin. Oncol.* **2006**, *132*, 57-68.
 35. O'Donovan, N.; Crown, J.; Stunell, H.; Hill, A. D.; McDermott, E.; O'Higgins, N.; Duffy, M. J. Caspase 3 in breast cancer. *Clin. Cancer Res.* **2003**, *9*, 738-742.
 36. Zapata, J. M.; Krajewska, M.; Krajewski, S.; Huang, R. P.; Takayama, S.; Wang, H. G.; Adamson, E.; Reed, J. C. Expression of multiple apoptosis-regulatory genes in human breast cancer cell lines and primary tumors. *Breast Cancer Res. Treat.* **1998**, *47*, 129-140.
 37. Krajewski, S.; Krajewska, M.; Turner, B. C.; Pratt, C.; Howard, B.; Zapata, J. M.; Frenkel, V.; Robertson, S.; Ionov, Y.; Yamamoto, H.; Perucho, M.; Takayama, S.; Reed, J. C. Prognostic significance of apoptosis regulators in breast cancer. *Endocr. Relat. Cancer* **1999**, *6*, 29-40.
 38. Nakopoulou, L.; Alexandrou, P.; Stefanaki, K.; Panayotopoulou, E.; Lazaris, A. C.; Davaris, P. S. Immunohistochemical expression of caspase-3 as an adverse indicator of the clinical outcome in human breast cancer. *Pathobiology* **2001**, *69*, 266-273.
 39. Jiang, H.; Gong, M.; Cui, Y.; Ma, K.; Chang, D.; Wang, T. Y. Upregulation of caspase-3 expression in esophageal cancer correlates with favorable prognosis: an immunohistochemical study from a high incidence area in northern China. *Dis. Esophagus* **2010**, *23*, 487-492.
 40. Roy, S.; Bayly, C. I.; Gareau, Y.; Houtzager, V. M.; Kargman, S.; Keen, S. L.; Rowland, K.; Seiden, I. M.; Thornberry, N. A.; Nicholson, D. W. Maintenance of caspase-3 proenzyme dormancy by an intrinsic "safety catch" regulatory tripeptide. *Proc. Natl. Acad. Sci. U.S.A.* **2001**, *98*, 6132-6137.
 41. Sadowska, A.; Car, H.; Pryczynicz, A.; Guzinska-Ustymowicz, K.; Kowal, K. W.; Cepowicz, D.; Kedra, B. Expression of apoptotic proteins in human colorectal cancer and metastatic lymph nodes. *Pathol. Res. Pract.* **2014**, *210*, 576-581.
 42. Hector, S.; Conlon, S.; Schmid, J.; Dicker, P.; Cummins, R. J.; Concannon, C. G.; Johnston, P. G.; Kay, E. W.; Prehn, J. H. Apoptosome-dependent caspase activation proteins as prognostic markers in Stage II and III colorectal cancer. *Br. J. Cancer* **2012**, *106*, 1499-1505.
 43. Peterson, Q. P.; Goode, D. R.; West, D. C.; Ramsey, K. N.; Lee, J. J. Y.; Hergenrother, P. J. PAC-1 activates procaspase-3 in vitro through relief of zinc-mediated inhibition. *J. Mol. Biol.* **2009**, *388*, 144-158.
 44. Peterson, Q. P.; Hsu, D. C.; Goode, D. R.; Novotny, C. J.; Totten, R. K.; Hergenrother, P. J. Procaspase-3 activation as an anti-cancer strategy: structure-activity relationship of

Procaspase-Activating Compound 1 (PAC-1) and its cellular co-localization with caspase-3. *J. Med. Chem.* **2009**, *52*, 5721-5731.

45. Peterson, Q. P.; Hsu, D. C.; Novotny, C. J.; West, D. C.; Kim, D.; Schmit, J. M.; Dirikolu, L.; Hergenrother, P. J.; Fan, T. M. Discovery and canine preclinical assessment of a nontoxic procaspase-3-activating compound. *Cancer Res.* **2010**, *70*, 7232-7241.

46. Lucas, P. W.; Schmit, J. M.; Peterson, Q. P.; West, D. C.; Hsu, D. C.; Novotny, C. J.; Dirikolu, L.; Churchwell, M. I.; Doerge, D. R.; Garrett, L. D.; Hergenrother, P. J.; Fan, T. M. Pharmacokinetics and derivation of an anticancer dosing regimen for PAC-1, a preferential small molecule activator of procaspase-3, in healthy dogs. *Invest. New Drugs* **2011**, *29*, 901-911.

47. West, D. C.; Qin, Y.; Peterson, Q. P.; Thomas, D. L.; Palchaudhuri, R.; Morrison, K. C.; Lucas, P. W.; Palmer, A. E.; Fan, T. M.; Hergenrother, P. J. Differential effects of procaspase-3 activating compounds in the induction of cancer cell death. *Mol. Pharmaceutics* **2012**, *9*, 1425-1434.

48. Wang, F. Y.; Wang, L. H.; Zhao, Y. F.; Li, Y.; Ping, G. F.; Xiao, S.; Chen, K.; Zhu, W. F.; Gong, P.; Yang, J. Y.; Wu, C. F. A novel small-molecule activator of procaspase-3 induces apoptosis in cancer cells and reduces tumor growth in human breast, liver and gallbladder cancer xenografts. *Mol. Oncol.* **2014**, *8*, 1640-1652.

49. Wang, F.; Liu, Y.; Wang, L.; Yang, J.; Zhao, Y.; Wang, N.; Cao, Q.; Gong, P.; Wu, C. Targeting procaspase-3 with WF-208, a novel PAC-1 derivative, causes selective cancer cell apoptosis. *J. Cell. Mol. Med.* [Online early access]. DOI: 10.1111/jcmm.12566. Published Online: March 8, 2015.

50. Zhang, B.; Zhao, Y. F.; Zhai, X.; Fan, W. J.; Ren, J. L.; Wu, C. F.; Gong, P. Design, synthesis and antiproliferative activities of diaryl urea derivatives bearing N-acylhydrazone moiety. *Chin. Chem. Lett.* **2012**, *23*, 915-918.

51. Zhang, B.; Zhao, Y. F.; Zhai, X.; Wang, L. H.; Yang, J. Y.; Tan, Z. H.; Gong, P. Design, synthesis and anticancer activities of diaryl urea derivatives bearing N-acylhydrazone moiety. *Chem. Pharm. Bull.* **2012**, *60*, 1046-1054.

52. Zhai, X.; Huang, Q.; Jiang, N.; Wu, D.; Zhou, H. Y.; Gong, P. Discovery of hybrid dual N-acylhydrazone and diaryl urea derivatives as potent antitumor agents: design, synthesis and cytotoxicity evaluation. *Molecules* **2013**, *18*, 2904-2923.

53. Huang, Q.; Fu, Q.; Liu, Y.; Bai, J.; Wang, Q.; Liao, H.; Gong, P. Design, synthesis and anticancer activity of novel 6-(aminophenyl)-2,4-bismorpholino-1,3,5-triazine derivatives bearing arylmethylene hydrazine moiety. *Chem. Res. Chin. Univ.* **2014**, *30*, 257-265.

54. Botham, R. C.; Fan, T. M.; Im, I.; Borst, L. B.; Dirikolu, L.; Hergenrother, P. J. Dual small-molecule targeting of procaspase-3 dramatically enhances zymogen activation and anticancer activity. *J. Am. Chem. Soc.* **2014**, *136*, 1312-1319.

55. Ma, J.; Zhang, G.; Han, X.; Bao, G.; Wang, L.; Zhai, X.; Gong, P. Synthesis and biological evaluation of benzothiazole derivatives bearing the ortho-hydroxy-N-acylhydrazone moiety as potent antitumor agents. *Arch. Pharm. Chem. Life Sci.* **2014**, *347*, 936-949.

56. Ma, J. J.; Chen, D.; Lu, K.; Wang, L. H.; Han, X. Q.; Zhao, Y. F.; Gong, P. Design, synthesis, and structure-activity relationships of novel benzothiazole derivatives bearing the ortho-hydroxy N-carbamoylhydrazone moiety as potent antitumor agents. *Eur. J. Med. Chem.* **2014**, *86*, 257-269.

57. Astrand, O. A. H.; Aziz, G.; Ali, S. F.; Paulsen, R. E.; Hansen, T. V.; Rongved, P. Synthesis and initial in vitro biological evaluation of two new zinc-chelating compounds: comparison with TPEN and PAC-1. *Bioorg. Med. Chem.* **2013**, *21*, 5175-5181.

58. Qin, M. Z.; Liao, W. K.; Xu, C.; Fu, B. L.; Ren, J. G.; Gu, Y. C.; Gong, P. Synthesis and biological evaluation of novel 4-(2-fluorophenoxy)-2-(1H-tetrazol-1-yl)pyridines bearing semicarbazone moieties as potent antitumor agents. *Arch. Pharm. Chem. Life Sci.* **2013**, *346*, 840-850.
59. Hao-ming, L.; Chun-ling, Y.; Xiao-ying, Z.; Ming-ming, Z.; Dan, J.; Jun-hai, X.; Xiao-hong, Y.; Song, L. Design, synthesis, and antitumor activity of a novel series of PAC-1 analogues. *Chem. Res. Chin. Univ.* **2013**, *29*, 906-910.
60. Razi, S. S.; Schwartz, G.; Boone, D.; Li, X.; Belsley, S.; Todd, G.; Connery, C. P.; Bhora, F. Y. Small molecule activation of procaspase-3 induces apoptosis in human lung adenocarcinoma: a tailored anti-cancer strategy. *J. Surg. Res.* **2010**, *158*, 402-403.
61. Razi, S. S.; Rehmani, S.; Li, X.; Park, K.; Schwartz, G. S.; Latif, M. J.; Bhora, F. Y. Antitumor activity of paclitaxel is significantly enhanced by a novel proapoptotic agent in non-small cell lung cancer. *J. Surg. Res.* **2015**, *194*, 622-630.
62. Razi, S. S.; Schwartz, G.; Li, X. G.; Boone, D.; Belsley, S.; Todd, G.; Connery, C. P.; Bhora, F. Y. Direct activation of procaspase-3 inhibits human lung adenocarcinoma in a murine model. *J. Am. Coll. Surgeons* **2010**, *211*, S36-S36.
63. Charkoudian, L. K.; Pham, D. M.; Franz, K. J. A pro-chelator triggered by hydrogen peroxide inhibits iron-promoted hydroxyl radical formation. *J. Am. Chem. Soc.* **2006**, *128*, 12424-12425.
64. Johnson, D. K.; Murphy, T. B.; Rose, N. J.; Goodwin, W. H.; Pickart, L. Cytotoxic chelators and chelates. 1. Inhibition of DNA synthesis in cultured rodent and human cells by aroylhydrazones and by a copper(II) complex of salicylaldehyde benzoyl hydrazone. *Inorg. Chim. Acta* **1982**, *67*, 159-165.
65. Peng, X.; Tang, X.; Qin, W.; Dou, W.; Guo, Y.; Zheng, J.; Liu, W.; Wang, D. Aroylhydrazone derivative as fluorescent sensor for highly selective recognition of Zn²⁺ ions: syntheses, characterization, crystal structures and spectroscopic properties. *Dalton Trans.* **2011**, *40*, 5271-5277.
66. Muzio, M.; Salvesen, G. S.; Dixit, V. M. FLICE induced apoptosis in a cell-free system. Cleavage of caspase zymogens. *J. Biol. Chem.* **1997**, *272*, 2952-2956.
67. Perry, D. K.; Smyth, M. J.; Stennicke, H. R.; Salvesen, G. S.; Duriez, P.; Poirier, G. G.; Hannun, Y. A. Zinc is a potent inhibitor of the apoptotic protease, caspase-3. A novel target for zinc in the inhibition of apoptosis. *J. Biol. Chem.* **1997**, *272*, 18530-18533.
68. Huber, K. L.; Hardy, J. A. Mechanism of zinc-mediated inhibition of caspase-9. *Protein Sci.* **2012**, *21*, 1056-1065.
69. Velazquez-Delgado, E. M.; Hardy, J. A. Zinc-mediated allosteric inhibition of caspase-6. *J. Biol. Chem.* **2012**, *287*, 36000-36011.
70. Truong-Tran, A. Q.; Grosser, D.; Ruffin, R. E.; Murgia, C.; Zalewski, P. D. Apoptosis in the normal and inflamed airway epithelium: role of zinc in epithelial protection and procaspase-3 regulation. *Biochem. Pharmacol.* **2003**, *66*, 1459-1468.
71. Daniel, A. G.; Peterson, E. J.; Farrell, N. P. The bioinorganic chemistry of apoptosis: potential inhibitory zinc binding sites in caspase-3. *Angew. Chem. Int. Ed. Engl.* **2014**, *53*, 4098-4101.
72. Sjoli, S.; Solli, A. I.; Akselsen, O.; Jiang, Y.; Berg, E.; Hansen, T. V.; Sylte, I.; Winberg, J. O. PAC-1 and isatin derivatives are weak matrix metalloproteinase inhibitors. *Biochim. Biophys. Acta* **2014**, *1840*, 3162-3169.

73. Baell, J. B.; Holloway, G. A. New substructure filters for removal of pan assay interference compounds (PAINS) from screening libraries and for their exclusion in bioassays. *J. Med. Chem.* **2010**, *53*, 2719-2740.
74. Song, Z.; Chen, X. H.; Zhang, D.; Ren, L.; Fang, L. N.; Cheng, W. M.; Gong, P.; Bi, K. S. Kinetic study of the degradation of PAC-1 and identification of a degradation product in alkaline condition. *Chromatographia* **2009**, *70*, 1575-1580.
75. Goode, D. R.; Totten, R. K.; Heeres, J. T.; Hergenrother, P. J. Identification of promiscuous small molecule activators in high-throughput enzyme activation screens. *J. Med. Chem.* **2008**, *51*, 2346-2349.
76. Putinski, C.; Abdul-Ghani, M.; Stiles, R.; Brunette, S.; Dick, S. A.; Fernando, P.; Megeney, L. A. Intrinsic-mediated caspase activation is essential for cardiomyocyte hypertrophy. *Proc. Natl. Acad. Sci. U.S.A.* **2013**, *110*, E4079-E4087.
77. Franz, K. J. Clawing back: broadening the notion of metal chelators in medicine. *Curr. Opin. Chem. Biol.* **2013**, *17*, 143-149.
78. Richon, V. M. Cancer biology: mechanism of antitumour action of vorinostat (suberoylanilide hydroxamic acid), a novel histone deacetylase inhibitor. *Br. J. Cancer* **2006**, *95*, S2-S6.
79. Russell, R. G.; Watts, N. B.; Ebetino, F. H.; Rogers, M. J. Mechanisms of action of bisphosphonates: similarities and differences and their potential influence on clinical efficacy. *Osteoporosis Int.* **2008**, *19*, 733-759.
80. Huesca, M.; Lock, L. S.; Khine, A. A.; Viau, S.; Peralta, R.; Cukier, I. H.; Jin, H.; Al-Qawasmeh, R. A.; Lee, Y.; Wright, J.; Young, A. A novel small molecule with potent anticancer activity inhibits cell growth by modulating intracellular labile zinc homeostasis. *Mol. Cancer Ther.* **2009**, *8*, 2586-2596.
81. Yu, Y.; Wong, J.; Lovejoy, D. B.; Kalinowski, D. S.; Richardson, D. R. Chelators at the cancer coalface: desferrioxamine to triapine and beyond. *Clin. Cancer Res.* **2006**, *12*, 6876-6883.
82. Makhov, P.; Golovine, K.; Uzzo, R. G.; Rothman, J.; Crispen, P. L.; Shaw, T.; Scoll, B. J.; Kolenko, V. M. Zinc chelation induces rapid depletion of the X-linked inhibitor of apoptosis and sensitizes prostate cancer cells to TRAIL-mediated apoptosis. *Cell Death Differ.* **2008**, *15*, 1745-1751.
83. Hepowit, N. L.; Uthandi, S.; Miranda, H. V.; Toniutti, M.; Prunetti, L.; Olivarez, O.; De Vera, I. M.; Fanucci, G. E.; Chen, S.; Maupin-Furlow, J. A. Archaeal JAB1/MPN/MOV34 metalloenzyme (HvJAMM1) cleaves ubiquitin-like small archaeal modifier proteins (SAMPs) from protein-conjugates. *Mol. Microbiol.* **2012**, *86*, 971-987.
84. Lee, H. G.; Lee, J. H.; Jang, S. P.; Park, H. M.; Kim, S. J.; Kim, Y.; Kim, C.; Harrison, R. G. Zinc selective chemosensor based on pyridyl-amide fluorescence. *Tetrahedron* **2011**, *67*, 8073-8078.
85. Richardson, D. R.; Hefter, G. T.; May, P. M.; Webb, J.; Baker, E. Iron chelators of the pyridoxal isonicotinoyl hydrazone class. III. Formation constants with calcium(II), magnesium(II) and zinc(II). *Biol. Metals* **1989**, *2*, 161-167.
86. Cecchelli, R.; Berezowski, V.; Lundquist, S.; Culot, M.; Renftel, M.; Dehouck, M. P.; Fenart, L. Modelling of the blood-brain barrier in drug discovery and development. *Nat. Rev. Drug Discov.* **2007**, *6*, 650-661.
87. Qin, Y.; Dittmer, P. J.; Park, J. G.; Jansen, K. B.; Palmer, A. E. Measuring steady-state and dynamic endoplasmic reticulum and Golgi Zn²⁺ with genetically encoded sensors. *Proc. Natl. Acad. Sci. U.S.A.* **2011**, *108*, 7351-7356.

88. Cossu, F.; Malvezzi, F.; Canevari, G.; Mastrangelo, E.; Lecis, D.; Delia, D.; Seneci, P.; Scolastico, C.; Bolognesi, M.; Milani, M. Recognition of Smac-mimetic compounds by the BIR domain of cIAP1. *Protein Sci.* **2010**, *19*, 2418-2429.

Chapter 2. Synthetic and Spectroscopic Studies of PAC-1, and Synthesis of S-PAC-1

2.1. Introduction

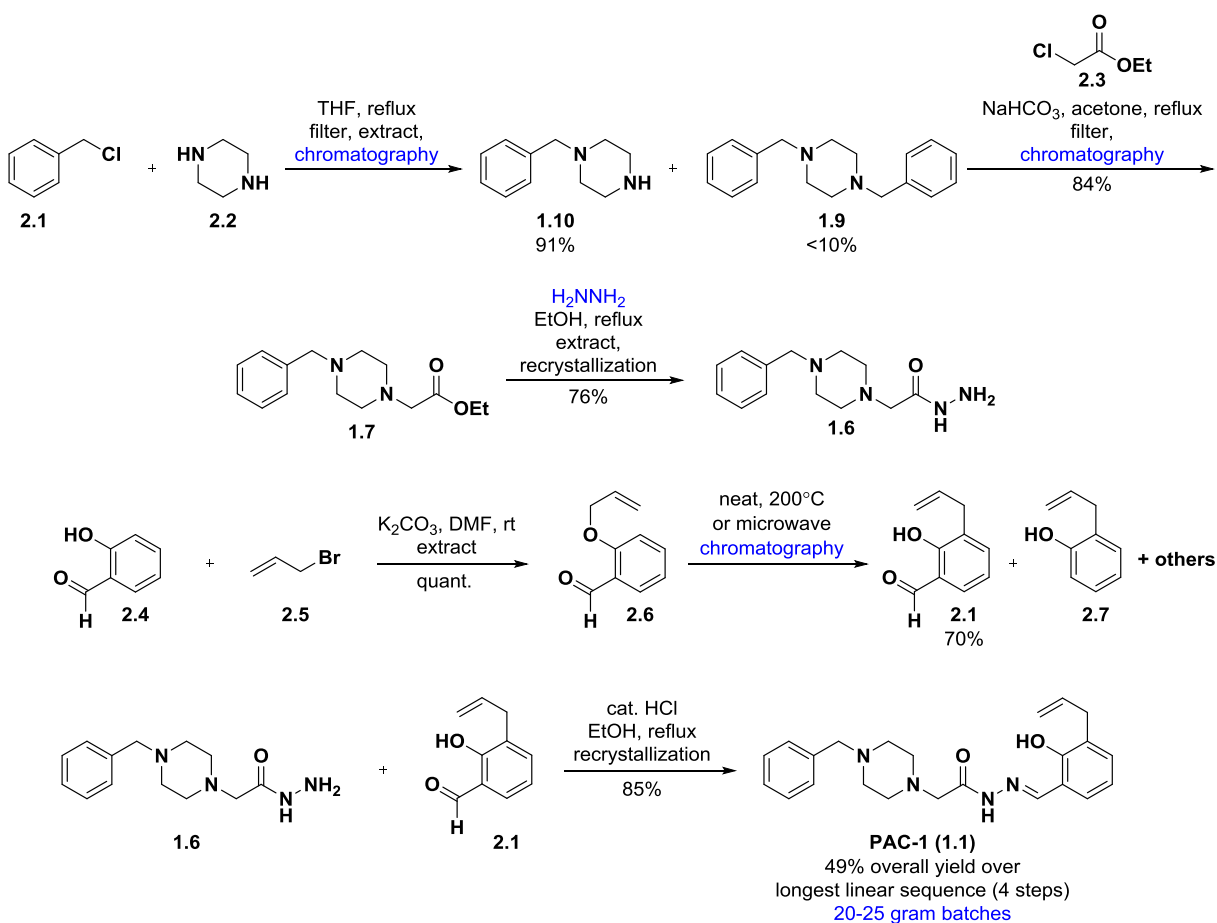
As discussed in Chapter 1, **PAC-1 (1.1)** was discovered as a small molecule capable of enhancing the enzymatic activity of procaspase-3 *in vitro*.¹ Based on promising results from murine anticancer efficacy experiments, clinical trials in canine and human cancer patients were planned. In order to facilitate these studies, it became necessary to develop an improved gram-scale synthetic route to **PAC-1**, as well as to improve upon the synthetic route toward **S-PAC-1**. In addition, it was necessary to determine the identity of two species in the ¹H- and ¹³C-NMR spectra of **PAC-1**. If these were truly two distinct species, the final product would need to be purified more rigorously, but if these were two interconverting isomers of **PAC-1**, then the purity would be acceptable.

2.2. Improved large-scale synthesis of PAC-1

2.2.1. First-generation synthesis of PAC-1

The synthesis of **PAC-1** involves the late-stage condensation of a hydrazide (**1.6**) and an aldehyde (**2.1**) to form the essential *ortho*-hydroxy-*N*-acylhydrazone (Scheme 2.1). The original synthetic route toward **PAC-1** is shown in Scheme 2.1. The synthesis of **PAC-1** begins by the reaction of benzyl chloride (**2.2**) with 6 equivalents of piperazine (**2.3**) to form 1-benzylpiperazine (**1.10**) in 91% yield, while also forming 1,4-dibenzylpiperazine (**1.9**) in <10% yield. The slow addition of benzyl chloride into a solution of excess piperazine is essential to favor the formation of **1.10** over **1.9**. A second alkylation of **1.10** with a slight excess of ethyl chloroacetate (**2.3**) gives disubstituted piperazine **1.7** in 84% yield, and subsequent reaction of the ethyl ester with 3 equivalents of anhydrous hydrazine gives hydrazide **1.6** in 76% yield.¹ Synthesis of the aldehyde fragment begins by the alkylation of salicylaldehyde (**2.4**) with allyl bromide (**2.5**) to give 2-allyloxybenzaldehyde (**2.6**) in high yield. Compound **2.6** is subjected to a Claisen rearrangement by heating with or without microwave irradiation to form 3-allylsalicylaldehyde (**2.1**) in 70% yield.^{2,3} Finally, aldehyde **2.1** is condensed with a slight excess of hydrazide **1.6** with catalytic hydrochloric acid, and recrystallization from 15:1 hexane:ethanol gives **PAC-1 (1.1)** in 85% yield. The synthesis of **PAC-1** proceeded in an overall yield of 49%

over the longest linear sequence of four steps. This strategy was successful for the generation of 20-25 gram batches of **PAC-1**.¹



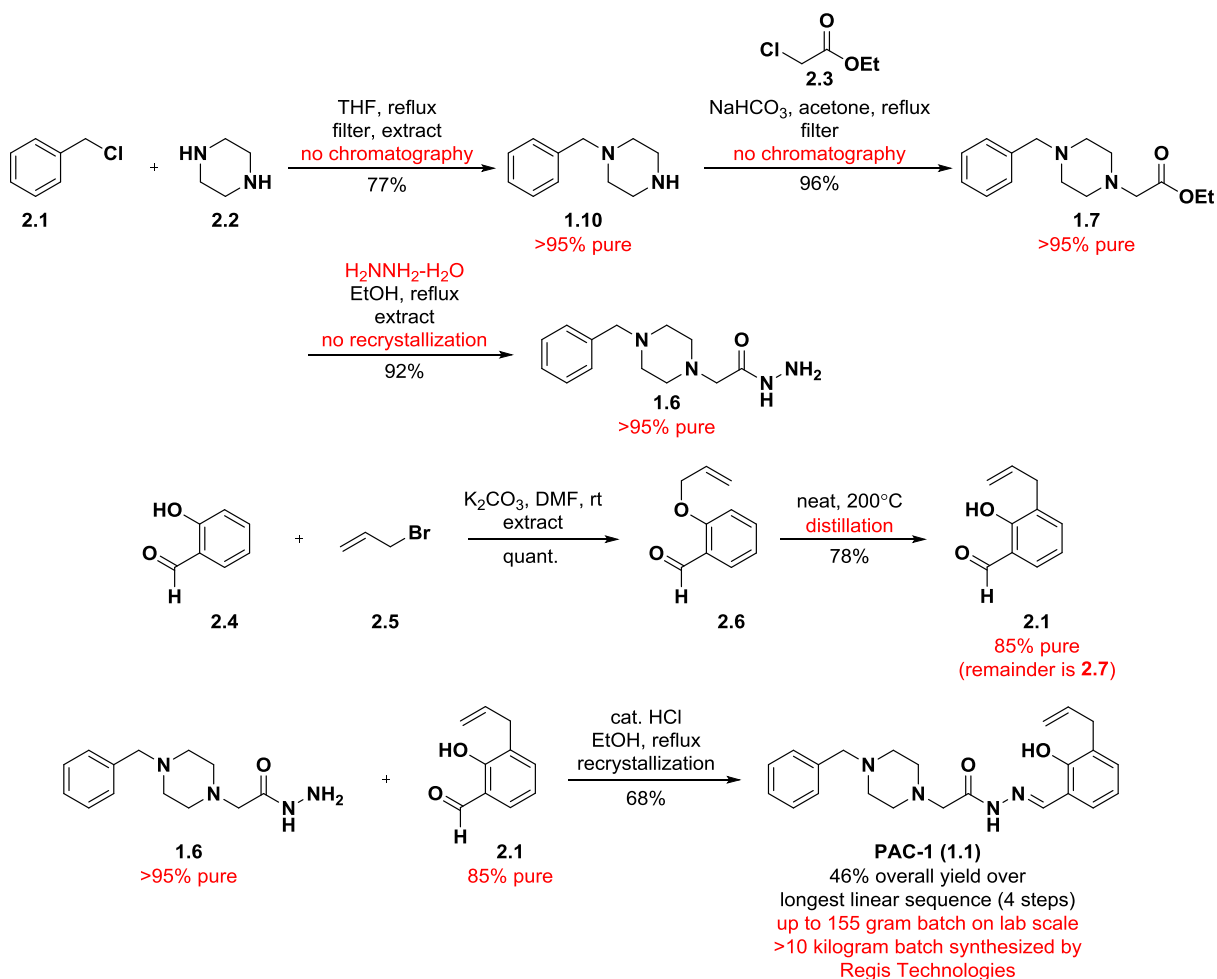
Scheme 2.1. First-generation synthesis of **PAC-1**.¹

2.2.2. Second-generation synthesis of PAC-1

The first-generation synthesis of **PAC-1** generated sufficient material to support initial experiments *in vitro*, in cell culture, and in mice.¹ However, studies in dogs required larger quantities of compound, and any clinical trials in human cancer patients would require even larger quantities. Therefore, it became necessary to modify the synthesis so that larger batches of **PAC-1** could be produced. The most significant challenges to increasing scale are highlighted in blue in Scheme 2.1: intermediates **1.10**, **1.7**, and **2.1** were purified by chromatography, which is challenging and expensive on large scale, and synthesis of hydrazide **1.6** involved the use of anhydrous hydrazine, which is expensive, dangerous, and unstable upon storage. In particular,

the highly polar intermediate **1.10** has a very high affinity for silica, requiring large amounts of polar eluent to elute the product, and intermediate **2.1** is difficult to separate from the major side product, 2-allylphenol (**2.7**). In addition, while recrystallization of hydrazide **1.6** was not a significant limitation of the first-generation synthesis, there was significant material that could not be recovered from the mother liquor.

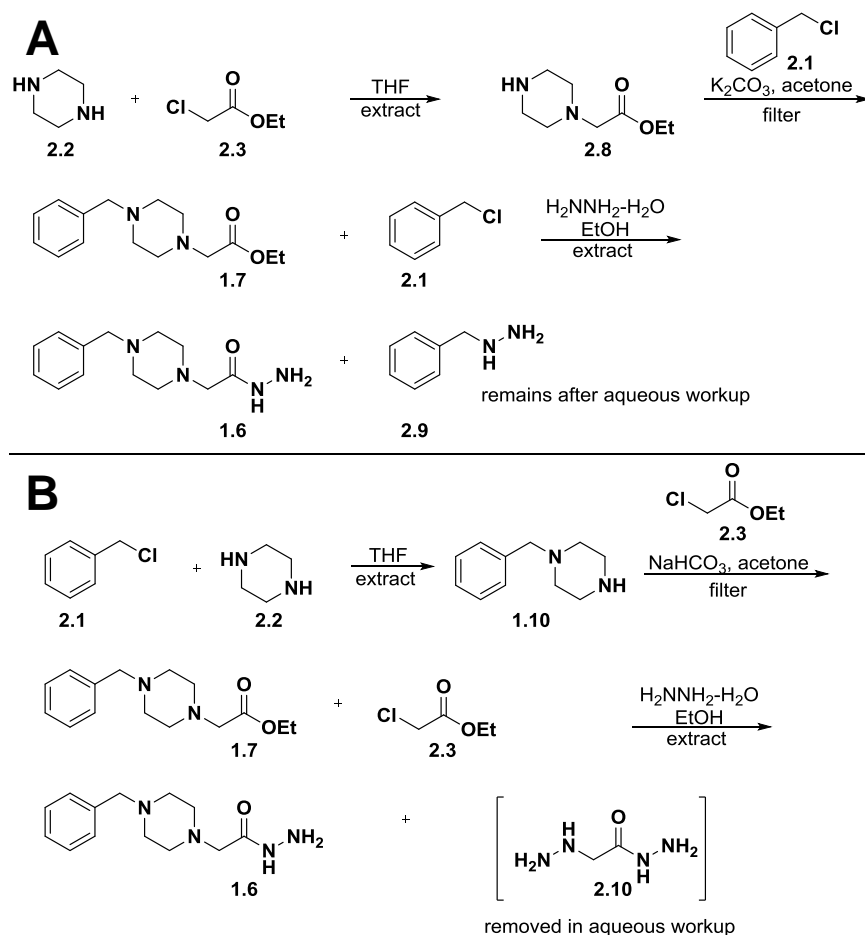
Fortunately, neither these challenging purifications nor reaction with anhydrous hydrazine proved necessary for the synthesis of **PAC-1**. The improved synthetic route is shown in Scheme 2.2, with modifications highlighted in red. After full consumption of benzyl chloride, excess piperazine was removed quantitatively by filtration and extraction to give intermediate **1.10** in high yield and high purity, with <5% **1.9**. Intermediate **1.10** was alkylated with 1 equivalent of ethyl chloroacetate to give intermediate **1.7** after filtration of inorganic solids. Instead of using anhydrous hydrazine, formation of hydrazide **1.6** was accomplished by reaction of **1.7** with hydrazine monohydrate, which is safer, less expensive, and more shelf-stable. In addition, the stoichiometry of the reaction was increased to 4 equivalents of hydrazine to ensure full conversion. Product of high purity was isolated after extraction, with no recrystallization necessary. Formation of intermediate **2.6** was already optimized, but synthesis of intermediate **2.1** remained the most significant challenge of the route. After the reaction was complete, distillation of the crude material provided a distillate consisting of **2.1** and **2.7** in a 6:1 ratio. Since **2.7** would not react with the hydrazide, crude **2.1** was condensed with **1.6** to yield **PAC-1**. In order to avoid wasting valuable intermediates **1.6** and **2.1**, the condensation was performed using a 1:1 ratio of hydrazide and aldehyde. It was also discovered that using heptane instead of hexane in the final recrystallization allowed for a slightly greater recovery of product, and heptane is less toxic *in vivo* than hexane. This route proceeded in 46% overall yield over the longest linear sequence of four steps and facilitated the synthesis of 155-gram batches on laboratory scale. The important advances included the elimination of all chromatographic purifications and one recrystallization, the removal of anhydrous hydrazine, and the ability to scale up six-fold on the laboratory scale.



Scheme 2.2. Second-generation synthesis of **PAC-1**.

In the optimized route toward **PAC-1**, piperazine was first alkylated with benzyl chloride, followed by ethyl chloroacetate, but the reverse order was also attempted (Scheme 2.3A). In this alternate route, piperazine was first alkylated with ethyl chloroacetate to form monosubstituted piperazine **2.8**. A second alkylation with benzyl chloride gave **1.7**, with a small amount of unreacted benzyl chloride. Reaction of the crude mixture of **1.7** and benzyl chloride with hydrazine gave hydrazide **1.6**, while the remaining benzyl chloride was converted to benzylhydrazine (**2.9**), which could not be removed via extraction or recrystallization. Removal of benzyl chloride from crude **1.7** was accomplished by acid-base extraction, but this procedure led to a significant loss of yield due to ester hydrolysis. However, alkylation with benzyl chloride first (Scheme 2.3B) solved this problem. In this route, **1.10** was formed first, followed by reaction with ethyl chloroacetate to form **1.7** with a small amount of unreacted ethyl

chloroacetate. Reaction with hydrazine then gave hydrazide **1.6**, along with a side product that is most likely **2.10**, but this material was never observed in the isolated material, and it is likely removed during aqueous extraction.



Scheme 2.3. A. Alkylation of piperazine with ethyl chloroacetate first gives a side product that cannot be easily removed. **B.** Alkylation of piperazine with benzyl chloride first leads to the isolation of pure **1.6**.

The optimized synthetic route toward **PAC-1** was adapted by Regis Technologies to produce a batch greater than 10 kilograms with only two modifications. The presence of 2-allylphenol in the final reaction makes recrystallization challenging due to trace 2-allylphenol in the final product, so intermediate **2.1** was purified by chromatography, although use of hexane and dichloromethane as the eluent allowed for a more facile separation than the original eluent of hexane and ethyl acetate. In addition, the relatively small increase in recovery when using

heptane in the final recrystallization did not overcome the increase in cost compared to hexane, so hexane was used instead.

2.3. Determination of *N*-acylhydrazone isomers by NMR spectroscopy

2.3.1. Assignment of NMR spectral resonances

In addition to the development of an improved large-scale synthesis of **PAC-1**, it was necessary to characterize the identity of the purified **PAC-1**. ¹H-NMR and ¹³C-NMR spectra of the purified **PAC-1** suggested that two species were present in solution, despite other analytical techniques suggesting a pure product. Since the active pharmaceutical ingredient needs to be of the highest possible purity for *in vivo* studies, it was necessary to determine whether the minor species was an impurity or a second conformer of **PAC-1**, although HPLC analysis of **PAC-1** showed a single peak, suggesting two interconverting species.

2.3.1.1. ¹H-NMR and ¹³C-NMR spectroscopy

In order to determine the identity of these species, it was necessary to assign all resonances in the ¹H- and ¹³C-NMR spectra. The numbering scheme for all atoms is shown in Figure 2.1A; Figure 2.1B shows the ¹H-NMR spectrum, acquired at 500 MHz in chloroform-*d*. Because the minor species is not present in a high enough concentration for all peaks to be easily visible, only the major isomer is considered in this analysis. Many peaks in the ¹H-NMR spectrum can be assigned based upon the analogous positions of these resonances in synthetic intermediates. The OH and NH resonances appear at 11.34 and 10.12 ppm, although it was not immediately clear which resonance corresponded to each atom. Hydrogen 10, corresponding to the hydrazone CH, appears at 8.34 ppm. Resonances corresponding to aromatic hydrogens appear between 6.5-7.5 ppm; the four hydrogens at positions 2 and 3 appear as a multiplet centered around 7.33 ppm, while hydrogen 1 appears as a multiplet centered at 7.27. The triplet at 6.84 ppm corresponds to hydrogen 13, while hydrogens 12 and 14 appear at 7.19 and 7.07 ppm, although it was not apparent which resonance corresponded to each atom. The single hydrogen atom 18 appears as a complex multiplet at 6.04 ppm, while the two hydrogen atoms on carbon 19 appear as a multiplet centered at 5.08 ppm. The doublet at 3.46 ppm corresponds to the two hydrogens on carbon 17. The remaining four resonances correspond to methylene groups

adjacent to the nitrogen atoms: the sharp singlets at 3.54 and 3.19 correspond to hydrogens at 5 and 8, while the broad singlets correspond to the hydrogens in the piperazine ring (6 and 7), although two-dimensional NMR analysis was necessary to unambiguously assign these resonances. Also visible are several resonances corresponding to hydrogen atoms in the minor isomer, denoted with the prime symbol: the phenol (OH') and hydrazone (10'), methylene 17', a second methylene correlating to either 5' or 8', and a broad peak corresponding to the piperazine hydrogens (6' or 7'). It is difficult to assign resonances in the ^{13}C -NMR spectrum (Figure 2.1C; acquired at 125 MHz in chloroform-*d*) via similar analysis, in part due to the proximity of many resonances, including five resonances within the range of 127-130 ppm (Figure 2.1C inset).

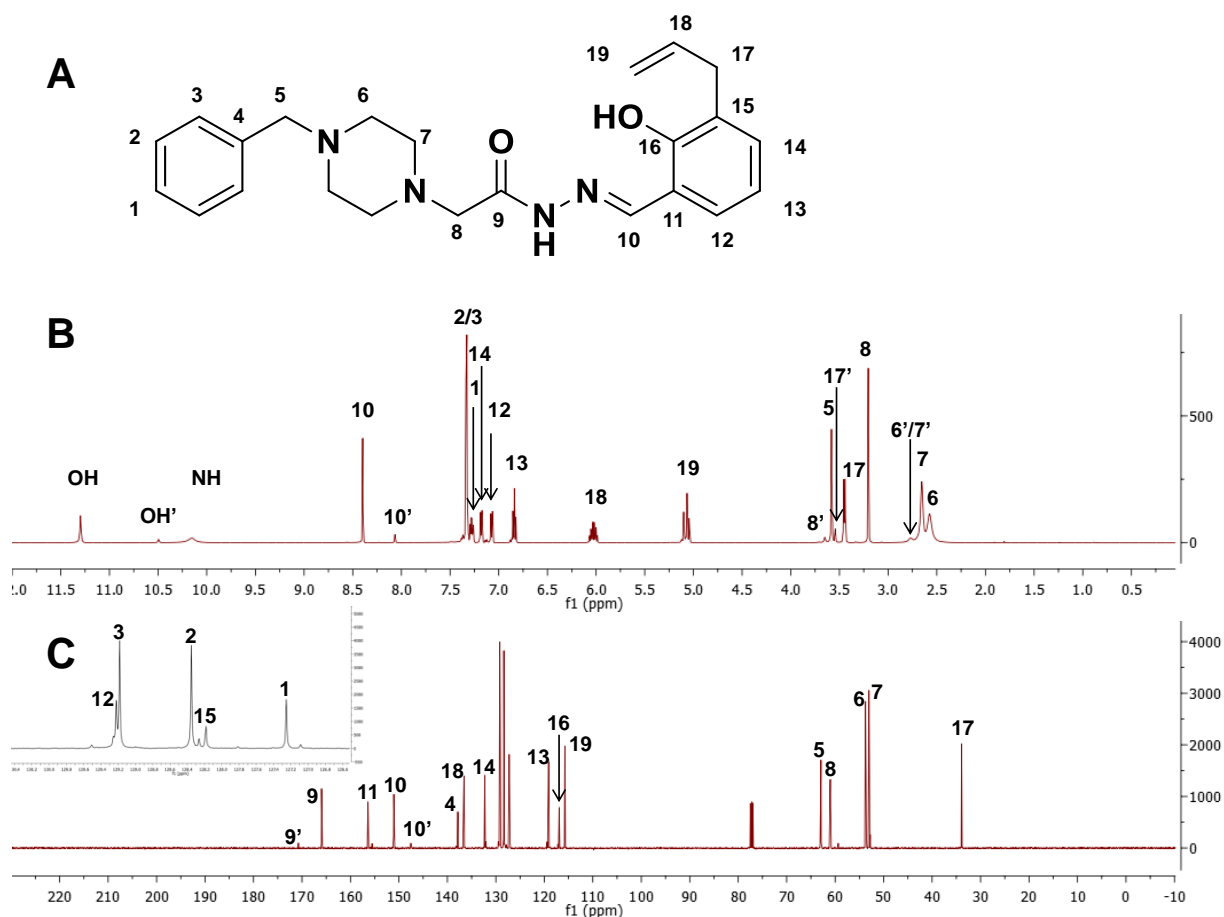


Figure 2.1. A. Atom numbering scheme, B. ^1H -NMR spectrum, and C. ^{13}C -NMR spectrum of PAC-1, with inset showing five peaks between 127-130 ppm in ^{13}C -NMR spectrum.

2.3.1.2. Two-dimensional heteronuclear spectroscopy

In order to unambiguously assign all resonances in the ^1H - and ^{13}C -NMR spectra, it was necessary to analyze **PAC-1** via two-dimensional NMR spectroscopy. Because most non-singlets in the ^1H -NMR spectrum had been assigned, $^1\text{H}/^1\text{H}$ -COSY analysis was not necessary. However, analysis via $^1\text{H}/^{13}\text{C}$ -heteronuclear correlation spectroscopy was useful for assigning all resonances. The full HSQC spectrum of **PAC-1** is shown in Figure 2.2. Based on these one-bond correlations, resonances for carbons 10 (151.1 ppm), 13 (119.1 ppm), 17 (33.9 ppm), 18 (136.6 ppm), and 19 (115.8 ppm) can be assigned. In addition, one-bond heteronuclear correlations were observed for resonances corresponding to atoms 5, 6, 7, and 8. Interestingly, the farther upfield hydrogen resonance in the piperazine ring correlates to the farther downfield carbon resonance. An expansion of the aromatic region is shown in Figure 2.2B. This spectrum indicates the assignment of carbon 1 at 127.3 ppm, while also indicating resonances corresponding to carbons 2, 3, 12, and 13.

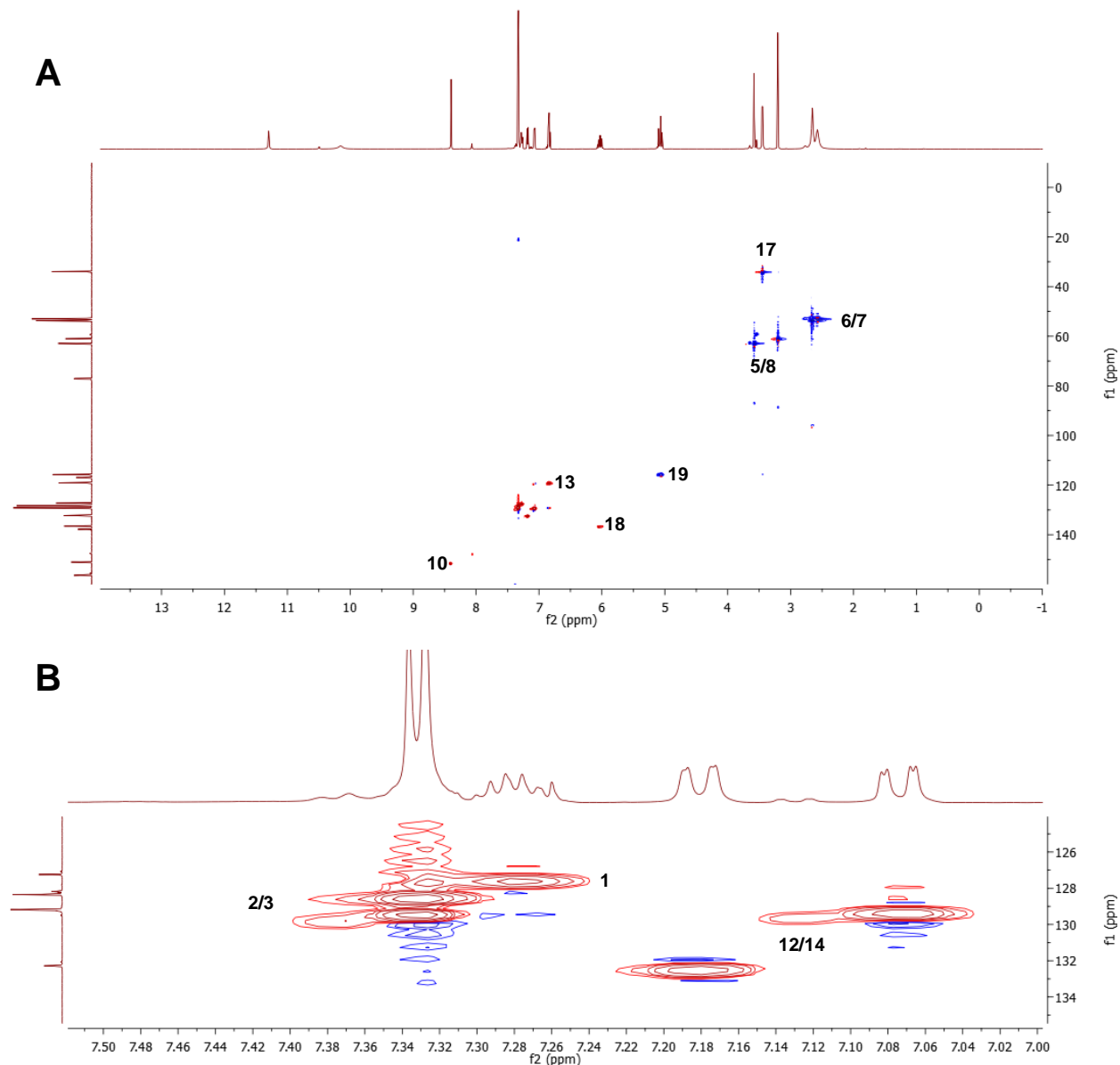


Figure 2.2. HSQC spectrum of **PAC-1**. **A.** Full spectrum. **B.** Expanded view of aromatic region.

The remaining resonances were assigned via HMBC spectroscopy (Figure 2.3; full spectrum in Figure 2.3A). An expansion around 3.1-3.7 ppm is shown in Figure 2.3B. The hydrogen at 3.54 ppm shows correlations with carbons at 53.1 ppm, 129.20 ppm, and 137.9 ppm, while the hydrogen at 3.19 ppm shows correlations with carbons at 53.8 ppm and 166.0 ppm. Because hydrogen resonance 5 is expected to correlate with three carbon resonances, while hydrogen resonance 8 is expected to correlate with two carbon resonances, hydrogen resonances at 3.54 ppm and 3.19 ppm can be assigned as hydrogens 5 and 8, respectively. The carbon

resonances at 53.8 ppm and 166.0 ppm can be assigned as carbons 7 and 9, respectively, due to their correlations to hydrogen resonance 8. Further, the carbon resonances at 53.1 ppm, 129.20 ppm, and 137.9 ppm can be assigned as carbons 6, 3, and 4, respectively, based upon their correlations to hydrogen 5 and relative chemical shifts, and assignment of 3 also gives definitive assignment of carbon 2 at 128.4 ppm. Hydrogen resonances 6 and 7 can be assigned via the HSQC results previously discussed.

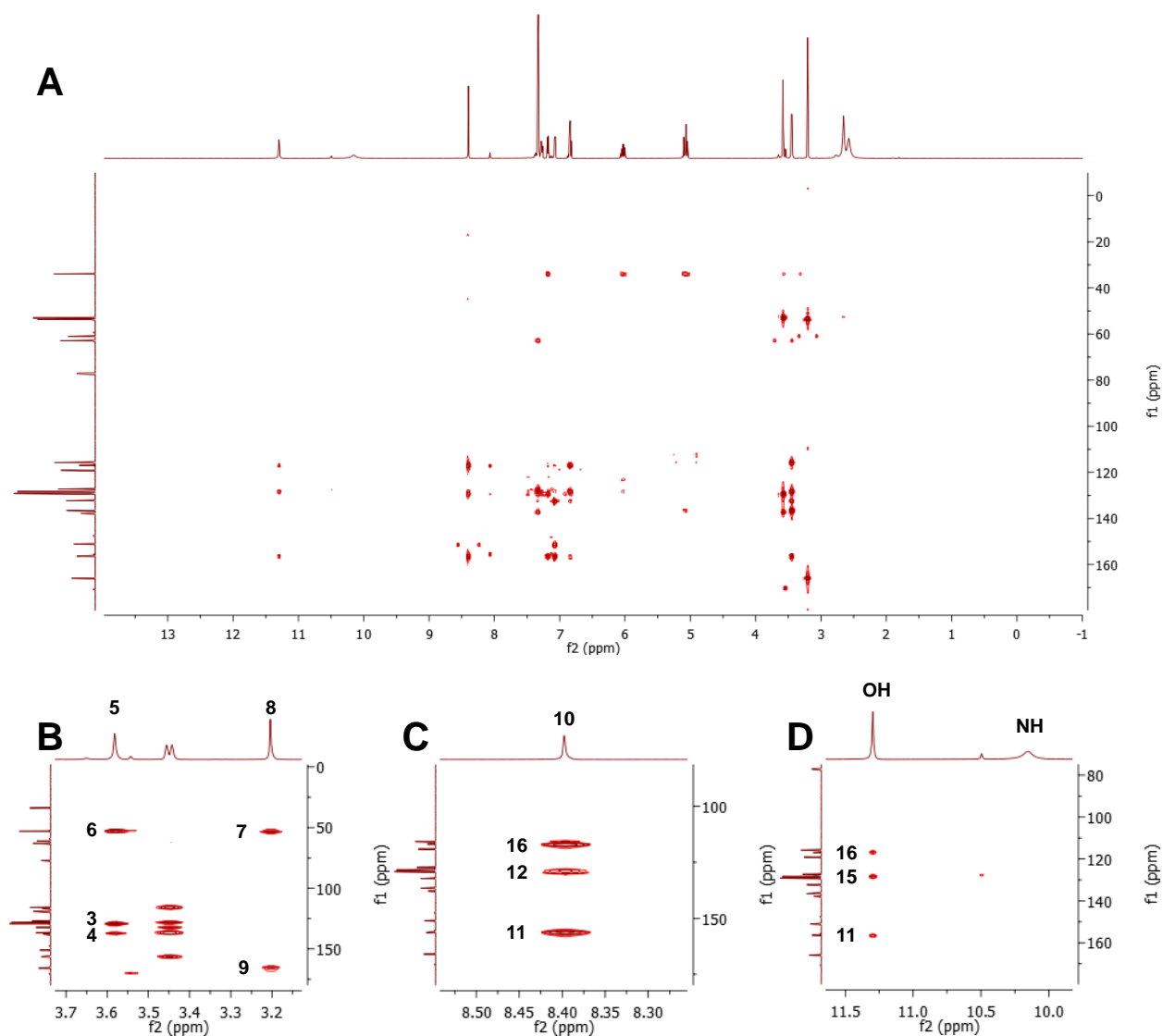


Figure 2.3. HMBC spectrum of PAC-1. **A.** Full spectrum. **B-D.** Expanded views.

Figure 2.3C shows an expansion of the HMBC spectrum around hydrogen 10. This hydrogen resonance correlates to carbon resonances at 117.0 ppm, 129.24 ppm, and 156.4 ppm;

hydrogen 10 is expected to correlate to carbons 11, 12, and 16. Carbon 16, bearing a hydroxyl group, is the most upfield of these, at 117.0 ppm, while carbon 11, bearing the electron-withdrawing hydrazone, is the most downfield, at 156.4 ppm. The remaining resonance, at 129.24 ppm, belongs to carbon 12, and assignment of carbon 12 also allows for the assignment of carbon 14 at 132.3 ppm; hydrogens 12 and 14 can be assigned based upon HSQC results. The last remaining carbon resonance, at 128.2 ppm, belongs to carbon 15.

Figure 2.3D shows the expansion of the HMBC spectrum between 9.8-11.7 ppm. The hydrogen resonance at 11.34 ppm exhibits correlations to carbons 11, 15, and 16, as would be expected for the OH, while the hydrogen resonance at 10.12 ppm, corresponding to the NH, correlates to no carbon resonances. The assignments are summarized in Table 2.1.

| Atom | $\delta^1\text{H}$ (ppm) | $\delta^{13}\text{C}$ (ppm) |
|------|--------------------------|-----------------------------|
| 1 | 7.27 | 127.3 |
| 2 | 7.33 | 128.4 |
| 3 | 7.33 | 129.2(0) |
| 4 | - | 137.9 |
| 5 | 3.54 | 63.0 |
| 6 | 2.54 | 53.1 |
| 7 | 2.62 | 53.8 |
| 8 | 3.19 | 61.0 |
| 9 | - | 166.0 |
| 10 | 8.34 | 151.1 |
| 11 | - | 156.4 |
| 12 | 7.07 | 129.2(4) |
| 13 | 6.84 | 119.1 |
| 14 | 7.19 | 132.3 |
| 15 | - | 128.2 |
| 16 | - | 117.0 |
| 17 | 3.46 | 33.9 |
| 18 | 6.04 | 136.6 |
| 19 | 5.08 | 115.8 |
| NH | 10.12 | - |
| OH | 11.34 | - |

Table 2.1. Assignment of resonances in ^1H - and ^{13}C -NMR spectra of PAC-1.

2.3.2. Interconversion of species by exchange spectroscopy

Assignment of resonances in the ^1H -NMR spectrum facilitated further NMR study of the two species present in the spectrum. Exchange spectroscopy (EXSY) was used to determine

whether the two species underwent chemical exchange. EXSY is a dynamic NMR technique used to identify resonances corresponding to two or more nuclei undergoing chemical exchange on the NMR timescale. The pulse sequence is identical to the NOESY experiment; however, in contrast to observed NOE interactions, resonances corresponding to nuclei undergoing chemical exchange will appear in phase with each other. For the EXSY experiment with **PAC-1**, the hydrazone CH (hydrogen atom 10) was chosen because of the large difference in chemical shift for resonances corresponding to the major species (8.34 ppm) and minor species (7.91 ppm) and the isolation of these resonances from other resonances in the spectrum. The EXSY spectra are shown in Figure 2.4. Irradiation of the peaks at both 8.39 ppm (Figure 2.4A) and 7.95 ppm (Figure 2.4B) results in the in-phase appearance of the non-irradiated peak. This result confirms that the two species present correspond to interconverting isomers of **PAC-1**.

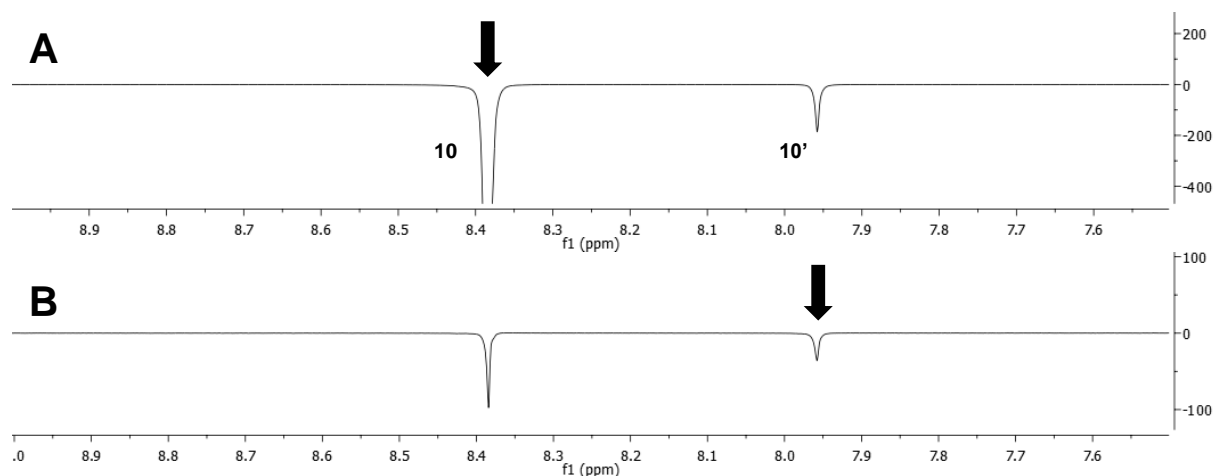


Figure 2.4. EXSY spectrum of **PAC-1** following irradiation at **A.** 8.39 ppm and **B.** 7.95 ppm. Irradiated peaks are indicated with a black arrow.

2.3.3. Assignment of isomers by chemical shifts

The interconverting species most likely correspond to two isomers of the *N*-acylhydrazone. It is known that two isomers (*E* and *Z*) can exist at the hydrazone C-N double bond, while two isomers can also exist at the amide C-N single bond (*syn* and *antiperiplanar*; relating to the configuration of the carbonyl oxygen and the amide hydrogen), for a total of four possible isomers (general *N*-acylhydrazone isomers in Figure 2.5A; isomers of **PAC-1** in figure 2.5B). It is known that interconversion between *syn* and *anti* isomers is rapid, while

interconversion between *E* and *Z* isomers is slow; in fact, *E-Z* isomerization is slow enough that the isomers are separable by HPLC.⁴ The interconversion of the two **PAC-1** isomers on the NMR timescale strongly suggests a *syn/anti* relationship between the two isomers.

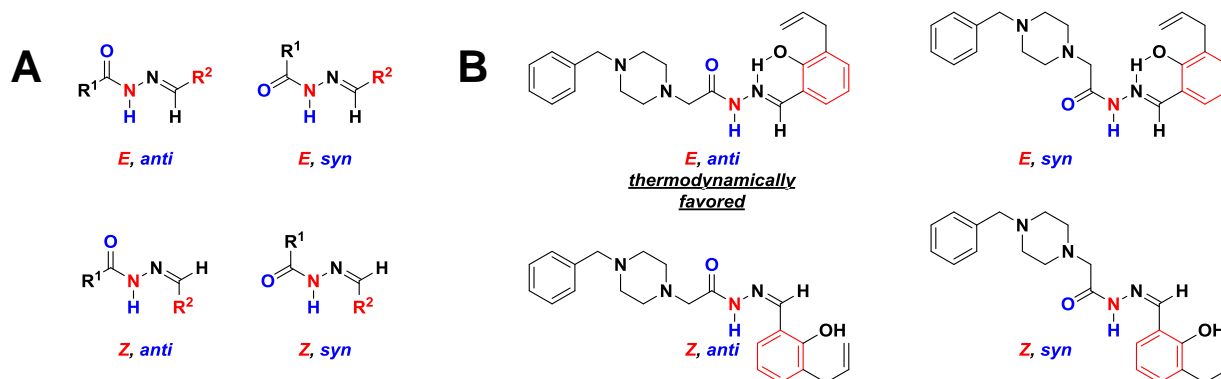


Figure 2.5. Four possible configurational isomers of *N*-acylhydrazones, for **A.** general structure and **B.** **PAC-1**.

The *E* isomers are favored for *N*-acylhydrazones derived from aromatic aldehydes due to minimization of steric interactions, with the (*E, anti*) conformation favored over the (*E, syn*) conformation.⁴⁻⁷ In addition, the *E* isomers are favored over the *Z* isomers for *ortho*-hydroxy-*N*-acylhydrazones due to the presence of an intramolecular hydrogen bond between the hydrazone nitrogen atom and the hydroxyl hydrogen atom not possible in the *Z* isomer. This intramolecular hydrogen bond results in a sharper, more downfield resonance for the hydroxyl hydrogen atom in the NMR spectrum, as compared to a non-hydrogen bonded phenol, which would be broader and farther upfield. The resonances corresponding to the phenolic hydrogens for the major and minor isomer of **PAC-1** appear at 11.34 and 10.50 ppm, respectively, while analogous resonances in spectra for **PAC-1** derivatives that lack the hydrazone, and thus lack the ability to hydrogen bond, appear between 9.0-9.5 ppm.⁸ This provides strong evidence to suggest that **PAC-1** exists as a mixture of (*E, anti*) and (*E, syn*) isomers.

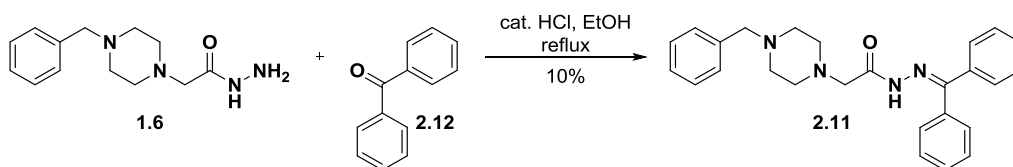
The carbonyl carbon (carbon 9) and hydrogens adjacent to the carbonyl (hydrogens 8) are also diagnostic for the *syn* and *anti* isomers. Resonances for both carbonyl carbons and adjacent hydrogens for *syn* isomers of *N*-acylhydrazones are shifted downfield relative to corresponding resonances for *anti* isomers, because the $N^+=C-O^-$ resonance form contributes less to the *syn* isomers than to the *anti* isomers.^{4, 5, 7, 9} Hydrogen resonance 8 appears at 3.19 ppm, while

hydrogen resonance 8' appears at 3.52 ppm. Similarly, carbon resonance 9 appears at 166.0 ppm, while carbon resonance 9' appears at 170.7 ppm. Since the resonances for the minor isomer for both of these diagnostic signals appear downfield relative to the resonances for the major isomer, it is most likely that the major isomer has the (*E*, *anti*) configuration, while the minor isomer has the (*E*, *syn*) configuration.

The hydrogen and carbon chemical shifts for the hydrazone (carbon and hydrogen 10) are also important in assigning the isomers. The differences in chemical shifts between *syn* and *anti* isomers are expected to be less than 0.5 ppm for hydrogens and less than 5 ppm for carbons, while the differences between *E* and *Z* isomers are expected to be closer to 1 ppm for hydrogens and 10 ppm for carbons. The chemical shifts appear in the order (*E*, *anti*) > (*E*, *syn*) > (*Z*, *anti*) > (*Z*, *syn*) for both hydrogens and carbons.⁷ The distance between hydrogen 10 and hydrogen 10' for **PAC-1** is approximately 0.4 ppm, while the distance between carbon 10 and carbon 10' is approximately 4 ppm, both of which strongly suggest a *syn/anti* relationship between the two isomers. Further, hydrogen 10 of **PAC-1** appears at 8.39 ppm, and only the hydrogen for the (*E*, *anti*) isomer is expected to appear this far downfield.⁷ Taken together, these results strongly suggest that the major isomer of **PAC-1** exists in the (*E*, *anti*) configuration, while the minor isomer exists in the (*E*, *syn*) configuration.

2.3.4. Diphenylmethylenes hydrazone

In order to support the assignment of the isomers, compound **2.8**, a diphenylmethylenes hydrazone, was synthesized via the condensation of hydrazide **1.6** and benzophenone (**2.9**, Scheme 2.3). The reaction proceeded in only 10% yield; it is likely that the steric interactions between the added phenyl ring and the NH that disfavor formation of *Z*-hydrazones made formation of this product more difficult or made hydrolysis to the starting materials more facile. Because both substituents at the hydrazone carbon are identical, compound **2.8** does not exhibit different *E* and *Z* isomers. Therefore, the existence of two isomers of compound **2.8** would strongly suggest that **PAC-1** exists as a mixture of *syn* and *anti* isomers.



Scheme 2.4. Synthesis of **2.11**.

The $^1\text{H-NMR}$ spectrum of **2.8** is shown in Figure 2.6A. While the major isomer of **2.8** is present in a much higher proportion, the presence of a minor isomer is clear; four singlets, corresponding to two methylene groups on each of the two isomers, are observed between 3.0-4.0 ppm. An EXSY experiment irradiating either the major isomer (Figure 2.6B) or the minor isomer (Figure 2.6C) indicates that the two isomers exchange on the NMR timescale.

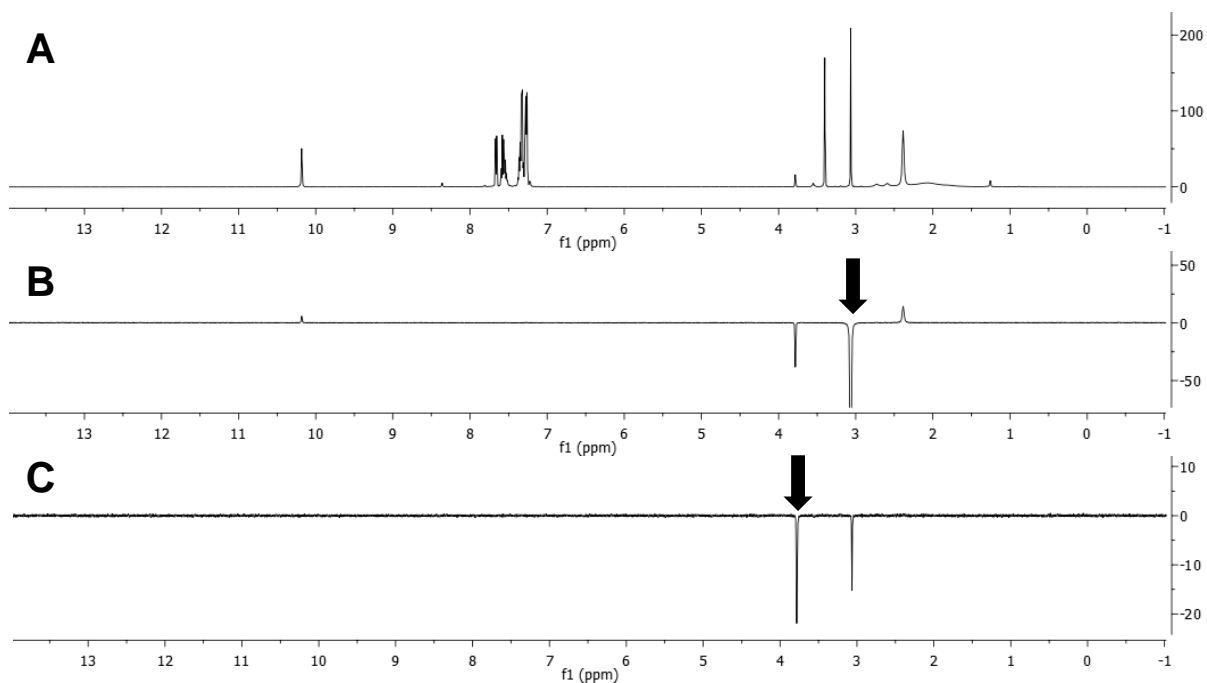
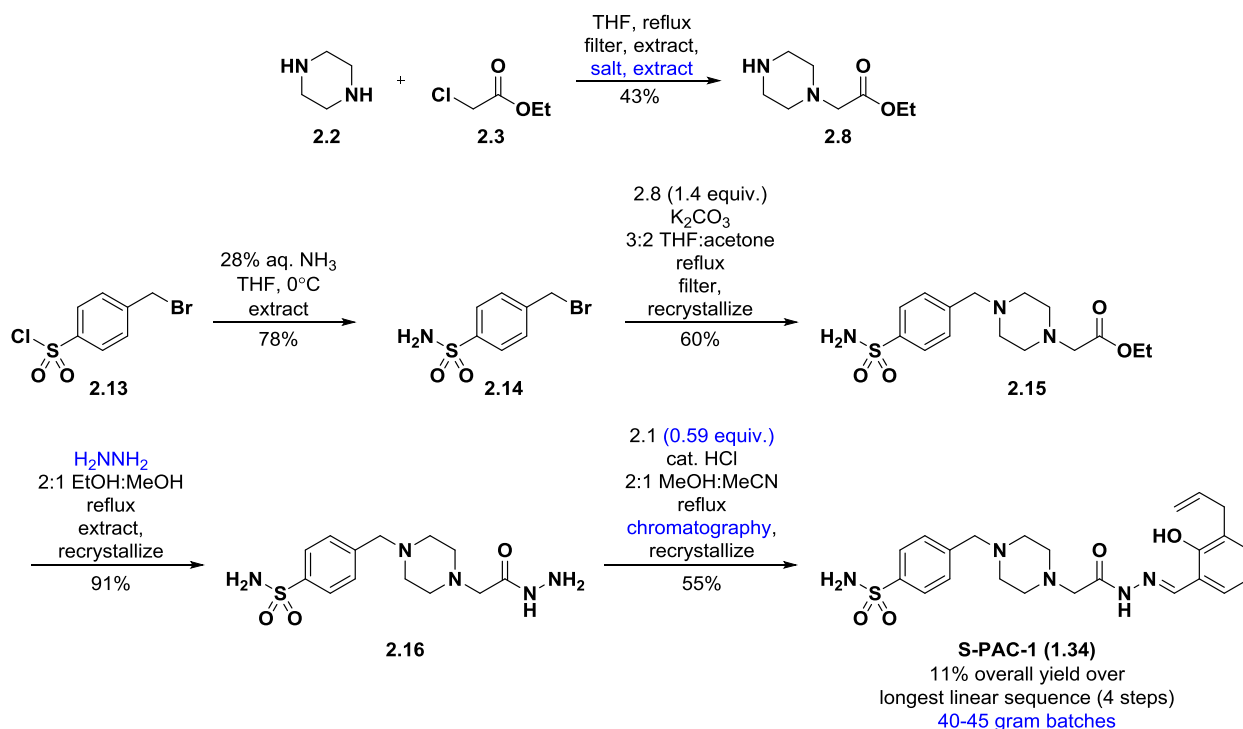


Figure 2.6. A. $^1\text{H-NMR}$ spectrum of **2.11**. B.-C. EXSY spectra of **2.11** with irradiation at B. 3.07 ppm and C. 3.78 ppm. Irradiated peaks are indicated with black arrows.

2.4. Improved large-scale synthesis of S-PAC-1

2.4.1. First-generation synthesis of S-PAC-1

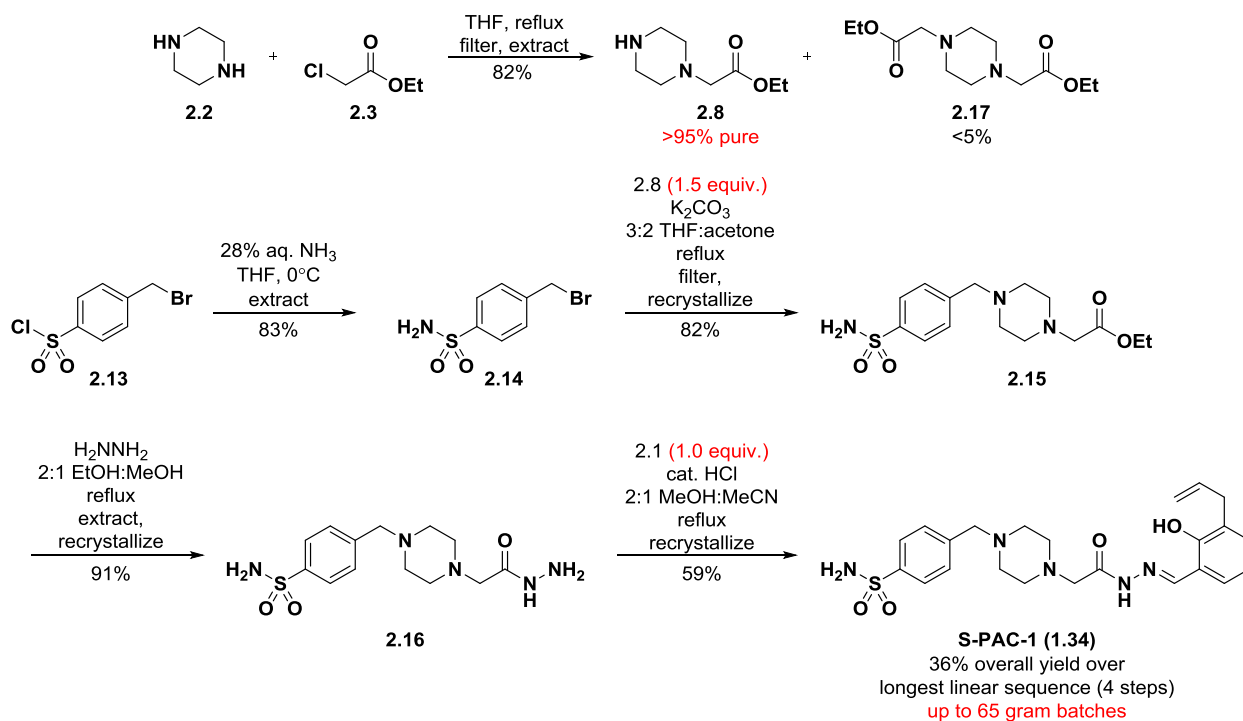
In order to support clinical studies of **S-PAC-1** in canine cancer patients, it was necessary to improve upon the synthesis of this compound as well. The initial synthetic route toward **S-PAC-1** is shown in Scheme 2.5.² The synthesis begins with the alkylation of piperazine (**2.2**) with ethyl chloroacetate (**2.3**) to form monosubstituted piperazine **2.8** in 43% yield. Sulfonyl chloride **2.13** is converted to sulfonamide **2.14** in high yield by reaction with aqueous ammonia, and alkylation of **2.8** with **2.14** gives disubstituted piperazine **2.15**. Reaction of the ester with anhydrous hydrazine gives hydrazide **2.16**, and condensation of the hydrazide with aldehyde **2.1** gives **S-PAC-1**. The route was used to prepare the compound in batches of 40-45 grams in an 11% overall yield over the longest linear sequence of four steps beginning with ethyl chloroacetate.²



Scheme 2.5. First-generation synthesis of **S-PAC-1**.²

2.4.2. Second-generation synthesis of S-PAC-1

Sufficient quantities of **S-PAC-1** were produced via the above synthetic route to supply the initial canine clinical trial. However, a larger trial was planned, and it became necessary to produce larger batches of compound to supply these efforts. The major challenges in scalability are highlighted in blue in Scheme 2.4. The most significant loss in yield occurs in the formation of monosubstituted piperazine **2.8**. While the formation of **2.8** is highly efficient, it is necessary to purify by acid-base extraction to remove disubstituted piperazine **2.17** (Scheme 2.6), which results in significant hydrolysis of the ester. In addition, the use of anhydrous hydrazine for formation of hydrazide **2.16** is not optimal for the reasons discussed in the **PAC-1** synthesis. Finally, the use of excess hydrazide **2.16** in the final condensation reaction to form **S-PAC-1** makes production of large quantities of compound challenging, since it is difficult to recover the excess unreacted starting material, and nearly half of the hydrazide is discarded. The excess hydrazide makes it necessary to purify the final product by chromatography, which also limits the scalability.



Scheme 2.6. Second-generation synthesis of **S-PAC-1**.

The improved synthesis of **S-PAC-1** is shown in Scheme 2.6. As with the formation of monosubstituted piperazine **1.10** in the synthesis of **PAC-1**, compound **2.8** could be isolated at greater than 95% purity after initial extraction, with less than 5% **2.17**. Use of this material in the next reaction, along with a slight increase to 1.5 equivalents of **2.8**, led to an isolated yield of 82% of **2.15**, an increase from the 60% isolated yield in the initial synthesis. Finally, reacting hydrazide **2.14** with aldehyde **2.1** in a 1:1 molar ratio eliminated the need for chromatography and reduced the amount of unreacted **2.14** that was discarded. Overall, the batch size was increased to a maximum of 65 grams, with a 36% overall yield over the longest linear sequence of four steps from ethyl chloroacetate. It is possible that further optimizations could be made, including the use of hydrazine monohydrate rather than anhydrous hydrazine, as well as efforts toward a higher recovery of **S-PAC-1** during the final recrystallization.

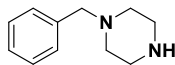
2.5. Materials and methods

2.5.1. Chemical information

General All reactions requiring anhydrous conditions were conducted under a positive atmosphere of nitrogen or argon in oven-dried glassware. Standard syringe techniques were used for anhydrous addition of liquids. Unless otherwise noted, all starting materials, solvents, and reagents were acquired from commercial suppliers and used without further purification. Flash chromatography was performed using 230-400 mesh silica gel.

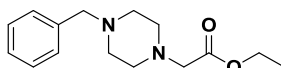
Compound Analysis All NMR experiments were recorded in CDCl₃ (Sigma or Cambridge), (CD₃)₂CO (Sigma or Cambridge), or CD₃OD (Cambridge) on a Varian Unity 500 MHz spectrometer with residual undeuterated solvent as the internal reference for ¹H-NMR (CDCl₃ – 7.26 ppm; (CD₃)₂CO – 2.04 ppm; CD₃OD – 3.30 ppm) and ¹³C-NMR (CDCl₃ – 77.23 ppm (CD₃)₂CO – 29.80 ppm; CD₃OD – 49.00 ppm). Chemical shift, δ (ppm); coupling constants, J (Hz); multiplicity (s = singlet, d = doublet, t = triplet, q = quartet, quint = quintet, sext = sextet, m = multiplet, br = broad); and integration are reported. High-resolution mass spectral data was recorded on a Micromass Q-ToF Ultima hybrid quadrupole/time-of-flight ESI mass spectrometer or a Micromass 70-VSE at the University of Illinois Mass Spectrometry Laboratory.

1-benzylpiperazine (1.10)



To a 5L three-necked round-bottom flask with a mechanical stirrer and condenser were added piperazine (**2.2**, 517 g, 6000 mmol, 6.0 equiv.) and THF (2.5 L, 0.4 M). The third neck was sealed with a septum, and the mixture was stirred at reflux until all piperazine dissolved. Benzyl chloride (**2.1**, 127 g, 116 mL, 1000 mmol, 1.0 equiv.) was added dropwise with stirring via addition funnel over 30 minutes. The reaction mixture was stirred at reflux for an additional hour after addition was complete. The reaction mixture was cooled to room temperature. The solid was filtered and washed with THF. The filtrate was filtered a second time. The second filtrate was concentrated and partitioned between CH₂Cl₂ (400 mL) and saturated Na₂CO₃ (400 mL). H₂O (400 mL) was added to dissolve all remaining solid. The layers were separated, and the aqueous layer was extracted with CH₂Cl₂ (3 x 300 mL). The combined organic layers were washed with brine (3 x 300 mL), dried over MgSO₄, filtered, and concentrated to yield **1.10** (135.92 g, 77.2%) as a pale yellow oil at >95% purity (as assessed by ¹H-NMR; remainder was **1.9**), which was used without further purification. ¹H-NMR (500 MHz, CDCl₃): δ 7.33-7.29 (m, 4H), 7.26-7.23 (m, 1H), 3.49 (s, 2H), 2.88 (br t, 4H, *J* = 4.5 Hz), 2.41 (br s, 4H), 1.63 (br s, 1H). ¹³C-NMR (125 MHz, CDCl₃): δ 138.3, 129.4, 128.4, 127.2, 63.9, 54.7, 46.3. HRMS (ESI): 177.1379 (M+H)⁺; calcd. for C₁₁H₁₇N₂: 177.1386.

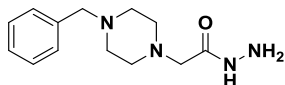
Ethyl 2-(4-benzylpiperazin-1-yl)acetate (1.7)



To a 3L three-necked round-bottom flask with a mechanical stirrer and condenser were added **1.10** (79.25 g, 448 mmol, 1.0 equiv.), NaHCO₃ (56.5 g, 673 mmol, 1.5 equiv.), and acetone (900 mL, 0.5 M). The mixture was stirred, and ethyl chloroacetate (**2.3**, 54.7 g, 47.6 mL, 448 mmol, 1.0 equiv.) was added dropwise via addition funnel over 10 minutes. The reaction mixture was stirred at reflux overnight. The reaction mixture was cooled to room temperature. The solid was vacuum filtered and washed with acetone. The filtrate was concentrated to yield **1.7** (113.3 g, 96.4%) as a dark yellow-orange liquid at >90% purity (as assessed by ¹H-NMR; remainder was **1.9** and excess unreacted **2.3**), which was used without further purification. ¹H-NMR (500 MHz, CDCl₃): δ 7.32-7.29 (m, 4H), 7.26-7.23 (m, 1H), 4.20 (q, 2H, *J* = 7.0 Hz), 3.53 (s, 2H), 3.20 (s,

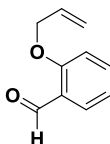
2H), 2.61 (br s, 4H), 2.54 (br s, 4H), 1.26 (t, 3H, $J = 7.0$ Hz). $^{13}\text{C-NMR}$ (125 MHz, CDCl_3): δ 170.5, 138.2, 129.4, 128.4, 127.3, 63.2, 60.8, 59.8, 53.3, 53.0, 14.5. HRMS (ESI): 263.1752 ($\text{M}+\text{H}$) $^+$; calcd. for $\text{C}_{15}\text{H}_{23}\text{N}_2\text{O}_2$: 263.1754.

2-(4-benzylpiperazin-1-yl)acetohydrazide (**1.6**)



To a 3L three-necked round-bottom flask with a mechanical stirrer and condenser were added **1.7** (140 g, 534 mmol, 1.0 equiv.) and EtOH (1068 mL, 0.5 M). The solution was stirred, and hydrazine monohydrate (107 g, 104 mL, 2136 mmol, 4.0 equiv.) was added dropwise via addition funnel over 30 minutes. The reaction mixture was stirred at reflux overnight. The reaction mixture was cooled to room temperature and concentrated. The resulting solid was partitioned between CH_2Cl_2 (250 mL) and 1:1 brine:0.1 M KOH (200 mL). The layers were separated, and the aqueous layer was extracted with CH_2Cl_2 (2 x 200 mL). The combined organic layers were dried over MgSO_4 , filtered, and concentrated to yield **1.6** (122.78 g, 92.3%) as a white solid, which was used without further purification. $^1\text{H-NMR}$ (500 MHz, CDCl_3): δ 8.12 (br s, 1H), 7.34-7.31 (m, 4H), 7.29-7.25 (m, 1H), 3.84 (br s, 2H), 3.53 (s, 2H), 3.08 (s, 2H), 2.56 (br s, 4H), 2.50 (br s, 4H). $^{13}\text{C-NMR}$ (125 MHz, CDCl_3): δ 170.7, 138.0, 129.3, 128.4, 127.3, 63.0, 60.8, 53.8, 53.2. HRMS (ESI): 249.1708 ($\text{M}+\text{H}$) $^+$; calcd. for $\text{C}_{13}\text{H}_{21}\text{N}_4\text{O}$: 249.1710.

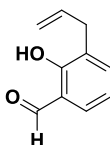
2-(allyloxy)benzaldehyde (**2.6**)



To a 2L three-necked round-bottom flask with a mechanical stirrer and condenser were added K_2CO_3 (173 g, 1250 mmol, 1.25 equiv.), DMF (250 mL), and salicylaldehyde (**2.4**, 122 g, 106 mmol, 1000 mmol, 1.0 equiv.). The mixture was stirred, and allyl bromide (**2.5**, 145 g, 104 mL, 1200 mmol, 1.2 equiv.) was added dropwise via addition funnel over 2 hours. The reaction mixture was stirred at room temperature overnight. The reaction mixture was diluted with H_2O (1L) and extracted with EtOAc (4 x 250 mL). The combined organic layers were washed with H_2O (2 x 200 mL), 0.1 M KOH (2 x 200 mL), H_2O (2 x 200 mL), and brine (2 x 200 mL), dried over MgSO_4 , filtered, and concentrated to yield **2.6** (154.87 g, 95.6%) as a dark brown liquid, which was used without further purification. $^1\text{H-NMR}$ (500 MHz, CDCl_3): δ 10.54 (s, 1H), 7.84

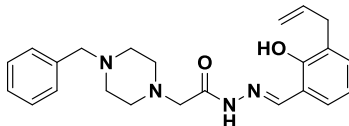
(dd, 1H, $J = 1.5, 7.5$ Hz), 7.53 (dt, 1H, $J = 1.5, 7.0$ Hz), 7.03 (t, 1H, $J = 7.5$ Hz), 6.98 (d, 1H, $J = 8.0$ Hz), 6.08 (tdd, 1H, $J = 5.0, 10.5, 17.5$ Hz), 5.45 (qd, 1H, $J = 1.5, 17.0$ Hz), 5.34 (qd, 1H, $J = 1.5, 10.5$ Hz), 4.66 (td, 2H, $J = 1.5, 5.0$ Hz). ^{13}C -NMR (125 MHz, CDCl_3): δ 190.0, 161.1, 136.0, 132.6, 128.6, 125.3, 121.1, 118.3, 113.0, 69.4. HRMS (EI): 162.0679 (M) $^+$; calcd. for $\text{C}_{10}\text{H}_{10}\text{O}_2$: 162.0681.

3-allylsalicylaldehyde (**2.1**)



2.6 (154 g, 950 mmol, 1.0 equiv.) was stirred at 200°C overnight. The reaction mixture was cooled to room temperature. Purification by vacuum distillation (b.p. = 95-105°C at 1 torr) yielded **2.1** (127.80 g, 83.0%) as a yellow liquid at 85% purity (remainder was **2.7**), which was used without further purification. ^1H -NMR (500 MHz, CDCl_3): δ 11.31 (s, 1H), 9.89 (s, 1H), 7.44 (dd, 1H, $J = 1.5, 7.5$ Hz), 7.41 (dd, 1H, $J = 1.0, 7.5$ Hz), 6.97 (t, 1H, $J = 7.5$ Hz), 6.00 (tdd, 1H, $J = 6.5, 10.0, 16.5$ Hz), 5.12-5.10 (m, 1H), 5.09-5.08 (m, 1H), 3.44 (d, 2H, $J = 7.0$ Hz). ^{13}C -NMR (125 MHz, CDCl_3): δ 196.9, 159.7, 137.4, 136.0, 132.1, 129.0, 120.5, 119.8, 116.5, 33.3. HRMS (ESI): 163.0765 ($\text{M}+\text{H}$) $^+$; calcd. for $\text{C}_{10}\text{H}_{11}\text{O}_2$: 163.0754.

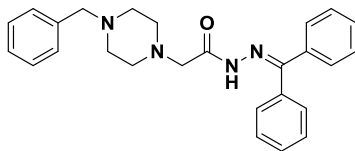
N'-(3-allyl-2-hydroxybenzylidene)-2-(4-benzylpiperazin-1-yl)acetohydrazide (**PAC-1**, **1.1**)



To a 3L three-necked round-bottom flask with a mechanical stirrer and condenser were added **1.6** (72.8 g, 293 mmol, 1.0 equiv.), **2.1** (47.5 g, 293 mmol, 1.0 equiv.), and EtOH (1200 mL, 0.15 M). The solution was stirred, and 1 M HCl (20.5 mL, 20.5 mmol, 0.070 equiv.) was added dropwise. The reaction mixture was stirred at reflux overnight. The reaction mixture was cooled to room temperature and concentrated. Recrystallization from 15:1 heptane:EtOH yielded **PAC-1** (**1.1**, 78.5 g, 68.3%) as a white solid, which was an interconverting mixture of two isomers. Spectral data for major isomer: ^1H -NMR (500 MHz, CDCl_3): δ 11.27 (s, 1H), 10.04 (br s, 1H), 8.40 (s, 1H), 7.35-7.32 (m, 4H), 7.29-7.26 (m, 1H), 7.19 (dd, 1H, $J = 1.0, 7.5$ Hz), 7.08 (dd, 1H, $J = 1.5, 8.0$ Hz), 6.85 (t, 1H, $J = 7.5$ Hz), 6.04 (tdd, 1H, $J = 6.5, 10.0, 16.5$ Hz), 5.12-5.05 (m, 2H), 3.55 (s, 2H), 3.46 (d, 2H, $J = 6.5$ Hz), 3.19 (s, 2H), 2.63 (br s, 4H), 2.54 (br s, 4H). ^{13}C -

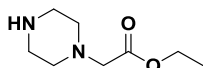
NMR (125 MHz, CDCl₃): δ 166.0, 156.6, 151.5, 137.9, 136.7, 132.5, 129.3, 129.3, 128.5, 128.4, 127.4, 119.2, 117.1, 115.8, 63.1, 61.2, 53.9, 53.2, 34.0. HRMS (ESI): 393.2291 (M+H)⁺; calcd. for C₂₃H₂₉N₄O₂: 393.2291.

2-(4-benzylpiperazin-1-yl)-N'-(diphenylmethylene)acetohydrazide (2.11)



To a round-bottom flask were added **1.6** (124 mg, 0.50 mmol, 1.0 equiv.), EtOH (3 mL, 0.15 M), benzophenone (**2.12**, 91 mg, 0.50 mmol, 1.0 equiv.), and 1.2 M HCl (29 μL, 0.035 mmol, 0.070 equiv.). The reaction mixture was stirred at reflux for 3 days. The reaction mixture was then concentrated. Purification by silica gel column chromatography (0-10% MeOH/EtOAc) yielded **2.11** (21 mg, 10.3%) as a white solid. ¹H-NMR (500 MHz, CDCl₃) δ 10.18 (s, 1H), 7.68-7.64 (m, 2H), 7.60-7.50 (m, 3H), 7.38-7.30 (m, 5H), 7.30-7.25 (m, 5H), 3.40 (s, 2H), 3.07 (s, 2H), 2.39 (br s, 4H), 2.07 (br s, 2H). ¹³C-NMR (125 MHz, CDCl₃) δ 166.4, 155.0, 137.9, 136.8, 133.0, 130.14, 130.06, 129.9, 129.3, 128.5, 128.38, 128.37, 128.2, 127.4, 63.0, 60.9, 53.5, 52.8. HRMS (ESI): 413.2343 (M+1); calcd. for C₂₆H₂₉N₄O: 413.2336.

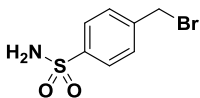
Ethyl 2-(piperazin-1-yl)acetate (2.8)



To a 5L three-necked round-bottom flask with a mechanical stirrer and condenser were added piperazine (**2.2**, 362 g, 4200 mmol, 6.0 equiv.) and THF (2100 mL). The third neck was sealed with a septum, and the mixture was stirred at reflux until all piperazine dissolved (approx. 1 hour). The heat source was removed, and ethyl chloroacetate (**2.3**, 74.4 mL, 700 mmol, 1.0 equiv.) was added dropwise with stirring via addition funnel (approx. 30 minutes). A white solid formed immediately upon addition of ethyl chloroacetate. ¹H-NMR showed complete consumption of ethyl chloroacetate after addition was complete. The reaction mixture was cooled to room temperature. The solid was filtered and washed with THF. The filtrate was concentrated and partitioned between CH₂Cl₂ (300 mL) and sat. Na₂CO₃ (300 mL), and H₂O (500 mL) was added to dissolve the remaining solid. The layers were separated, and the aqueous layer was extracted with CH₂Cl₂ (3 x 250 mL). The combined organic layers were washed with brine (3 x 150 mL), dried over MgSO₄, filtered, and concentrated to yield **2.8** (99.14 g, 82.2%) as

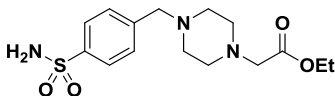
a pale yellow oil at >95% purity, which was used without further purification. $^1\text{H-NMR}$ (500 MHz, CDCl_3) δ 4.17 (q, 2H, $J = 7.0$ Hz), 3.18 (s, 2H), 2.94 (t, 4H, $J = 5.0$ Hz), 2.55 (br s, 4H), 2.18 (br s, 1H), 1.26 (t, 3H, $J = 7.5$ Hz). $^{13}\text{C-NMR}$ (125 MHz, CDCl_3) δ 170.5, 60.8, 60.2, 54.2, 46.0, 14.4.

4-(bromomethyl)benzenesulfonamide (**2.14**)



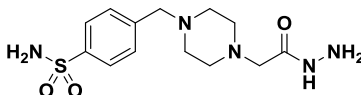
To a round-bottom flask were added 4-(bromomethyl)benzenesulfonyl chloride (**2.13**, 100 g, 371 mmol) and THF (1340 mL). The solution was stirred at 0°C , and 28% aqueous ammonia (94 mL, 1.48 mol, 4.0 equiv.) was added dropwise, during which time a white solid formed in the flask. The reaction mixture was stirred at 0°C for 1 hour. The reaction was quenched by the addition of water (300 mL). The mixture was extracted with EtOAc (2 x 100 mL). The combined organic layers were washed with water (100 mL) and brine (2 x 100 mL), dried over MgSO_4 , filtered, and concentrated to afford **2.14** (76.56 g, 82.5%) as a white solid. $^1\text{H-NMR}$ (500 MHz, $(\text{CD}_3)_2\text{CO}$) δ 7.87 (d, 2H, $J = 8.5$ Hz), 7.64 (d, 2H, $J = 8.5$ Hz), 6.65 (br s, 2H), 4.70 (s, 2H). $^{13}\text{C-NMR}$ (125 MHz, $(\text{CD}_3)_2\text{CO}$) δ 144.7, 143.2, 130.4, 127.3, 32.8.

Ethyl 2-(4-(4-sulfamoylbenzyl)piperazin-1-yl)acetate (**2.15**)



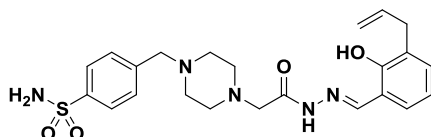
To a 3L three-necked round-bottom flask with a mechanical stirrer and condenser were added **2.14** (78.3 g, 313 mmol, 1.0 equiv.), K_2CO_3 (103.7 g, 751 mmol, 3.0 equiv.), 3:2 THF:acetone (1565 mL, 0.2 M), and **2.8** (80.9 g, 470 mmol, 1.5 equiv.). The reaction mixture was stirred at reflux overnight. The reaction mixture was cooled to rt. The solid was filtered and washed with acetone, and the filtrate was concentrated. Recrystallization from EtOH afforded **2.15** (88 g, 82%) as an off-white solid. $^1\text{H-NMR}$ (500 MHz, CD_3OD) δ 7.85 (d, 2H, $J = 8.5$ Hz), 7.51 (d, 2H, $J = 8.5$ Hz), 4.16 (q, 2H, $J = 7.0$ Hz), 3.60 (s, 2H), 3.22 (s, 2H), 2.62 (br s, 4H), 2.52 (br s, 4H), 1.25 (t, 3H, $J = 7.0$ Hz). $^{13}\text{C-NMR}$ (125 MHz, CD_3OD) δ 171.5, 144.0, 143.5, 130.9, 127.2, 63.0, 61.2, 59.7, 53.7, 53.5, 14.5.

4-((4-(2-hydrazinyl-2-oxoethyl)piperazin-1-yl)methyl)benzenesulfonamide (**2.16**)



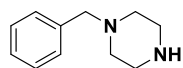
To a 2L three-necked round-bottom flask with a mechanical stirrer and condenser were added **2.15** (88 g, 258 mmol, 1.0 equiv.) and 2:1 EtOH:MeOH (520 mL, 0.5 M). The solution was stirred, and anhydrous hydrazine (33 mL, 1031 mmol, 4.0 equiv.) was added dropwise via addition funnel. The reaction mixture was stirred at reflux overnight. The reaction mixture was cooled to rt and concentrated. Recrystallization from MeOH afforded **2.16** (77.15 g, 91.4%) as a white solid. ¹H-NMR (500 MHz, CD₃OD) δ 7.85 (d, 2H, *J* = 8.5 Hz), 7.51 (d, 2H, *J* = 8.5 Hz), 3.60 (s, 2H), 3.03 (s, 2H), 2.53 (br s, 8H). ¹³C-NMR (125 MHz, CD₃OD) δ 171.4, 144.0, 143.5, 130.9, 127.2, 63.0, 61.0, 54.1, 53.8.

4-((4-(2-(2-(3-allyl-2-hydroxybenzylidene)hydrazinyl)-2-oxoethyl)piperazin-1-yl)methyl)benzenesulfonamide (S-PAC-1, 1.34)

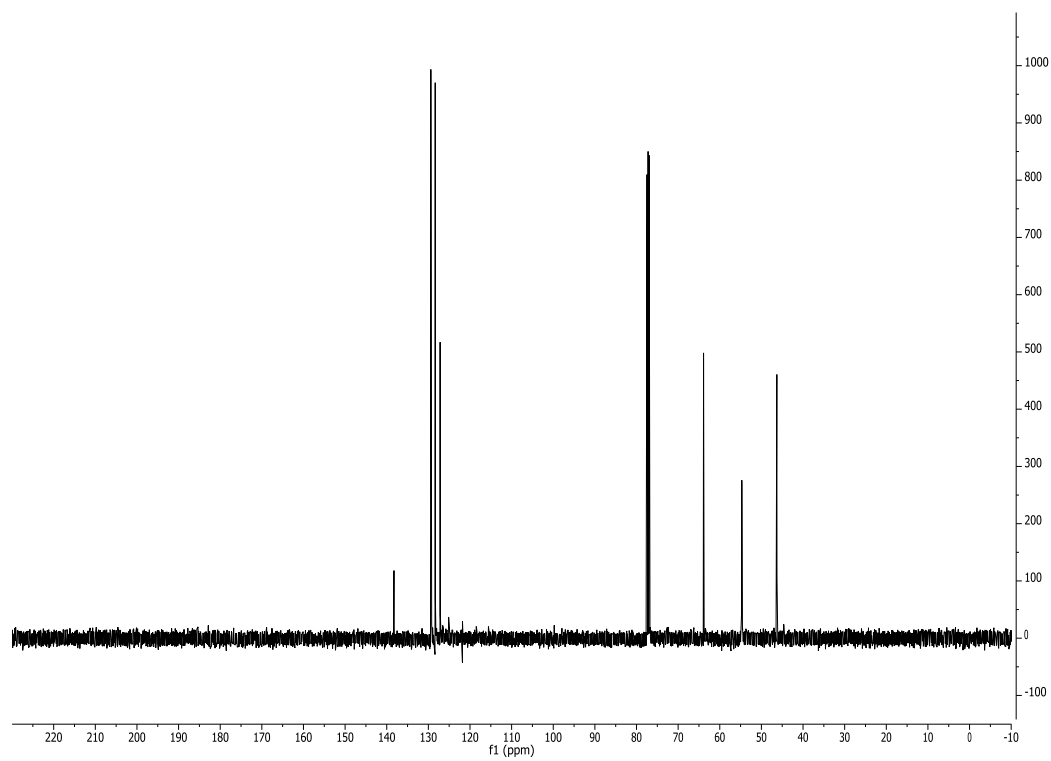
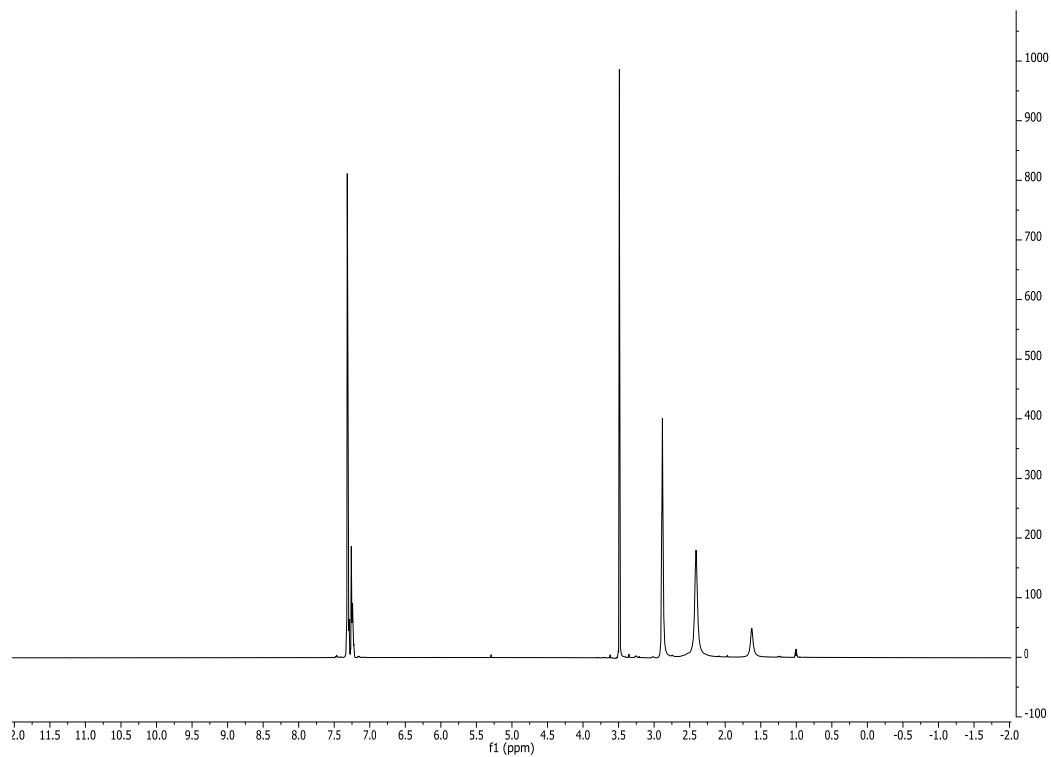


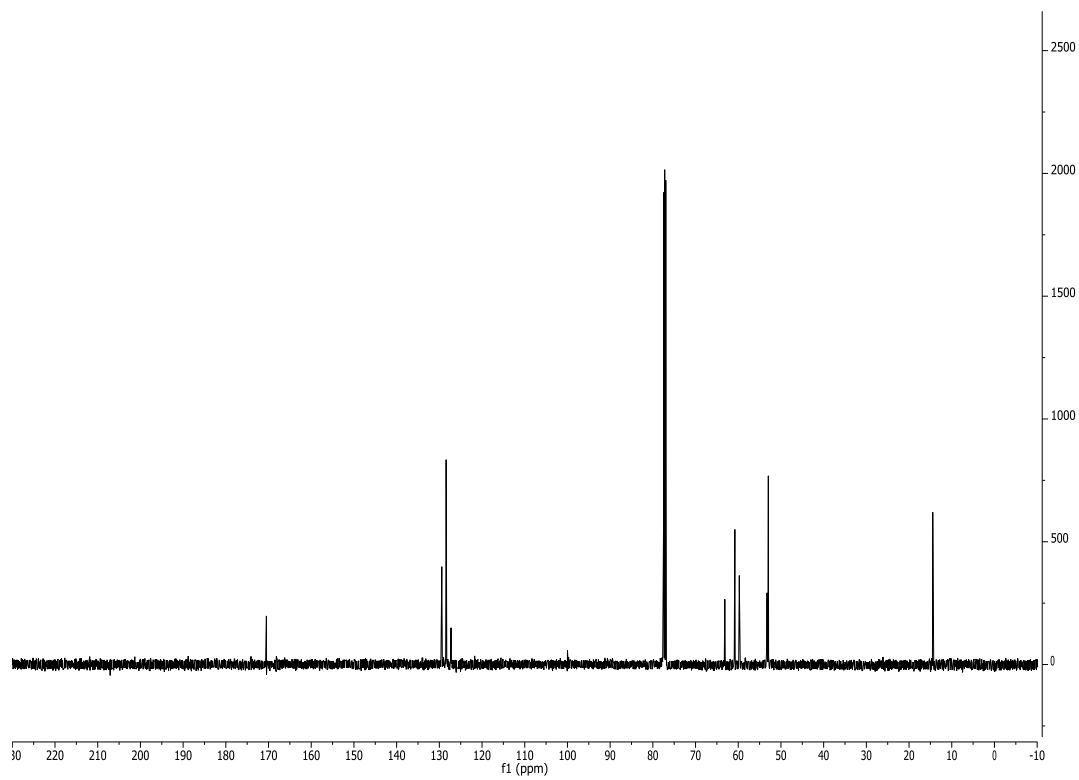
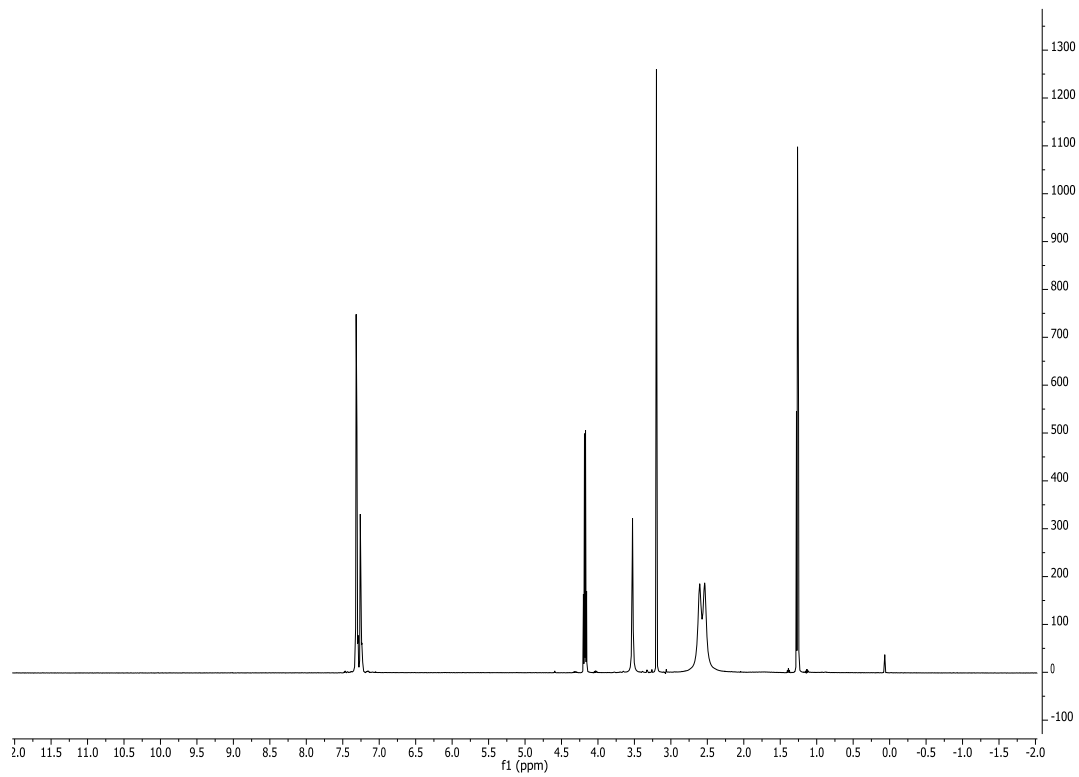
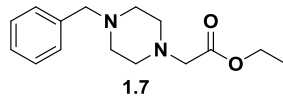
To a round-bottom flask were added **2.16** (77.15 g, 236.7 mmol, 1.0 equiv.), **2.1** (38.39 g, 236.7 mmol, 1.0 equiv.), 2:1 MeOH:MeCN (1580 mL, 0.15 M), and 1.2 M HCl (16.6 mL, 16.6 mmol, 0.070 equiv.). The reaction mixture was stirred at reflux overnight. The reaction mixture was cooled to rt and concentrated. Purification by recrystallization from MeOH yielded **S-PAC-1** (65.56 g, 58.7%) as a white solid. ¹H-NMR (500 MHz, (CD₃)₂CO) δ 11.84 (s, 1H), 10.78 (br s, 1H), 8.49 (s, 1H), 7.84 (d, 2H, *J* = 8.0 Hz), 7.51 (d, 2H, *J* = 8.0 Hz), 7.17 (d, 2H, *J* = 7.5 Hz), 6.85 (t, 1H, *J* = 7.5 Hz), 6.55 (br s, 2H), 6.01 (tdd, 1H, *J* = 6.5, 10.0, 16.5 Hz), 5.09-5.05 (m, 1H), 5.01-4.98 (m, 1H), 3.59 (s, 2H), 3.41 (d, 2H, *J* = 7.0 Hz), 3.17 (s, 2H), 2.61 (br s, 4H), 2.51 (br s, 4H). ¹³C-NMR (125 MHz, (CD₃)₂CO) δ 166.4, 157.0, 150.7, 144.0, 143.8, 137.6, 132.4, 129.9, 129.9, 128.5, 126.8, 119.8, 118.4, 115.7, 62.6, 61.7, 54.3, 53.6, 34.4. HRMS (ESI): 472.2014 (M+1); calcd. for C₂₃H₃₀N₅O₄S: 472.2019.

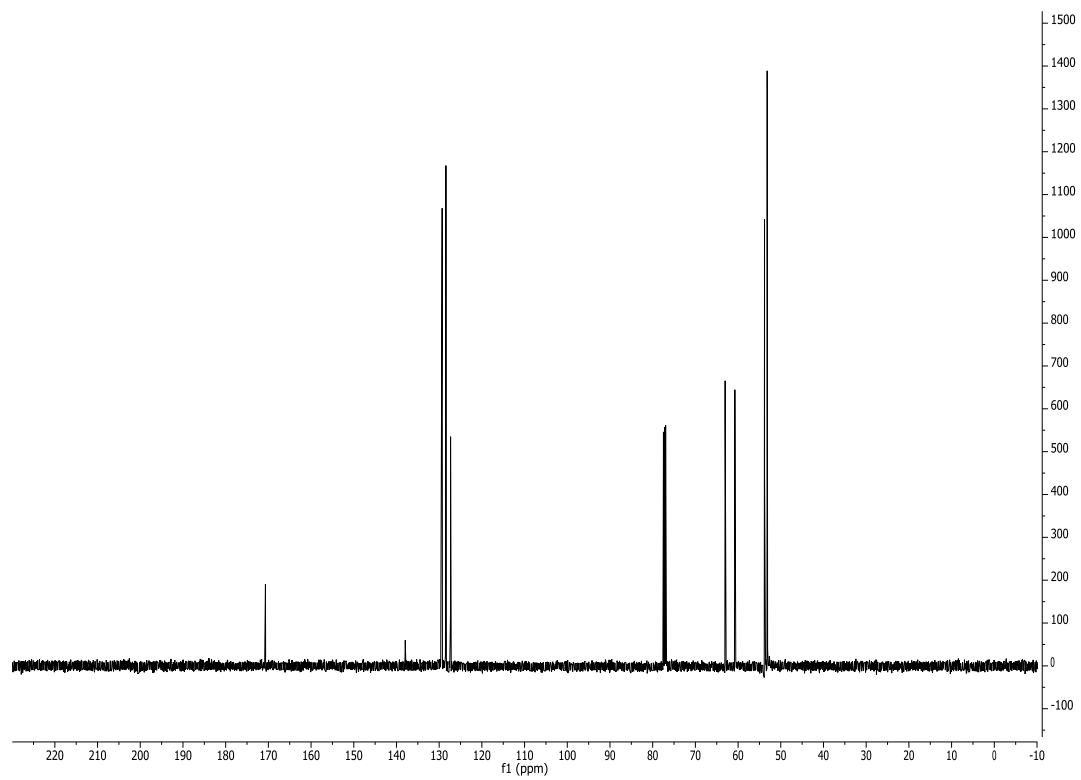
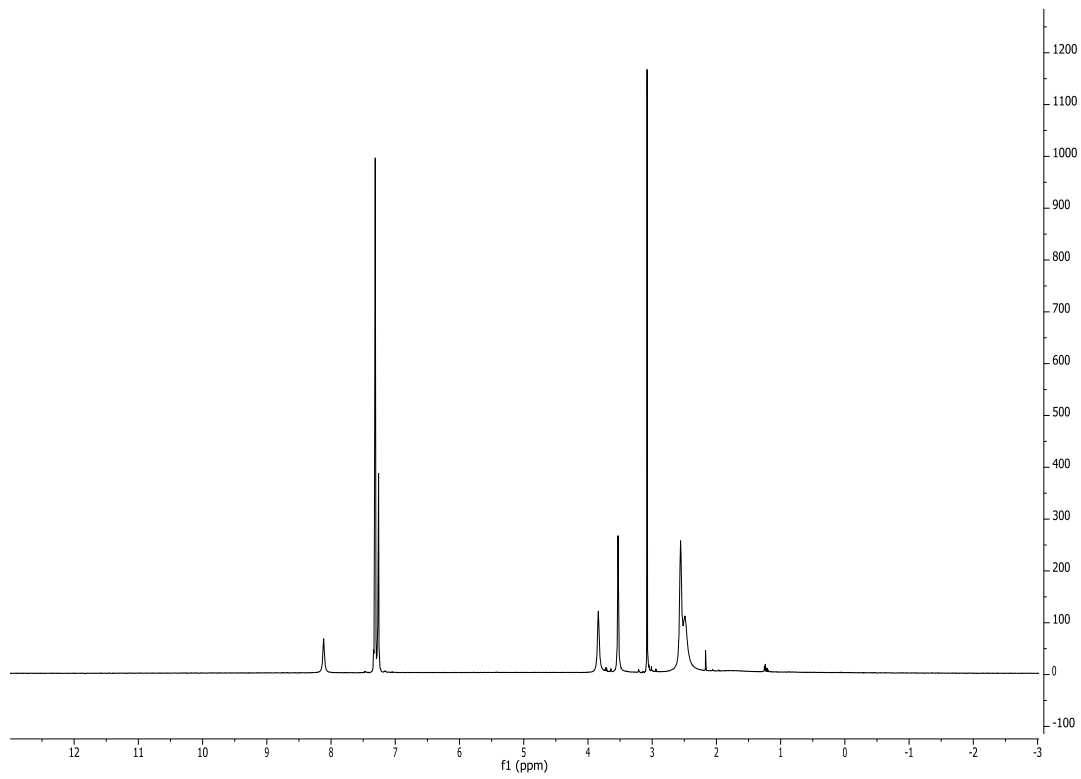
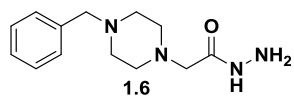
2.5.2. Spectra

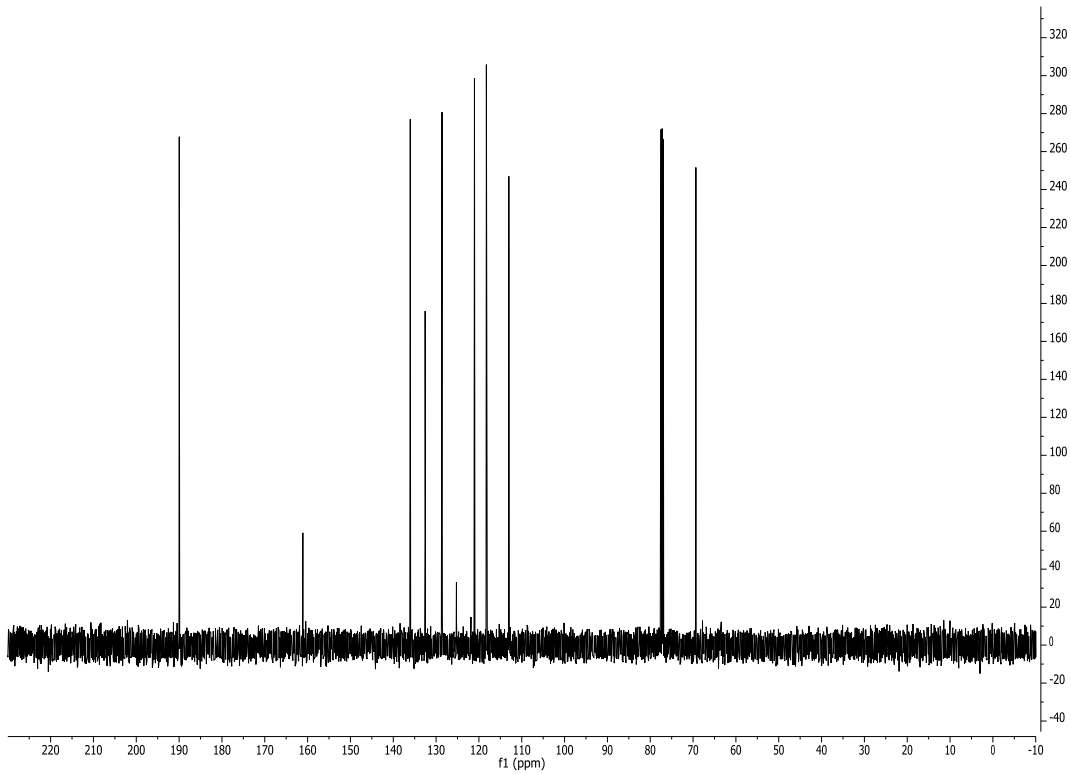
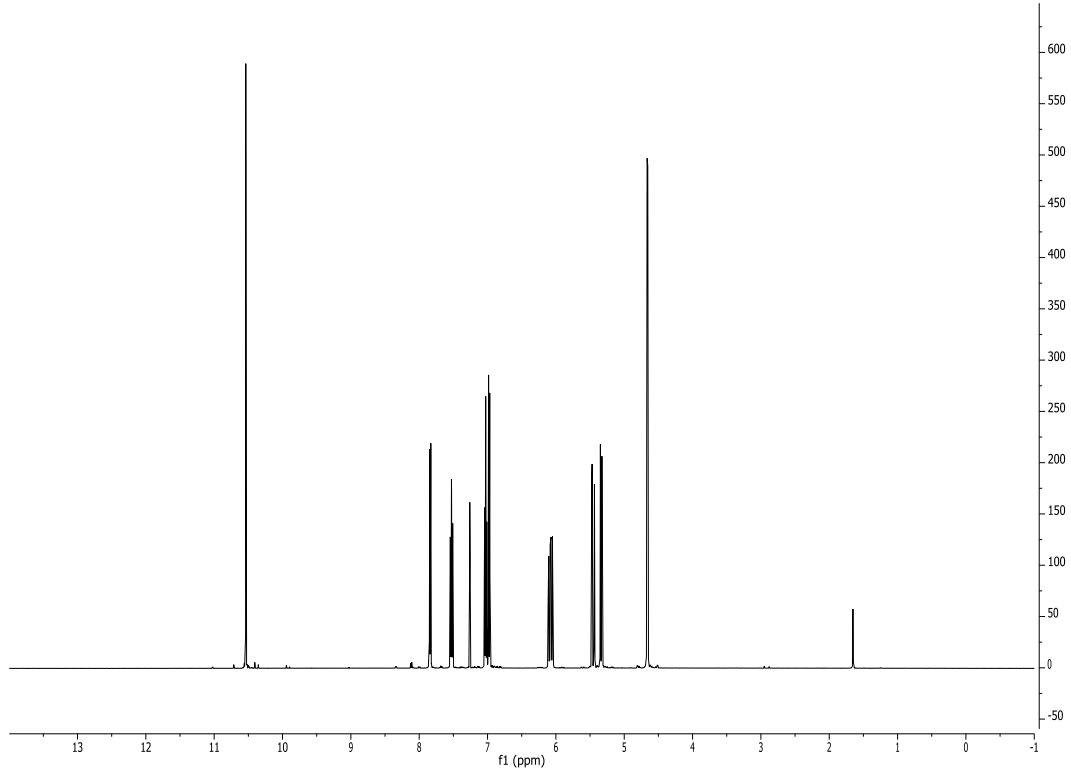
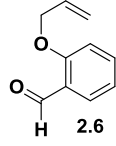


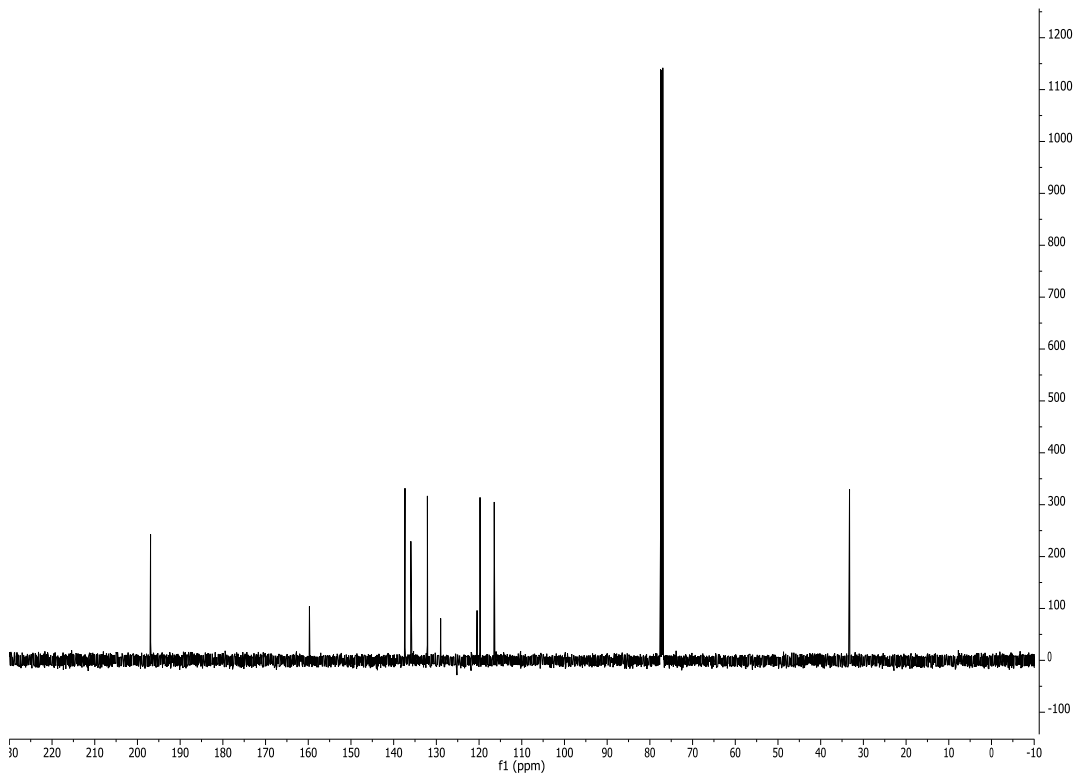
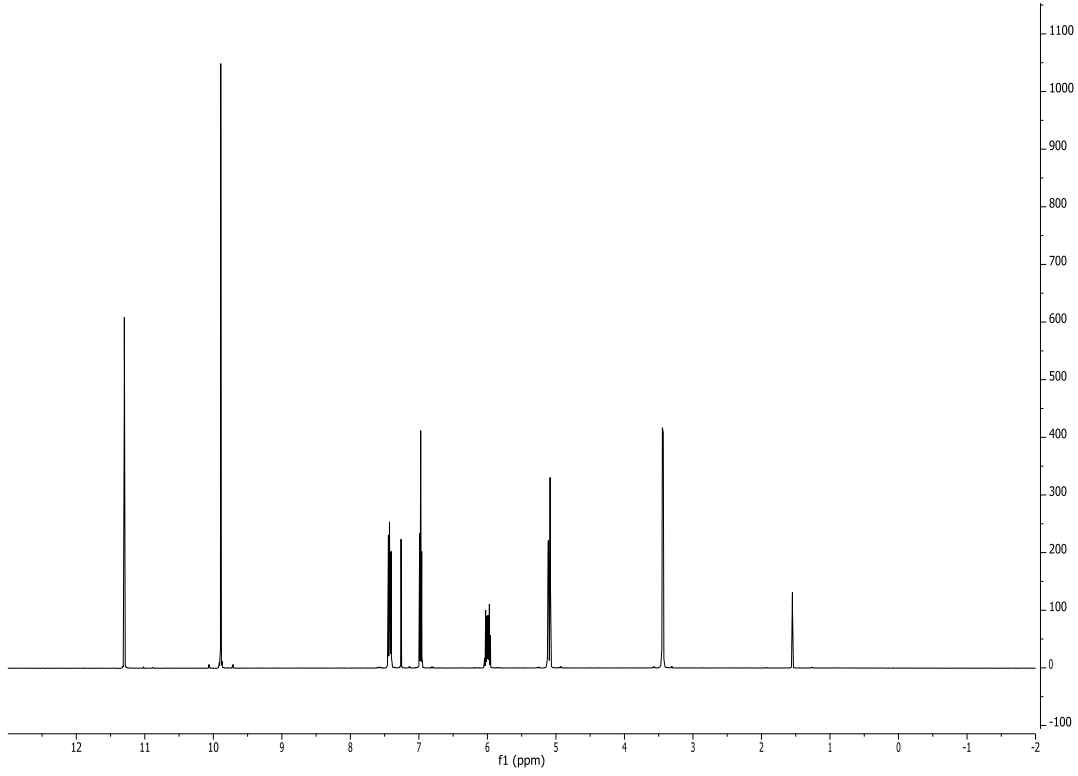
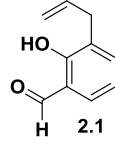
1.10

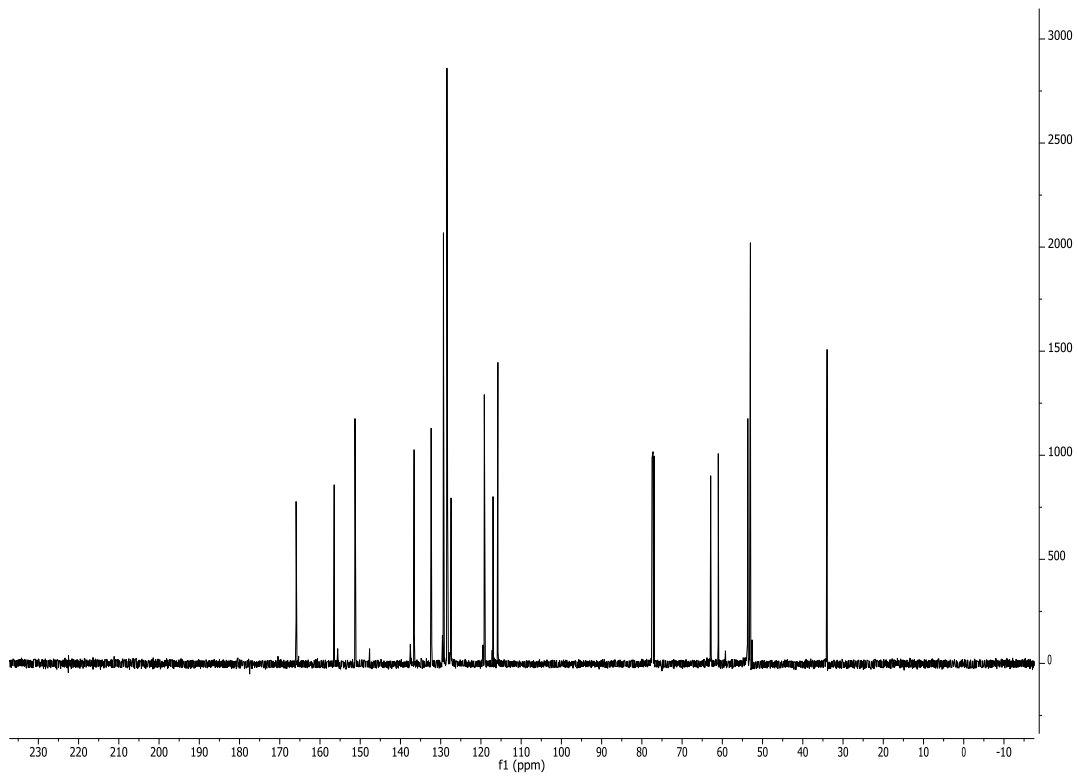
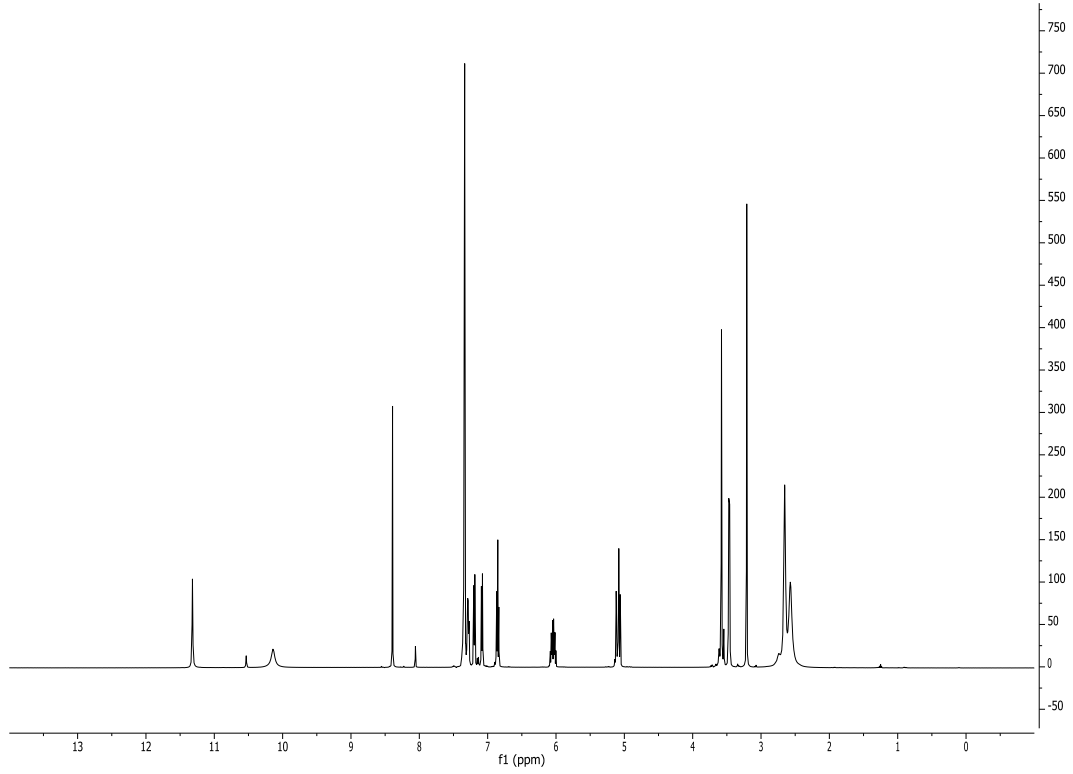
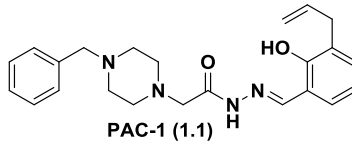


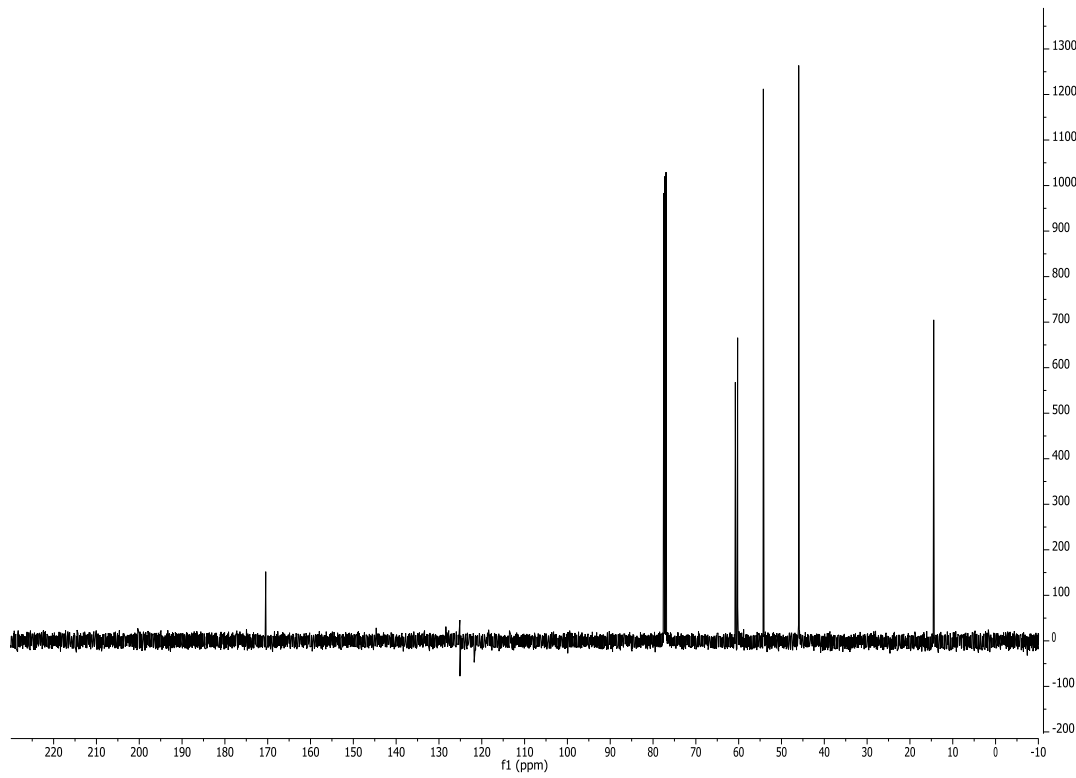
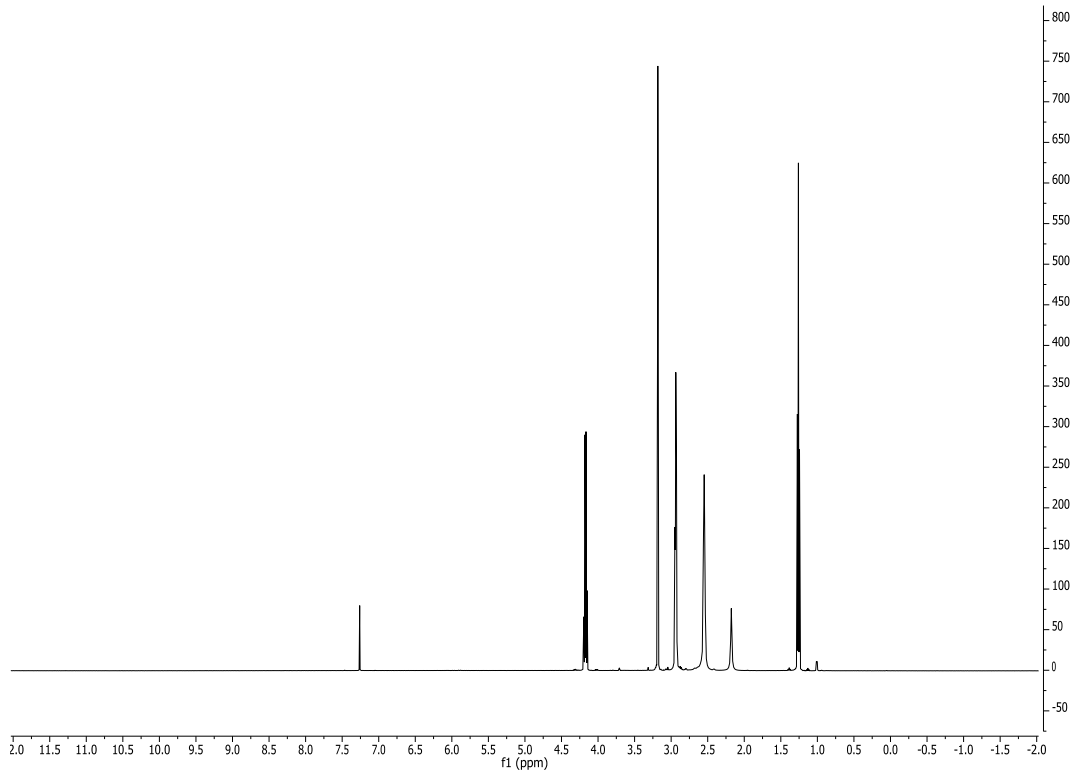
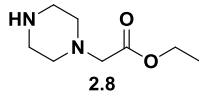


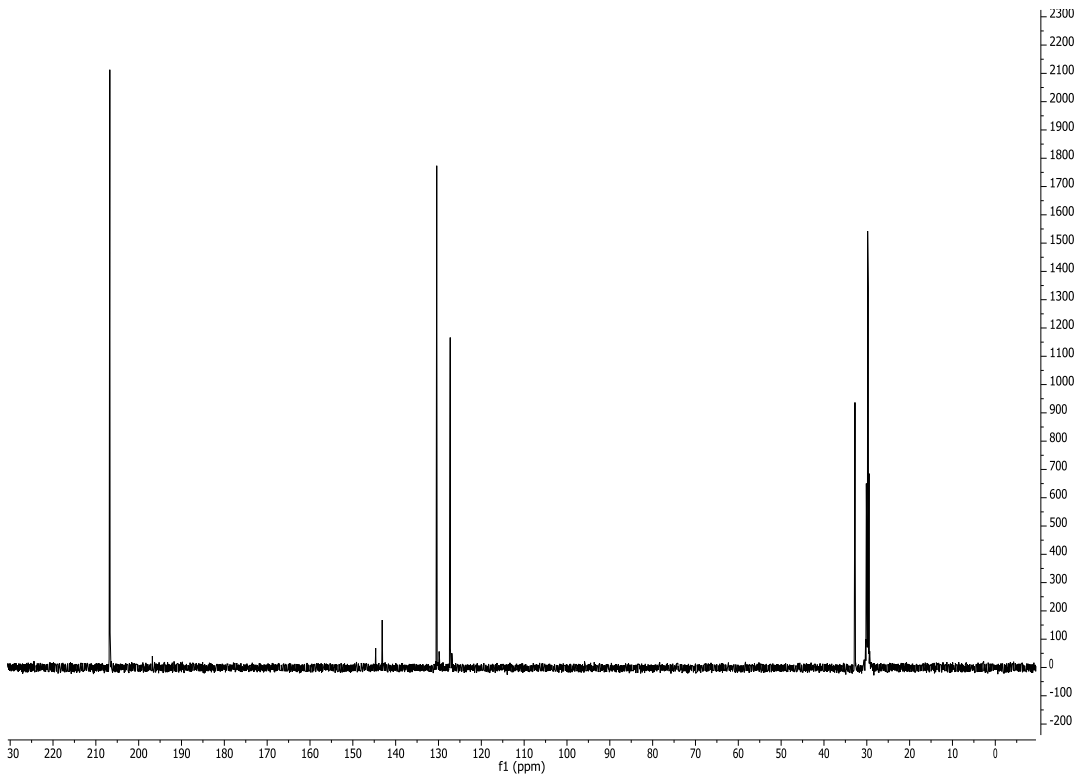
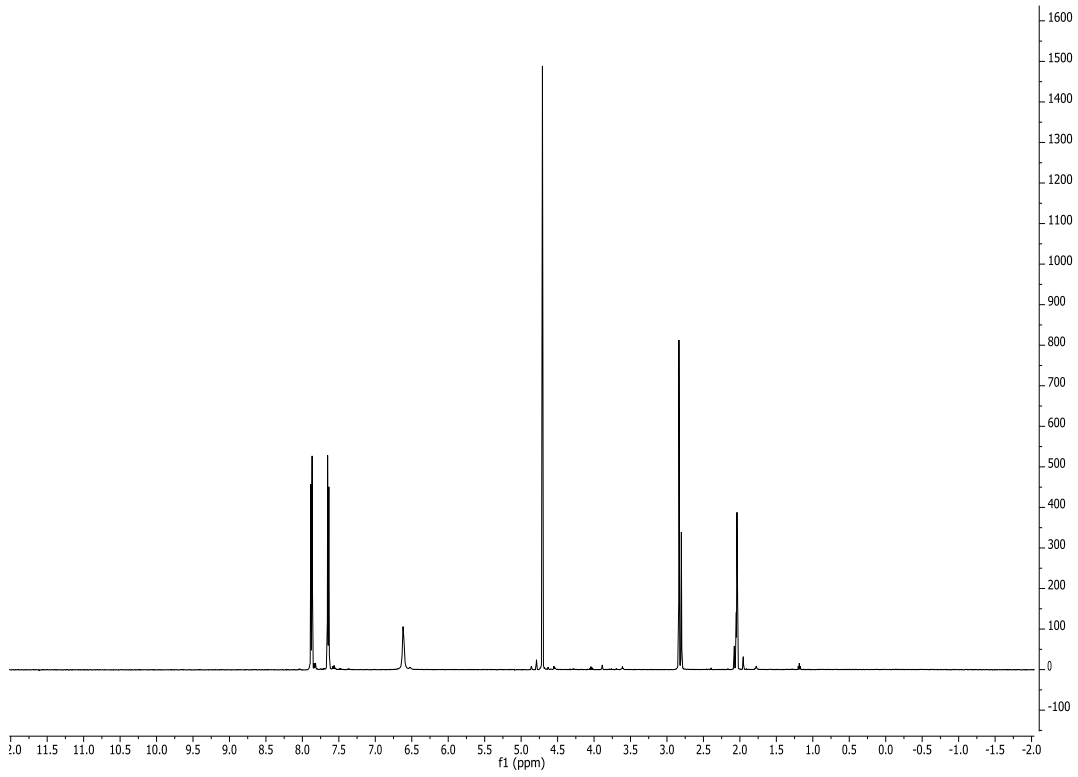
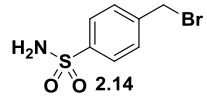


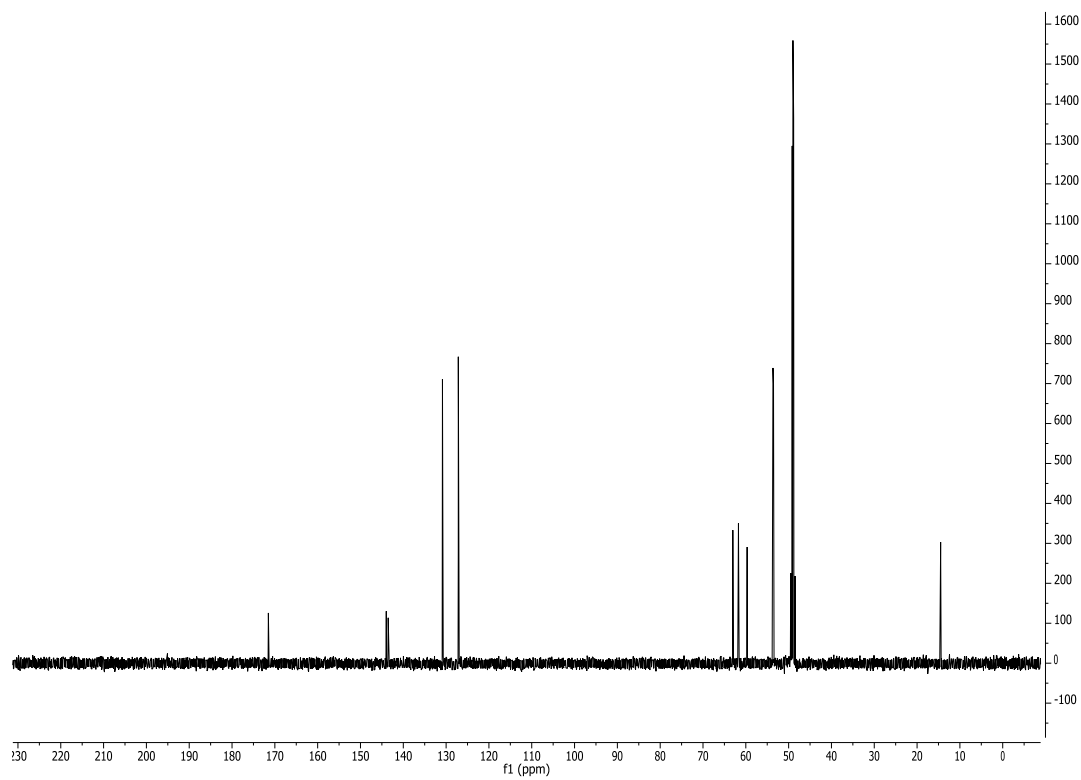
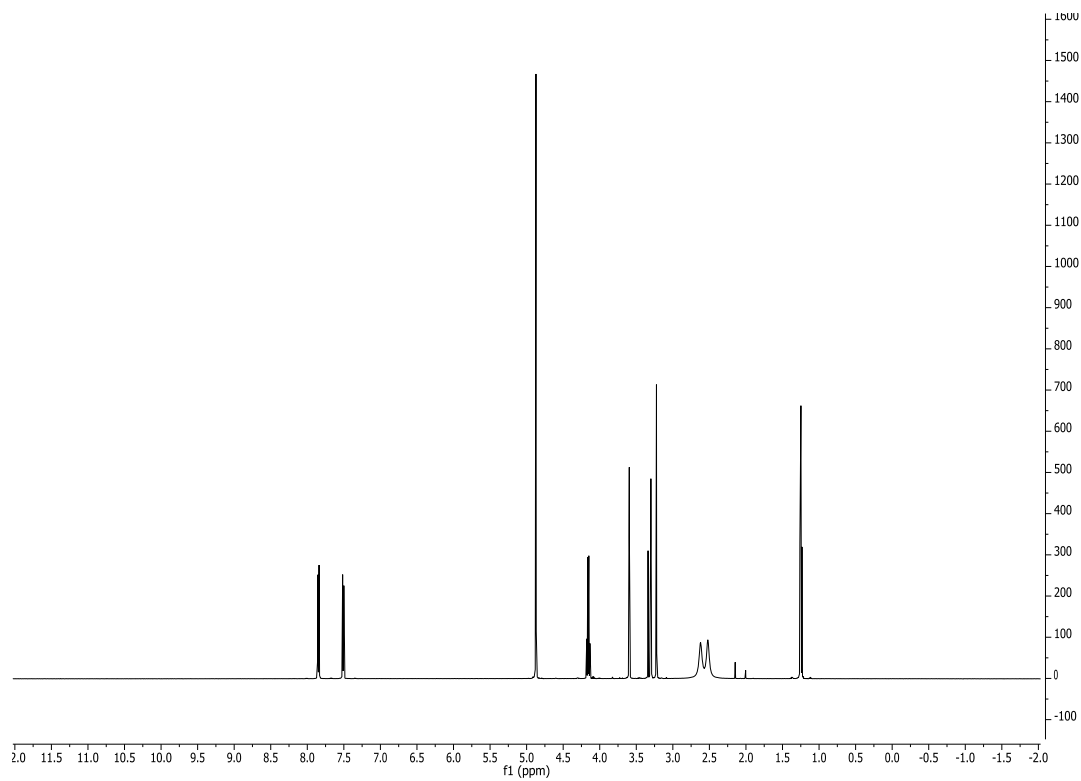
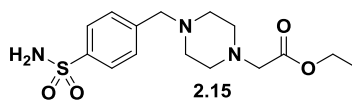


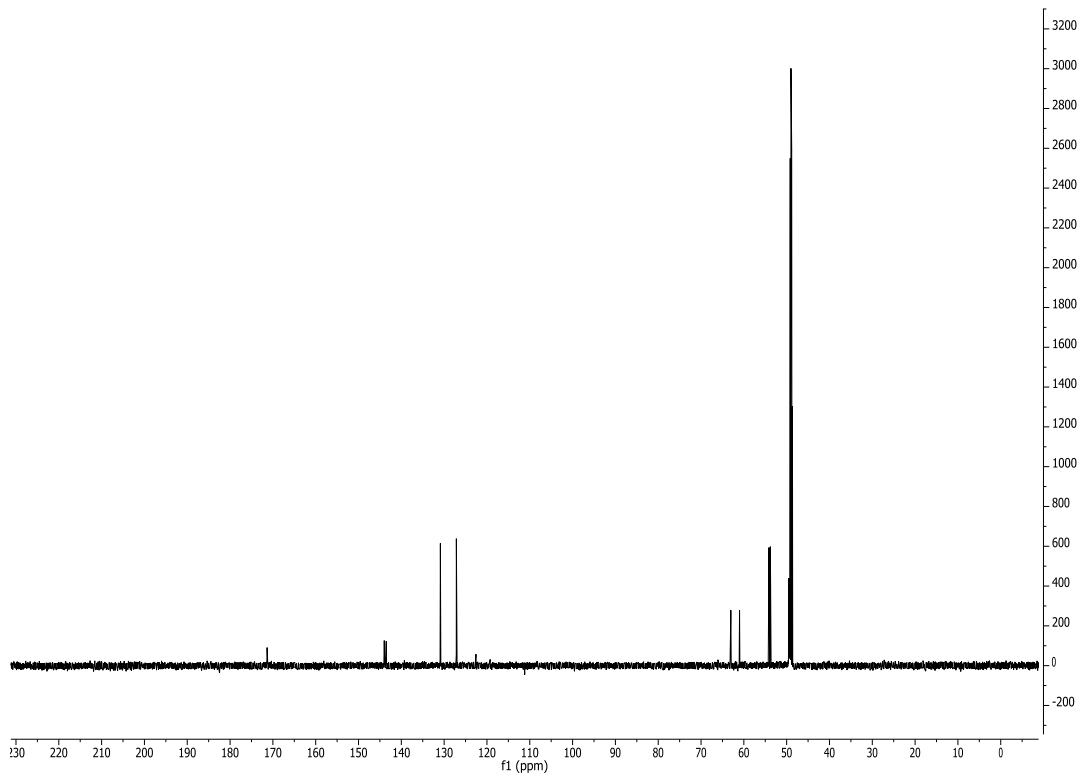
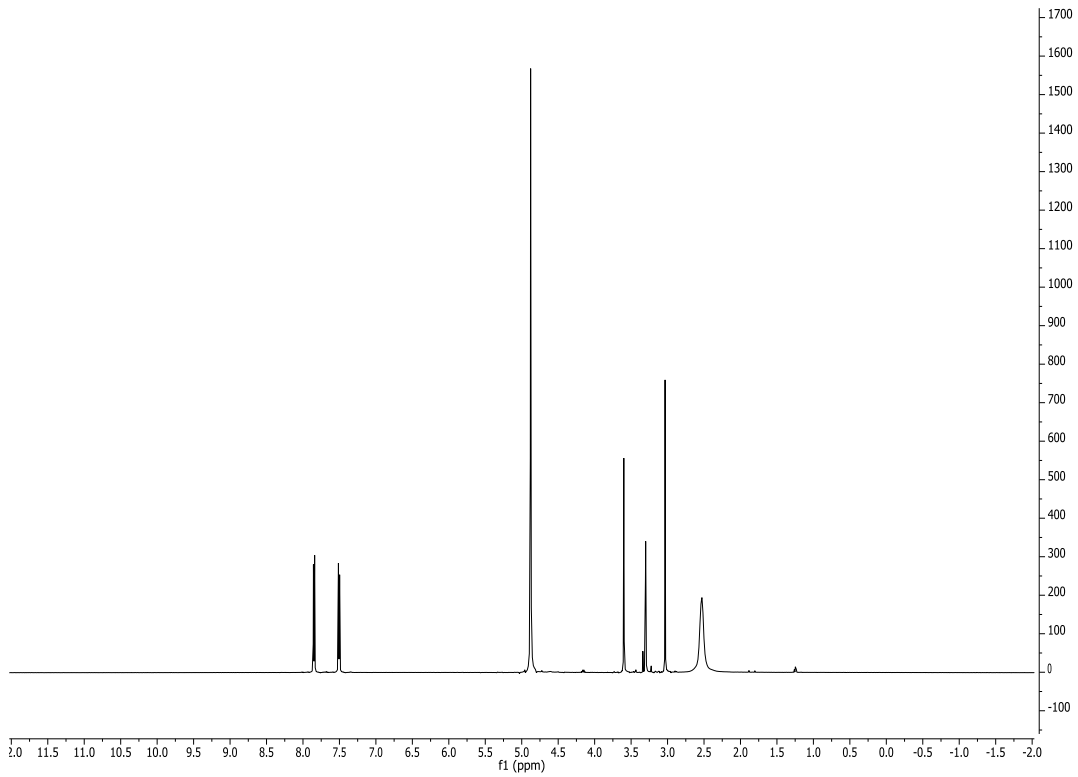
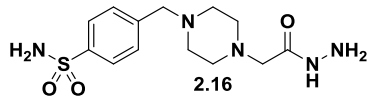


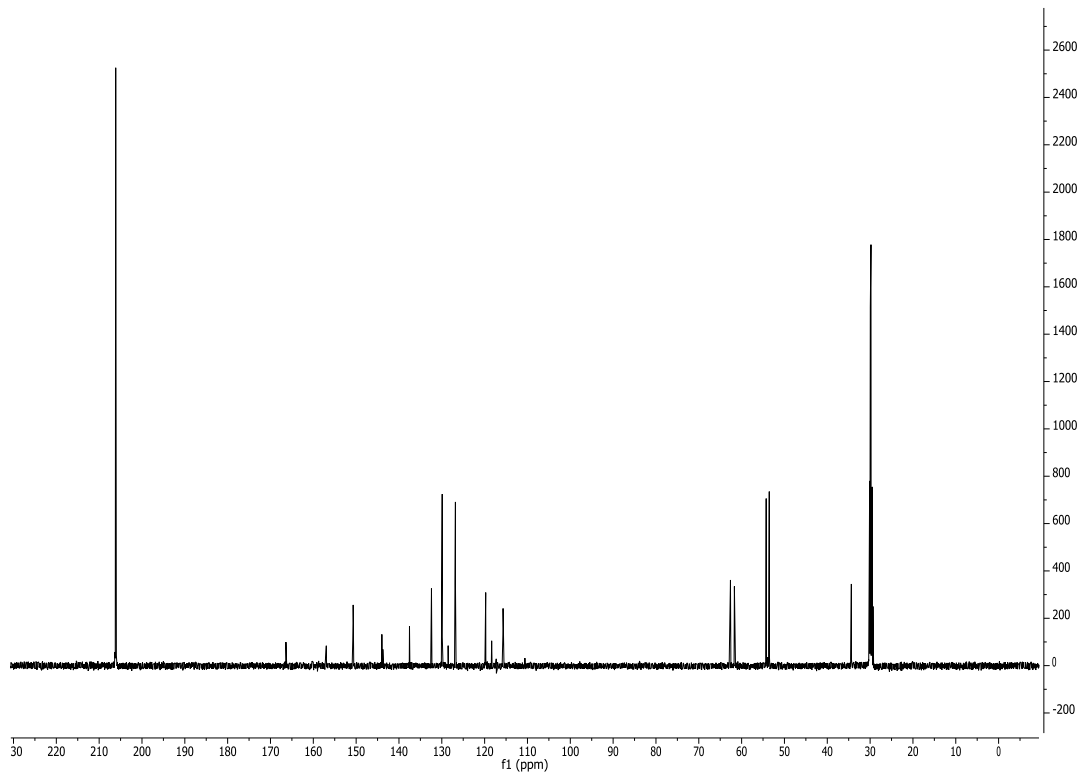
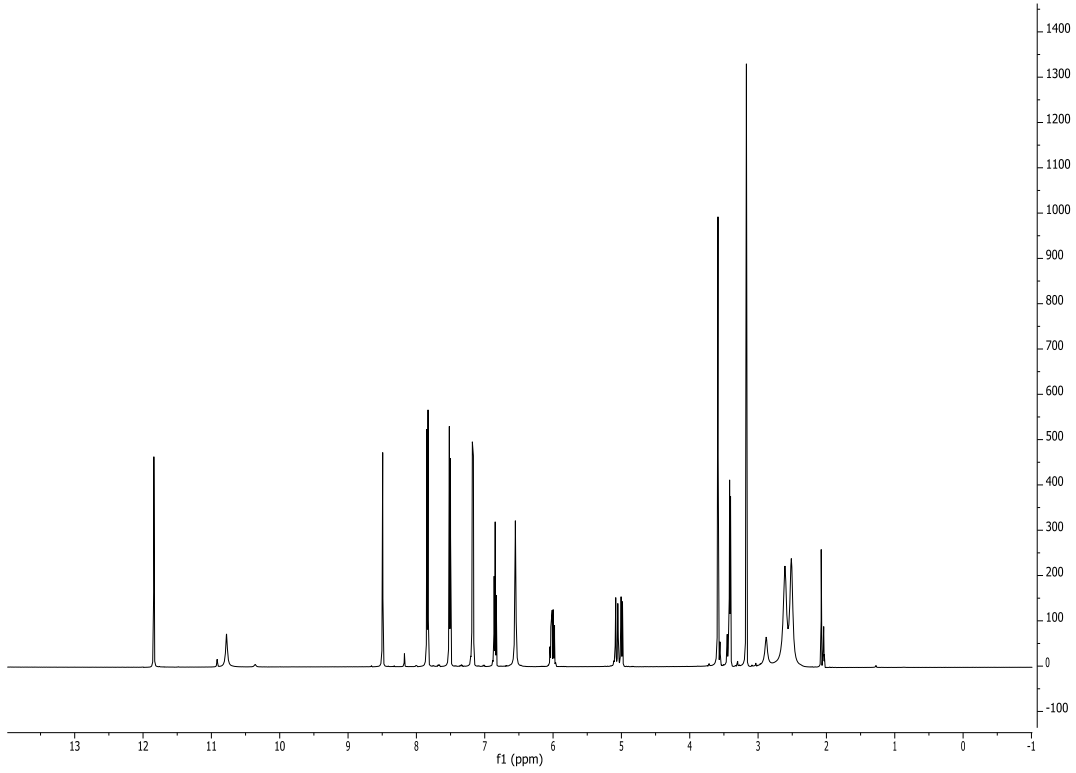
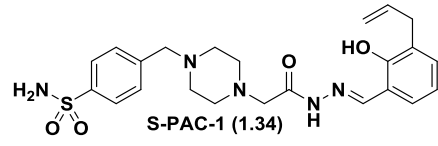












2.6. References

1. Putt, K. S.; Chen, G. W.; Pearson, J. M.; Sandhorst, J. S.; Hoagland, M. S.; Kwon, J. T.; Hwang, S. K.; Jin, H.; Churchwell, M. I.; Cho, M. H.; Doerge, D. R.; Helferich, W. G.; Hergenrother, P. J. Small-molecule activation of procaspase-3 to caspase-3 as a personalized anticancer strategy. *Nat. Chem. Biol.* **2006**, *2*, 543-550.
2. Peterson, Q. P.; Hsu, D. C.; Novotny, C. J.; West, D. C.; Kim, D.; Schmit, J. M.; Dirikolu, L.; Hergenrother, P. J.; Fan, T. M. Discovery and canine preclinical assessment of a nontoxic procaspase-3-activating compound. *Cancer Res.* **2010**, *70*, 7232-7241.
3. Dauzonne, D.; Folleas, B.; Martinez, L.; Chabot, G. G. Synthesis and in vitro cytotoxicity of a series of 3-aminoflavones. *Eur. J. Med. Chem.* **1997**, *32*, 71-82.
4. Palla, G.; Predieri, G.; Domiano, P.; Vignali, C.; Turner, W. Conformational Behavior and E/Z Isomerization of N-Acyl and N-Aroylhydrazones. *Tetrahedron* **1986**, *42*, 3649-3654.
5. Palla, G.; Pelizzi, C.; Predieri, G.; Vignali, C. Conformational Study on N-Acylhydrazones of Aromatic-Aldehydes by Nmr-Spectroscopy. *Gazz. Chim. Ital.* **1982**, *112*, 339-341.
6. Lopes, A. B.; Miguez, E.; Kummerle, A. E.; Rumjanek, V. M.; Fraga, C. A.; Barreiro, E. J. Characterization of amide bond conformers for a novel heterocyclic template of N-acylhydrazone derivatives. *Molecules* **2013**, *18*, 11683-11704.
7. Syakaev, V. V.; Podyachev, S. N.; Buzykin, B. I.; Latypov, S. K.; Habicher, W. D.; Konovalov, A. I. NMR study of conformation and isomerization of aryl- and heteroarylaldehyde 4-tert-butylphenoxyacetylhydrazones. *J. Mol. Struct.* **2006**, *788*, 55-62.
8. Peterson, Q. P.; Hsu, D. C.; Goode, D. R.; Novotny, C. J.; Totten, R. K.; Hergenrother, P. J. Procaspase-3 activation as an anti-cancer strategy: structure-activity relationship of Procaspase-Activating Compound 1 (PAC-1) and its cellular co-localization with caspase-3. *J. Med. Chem.* **2009**, *52*, 5721-5731.
9. Zhou, M. Q.; Eun, Y. J.; Guzei, I. A.; Weibel, D. B. Structure-Activity Studies of Divin: An Inhibitor of Bacterial Cell Division. *ACS Med. Chem. Lett.* **2013**, *4*, 880-885.

Chapter 3. Parallel Synthesis and Biological Evaluation of 837 Analogues of PAC-1

Portions of this chapter are reproduced with permission from literature (Hsu, D. C.; Roth, H. S.; West, D. C.; Botham, R. C.; Novotny, C. J.; Schmid, S. C.; Hergenrother, P. J. Parallel synthesis and biological evaluation of 837 analogues of Procaspase-Activating Compound 1 (PAC-1). *ACS Comb. Sci.* **2012**, 14, 44-50.).¹ Library synthesis was performed in collaboration with Dr. Danny C. Hsu, Dr. Diana C. West, Chris J. Novotny, and Steven C. Schmid. Biological evaluation was performed by Dr. Danny C. Hsu, Dr. Diana C. West, and Rachel C. Botham. Animal experiments were performed by Prof. Timothy M. Fan.

3.1. Combinatorial library design and synthesis

3.1.1. Library design

Given initial promising results with **PAC-1** and **S-PAC-1**, efforts were undertaken to develop **PAC-1** derivatives with improved properties, including potency, metabolic stability, and tolerability. In order to expand upon previously determined structure-activity relationships² and identify a highly potent derivative, a library of diverse **PAC-1** analogues was designed. As the maximal cytotoxicity of **S-PAC-1** is not reached until at least 24 hours,³ and both **PAC-1** and **S-PAC-1** exhibit short half-lives of 1-2 hours *in vivo*,^{3, 4} a secondary goal of this study was to identify **PAC-1** analogues that could induce apoptosis more rapidly. Reported synthetic routes to **PAC-1** and **S-PAC-1**, as well as other **PAC-1** analogues, utilize the condensation of a hydrazide and an aldehyde as the final step in the synthetic scheme.^{1-3, 5-15} The modular nature of the **PAC-1** synthesis allows for a diverse array of functional groups to be conveniently incorporated into the **PAC-1** scaffold without altering the core *ortho*-hydroxy *N*-acylhydrazone motif essential for procaspase-3 activation and induction of apoptosis.² As shown in Figure 3.1, 31 hydrazides (**3.1**{1-31}) and 27 aldehydes (**3.2**{1-27}) were selected for building the library of 837 **PAC-1** analogues.

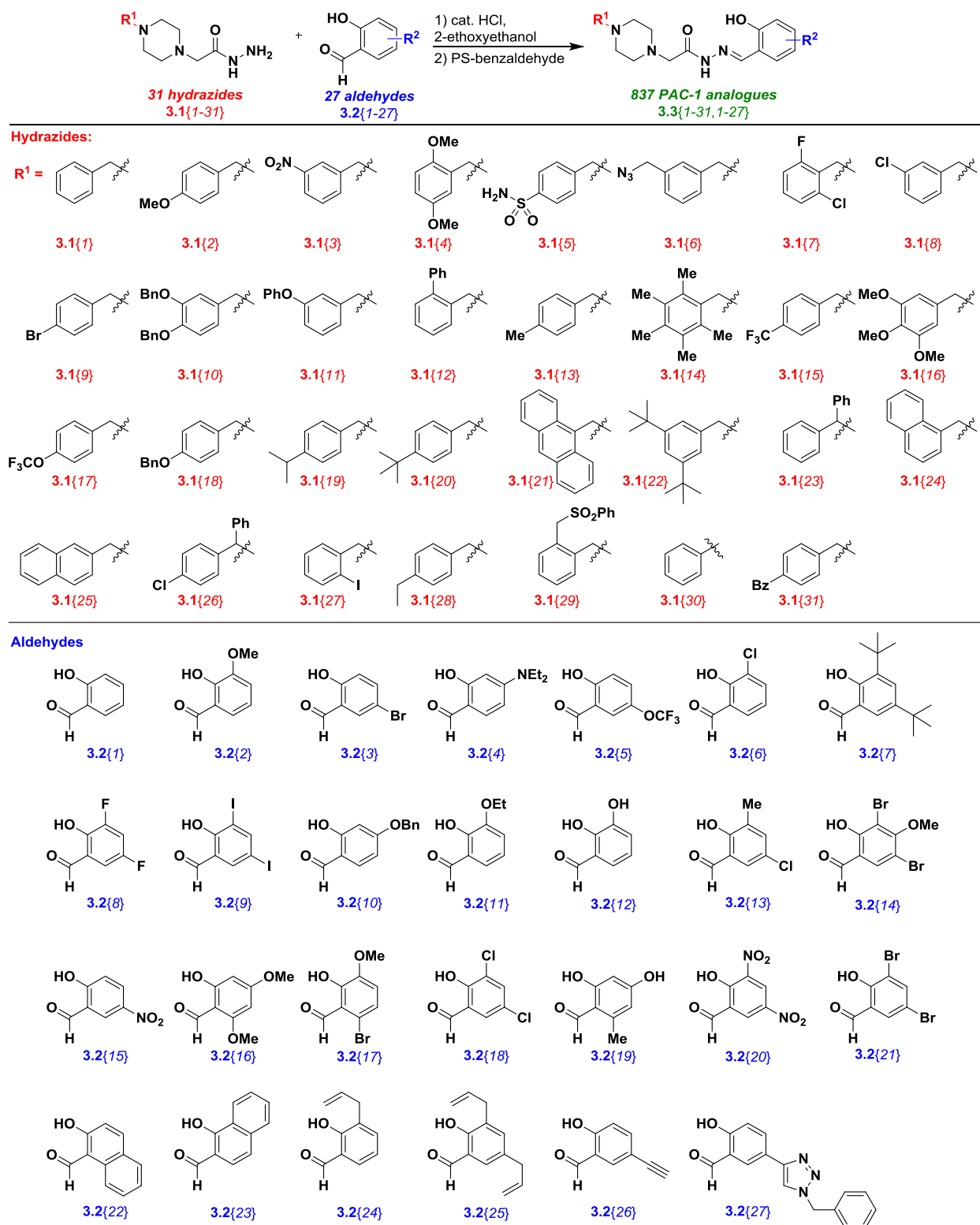
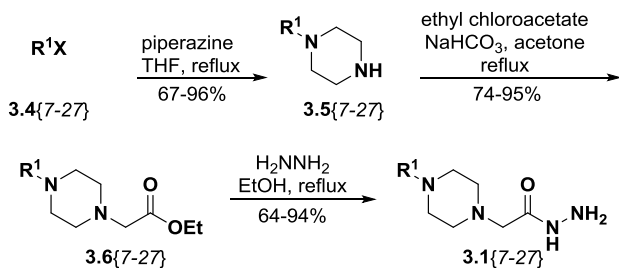


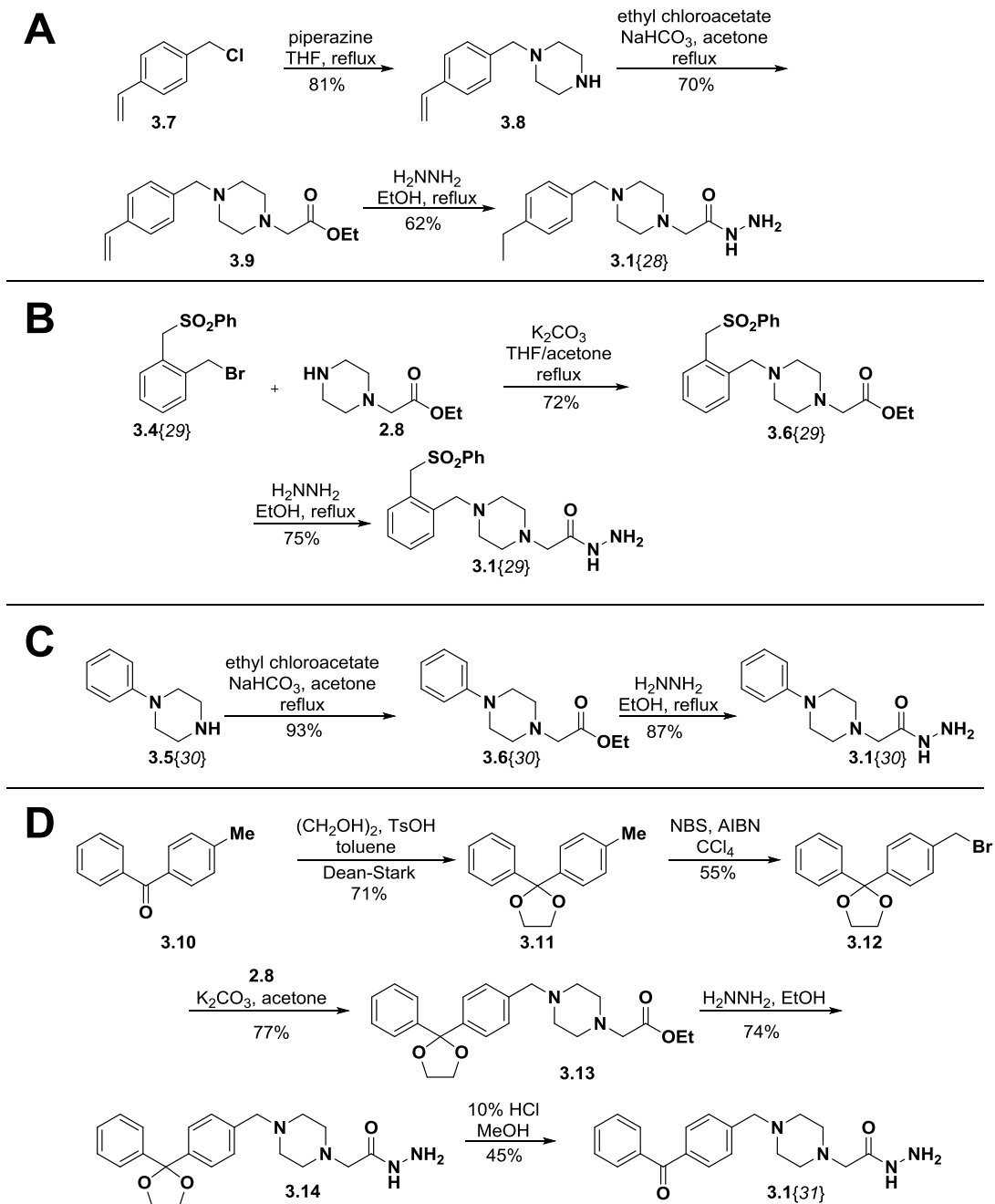
Figure 3.1. Hydrazides and aldehydes used to construct 837-membered combinatorial library of PAC-1 analogues.¹

3.1.2. Synthesis of library building blocks

The hydrazide building blocks were constructed from commercially available benzyl halide starting materials. The syntheses of hydrazides **3.1**{1-6} have been reported previously.^{2,3,5} Hydrazides **3.1**{7-27} were synthesized according to Scheme 3.1. Substituted benzyl halides **3.4**{7-27} first reacted with piperazine to form substituted benzylpiperazines **3.5**{7-27}. A second alkylation of the piperazine ring with ethyl chloroacetate gave disubstituted piperazines **3.6**{7-27}, and the esters were then converted to hydrazides **3.1**{7-27} by reaction with hydrazine. The synthetic routes toward hydrazides **3.1**{28-31} are detailed in Scheme 3.2. Synthesis of hydrazide **3.1**{28} began by the alkylation of piperazine with 4-vinylbenzyl chloride (**7**) to form monosubstituted piperazine **3.8** (Scheme 3.2A). A second alkylation with ethyl chloroacetate formed ester **3.9**, and reaction with hydrazine formed the hydrazide and reduced the olefin, giving hydrazide **3.1**{28}. The reduction of olefins with hydrazine typically involves the addition of an oxidizing agent,¹⁶ but the presence of atmospheric oxygen was sufficient to achieve this transformation. Synthesis of hydrazide **3.1**{29} (Scheme 3.2B) began with the reaction of monosubstituted piperazine **2.8** with benzyl bromide **3.4**{29} to form intermediate **3.6**{29}. Reaction of **3.6**{29} with hydrazine then formed hydrazide **3.1**{29}. Hydrazide **3.1**{30} (Scheme 3.2C) was synthesized beginning with the reaction of 1-phenylpiperazine (**3.5**{30}) with ethyl chloroacetate to give disubstituted piperazine **3.6**{30}, and reaction with hydrazine formed hydrazide **3.1**{30}. Hydrazide **3.1**{31}, was synthesized by first protecting 4-methylbenzophenone (**3.10**) as the ethylene acetal (**3.11**), as shown in Scheme 3.2D. This compound was brominated under radical conditions to give benzyl bromide **3.12**. Reaction with monosubstituted piperazine **2.8** gave intermediate **3.13**, and reaction with hydrazine gave hydrazide **3.14**. Deprotection of the acetal with aqueous acid gave hydrazide **3.1**{31}.



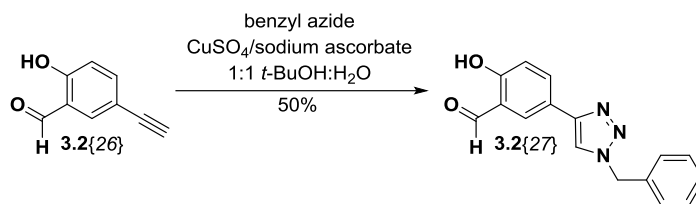
Scheme 3.1. Synthesis of hydrazides **3.1**{7-27}.¹



Scheme 3.2. Synthesis of hydrazides **A. 3.1{28}**, **B. 3.1{29}**, **C. 3.1{30}**, and **D. 3.1{31}**.¹

The structure-activity relationships of **PAC-1** derived from the synthesis and evaluation of ~30 compounds demonstrated the necessity of the *ortho*-hydroxyl group,² so 27 salicylaldehyde building blocks were selected for library construction. Aldehydes **3.2{1-23}** were obtained from commercial sources, and the syntheses of aldehydes **3.2{24-26}** have been

reported previously.^{2, 3, 17} Aldehyde **3.2{27}** was synthesized via copper-catalyzed cycloaddition of aldehyde **3.2{26}** with benzyl azide, as shown in Scheme 3.3.



Scheme 3.3. Synthesis of aldehyde **3.2{27}**.¹

3.1.3. Synthesis of library members

Using a Büchi Syncore parallel synthesizer, each hydrazide was condensed with each aldehyde, with over 80 reactions performed simultaneously. Each aldehyde (5-15 mg) was allowed to react with excess hydrazide (1.7 equiv.), and mass spectrometry was used to monitor the disappearance of the aldehyde from the reaction mixture. When the aldehyde had reacted completely, polystyrene-bound benzaldehyde was added as a scavenger resin to react with and remove the excess hydrazide. When mass spectrometry showed no hydrazide remaining, the beads were removed by filtration, and the solutions were dried under high vacuum. Each of the 837 compounds was assessed by HPLC/MS. The purity of each compound is listed in Table 3.1, and the expected and observed molecular ions are listed in Tables 3.2 and 3.3, respectively. The library members had an average purity of 91%.

| | 3.2(1) | 3.2(2) | 3.2(3) | 3.2(4) | 3.2(5) | 3.2(6) | 3.2(7) | 3.2(8) | 3.2(9) | 3.2(10) | 3.2(11) | 3.2(12) | 3.2(13) | 3.2(14) | 3.2(15) | 3.2(16) | 3.2(17) | 3.2(18) | 3.2(19) | 3.2(20) | 3.2(21) | 3.2(22) | 3.2(23) | 3.2(24) | 3.2(25) | 3.2(26) | 3.2(27) |
|---------|--------|--------|--------|--------|--------|--------|--------|--------|--------|---------|---------|---------|---------|---------|---------|---------|---------|---------|---------|---------|---------|---------|---------|---------|---------|---------|---------|
| 3.1(1) | 91 | 93 | 90 | 85 | 91 | 92 | 98 | 96 | 92 | 95 | 99 | 96 | 95 | 96 | 98 | 86 | 95 | 98 | 93 | 97 | 95 | 95 | 95 | 97 | 99 | 90 | 100 |
| 3.1(2) | 92 | 91 | 90 | 91 | 93 | 95 | 99 | 96 | 95 | 92 | 96 | 94 | 99 | 93 | 91 | 86 | 90 | 93 | 93 | 90 | 91 | 95 | 93 | 93 | 71 | 96 | 96 |
| 3.1(3) | 91 | 94 | 91 | 95 | 79 | 88 | 97 | 89 | 91 | 91 | 97 | 83 | 99 | 99 | 85 | 90 | 87 | 86 | 80 | 90 | 87 | 87 | 87 | 92 | 86 | 88 | 91 |
| 3.1(4) | 93 | 98 | 96 | 99 | 96 | 98 | 99 | 96 | 90 | 99 | 100 | 91 | 94 | 92 | 93 | 90 | 95 | 91 | 88 | 95 | 89 | 90 | 88 | 96 | 86 | 93 | 98 |
| 3.1(5) | 94 | 96 | 97 | 93 | 90 | 97 | 100 | 98 | 90 | 98 | 97 | 93 | 61 | 96 | 98 | 90 | 96 | 97 | 91 | 97 | 97 | 88 | 88 | 88 | 89 | 90 | 89 |
| 3.1(6) | 98 | 98 | 97 | 72 | 95 | 100 | 97 | 90 | 94 | 95 | 98 | 96 | 95 | 96 | 92 | 100 | 100 | 95 | 92 | 92 | 97 | 95 | 92 | 90 | 80 | 83 | 89 |
| 3.1(7) | 93 | 98 | 93 | 98 | 93 | 96 | 98 | 98 | 96 | 98 | 100 | 97 | 100 | 94 | 98 | 83 | 96 | 97 | 86 | 92 | 100 | 93 | 99 | 93 | 97 | 89 | 96 |
| 3.1(8) | 89 | 93 | 91 | 90 | 90 | 94 | 96 | 95 | 90 | 95 | 93 | 92 | 97 | 93 | 94 | 81 | 90 | 94 | 85 | 98 | 97 | 96 | 96 | 93 | 96 | 85 | 84 |
| 3.1(9) | 92 | 90 | 88 | 92 | 82 | 91 | 96 | 92 | 94 | 92 | 92 | 93 | 92 | 90 | 92 | 92 | 90 | 90 | 96 | 93 | 89 | 82 | 90 | 88 | 90 | 82 | 87 |
| 3.1(10) | 92 | 88 | 84 | 90 | 93 | 90 | 93 | 91 | 89 | 84 | 90 | 93 | 91 | 83 | 91 | 77 | 85 | 83 | 88 | 85 | 87 | 89 | 92 | 97 | 90 | 91 | 90 |
| 3.1(11) | 91 | 92 | 86 | 90 | 89 | 91 | 96 | 92 | 90 | 89 | 93 | 96 | 96 | 92 | 91 | 90 | 88 | 94 | 89 | 90 | 91 | 95 | 91 | 92 | 88 | 90 | 88 |
| 3.1(12) | 84 | 86 | 83 | 87 | 95 | 85 | 90 | 86 | 87 | 87 | 83 | 96 | 89 | 85 | 81 | 86 | 86 | 94 | 86 | 100 | 90 | 87 | 90 | 90 | 82 | 88 | 83 |
| 3.1(13) | 95 | 86 | 86 | 92 | 89 | 91 | 96 | 95 | 90 | 86 | 93 | 91 | 90 | 89 | 94 | 91 | 85 | 84 | 90 | 100 | 86 | 90 | 90 | 90 | 91 | 83 | 98 |
| 3.1(14) | 99 | 90 | 95 | 93 | 92 | 97 | 93 | 94 | 98 | 96 | 92 | 95 | 99 | 89 | 87 | 95 | 85 | 90 | 87 | 86 | 92 | 95 | 99 | 95 | 94 | 82 | 88 |
| 3.1(15) | 98 | 87 | 85 | 99 | 94 | 86 | 92 | 93 | 82 | 88 | 93 | 99 | 95 | 82 | 87 | 84 | 90 | 88 | 92 | 100 | 91 | 91 | 90 | 93 | 96 | 93 | 98 |
| 3.1(16) | 95 | 95 | 88 | 85 | 87 | 91 | 92 | 95 | 85 | 93 | 90 | 87 | 94 | 74 | 87 | 59 | 82 | 88 | 88 | 91 | 83 | 85 | 86 | 93 | 80 | 93 | 93 |
| 3.1(17) | 86 | 95 | 89 | 73 | 84 | 92 | 95 | 92 | 86 | 82 | 89 | 97 | 93 | 80 | 84 | 86 | 86 | 90 | 87 | 100 | 81 | 86 | 88 | 89 | 89 | 80 | 97 |
| 3.1(18) | 82 | 100 | 85 | 85 | 100 | 100 | 100 | 100 | 85 | 94 | 100 | 94 | 100 | 100 | 100 | 52 | 100 | 100 | 85 | 100 | 94 | 88 | 100 | 100 | 83 | 91 | 95 |
| 3.1(19) | 93 | 99 | 100 | 70 | 100 | 92 | 94 | 94 | 87 | 99 | 93 | 98 | 100 | 93 | 92 | 83 | 88 | 97 | 66 | 100 | 92 | 75 | 99 | 98 | 90 | 87 | 98 |
| 3.1(20) | 99 | 98 | 93 | 86 | 84 | 96 | 90 | 85 | 92 | 90 | 91 | 89 | 100 | 98 | 90 | 86 | 89 | 99 | 86 | 99 | 95 | 86 | 99 | 98 | 92 | 90 | 87 |
| 3.1(21) | 88 | 83 | 89 | 85 | 93 | 85 | 88 | 90 | 100 | 86 | 99 | 100 | 92 | 92 | 100 | 85 | 100 | 96 | 67 | 95 | 92 | 84 | 93 | 93 | 92 | 92 | 86 |
| 3.1(22) | 88 | 96 | 85 | 86 | 89 | 90 | 86 | 90 | 86 | 87 | 91 | 95 | 90 | 86 | 90 | 72 | 84 | 85 | 87 | 92 | 87 | 86 | 86 | 89 | 88 | 95 | 85 |
| 3.1(23) | 88 | 86 | 84 | 87 | 91 | 85 | 98 | 92 | 93 | 98 | 87 | 88 | 96 | 81 | 88 | 90 | 86 | 96 | 90 | 100 | 97 | 83 | 84 | 98 | 85 | 81 | 90 |
| 3.1(24) | 89 | 91 | 98 | 96 | 97 | 94 | 99 | 92 | 96 | 97 | 95 | 95 | 89 | 86 | 94 | 81 | 89 | 84 | 86 | 96 | 81 | 97 | 97 | 96 | 93 | 96 | 95 |
| 3.1(25) | 100 | 96 | 96 | 93 | 95 | 96 | 98 | 91 | 91 | 95 | 97 | 95 | 92 | 92 | 95 | 82 | 90 | 90 | 87 | 94 | 90 | 93 | 94 | 94 | 86 | 92 | 88 |
| 3.1(26) | 90 | 93 | 88 | 87 | 83 | 88 | 96 | 86 | 93 | 90 | 94 | 91 | 97 | 90 | 83 | 89 | 87 | 85 | 91 | 97 | 89 | 88 | 91 | 94 | 91 | 89 | 92 |
| 3.1(27) | 93 | 92 | 92 | 87 | 80 | 94 | 95 | 91 | 89 | 90 | 92 | 92 | 91 | 88 | 94 | 89 | 90 | 90 | 91 | 94 | 90 | 88 | 89 | 90 | 95 | 82 | 95 |
| 3.1(28) | 86 | 83 | 98 | 82 | 86 | 97 | 86 | 94 | 87 | 84 | 66 | 88 | 86 | 86 | 93 | 85 | 96 | 91 | 85 | 100 | 86 | 55 | 85 | 81 | 94 | 88 | 90 |
| 3.1(29) | 86 | 91 | 93 | 88 | 86 | 94 | 98 | 90 | 94 | 89 | 91 | 93 | 83 | 91 | 90 | 90 | 87 | 86 | 89 | 98 | 87 | 95 | 95 | 89 | 87 | 84 | 88 |
| 3.1(30) | 87 | 92 | 85 | 86 | 90 | 90 | 95 | 90 | 93 | 83 | 91 | 92 | 86 | 85 | 93 | 82 | 97 | 91 | 80 | 88 | 88 | 82 | 93 | 89 | 90 | 81 | 98 |
| 3.1(31) | 82 | 83 | 83 | 90 | 82 | 86 | 96 | 83 | 86 | 90 | 92 | 94 | 84 | 91 | 79 | 84 | 89 | 80 | 84 | 95 | 89 | 91 | 87 | 91 | 99 | 93 | 90 |

Table 3.1. Percent purity of PAC-1 analogues (determined by LC/MS).¹

| | 3.2(1) | 3.2(2) | 3.2(3) | 3.2(4) | 3.2(5) | 3.2(6) | 3.2(7) | 3.2(8) | 3.2(9) | 3.2(10) | 3.2(11) | 3.2(12) | 3.2(13) | 3.2(14) | 3.2(15) | 3.2(16) | 3.2(17) | 3.2(18) | 3.2(19) | 3.2(20) | 3.2(21) | 3.2(22) | 3.2(23) | 3.2(24) | 3.2(25) | 3.2(26) | 3.2(27) |
|---------|--------|--------|--------|--------|--------|--------|--------|--------|--------|---------|---------|---------|---------|---------|---------|---------|---------|---------|---------|---------|---------|---------|---------|---------|---------|---------|---------|
| 3.1(1) | 353.2 | 383.2 | 431.1 | 424.3 | 437.2 | 387.2 | 465.4 | 389.2 | 605.0 | 459.2 | 397.2 | 369.2 | 401.2 | 541.0 | 398.2 | 413.2 | 461.1 | 421.1 | 383.2 | 443.2 | 511.0 | 403.2 | 403.2 | 393.2 | 433.3 | **400.2 | 510.3 |
| 3.1(2) | 383.2 | 413.2 | 461.1 | 454.3 | 467.2 | 417.2 | 495.3 | 419.2 | 635.0 | 489.2 | 427.2 | 399.2 | 431.2 | 571.0 | 428.2 | 443.2 | 491.1 | 451.1 | 413.2 | *496.2 | 541.0 | 433.2 | 433.2 | 423.2 | 463.3 | **425.2 | 540.3 |
| 3.1(3) | 398.2 | 428.2 | 476.1 | 469.3 | 482.2 | 432.1 | 510.3 | 434.2 | 650.0 | 504.2 | 442.2 | 414.2 | 446.2 | 586.0 | 443.2 | 458.2 | 506.1 | 466.1 | 428.2 | 488.2 | 556.0 | 448.2 | 448.2 | 438.2 | 478.2 | **440.2 | 555.2 |
| 3.1(4) | 413.2 | 443.2 | 491.1 | 484.3 | 497.2 | 447.2 | 525.3 | 449.2 | 665.0 | 519.3 | 457.2 | 429.2 | 461.2 | 601.0 | 458.2 | 473.2 | 521.1 | 481.1 | 443.2 | 503.2 | 571.0 | 463.2 | 463.2 | 453.2 | 493.3 | **455.2 | 570.3 |
| 3.1(5) | 432.2 | 462.2 | 510.1 | 503.2 | 516.2 | 466.1 | 544.3 | 468.1 | 684.0 | 538.2 | 476.2 | 448.2 | 480.1 | 620.0 | 477.2 | 492.2 | 540.1 | 500.1 | 462.2 | 522.1 | 590.0 | 482.2 | 482.2 | 472.2 | 512.2 | **474.2 | 589.2 |
| 3.1(6) | 408.2 | 438.2 | 486.1 | 479.3 | 492.2 | 442.2 | 520.3 | 444.2 | 660.0 | 514.3 | 452.2 | 424.2 | 456.2 | 596.0 | 453.2 | 468.2 | 516.1 | 476.1 | 438.2 | 498.2 | 566.0 | 458.2 | 458.2 | 448.2 | 488.3 | **450.2 | 565.3 |
| 3.1(7) | 405.1 | 435.2 | 485.1 | 476.2 | 489.1 | 439.1 | 517.3 | 441.1 | 656.9 | 511.2 | 449.2 | 421.1 | 453.1 | 593.0 | 450.1 | 465.2 | 515.1 | 473.1 | 435.2 | 495.1 | 563.0 | 455.2 | 455.2 | 445.2 | 485.2 | **447.1 | 562.2 |
| 3.1(8) | 387.2 | 417.2 | 467.1 | 458.2 | 471.1 | 421.1 | 499.3 | 423.1 | 638.9 | 493.3 | 431.2 | 403.2 | 435.1 | 575.0 | 432.1 | 447.2 | 497.1 | 455.1 | 417.2 | 477.1 | 545.0 | 437.2 | 437.2 | 427.2 | 467.2 | **429.2 | 544.2 |
| 3.1(9) | 431.1 | 461.1 | 511.0 | 502.2 | 515.1 | 467.1 | 543.3 | 467.1 | 682.9 | 537.1 | 475.1 | 447.1 | 481.0 | 618.9 | 476.1 | 491.1 | 541.0 | 501.0 | 461.1 | 521.1 | 588.9 | 481.1 | 481.1 | 471.1 | 511.1 | **473.1 | 588.2 |
| 3.1(10) | 565.3 | 595.3 | 643.2 | 636.4 | 649.3 | 599.2 | 677.4 | 601.3 | 817.1 | 671.3 | 609.3 | 581.3 | 613.3 | 753.1 | 610.3 | 625.3 | 673.2 | 633.2 | 595.3 | 655.2 | 723.1 | 615.3 | 615.3 | 605.3 | 645.3 | **607.3 | 722.3 |
| 3.1(11) | 445.2 | 475.2 | 523.1 | 515.3 | 529.2 | 479.2 | 557.3 | 481.2 | 697.0 | 551.3 | 489.2 | 461.2 | 493.2 | 633.1 | 490.2 | 505.2 | 553.1 | 513.1 | 475.2 | 535.2 | 603.0 | 495.2 | 495.2 | 485.3 | 525.3 | **487.2 | 602.3 |
| 3.1(12) | 429.2 | 459.2 | 507.1 | 500.3 | 513.2 | 463.2 | 541.4 | 465.2 | 681.0 | 535.3 | 473.3 | 445.2 | 477.2 | 617.1 | 474.2 | 489.2 | 537.1 | 497.1 | 459.2 | 519.2 | 587.0 | 479.2 | 479.2 | 469.3 | 509.3 | 453.2 | 586.3 |
| 3.1(13) | 367.2 | 397.2 | 445.1 | 438.3 | 451.2 | 401.2 | 479.3 | 403.2 | 619.0 | 473.3 | 411.2 | 383.2 | 415.2 | 555.0 | 412.2 | 427.2 | 475.1 | 435.1 | 397.2 | 457.2 | 525.0 | 417.2 | 417.2 | 407.2 | 447.3 | **409.2 | 524.3 |
| 3.1(14) | 423.3 | 453.3 | 501.2 | 494.3 | 507.3 | 457.2 | 535.4 | 459.3 | 675.1 | 529.3 | 467.3 | 439.3 | 471.2 | 611.1 | 468.3 | 483.3 | 531.2 | 491.2 | 453.3 | 513.2 | 581.1 | 473.3 | 473.3 | 463.3 | 503.3 | **465.3 | 580.3 |
| 3.1(15) | 421.2 | 451.2 | 499.1 | 492.3 | 505.2 | 455.1 | 533.3 | 457.2 | 673.0 | 527.2 | 465.2 | 437.2 | 469.2 | 609.0 | 466.2 | 481.2 | 529.1 | 489.1 | 451.2 | 511.2 | 579.0 | 471.2 | 471.2 | 461.2 | 501.2 | **463.2 | 578.2 |
| 3.1(16) | 443.2 | 473.2 | 521.1 | 514.3 | 527.2 | 477.2 | 555.4 | 479.2 | 695.0 | 549.3 | 487.3 | 459.2 | 491.2 | 631.1 | 488.2 | 503.2 | 551.1 | 511.1 | 473.2 | 533.2 | 601.0 | 493.2 | 493.2 | 483.3 | 523.3 | **484.2 | 600.3 |
| 3.1(17) | 437.2 | 467.2 | 515.1 | 508.3 | 521.2 | 471.1 | 549.3 | 473.2 | 689.0 | 543.2 | 481.2 | 453.2 | 485.2 | 625.0 | 482.2 | 497.2 | 545.1 | 505.1 | 467.2 | 527.1 | 595.0 | 487.2 | 487.2 | 477.2 | 517.2 | **479.2 | 594.2 |
| 3.1(18) | 459.2 | 489.2 | 537.1 | 530.3 | 543.2 | 493.2 | 571.4 | 495.2 | 711.0 | 565.3 | 503.3 | 475.2 | 507.2 | 647.1 | 504.2 | 519.3 | 567.2 | 527.2 | 489.2 | 549.2 | 617.1 | 509.3 | 509.3 | 499.3 | 539.3 | **501.2 | 616.3 |
| 3.1(19) | 395.2 | 425.3 | 473.2 | 466.3 | 479.2 | 429.2 | 507.4 | 431.2 | 647.0 | 501.3 | 439.3 | 411.2 | 443.2 | 583.1 | 440.2 | 455.3 | 503.2 | 463.2 | 425.3 | 485.2 | 553.1 | 445.3 | 445.3 | 435.2 | 475.3 | **437.2 | 552.3 |
| 3.1(20) | 409.3 | 439.3 | 487.2 | 480.3 | 493.2 | 443.2 | 521.4 | 445.2 | 661.1 | 515.3 | 453.3 | 425.3 | 457.2 | 597.1 | 454.3 | 469.3 | 517.2 | 477.2 | 439.3 | 499.2 | 567.1 | 459.3 | 459.3 | 449.3 | 489.3 | **451.3 | 566.3 |
| 3.1(21) | 453.2 | 483.2 | 531.1 | 524.3 | 537.2 | 487.2 | 565.4 | 489.2 | 705.0 | 559.3 | 497.3 | 469.2 | 501.2 | 641.1 | 498.2 | 513.2 | 561.1 | 521.1 | 483.2 | 543.2 | 611.0 | 503.2 | 503.2 | 493.3 | 533.3 | **495.2 | 610.3 |
| 3.1(22) | 465.3 | 495.3 | 543.2 | 536.4 | 549.3 | 499.3 | 577.4 | 501.3 | 717.1 | 571.4 | 509.3 | 481.3 | 513.3 | 653.1 | 510.3 | 525.3 | 573.2 | 533.2 | 495.3 | 555.3 | 623.1 | 515.3 | 515.3 | 505.4 | 545.4 | **507.3 | 622.4 |
| 3.1(23) | 429.2 | 459.2 | 507.1 | 500.3 | 513.2 | 463.2 | 541.4 | 465.2 | 681.0 | 535.3 | 473.3 | 445.2 | 477.2 | 617.1 | 474.2 | 489.2 | 537.1 | 497.1 | 459.2 | 519.2 | 587.0 | 479.2 | 479.2 | 469.3 | 509.3 | **471.2 | 586.3 |
| 3.1(24) | 403.2 | 433.2 | 481.1 | 474.3 | 487.2 | 437.2 | 515.3 | 439.2 | 655.0 | 509.3 | 447.2 | 419.2 | 451.2 | 591.0 | 448.2 | 463.2 | 511.1 | 471.1 | 433.2 | 493.2 | 561.0 | 453.2 | 453.2 | 443.2 | 483.3 | **445.2 | 560.3 |
| 3.1(25) | 403.2 | 433.2 | 481.1 | 474.3 | 487.2 | 437.2 | 515.3 | 439.2 | 655.0 | 509.3 | 447.2 | 419.2 | 451.2 | 591.0 | 448.2 | 463.2 | 511.1 | 471.1 | 433.2 | 493.2 | 561.0 | 453.2 | 453.2 | 443.2 | 483.3 | **445.2 | 560.3 |
| 3.1(26) | 463.2 | 493.2 | 543.1 | 534.3 | 547.2 | 497.1 | 575.3 | 499.2 | 715.0 | 569.2 | 507.2 | 479.2 | 511.2 | 651.0 | 508.2 | 523.2 | 573.1 | 531.1 | 493.2 | 553.2 | 621.0 | 513.2 | 513.2 | 503.2 | 543.2 | **505.2 | 620.3 |
| 3.1(27) | 479.1 | 509.1 | 557.0 | 550.2 | 563.1 | 513.1 | 591.2 | 515.1 | 730.9 | 585.1 | 523.1 | 495.1 | 527.1 | 667.0 | 524.1 | 539.1 | 587.0 | 547.0 | 509.1 | 569.1 | 636.9 | 529.1 | 529.1 | 519.1 | 559.2 | **521.1 | 636.2 |
| 3.1(28) | 381.2 | 411.2 | 459.1 | 452.3 | 425.2 | 415.2 | 493.4 | 417.2 | 633.0 | 487.3 | 425.3 | 397.2 | 429.2 | 569.1 | 426.2 | 441.2 | 489.1 | 449.1 | 411.2 | 471.2 | 539.0 | 431.2 | 431.2 | 421.3 | 461.3 | 405.2 | 538.3 |
| 3.1(29) | 507.2 | 537.2 | 585.1 | 578.3 | 591.2 | 541.2 | 619.3 | 543.2 | 759.0 | 613.2 | 551.2 | 523.2 | 555.2 | 695.0 | 552.2 | 567.2 | 615.1 | 575.1 | 537.2 | 597.2 | 665.0 | 557.2 | 557.2 | 547.2 | 587.3 | **549.2 | 664.3 |
| 3.1(30) | 339.2 | 369.2 | 417.1 | 410.3 | 423.2 | 373.1 | 451.3 | 375.2 | 591.0 | 445.2 | 383.2 | 355.2 | 387.2 | 527.0 | 384.2 | 399.2 | 447.1 | 407.1 | 369.2 | 429.1 | 497.0 | 389.2 | 389.2 | 379.2 | 419.2 | **381.2 | 496.2 |
| 3.1(31) | 457.2 | 487.2 | 535.1 | 528.3 | 541.2 | 491.2 | 569.3 | 493.2 | 709.0 | 563.3 | 501.2 | 473.2 | 505.2 | 645.1 | 502.2 | 517.2 | 565.1 | 525.1 | 487.2 | 547.2 | 615.0 | 507.2 | 507.2 | 497.3 | 537.3 | **499.2 | 614.3 |

Table 3.2. Expected m/z for mass spectrometry of **PAC-1** analogues. All masses are [M+H]⁺ except as noted: *=[M+Na]⁺ and **=[M+H₂O+H]⁺.¹

| | 3.2(1) | 3.2(2) | 3.2(3) | 3.2(4) | 3.2(5) | 3.2(6) | 3.2(7) | 3.2(8) | 3.2(9) | 3.2(10) | 3.2(11) | 3.2(12) | 3.2(13) | 3.2(14) | 3.2(15) | 3.2(16) | 3.2(17) | 3.2(18) | 3.2(19) | 3.2(20) | 3.2(21) | 3.2(22) | 3.2(23) | 3.2(24) | 3.2(25) | 3.2(26) | 3.2(27) |
|---------|--------|--------|--------|--------|--------|--------|--------|--------|--------|---------|---------|---------|---------|---------|---------|---------|---------|---------|---------|---------|---------|---------|---------|---------|---------|---------|---------|
| 3.1(7) | 353.3 | 383.3 | 431.2 | 424.3 | 437.3 | 387.3 | 465.4 | 389.2 | 605.2 | 459.4 | 397.3 | 369.3 | 401.3 | 541.2 | 398.3 | 413.3 | 461.2 | 421.2 | 383.3 | 443.3 | 511.1 | 403.3 | 403.3 | 393.3 | 433.3 | **425.1 | 510.2 |
| 3.1(2) | 383.1 | 413.1 | 461.2 | 454.2 | 467.1 | 417.1 | 495.3 | 419.1 | 635.0 | 489.2 | 427.2 | 399.1 | 431.1 | 571.0 | 428.1 | 443.2 | 491.2 | 451.1 | 413.1 | **495.1 | 542.0 | 433.2 | 433.2 | 423.2 | 463.1 | **440.1 | 540.1 |
| 3.1(3) | 398.3 | 428.3 | 476.3 | 469.3 | 482.3 | 432.2 | 510.4 | 434.3 | 650.0 | 504.3 | 442.3 | 414.2 | 446.3 | 586.1 | 443.3 | 458.3 | 506.2 | 466.2 | 428.3 | 488.3 | 556.1 | 448.3 | 448.3 | 438.3 | 478.1 | **440.1 | 555.2 |
| 3.1(4) | 413.3 | 443.3 | 491.3 | 484.4 | 497.3 | 447.3 | 525.4 | 449.2 | 665.1 | 519.3 | 457.3 | 429.3 | 461.3 | 601.2 | 458.2 | 473.3 | 521.3 | 481.1 | 443.1 | 503.1 | 570.9 | 463.2 | 463.2 | 453.3 | 493.2 | **455.1 | 570.2 |
| 3.1(5) | 432.1 | 462.1 | 510.0 | 503.2 | 516.1 | 466.1 | 544.2 | 468.1 | 683.9 | 538.2 | 476.1 | 448.1 | 480.1 | 620.0 | 477.1 | 492.1 | 540.0 | 500.1 | 462.1 | 522.1 | 590.0 | 482.1 | 482.1 | 472.1 | 512.2 | **474.1 | 589.1 |
| 3.1(6) | 408.1 | 438.1 | 486.0 | 479.2 | 492.1 | 442.1 | 520.2 | 444.1 | 659.9 | 514.1 | 452.1 | 424.1 | 456.1 | 595.9 | 453.1 | 468.1 | 516.0 | 476.1 | 438.1 | 498.1 | 566.0 | 458.1 | 458.1 | 448.1 | 488.2 | **450.1 | 565.2 |
| 3.1(7) | 405.2 | 435.2 | 485.2 | 476.3 | 489.3 | 439.2 | 517.4 | 441.3 | 657.1 | 511.3 | 449.3 | 421.2 | 453.2 | 593.1 | 450.3 | 465.3 | 515.1 | 473.2 | 435.2 | 495.2 | 563.0 | 455.2 | 455.2 | 445.3 | 485.2 | **447.1 | 562.2 |
| 3.1(8) | 387.2 | 417.2 | 467.1 | 458.2 | 471.2 | 421.1 | 499.3 | 423.2 | 639.0 | 493.2 | 431.2 | 403.2 | 435.2 | 575.0 | 432.2 | 447.2 | 497.1 | 455.2 | 417.2 | 477.2 | 545.0 | 437.2 | 437.2 | 427.2 | 467.2 | **429.1 | 544.1 |
| 3.1(9) | 431.1 | 461.1 | 511.0 | 502.2 | 515.1 | 467.1 | 543.3 | 467.1 | 683.0 | 537.2 | 475.1 | 447.1 | 481.0 | 619.0 | 476.2 | 491.1 | 541.0 | 501.0 | 461.1 | 521.2 | 589.0 | 481.2 | 481.2 | 471.1 | 511.1 | **473.1 | 588.1 |
| 3.1(10) | 565.1 | 595.1 | 643.0 | 636.2 | 649.1 | 599.1 | 677.2 | 601.1 | 817.0 | 671.2 | 609.1 | 581.1 | 613.1 | 753.0 | 610.0 | 625.1 | 673.1 | 633.0 | 595.1 | 655.0 | 723.0 | 615.1 | 615.1 | 605.1 | 645.1 | **607.1 | 722.2 |
| 3.1(11) | 445.2 | 475.2 | 523.2 | 516.2 | 529.2 | 479.2 | 557.4 | 481.2 | 697.0 | 551.2 | 489.2 | 461.2 | 493.2 | 633.1 | 490.2 | 505.2 | 553.2 | 513.3 | 475.1 | **539.8 | 603.1 | 495.1 | 495.3 | 485.3 | 525.2 | **487.2 | 602.3 |
| 3.1(12) | 429.2 | 459.3 | 507.2 | 500.3 | 513.2 | 463.2 | 541.4 | 465.2 | 681.0 | 535.3 | 473.3 | 445.2 | 477.2 | 617.1 | 474.2 | 489.3 | 537.2 | 497.2 | 459.3 | 519.2 | 587.1 | 479.3 | 479.3 | 469.3 | 509.2 | 453.1 | 586.3 |
| 3.1(13) | 367.2 | 397.2 | 445.2 | 438.3 | 451.2 | 401.2 | 479.4 | 403.2 | 619.0 | 473.3 | 411.2 | 383.2 | 415.2 | 555.1 | 412.2 | 427.2 | 475.2 | 435.2 | 397.2 | 457.2 | 525.1 | 417.3 | 417.3 | 407.2 | 447.2 | **409.1 | 524.2 |
| 3.1(14) | 423.2 | 453.2 | 501.2 | 494.2 | 507.1 | 457.3 | 535.3 | 459.1 | 675.0 | 529.2 | 467.2 | 439.2 | 471.2 | 611.1 | 468.2 | 483.2 | 531.2 | 491.2 | 453.2 | 513.1 | 581.2 | 473.2 | 473.2 | 463.3 | 503.3 | **465.1 | 580.2 |
| 3.1(15) | 421.2 | 451.2 | 499.2 | 492.2 | 505.2 | 455.2 | 533.3 | 457.2 | 673.0 | 527.2 | 465.2 | 437.2 | 469.2 | 609.1 | 466.3 | 481.2 | 529.2 | 489.2 | 451.2 | 511.2 | 579.1 | 471.3 | 471.3 | 461.2 | 501.2 | **463.1 | 578.2 |
| 3.1(16) | 443.2 | 473.2 | 521.2 | 514.3 | 527.1 | 477.1 | 555.3 | 479.1 | 695.0 | 549.2 | 487.2 | 459.2 | 491.2 | 631.0 | 488.1 | 503.2 | 551.2 | 511.1 | 473.2 | **493.1 | 601.0 | 493.2 | 493.2 | 483.2 | 523.1 | **485.1 | 600.2 |
| 3.1(17) | 437.2 | 467.3 | 515.2 | 508.3 | 521.2 | 471.2 | 549.4 | 473.2 | 689.0 | 543.3 | 481.3 | 453.2 | 485.2 | 625.1 | 482.2 | 497.2 | 545.2 | 505.3 | 467.2 | 527.2 | 595.1 | 487.3 | 487.3 | 477.3 | 517.2 | **479.1 | 594.2 |
| 3.1(18) | 459.2 | 489.3 | 537.1 | 530.4 | 543.2 | 493.2 | 571.4 | 495.2 | 711.0 | 565.3 | 503.3 | 475.2 | 507.2 | 647.1 | 504.2 | 519.2 | 567.2 | 527.2 | 489.2 | 549.2 | 617.0 | 509.3 | 509.3 | 499.3 | 539.1 | **501.1 | 616.2 |
| 3.1(19) | 395.3 | 425.3 | 473.3 | 466.3 | 479.3 | 429.3 | 507.4 | 431.3 | 641.1 | 501.3 | 439.3 | 411.3 | 443.3 | 583.2 | 440.3 | 455.3 | 503.3 | 463.3 | 425.3 | 485.3 | 553.2 | 445.3 | 445.3 | 435.3 | 475.2 | **437.2 | 552.2 |
| 3.1(20) | 409.3 | 439.4 | 487.4 | 480.4 | 493.3 | 443.3 | 521.5 | 445.3 | 661.2 | 515.4 | 453.4 | 425.3 | 457.3 | 597.2 | 454.3 | 469.3 | 517.3 | 477.3 | 439.3 | 499.2 | 567.2 | 459.3 | 459.3 | 449.3 | 489.2 | **451.2 | 566.3 |
| 3.1(21) | 453.1 | 483.2 | 531.2 | 524.2 | 537.2 | 487.2 | 565.3 | 489.1 | 705.0 | 559.2 | 497.2 | 469.1 | 501.2 | 641.1 | 498.1 | 513.2 | 561.2 | 521.2 | 483.1 | 543.1 | 611.1 | 503.2 | 503.2 | 493.2 | 533.1 | **495.0 | 610.1 |
| 3.1(22) | 465.4 | 495.4 | 543.4 | 536.4 | 549.4 | 499.5 | 577.5 | 501.4 | 717.2 | 571.5 | 509.4 | 481.4 | 513.5 | 653.3 | 510.4 | 525.4 | 573.5 | 533.4 | 495.4 | 555.3 | 623.3 | 515.4 | 515.4 | 505.5 | 545.3 | **507.3 | 622.3 |
| 3.1(23) | 429.2 | 459.2 | 507.2 | 500.3 | 513.2 | 463.2 | 541.4 | 465.2 | 681.0 | 535.3 | 473.3 | 445.2 | 477.2 | 617.3 | 474.2 | 489.2 | 537.2 | 497.2 | 459.2 | 519.1 | 587.1 | 479.2 | 479.2 | 469.3 | 509.1 | **471.0 | 586.1 |
| 3.1(24) | 403.3 | 443.3 | 481.4 | 474.3 | 487.3 | 437.3 | 515.4 | 439.3 | 655.1 | 509.4 | 447.3 | 419.3 | 451.3 | 591.2 | 448.2 | 463.3 | 511.4 | 471.3 | 433.3 | 493.3 | 561.2 | 453.3 | 453.3 | 443.3 | 483.2 | **445.2 | 560.2 |
| 3.1(25) | 403.3 | 433.3 | 481.3 | 474.3 | 487.3 | 437.3 | 515.4 | 439.3 | 655.1 | 509.4 | 447.3 | 419.3 | 451.3 | 591.2 | 448.2 | 463.3 | 511.0 | 471.3 | 433.3 | 493.3 | 561.2 | 453.3 | 453.3 | 443.3 | 483.2 | **445.2 | 560.2 |
| 3.1(26) | 463.1 | 493.2 | 543.1 | 534.2 | 547.1 | 497.1 | 575.3 | 499.1 | 714.9 | 569.2 | 507.2 | 479.1 | 511.1 | 651.0 | 508.1 | 523.2 | 573.1 | 531.1 | 493.1 | 553.1 | 621.0 | 513.2 | 513.2 | 503.1 | 543.0 | **505.0 | 620.1 |
| 3.1(27) | 479.2 | 509.2 | 557.2 | 550.2 | 563.2 | 513.2 | 591.3 | 515.2 | 731.0 | 585.2 | 523.2 | 495.2 | 527.2 | 667.1 | 524.2 | 539.2 | 587.3 | 547.2 | 509.2 | 569.0 | 637.1 | 529.2 | 529.2 | 519.2 | 559.1 | **521.0 | 636.1 |
| 3.1(28) | 381.3 | 411.3 | 459.3 | 452.3 | 425.2 | 415.3 | 493.4 | 417.3 | 633.1 | 487.4 | 425.2 | 397.2 | 429.3 | 569.2 | 426.2 | 441.2 | 489.1 | 449.3 | 411.3 | 471.3 | 539.2 | 431.2 | 431.3 | 421.3 | 461.2 | 405.2 | 538.2 |
| 3.1(29) | 507.3 | 537.3 | 585.4 | 578.4 | 591.3 | 541.4 | 619.5 | 543.3 | 759.2 | 613.4 | 551.3 | 523.3 | 555.4 | 695.3 | 552.3 | 567.3 | 615.4 | 575.4 | 537.3 | 597.3 | 665.2 | 557.4 | 557.4 | 547.4 | 587.2 | **549.2 | 664.2 |
| 3.1(30) | 339.1 | 369.1 | 417.1 | 410.1 | 423.1 | 373.1 | 451.2 | 375.1 | 590.9 | 445.1 | 383.1 | 355.1 | 387.1 | 527.0 | 384.1 | 399.1 | 447.0 | 407.0 | 369.1 | 429.1 | 497.0 | 389.1 | 389.1 | 379.1 | 419.2 | **381.1 | 496.2 |
| 3.1(31) | 457.2 | 487.2 | 535.0 | 528.2 | 541.2 | 491.1 | 569.3 | 493.2 | 709.0 | 563.2 | 501.2 | 473.2 | 505.1 | 645.0 | 502.2 | 517.2 | 565.1 | 525.1 | 487.2 | 547.2 | 615.0 | 507.2 | 507.2 | 497.2 | 537.2 | **499.2 | 614.3 |

Table 3.3. Observed m/z for mass spectrometry of **PAC-1** analogues. All masses are [M+H]⁺ except as noted: *=[M+Na]⁺ and **=[M+H₂O+H]⁺. ***The correct m/z was not observed for these compounds.¹

3.2. Cell culture evaluation of library

With 837 **PAC-1** analogues in hand, compounds were evaluated for their ability to induce apoptosis in cell culture. U-937 human lymphoma cells were exposed to the compounds for 24 hours at a concentration of 20 μM. Both **PAC-1** and **S-PAC-1** display moderate potency (~50% cell death) versus this cell line under these conditions. Apoptotic cell death was assessed by flow cytometry, using Annexin V-FITC/propidium iodide staining. The full set of results is available in Table 3.4. Through this screening process, 61 compounds were identified that induced >80% cell death under these conditions, and re-screening the hits (Table 3.5) confirmed six potent **PAC-1** derivatives (**3.3{2,7}**, **3.3{4,7}**, **3.3{18,7}**, **3.3{20,24}**, **3.3{25,7}**, and **3.3{28,7}**).

| | 3.2(1) | 3.2(2) | 3.2(3) | 3.2(4) | 3.2(5) | 3.2(6) | 3.2(7) | 3.2(8) | 3.2(9) | 3.2(10) | 3.2(11) | 3.2(12) | 3.2(13) | 3.2(14) | 3.2(15) | 3.2(16) | 3.2(17) | 3.2(18) | 3.2(19) | 3.2(20) | 3.2(21) | 3.2(22) | 3.2(23) | 3.2(24) | 3.2(25) | 3.2(26) | 3.2(27) |
|---------|--------|--------|--------|--------|--------|--------|--------|--------|--------|---------|---------|---------|---------|---------|---------|---------|---------|---------|---------|---------|---------|---------|---------|---------|---------|---------|---------|
| 3.1(1) | 5 | 5 | 32 | 68 | 42 | 10 | 92 | 9 | 11 | 43 | 7 | 14 | 26 | 37 | 11 | 10 | 15 | 35 | 17 | 7 | 47 | 39 | 36 | 34 | 84 | 3 | 33 |
| 3.1(2) | 9 | 8 | 39 | 70 | 71 | 14 | 92 | 27 | 80 | 85 | 31 | 35 | 81 | 42 | 8 | 18 | 20 | 62 | 38 | 10 | 58 | 67 | 70 | 42 | 57 | 9 | 37 |
| 3.1(3) | 7 | 5 | 57 | 87 | 50 | 5 | 30 | 20 | 40 | 70 | 15 | 46 | 26 | 26 | 4 | 3 | 35 | 68 | 22 | 7 | 82 | 76 | 81 | 30 | 9 | 7 | 40 |
| 3.1(4) | 9 | 4 | 75 | 84 | 62 | 7 | 99 | 30 | 61 | 66 | 7 | 50 | 42 | 51 | 5 | 6 | 20 | 46 | 25 | 6 | 41 | 84 | 67 | 26 | 35 | 4 | 28 |
| 3.1(5) | 3 | 3 | 5 | 51 | 3 | 3 | 65 | 3 | 4 | 57 | 5 | 4 | 3 | 3 | 3 | 4 | 3 | 3 | 4 | 3 | 3 | 21 | 40 | 5 | 4 | 6 | 3 |
| 3.1(6) | 7 | 4 | 35 | 66 | 58 | 5 | 78 | 26 | 45 | 58 | 11 | 55 | 48 | 25 | 6 | 37 | 9 | 43 | 40 | 2 | 46 | 73 | 51 | 24 | 4 | 3 | 46 |
| 3.1(7) | 31 | 13 | 74 | 55 | 67 | 11 | 31 | 41 | 59 | 91 | 93 | 55 | 69 | 74 | 25 | 48 | 39 | 90 | 72 | 34 | 76 | 71 | 71 | 33 | 72 | 14 | 54 |
| 3.1(8) | 39 | 37 | 73 | 46 | 48 | 30 | 75 | 28 | 60 | 71 | 52 | 53 | 56 | 50 | 23 | 32 | 41 | 63 | 47 | 6 | 60 | 80 | 69 | 31 | 69 | 71 | 53 |
| 3.1(9) | 62 | 41 | 64 | 92 | 66 | 27 | 92 | 49 | 60 | 41 | 7 | 60 | 67 | 47 | 38 | 68 | 26 | 13 | 74 | 3 | 42 | 42 | 66 | 54 | 55 | 67 | 65 |
| 3.1(10) | 54 | 61 | 70 | 79 | 71 | 67 | 76 | 70 | 56 | 69 | 58 | 79 | 92 | 67 | 55 | 58 | 57 | 54 | 59 | 3 | 63 | 57 | 79 | 70 | 64 | 71 | 60 |
| 3.1(11) | 24 | 11 | 69 | 76 | 74 | 21 | 74 | 57 | 65 | 46 | 47 | 73 | 70 | 42 | 22 | 63 | 26 | 43 | 36 | 6 | 36 | 65 | 69 | 22 | 59 | 42 | 66 |
| 3.1(12) | 8 | 8 | 20 | 83 | 13 | 7 | 8 | 45 | 57 | 47 | 33 | 31 | 16 | 42 | 6 | 27 | 9 | 10 | 14 | 6 | 8 | 9 | 15 | 11 | 5 | 11 | 70 |
| 3.1(13) | 10 | 7 | 35 | 69 | 61 | 7 | 89 | 11 | 56 | 62 | 8 | 13 | 28 | 23 | 4 | 16 | 13 | 25 | 26 | 4 | 40 | 7 | 10 | 42 | 63 | 6 | 58 |
| 3.1(14) | 23 | 38 | 44 | 59 | 20 | 29 | 3 | 62 | 49 | 59 | 20 | 62 | 19 | 56 | 41 | 44 | 33 | 6 | 7 | 3 | 3 | 33 | 5 | 12 | 45 | 30 | 49 |
| 3.1(15) | 30 | 42 | 51 | 46 | 57 | 37 | 74 | 38 | 55 | 55 | 67 | 14 | 62 | 82 | 13 | 48 | 34 | 36 | 56 | 3 | 46 | 68 | 60 | 74 | 63 | 66 | 51 |
| 3.1(16) | 2 | 3 | 25 | 69 | 9 | 4 | 88 | 10 | 35 | 47 | 3 | 13 | 11 | 5 | 3 | 4 | 5 | 6 | 4 | 3 | 5 | 4 | 8 | 12 | 44 | 4 | 3 |
| 3.1(17) | 26 | 40 | 64 | 60 | 69 | 53 | 68 | 52 | 53 | 40 | 38 | 65 | 57 | 35 | 21 | 44 | 26 | 43 | 32 | 3 | 47 | 30 | 27 | 73 | 71 | 79 | 48 |
| 3.1(18) | 18 | 43 | 37 | 60 | 71 | 30 | 97 | 37 | 71 | 13 | 47 | 47 | 58 | 68 | 26 | 23 | 53 | 48 | 22 | 7 | 66 | 78 | 84 | 77 | 67 | 53 | 64 |
| 3.1(19) | 72 | 54 | 80 | 86 | 58 | 55 | 77 | 38 | 81 | 69 | 62 | 55 | 79 | 42 | 26 | 31 | 50 | 52 | 45 | 6 | 65 | 60 | 68 | 89 | 80 | 80 | 64 |
| 3.1(20) | 75 | 45 | 90 | 94 | 76 | 74 | 90 | 63 | 84 | 63 | 81 | 62 | 93 | 83 | 45 | 55 | 22 | 78 | 75 | 5 | 81 | 69 | 71 | 98 | 78 | 73 | 59 |
| 3.1(21) | 3 | 44 | 52 | 79 | 31 | 42 | 5 | 43 | 51 | 32 | 59 | 56 | 19 | 39 | 69 | 44 | 35 | 43 | 4 | 6 | 37 | 81 | 46 | 8 | 5 | 9 | 12 |
| 3.1(22) | 83 | 78 | 76 | 65 | 72 | 72 | 16 | 74 | 74 | 74 | 74 | 72 | 63 | 59 | 59 | 65 | 62 | 20 | 56 | 3 | 64 | 61 | 83 | 69 | 11 | 43 | 64 |
| 3.1(23) | 55 | 62 | 63 | 74 | 64 | 58 | 6 | 53 | 38 | 48 | 59 | 61 | 43 | 66 | 58 | 80 | 62 | 69 | 37 | 6 | 86 | 70 | 84 | 17 | 5 | 13 | 23 |
| 3.1(24) | 38 | 45 | 64 | 77 | 64 | 34 | 13 | 52 | 55 | 50 | 59 | 54 | 39 | 41 | 38 | 47 | 44 | 54 | 56 | 6 | 61 | 51 | 73 | 50 | 5 | 6 | 55 |
| 3.1(25) | 40 | 60 | 61 | 52 | 77 | 41 | 87 | 36 | 83 | 50 | 59 | 45 | 77 | 58 | 31 | 59 | 47 | 68 | 66 | 7 | 60 | 75 | 85 | 72 | 48 | 51 | 69 |
| 3.1(26) | 78 | 64 | 81 | 80 | 75 | 64 | 3 | 58 | 63 | 62 | 63 | 68 | 29 | 67 | 69 | 36 | 64 | 63 | 55 | 4 | 27 | 46 | 74 | 97 | 6 | 8 | 33 |
| 3.1(27) | 20 | 29 | 54 | 76 | 38 | 35 | 7 | 46 | 43 | 81 | 54 | 53 | 32 | 63 | 20 | 61 | 54 | 57 | 60 | 6 | 56 | 58 | 51 | 7 | 7 | 71 | 53 |
| 3.1(28) | 4 | 4 | 50 | 53 | 2 | 5 | 96 | 16 | 62 | 52 | 4 | 27 | 34 | 21 | 2 | 3 | 3 | 51 | 6 | 4 | 46 | 7 | 67 | 76 | 3 | 75 | 74 |
| 3.1(29) | 11 | 14 | 19 | 80 | 62 | 10 | 11 | 20 | 99 | 28 | 53 | 88 | 33 | 38 | 10 | 46 | 21 | 14 | 51 | 4 | 11 | 77 | 68 | 40 | 45 | 16 | 14 |
| 3.1(30) | 2 | 3 | 20 | 67 | 9 | 4 | 31 | 3 | 33 | 55 | 5 | 39 | 5 | 45 | 10 | 34 | 27 | 42 | 10 | 3 | 19 | 70 | 31 | 4 | 4 | 5 | 5 |
| 3.1(31) | 65 | 57 | 81 | 82 | 70 | 47 | 81 | 69 | 71 | 75 | 71 | 70 | 62 | 68 | 14 | 79 | 42 | 75 | 68 | 4 | 97 | 77 | 73 | 75 | 31 | 7 | 55 |

Table 3.4. Percent cell death induced by PAC-1 analogues. U-937 cells were treated with compounds (20 μ M) for 24 hours, and cell viability was determined by Annexin V-FITC/propidium iodide staining.¹

| compound | % Cell Death | compound | % Cell Death |
|------------|--------------|------------|--------------|
| PAC-1 | 47 | 3.3{20,3} | 49 |
| S-PAC-1 | 14 | 3.3{20,4} | 62 |
| 3.3{2,7} | 94 | 3.3{20,7} | 46 |
| 3.3{2,9} | 52 | 3.3{20,9} | 47 |
| 3.3{2,10} | 35 | 3.3{20,11} | 41 |
| 3.3{2,13} | 24 | 3.3{20,13} | 55 |
| 3.3{3,4} | 30 | 3.3{20,14} | 40 |
| 3.3{3,21} | 28 | 3.3{20,21} | 41 |
| 3.3{3,23} | 35 | 3.3{20,22} | 40 |
| 3.3{4,4} | 28 | 3.3{20,24} | 91 |
| 3.3{4,7} | 92 | 3.3{22,1} | 44 |
| 3.3{4,22} | 34 | 3.3{22,23} | 45 |
| 3.3{5,7} | 69 | 3.3{23,16} | 30 |
| 3.3{7,10} | 33 | 3.3{23,21} | 33 |
| 3.3{7,11} | 26 | 3.3{23,23} | 35 |
| 3.3{7,18} | 34 | 3.3{25,7} | 87 |
| 3.3{9,4} | 33 | 3.3{25,9} | 36 |
| 3.3{10,4} | 61 | 3.3{25,23} | 36 |
| 3.3{10,13} | 71 | 3.3{26,3} | 31 |
| 3.3{12,4} | 36 | 3.3{26,4} | 38 |
| 3.3{13,7} | 58 | 3.3{26,24} | 19 |
| 3.3{15,14} | 42 | 3.3{27,10} | 34 |
| 3.3{16,7} | 43 | 3.3{28,7} | 96 |
| 3.3{17,26} | 39 | 3.3{28,8} | 33 |
| 3.3{18,7} | 94 | 3.3{29,4} | 33 |
| 3.3{18,23} | 33 | 3.3{29,9} | 38 |
| 3.3{19,3} | 42 | 3.3{29,12} | 31 |
| 3.3{19,4} | 48 | 3.3{31,3} | 35 |
| 3.3{19,9} | 48 | 3.3{31,4} | 36 |
| 3.3{19,24} | 52 | 3.3{31,7} | 45 |
| 3.3{19,25} | 48 | 3.3{31,21} | 34 |
| 3.3{19,26} | 40 | | |

Table 3.5. Results of re-screen of hit compounds identified from combinatorial library. U-937 cells were treated with compounds (20 μ M) for 24 hours, and cell viability was determined by Annexin V-FITC/propidium iodide staining. Confirmed hits are highlighted in red.¹

3.3. Cell culture, *in vitro*, and *in silico* evaluation of hit compounds

After re-synthesis of the hits, analytically pure samples of the compounds were evaluated in further biological assays. These structures and the biological results are shown in Table 3.6. The compounds were evaluated, at a range of concentrations, for their ability to induce cell death in U-937 cells. All six of these hits were found to be two- to four-fold more potent in cell culture than PAC-1 and S-PAC-1 in a 72-hour treatment.

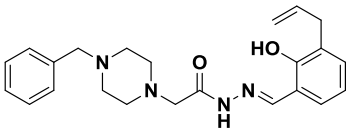
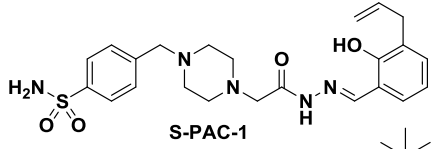
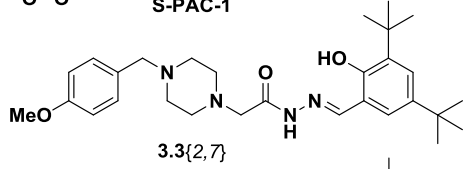
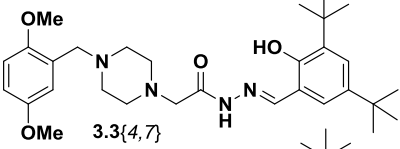
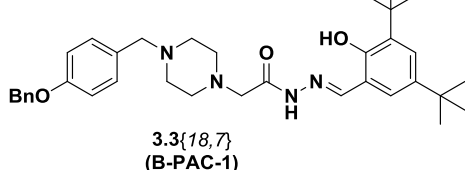
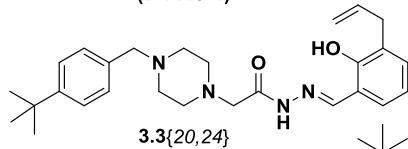
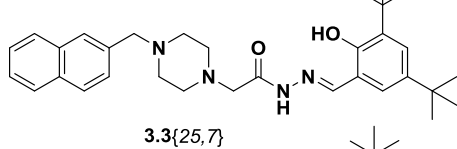
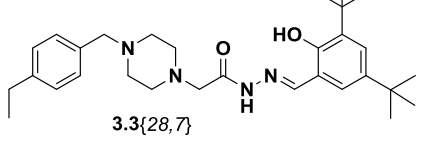
| | 72-hour IC ₅₀ (μM) | % Cell Death (24 h, 7.5 μM) | %Procaspase-3 Activity (25 μM) | Predicted logBB |
|--|----------------------------------|--------------------------------|--------------------------------------|--------------------|
|  PAC-1 | 3.8 ± 0.4 | 21 | 42 ± 1.8 | -0.37 |
|  S-PAC-1 | 4.4 ± 0.7 | 23 | 4 ± 0.6 | -1.59 |
|  3.3{2,7} | 1.8 ± 0.2 | 90 | 53 ± 4.1 | -0.24 |
|  3.3{4,7} | 1.6 ± 0.2 | 53 | 64 ± 2.5 | -0.37 |
|  3.3{18,7} (B-PAC-1) | 1.4 ± 0.2 | 97 | 36 ± 1.6 | +0.01 |
|  3.3{20,24} | 0.9 ± 0.03 | 83 | 82 ± 2.4 | -0.15 |
|  3.3{25,7} | 1.0 ± 0.04 | 50 | 69 ± 5.3 | +0.04 |
|  3.3{28,7} | 2.0 ± 0.2 | 70 | 60 ± 2.4 | +0.05 |

Table 3.6. Six library compounds induce potent cell death of U-937 cells (human lymphoma) in both 24-h^a and 72-h^b experiments and enhance enzymatic activity of procaspase-3 *in vitro*.^c Results adapted from literature.¹ Predicted BBB permeability was also calculated for all compounds.^d

(a) Cell viability determined by Annexin V-FITC/propidium iodide staining.

(b) Biomass quantified using the sulforhodamine B assay.

(c) Compounds were tested at a concentration of 50 μM with 1 μM procaspase-3 (wild-type) and 3.5 μM ZnSO_4 . Cleavage of the Ac-DEVD-pNA substrate was monitored at 405 nm and normalized to a DMSO-treated control (0%) and a zinc-free control (100%).¹

(d) Calculated using equation 3.2:¹⁸

$$\text{predicted logBB} = (-0.0148 \times \text{PSA}) + (0.152 \times \text{ClogP}) + 0.139.$$

In a second experiment, flow cytometry analysis with Annexin V-FITC/propidium iodide was performed on U-937 cells that were exposed to the compounds at a single concentration (7.5 μM) for 24 hours (Table 3.6 and Figure 3.2). As demonstrated by the histograms in Figure 3.2, the majority of the compound-treated cells were undergoing apoptosis within 24 hours (cells in the lower right quadrant of the histogram – Annexin V positive, propidium iodide negative), or were in a late apoptotic/necrotic stage (upper right quadrant – Annexin V positive, propidium iodide positive). The novel analogues were found to be more potent than **PAC-1** under these 24 hour conditions.

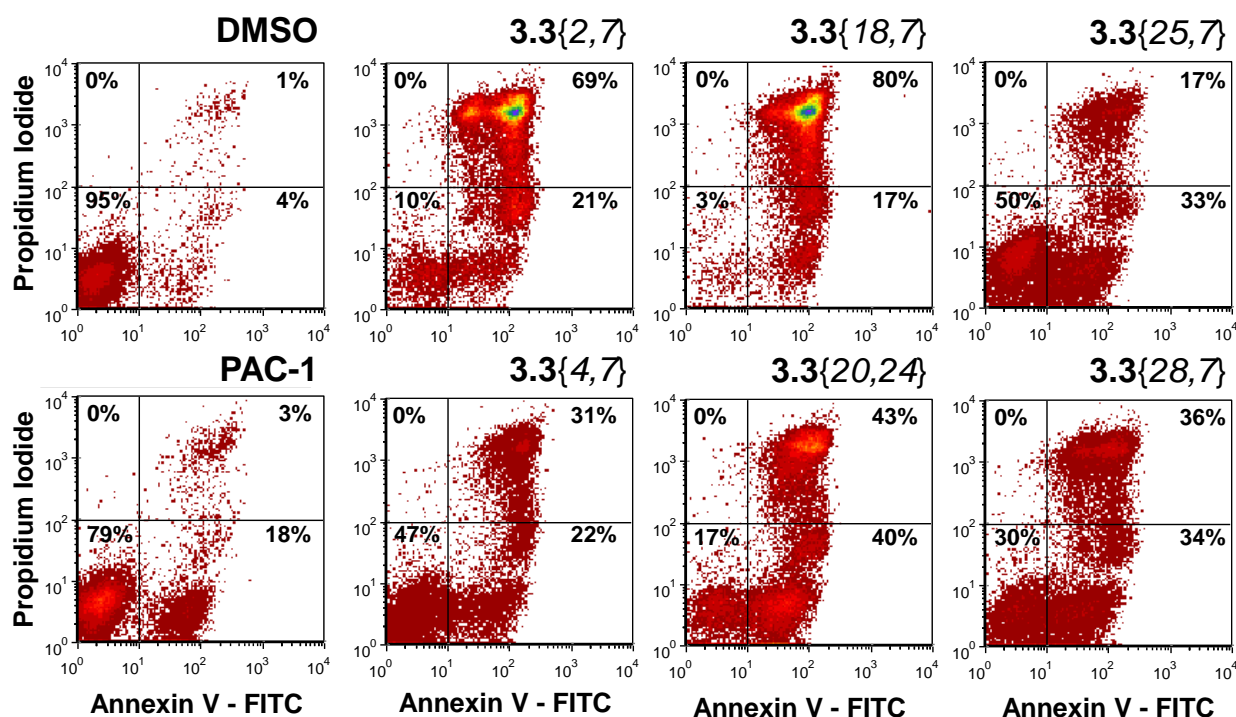


Figure 3.2. Annexin V-FITC/propidium iodide staining of U-937 cells treated with 7.5 μM of each compound for 24 hours.¹

The six confirmed hits were then evaluated *in vitro* for their ability to relieve zinc-mediated inhibition of procaspase-3 (Table 3.6 and Figure 3.3). In this experiment, procaspase-3 was incubated with ZnSO₄, conditions under which procaspase-3 has >95% reduction in enzymatic activity.^{2, 19} All compounds were able to restore procaspase-3 enzymatic activity under these conditions (as assessed by the cleavage of the colorimetric caspase-3 substrate Ac-DEVD-pNA, synthesized as previously reported²⁰), and five of the six hit compounds showed greater activity than **PAC-1** in this assay. These data indicate that the compounds enhance the activity of procaspase-3 *in vitro* through chelation of inhibitory zinc, and suggest that in the cell the compounds chelate zinc from the labile pool, allowing procaspase-3 to be processed to active caspase-3, leading to apoptotic cell death.

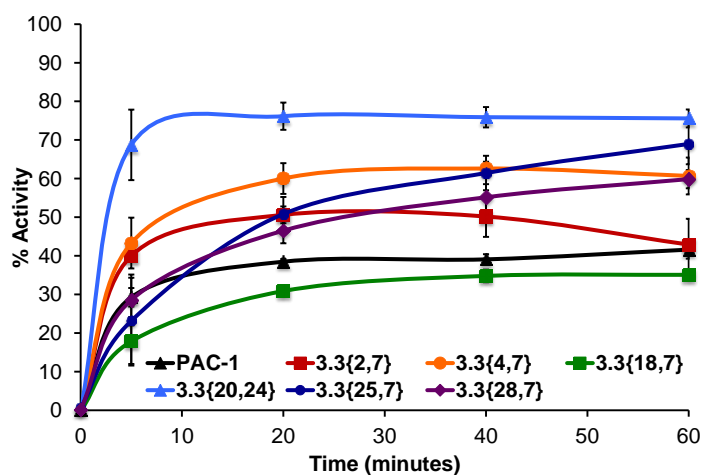


Figure 3.3. Relief of zinc-mediated inhibition of 1 μ M procaspase-3 (wild-type) by **PAC-1** and hit compounds, as measured by the processing of the Ac-DEVD-pNA substrate. Compounds were tested at a concentration of 50 μ M with 3.5 μ M ZnSO₄ and normalized to a DMSO-treated control (0%) and a zinc-free control (100%), and substrate cleavage was monitored at 405 nm.¹

Finally, because **PAC-1** and derivatives are under investigation both for tumors of the central nervous system and for the remainder of the body, it is important to determine whether any **PAC-1** derivative will enter the brain. The ability of a small molecule to penetrate the blood-brain barrier (BBB) is commonly represented as logBB (Equation 3.1):

$$\log_{10}BB = \log_{10}([\text{compound}]_{\text{brain}}/[\text{compound}]_{\text{blood}}) \quad (\text{Equation 3.1})$$

where $[\text{compound}]_{\text{brain}}$ and $[\text{compound}]_{\text{blood}}$ represent concentrations of the analyte in the brain and the blood, respectively. A negative $\log_{10}BB$ value indicates that the concentration is higher in the blood, while a positive value indicates higher concentration in the brain, and equal concentrations in brain and blood result in a $\log_{10}BB$ of 0.²¹ The prediction algorithm used herein (Equation 3.2) involves polar surface area (PSA) and the calculated logarithm of the octanol/water partition coefficient (AlogP):¹⁸

$$\text{predicted } \log_{10}BB = (-0.0148 \times \text{PSA}) + (0.152 \times \text{AlogP}) + 0.139 \quad (\text{Equation 3.2})$$

The PSA and AlogP values for **PAC-1** and derivatives were calculated using the Schrodinger software, and insertion of these values into Equation 3.2 gave the predicted $\log_{10}BB$ values (Table 3.6). **PAC-1** has a predicted $\log_{10}BB$ value of -0.37, which is very close to the experimentally determined value of -0.36.²² In general, the six hits contain relatively hydrophobic substituents, and five of them have predicted $\log_{10}BB$ values substantially higher than that of **PAC-1**. Compound **3.3**{4,7} contains two relatively polar methoxy substituents, which offset the highly hydrophobic *tert*-butyl substituents, and the predicted $\log_{10}BB$ value is identical to that of **PAC-1**.

3.4. Evaluation of **B-PAC-1**

Because it was potent in cell culture, stable in rat liver microsomes, and well tolerated in mice following a single 100 mg/kg i.p. dose, compound **3.3**{18,7} was selected for further evaluation and given the name **B-PAC-1** (referring to the benzyloxy and butyl substituents). The pharmacokinetics of **B-PAC-1** were evaluated following i.v. and oral administration, and compared to equivalent doses of **PAC-1** (Figure 3.4A). Pharmacokinetic curves for **PAC-1** show an initial increase in concentration, followed by a rapid decrease, and the compound is not detectable in serum later than four hours post-administration following i.v. or oral administration. In contrast, **B-PAC-1** achieves a lower maximum concentration upon i.v. or oral administration as compared to **PAC-1**, but the serum concentrations remain relatively constant

between two and eight hours post-administration. These flat concentration-time curves are unusual, and further studies are necessary to fully understand the pharmacokinetics of **B-PAC-1**.

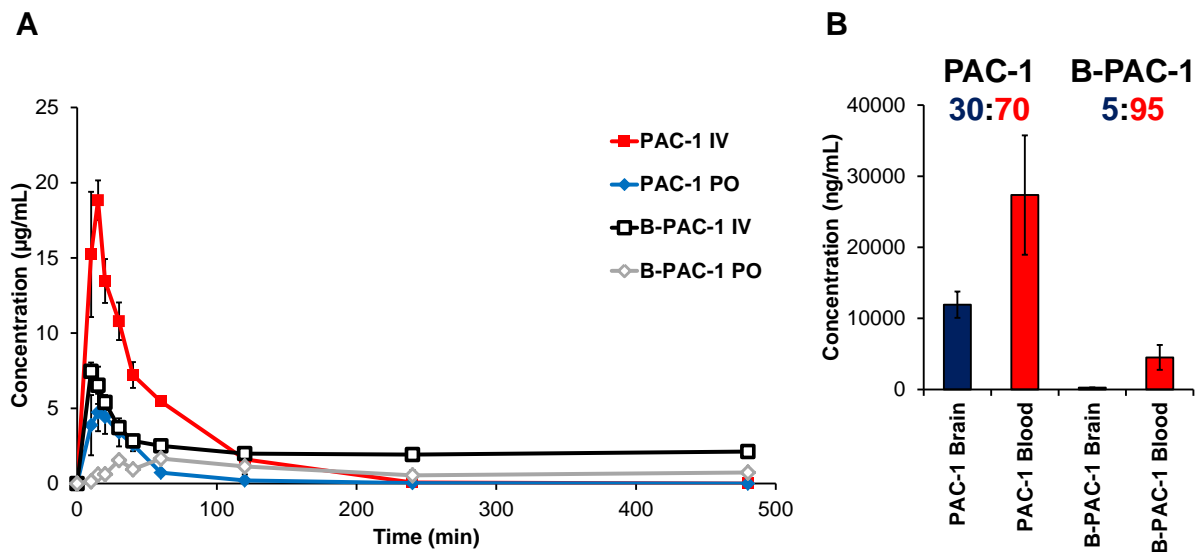


Figure 3.4. *In vivo* evaluation of **PAC-1** and **B-PAC-1**. **A.** Comparison of pharmacokinetics. Mice received **PAC-1** or **B-PAC-1** at 50 mg/kg (dissolved in HP β CD) at 50 mg/kg via lateral tail vein injection or oral gavage. **B.** Comparison of BBB permeability. Mice received **PAC-1** or **B-PAC-1** at 75 mg/kg (dissolved in HP β CD) via lateral tail vein injection. Concentrations of compounds within serum and brain tissue 5 minutes post-injection. Results for **PAC-1** BBB permeability from literature.²² Error bars indicate standard deviation ($n \geq 3$).

In addition, the BBB permeability of **B-PAC-1** was determined and compared to the previously determined results for **PAC-1** (Figure 3.4B).²² Mice were administered compound at 75 mg/kg, and then sacrificed after 5 minutes. Brain and blood samples were collected, and concentrations were determined by HPLC. **PAC-1** shows a 30:70 distribution between brain and blood,²² while **B-PAC-1** shows a distribution of 5:95 between brain and blood. The experimental results for **B-PAC-1** strongly contrast the calculation derived from the prediction algorithm, which predicts approximately 50:50 distribution between brain and blood. This discrepancy may be due to the relatively large size of **B-PAC-1**, which the algorithm does not consider. It has been suggested that compounds that cross the BBB should have molecular weights below 450.²¹ **PAC-1**, with a molecular weight of 392, is small enough to enter the brain, but **B-PAC-1** has a

molecular weight of 570, well above the cutoff, and it is excluded despite its increased hydrophobicity. The decreased BBB permeability is consistent with the lack of observed neuroexcitation in response to the compound and provides support for the evaluation of **B-PAC-1** in diverse tumor types not in the central nervous system. Evaluation in primary leukemic lymphocytes has shown promise,²³ and further experiments are underway.

3.5. Discussion

The modular nature of the **PAC-1** synthesis allows for the assembly of **PAC-1** derivatives via the late-stage condensation of a hydrazide with an aldehyde to form the essential *ortho*-hydroxy-*N*-acylhydrazone, which has been utilized for the construction of many **PAC-1** derivatives.^{1-3, 5-15} This allows for the creation of a large number of diverse molecules from a relatively small number of building blocks, as the diversification occurs during the final synthetic step. In this report, a total of 58 building blocks (31 hydrazides and 27 aldehydes) were used to produce 837 **PAC-1** derivatives.¹

For compound libraries of this size, traditional methods of synthesis and purification are impractical; reaction flasks would require a large amount of space, and chromatographic purification of all of the library members would be costly and would likely require months to complete. Therefore, a strategy was developed that allowed for the rapid and efficient generation of **PAC-1** derivatives. Each aldehyde was reacted with an excess of each hydrazide, and when consumption of the aldehyde was complete, resin-bound aldehyde was added to scavenge the remaining hydrazide, forming solid-phase hydrazones that could be removed by filtration. Using a parallel synthesizer, it was possible to perform 80 reactions simultaneously. The entire process was complete in approximately one week, which represents a significantly shorter time than would be required for the synthesis of 80 **PAC-1** analogues using chromatographic purification. While this report described the creation of **PAC-1** derivatives, the strategy represents a general method for the synthesis of combinatorial libraries of diverse compounds. In theory, this strategy could be adopted for other reactions of two compatible building blocks, including alkylations, acylations, reductive aminations, or dipolar cycloadditions, and a scavenger resin could remove excess unreacted starting materials. However, one main reason the strategy was successful for this application is because of the efficiency of hydrazone formation, and it may be more

challenging to apply this strategy to less robust reactions, such as metal-catalyzed cross-couplings or alkene metathesis reactions.

The resin purification strategy generated compounds of relatively high purity, and compounds of the highest possible purity were not necessary for the initial cell death screen. Secondary assays required compounds of higher purity, so the six hit compounds were resynthesized and purified more rigorously. If the goal in a drug discovery campaign is the rapid generation of large numbers of derivatives in order to identify a smaller number of active compounds, then the strategy described herein is a useful method. However, if a more thorough understanding of structure-activity relationships for a given compound series through complex biochemical assays is required, compounds generated via this method may not be pure enough, and traditional methods for purification may be more appropriate. An application of the traditional synthetic approach for **PAC-1** derivatives is presented in Chapter 4.

The six compounds shown in Table 3.6 emerged from the combinatorial library; these compounds are two- to four-fold more potent than **PAC-1** at induction of cancer cell death in both 24-hour and 72-hour assays. Of note, five of the six hit compounds contain two *tert*-butyl substituents on the benzylidene ring, while the sixth contains a *tert*-butyl substituent on the benzyl ring. There are several marketed drugs containing aryl *tert*-butyl groups, including the antihistamine buclizine, the CFTR potentiator ivacaftor for the treatment of cystic fibrosis, and the mutant B-Raf kinase inhibitor dabrafenib for the treatment of metastatic melanoma. However, introduction of the *tert*-butyl substituent is often accompanied by a substantial increase in logD and logP, which can lead to decreased aqueous solubility and increased rate of metabolism. Several bioisosteric replacements for the *tert*-butyl group have been proposed, many of which rely on fluorine substitution to reduce hydrophobicity and block undesired metabolism.²⁴ It is possible that these isosteric replacements could be beneficial for further development of the **PAC-1** derivatives described herein, although at least one compound, **B-PAC-1**, is not cleared rapidly from circulation.

Given the general hydrophobicity of the hit compounds relative to **PAC-1**, it is possible that the enhanced potency and rate of cell death are driven by enhanced cell permeability. These qualities are likely to be advantageous as the compounds are moved forward *in vivo*. In addition, it is possible that other members of this library will emerge as viable *in vivo* candidates as alternate properties (such as propensity to cross the blood-brain barrier, improved metabolic

stability, improved solubility/formulation for *in vivo* studies, etc.) are examined. Thus, this library of 837 compounds represents a rich source from which to develop next-generation procaspase-3 activating compounds.

3.6. Materials and methods

3.6.1. Chemical information

General All reactions requiring anhydrous conditions were conducted under a positive atmosphere of nitrogen or argon in oven-dried glassware. Standard syringe techniques were used for anhydrous addition of liquids. Unless otherwise noted, all starting materials, solvents, and reagents were acquired from commercial suppliers and used without further purification. Flash chromatography was performed using 230-400 mesh silica gel. A full set of experimental details is available in the literature.¹

Compound Analysis All NMR experiments were recorded in CDCl₃ (Sigma or Cambridge) on a Varian Unity 500 MHz spectrometer with residual undeuterated solvent as the internal reference for ¹H-NMR (7.26 ppm) and ¹³C-NMR (77.23 ppm). Chemical shift, δ (ppm); coupling constants, *J* (Hz); multiplicity (s = singlet, d = doublet, t = triplet, q = quartet, quint = quintet, sext = sextet, m = multiplet, br = broad); and integration are reported. High-resolution mass spectral data was recorded on a Micromass Q-ToF Ultima hybrid quadrupole/time-of-flight ESI mass spectrometer or a Micromass 70-VSE at the University of Illinois Mass Spectrometry Laboratory.

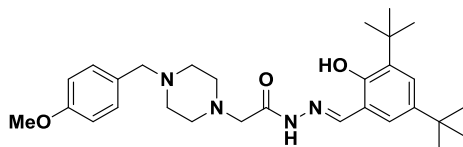
General Procedure A: Synthesis of PAC-1 analogue library.

To a 16 × 150 mm test tube were added hydrazide (1.7 equiv.), aldehyde (1.0 equiv.), 2-ethoxyethanol (1 mL), and 1.2 M HCl (10 mol %). The tubes were shaken on a Büchi Syncore parallel synthesizer at 110 °C until all aldehyde had reacted (monitoring by ESI-MS). The reaction mixture was cooled to room temperature, and polystyrene-benzaldehyde (3.5 equiv.) was added. The reaction mixture was shaken at 25–80°C until no hydrazide remained (monitoring by ESI-MS). The reaction mixture was cooled to room temperature, and the resin was filtered and washed with 2-ethoxyethanol. The filtrate was dried under high vacuum to afford the PAC-1 analogue.

General Procedure B: Synthesis of hit compounds.

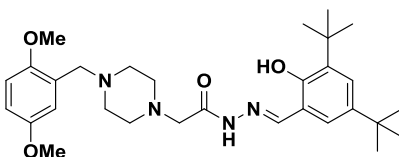
To a stirred solution of hydrazide (1.0 equiv.) and aldehyde (1.0 equiv.) in EtOH (0.15 M) was added 1.2 M HCl (7 mol%). The reaction mixture was stirred at reflux overnight. The reaction mixture was cooled to room temperature and concentrated. The crude product was purified by silica gel column chromatography to yield pure **PAC-1** analogue.

***N'*-(3,5-di-tert-butyl-2-hydroxybenzylidene)-2-(4-(4-methoxybenzyl)piperazin-1-yl)acetohydrazide (3.3{2,7})**



Synthesized according to General Procedure B: hydrazide (**3.1{2}**, 112 mg, 0.40 mmol, 1.0 equiv.), aldehyde (**3.2{7}**, 94 mg, 0.40 mmol, 1.0 equiv.), EtOH (3 mL, 0.15 M), 1.2 M HCl (7 mol%). A white crystalline solid formed upon cooling. The crystals were filtered and washed with cold EtOH to yield **3.3{2,7}** (118 mg, 59.0%) as a white solid without further purification. ¹H-NMR (500 MHz, CDCl₃): δ 11.32 (br s, 1H), 9.98 (br s, 1H), 8.44 (s, 1H), 7.38 (d, 1H, *J* = 2.0 Hz), 7.23 (d, 2H, *J* = 9.0 Hz), 7.05 (d, 1H, *J* = 2.5 Hz), 6.87 (d, 2H, *J* = 8.5 Hz), 3.81 (s, 3H), 3.49 (s, 2H), 3.19 (s, 2H), 2.62 (br s, 4H), 2.51 (br s, 4H), 1.44 (s, 9H), 1.30 (s, 9H). ¹³C-NMR (125 MHz, CDCl₃): δ 165.6, 158.7, 155.5, 152.4, 140.7, 136.8, 130.2, 129.6, 126.8, 125.6, 116.3, 113.6, 62.2, 60.9, 55.2, 53.6, 52.8, 35.0, 34.1, 31.4, 29.3. HRMS (ESI): 495.3340 (M+H)⁺; calcd. for C₂₉H₄₃N₄O₃: 495.3335.

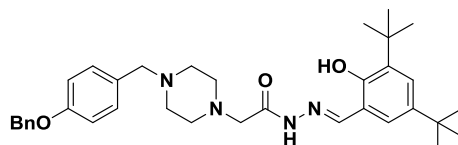
***N'*-(3,5-di-tert-butyl-2-hydroxybenzylidene)-2-(4-(2,5-dimethoxybenzyl)piperazin-1-yl)acetohydrazide (3.3{4,7})**



Synthesized according to General Procedure B: hydrazide (**3.1{4}**, 100 mg, 0.32 mmol, 1.0 equiv.), aldehyde (**3.2{7}**, 75 mg, 0.32 mmol, 1.0 equiv.), EtOH (2.2 mL, 0.15 M), 1.2 M HCl (7 mol%). Purification by silica gel column chromatography (gradient, 0-10% MeOH/EtOAc) yielded **3.3{4,7}** (106 mg, 63.2%) as a white solid. ¹H-NMR (500 MHz, CDCl₃): δ 11.34 (br s, 1H), 10.02 (br s, 1H), 8.43 (s, 1H), 7.38 (d, 1H, *J* = 2.5 Hz), 7.05 (d, 1H, *J* = 2.0 Hz), 6.97 (d, 1H, *J* = 3.0 Hz), 6.82 (d, 1H, *J* = 8.0 Hz), 6.77 (dd, 1H, *J* = 3.0, 8.0 Hz), 3.79 (s, 3H), 3.78 (s,

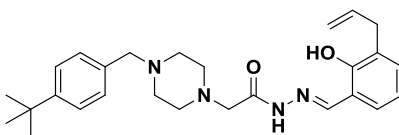
3H), 3.59 (s, 2H), 3.19 (s, 2H), 2.64 (br s, 4H), 2.59 (br s, 4H), 1.44 (s, 9H), 1.30 (s, 9H). ¹³C-NMR (125 MHz, CDCl₃): δ 165.7, 155.5, 153.5, 152.5, 152.0, 140.7, 136.8, 127.1, 126.8, 125.6, 116.5, 116.3, 112.2, 111.6, 60.9, 56.1, 55.8, 55.7, 53.7, 52.9, 35.1, 34.1, 31.4, 29.4. HRMS (ESI): 525.3449 (M+H)⁺; calcd. for C₃₀H₄₅N₄O₄: 525.3441.

2-(4-(4-(benzyloxy)benzyl)piperazin-1-yl)-N'-(3,5-di-tert-butyl-2-hydroxybenzylidene)acetohydrazide (3.3{18,7})



Synthesized according to General Procedure B: hydrazide (**3.1{18}**) 100 mg, 0.29 mmol, 1.0 equiv.), aldehyde (**3.2{7}**), 68 mg, 0.29 mmol, 1.0 equiv.), EtOH (2 mL, 0.15 M), 1.2 M HCl (7 mol%). Purification by silica gel column chromatography (gradient, 0-10% MeOH/EtOAc) yielded **3.3{18,7}** (97 mg, 58.7%) as a white solid. ¹H-NMR (500 MHz, CDCl₃): δ 11.38 (br s, 1H), 10.03 (br s, 1H), 8.43 (s, 1H), 7.45 (d, 2H, *J* = 7.0 Hz), 7.42-7.39 (m, 3H), 7.34 (t, 1H, *J* = 7.0 Hz), 7.24 (d, 2H, *J* = 8.5 Hz), 7.07 (d, 1H, *J* = 2.0 Hz), 6.96 (d, 2H, *J* = 8.5 Hz), 5.07 (s, 2H), 3.50 (s, 2H), 3.20 (s, 2H), 2.63 (br s, 4H), 2.53 (br s, 4H), 1.46 (s, 9H), 1.32 (s, 9H). ¹³C-NMR (125 MHz, CDCl₃): δ 165.7, 158.0, 155.5, 152.5, 140.7, 137.0, 136.8, 130.2, 130.0, 128.5, 127.9, 127.4, 126.8, 125.6, 116.3, 114.5, 70.0, 62.2, 60.9, 53.6, 52.8, 35.1, 34.1, 31.4, 29.4. HRMS (ESI): 571.3652 (M+H)⁺; calcd. for C₃₅H₄₇N₄O₃: 571.3648.

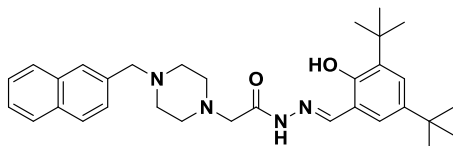
N'-(3-allyl-2-hydroxybenzylidene)-2-(4-(4-(tert-butyl)benzyl)piperazin-1-yl)acetohydrazide (3.3{20,24})



Synthesized according to General Procedure B: hydrazide (**3.1{20}**), 100 mg, 0.33 mmol, 1.0 equiv.), aldehyde (**3.2{24}**), 53.5 mg, 0.33 mmol, 1.0 equiv.), EtOH (2.2 mL, 0.15 M), 1.2 M HCl (7 mol%). Purification by silica gel column chromatography (gradient, 0-10% MeOH/EtOAc) yielded **3.3{20,24}** (102 mg, 68.9%) as a light brown solid. ¹H-NMR (500 MHz, CDCl₃): δ 11.31 (br s, 1H), 10.09 (br s, 1H), 8.38 (s, 1H), 7.36 (d, 2H, *J* = 8.5 Hz), 7.25 (d, 2H, *J* = 8.5 Hz), 7.19 (d, 1H, *J* = 7.5 Hz), 7.08 (dd, 1H, *J* = 1.5, 7.5 Hz), 6.85 (t, 1H, *J* = 7.5 Hz), 6.04 (tdd, 1H, *J* = 6.5, 10.0, 16.5 Hz), 5.12-5.06 (m, 2H), 3.52 (s, 2H), 3.47 (d, 2H, *J* = 6.5 Hz), 3.20 (s, 2H), 2.63

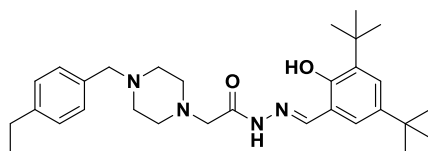
(br s, 4H), 2.54 (br s, 4H), 1.33 (s, 9H). ^{13}C -NMR (125 MHz, CDCl_3): δ 165.8, 156.3, 151.1, 150.0, 136.4, 134.6, 132.2, 129.1, 128.7, 128.1, 125.1, 118.9, 116.8, 115.6, 62.5, 60.9, 53.6, 53.0, 34.4, 33.8, 31.3. HRMS (ESI): 449.2915 ($\text{M}+\text{H}$) $^+$; calcd. for $\text{C}_{27}\text{H}_{37}\text{N}_4\text{O}_2$: 449.2917.

***N'*-(3,5-di-tert-butyl-2-hydroxybenzylidene)-2-(4-(naphthalen-2-ylmethyl)piperazin-1-yl)acetohydrazide (3.3{25,7})**



Synthesized according to General Procedure B: hydrazide (**3.1{25}**), 100 mg, 0.34 mmol, 1.0 equiv.), aldehyde (**3.2{7}**), 80 mg, 0.34 mmol, 1.0 equiv.), EtOH (2.3 mL, 0.15 M), 1.2 M HCl (7 mol%). Purification by silica gel column chromatography (gradient, 0-10% MeOH/EtOAc) yielded **3.3{25,7}** (142 mg, 81.3%) as a white solid. ^1H -NMR (500 MHz, CDCl_3): δ 11.40 (br s, 1H), 10.05 (br s, 1H), 8.43 (s, 1H), 7.86-7.83 (m, 3H), 7.75 (s, 1H), 7.53-7.43 (m, 3H), 7.41 (d, 1H, $J = 2.5$ Hz), 7.07 (d, 1H, $J = 2.5$ Hz), 3.72 (s, 2H), 3.21 (s, 2H), 2.65 (br s, 4H), 2.59 (br s, 4H), 1.47 (s, 9H), 1.33 (s, 9H). ^{13}C -NMR (125 MHz, CDCl_3): δ 165.6, 155.5, 152.4, 140.7, 136.8, 135.3, 133.2, 132.7, 127.9, 127.6, 127.6, 127.6, 127.3, 126.8, 126.0, 125.6, 125.6, 116.3, 62.9, 60.9, 53.6, 53.0, 35.0, 34.1, 31.4, 29.4. HRMS (ESI): 515.3389 ($\text{M}+\text{H}$) $^+$; calcd. for $\text{C}_{32}\text{H}_{43}\text{N}_4\text{O}_2$: 515.3386.

***N'*-(3,5-di-tert-butyl-2-hydroxybenzylidene)-2-(4-(4-ethylbenzyl)piperazin-1-yl)acetohydrazide (3.3{28,7})**



Synthesized according to General Procedure B: hydrazide (**3.1{28}**), 26 mg, 0.094 mmol, 1.0 equiv.), aldehyde (**3.2{7}**), 22 mg, 0.094 mmol, 1.0 equiv.), EtOH (1 mL), 1.2 M HCl (7 mol%). Purification by silica gel column chromatography (gradient, 0-10% MeOH/EtOAc) yielded **3.3{28,7}** (34.6 mg, 75%) as a white solid. ^1H -NMR (500 MHz, CDCl_3): δ 11.33 (br s, 1H), 10.00 (br s, 1H), 8.43 (s, 1H), 7.38 (d, 1H, $J = 2.0$ Hz), 7.23 (d, 2H, $J = 8.0$ Hz), 7.17 (d, 2H, $J = 8.0$ Hz), 7.05 (d, 1H, $J = 2.5$ Hz), 3.52 (s, 2H), 3.19 (s, 2H), 2.65 (q, 2H, $J = 7.5$ Hz), 2.63 (br s, 4H), 2.53 (br s, 4H), 1.44 (s, 9H), 1.30 (s, 9H), 1.24 (t, 3H, $J = 7.5$ Hz). ^{13}C -NMR (125 MHz, CDCl_3): δ 165.7, 155.6, 152.6, 143.2, 140.7, 136.9, 134.9, 129.1, 127.8, 126.9, 125.6, 116.3,

62.6, 61.0, 53.7, 53.0, 35.1, 34.1, 31.5, 29.4, 28.5, 15.6. HRMS (ESI): 493.3550 (M+H)⁺; calcd. for C₃₀H₄₅N₄O₂: 493.3543.

3.6.2. Biological evaluation

Materials All reagents were obtained from Fisher unless otherwise indicated. All buffers were made with MilliQ purified water. Ac-DEVD-pNA was synthesized as previously described.²⁰ Luria broth (LB) was obtained from EMD. Doxorubicin was obtained from Sigma. Caspase Activity Buffer contains 50 mM HEPES, 300 mM NaCl, 1.5mM TCEP, 0.01% TritonX-100 and is Chelex® treated. Ni NTA Binding Buffer contains 50 mM Tris (pH 8.0), 300 mM NaCl, and 10mM imidazole. Ni NTA Wash Buffer contains 50 mM Tris (pH 8.0), 300 mM NaCl, and 50 mM imidazole. Ni NTA Elution Buffer contains 50 mM Tris (pH 8.0), 300 mM NaCl, and 500 mM imidazole. Annexin V Binding Buffer contains 10 mM HEPES pH 7.4, 140 mM NaCl, 2.5 mM CaCl₂, 0.1% BSA. The C-terminal 6xHis-tagged procaspase-3 proteins were expressed as described below.

Cell Culture U-937 cells were obtained from the American Type Culture Collection and maintained at low passage number. Cultures were maintained in RPMI 1640 supplemented with 10% fetal bovine serum and 1% penicillin-streptomycin and grown at 37°C and 5% CO₂.

Cell Death Assay for Initial Screen Compound (2 µL of a 10 mM DMSO solution) was added in singlet by direct addition to a well containing 998 µL U-937 cells (1x10⁶) in RPMI 1640 media (10% FBS) at a final compound concentration of 20 µM. After incubation at 37°C for 24 h, the cells were transferred to flow cytometry tubes, washed, and resuspended in Annexin V binding buffer. The cells were double stained with FITC-Annexin V and propidium iodide and a cell population of at least 10,000 events was collected by the LSR II flow cytometer. Percent viable cells (Annexin V- negative, propidium iodide - negative) were determined using FCS Express software.

72hr IC₅₀ Cell Death Assay U-937 human lymphoma cells were plated into the wells of 96 well plate at a density of 15,000 cells per well in 99 µL of RPMI 1640 growth media with 10% FBS and 1% pen-strep. To each well was added 1 µL of compound stock solutions in DMSO at varying concentrations such that the cells were treated with concentrations between 0 µM and 100 µM compound. Each concentration was tested in quintuplicate per plate. In each plate 5 wells received 20 µM doxorubicin as a positive death control and 5 wells received 1 µL of

DMSO as a negative control. The plates were then incubated at 37°C and 5% CO₂ for 72 hours. After the 72 hour incubation period, the plates were analyzed using a Sulforhodamine B assay.²⁵ Specifically, to each well of the plate 25 µL of a 50% (w/v) solution of trichloroacetic acid in H₂O was added and the plates were incubated for 4 hours at 4°C. The plates were then washed gently with H₂O five times. The plates were allowed to air dry after which 100 µL of a 0.057% (w/v) Sulforhodamine B in a 1% (v/v) acetic acid solution was added to each well for 30 minutes at room temperature. The plates were gently washed 5 times with 1% (v/v) acetic acid and air dried. 200 µL of 10 mM Tris base (pH 10.4) was added to each well and the plates were placed on an orbital shaker for thirty minutes. The level of SRB was quantified fluorometrically at excitation and emission wavelengths 488 and 585nm, respectively, on a Molecular Devices plate reader and the percent cell death calculated and normalized to the positive control (100% cell death) and the negative control (0% cell death). The percent cell death was averaged for each compound concentration and plotted as a function of compound concentration. The data were fit to a logistical dose response curve using Table curve 2D and the IC₅₀ value was calculated. The experiment was repeated three times and the average of the calculated IC₅₀ values was reported. The standard error of the mean (SEM) was determined and reported for the triplicate experiments.

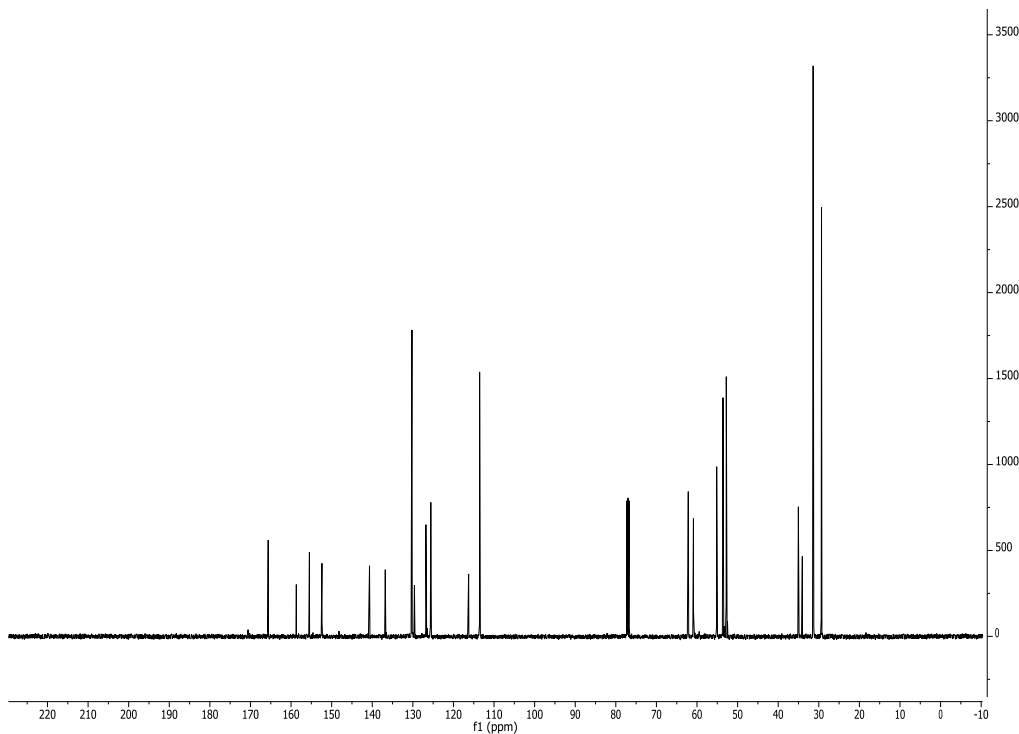
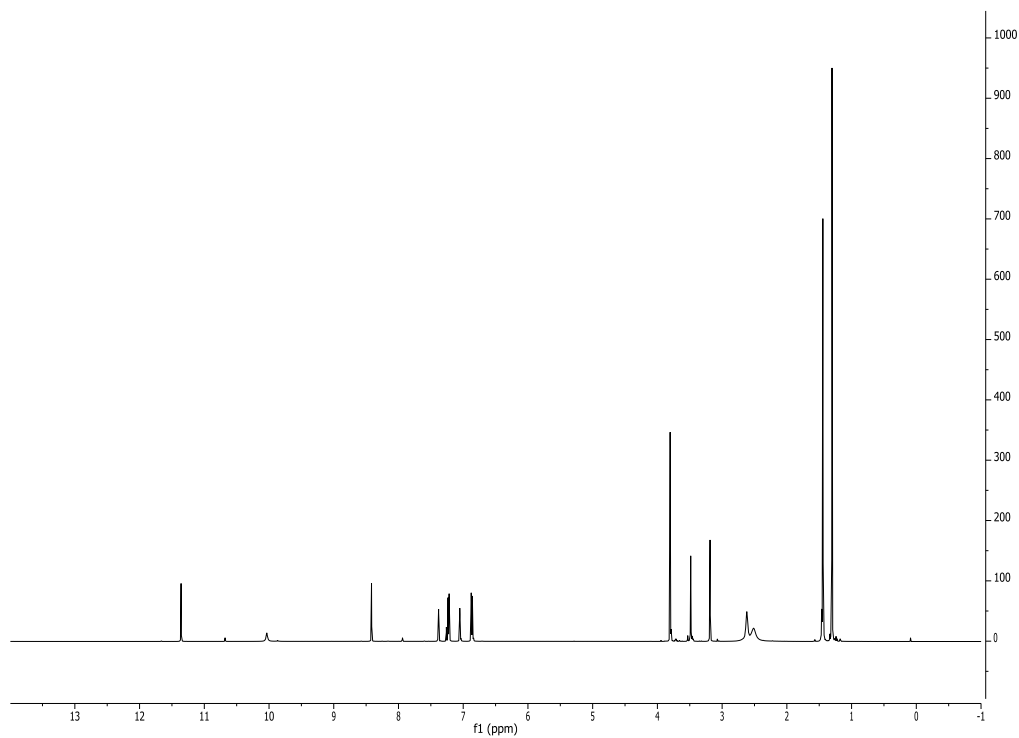
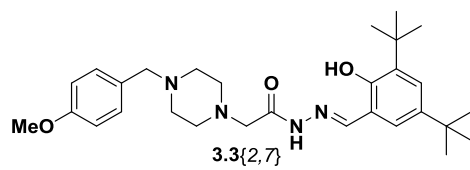
Induction of Apoptosis by Hit Compounds U-937 Cells (1 mL of 6 x 10⁵ cells/mL) were treated with 10 µL of 750µM DMSO solutions of the compounds to achieve a final concentration of 7.5 µM. The cells were incubated at 37 °C for 24 hours. The cells were harvested via centrifugation (200g for 5 min), washed with PBS (2 mL), and resuspended in 450 µL Annexin V Binding Buffer. To each sample was added 3.5 µL of FITC conjugated Annexin V stain (Southern Biotech) and 3.5 µL of propidium iodide (Sigma) to a final concentration of 50 µg/mL. Cell populations were analyzed on a Benton Dickinson LSR II cell flow cytometer.

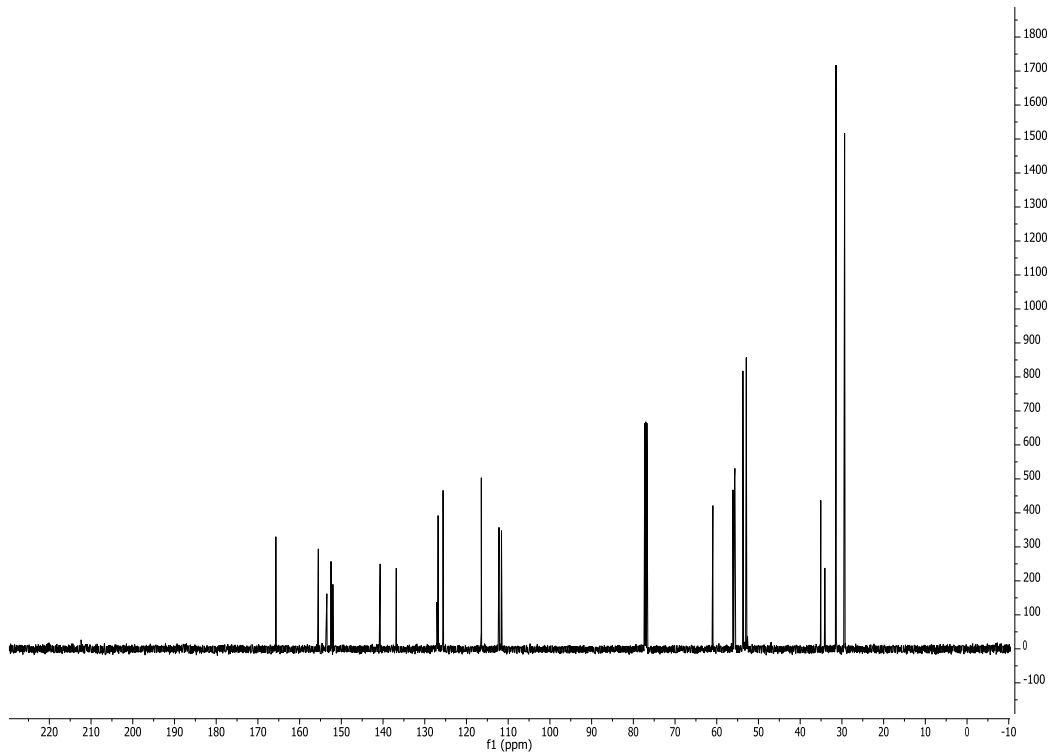
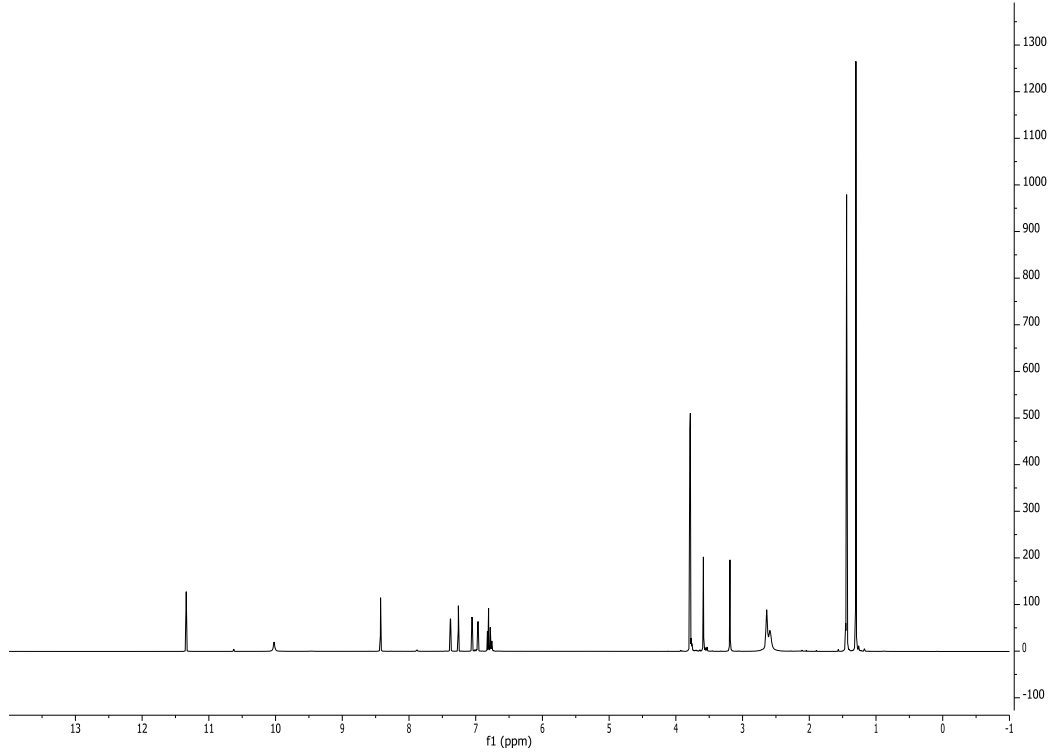
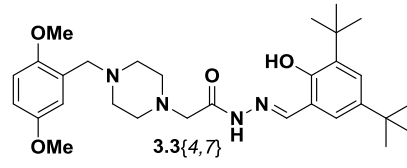
Recombinant Expression and Purification of Procaspace-3 Adapted from reference.⁵ A 20 mL volume of an overnight culture of *Rosetta E. coli* containing the procaspase-3 (wild-type) expression plasmid was seeded into 2 L of LB media containing ampicillin. The culture was grown to an OD₆₀₀ = 1.0, at which point protein expression was induced via addition of IPTG (to 1 mM); the culture was allowed to grow for 30 additional minutes. Cells were then harvested (10 minute spins at 10,000xg and re-suspended in NTA binding buffer (300 mM NaCl, 50 mM Tris, 10 mM imidazole, pH 8.0). The cells were lysed on ice via sonication. The cell lysate was

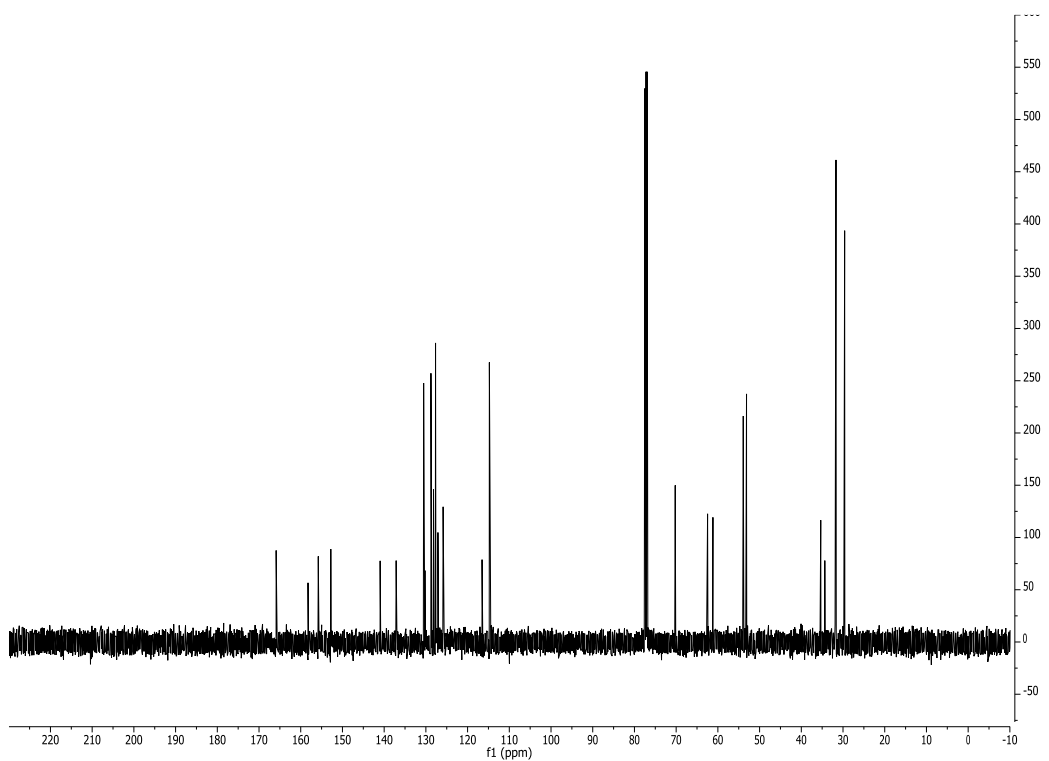
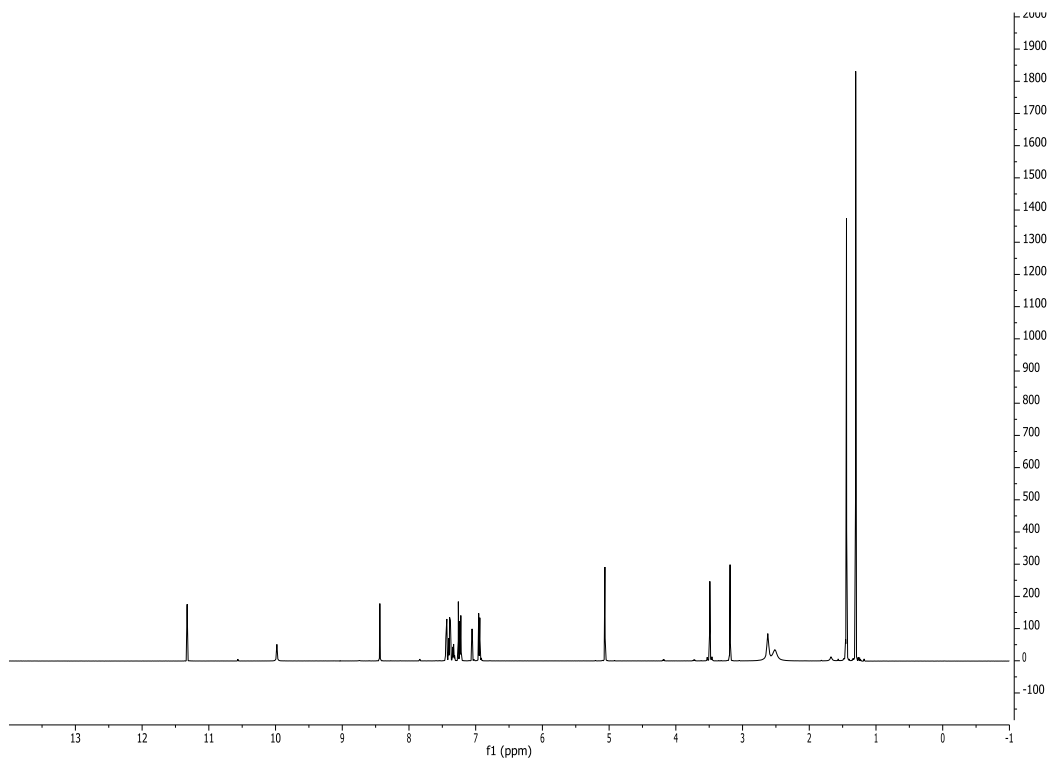
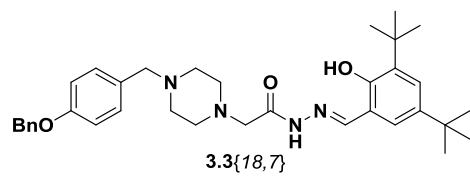
then spun at 35,000xg for 35 min. The supernatant was decanted and 1 mL of nickel-NTA resin was added. The cell lysate was incubated for 45 minutes at 4°C. The resin was loaded on a column, washed with 10 mL NTA binding buffer followed by 10 mL NTA wash buffer (300 mM NaCl, 50 mM Tris, 50 mM imidazole, pH 8.0). The proteins were eluted in 0.5 mL fractions with 10 mL of NTA elution buffer (300 mM NaCl, 50 mM Tris, 500 mM imidazole, pH 8.0). Fractions containing protein were pooled and further purified to remove any contaminating zinc by applying the protein to a PD-10 column (GE Healthcare) charged with Caspase Activity Buffer that had been treated with Chelex ® resin. The resulting concentration was determined using the Edelhoch method and the molar absorptivity of procaspase-3 of 26150 M⁻¹ cm⁻¹. Protein stocks were flash-frozen in liquid nitrogen and stored at -80°C

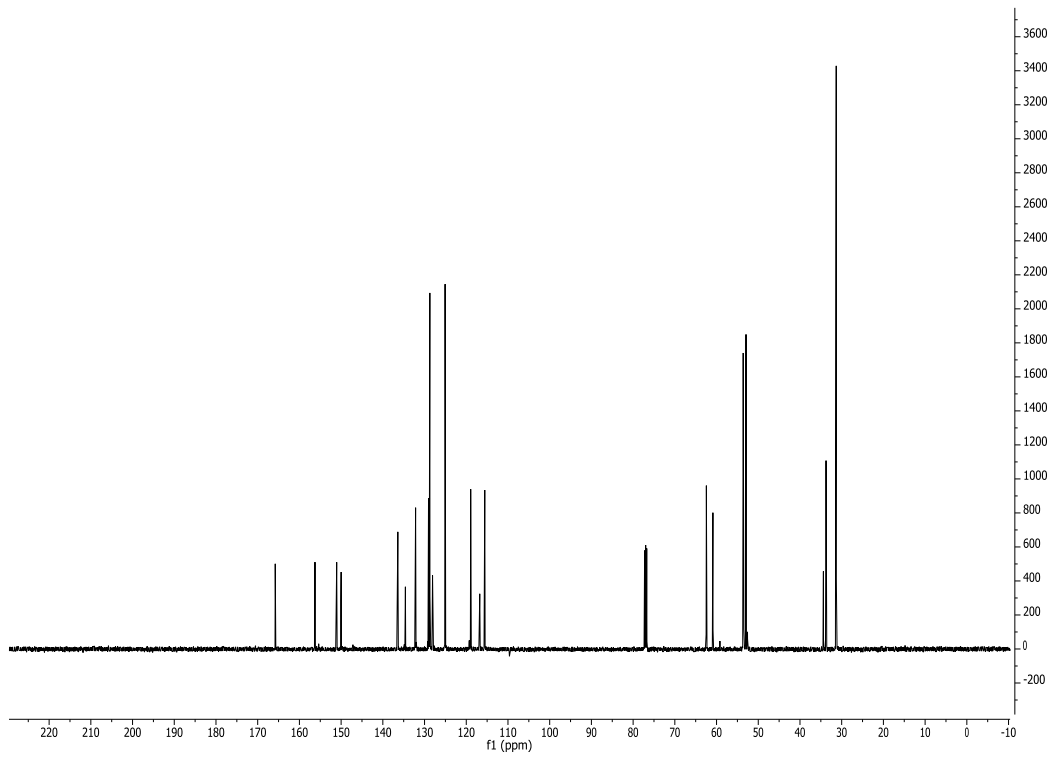
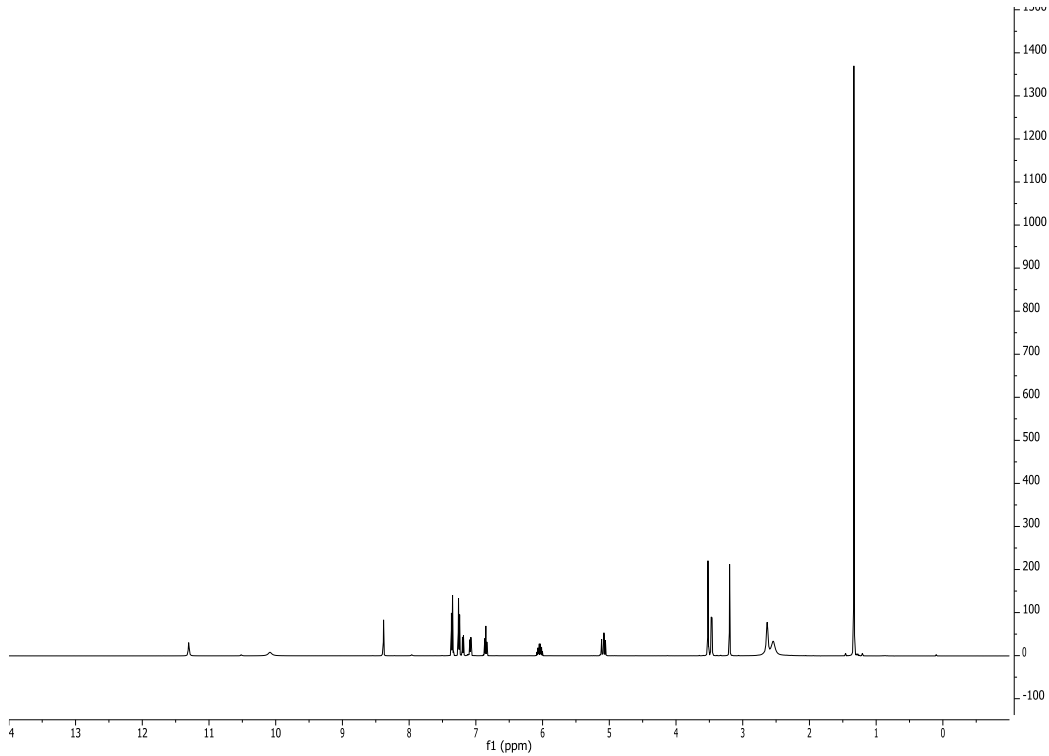
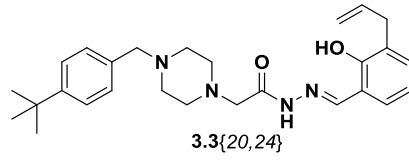
Procaspase-3 Activity Assay In a 384-well plate recombinantly expressed, zinc-free procaspase-3 (wild type, at 1 µM) in Caspase Activity Buffer (50mM HEPES, 300mM NaCl, 1.5mM TCEP, 0.01% TritonX-100) was incubated at 37 °C in the presence of 3.5 µM ZnSO₄ and the basal activity was assessed via the addition of Ac-DEVD-pNA (final concentration in well of 200 µM). The absorbance at 405nm was monitored with a SpectraMax plate reader (Molecular Devices). After the basal activity was determined, DMSO, **PAC-1** and analogues were added to each sample to a final concentration of 25 µM. Activity of each treatment was assessed at 5, 20, 40 and 60 minutes via 5-minute kinetic reads. The slope of each data set was used to determine the activity of the protein. Activity was normalized to a percent activity at each time point using a zinc-free sample and a zinc-inhibited sample treated with DMSO.

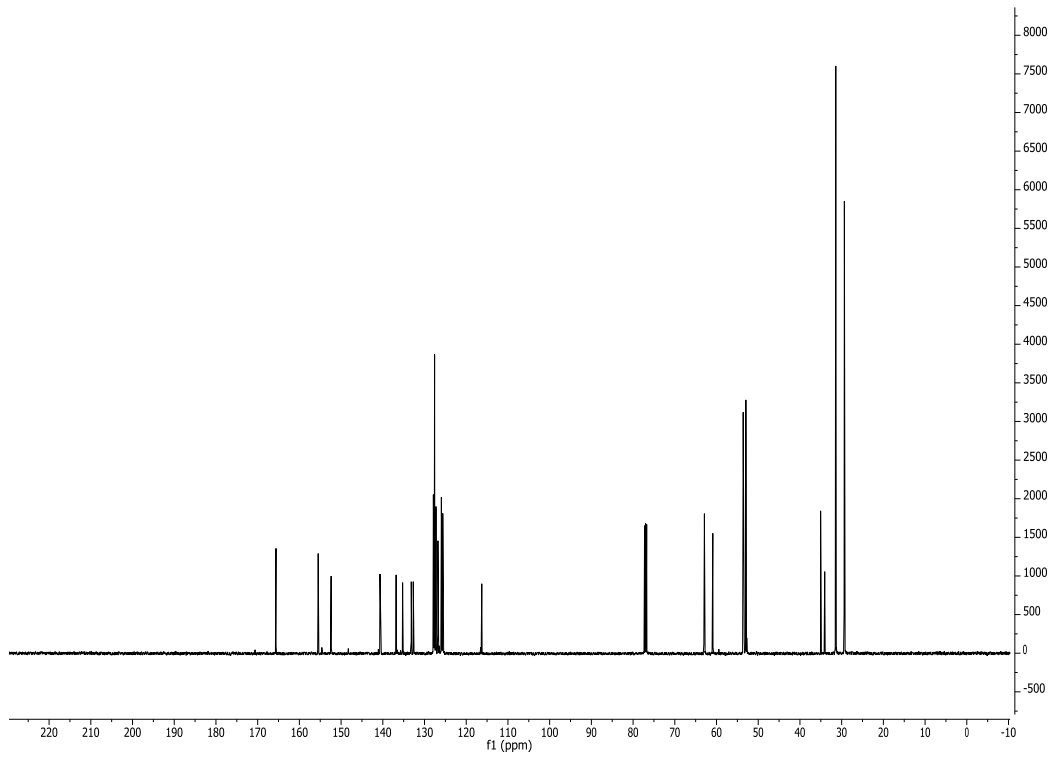
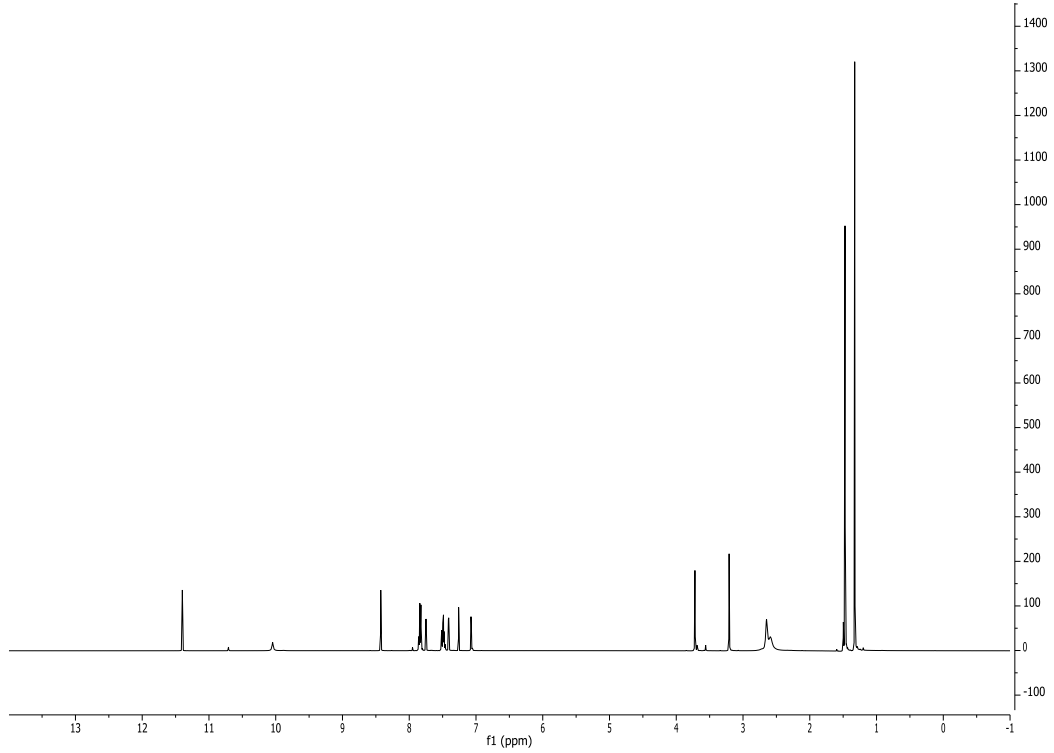
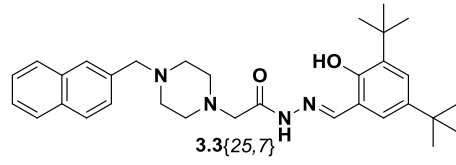
3.6.3. Spectra

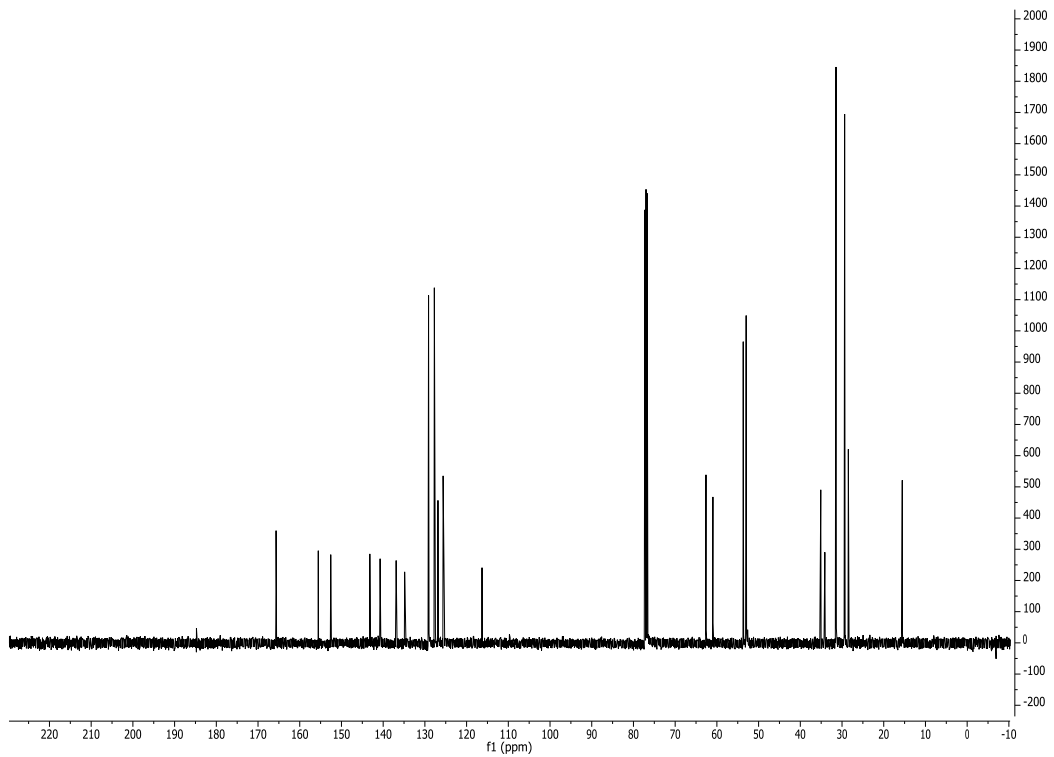
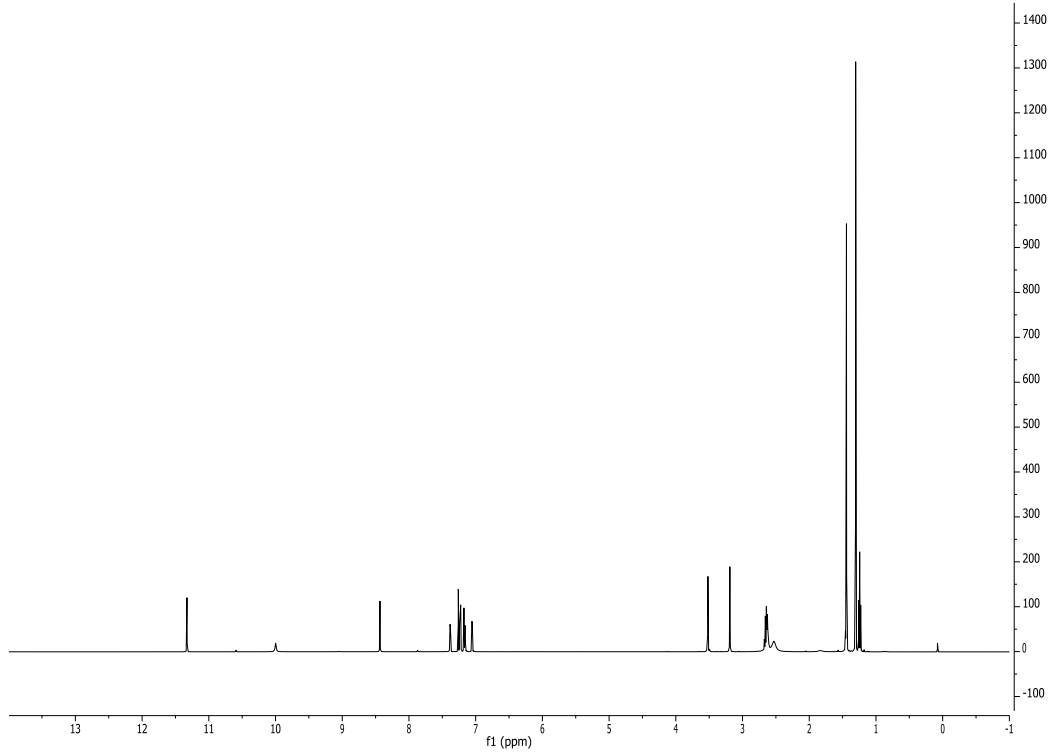
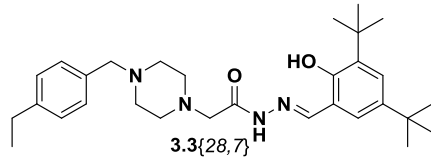












3.7. References

1. Hsu, D. C.; Roth, H. S.; West, D. C.; Botham, R. C.; Novotny, C. J.; Schmid, S. C.; Hergenrother, P. J. Parallel synthesis and biological evaluation of 837 analogues of Procaspase-Activating Compound 1 (PAC-1). *ACS Comb. Sci.* **2012**, *14*, 44-50.
2. Peterson, Q. P.; Hsu, D. C.; Goode, D. R.; Novotny, C. J.; Totten, R. K.; Hergenrother, P. J. Procaspase-3 activation as an anti-cancer strategy: structure-activity relationship of Procaspase-Activating Compound 1 (PAC-1) and its cellular co-localization with caspase-3. *J. Med. Chem.* **2009**, *52*, 5721-5731.
3. Peterson, Q. P.; Hsu, D. C.; Novotny, C. J.; West, D. C.; Kim, D.; Schmit, J. M.; Dirikolu, L.; Hergenrother, P. J.; Fan, T. M. Discovery and canine preclinical assessment of a nontoxic procaspase-3-activating compound. *Cancer Res.* **2010**, *70*, 7232-7241.
4. Lucas, P. W.; Schmit, J. M.; Peterson, Q. P.; West, D. C.; Hsu, D. C.; Novotny, C. J.; Dirikolu, L.; Churchwell, M. I.; Doerge, D. R.; Garrett, L. D.; Hergenrother, P. J.; Fan, T. M. Pharmacokinetics and derivation of an anticancer dosing regimen for PAC-1, a preferential small molecule activator of procaspase-3, in healthy dogs. *Invest. New Drugs* **2011**, *29*, 901-911.
5. Putt, K. S.; Chen, G. W.; Pearson, J. M.; Sandhorst, J. S.; Hoagland, M. S.; Kwon, J. T.; Hwang, S. K.; Jin, H.; Churchwell, M. I.; Cho, M. H.; Doerge, D. R.; Helferich, W. G.; Hergenrother, P. J. Small-molecule activation of procaspase-3 to caspase-3 as a personalized anticancer strategy. *Nat. Chem. Biol.* **2006**, *2*, 543-550.
6. Zhang, B.; Zhao, Y. F.; Zhai, X.; Fan, W. J.; Ren, J. L.; Wu, C. F.; Gong, P. Design, synthesis and antiproliferative activities of diaryl urea derivatives bearing N-acylhydrazone moiety. *Chin. Chem. Lett.* **2012**, *23*, 915-918.
7. Zhang, B.; Zhao, Y. F.; Zhai, X.; Wang, L. H.; Yang, J. Y.; Tan, Z. H.; Gong, P. Design, synthesis and anticancer activities of diaryl urea derivatives bearing N-acylhydrazone moiety. *Chem. Pharm. Bull.* **2012**, *60*, 1046-1054.
8. Hao-ming, L.; Chun-ling, Y.; Xiao-ying, Z.; Ming-ming, Z.; Dan, J.; Jun-hai, X.; Xiao-hong, Y.; Song, L. Design, synthesis, and antitumor activity of a novel series of PAC-1 analogues. *Chem. Res. Chin. Univ.* **2013**, *29*, 906-910.
9. Astrand, O. A. H.; Aziz, G.; Ali, S. F.; Paulsen, R. E.; Hansen, T. V.; Rongved, P. Synthesis and initial in vitro biological evaluation of two new zinc-chelating compounds: comparison with TPEN and PAC-1. *Bioorg. Med. Chem.* **2013**, *21*, 5175-5181.
10. Zhai, X.; Huang, Q.; Jiang, N.; Wu, D.; Zhou, H. Y.; Gong, P. Discovery of hybrid dual N-acylhydrazone and diaryl urea derivatives as potent antitumor agents: design, synthesis and cytotoxicity evaluation. *Molecules* **2013**, *18*, 2904-2923.
11. Ma, J.; Zhang, G.; Han, X.; Bao, G.; Wang, L.; Zhai, X.; Gong, P. Synthesis and biological evaluation of benzothiazole derivatives bearing the ortho-hydroxy-N-acylhydrazone moiety as potent antitumor agents. *Arch. Pharm. Chem. Life Sci.* **2014**, *347*, 936-949.
12. Ma, J. J.; Chen, D.; Lu, K.; Wang, L. H.; Han, X. Q.; Zhao, Y. F.; Gong, P. Design, synthesis, and structure-activity relationships of novel benzothiazole derivatives bearing the ortho-hydroxy N-carbamoylhydrazone moiety as potent antitumor agents. *Eur. J. Med. Chem.* **2014**, *86*, 257-269.
13. Sjoli, S.; Solli, A. I.; Akselsen, O.; Jiang, Y.; Berg, E.; Hansen, T. V.; Sylte, I.; Winberg, J. O. PAC-1 and isatin derivatives are weak matrix metalloproteinase inhibitors. *Biochim. Biophys. Acta* **2014**, *1840*, 3162-3169.
14. Wang, F. Y.; Wang, L. H.; Zhao, Y. F.; Li, Y.; Ping, G. F.; Xiao, S.; Chen, K.; Zhu, W. F.; Gong, P.; Yang, J. Y.; Wu, C. F. A novel small-molecule activator of procaspase-3 induces

apoptosis in cancer cells and reduces tumor growth in human breast, liver and gallbladder cancer xenografts. *Mol. Oncol.* **2014**, 8, 1640-1652.

15. Wang, F.; Liu, Y.; Wang, L.; Yang, J.; Zhao, Y.; Wang, N.; Cao, Q.; Gong, P.; Wu, C. Targeting procaspase-3 with WF-208, a novel PAC-1 derivative, causes selective cancer cell apoptosis. *J. Cell. Mol. Med.* [Online early access]. DOI: 10.1111/jcmm.12566. Published Online: March 8, 2015.

16. Miller, C. E. Hydrogenation with Diimide. *J. Chem. Educ.* **1965**, 42, 254-259.

17. Chang, K. H.; Huang, C. C.; Liu, Y. H.; Hu, Y. H.; Chou, P. T.; Lin, Y. C. Synthesis of photo-luminescent Zn(II) Schiff base complexes and its derivative containing Pd(II) moiety. *Dalton Trans.* **2004**, 1731-1738.

18. Clark, D. E. Rapid calculation of polar molecular surface area and its application to the prediction of transport phenomena. 2. Prediction of blood-brain barrier penetration. *J. Pharm. Sci.* **1999**, 88, 815-821.

19. Peterson, Q. P.; Goode, D. R.; West, D. C.; Ramsey, K. N.; Lee, J. J. Y.; Hergenrother, P. J. PAC-1 activates procaspase-3 in vitro through relief of zinc-mediated inhibition. *J. Mol. Biol.* **2009**, 388, 144-158.

20. Peterson, Q. P.; Goode, D. R.; West, D. C.; Botham, R. C.; Hergenrother, P. J. Preparation of the caspase-3/7 substrate Ac-DEVD-pNA by solution-phase peptide synthesis. *Nat. Protoc.* **2010**, 5, 294-302.

21. Clark, D. E. In silico prediction of blood-brain barrier permeation. *Drug Discov. Today* **2003**, 8, 927-933.

22. West, D. C.; Qin, Y.; Peterson, Q. P.; Thomas, D. L.; Palchoudhuri, R.; Morrison, K. C.; Lucas, P. W.; Palmer, A. E.; Fan, T. M.; Hergenrother, P. J. Differential effects of procaspase-3 activating compounds in the induction of cancer cell death. *Mol. Pharmaceutics* **2012**, 9, 1425-1434.

23. Patel, V.; Balakrishnan, K.; Keating, M. J.; Wierda, W. G.; Gandhi, V. Expression of executioner procaspases and their activation by a procaspase activating compound in chronic lymphocytic leukemia cells. *Blood* **2015**, 125, 1126-1136.

24. Westphal, M. V.; Wolfstadter, B. T.; Plancher, J. M.; Gatfield, J.; Carreira, E. M. Evaluation of tert-Butyl Isosteres: Case Studies of Physicochemical and Pharmacokinetic Properties, Efficacies, and Activities. *ChemMedChem* **2015**, 10, 461-469.

25. Vichai, V.; Kirtikara, K. Sulforhodamine B colorimetric assay for cytotoxicity screening. *Nat. Protoc.* **2006**, 1, 1112-1116.

Chapter 4. Removal of metabolic liabilities enables development of PAC-1 derivatives with improved pharmacokinetics

Portions of this chapter are reproduced with permission from literature (Roth, H. S.; Botham, R. C.; Schmid, S. C.; Fan, T. M.; Dirikolu, L.; Hergenrother, P. J. Removal of metabolic liabilities enables development of derivatives of Procaspase-Activating Compound 1 (PAC-1) with improved pharmacokinetics. *J. Med. Chem.* **2015**, 58(9), 4046-4065.)¹ Cytotoxicity screen for first library was performed by Rachel C. Botham. Animal experiments were performed by Rachel C. Botham and Prof. Timothy M. Fan. Pharmacokinetic analysis was performed by Prof. Levent Dirikolu.

4.1. Introduction

While studies with **PAC-1** and **S-PAC-1** have been encouraging, a challenge in using these compounds in animals is the relatively short *in vivo* half-lives of both **PAC-1** (2.1 ± 0.3 h in dogs)² and **S-PAC-1** (1.09 ± 0.02 h in dogs)³ following IV administration. A study in rats identified three main pathways of metabolism for **PAC-1**, including oxidative *N*-dealkylation, olefin oxidation, and arene oxidation (Figure 4.1).⁴ While many of these metabolites may be active based on the predicted structure-activity relationships, the alcohols and secondary amines resulting from these metabolites provide sites for conjugation, including sulfation and glucuronidation; these conjugates are then cleared from circulation. The metabolic liabilities present in **PAC-1** likely contribute to its pharmacokinetic profile, necessitating relatively large doses to achieve therapeutic levels *in vivo*. A **PAC-1** analogue lacking some of these liabilities may allow for lower or less frequent dosing, which could potentially reduce toxicity.

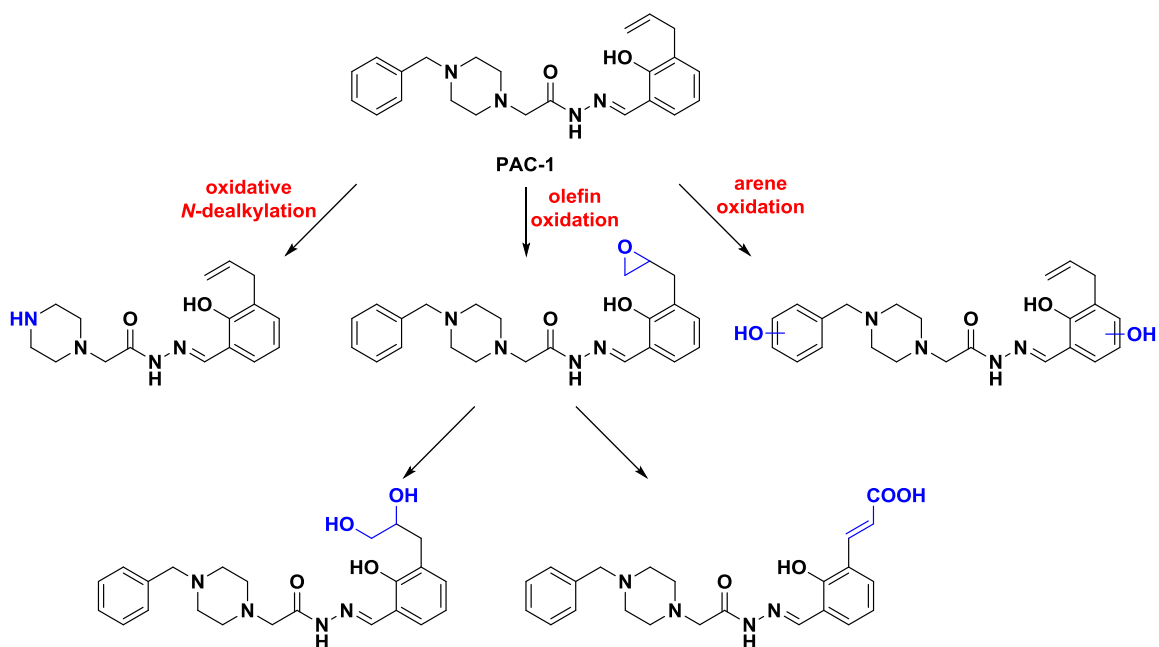


Figure 4.1. PAC-1 is susceptible to enzymatic oxidation *in vitro* and *in vivo*, giving metabolites that result from *N*-dealkylation, olefin oxidation, and arene oxidation.^{1,4}

4.2. First-generation library for enhancement of metabolic stability

4.2.1. Compound design and synthesis

The structure-activity relationships of **PAC-1** indicate that modifications to the aryl rings can be tolerated, as long as the core *ortho*-hydroxy-*N*-acylhydrazone remains intact.^{3, 5-7} The synthetic strategy that has been adopted to access these active compounds involves the late-stage condensation of a hydrazide and an aldehyde to form the key *ortho*-hydroxy-*N*-acylhydrazone.^{3, 5, 6, 8-16} This strategy was useful for the generation of a large combinatorial library of 837 diverse **PAC-1** analogues, as discussed in Chapter 3.⁸ For the study described in this chapter, the library design was focused on the creation of derivatives with systematic removal of the metabolic liabilities. The initial library of **PAC-1** analogues (Figure 4.2) was constructed from six hydrazides (**1.6**, **2.16**, **4.1a-d**) and five aldehydes (**2.1**, **4.2a-d**). In order to avoid oxidative *N*-dealkylation, the benzyl moiety was modified to a benzoyl (as in **4.1a**, and **4.1c**), hypothesized to be more resistant to oxidation,¹⁷ or substituted with *ortho*-chlorine substituents (as in **4.1d**), hypothesized to block oxidation due to steric effects. In order to avoid olefin oxidation, the allyl group was reduced to a propyl group (as in **4.2a**) or removed entirely (as in **4.2b** and **4.2c**).

Finally, in order to block arene oxidation, building blocks were introduced containing nitrile substituents (**4.1b-c**, **4.2b**), which have been shown to resist metabolic oxidation.¹⁸ A secondary goal of this library was to identify derivatives with improved aqueous solubility, so building blocks containing polar substituents (including **2.16**, **4.1b-c**, and **4.2b-d**) were employed. Multiple derivatives were synthesized containing only one modification to the **PAC-1** core, so that the effect of individual changes could be systematically evaluated.

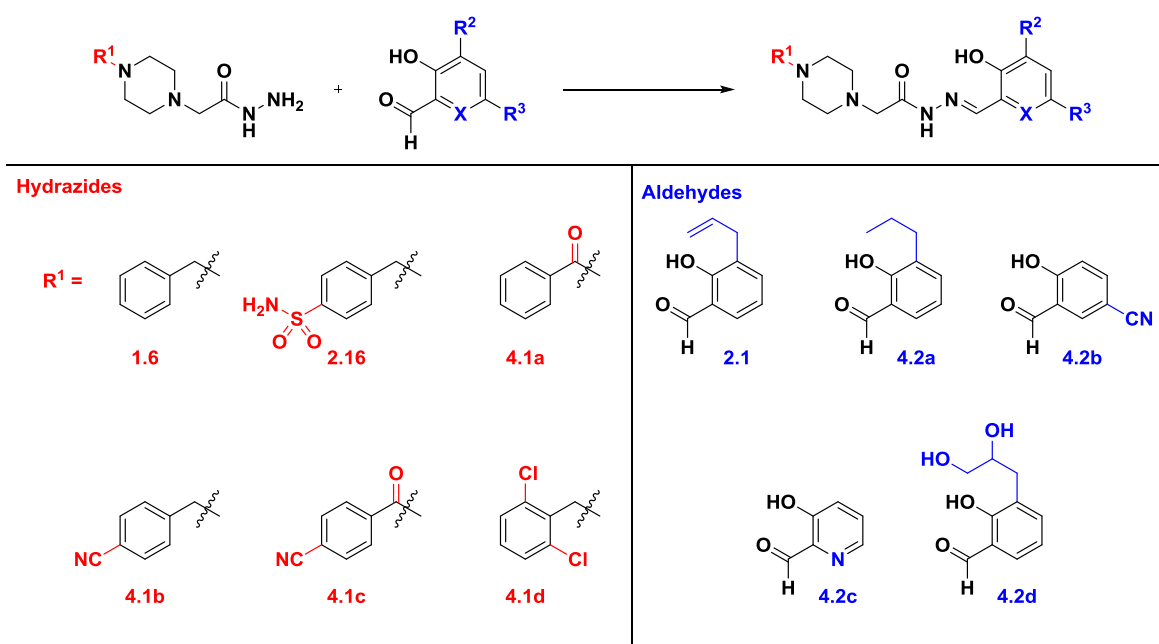
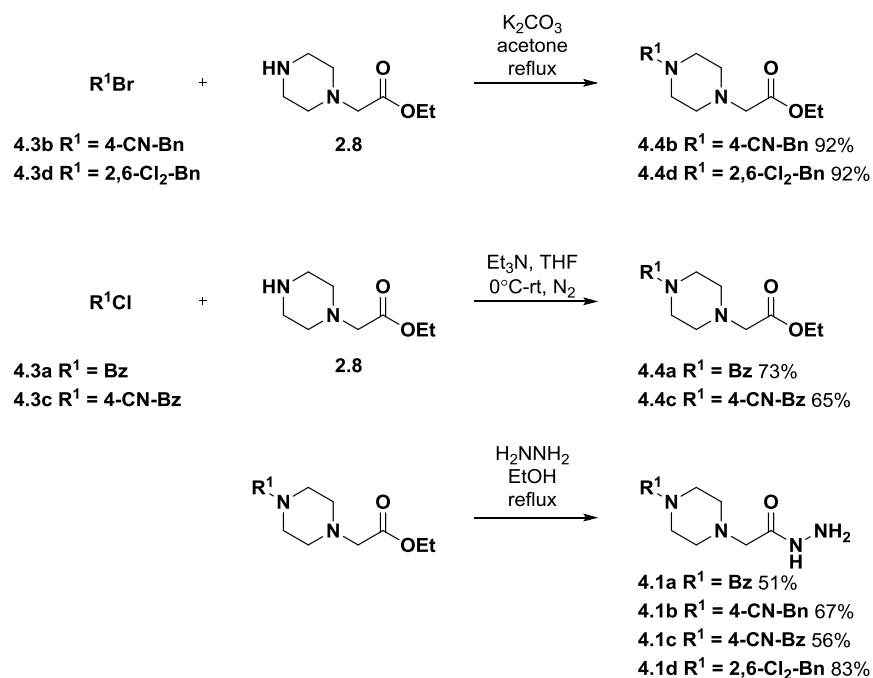


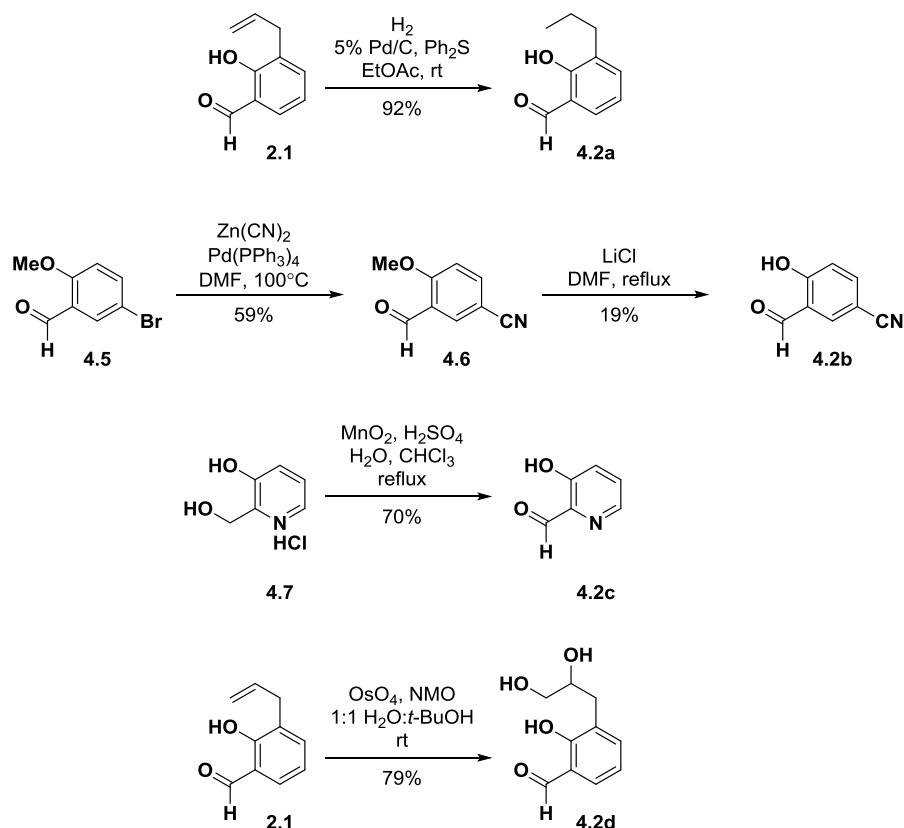
Figure 4.2. Design of first-generation library of **PAC-1** derivatives designed to display enhanced metabolic stability.¹

The hydrazides were synthesized according to Scheme 4.1. Alkylation of monosubstituted piperazine **2.8** with substituted benzyl bromides **4.3b** and **4.3d** gave dialkylated piperazines **4.4b** and **4.4d**. Acylation of **2.8** with benzoyl chlorides **4.3a** and **4.3c** gave amides **4.4a** and **4.4c**. Finally, reaction of ethyl esters **4.4a-d** with anhydrous hydrazine gave hydrazides **4.1a-d**.



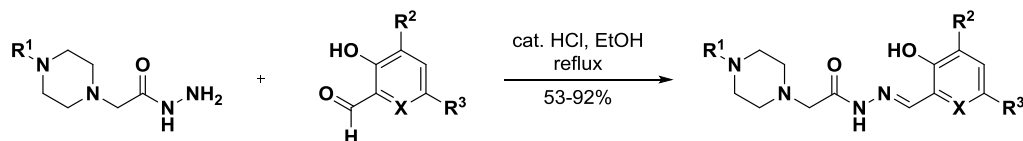
Scheme 4.1. Synthesis of hydrazide building blocks.¹

Synthesis of the aldehyde building blocks is shown in Scheme 4.2. Hydrogenation of **2.1** with diphenyl sulfide as a catalyst poison allowed for chemoselective reduction of the olefin,¹⁹ giving aldehyde **4.2a** in high yield. Synthesis of aldehyde **4.2b** began with the Negishi-like coupling of bromide **4.5** with zinc cyanide to give nitrile **4.6**, and demethylation with lithium chloride gave **4.2b**. Manganese(IV) oxide-mediated oxidation of alcohol **4.7** gave aldehyde **4.2c**, and dihydroxylation of **2.1** with osmium tetroxide gave **4.2d**.



Scheme 4.2. Synthesis of aldehyde building blocks.¹

The **PAC-1** derivatives (**4.8-4.31**) were synthesized by condensation of each hydrazide with one molar equivalent of each aldehyde in the presence of catalytic HCl (Table 4.1). Sufficient quantities of **4.2b** were not generated to react with all hydrazides, so this compound was only condensed with hydrazides **1.6** and **2.16**, to give **PAC-1** derivatives **4.24** and **4.25**. However, each of the other four aldehydes was condensed with each of the six hydrazides, to give a total of 26 **PAC-1** derivatives. Reactions were performed on 0.5-1.0 mmol scale and purified by chromatography, with the exception of **PAC-1** and **S-PAC-1**, which were synthesized on multi-gram scale and purified by recrystallization, as discussed in Chapter 2.



| compound | R ¹ | R ² | R ³ | X | Condensation % Yield | Predicted logBB | % Cytotoxicity (72h at 5 μM) |
|----------------|---------------------------------------|---------------------------|----------------|----|----------------------|-----------------|------------------------------|
| PAC-1 | Bn | All | H | CH | 85 | -0.37 | 57 |
| S-PAC-1 | 4-SO ₂ NH ₂ -Bn | All | H | CH | 59 | -1.59 | 56 |
| 4.8 | Bz | All | H | CH | 70 | -0.72 | 58 |
| 4.9 | 4-CN-Bn | All | H | CH | 88 | -0.74 | 56 |
| 4.10 | 4-CN-Bz | All | H | CH | 88 | -1.09 | 62 |
| 4.11 | 2,6-Cl ₂ -Bn | All | H | CH | 85 | -0.17 | 66 |
| 4.12 | Bn | Pr | H | CH | 87 | -0.31 | 74 |
| 4.13 | 4-SO ₂ NH ₂ -Bn | Pr | H | CH | 89 | -1.53 | 68 |
| 4.14 | Bz | Pr | H | CH | 86 | -0.66 | 60 |
| 4.15 | 4-CN-Bn | Pr | H | CH | 89 | -0.68 | 58 |
| 4.16 | 4-CN-Bz | Pr | H | CH | 87 | -1.03 | 57 |
| 4.17 | 2,6-Cl ₂ -Bn | Pr | H | CH | 53 | -0.11 | 66 |
| 4.18 | Bn | H | CN | CH | 85 | -0.89 | 20 |
| 4.19 | 4-SO ₂ NH ₂ -Bn | H | CN | CH | 75 | -2.11 | 8 |
| 4.20 | Bn | H | H | N | 84 | -1.25 | 36 |
| 4.21 | 4-SO ₂ NH ₂ -Bn | H | H | N | 72 | -2.45 | 3 |
| 4.22 | Bz | H | H | N | 55 | -1.60 | 8 |
| 4.23 | 4-CN-Bn | H | H | N | 87 | -1.60 | 25 |
| 4.24 | 4-CN-Bz | H | H | N | 73 | -1.96 | 0 |
| 4.25 | 2,6-Cl ₂ -Bn | H | H | N | 91 | -1.04 | 56 |
| 4.26 | Bn | 2,3-(OH) ₂ -Pr | H | CH | 79 | -0.74 | 0 |
| 4.27 | 4-SO ₂ NH ₂ -Bn | 2,3-(OH) ₂ -Pr | H | CH | 78 | -1.96 | 0 |
| 4.28 | Bz | 2,3-(OH) ₂ -Pr | H | CH | 92 | -1.08 | 4 |
| 4.29 | 4-CN-Bn | 2,3-(OH) ₂ -Pr | H | CH | 61 | -1.11 | 20 |
| 4.30 | 4-CN-Bz | 2,3-(OH) ₂ -Pr | H | CH | 71 | -1.46 | 11 |
| 4.31 | 2,6-Cl ₂ -Bn | 2,3-(OH) ₂ -Pr | H | CH | 84 | -0.53 | 0 |

Table 4.1. Structures, isolated yields, predicted BBB permeability,^a and cytotoxicity^b of first-generation **PAC-1** derivatives for the enhancement of metabolic stability.

(a) Calculated using Equation 3.2:²⁰

$$\text{predicted logBB} = (-0.0148 \times \text{PSA}) + (0.152 \times \text{ClogP}) + 0.139.$$

(b) U-937 cells treated with compounds (5 μM) for 72 hours. Biomass quantified via sulforhodamine B assay.¹

4.2.2. Evaluation of library

Because **PAC-1** and derivatives are under investigation both for tumors of the central nervous system and for the remainder of the body, it is important to determine whether any **PAC-1** derivative will enter the brain. As discussed in Chapter 3, the ability of a small molecule to penetrate the blood-brain barrier (BBB) is commonly represented as logBB, and predicted logBB was calculated using Equation 3.2 (reproduced below):²⁰

$$\text{predicted logBB} = (-0.0148 \times \text{PSA}) + (0.152 \times \text{AlogP}) + 0.139 \quad (\text{Equation 3.2})^{20}$$

The PSA and AlogP values for **PAC-1** and derivatives were calculated using the Schrodinger software, and insertion of these values into Equation 3.2 gave the predicted logBB values (Table 4.1). **PAC-1** has a predicted logBB value of -0.37, which is very close to the experimentally determined value of -0.36.²¹ As expected, substitution with polar groups, including the pyridyl, dihydroxypropyl, and sulfonamide, leads to a decrease in predicted BBB permeability, while substitution with nonpolar substituents, including dichloro and propyl, leads to an increase in predicted BBB permeability.

The compounds were then evaluated for their ability to induce apoptosis in cell culture. U-937 human lymphoma cells were incubated with each compound at 5 μ M for 72 hours; **PAC-1** and **S-PAC-1** each induce approximately 50% cell death under these conditions. The results of the screen are shown in Table 4.1. Of the 24 novel analogues, 11 compounds were at least as potent as **PAC-1** and **S-PAC-1**. Each of these analogues contains a relatively hydrophobic substituent (allyl, propyl, or chlorine), and cell permeability likely contributes to the potency of these analogues relative to the less potent compounds. Because most of the compounds derived from aldehydes **4b**, **4c**, and **4d** induced apoptosis to a minimal degree, these analogues were not included in further biological evaluation.

The remaining 12 compounds (**PAC-1**, **S-PAC-1**, and **4.8-4.17**) were evaluated in rat liver microsomes. Compounds were incubated for 3 hours at 10 μ M, and products were analyzed by LC/MS. The metabolites observed from **PAC-1** matched well with the reported transformations from the experiment in rats:⁴ there was a metabolite corresponding to removal of the benzyl group, a metabolite corresponding to dihydroxylation of the olefin, and several metabolites from monooxygenation of **PAC-1**. In general, most of the modifications were successful in blocking the undesired transformations; the amide substitution eliminated the oxidative *N*-dealkylation, no dihydroxylated species were observed from propyl-substituted compounds, and the nitrile substitution reduced the number of monooxygenated species. However, the dichloro substitution was not successful in preventing *N*-dealkylation, as the dealkylated metabolite was still observed for these compounds (**4.11** and **4.17**). Further, the degree of monooxygenation increased, and metabolites were observed containing two additional oxygen atoms for these derivatives, unlike any of the other **10** compounds evaluated. For this

reason, **PAC-1** derivatives containing the dichlorobenzyl substituent were not evaluated in further experiments.

4.3. Second-generation library for enhancement of metabolic stability

4.3.1. Compound design and synthesis

The experiments performed with the initial set of **PAC-1** derivatives allowed for a greater understanding of the structure-activity relationships and guided an improved library design. Because of the poor *in vitro* metabolic stability, compounds containing the 2,6-dichlorobenzyl substituent were removed, and due to reduced cell culture potency, compounds constructed from aldehydes **4.2b-d** were removed, and increased solubility was no longer a criterion for advancement of compounds. Additional strategies for blocking arene oxidation were desired, and it appeared that polar substituents tended to reduce potency, so fluorine and trifluoromethyl substituents were added to the aromatic rings.

The new library for the enhancement of metabolic stability (Figure 4.3) consisted of 45 **PAC-1** analogues, constructed from nine hydrazides and five aldehydes. Five hydrazides (**1.6**, **2.16** and **4.1a-c**) and two aldehydes (**2.1** and **4.2a**) remained from the previous library. Added hydrazides included those containing 4-fluorobenzyl (**4.1e**), 4-fluorobenzoyl (**4.1f**), 4-(trifluoromethyl)benzyl (**3.1{15}**), and 4-(trifluoromethyl)benzoyl (**4.1g**) substituents. Added salicylaldehydes contained a fluorine in the 5-position, either with no other substitution on the ring (**4.2e**), or with allyl (**4.2f**) or *n*-propyl (**4.2g**) substituents in the 3-position.

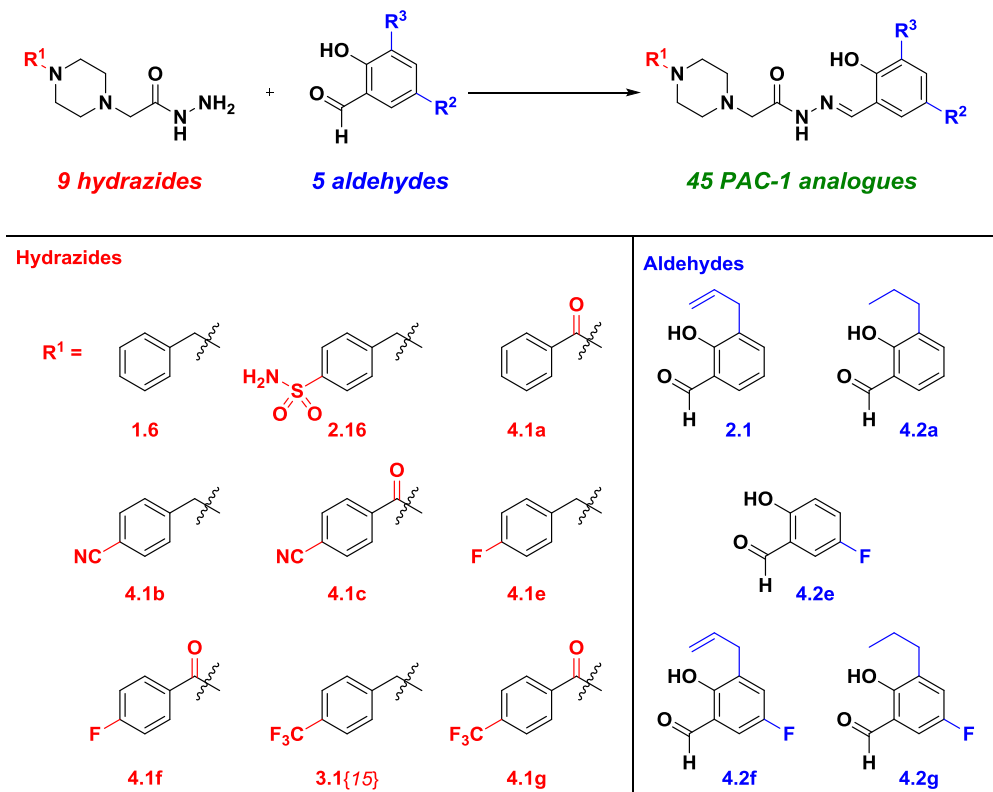
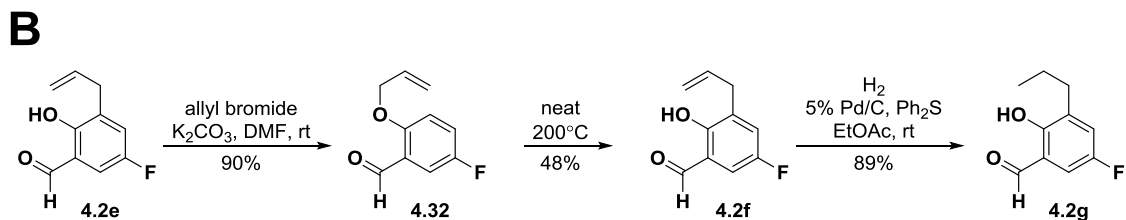
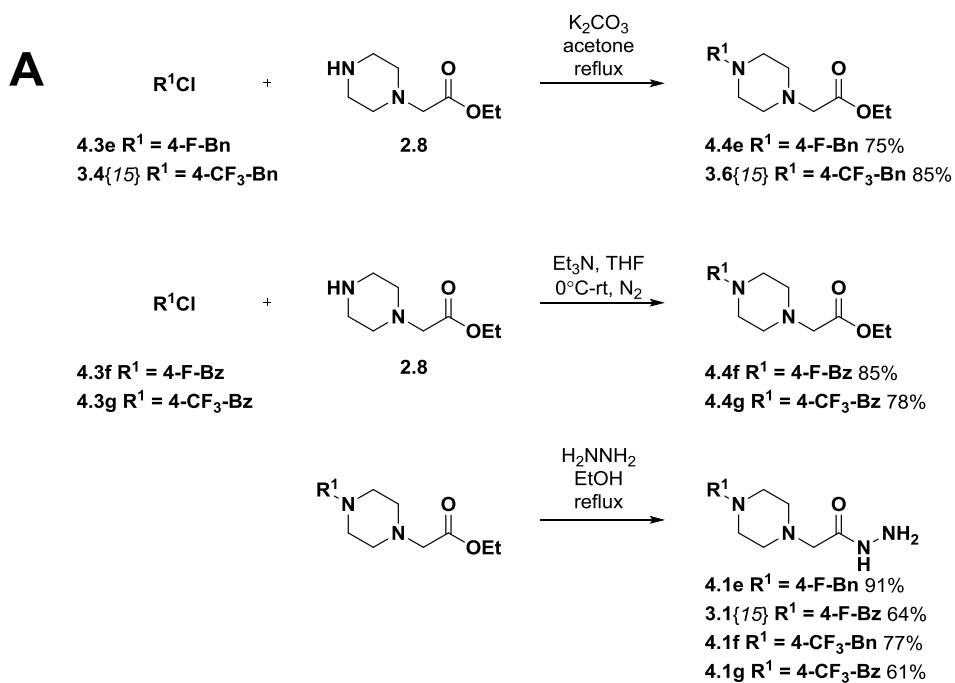
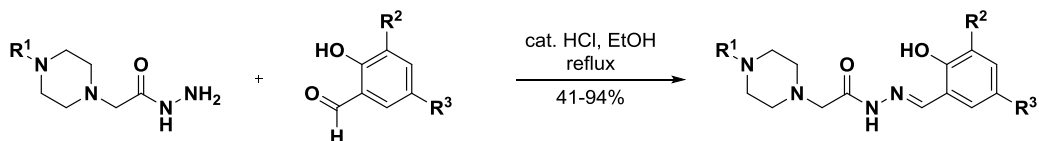


Figure 4.3. Nine hydrazides and five aldehydes were used to construct a library of 45 **PAC-1** derivatives designed to display enhanced metabolic stability by blocking oxidative *N*-dealkylation, olefin oxidation, and/or arene oxidation.¹

Synthesis of the added building blocks (Scheme 4.3) was adapted from previous routes. The added hydrazides were synthesized according to Scheme 4.3A. Alkylation of **2.8** with substituted benzyl chlorides **4.3e** and **3.4{15}** gave dialkylated piperazines **4.4e** and **3.6{15}**, respectively, while acylation of **2.8** with substituted benzoyl chlorides **4.3f-g** gave amides **4.4f-g**, respectively. Reaction of these four esters with anhydrous hydrazine gave the four new hydrazides. The additional aldehydes (Scheme 4.3B) were synthesized beginning with the alkylation of commercially available building block 5-fluorosalicylaldehyde (**4.2e**) with allyl bromide to give ether **4.32**. This compound underwent a Claisen rearrangement upon heating to give **4.2f**, and chemoselective hydrogenation gave **4.2g**. Each of the nine hydrazides was condensed with each of the five aldehydes to give a total of 45 **PAC-1** derivatives, including 10 from the initial library (Table 4.2).



Scheme 4.3. A. Synthesis of hydrazide building blocks. **B.** Synthesis of aldehyde building blocks.¹



| compound | R ¹ | R ² | R ³ | Condensation % Yield |
|----------|---------------------------------------|----------------|----------------|-------------------------|
| PAC-1 | Bn | H | All | 85 |
| S-PAC-1 | 4-SO ₂ NH ₂ -Bn | H | All | 59 |
| 4.8 | Bz | H | All | 70 |
| 4.9 | 4-CN-Bn | H | All | 88 |
| 4.10 | 4-CN-Bz | H | All | 88 |
| 1.14a | 4-F-Bn | H | All | 89 |
| 4.33 | 4-F-Bz | H | All | 81 |
| 4.34 | 4-CF ₃ -Bn | H | All | 54 |
| 4.35 | 4-CF ₃ -Bz | H | All | 89 |
| 4.12 | Bn | H | <i>n</i> -Pr | 87 |
| 4.13 | 4-SO ₂ NH ₂ -Bn | H | <i>n</i> -Pr | 89 |
| 4.14 | Bz | H | <i>n</i> -Pr | 86 |
| 4.15 | 4-CN-Bn | H | <i>n</i> -Pr | 89 |
| 4.16 | 4-CN-Bz | H | <i>n</i> -Pr | 87 |
| 4.36 | 4-F-Bn | H | <i>n</i> -Pr | 66 |
| 4.37 | 4-F-Bz | H | <i>n</i> -Pr | 62 |
| 4.38 | 4-CF ₃ -Bn | H | <i>n</i> -Pr | 41 |
| 4.39 | 4-CF ₃ -Bz | H | <i>n</i> -Pr | 91 |
| 4.40 | Bn | F | H | 94 |
| 4.41 | 4-SO ₂ NH ₂ -Bn | F | H | 82 |
| 4.42 | Bz | F | H | 82 |
| 4.43 | 4-CN-Bn | F | H | 86 |
| 4.44 | 4-CN-Bz | F | H | 70 |
| 4.45 | 4-F-Bn | F | H | 78 |
| 4.46 | 4-F-Bz | F | H | 50 |
| 4.47 | 4-CF ₃ -Bn | F | H | 89 |
| 4.48 | 4-CF ₃ -Bz | F | H | 77 |
| 4.49 | Bn | F | All | 91 |
| 4.50 | 4-SO ₂ NH ₂ -Bn | F | All | 87 |
| 4.51 | Bz | F | All | 88 |
| 4.52 | 4-CN-Bn | F | All | 75 |
| 4.53 | 4-CN-Bz | F | All | 87 |
| 4.54 | 4-F-Bn | F | All | 82 |
| 4.55 | 4-F-Bz | F | All | 74 |
| 4.56 | 4-CF ₃ -Bn | F | All | 74 |
| 4.57 | 4-CF ₃ -Bz | F | All | 56 |
| 4.58 | Bn | F | <i>n</i> -Pr | 85 |
| 4.59 | 4-SO ₂ NH ₂ -Bn | F | <i>n</i> -Pr | 90 |
| 4.60 | Bz | F | <i>n</i> -Pr | 89 |
| 4.61 | 4-CN-Bn | F | <i>n</i> -Pr | 82 |
| 4.62 | 4-CN-Bz | F | <i>n</i> -Pr | 87 |
| 4.63 | 4-F-Bn | F | <i>n</i> -Pr | 94 |
| 4.64 | 4-F-Bz | F | <i>n</i> -Pr | 88 |
| 4.65 | 4-CF ₃ -Bn | F | <i>n</i> -Pr | 77 |
| 4.66 | 4-CF ₃ -Bz | F | <i>n</i> -Pr | 57 |

Table 4.2. Synthesis of 45 PAC-1 derivatives designed to display enhanced metabolic stability.¹

4.3.2. Evaluation of library *in silico*, in cell culture, and *in vitro*

With the 45 compounds in hand, evaluation of the library was initiated, beginning with calculation of the predicted BBB permeability. Calculation of these values was performed as previously; the PSA and AlogP values for the compounds were calculated using the Schrodinger software, and Equation 3.2 was used to calculate the predicted logBB values (Table 4.3). Replacement of hydrogen with fluorine led to a minimal increase in predicted logBB, as demonstrated by **PAC-1** and **1.14a**. However, replacement of hydrogen with a trifluoromethyl group, as with compound **4.34**, led to a larger increase in predicted BBB permeability.

| compound | Predicted logBB | U-937 72h IC ₅₀ (μM) | RLM 3h % Stability | mouse toxicity IP 200 mg/kg (except as noted) |
|----------|-----------------|---------------------------------|--------------------|---|
| PAC-1 | -0.37 | 10.2 ± 0.3 | 38 ± 2 | severe - E |
| S-PAC-1 | -1.59 | 8.9 ± 0.6 | 84 ± 1 | none |
| 4.8 | -0.72 | 12.1 ± 1.3 | 89 ± 4 | severe - D |
| 4.9 | -0.74 | 13.7 ± 0.9 | 48 ± 2 | mild |
| 4.10 | -1.09 | 13.1 ± 3.7 | 90 ± 4 | lethal -D |
| 1.14a | -0.34 | 11.1 ± 2.1 | 31 ± 1 | **severe - E |
| 4.33 | -0.69 | 10.2 ± 1.7 | 86 ± 2 | moderate - D |
| 4.34 | -0.22 | 15.3 ± 6.7 | 16 ± 1 | lethal - E |
| 4.35 | -0.58 | 6.6 ± 1.9 | 85 ± 6 | *lethal - D |
| 4.12 | -0.31 | 9.6 ± 2.1 | 30 ± 1 | moderate - E |
| 4.13 | -1.53 | 4.9 ± 0.4 | 61 ± 2 | N.D. |
| 4.14 | -0.66 | 9.4 ± 1.3 | 71 ± 3 | N.D. |
| 4.15 | -0.68 | 9.0 ± 1.2 | 30 ± 2 | N.D. |
| 4.16 | -1.03 | 12.8 ± 2.7 | 61 ± 3 | N.D. |
| 4.36 | -0.28 | 10.0 ± 1.7 | 24 ± 2 | lethal - E |
| 4.37 | -0.63 | 7.3 ± 0.9 | 69 ± 4 | N.D. |
| 4.38 | -0.17 | 4.1 ± 0.4 | 15 ± 2 | lethal - E |
| 4.39 | -0.52 | 4.8 ± 1.2 | 64 ± 1 | *lethal - E |
| 4.40 | -0.49 | 17.0 ± 1.4 | 64 ± 4 | severe - E |
| 4.41 | -1.71 | 19.6 ± 3.8 | 85 ± 6 | lethal - D |
| 4.42 | -0.84 | 15.7 ± 2.6 | 88 ± 1 | N.D. |
| 4.43 | -0.86 | 13.5 ± 1.0 | 79 ± 4 | lethal - D |
| 4.44 | -1.21 | 15.3 ± 1.3 | 88 ± 4 | N.D. |
| 4.45 | -0.46 | 11.7 ± 1.4 | 62 ± 2 | severe - E |
| 4.46 | -0.81 | 15.3 ± 0.8 | 86 ± 2 | N.D. |
| 4.47 | -0.35 | 4.7 ± 0.3 | 30 ± 5 | severe - E |
| 4.48 | -0.70 | 8.7 ± 0.5 | 87 ± 3 | moderate - D |
| 4.49 | -0.34 | 9.5 ± 0.9 | 56 ± 1 | lethal - E |
| 4.50 | -1.56 | 9.8 ± 1.3 | 89 ± 3 | lethal - D |
| 4.51 | -0.69 | 8.6 ± 2.0 | 93 ± 7 | moderate - D |
| 4.52 | -0.71 | 12.7 ± 2.0 | 65 ± 2 | N.D. |
| 4.53 | -1.06 | 10.1 ± 2.0 | 95 ± 4 | mild |
| 4.54 | -0.30 | 10.3 ± 4.1 | 57 ± 1 | ***severe - E |
| 4.55 | -0.66 | 8.5 ± 1.4 | 92 ± 3 | severe - D |
| 4.56 | -0.19 | 3.4 ± 0.6 | 49 ± 3 | *lethal - E (IV) |
| 4.57 | -0.55 | 6.5 ± 0.6 | 90 ± 2 | moderate - D |
| 4.58 | -0.28 | 8.9 ± 1.2 | 49 ± 6 | lethal - E |
| 4.59 | -1.50 | 8.7 ± 0.4 | 62 ± 3 | N.D. |
| 4.60 | -0.63 | 12.3 ± 1.0 | 86 ± 5 | moderate - D |
| 4.61 | -0.65 | 11.2 ± 0.9 | 49 ± 5 | N.D. |
| 4.62 | -1.00 | 9.4 ± 1.2 | 66 ± 3 | mild |
| 4.63 | -0.25 | 7.5 ± 0.7 | 48 ± 1 | ***severe - E |
| 4.64 | -0.60 | 7.5 ± 1.4 | 67 ± 3 | severe - D |
| 4.65 | -0.13 | 3.9 ± 0.6 | 40 ± 1 | lethal - E |
| 4.66 | -0.49 | 5.2 ± 0.6 | 64 ± 5 | lethal - E |

Table 4.3. Predicted BBB permeability,^a cytotoxicity,^b rat liver microsome stability,^c and mouse toxicity^d of PAC-1 derivatives for the enhancement of metabolic stability.

(a) Calculated using Equation 3.2:²⁰

$$\text{predicted logBB} = (-0.0148 \times \text{PSA}) + (0.152 \times \text{ClogP}) + 0.139.$$

(b) U-937 cells treated with compounds for 72 hours. Biomass quantified via sulforhodamine B assay. IC₅₀ values shown are mean ± s.e.m. (n = 3).

(c) Rat liver microsomes treated with compounds (10 μ M) for 3 hours. Percent stability values shown are mean \pm s.e.m. (n = 3).

(d) Compounds formulated at 5 mg/mL in 200 mg/mL aqueous HP β CD (pH 5.5). Mice dosed with compounds via i.p. injection at 200 mg/kg (except as noted: *100 mg/kg, **10 mg/mL solution, ***125 mg/kg). E = excitatory, D = depressive, N.D. = not determined.¹

Following these calculations, the biological activity of the compounds was evaluated. First, the ability of the compounds to induce cell death in U-937 (human lymphoma) cells in culture was determined (Table 4.3). Each of the compounds was found to induce dose-dependent cell death under these conditions, and most of the compounds were approximately as potent as **PAC-1** and **S-PAC-1**, confirming the previously determined SAR.^{3, 5, 6, 8}

Next, the metabolic stability of the compounds was evaluated in rat liver microsomes. The compounds were evaluated after a 3 hour treatment at 10 μ M, and metabolites were observed by LC/MS. The beta-adrenergic antagonist (\pm)-propranolol hydrochloride was included as a positive control;²² approximately 20% of the control remained. The results of this assay are shown in Table 1. Compounds that contained benzoyl substituents were significantly more stable than analogous compounds containing benzyl groups; for example, compound **4.8** was more stable than **PAC-1**, and compound **4.53** was more stable than compound **4.52**. The propyl-containing compounds were less stable than the allyl-containing compounds (e.g., **PAC-1** was more stable than compound **4.12**), although the dihydroxylated metabolites were not observed for propyl-substituted compounds. In addition, **S-PAC-1** was relatively stable in the liver microsomes, despite the short *in vivo* half-life of the compound,³ suggesting that clearance mechanisms other than oxidative metabolism play a greater role in the elimination of **S-PAC-1** from treated animals.

The results of selected liver microsome experiments are shown in Figure 4.4. **PAC-1** (Figure 4.4A) was 38% stable in the assay, and several metabolites, including an *N*-dealkylated product, a dihydroxylated product, and multiple monooxygenated products, were observed. **S-PAC-1** (Figure 4.4B) was found to be more stable than **PAC-1**, and fewer metabolites were observed. One of the modifications that improved stability to the greatest degree was the addition of the benzoyl in place of the benzyl substituent, as demonstrated with compound **4.8** (Figure 4.4C). This modification prevented the *N*-dealkylation completely and increased stability to 89%

during the three-hour incubation. In addition, compounds with a benzoyl substituent had fewer monooxygenated species than **PAC-1**, as the amide likely acted to deactivate the aromatic ring towards oxidation. The addition of fluorine to the benzylidene ring, as in compound **4.40** (Figure 4.4D), was also successful in reducing the number of monooxygenated metabolites, and as expected, dihydroxylated metabolites were not formed from compounds lacking the allyl group. Finally, combining multiple modifications, as in compounds **4.33** (Figure 4.4E) and **4.53** (Figure 4.4F), led to highly stable compounds that gave significantly fewer metabolites in the liver microsome experiment.

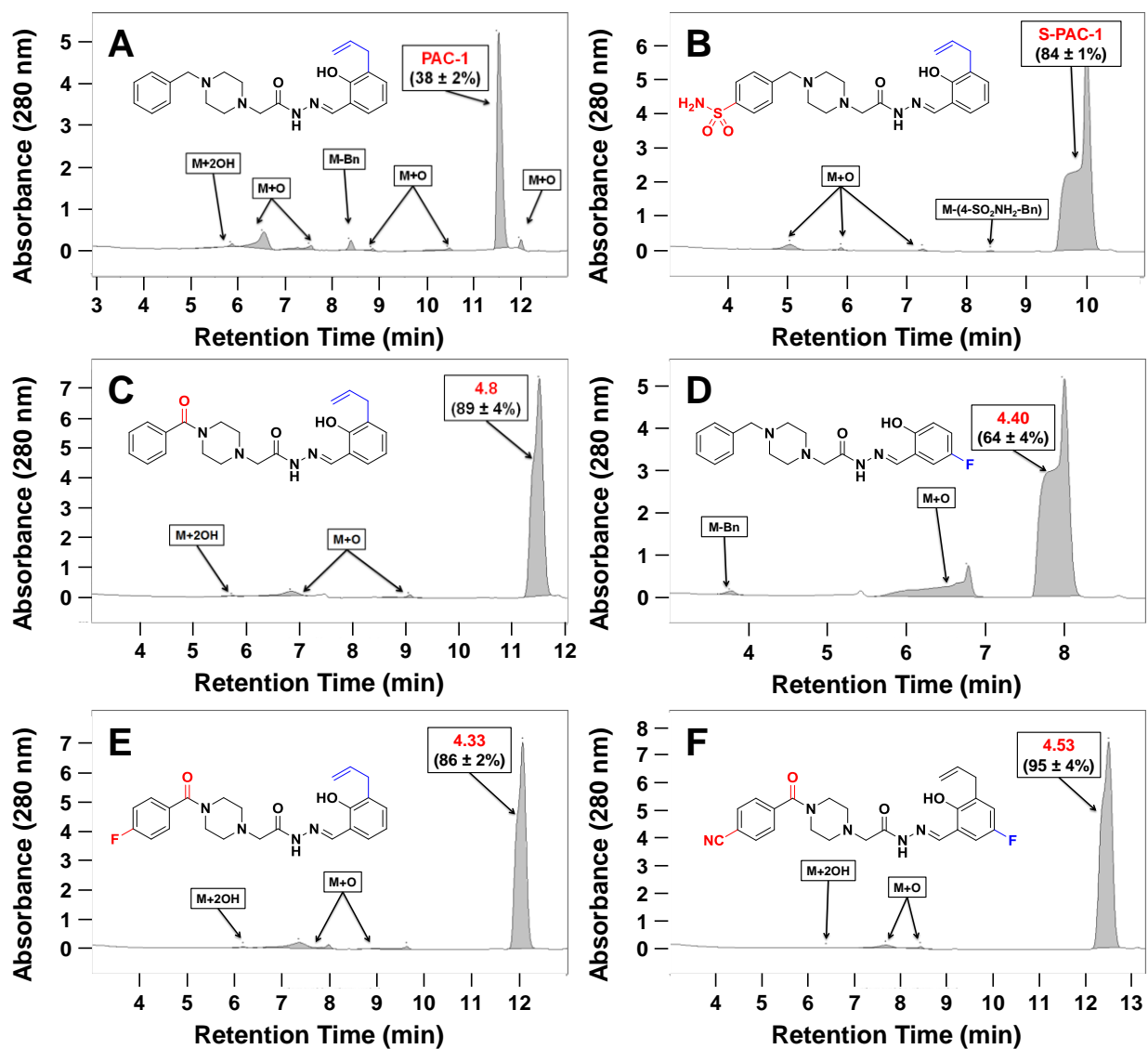


Figure 4.4. Metabolic stability of **PAC-1** and derivatives was evaluated in rat liver microsomes at 10 μ M for 3 hours. LC/MS results of liver microsome experiments for **A. PAC-1**, **B. S-PAC-1**, **C. 4.8**, **D. 4.40**, **E. 4.33**, and **F. 4.53** are shown. Data shown are representative of three independent experiments.¹

4.3.3. Compound tolerability in mice

After determination of the cytotoxicity and *in vitro* metabolic stability of the 45 compounds, several of the compounds were evaluated in mice (C57BL/6) to determine the tolerability (Table 4.3); compounds with improved tolerability would be considered for further evaluation. Compounds were formulated at 5 mg/mL in 200 mg/mL aqueous HP β CD (pH 5.5),

and a dose of 200 mg/kg was administered to mice via i.p. injection (exceptions to this protocol are noted in Table 4.3). This dose of **PAC-1** induces severe but transient neuroexcitation; no adverse effects to **S-PAC-1** are observed at this dose. Responses to compounds were graded as mild, moderate, or severe; compounds that were lethal are also noted. Responses above mild toxicity were classified as excitatory (E) or depressive (D).

In general, most of the compounds predicted to be BBB permeable were not well tolerated. Every compound with a predicted logBB value above -0.55 was evaluated in mice, because of the desire for a BBB-permeable compound for the treatment of brain tumors. Each of these compounds induced the excitatory phenotype in animals, with the exception of compound **4.35**; however, this compound was lethal at the lower dose of 100 mg/kg. Further, no compound that induced neuroexcitation had a predicted logBB value below -0.55. Compound **4.57**, with a predicted logBB value of -0.55, induced a depressive phenotype. The only compound with a predicted logBB value above -0.55 that showed improved tolerability as compared to **PAC-1** was compound **4.12**, with moderate toxicity; all others induced severe toxicity or were lethal to the animals.

Because of promising results from cell culture and liver microsome experiments, several compounds with lower predicted BBB permeability were also evaluated in mice. Each compound with a predicted logBB value below -0.55 that was evaluated in mice induced the depressive phenotype similar to elevated doses of **S-PAC-1**. However, the relationship between predicted BBB permeability and degree of toxicity was less clear for these compounds. Six additional compounds (**4.33**, **4.48**, **4.51**, **4.53**, **4.60**, and **4.62**) were found to be tolerated better than **PAC-1** at the 200 mg/kg dose.

4.4. Evaluation of compound 4.12

Because it had slightly improved tolerability as compared to **PAC-1**, but it was still predicted to cross the BBB, compound **4.12** (structure in Figure 4.5C) was evaluated further as a potential agent for the treatment of brain tumors. The ability of **PAC-1** and **4.12** to induce apoptosis was evaluated in five glioma-derived cell lines from human and murine origin, as well as a diverse array of human cell lines from six other cancer types. As shown in Table 4.4, compound **4.12** displayed comparable potency to that of **PAC-1** in all 12 cell lines tested. The

compounds showed low micromolar IC₅₀ values against all cell lines, providing support for the evaluation of these compounds as anticancer agents.

| Cell Line | Species | Origin | 72-hour IC ₅₀ (μM) | |
|------------|---------|--------------|-------------------------------|------------|
| | | | PAC-1 | 4.12 |
| D54 | Human | Glioblastoma | 4.0 ± 0.8 | 3.5 ± 1.3 |
| U-87 MG | Human | Glioblastoma | 9.1 ± 0.5 | 5.6 ± 1.7 |
| U-118 MG | Human | Glioblastoma | 13.4 ± 0.9 | 12.2 ± 3.0 |
| 9L | Rat | Gliosarcoma | 4.6 ± 0.2 | 3.2 ± 0.7 |
| GL261 | Mouse | Glioma | 0.4 ± 0.1 | 0.4 ± 0.2 |
| U-937 | Human | Lymphoma | 10.2 ± 0.3 | 9.6 ± 2.1 |
| MDA-MB-231 | Human | Breast | 5.1 ± 0.8 | 3.3 ± 0.7 |
| A549 | Human | Lung | 3.6 ± 0.2 | 2.1 ± 0.4 |
| IGROV-1 | Human | Ovarian | 2.7 ± 0.4 | 1.7 ± 0.4 |
| HOS | Human | Osteosarcoma | 1.2 ± 0.2 | 0.7 ± 0.07 |
| 143B | Human | Osteosarcoma | 1.3 ± 0.1 | 1.1 ± 0.1 |
| MIA PaCa-2 | Human | Pancreatic | 4.2 ± 1.8 | 2.0 ± 0.3 |

Table 4.4. PAC-1 and 4.12 are potent in a variety of cancer cell lines. Cells treated with compounds for 72 hours. Biomass quantified by sulforhodamine B assay. IC₅₀ values shown are mean ± s.e.m. (n = 3).

4.5. Blood-brain barrier permeability of selected derivatives

In order to determine whether compound 4.12 would be a promising candidate as a therapeutic agent for the treatment of brain tumors, the BBB permeability of this compound was assessed in mice (Figure 4.5A). Mice were administered compound at 75 mg/kg via i.v. injection and sacrificed after 5 minutes. Brain and blood samples were collected, and concentrations were determined by HPLC. PAC-1 shows a 30:70 distribution between brain and blood, while S-PAC-1 shows a distribution of less than 1:99.²¹ The brain:blood distribution of compound 4.12 was 23:77. The compound is slightly less BBB permeable than PAC-1, which may be sufficient to explain the lower toxicity of this compound. For this reason, development of compound 4.12 was not pursued further.

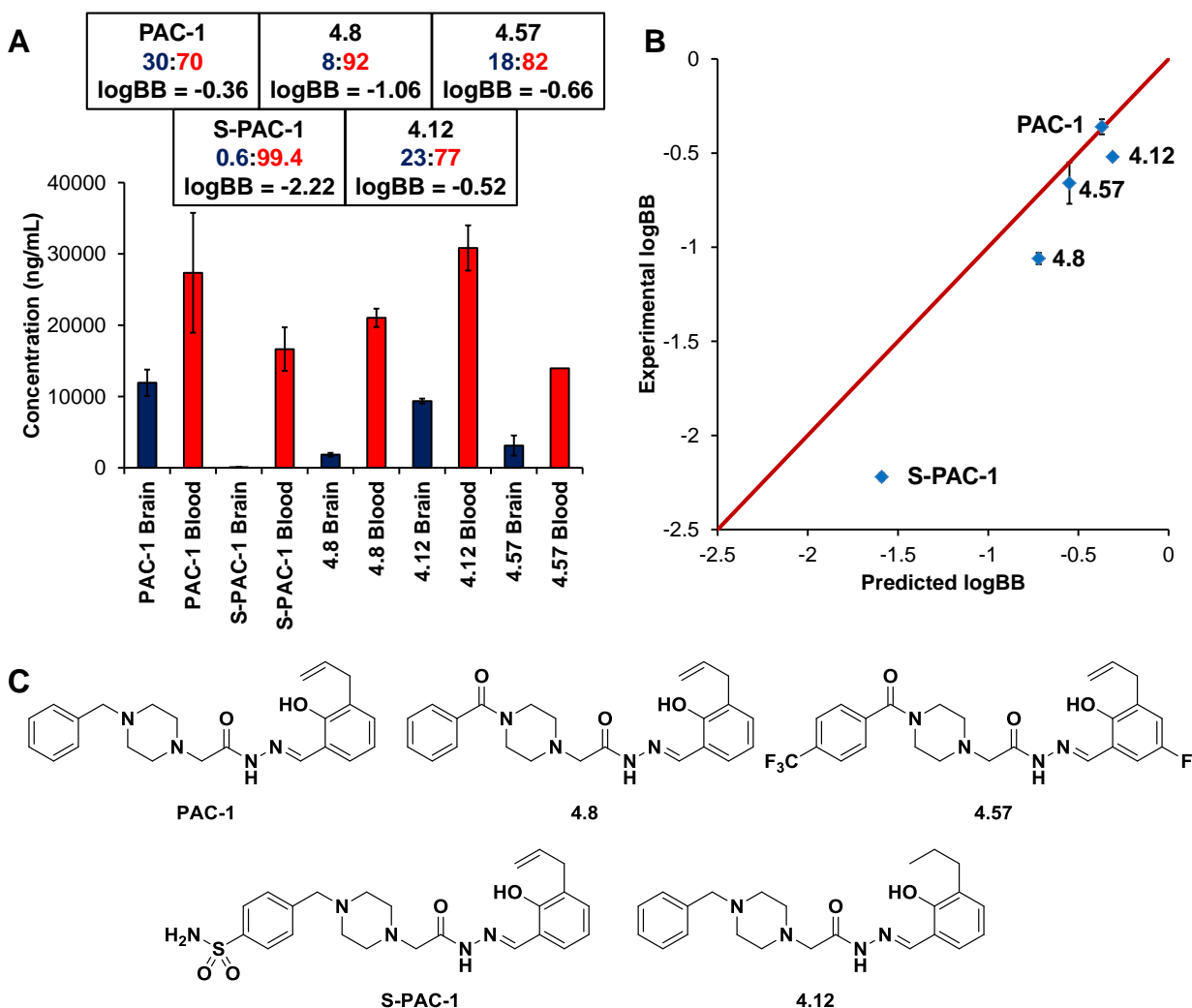


Figure 4.5. BBB permeability *in vivo* for **PAC-1** and derivatives. **A.** Brain/blood distribution for derivatives. **B.** Comparison of predicted and experimentally determined BBB permeability. Red line indicates identical predicted and experimental logBB values. **C.** Structures of derivatives evaluated. C57BL/6 mice received compound at 75 mg/kg (dissolved in HP β CD) via lateral tail vein injection. Concentrations of compounds within serum and brain tissue determined 5 minutes post-injection. Results from **PAC-1** and **S-PAC-1** were reported previously.²¹ Error bars indicate standard deviation ($n \geq 4$).

In addition, the BBB permeability of compounds **4.8** and **4.57** was evaluated via the same method (Figure 4.5A). Compound **4.8** differs from **PAC-1** only by the replacement of the benzyl with a benzoyl substituent, so the effect of this substitution on BBB permeability was assessed. The brain:blood distribution of compound **4.8** was 8:92, indicating that the amide-containing

compounds should be less BBB permeable than analogous compounds containing benzyl substituents. Further, compound **4.57** was of interest due to cell culture potency, liver microsome stability, and improved tolerability as compared to **PAC-1**, so the BBB permeability was assessed to determine whether compound **4.57** would be a promising candidate for the treatment of brain tumors. The brain:blood distribution of **4.57** was 18:82; while this is lower than the BBB permeability of **PAC-1**, it is possible that this level of compound in the brain could be sufficient for treatment of brain tumors. However, compound **4.57** was found to induce hemolysis in the treated animals, so the compound was not evaluated further.

The experimentally determined brain:blood distribution ratios were converted to logBB values and compared to the predicted values calculated previously (Figure 4.5B). The red diagonal line in Figure 4.5B indicates a case in which the predicted values match the experimental values, and the farther away a data point lies from the diagonal, the farther the predicted value is from the experimental value. The algorithm was highly predictive for **PAC-1**, as the predicted value of -0.37 was very close to the experimental value of -0.36. **S-PAC-1** was predicted to show very low permeability (approximately 2.5%), and the experiment demonstrated that less than 1% enters the brain. Each of the other three compounds evaluated was relatively close to the diagonal, although the concentration of each compound in the brain was less than what was predicted.

4.6. Secondary biological assays

As discussed in Section 4.3.3, six compounds (**4.33**, **4.48**, **4.51**, **4.53**, **4.60**, and **4.62**; structures in Table 4.5) were identified that were metabolically stable *in vitro*, and well tolerated *in vivo*. However, due to the high toxicity at lower doses of compounds **4.35** and **4.39**, as well as the hemolysis induced by **4.57**, compounds containing the 4-(trifluoromethyl)benzoyl substituent, including compound **4.48**, were not pursued further. In addition, compound **4.60** was removed from consideration due to slightly decreased potency compared to the rest of the well-tolerated derivatives.

Because of their high stability, comparable potency, and improved *in vivo* tolerability as compared to **PAC-1**, compounds **4.33**, **4.51**, **4.53**, and **4.62** were selected for further investigation. In order to confirm that the hit compounds act similarly to **PAC-1**, the compounds were evaluated for their ability to chelate zinc *in vitro*, activate executioner caspases in whole

cells, and induce apoptosis in cancer cells. Zinc binding was determined using an EGTA titration experiment.²³ In this experiment, varying concentrations of $\text{Zn}(\text{OTf})_2$ were added to each well of a 96-well plate with a HEPES-buffered solution containing EGTA and **PAC-1** derivative, and the fluorescence of the complex was analyzed, a slight variant of our previous protocol for assessment of zinc binding.⁶ As shown in Table 4.5, **PAC-1** binds zinc with a K_d of 1.28 ± 0.03 nM, while **S-PAC-1** binds zinc with a K_d of 2.72 ± 0.13 nM. Each of the four new compounds displays affinity for zinc in the range of 1-2 nM. Inactive derivative **PAC-1a** does not bind zinc, as shown previously.⁶

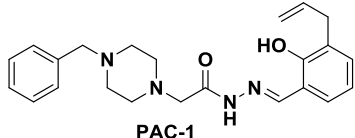
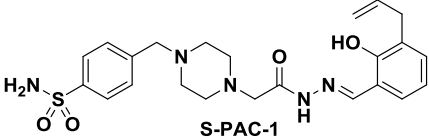
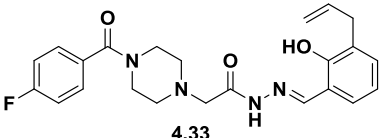
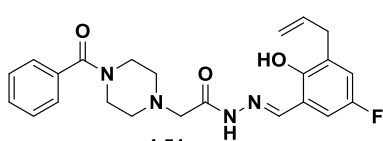
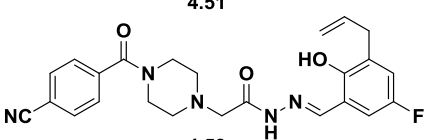
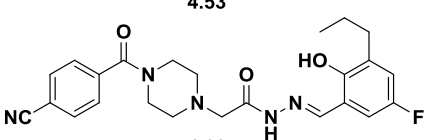
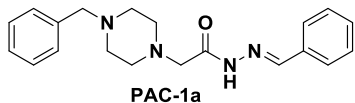
| | Zn ²⁺ K _d (nM) | % Caspase-3/-7 Activity | Predicted logBB |
|---|---|----------------------------|--------------------|
|  PAC-1 | 1.28 ± 0.03 | 87 ± 7 | -0.37 |
|  S-PAC-1 | 2.72 ± 0.13 | 64 ± 11 | -1.59 |
|  4.33 | 1.46 ± 0.07 | 64 ± 4 | -0.69 |
|  4.51 | 1.07 ± 0.09 | 67 ± 6 | -0.69 |
|  4.53 | 1.37 ± 0.10 | 83 ± 3 | -1.06 |
|  4.62 | 1.37 ± 0.03 | 81 ± 4 | -1.00 |
|  PAC-1a | >10 ⁶ | 3 ± 0.1 | -0.18 |

Table 4.5. Zinc chelation,^a caspase activation,^b and predicted BBB permeability of **PAC-1** derivatives.

(a) Increasing amounts of Zn(OTf)₂ added to a buffered solution of EGTA (7.3 mM) and **PAC-1** derivative (100 μM). K_d was determined by comparing fluorescence intensity (ex. 410 nm, em.

475 nm) and free zinc concentration.

(b) U-937 cells treated with compounds (30 μM) for 16 hours, then lysed. Caspase-3/7 activity assessed by cleavage of fluorogenic substrate Ac-DEVD-AFC.¹

(c) Calculated using Equation 3.2:²⁰

$$\text{predicted logBB} = (-0.0148 \times \text{PSA}) + (0.152 \times \text{ClogP}) + 0.139.$$

In addition, the ability of compounds to activate executioner caspases in whole cells was evaluated. Cells were treated with compound for 0 or 16 hours, then the cells were lysed, and cleavage of the fluorescent caspase-3/-7 substrate Ac-DEVD-AFC was analyzed via kinetic reads. The percent activity at 16 hours was normalized to the slope of each compound at 0 hours (0% activity) and the slope of the positive control compound staurosporine at 16 hours (100% activity). As shown in Table 4.5 and Figure 4.6, **PAC-1** induces nearly 90% caspase activation, while each of the other active compounds induces greater than 60% activation of the executioner caspases. As expected, treatment with DMSO alone or **PAC-1a** induces minimal caspase activity in the cells.

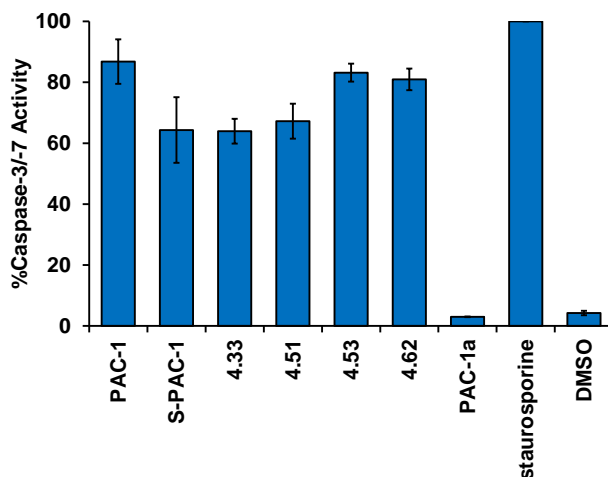


Figure 4.6. **PAC-1** and active derivatives activate executioner caspases in cells. U-937 cells were treated with compounds (30 μ M for **PAC-1** derivatives, 1 μ M for staurosporine) for 16 hours, and then lysed. Caspase-3/7 activity was assessed by cleavage of the fluorogenic substrate Ac-DEVD-AFC. Cells treated with vehicle alone or inactive derivative **PAC-1a** show minimal caspase activity after 16 hours. Values shown are mean \pm s.e.m. (n = 3).¹

In order to confirm that the compounds induced cell death via apoptosis, U-937 cells were treated with compounds at 50 μ M for 12 hours, and cells were assessed by Annexin V-FITC/propidium iodide staining (Figure 4.7). Each of these compounds induced approximately 50% cell death under these conditions, and the presence of large populations in the lower right quadrants of the histograms (Annexin V-FITC positive, propidium iodide negative) confirms that the compounds induce apoptosis in these cancer cells.

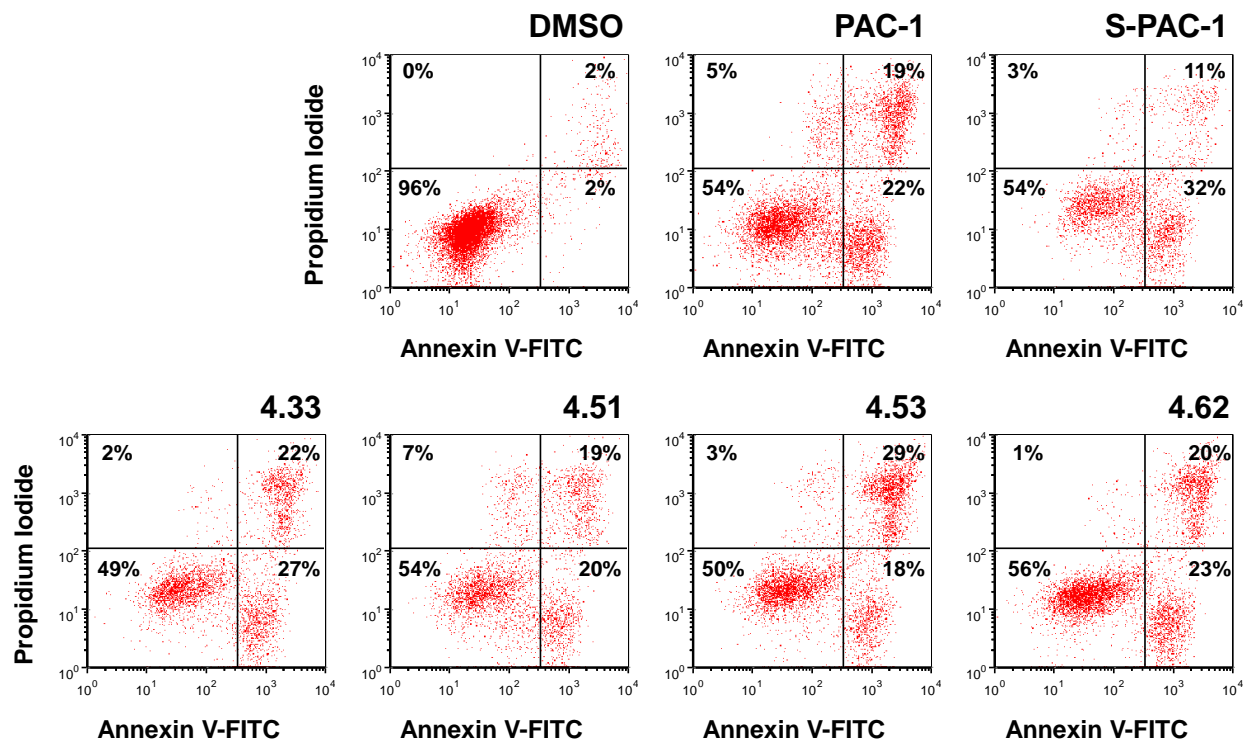


Figure 4.7. PAC-1 and derivatives induce apoptosis in U-937 cells. Cells were treated for 12 hours at 50 μ M, and viability was assessed by Annexin V-FITC/propidium iodide staining. Data shown are representative of three independent experiments.¹

As many PAC-1 derivatives show activity against white blood cell cancer lines^{3, 5, 6, 8, 10, 13-16, 24} and patient-derived leukemic lymphocytes²⁵ in culture, the compounds were evaluated for their ability to induce cell death in a panel of lymphoma and leukemia cell lines, including Jurkat (human leukemia), GL-1 (dog lymphoma), OSW (dog lymphoma), and EL4 (mouse lymphoma) cells, in order to complement the previously determined IC₅₀ values in U-937 (human lymphoma) cells. As shown in Table 4.6, the compounds displayed comparable potency against each given cell line. These results provide further support to the previously determined structure-activity relationships, as the modifications to improve metabolic stability had minimal effect on the activity of the new compounds, and further suggest the potential of PAC-1 and derivatives for the treatment of white blood cell cancers.

| Cell line | Species | Origin | 72-hour IC ₅₀ (μM) | | | | | |
|-----------|---------|----------|-------------------------------|-----------|------------|------------|------------|-----------|
| | | | PAC-1 | S-PAC-1 | 4.33 | 4.51 | 4.53 | 4.62 |
| U-937 | human | lymphoma | 10.2 ± 0.3 | 8.9 ± 0.6 | 10.2 ± 1.7 | 8.6 ± 2.0 | 10.1 ± 2.0 | 9.4 ± 1.2 |
| Jurkat | human | leukemia | 4.4 ± 0.6 | 4.5 ± 1.2 | 4.0 ± 0.5 | 4.1 ± 0.7 | 3.5 ± 0.2 | 3.4 ± 0.6 |
| GL-1 | dog | lymphoma | 3.0 ± 0.1 | 3.2 ± 0.2 | 3.0 ± 0.1 | 3.4 ± 0.2 | 2.4 ± 0.4 | 2.2 ± 0.3 |
| OSW | dog | lymphoma | 10.0 ± 0.8 | 9.8 ± 0.1 | 9.3 ± 0.2 | 10.0 ± 0.6 | 9.5 ± 0.7 | 8.5 ± 0.7 |
| EL4 | mouse | lymphoma | 6.5 ± 0.5 | 7.9 ± 0.5 | 6.5 ± 0.8 | 7.3 ± 1.2 | 5.1 ± 0.4 | 4.7 ± 0.7 |

Table 4.6. PAC-1 and derivatives are cytotoxic to white blood cell cancer lines in culture. Cells treated with compounds for 72 hours. Biomass quantified by sulforhodamine B assay. IC₅₀ values shown are mean ± s.e.m. (n = 3).¹

4.7. Pharmacokinetics

Because compounds **4.34**, **4.52**, **4.54**, and **4.63** all chelate zinc *in vitro* and activate executioner caspases to induce apoptosis in cancer cell lines, all four of the hit compounds were studied further *in vivo*. The pharmacokinetics of the four compounds plus **PAC-1** and **S-PAC-1** were evaluated in mice at a dose of 25 mg/kg (IV injection), and the results are shown in Figure 4.8 and Table 4.7. **PAC-1** and **S-PAC-1** were cleared rapidly and were no longer detectable after 5 and 6 hours post-treatment, respectively. In contrast, detectable levels of each of the four new derivatives remained in circulation for at least 8 hours post-treatment.

The elimination half-life of **PAC-1** was 24.6 ± 0.9 minutes, and the half-life of **S-PAC-1** was 38.1 ± 3.3 minutes. Each of the four new derivatives displayed half-lives of at least 88 minutes, with compound **4.62** having the longest half-life at 122.3 ± 1.4 minutes. In addition, AUC values from intravenous administration for the four new derivatives were all considerably higher than that of **PAC-1**. Compounds **4.33**, **4.53**, and **4.62** were also found to display increased oral bioavailability as compared to **PAC-1** and **S-PAC-1**.

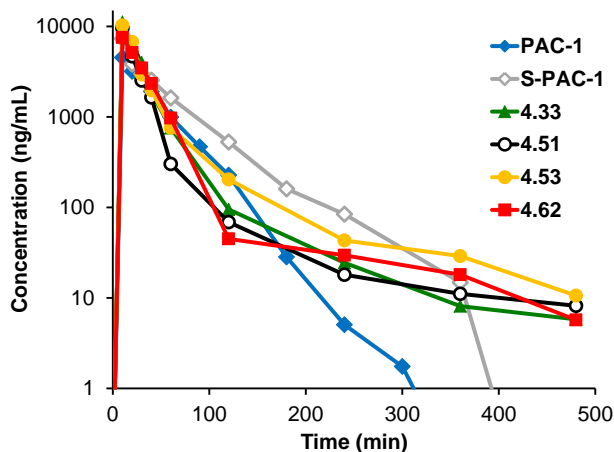


Figure 4.8. Pharmacokinetic profiles of **PAC-1** and selected derivatives following 25 mg/kg intravenous dose (n = 2). Detectable levels of the novel derivatives are present in serum for at least 8 hours post-treatment, while **PAC-1** and **S-PAC-1** are no longer detectable after 5 and 6 hours post-treatment, respectively.¹

| compound | $t_{1/2}$ (min) | AUC (IV) (min* μ g/mL) | AUC (PO) (min* μ g/mL) | %F _{oral} | Predicted logBB |
|----------------|--------------------|-------------------------------|-------------------------------|--------------------|--------------------|
| PAC-1 | 24.6 \pm 0.9 | 210.3 \pm 9.3 | 31.6 \pm 1.6 | 15.1 \pm 1.4 | -0.37 |
| S-PAC-1 | 38.1 \pm 3.3 | 446.0 \pm 114.1 | 54.0 \pm 12.4 | 12.9 \pm 6.1 | -1.59 |
| 4.33 | 89.5 \pm 19.3 | 362.3 \pm 55.8 | 92.2 \pm 6.0 | 25.6 \pm 2.3 | -0.69 |
| 4.51 | 120.5 \pm 16.3 | 291.0 \pm 40.6 | 25.7 \pm 18.3 | 8.5 \pm 5.1 | -0.69 |
| 4.53 | 88.7 \pm 3.3 | 364.9 \pm 5.6 | 105.2 \pm 24.2 | 28.8 \pm 6.2 | -1.06 |
| 4.62 | 122.3 \pm 1.4 | 313.4 \pm 5.5 | 113.0 \pm 3.7 | 36.1 \pm 0.5 | -1.00 |

Table 4.7. Pharmacokinetic parameters and predicted BBB permeability for **PAC-1** and selected derivatives.

25 mg/kg dose was administered via intravenous injection or oral gavage. Values shown are mean \pm standard deviation (n = 2).¹

4.8. Discussion

The introduction of substituents designed to block oxidative metabolism is among the most attractive methods to improve the pharmacokinetic profile for a compound of interest, as the drug can pass through the liver without being modified and remain in circulation for longer periods of time. The knowledge of the metabolites formed from **PAC-1** *in vivo* facilitated the design of a library of **PAC-1** derivatives whose members lacked many of the metabolic liabilities present on the parent compound. The flexible, modular nature of the **PAC-1** synthesis allowed for the rapid generation of 61 derivatives from ten hydrazides and eight aldehydes.

Cell culture evaluation confirmed previously determined structure-activity relationships, in that substituents could be introduced to the aromatic rings without abolishing activity if the core *ortho*-hydroxy-*N*-acylhydrazone remained intact. In general, removal of the allyl group led to a decrease in cell culture potency, consistent with previous reports,^{5, 6} although reduction to the fully saturated propyl group was tolerated in the cell culture experiment. It is likely that the increased hydrophobicity of the alkyl chain contributes to increased cell permeability, as the allyl group does not affect the ability of **PAC-1** to bind zinc.⁶ This was especially apparent in the initial library, as compounds derived from aldehydes **4b**, **4c**, and **4d** induced minimal cell death under the conditions evaluated.

The benzoyl-containing compounds displayed similar cell culture activity to **PAC-1**. This substitution changes the electronics at both the arene and the piperazine nitrogen; the role of the benzylpiperazine in **PAC-1** activity merits further evaluation. Evaluation of the metabolic stability of the library members in rat liver microsomes suggested that *N*-dealkylation was the main route of metabolism *in vitro*; the **PAC-1** derivatives containing benzoyl substituents were more stable than those containing benzyl substituents. These substitutions also reduced the extent of arene oxidation, providing further support for advancement of these compounds. In contrast, the dichloro substitution was unsuccessful in preventing *N*-dealkylation, and the extent of arene oxidation increased for these compounds relative to derivatives containing an unsubstituted benzyl ring.

Experiments in mice demonstrated that most compounds with predicted logBB values above -0.55 induced neuroexcitation, and responses to most of these compounds were at least as severe as the toxicity induced by **PAC-1**. In contrast, no compound with a logBB value of -0.55 or lower induced neuroexcitation in mice, suggesting this level as a threshold for induction of neuroexcitation. Compound **4.12** was slightly less neurotoxic than **PAC-1**, but it was also slightly less BBB permeable. This concentration difference in the brain may represent a second threshold for the severity of neurotoxicity, or **4.12** may interact more weakly with the biological macromolecule responsible for neuroexcitation. Further experiments are necessary to fully understand the nature of this toxicity; preliminary efforts toward this goal will be discussed in Chapter 5.

Four compounds (**4.33**, **4.51**, **4.53**, and **4.62**) were identified with favorable cell culture potency, *in vitro* metabolic stability, and *in vivo* tolerability. Each of these compounds contained

the benzoyl substitution, as well as at least one arene substituent (fluorine and/or nitrile) not present on **PAC-1**. The introduction of fluorine is common in medicinal chemistry, especially the use of aryl fluorides to block undesired metabolic arene oxidation, as in the cholesterol-lowering drug ezetimibe.²⁶ Aryl nitriles are also commonly employed to accomplish this goal, as nitriles typically pass through the body unmodified, and the electron-withdrawing nature of the group deactivates the arene towards oxidative metabolism at other sites.¹⁸ Trifluoromethyl groups can deactivate arenes similarly in certain cases,²⁷ and *in vitro* results with the (trifluoromethyl)benzoyl-containing **PAC-1** derivatives were encouraging. However, these compounds were not evaluated further due to unacceptable levels of toxicity *in vivo*.

Further evaluation of the four lead compounds demonstrated that they chelate zinc, activate executioner caspases in whole cells, and induce apoptosis similarly to **PAC-1** and **S-PAC-1**. The four derivatives displayed three- to five-fold higher elimination half-lives and up to two-fold higher AUC values compared to **PAC-1**. Results from the liver microsome experiment were mostly consistent with the observed *in vivo* pharmacokinetic profiles from experiments in mice: fewer metabolites formed from the new derivatives than from **PAC-1** *in vitro*, and the compounds remained in serum for longer periods of time than **PAC-1**. In contrast, **S-PAC-1** was stable in the liver microsome assay but had a relatively short *in vivo* half-life. This suggests that the main mode of clearance for **S-PAC-1** may not be via oxidative metabolism; instead, the compound may be excreted without modification. A more thorough understanding of this phenomenon may allow for the design of **PAC-1** derivatives that improve upon the pharmacokinetics even further than those described in this report. The rapid clearance of **PAC-1** and **S-PAC-1** from circulation makes them challenging to evaluate in certain efficacy models *in vivo*; these studies typically require large doses of compound, thereby increasing the potential for toxicity. The four novel derivatives remain in circulation for longer than either **PAC-1** or **S-PAC-1**, and thus offer promise as novel therapeutic agents for the treatment of cancer.

4.9. Materials and methods

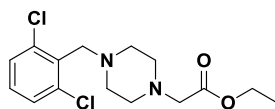
4.9.1. Chemical information

General All reactions requiring anhydrous conditions were conducted under a positive atmosphere of nitrogen or argon in oven-dried glassware. Standard syringe techniques were used

for anhydrous addition of liquids. Unless otherwise noted, all starting materials, solvents, and reagents were acquired from commercial suppliers and used without further purification. Flash chromatography was performed using 230-400 mesh silica gel. Experimental details for compounds not in literature¹ are provided below.

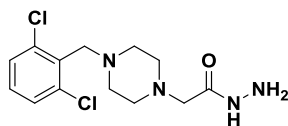
Compound Analysis All NMR experiments were recorded in CDCl₃ (Sigma or Cambridge) or (CD₃)₂CO (Sigma or Cambridge) on a Varian Unity 500 MHz spectrometer with residual undeuterated solvent as the internal reference for ¹H-NMR (CDCl₃ – 7.26 ppm; (CD₃)₂CO – 2.04 ppm) and ¹³C-NMR (CDCl₃ – 77.23 ppm; (CD₃)₂CO – 29.80 ppm). Chemical shift, δ (ppm); coupling constants, *J* (Hz); multiplicity (s = singlet, d = doublet, t = triplet, q = quartet, quint = quintet, sext = sextet, m = multiplet, br = broad); and integration are reported. High-resolution mass spectral data was recorded on a Micromass Q-ToF Ultima hybrid quadrupole/time-of-flight ESI mass spectrometer or a Micromass 70-VSE at the University of Illinois Mass Spectrometry Laboratory.

Ethyl 2-(4-(2,6-dichlorobenzyl)piperazin-1-yl)acetate (**4.4d**)



To a round-bottom flask were added 2,6-dichlorobenzyl bromide (**4.3d**, 2.0 g, 8.34 mmol, 1.0 equiv.), **2.8** (2.15 g, 12.5 mmol, 1.5 equiv.), K₂CO₃ (3.46 g, 25.0 mmol, 3.0 equiv.), and acetone (40 mL, 0.2 M). The reaction mixture was stirred at reflux overnight. The reaction mixture was then cooled to rt. The solid was filtered and washed with acetone, and the filtrate was concentrated. Purification by silica gel column chromatography (25-50% EtOAc/hexanes) gave **4.4d** (2.54 g, 92.0%) as a colorless oil. ¹H-NMR (500 MHz, CDCl₃) δ 7.29 (d, 2H, *J* = 8.0 Hz), 7.13 (t, 1H, *J* = 8.0 Hz), 4.17 (q, 2H, *J* = 7.0 Hz), 3.76 (s, 2H), 3.17 (s, 2H), 2.66 (br s, 4H), 2.55 (br s, 4H), 1.26 (t, 3H, *J* = 7.0 Hz). ¹³C-NMR (125 MHz, CDCl₃) δ 170.6, 137.2, 134.6, 129.0, 128.6, 60.8, 59.8, 56.6, 53.4, 52.9, 14.5.

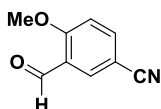
2-(4-(2,6-dichlorobenzyl)piperazin-1-yl)acetohydrazide (**4.1d**)



To a round-bottom flask were added **4.4d** (2.54 g, 7.67 mmol, 1.0 equiv.), EtOH (15 mL, 0.5 M), and anhydrous hydrazine (0.97 mL, 30.7 mmol, 4.0 equiv.). The reaction mixture was stirred at

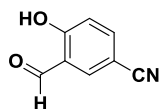
reflux overnight. The reaction mixture was cooled to rt and concentrated. The crude residue was partitioned between CH_2Cl_2 (20 mL)/1:1 brine:0.1M KOH (20 mL). The layers were separated, and the aqueous layer was extracted with CH_2Cl_2 (2 x 20 mL). The combined organic layers were dried over MgSO_4 , filtered, and concentrated. **4.1d** (2.01 g, 82.6%) was obtained as a white solid after extraction without further purification. $^1\text{H-NMR}$ (500 MHz, CDCl_3) δ 8.17 (s, 1H), 7.30 (d, 2H, $J = 8.0$ Hz), 7.14 (t, 1H, $J = 8.0$ Hz), 3.85 (br s, 2H), 3.75 (s, 2H), 3.08 (s, 2H), 2.60 (br s, 4H), 2.50 (br s, 4H). $^{13}\text{C-NMR}$ (125 MHz, CDCl_3) δ 170.8, 137.2, 134.3, 129.1, 128.6, 60.8, 56.5, 53.9, 53.1.

3-formyl-4-methoxybenzonitrile (4.6)



To an oven-dried round-bottom flask were added 5-bromo-2-methoxybenzaldehyde (**4.5**, 4.30 g, 20.0 mmol, 1.0 equiv.), $\text{Zn}(\text{CN})_2$ (2.35 g, 20.0 mmol, 1.0 equiv.), $\text{Pd}(\text{PPh}_3)_4$ (924 mg, 0.80 mmol, 0.040 equiv.), and anhydrous DMF (50 mL). The mixture was deoxygenated by the freeze-pump-thaw method. The reaction mixture was then stirred overnight at 100°C under N_2 . The reaction mixture was cooled to room temperature, diluted with H_2O (100 mL), and extracted with EtOAc (4 x 100 mL). The combined organic layers were washed with H_2O (4 x 50 mL) and brine (50 mL), dried over MgSO_4 , filtered, and concentrated. The product was purified by silica gel column chromatography (20-30% EtOAc/hexanes) to yield **4.6** (1.91 g, 59.2%) as a white solid. $^1\text{H-NMR}$ (500 MHz, CDCl_3) δ 10.40 (s, 1H), 8.08 (d, 1H, $J = 2.0$ Hz), 7.81 (dd, 1H, $J = 2.0, 9.0$ Hz), 7.10 (d, 1H, $J = 9.0$ Hz), 4.01 (s, 3H). $^{13}\text{C-NMR}$ (125 MHz, CDCl_3) δ 187.8, 164.3, 139.2, 133.0, 125.3, 118.2, 113.0, 104.8, 56.5.

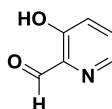
3-formyl-4-hydroxybenzonitrile (4.2b)



To a round-bottom flask were added **4.6** (1.61 g, 10.0 mmol, 1.0 equiv.), LiCl (1.27 g, 30.0 mmol, 3.0 equiv.), and DMF (25 mL, 0.4 M). The reaction mixture was stirred at reflux overnight. The reaction mixture was cooled to room temperature, acidified ($\text{pH} \leq 1$) with 1 M HCl (25 mL), and extracted with EtOAc (6 x 25 mL). The combined organic layers were washed with H_2O (3 x 25 mL) and brine (25 mL), dried over MgSO_4 , filtered, and concentrated. The

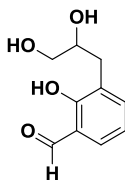
crude product was purified by silica gel column chromatography (gradient, 10-30% EtOAc/hexanes) to yield **4.2b** (274 mg, 18.7%) as a white solid. ¹H-NMR (500 MHz, CDCl₃) δ 11.46 (br s, 1H), 9.93 (s, 1H), 7.94 (d, 1H, *J* = 2.0 Hz), 7.77 (dd, 1H, *J* = 2.0, 8.0 Hz), 7.11 (d, 1H, *J* = 8.0 Hz). ¹³C-NMR (125 MHz, CDCl₃) δ 195.5, 164.8, 139.6, 138.5, 120.8, 119.6, 117.9, 104.1.

3-hydroxypicolinaldehyde (**4.2c**)



To a round-bottom flask were added 85% pure 3-hydroxy-2-(hydroxymethyl)pyridine hydrochloride (**4.7**, 5.0 g, 26.3 mmol, 1.0 equiv.), water (75 mL), and CHCl₃ (100 mL). The mixture was stirred, and activated MnO₂ (6.86 g, 78.9 mmol, 3.0 equiv.) was added. Concentrated H₂SO₄ (0.70 mL, 13.2 mmol, 0.5 equiv.) in water (25 mL) was added dropwise to the mixture. The reaction mixture was stirred at reflux for 2.5 hours. The mixture was cooled to room temperature. Brine (100 mL) was added, and the layers were separated. The aqueous layer was extracted with CHCl₃ (4 x 100 mL). The combined organic layers were dried over Na₂SO₄, filtered, and concentrated to yield **4.2c** (2.28 g, 70.4%) as a brown solid. ¹H-NMR (500 MHz, CDCl₃) δ 10.70 (br s, 1H), 10.04 (s, 1H), 8.32 (d, 1H, *J* = 3.5 Hz), 7.42 (dd, 1H, *J* = 4.0, 9.0 Hz), 7.34 (d, 1H, *J* = 8.5 Hz). ¹³C-NMR (125 MHz, CDCl₃) δ 198.9, 158.8, 142.7, 136.9, 130.2, 126.2.

3-(2,3-dihydroxypropyl)-2-hydroxybenzaldehyde (**4.2d**)



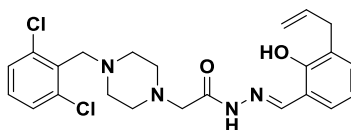
To a round-bottom flask were added **2.1** (2.43 g, 15.0 mmol, 1.0 equiv.), 4-methylmorpholine *N*-oxide (3.51 g, 30.0 mmol, 2.0 equiv.), and 1:1 *t*-BuOH:H₂O (150 mL, 0.1 M). The mixture was stirred, and a solution of OsO₄ (2.5% w/w in *t*-BuOH, 1.9 mL, 0.15 mmol, 0.010 equiv.) was added dropwise. The reaction mixture was capped and stirred overnight at room temperature. The reaction was quenched by the addition of saturated Na₂SO₃, capped, and stirred overnight at room temperature. The reaction mixture was then extracted with EtOAc (6 x 50 mL). The combined organic layers were washed with brine (50 mL), dried over MgSO₄, filtered, and

concentrated. Purification by silica gel column chromatography (gradient, 25-100% EtOAc/hexanes) afforded **4.2d** (2.32 g, 78.9%) as a white solid. ¹H-NMR (500 MHz, CDCl₃) δ 11.39 (br s, 1H), 9.85 (s, 1H), 7.46-7.43 (m, 2H), 6.97 (t, 1H, *J* = 7.5 Hz), 3.97 (m, 1H), 3.61 (dd, 1H, *J* = 2.5, 11.5 Hz), 3.48 (dd, 1H, *J* = 6.5, 11.5 Hz), 3.18 (br s, 1H), 3.03 (br s, 1H), 2.87 (dd, 1H, *J* = 5.5, 13.5 Hz), 2.81 (dd, 1H, *J* = 7.5, 13.5 Hz). ¹³C-NMR (125 MHz, CDCl₃) δ 197.0, 159.8, 138.9, 132.5, 126.8, 120.5, 120.1, 71.9, 66.0, 33.3.

General Procedure A: Synthesis of PAC-1 analogues

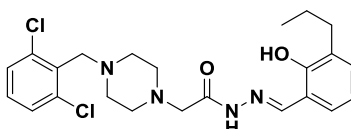
To a 16 x 150 mm test tube were added hydrazide (1.0 equiv.), aldehyde (1.0 equiv.), EtOH or 2:1 MeOH:MeCN (0.15 M), and 1.2 M HCl (7 mol%). The reaction mixture was shaken overnight at reflux on a Büchi Syncore parallel synthesizer. The reaction mixture was cooled to room temperature, concentrated, and purified by silica gel column chromatography or recrystallization to yield pure **PAC-1** analogue.

***N'*-(3-allyl-2-hydroxybenzylidene)-2-(4-(2,6-dichlorobenzyl)piperazin-1-yl)acetohydrazide (4.11)**



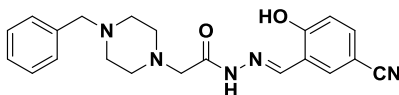
Synthesized according to General Procedure A, but in a round-bottom flask: **4.1d** (317 mg, 1.0 mmol, 1.0 equiv.), **2.1** (162 mg, 1.0 mmol, 1.0 equiv.), 1.2 M HCl (58 μL, 0.070 mmol, 0.070 equiv.), EtOH (7 mL, 0.15 M). Purification by silica gel column chromatography (0-5% MeOH/EtOAc) yielded **4.11** (392 mg, 85.1%) as an off-white solid. ¹H-NMR (500 MHz, CDCl₃) δ 11.25 (s, 1H), 10.10 (br s, 1H), 8.45 (s, 1H), 7.32 (d, 2H, *J* = 8.0 Hz), 7.19 (dd, 1H, *J* = 1.0, 7.5 Hz), 7.16 (t, 1H, *J* = 8.0 Hz), 7.11 (dd, 1H, *J* = 1.5, 8.0 Hz), 6.86 (t, 1H, *J* = 7.5 Hz), 6.04 (tdd, 1H, *J* = 6.5, 10.0, 16.5 Hz), 5.11-5.05 (m, 2H), 3.80 (s, 2H), 3.46 (d, 2H, *J* = 6.5 Hz), 3.19 (br s, 2H), 2.68 (br s, 4H), 2.62 (br s, 4H). ¹³C-NMR (125 MHz, CDCl₃) δ 166.0, 156.7, 151.6, 137.2, 136.8, 134.2, 132.5, 129.4, 129.2, 128.6, 128.5, 119.2, 117.1, 115.8, 61.2, 56.5, 54.0, 53.1, 34.1. HRMS (ESI): 461.1514 (M+1); calcd. for C₂₃H₂₇Cl₂N₄O₂: 461.1511.

2-(4-(2,6-dichlorobenzyl)piperazin-1-yl)-*N'*-(2-hydroxy-3-propylbenzylidene)acetohydrazide (4.17)



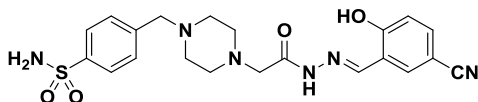
Synthesized according to General Procedure A: **4.1d** (159 mg, 0.50 mmol, 1.0 equiv.), **4.2a** (82 mg, 0.50 mmol, 1.0 equiv.), 1.2 M HCl (29 μ L, 0.035 mmol, 0.070 equiv.), EtOH (3 mL, 0.15 M). Purification by silica gel column chromatography (50-75% EtOAc/hexanes) yielded **4.17** (124 mg, 53.3%) as a white solid. $^1\text{H-NMR}$ (500 MHz, CDCl_3) δ 11.20 (s, 1H), 10.05 (br s, 1H), 8.40 (s, 1H), 7.31 (d, 2H, $J = 8.0$ Hz), 7.18-7.14 (m, 2H), 7.08 (dd, 1H, $J = 1.5, 8.0$ Hz), 6.84 (t, 1H, $J = 7.5$ Hz), 3.79 (s, 2H), 3.17 (s, 2H), 2.68-2.65 (m, 6H), 2.59 (br s, 4H), 1.66 (sext, 2H, $J = 7.5$ Hz), 0.96 (t, 3H, $J = 7.5$ Hz). $^{13}\text{C-NMR}$ (125 MHz, CDCl_3) δ 166.0, 156.9, 151.6, 137.1, 134.2, 132.7, 130.9, 129.2, 129.0, 128.6, 119.0, 116.9, 61.1, 56.5, 53.9, 53.2, 32.1, 22.9, 14.3. HRMS (ESI): 463.1670 (M+1); calcd. for $\text{C}_{23}\text{H}_{29}\text{Cl}_2\text{N}_4\text{O}_2$: 463.1668.

2-(4-benzylpiperazin-1-yl)-N'-(5-cyano-2-hydroxybenzylidene)acetohydrazide (4.18)



Synthesized according to General Procedure A: **1.6** (248 mg, 1.0 mmol, 1.0 equiv.), **4.2b** (147 mg, 1.0 mmol, 1.0 equiv.), 1.2 M HCl (58 μ L, 0.070 mmol, 0.070 equiv.), EtOH (7 mL, 0.15 M). Purification by silica gel column chromatography (gradient, 0-20% MeOH/EtOAc) yielded **4.18** (319.2 mg, 84.7%) as a yellow solid. $^1\text{H-NMR}$ (500 MHz, CDCl_3) δ 11.54 (br s, 1H), 10.24 (br s, 1H), 8.47 (s, 1H), 7.55-7.51 (m, 2H), 7.34-7.30 (m, 4H), 7.28-7.25 (m, 1H), 7.04 (d, 1H, $J = 9.5$ Hz), 3.55 (s, 2H), 3.21 (s, 2H), 2.63 (br s, 4H), 2.54 (br s, 4H). $^{13}\text{C-NMR}$ (125 MHz, CDCl_3) δ 166.5, 162.1, 148.8, 137.7, 135.2, 135.1, 129.3, 128.5, 127.4, 118.8, 118.8, 118.4, 103.0, 63.0, 61.1, 53.9, 53.0. HRMS (ESI): 378.1925 (M+1); calcd. for $\text{C}_{21}\text{H}_{24}\text{N}_5\text{O}_2$: 378.1930.

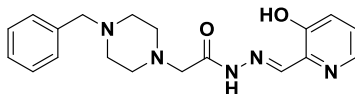
4-((4-(2-(2-(5-cyano-2-hydroxybenzylidene)hydrazinyl)-2-oxoethyl)piperazin-1-yl)methyl)benzenesulfonamide (4.19)



Synthesized according to General Procedure A: **2.16** (327 mg, 1.0 mmol, 1.0 equiv.), **2.1** (147 mg, 1.0 mmol, 1.0 equiv.), 1.2 M HCl (58 μ L, 0.070 mmol, 0.070 equiv.), 2:1 MeOH:MeCN (7 mL, 0.15 M). Purification by silica gel column chromatography (gradient, 0-20% MeOH/EtOAc) yielded **4.19** (343 mg, 75.0%) as a yellow solid. $^1\text{H-NMR}$ (500 MHz, $(\text{CD}_3)_2\text{CO}$) δ 12.31 (br s, 1H), 11.09 (br s, 1H), 8.56 (s, 1H), 7.84 (d, 2H, $J = 8.0$ Hz), 7.77 (s, 1H), 7.64 (d, 2H, $J = 8.0$ Hz), 7.50 (d, 2H, $J = 8.5$ Hz), 7.06 (d, 1H, $J = 8.5$ Hz), 6.59 (br s, 2H), 3.58 (s, 2H), 3.21 (s, 2H), 2.60 (br s, 4H), 2.51 (br s, 4H). $^{13}\text{C-NMR}$ (125 MHz, $(\text{CD}_3)_2\text{CO}$) δ 167.0, 162.6, 148.5, 143.8,

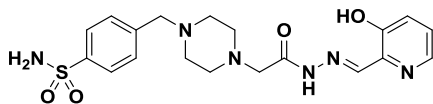
143.7, 135.9, 135.3, 129.9, 126.8, 119.9, 119.2, 119.0, 103.3, 62.5, 61.5, 54.1, 53.4. HRMS (ESI): 457.1655 (M+1); calcd. for C₂₁H₂₅N₆O₄S: 457.1658.

2-(4-benzylpiperazin-1-yl)-N'-((3-hydroxypyridin-2-yl)methylene)acetohydrazide (4.20)



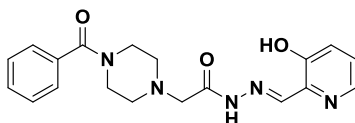
Synthesized according to General Procedure A: **1.6** (124 mg, 0.50 mmol, 1.0 equiv.), **4.2c** (62 mg, 0.50 mmol, 1.0 equiv.), 1.2 M HCl (29 μ L, 0.035 mmol, 0.070 equiv.), EtOH (3 mL, 0.15 M). Purification by silica gel column chromatography (gradient, 0-25% MeOH/EtOAc) yielded **4.20** (141 mg, 79.4%) as a yellow solid. ¹H-NMR (500 MHz, CDCl₃) δ 10.84 (br s, 1H), 10.31 (br s, 1H), 8.41 (s, 1H), 8.18 (dd, 1H, *J* = 1.5, 4.5 Hz), 7.34-7.30 (m, 4H), 7.28-7.24 (m, 1H), 7.21 (dd, 1H, *J* = 4.5, 8.0 Hz), 7.10 (dd, 1H, *J* = 1.5, 7.5 Hz), 3.54 (s, 2H), 3.21 (s, 2H), 2.63 (br s, 4H), 2.52 (br s, 4H). ¹³C-NMR (125 MHz, CDCl₃) δ 166.2, 155.8, 151.1, 141.4, 137.8, 136.4, 129.3, 128.5, 127.4, 125.8, 124.9, 63.0, 61.0, 53.8, 53.2. HRMS (ESI): 354.1927 (M+1); calcd. for C₁₉H₂₄N₅O₂: 354.1930.

4-((4-(2-(2-((3-hydroxypyridin-2-yl)methylene)hydrazinyl)-2-oxoethyl)piperazin-1-yl)methyl)benzenesulfonamide (4.21)



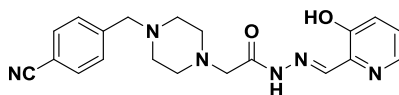
Synthesized according to General Procedure A: **2.16** (164 mg, 0.50 mmol, 1.0 equiv.), **4.2c** (62 mg, 0.50 mmol, 1.0 equiv.), 1.2 M HCl (29 μ L, 0.035 mmol, 0.070 equiv.), 2:1 MeOH:MeCN (3 mL, 0.15 M). Purification by silica gel column chromatography (gradient, 0-30% MeOH/EtOAc) yielded **4.21** (169 mg, 78.2%) as a yellow solid. ¹H-NMR (500 MHz, (CD₃)₂CO) δ 11.46 (br s, 1H), 11.12 (br s, 1H), 8.57 (s, 1H), 8.16 (dd, 1H, *J* = 1.5, 4.5 Hz), 7.84 (d, 2H, *J* = 8.5 Hz), 7.51 (d, 2H, *J* = 8.0 Hz), 7.31 (dd, 1H, *J* = 1.5, 8.5 Hz), 7.28 (dd, 1H, *J* = 4.5, 8.5 Hz), 6.57 (br s, 2H), 3.58 (s, 2H), 3.21 (s, 2H), 2.60 (br s, 4H), 2.51 (br s, 4H). ¹³C-NMR (125 MHz, CDCl₃) δ 166.9, 156.1, 151.1, 144.0, 143.8, 141.9, 137.9, 129.9, 126.8, 126.0, 124.7, 62.6, 61.7, 54.2, 53.5. HRMS (ESI): 433.1656 (M+1); calcd. for C₁₉H₂₅N₆O₄S: 433.1658.

2-(4-benzoylpiperazin-1-yl)-N'-((3-hydroxypyridin-2-yl)methylene)acetohydrazide (4.22)



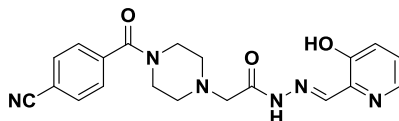
Synthesized according to General Procedure A: **4.1a** (131 mg, 0.50 mmol, 1.0 equiv.), **4.2c** (62 mg, 0.50 mmol, 1.0 equiv.), 1.2 M HCl (29 μ L, 0.035 mmol, 0.070 equiv.), EtOH (3 mL, 0.15 M). Purification by silica gel column chromatography (gradient, 0-20% MeOH/EtOAc) yielded **4.22** (169 mg, 91.8%) as a yellow solid. $^1\text{H-NMR}$ (500 MHz, CDCl_3) δ 10.96 (br s, 1H), 10.59 (br s, 1H), 8.44 (s, 1H), 8.13 (dd, 1H, $J = 4.0, 11.5$ Hz), 7.42-7.37 (m, 5H), 7.29 (d, 1H, $J = 8.0$ Hz), 7.19 (dd, 1H, $J = 4.5, 8.5$ Hz), 3.82 (br s, 2H), 3.50 (br s, 2H), 3.23 (s, 2H), 2.64 (br s, 2H), 2.54 (br s, 2H). $^{13}\text{C-NMR}$ (125 MHz, CDCl_3) δ 170.7, 165.8, 155.8, 151.3, 147.7, 141.3, 136.3, 135.3, 130.2, 128.8, 127.1, 125.8, 125.0, 60.8, 53.7 (br), 47.8 (br), 42.2 (br). HRMS (ESI): 368.1720 (M+1); calcd. for $\text{C}_{19}\text{H}_{22}\text{N}_5\text{O}_3$: 368.1723.

2-(4-(4-cyanobenzyl)piperazin-1-yl)-N'-((3-hydroxypyridin-2-yl)methylene)acetohydrazide (4.23)



Synthesized according to General Procedure A: **4.1b** (273 mg, 1.0 mmol, 1.0 equiv.), **4.2c** (123 mg, 1.0 mmol, 1.0 equiv.), 1.2 M HCl (58 μ L, 0.070 mmol, 0.070 equiv.), EtOH (7 mL, 0.15 M). Purification by silica gel column chromatography (gradient, 0-30% MeOH/EtOAc) yielded **4.23** (229 mg, 60.6%) as a yellow solid. $^1\text{H-NMR}$ (500 MHz, CDCl_3) δ 10.82 (br s, 1H), 10.36 (br s, 1H), 8.42 (s, 1H), 8.17 (d, 1H, $J = 4.0$ Hz), 7.59 (d, 2H, $J = 8.0$ Hz), 7.42 (d, 1H, $J = 8.0$ Hz), 7.31 (d, 1H, $J = 8.0$ Hz), 7.21 (d, 1H, $J = 4.5, 8.5$ Hz), 3.57 (s, 2H), 3.24 (s, 2H), 2.64 (br s, 4H), 2.52 (br s, 4H). $^{13}\text{C-NMR}$ (125 MHz, CDCl_3) δ 166.2, 155.8, 151.2, 143.6, 141.4, 136.3, 132.3, 129.6, 125.8, 125.0, 119.0, 111.2, 62.3, 60.8, 53.7, 53.2. HRMS (ESI): 379.1881 (M+1); calcd. for $\text{C}_{20}\text{H}_{23}\text{N}_6\text{O}_2$: 379.1882.

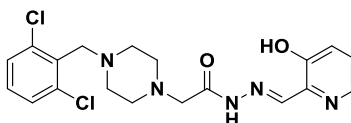
2-(4-(4-cyanobenzoyl)piperazin-1-yl)-N'-((3-hydroxypyridin-2-yl)methylene)acetohydrazide (4.24)



Synthesized according to General Procedure A: **4.1c** (287 mg, 1.0 mmol, 1.0 equiv.), **4.2c** (123 mg, 1.0 mmol, 1.0 equiv.), 1.2 M HCl (58 μ L, 0.070 mmol, 0.070 equiv.), EtOH (7 mL, 0.15 M). Purification by silica gel column chromatography (gradient, 0-30% MeOH/EtOAc) yielded **4.24** (279 mg, 71.1%) as a dark yellow solid. $^1\text{H-NMR}$ (500 MHz, CDCl_3) δ 10.91 (br s, 1H), 10.47

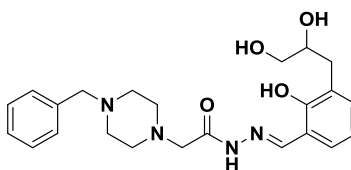
(br s, 1H), 8.44 (s, 1H), 8.17-8.09 (m, 1H), 7.69 (d, 2H, $J = 7.0$ Hz), 7.50-7.47 (m, 1H), 7.29-7.26 (m, 1H), 7.23-7.20 (m, 1H), 3.83 (br s, 2H), 3.42 (br s, 2H), 3.27 (s, 2H), 2.69 (br s, 2H), 2.56 (br s, 4H). ^{13}C -NMR (125 MHz, CDCl_3) δ 168.5, 165.6, 155.7, 151.4, 141.3, 139.7, 136.2, 132.7, 127.9, 125.9, 125.0, 118.1, 113.9, 60.7, 53.7 (br), 47.5 (br), 42.2 (br). HRMS (ESI): 393.1672 (M+1); calcd. for $\text{C}_{20}\text{H}_{21}\text{N}_6\text{O}_3$: 393.1675.

2-(4-(2,6-dichlorobenzyl)piperazin-1-yl)-N'-((3-hydroxypyridin-2-yl)methylene)acetohydrazide (4.25)



Synthesized according to General Procedure A: **4.1d** (159 mg, 0.50 mmol, 1.0 equiv.), **4.2c** (62 mg, 0.50 mmol, 1.0 equiv.), 1.2 M HCl (29 μL , 0.035 mmol, 0.070 equiv.), EtOH (3 mL, 0.15 M). Purification by silica gel column chromatography (gradient, 0-20% MeOH/EtOAc) yielded **4.25** (177 mg, 83.7%) as a yellow solid. ^1H -NMR (500 MHz, CDCl_3) δ 10.82 (br s, 1H), 10.40 (br s, 1H), 8.43 (s, 1H), 8.18 (dd, 1H, $J = 1.0, 4.5$ Hz), 7.32 (d, 1H, $J = 8.0$ Hz), 7.29 (d, 2H, $J = 8.0$ Hz), 7.22 (dd, 1H, $J = 4.5, 8.5$ Hz), 7.14 (t, 1H, $J = 8.0$ Hz), 3.77 (s, 2H), 3.20 (s, 2H), 2.64 (br s, 4H), 2.59 (br s, 4H). ^{13}C -NMR (125 MHz, CDCl_3) δ 166.4, 155.8, 151.1, 141.4, 137.1, 137.1, 134.1, 129.2, 128.6, 125.8, 125.0, 60.9, 56.4, 53.9, 53.1. HRMS (ESI): 422.1152 (M+1); calcd. for $\text{C}_{19}\text{H}_{22}\text{Cl}_2\text{N}_5\text{O}_2$: 422.1151.

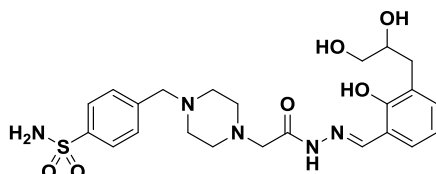
2-(4-benzylpiperazin-1-yl)-N'-((3-(2,3-dihydroxypropyl)-2-hydroxybenzylidene)acetohydrazide (4.26)



Synthesized according to General Procedure A: **1.6** (124 mg, 0.50 mmol, 1.0 equiv.), **4.2d** (98 mg, 0.50 mmol, 1.0 equiv.), 1.2 M HCl (29 μL , 0.035 mmol, 0.070 equiv.), EtOH (3 mL, 0.15 M). Purification by silica gel column chromatography (gradient, 0-20% MeOH/EtOAc) yielded **4.26** (178.9 mg, 84.0%) as an off-white solid. ^1H -NMR (500 MHz, CDCl_3) δ 11.49 (br s, 1H), 10.16 (br s, 1H), 8.36 (s, 1H), 7.34-7.30 (m, 4H), 7.28-7.25 (m, 1H), 7.21 (dd, 1H, $J = 1.5, 7.5$ Hz), 7.12 (dd, 1H, $J = 1.5, 7.5$ Hz), 6.86 (t, 1H, $J = 7.5$ Hz), 4.00-3.95 (m, 1H), 3.61 (dd, 1H, $J = 4.0, 11.5$ Hz), 3.54 (s, 2H), 3.50 (dd, 1H, $J = 6.0, 11.5$ Hz), 3.18 (s, 2H), 2.92 (dd, 1H, $J = 6.0,$

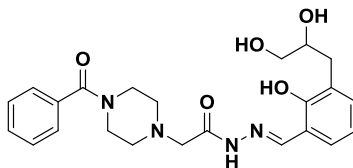
13.5 Hz), 2.87 (dd, 1H, $J = 7.0, 13.5$ Hz), 2.62 (br s, 4H), 2.53 (br s, 4H). $^{13}\text{C-NMR}$ (125 MHz, CDCl_3) δ 166.2, 156.6, 151.0, 137.8, 134.0, 129.8, 129.4, 128.5, 127.4, 126.3, 119.7, 117.3, 72.4, 66.0, 63.1, 61.1, 53.9, 53.1, 34.2. HRMS (ESI): 427.2336 ($M+1$); calcd. for $\text{C}_{23}\text{H}_{31}\text{N}_4\text{O}_4$: 427.2345.

4-((4-(2-(2-(3-(2,3-dihydroxypropyl)-2-hydroxybenzylidene)hydrazinyl)-2-oxoethyl)piperazin-1-yl)methyl)benzenesulfonamide (4.27)



Synthesized according to General Procedure A: **2.16** (164 mg, 0.50 mmol, 1.0 equiv.), **4.2d** (98 mg, 0.50 mmol, 1.0 equiv.), 1.2 M HCl (29 μL , 0.035 mmol, 0.070 equiv.), 2:1 MeOH:MeCN (3 mL, 0.15 M). Purification by silica gel column chromatography (gradient, 0-20% MeOH/EtOAc) yielded **4.27** (183 mg, 72.2%) as a yellow solid. $^1\text{H-NMR}$ (500 MHz, $(\text{CD}_3)_2\text{CO}$) δ 11.86 (br s, 1H), 10.82 (br s, 1H), 8.49 (s, 1H), 7.84 (d, 2H, $J = 8.0$ Hz), 7.51 (d, 2H, $J = 8.0$ Hz), 7.25 (dd, 1H, $J = 1.5, 7.5$ Hz), 7.17 (dd, 1H, $J = 1.5, 8.0$ Hz), 6.83 (t, 1H, $J = 7.5$ Hz), 6.57 (br s, 2H), 3.96-3.92 (m, 1H), 3.58 (s, 2H), 3.51 (dd, 1H, $J = 4.0, 11.0$ Hz), 3.43 (dd, 1H, $J = 6.5, 11.0$ Hz), 3.17 (s, 2H), 2.90 (dd, 1H, $J = 5.5, 13.5$ Hz), 2.74 (dd, 1H, $J = 7.5, 13.5$ Hz), 2.59 (br s, 4H), 2.51 (br s, 4H). $^{13}\text{C-NMR}$ (125 MHz, $(\text{CD}_3)_2\text{CO}$) δ 166.5, 157.3, 150.7, 144.0, 143.8, 134.2, 129.9, 129.9, 127.6, 126.8, 119.7, 118.4, 72.4, 66.8, 62.6, 61.6, 54.2, 53.5, 34.8. HRMS (ESI): 506.2072 ($M+1$); calcd. for $\text{C}_{23}\text{H}_{32}\text{N}_5\text{O}_6\text{S}$: 506.2073.

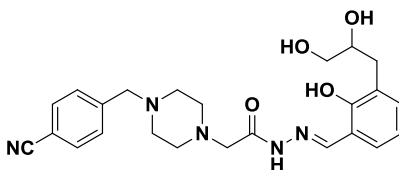
2-(4-benzoylpiperazin-1-yl)-N'-(3-(2,3-dihydroxypropyl)-2-hydroxybenzylidene)acetohydrazide (4.28)



Synthesized according to General Procedure A: **4.1a** (131 mg, 0.50 mmol, 1.0 equiv.), **4.2d** (98 mg, 0.50 mmol, 1.0 equiv.), 1.2 M HCl (29 μL , 0.035 mmol, 0.070 equiv.), EtOH (3 mL, 0.15 M). Purification by silica gel column chromatography (gradient, 0-20% MeOH/EtOAc) yielded **4.28** (121 mg, 55.0%) as a white solid. $^1\text{H-NMR}$ (500 MHz, $(\text{CD}_3)_2\text{CO}$) δ 11.86 (br s, 1H), 10.93 (br s, 1H), 8.47 (s, 1H), 7.44-7.39 (m, 5H), 7.25 (dd, 1H, $J = 1.5, 7.5$ Hz), 7.16 (dd, 1H, $J = 1.5,$

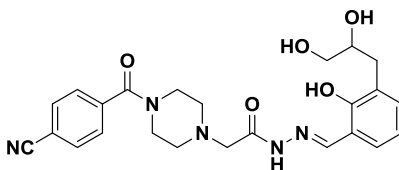
7.5 Hz), 6.83 (t, 1H, $J = 7.5$ Hz), 3.98-3.95 (m, 1H), 3.74 (br s, 2H), 3.64 (br s, 2H), 3.52-3.49 (m, 1H), 3.44-3.41 (m, 1H), 3.24 (s, 2H), 2.92 (dd, 2H, $J = 6.0, 13.0$ Hz), 2.74 (dd, 2H, $J = 7.5, 13.0$ Hz), 2.63 (br s, 4H). ^{13}C -NMR (125 MHz, $(\text{CD}_3)_2\text{CO}$) δ 170.2, 166.2, 157.3, 150.8, 137.3, 134.2, 130.3, 129.9, 129.2, 127.9, 127.6, 119.7, 118.3, 72.4, 66.8, 61.4, 54.1 (br), 48.2 (br), 42.5 (br), 34.8. HRMS (ESI): 441.2143 (M+1); calcd. for $\text{C}_{23}\text{H}_{29}\text{N}_4\text{O}_5$: 441.2138.

2-(4-(4-cyanobenzyl)piperazin-1-yl)-N'-(3-(2,3-dihydroxypropyl)-2-hydroxybenzylidene)acetohydrazide (4.29)



Synthesized according to General Procedure A: **4.1b** (273 mg, 1.0 mmol, 1.0 equiv.), **4.2d** (196 mg, 1.0 mmol, 1.0 equiv.), 1.2 M HCl (58 μL , 0.070 mmol, 0.070 equiv.), EtOH (7 mL, 0.15 M). Purification by silica gel column chromatography (gradient, 0-20% MeOH/EtOAc) yielded **4.29** (391 mg, 86.5%) as a light yellow solid. ^1H -NMR (500 MHz, CDCl_3) δ 11.45 (br s, 1H), 10.23 (br s, 1H), 8.31 (s, 1H), 7.59 (d, 2H, $J = 8.5$ Hz), 7.43 (d, 1H, $J = 8.0$ Hz), 7.17 (dd, 1H, $J = 1.0, 7.5$ Hz), 7.08 (dd, 1H, $J = 1.0, 7.5$ Hz), 6.81 (t, 1H, $J = 7.5$ Hz), 3.99-3.94 (m, 1H), 3.59 (dd, 1H, $J = 3.5, 11.5$ Hz), 3.56 (s, 2H), 3.47 (dd, 1H, $J = 6.0, 11.5$ Hz) 3.18 (s, 2H), 2.87 (dd, 1H, $J = 6.0, 14.0$ Hz), 2.82 (dd, 1H, $J = 7.0, 13.5$ Hz), 2.61 (br s, 4H), 2.50 (br s, 4H). ^{13}C -NMR (125 MHz, CDCl_3) δ 166.2, 156.5, 151.0, 143.9, 134.0, 132.3, 129.8, 129.6, 126.3, 119.7, 119.1, 117.2, 111.1, 72.3, 66.0, 62.4, 61.0, 53.7, 53.1, 34.1. HRMS (ESI): 452.2296 (M+1); calcd. for $\text{C}_{24}\text{H}_{30}\text{N}_5\text{O}_4$: 452.2298.

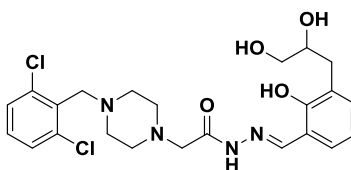
2-(4-(4-cyanobenzoyl)piperazin-1-yl)-N'-(3-(2,3-dihydroxypropyl)-2-hydroxybenzylidene)acetohydrazide (4.30)



Synthesized according to General Procedure A: **4.1c** (287 mg, 1.0 mmol, 1.0 equiv.), **4.2d** (196 mg, 1.0 mmol, 1.0 equiv.), 1.2 M HCl (58 μL , 0.070 mmol, 0.070 equiv.), EtOH (7 mL, 0.15 M). Purification by silica gel column chromatography (gradient, 0-20% MeOH/EtOAc) yielded **4.30** (341 mg, 73.4%) as a light yellow solid. ^1H -NMR (500 MHz, $(\text{CD}_3)_2\text{CO}$) δ 11.85 (br s, 1H),

10.95 (br s, 1H), 8.47 (s, 1H), 7.85 (d, 2H, $J = 8.0$ Hz), 7.61 (d, 2H, $J = 8.5$ Hz), 7.25 (d, 1H, $J = 7.5$ Hz), 7.15 (dd, 1H, $J = 1.5, 7.5$ Hz), 6.82 (t, 1H, $J = 7.5$ Hz), 3.96-3.92 (m, 1H), 3.78 (br s, 2H), 3.52-3.41 (m, 4H, CH_2-N), 3.25 (s, 2H), 2.90 (dd, 1H, $J = 6.0, 13.5$ Hz), 2.74 (dd, 1H, $J = 7.0, 13.5$ Hz), 2.68 (br s, 2H), 2.61 (br s, 2H). ^{13}C -NMR (125 MHz, $(CD_3)_2CO$) δ 168.5, 166.2, 157.3, 150.8, 141.6, 134.2, 133.2, 129.9, 128.8, 127.6, 119.7, 118.8, 118.3, 113.8, 72.4, 66.8, 61.3, 54.1 (br), 53.6 (br), 48.1 (br), 42.5 (br), 34.8. HRMS (ESI): 466.2088 (M+1); calcd. for $C_{24}H_{28}N_5O_5$: 466.2090.

2-(4-(2,6-dichlorobenzyl)piperazin-1-yl)-N'-(3-(2,3-dihydroxypropyl)-2-hydroxybenzylidene)acetohydrazide (4.31)



Synthesized according to General Procedure A: **4.1d** (159 mg, 0.50 mmol, 1.0 equiv.), **4.2d** (98 mg, 0.50 mmol, 1.0 equiv.), 1.2 M HCl (29 μ L, 0.035 mmol, 0.070 equiv.), EtOH (3 mL, 0.15 M). Purification by silica gel column chromatography (gradient, 0-20% MeOH/EtOAc) yielded **4.31** (225 mg, 90.6%) as a light yellow solid. 1H -NMR (500 MHz, $CDCl_3$) δ 11.47 (br s, 1H), 10.24 (br s, 1H), 8.34 (s, 1H), 7.29 (d, 2H, $J = 8.0$ Hz), 7.19 (dd, 1H, $J = 1.5, 7.5$ Hz), 7.14 (t, 1H, $J = 8.0$ Hz), 7.10 (dd, 1H, $J = 1.5, 7.5$ Hz), 6.83 (t, 1H, $J = 7.5$ Hz), 3.99-3.95 (m, 1H), 3.76 (s, 2H), 3.60 (dd, 1H, $J = 3.5, 11.5$ Hz), 3.48 (dd, 1H, $J = 6.0, 11.5$ Hz), 3.16 (s, 2H), 2.90 (dd, 1H, $J = 6.0, 13.5$ Hz), 2.84 (dd, 1H, $J = 7.0, 13.5$ Hz), 2.64 (br s, 4H), 2.57 (br s, 4H). ^{13}C -NMR (125 MHz, $CDCl_3$) δ 166.3, 156.6, 151.0, 137.1, 134.1, 134.0, 129.8, 129.2, 128.6, 126.3, 119.7, 117.3, 72.3, 66.0, 61.0, 56.4, 53.9, 53.0, 34.2. HRMS (ESI): 495.1563 (M+1); calcd. for $C_{23}H_{29}Cl_2N_4O_4$: 495.1566.

4.9.2. Biological evaluation

Materials All reagents were obtained from Fisher unless otherwise indicated. All buffers were made with MilliQ purified water. Annexin V Binding Buffer contains 10 mM HEPES (pH 7.4), 140 mM NaCl, 2.5 mM $CaCl_2$. Bifunctional cell lysis/caspase activity buffer contains 200 mM HEPES (pH 7.4), 400 mM NaCl, 40 mM DTT, 0.4 mM EDTA disodium salt dihydrate, 1% Triton-X-100, and 20 μ M Ac-DEVD-AFC (Enzo Life Sciences).

Liver Microsome Stability Assay A mixture of 0.1 M potassium phosphate buffer pH 7.4, NADP⁺ (final concentration 1.3 mM), MgCl₂ (final concentration 3.3 mM), glucose-6-phosphate (final concentration 3.3 mM), glucose-6-phosphate dehydrogenase (final concentration 0.4 U/mL), and a 10 mM solution of compound in DMSO (final concentration 10 μM; 0.1% DMSO) was incubated at 37°C in a shaking incubator for 5 min. The reactions were initiated by the addition of ice-cold liver microsomes (final protein concentration 1 mg/mL), to bring the total volume to 1 mL. A 450 μL aliquot was immediately removed, quenched with 450 μL of a 10 μM solution of **B-PAC-1**^{8, 25} in MeCN, mixed by inversion, and centrifuged at 10,000 x g for 3 min. 750 μL of the supernatant was removed for LC/MS analysis. The reactions were incubated at 37°C in a shaking incubator for 3 h. A second 450 μL aliquot was removed, quenched with 450 μL of a 10 μM solution of **B-PAC-1** in MeCN, mixed by inversion, and centrifuged at 10,000 x g for 3 min. 750 μL of the supernatant was removed for LC/MS analysis. Samples from the liver microsome assay were analyzed by LC/MS using an Agilent 1200 HPLC with DAD (monitoring at 280 nm) and an Agilent 6230 TOF MS, with an Agilent C18 column, 3.0 x 50 mm. Mobile phase A was 0.1% HCO₂H in H₂O, B was 0.1% HCO₂H in MeCN. A gradient was run from 5-50% B over 18 min, then 50-95% B for 2 min, then constant 95% B for 4 min, then 95-5% B for 1 min, then constant 5% B for 2 min. The ratio of the areas of analyte:internal standard at 3 hours was compared to the ratio at 0 hours to determine the percent compound remaining after 3 hours.

Cell Culture U-937, Jurkat, and EL4 cells were obtained from the American Type Culture Collection. GL-1 cells were provided by Dr. Steve Suter (North Carolina State University, Raleigh, NC). All cultures were maintained at low passage number in RPMI 1640 supplemented with 10% fetal bovine serum and 1% penicillin-streptomycin and grown at 37°C and 5% CO₂.

72hr IC₅₀ Cell Death Assay To each inner well of a 96-well plate was added 49 μL of RPMI 1640 complete growth media. To each inner well was added 1 μL of compound stock solutions in DMSO at nine concentrations such that the cells were treated with half-log concentrations between 0.01 μM and 100 μM compound. 50 μL of a suspension of cells at 300,000 cells/mL (for U-937, EL4, GL-1, and OSW cells) or 500,000 cells/mL (for Jurkat cells) were plated into the wells, for a final density of 15,000 or 25,000 cells per well, respectively. Each concentration was tested in triplicate per plate. In each plate 3 wells received 1 μL of a positive death control

and 3 wells received 1 μL DMSO as a live cell vehicle control. The outer wells were filled with sterile PBS pH 7.4 (100 or 200 μL), and the plates were then incubated at 37°C with 5% CO_2 for 72 hours. After the 72 hour incubation period, the plates were analyzed using a Sulforhodamine B assay.²⁸ Specifically, to each well of the plate 25 μL of a 50% (w/v) solution of trichloroacetic acid in H_2O was added and the plates were incubated for 4 hours at 4°C. The plates were then washed gently with H_2O five times. The plates were allowed to air dry after which 100 μL of a 0.057% (w/v) Sulforhodamine B in a 1% (v/v) acetic acid solution was added to each well for 30 minutes at room temperature. The plates were gently washed 5 times with 1% (v/v) acetic acid and air dried. 200 μL of 10 mM Tris base (pH 10.4) was added to each well and the plates were placed on a shaker for thirty minutes. For U-937 cells, the level of SRB was quantified fluorometrically (ex. 488 nm, em. 585 nm) on a Gemini EM Microplate Reader (Molecular Devices) plate reader. For all other cell lines, the level of SRB was quantified by absorbance at 510 nm on a SpectraMax Plus 384 Microplate Reader (Molecular Devices). The percent cell death was calculated and normalized to the positive control (100% cell death) and the negative control (0% cell death). The percent cell death was averaged for each compound concentration and plotted as a function of compound concentration. The data were fit to a logistical dose response curve using TableCurve 2D and the IC_{50} value was calculated. The experiment was repeated three times and the average of the calculated IC_{50} values was reported. The standard error of the mean (s.e.m.) was determined and reported for the triplicate experiments.

Induction of Apoptosis by Hit Compounds To each well of a 24-well plate for compound treatment was added 490 μL of RPMI-1640 complete growth media. To each well was then added 10 μL of 5 mM DMSO solutions to achieve a final compound concentration of 50 μM . 10 μL of DMSO was added to one well as a live cell vehicle control. 500 μL of a suspension of cells at 1.2×10^6 cells/mL were plated into the wells, for a final density of 600,000 cells per well. Wells not containing compounds were filled with 1 mL RPMI-1640 complete growth media, and spaces between wells were filled with 1 mL sterile PBS. The cells were incubated at 37 °C with 5% CO_2 for 12 hours. The cells were harvested via centrifugation (200 x g for 5 min), washed with PBS (2 mL), and resuspended in 450 μL Annexin V Binding Buffer containing 3.5 μL of FITC-conjugated Annexin V stain (Southern Biotech) and 2.25 μL of a 1 mg/mL solution of propidium iodide (Sigma) to a final concentration of 5 $\mu\text{g}/\text{mL}$. Samples were stored on ice until

assessment. Cell populations were analyzed on a Becton Dickinson LSR II cell flow cytometer. 10,000 events per sample were recorded.

EGTA Fluorescence Titration Assay This titration assay is based on a published protocol.²³ Buffer (50 mM HEPES, 100 mM KNO₃, 8.1 mM EGTA, pH 7.2) and solutions of compounds (1 mM in DMSO) and Zn(OTf)₂ (100 μM-1 M in H₂O) were prepared. The compound solutions were diluted ten-fold with buffer (final [compound] = 100 μM, final [EGTA] = 7.3 mM), and 198 μL of the resulting solution was added to each well of a 96-well plate. Each of 24 Zn(OTf)₂ solutions was added to four wells in each plate. The wells were allowed to equilibrate for 5 minutes, and the plates were analyzed via a Molecular Devices SpectraMax M3 fluorescent plate reader (ex. 410 nm, em. 475 nm). Fluorescence intensity at 475 nm of each of four technical replicates was plotted against free Zn²⁺ concentration ([Zn²⁺]_F), calculated using the MaxChelator program (maxchelator.stanford.edu). The data were analyzed using OriginPro 9.1 and fitted to a formation curve based on Equation 4.1:²³

$$I = (I_{\min}K_d + I_{\max}[Zn^{2+}]_F)/(K_d + [Zn^{2+}]_F) \quad (\text{Equation 4.1})$$

where I_{\min} and I_{\max} were defined as the fluorescence intensity of the free probe (**PAC-1** or derivative) and that of the Zn²⁺-probe complex, respectively.

Caspase Activity in Cell Lysate To each inner well of two 96-well plates was added 100 μL of a suspension of U-937 cells in phenol red-free RPMI-1640 complete growth media at 500,000 cells/mL (50,000 cells/well). Inner wells without compound were filled with 200 μL of media, and outer wells were filled with 200 μL of sterile PBS. The plates were incubated at 37°C with 5% CO₂ for 15 hours. Solutions of compounds (**PAC-1**, **S-PAC-1**, **4.33**, **4.51**, **4.53**, **4.62**, **PAC-1a**, staurosporine, or DMSO alone) in media were prepared at 3x final concentrations (3% DMSO), and 50 μL of each solution was added to the appropriate wells. Each compound was tested in six wells per plate. In the first plate, 50 μL of bifunctional cell lysis/caspase activity buffer was added to each treatment well. Fluorescence (ex. 400 nm, em. 505 nm) was monitored on an Analyst AD 96-384 plate reader via a 60-minute kinetic read, and the slope was used to determine caspase activity. The second plate was incubated at 37°C with 5% CO₂ for 16 hours, at

which time 50 μ L of bifunctional cell lysis/caspase activity buffer was added to each treatment well, and fluorescence was monitored as above. The slopes at 16 hours were normalized to the slopes of each compound at 0 hours (0% activity) and the staurosporine-treated samples at 16 hours (100% activity) to give percent caspase activity.

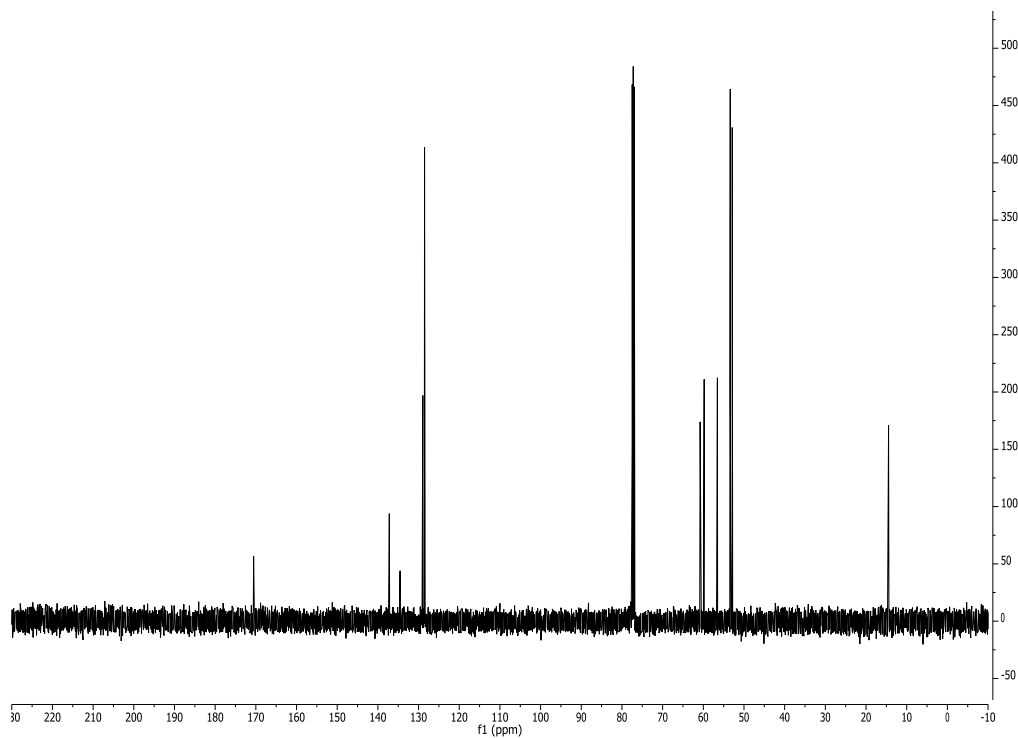
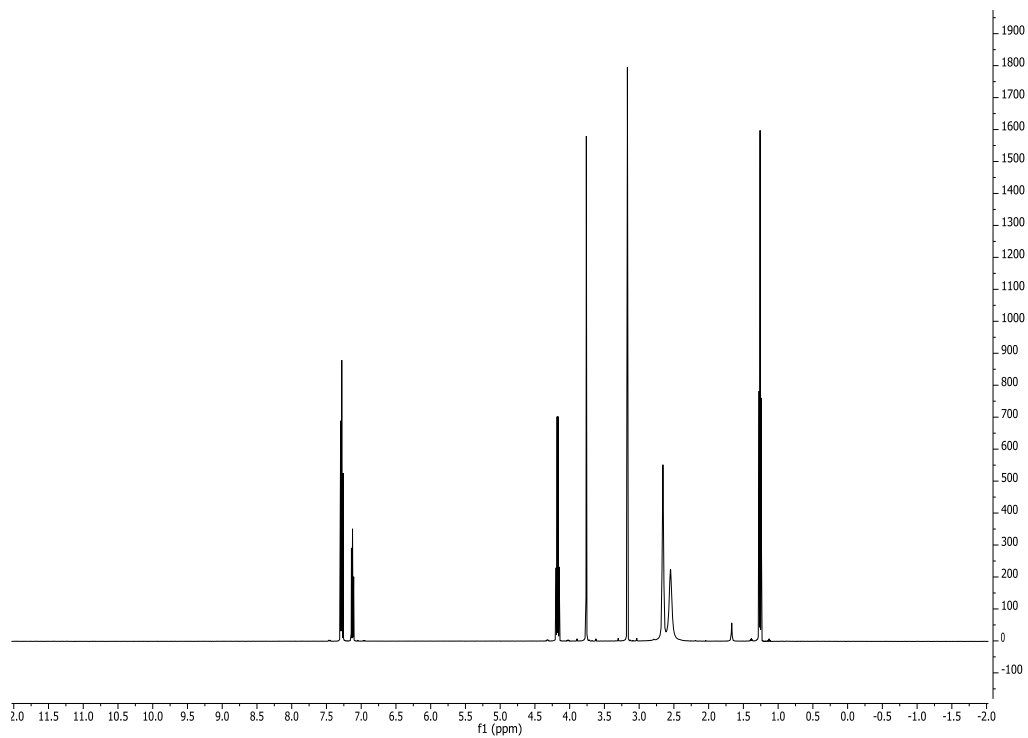
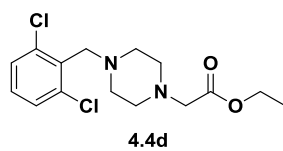
Evaluation of Compound Tolerability in vivo. All experimental procedures were reviewed and approved by the University of Illinois Institutional Animal Care and Use Committee. 8-10 week old C57BL/6 mice were used in all experiments (Charles River). Mice (n = 3/cohort) were evaluated for their ability to tolerate a single 200 mg/kg intraperitoneal dosage of compounds, formulated at 5 mg/mL in 200 mg/mL hydroxypropyl- β -cyclodextrin (HP β CD) at pH 5.5. Mice were treated and observed for clinical signs over 24 hours; specifically, they were observed continuously for the first hour, then at hours 2, 4, 6, 8, 12 and 24 hours post-treatment. Mice were further allowed 1 week to demonstrate delayed effects of treatment. Toxicity was classified as inducing either an ‘excitatory’ or a ‘depressive’ phenotype. The extent of response was graded from mild to severe.

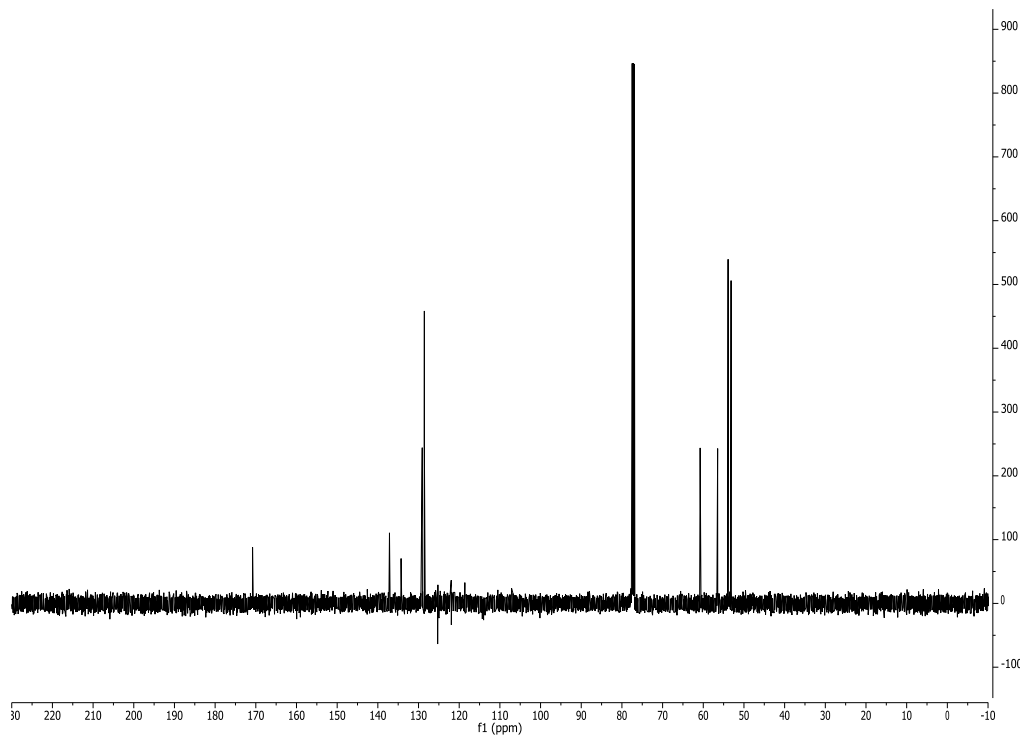
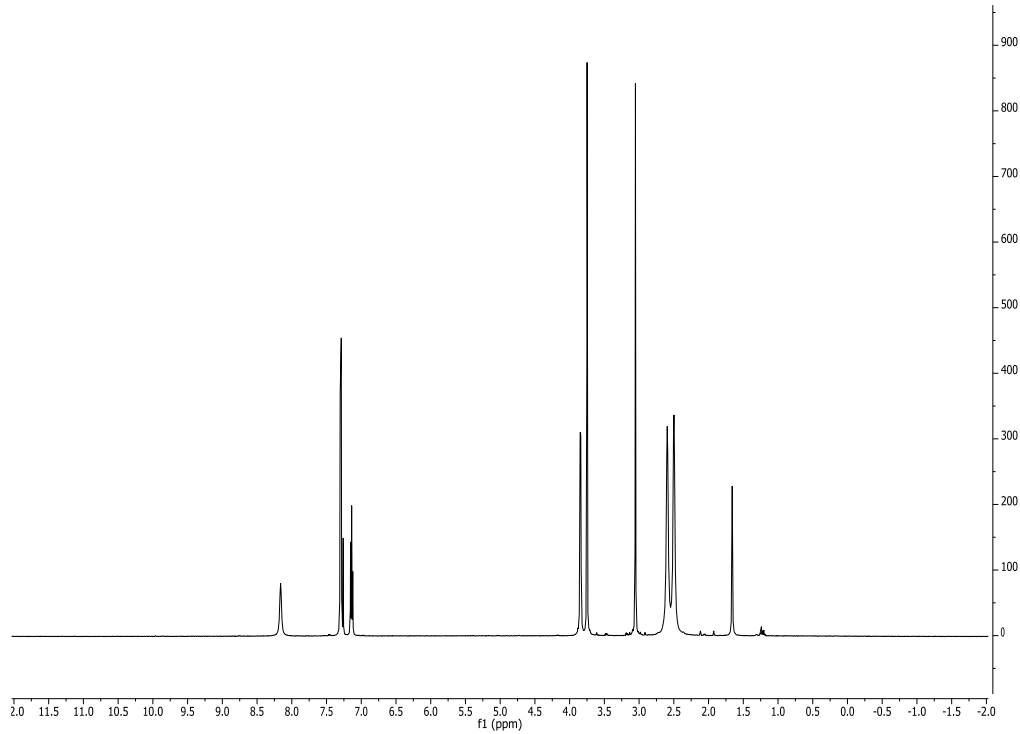
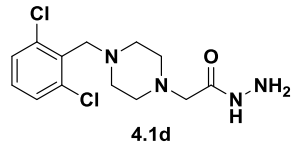
Pharmacokinetics of PAC-1 and Derivatives in Mice. Compounds were formulated at 5 mg/mL in 200 mg/mL HP β CD at pH 5.5. C57BL/6 mice (n = 2 per cohort per time point) were treated with a 25 mg/kg dose of **PAC-1** or derivative via tail vein injection or oral gavage. At specified time points, mice were sacrificed and blood was collected, centrifuged, and the EDTA plasma was frozen at -80°C until analysis.

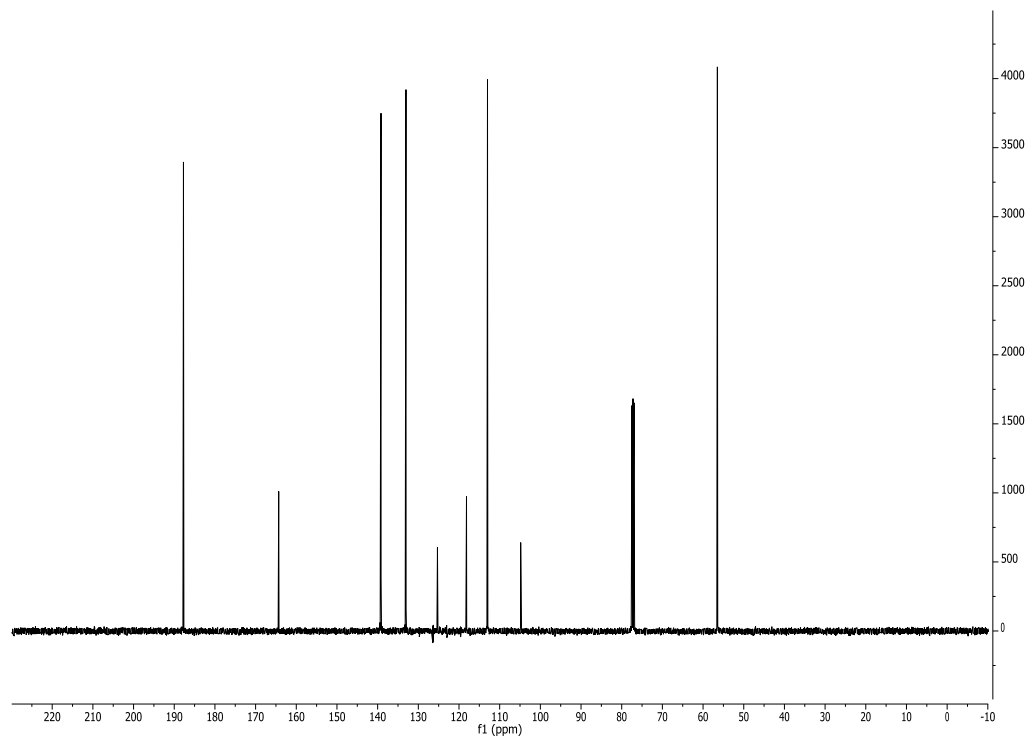
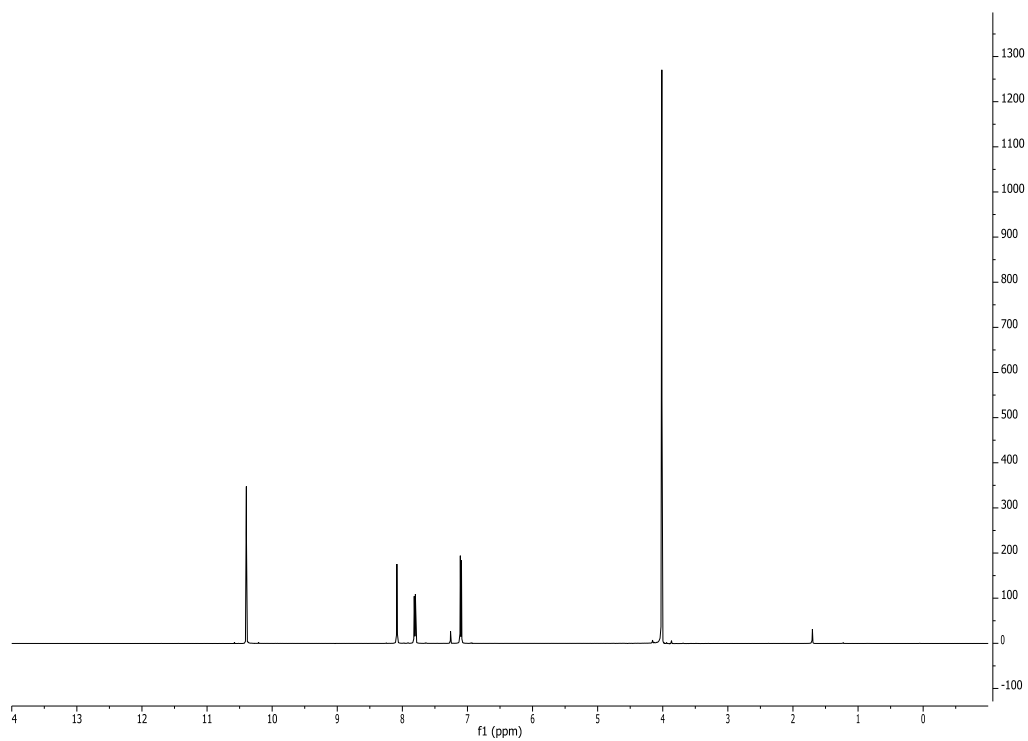
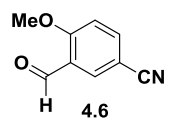
Assessment of serum concentrations of PAC-1 and derivatives. 2 μ L of a 10 μ g/mL solution of internal standard in 60:40 methanol:water (**PAC-1** was used as an internal standard for analysis of **S-PAC-1**; **S-PAC-1** was used as an internal standard for analysis of all other compounds) was added to a 10 μ L aliquot of serum. The proteins were precipitated by the addition of methanol (100 μ L). The sample was mixed by vortex and centrifuged to remove the proteins. The resulting supernatant was evaporated to complete dryness with a SpeedVac. The dried solid was then reconstituted in 100 μ L 60:40 methanol:water, followed by centrifugation. The supernatant was subject to instrument injection. Samples were analyzed with the 5500 QTRAP LC/MS/MS system (AB Sciex, Foster City, CA) in the Metabolomics Lab of the Roy J. Carver

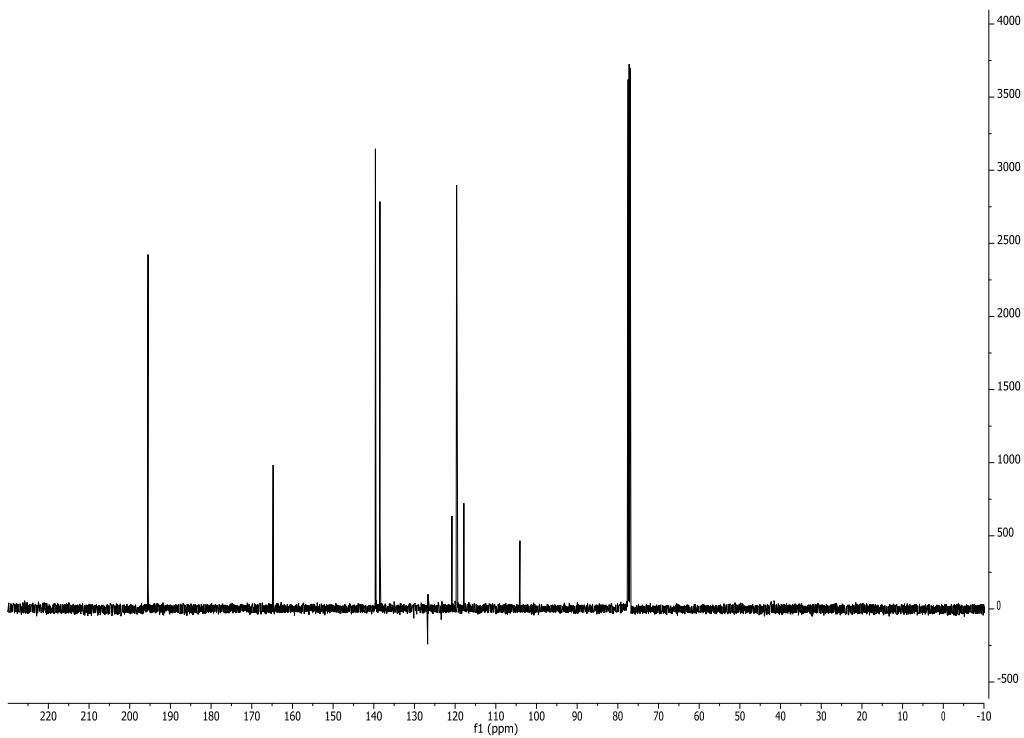
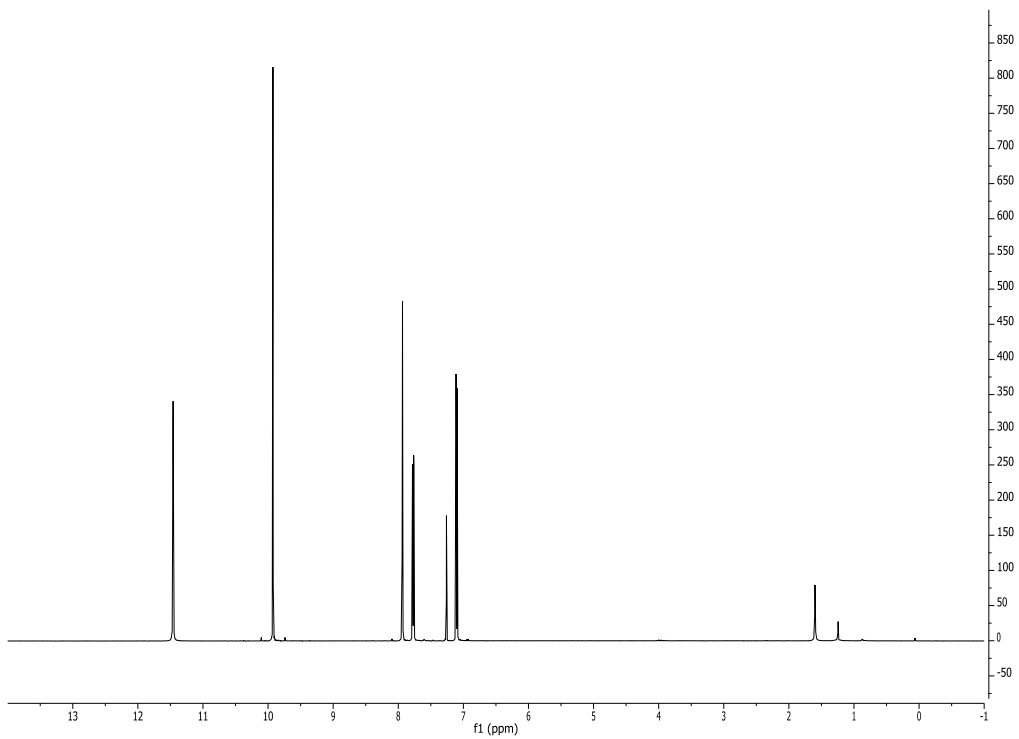
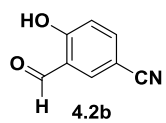
Biotechnology Center, University of Illinois at Urbana-Champaign. The 1200 series HPLC system (Agilent Technologies, Santa Clara, CA) includes a degasser, an autosampler, and a binary pump. The LC separation was performed on a Phenomenex 4u Polar-RP 80A column (4.6 x 100mm, 4 μ m, Torrance, CA) with mobile phase A (0.1% formic acid in water) and mobile phase B (methanol). The flow rate was 0.8 mL/min. The linear gradient was as follows: 0-1 min, 0% B; 5 min, 70% B; 7.5-10.5 min, 100% B; 10.6-15 min, 0% B. The autosampler was set at 5°C. The injection volume was 2 μ L. Mass spectra were acquired under negative electrospray ionization (ESI) with the ion spray voltage of -4500 V. The source temperature was 600°C. The curtain gas, ion source gas 1, and ion source gas 2 were 35, 50, and 65, respectively. Multiple reaction monitoring (MRM) was used for quantitation: **PAC-1**: m/z 391.1-->m/z 232.0; **S-PAC-1**: m/z 470.2-->m/z 311.1; compound **7**: m/z 423.1-->m/z 264.1; compound **30**: m/z 423.1-->m/z 246.1; compound **32**: m/z 448.1-->m/z 271.1; compound **41**: m/z 450.1-->m/z 271.1.

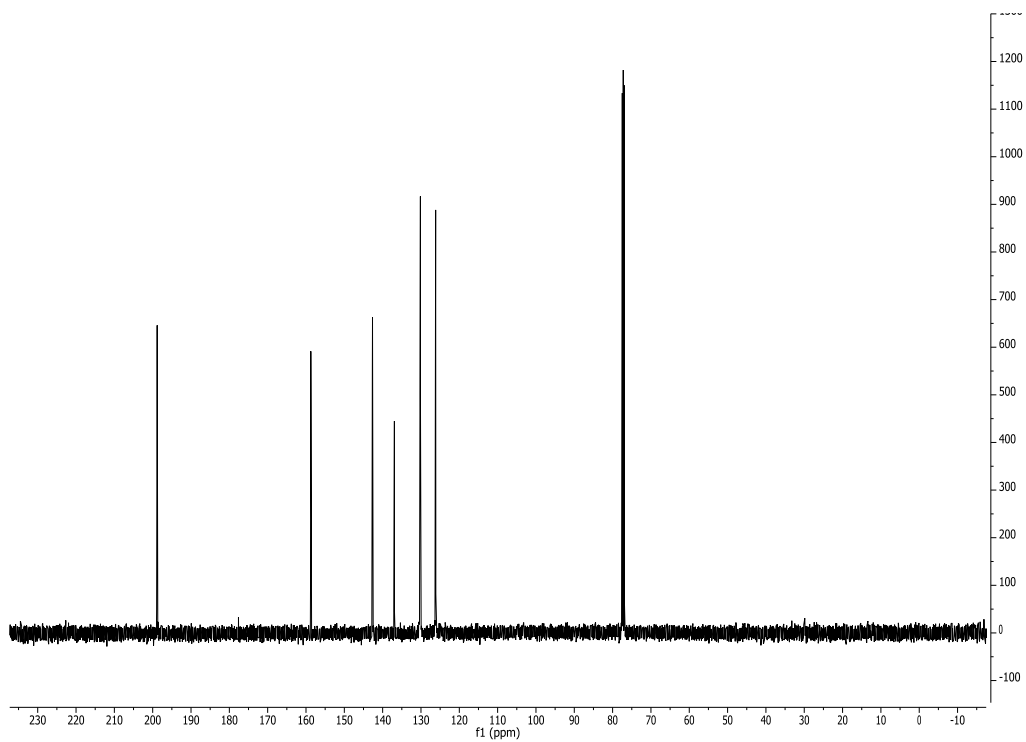
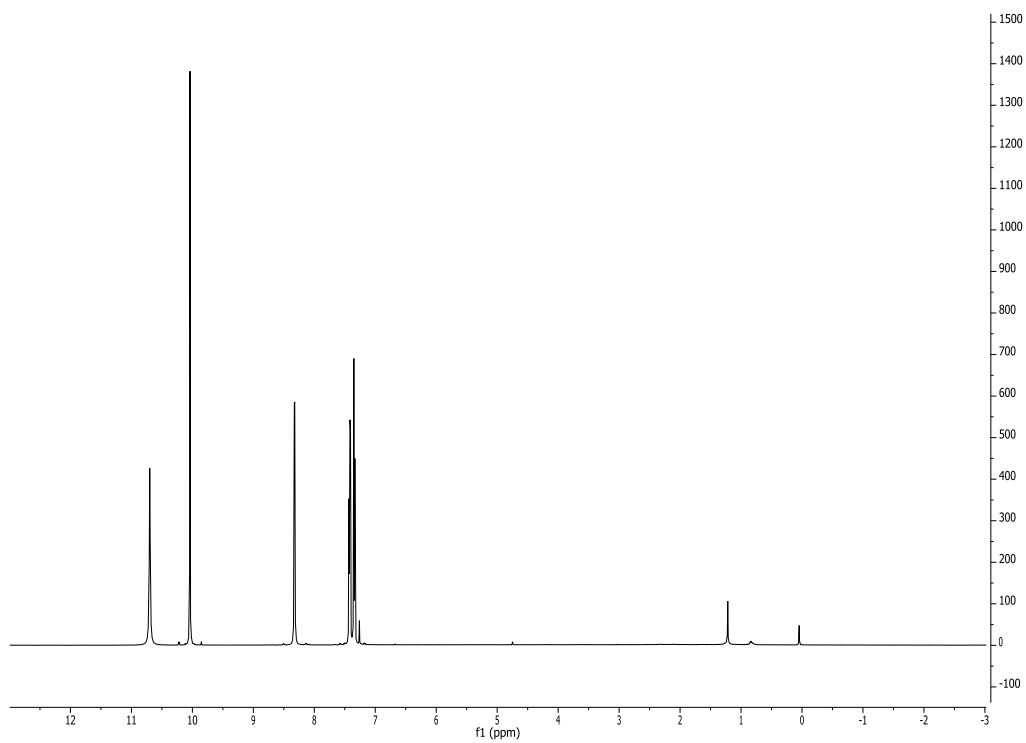
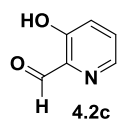
4.9.3. Spectra

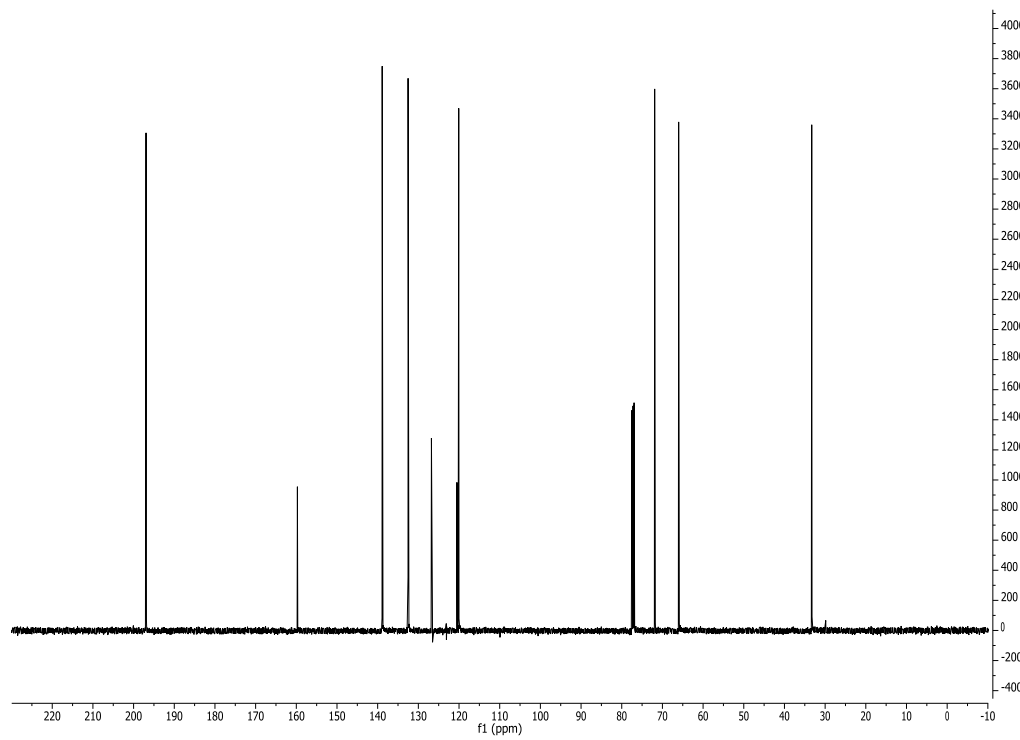
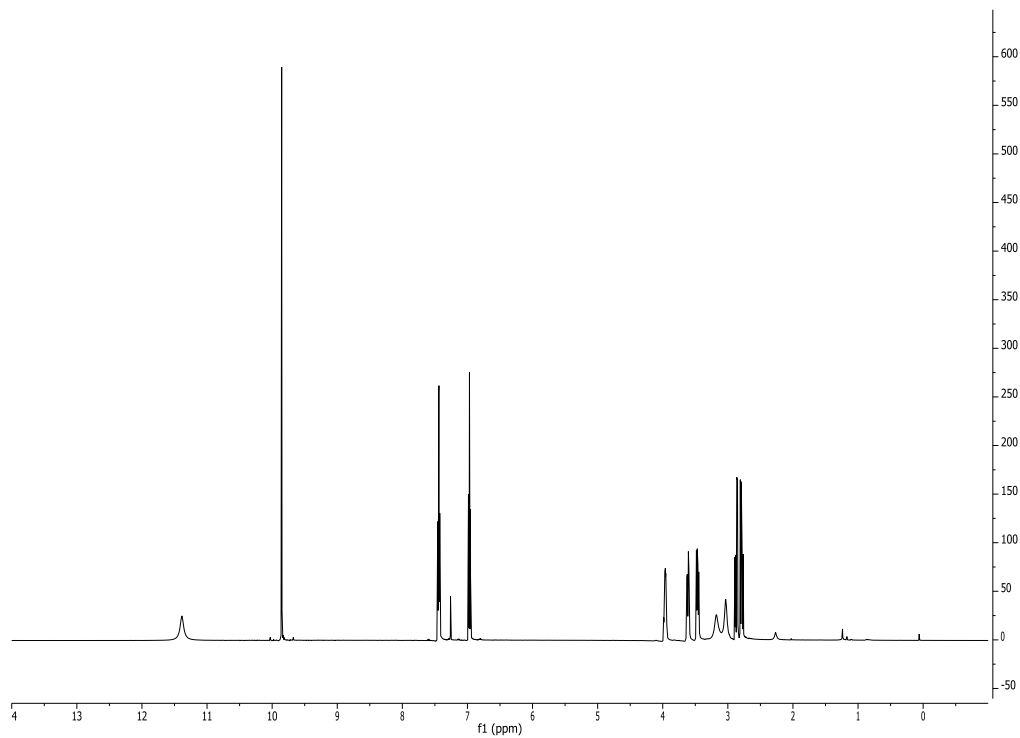
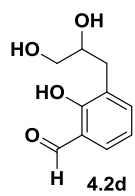


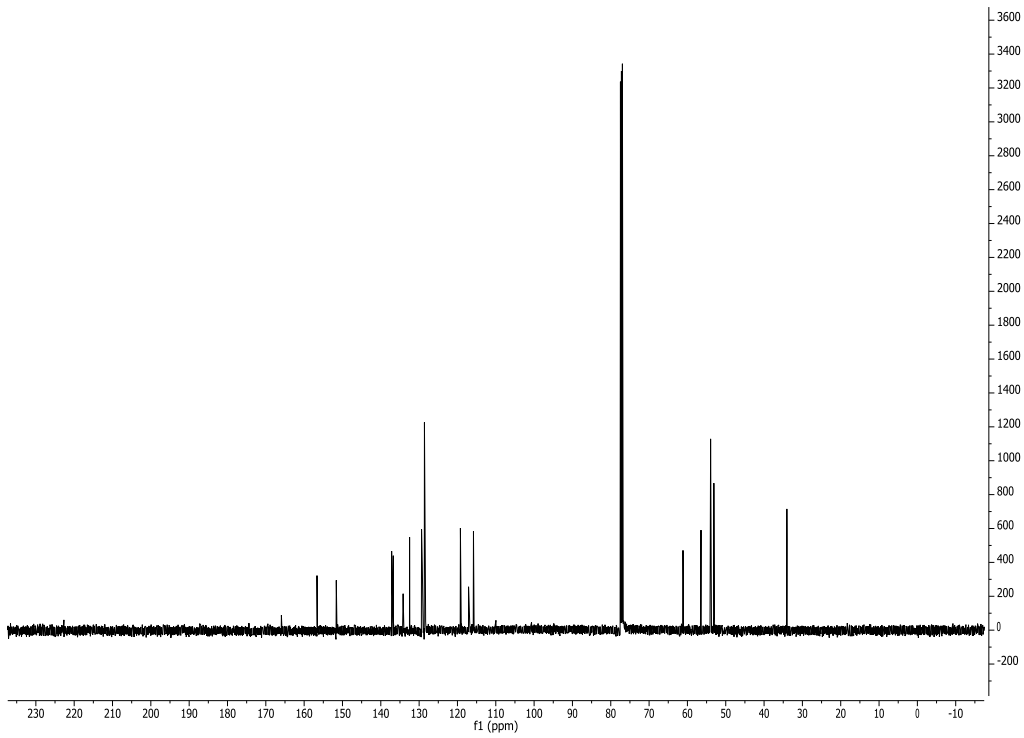
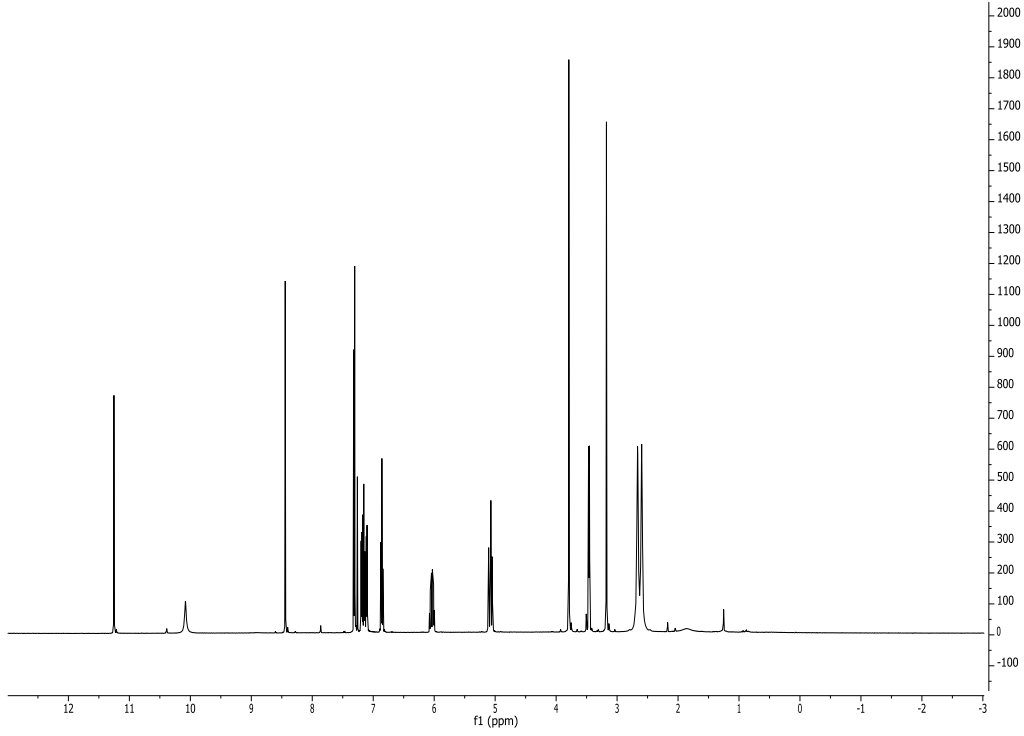
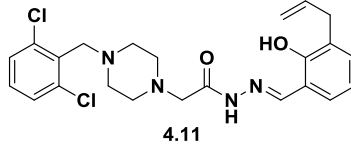


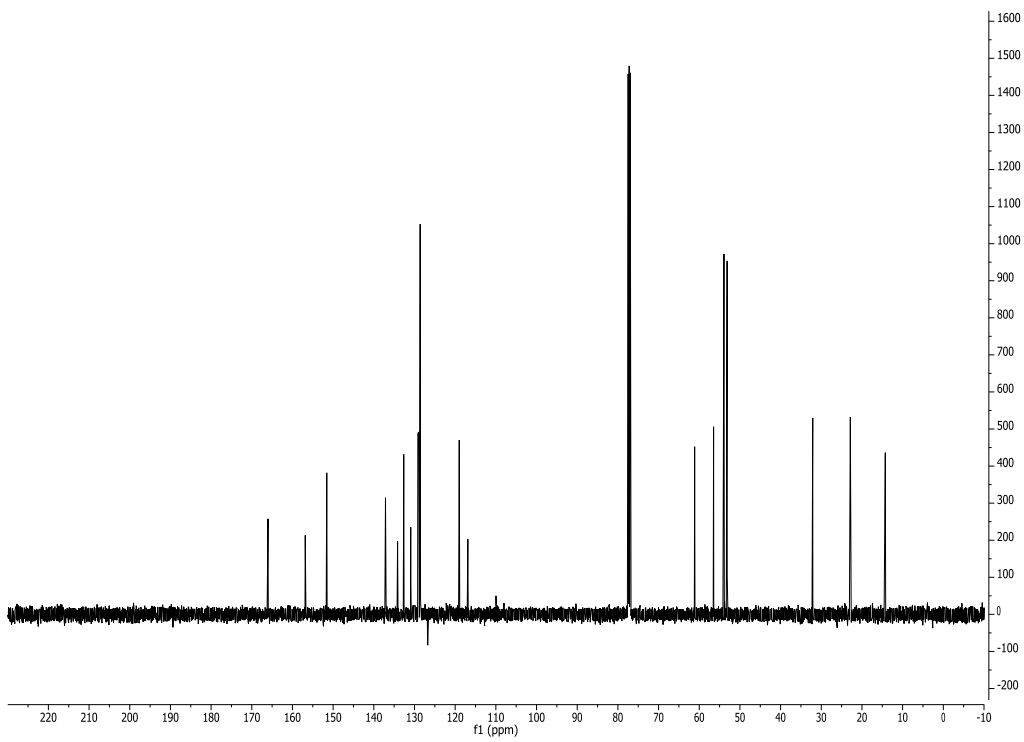
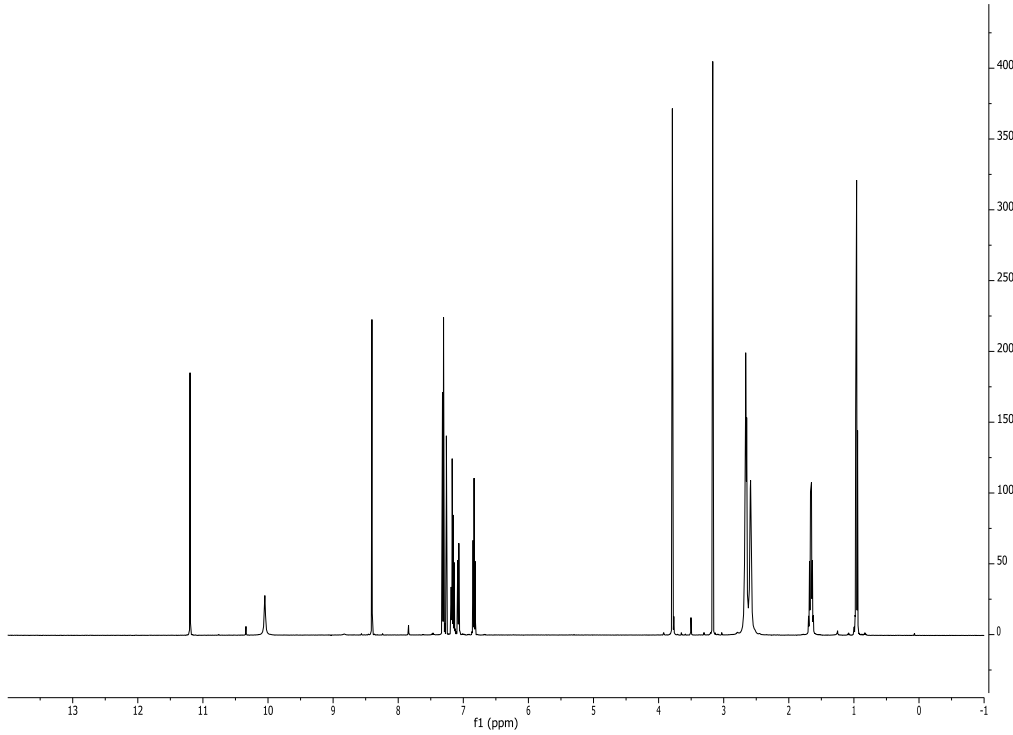
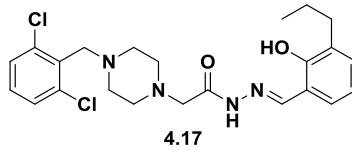


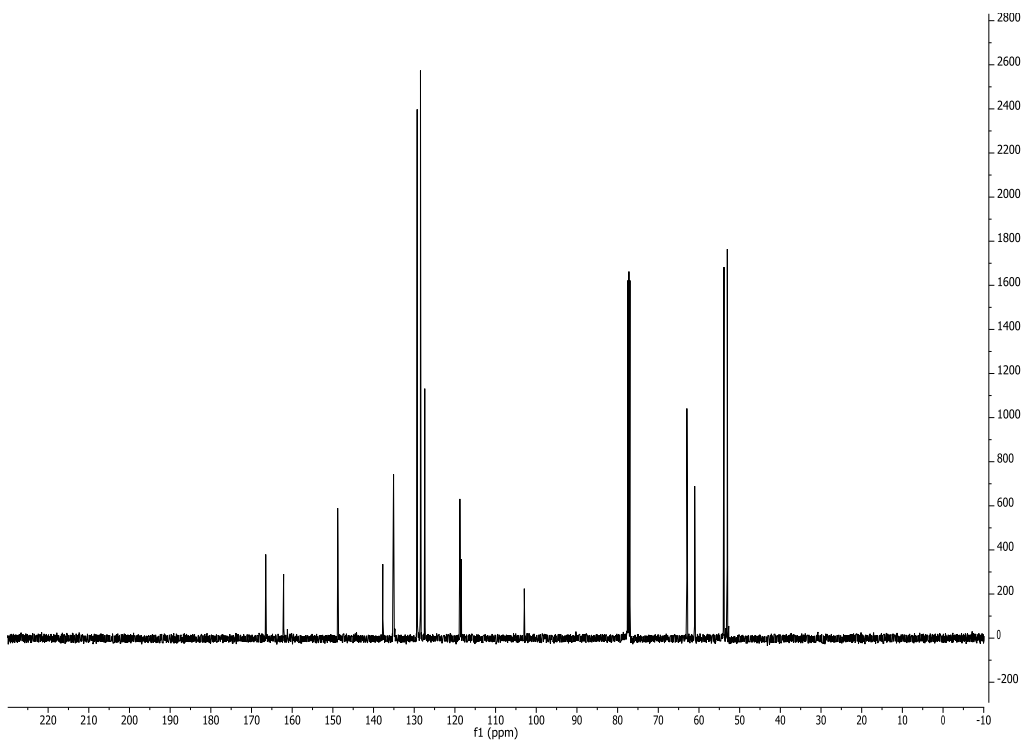
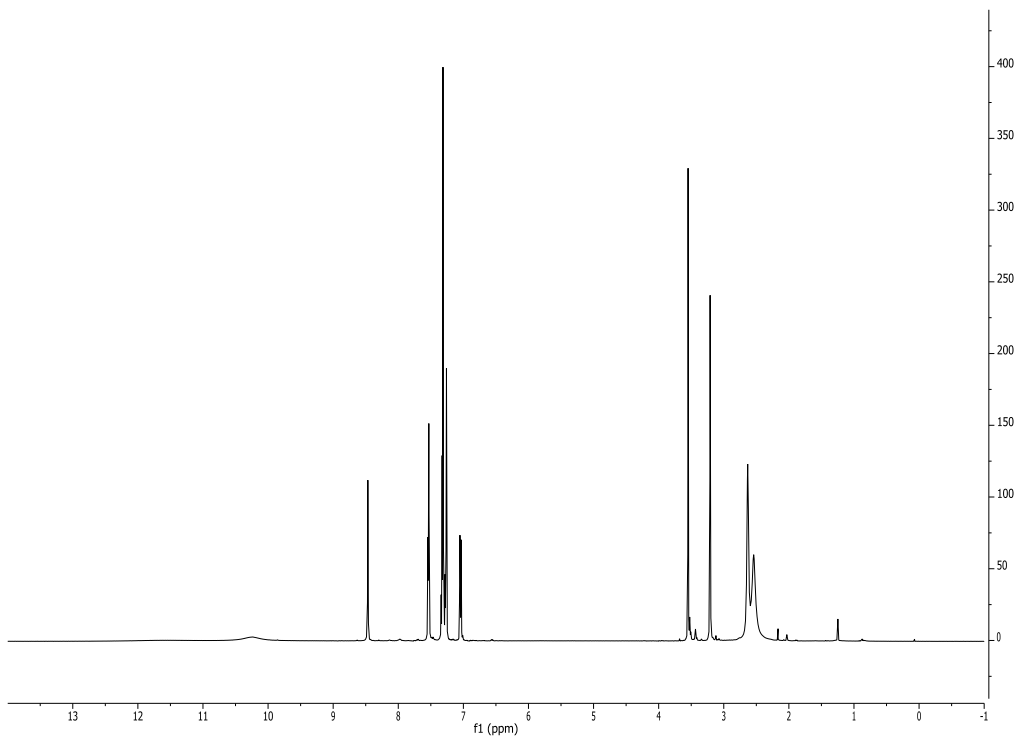
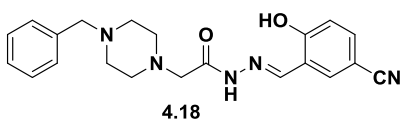


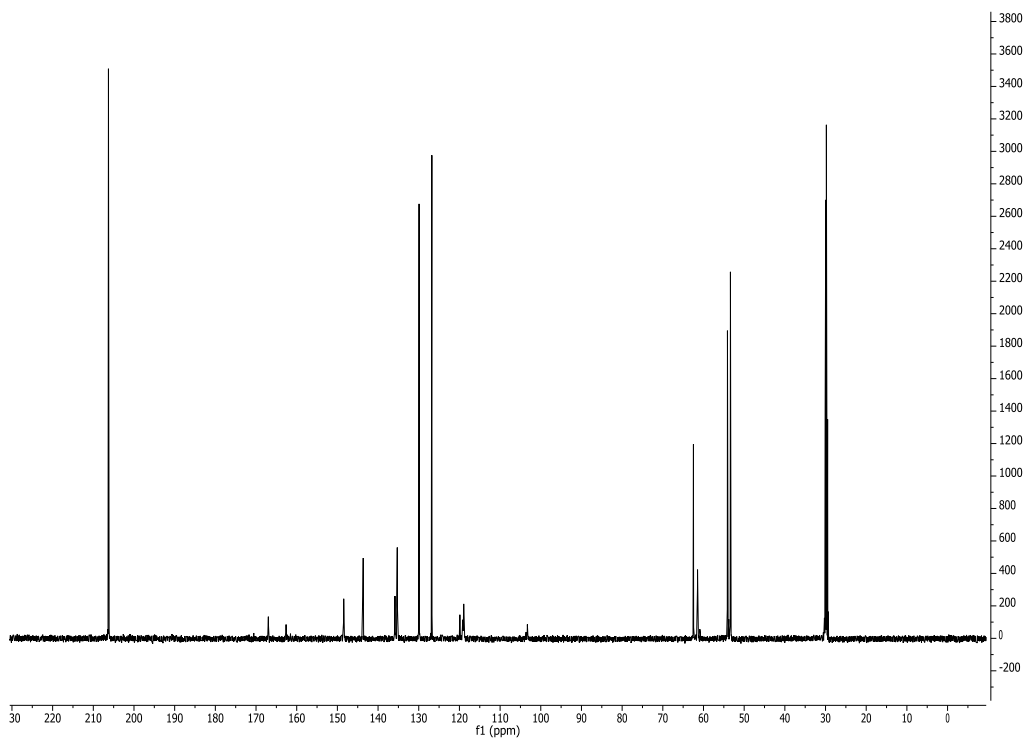
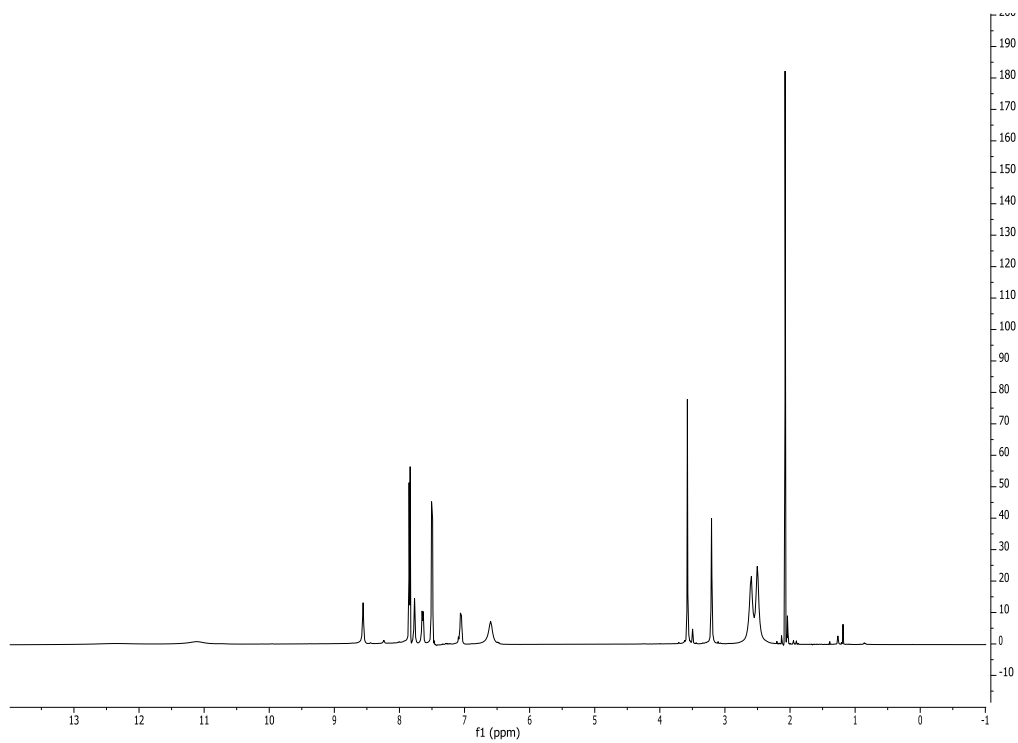
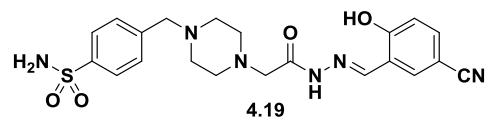


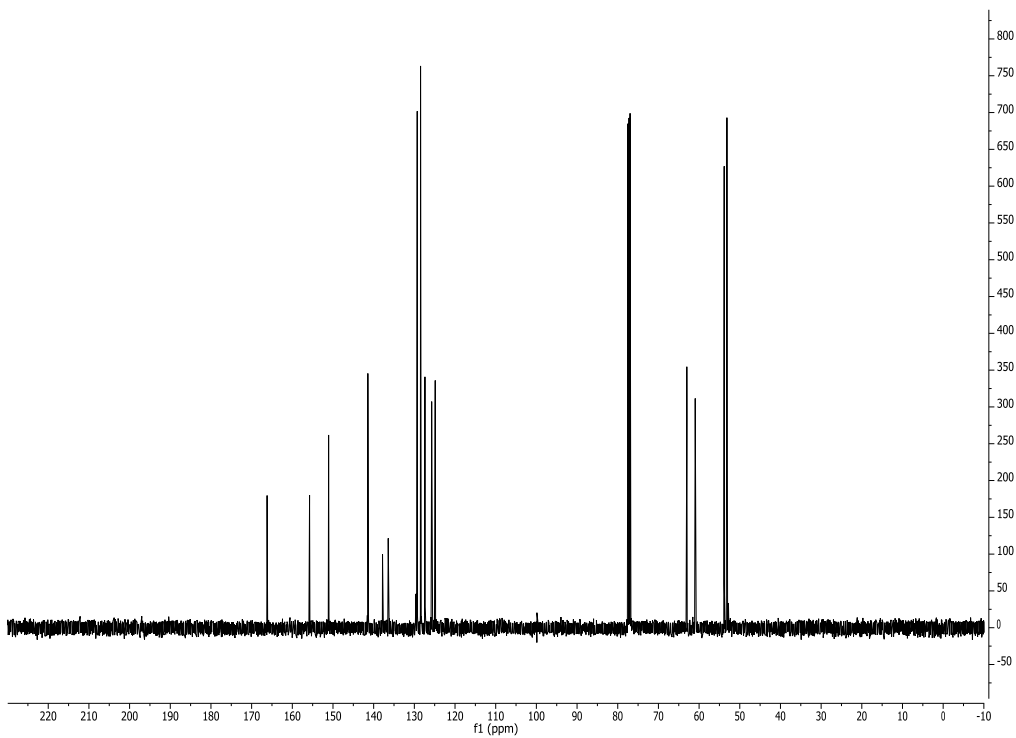
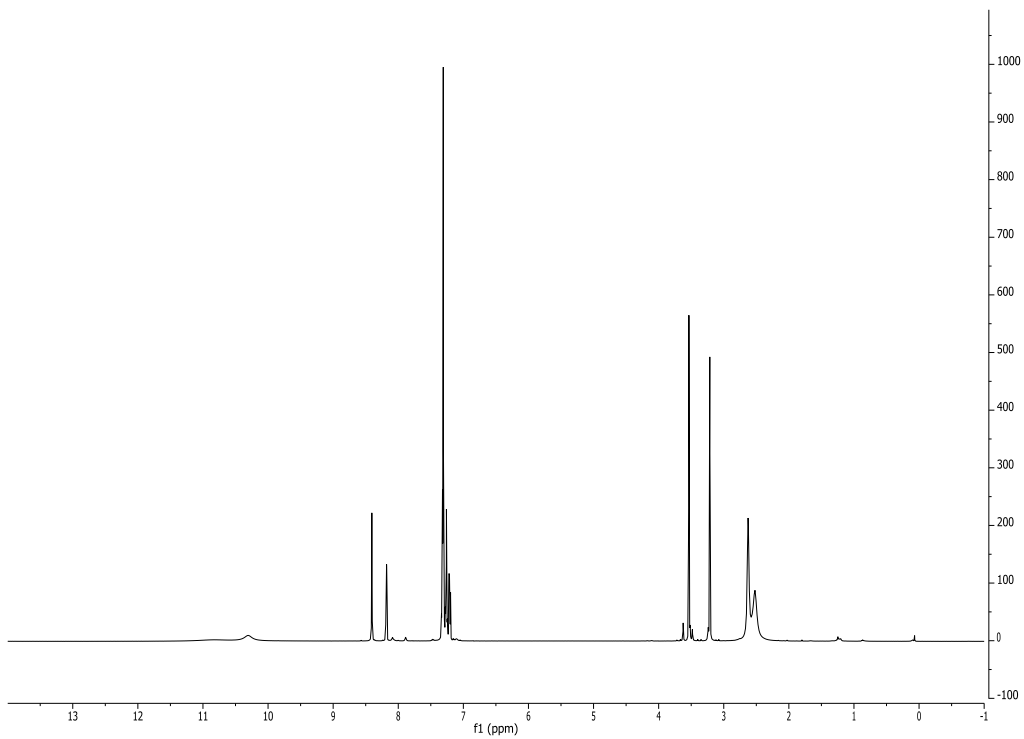
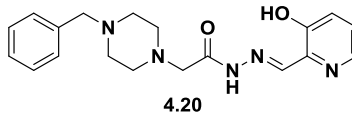


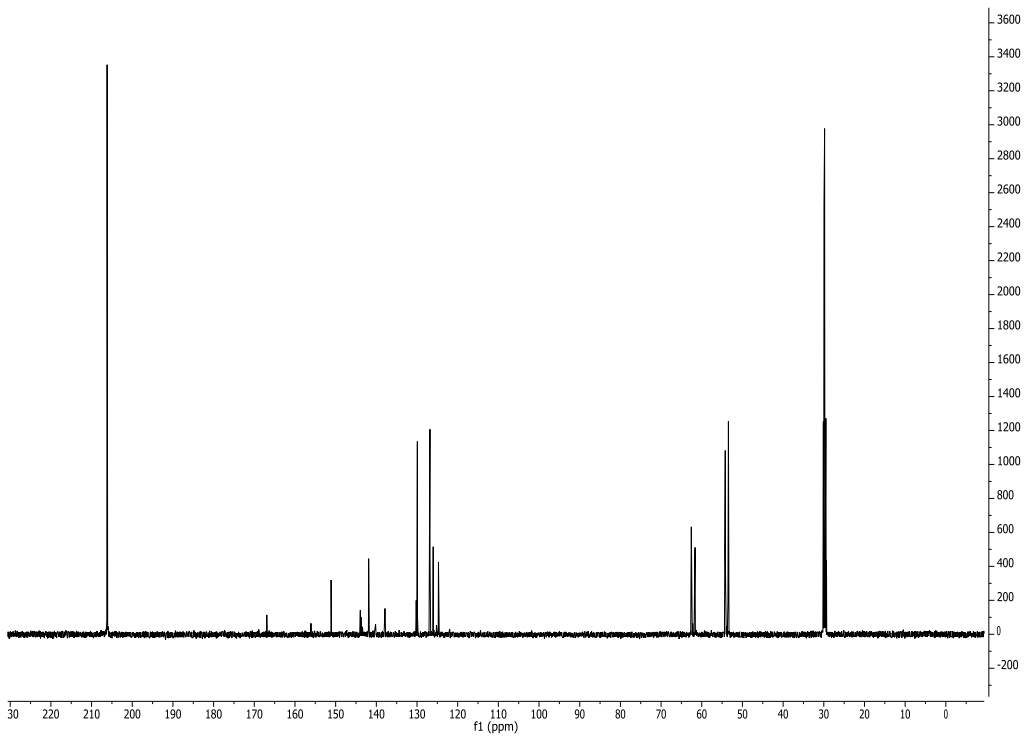
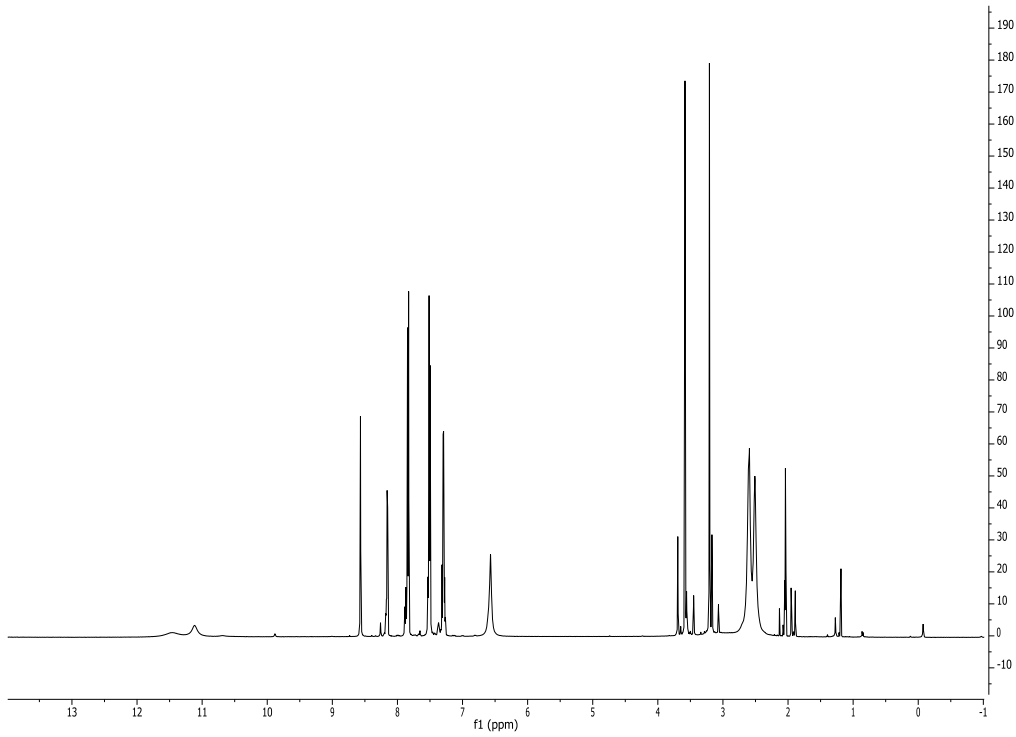
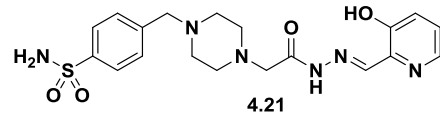


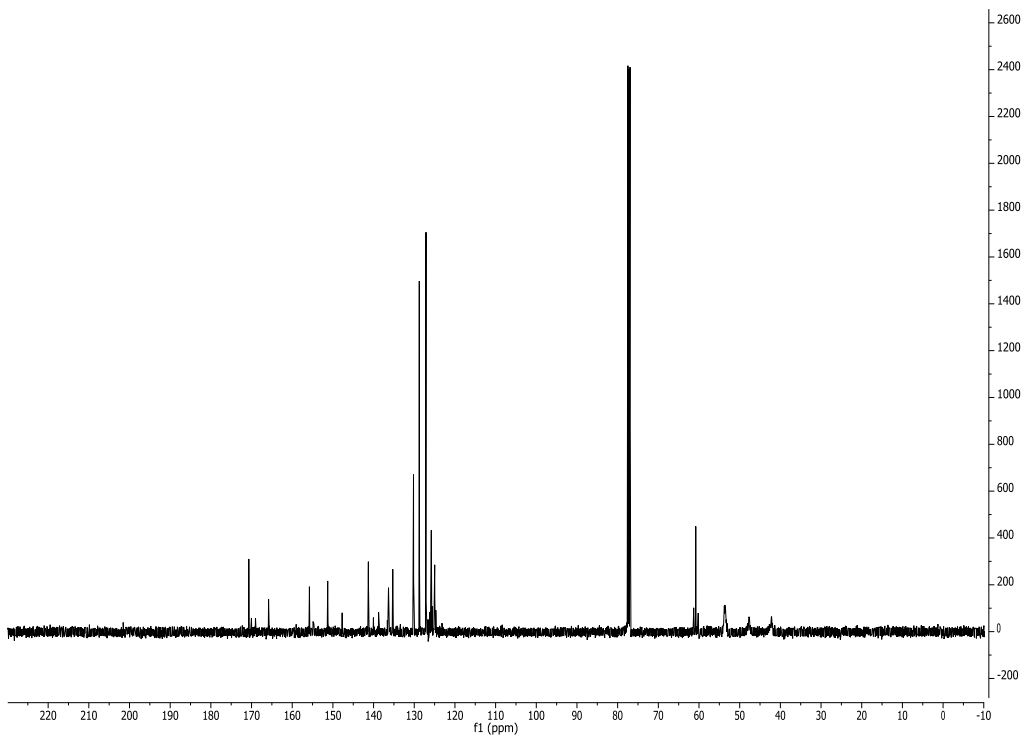
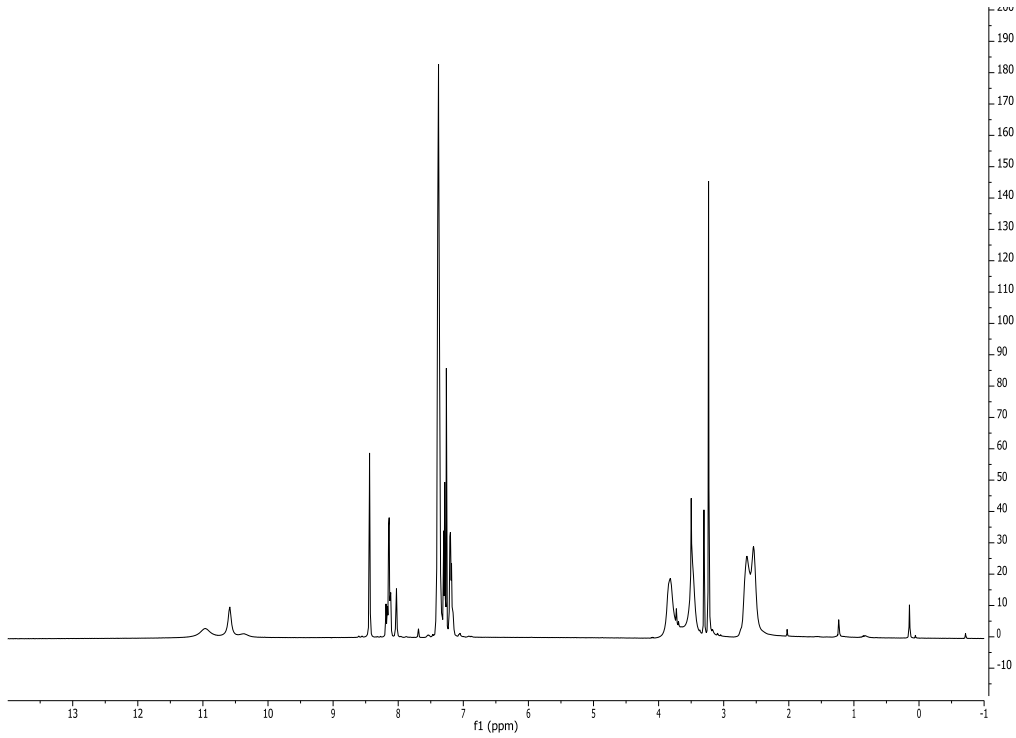
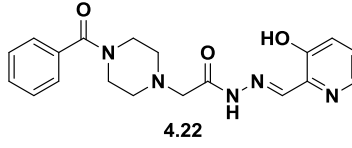


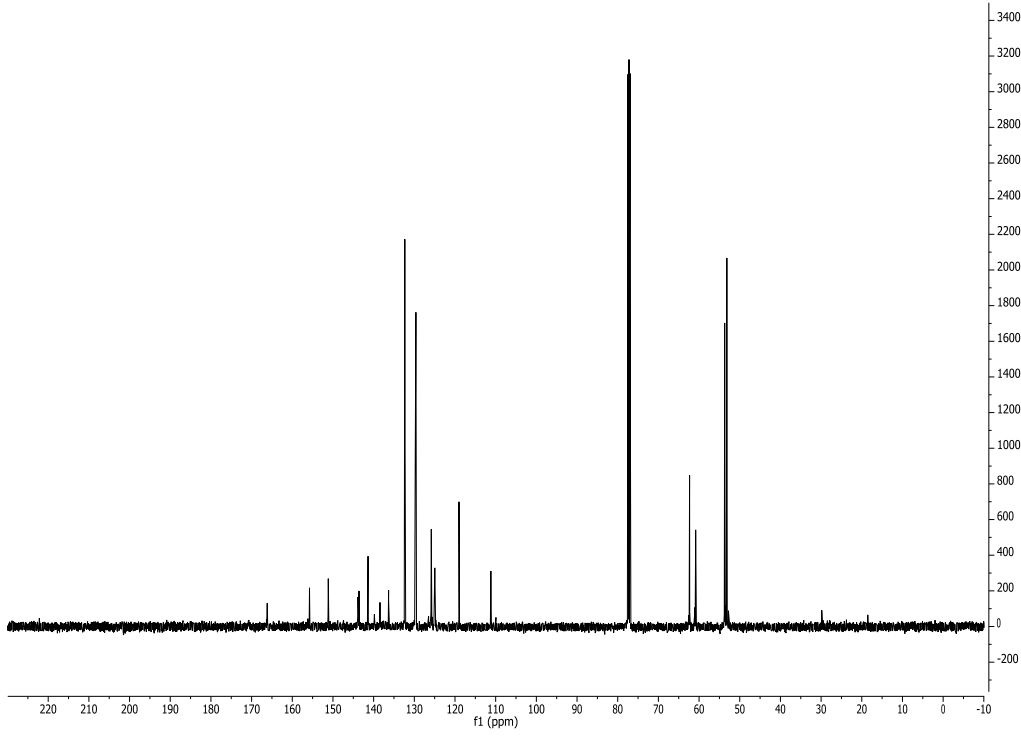
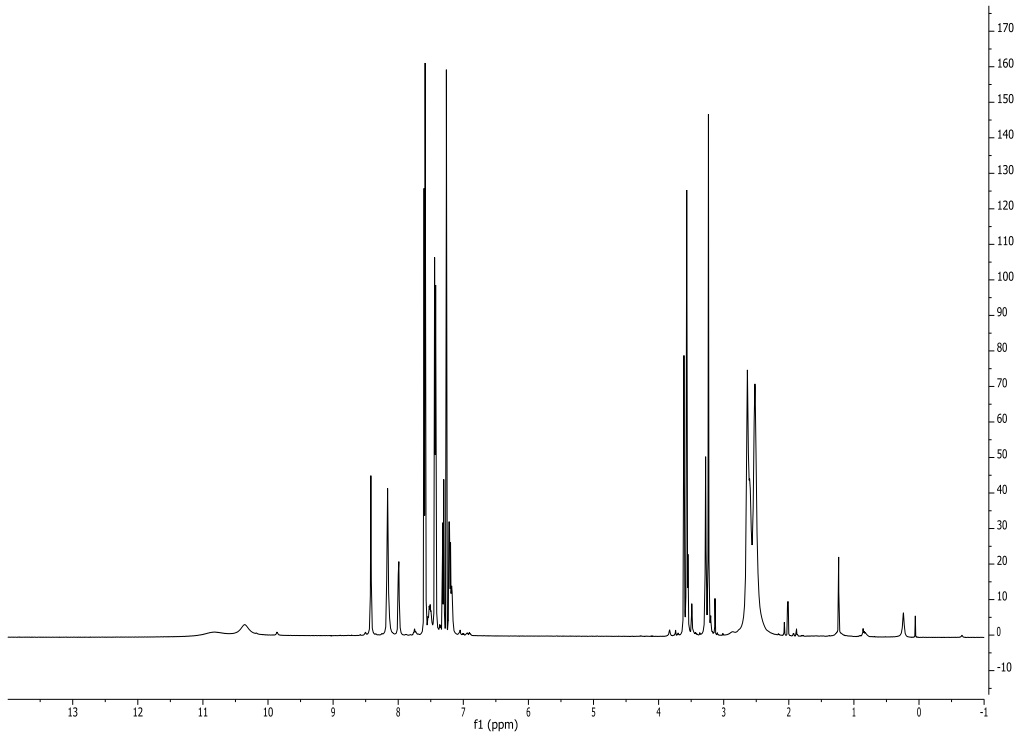
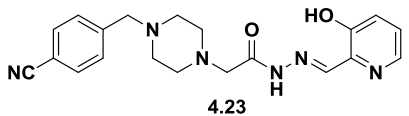


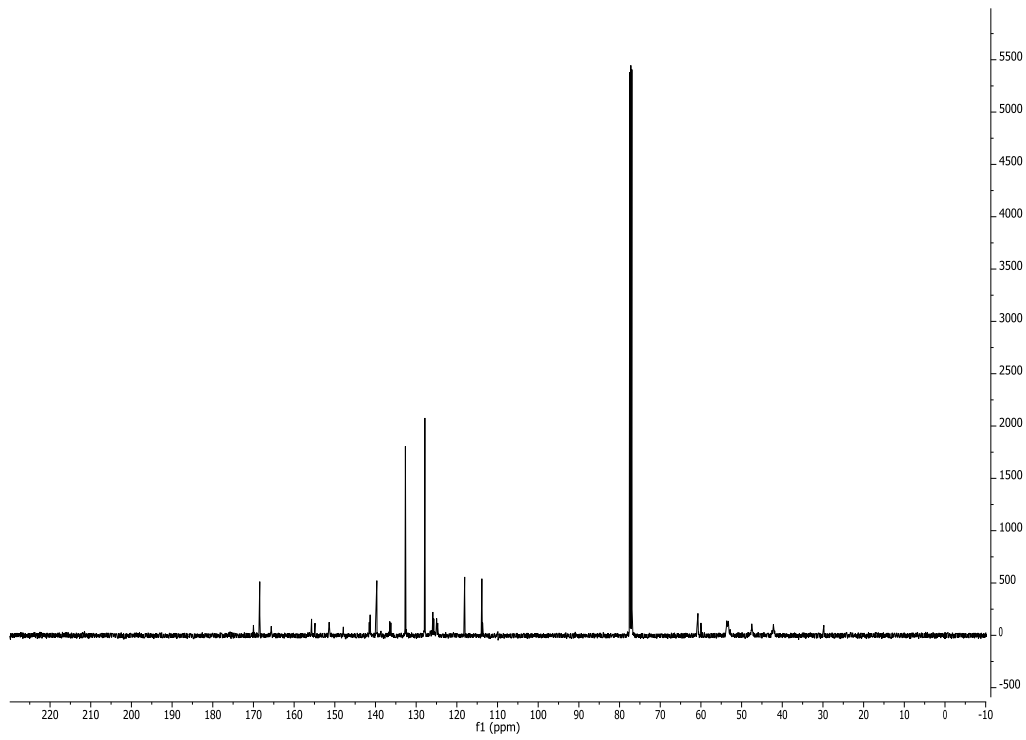
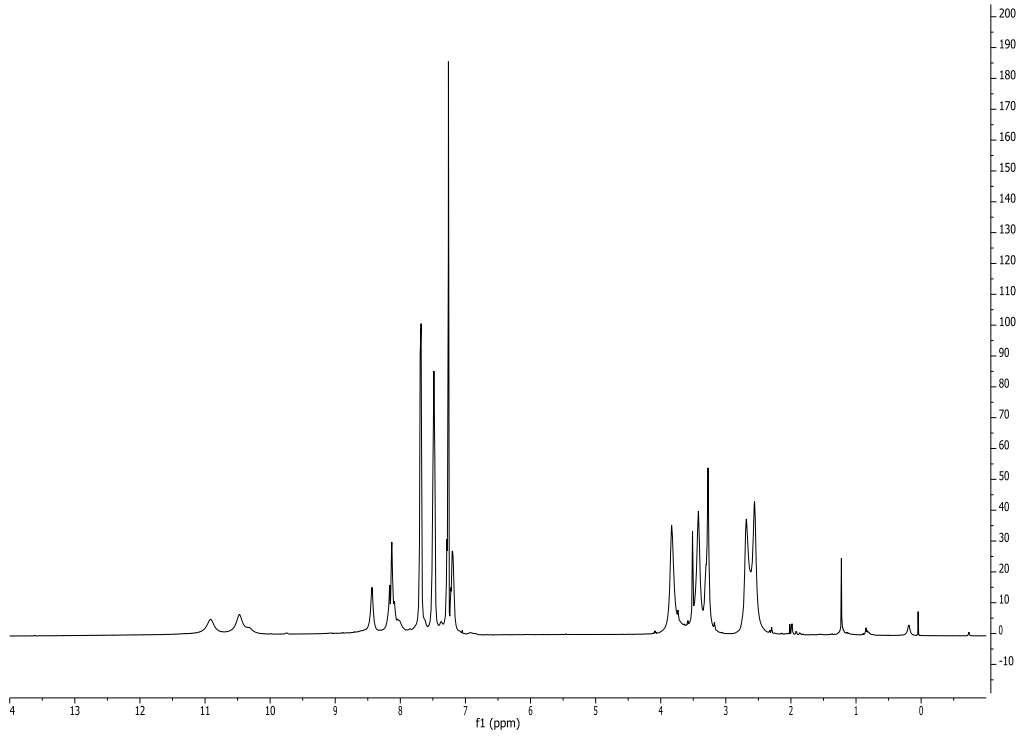
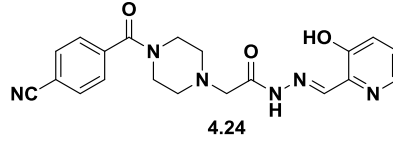


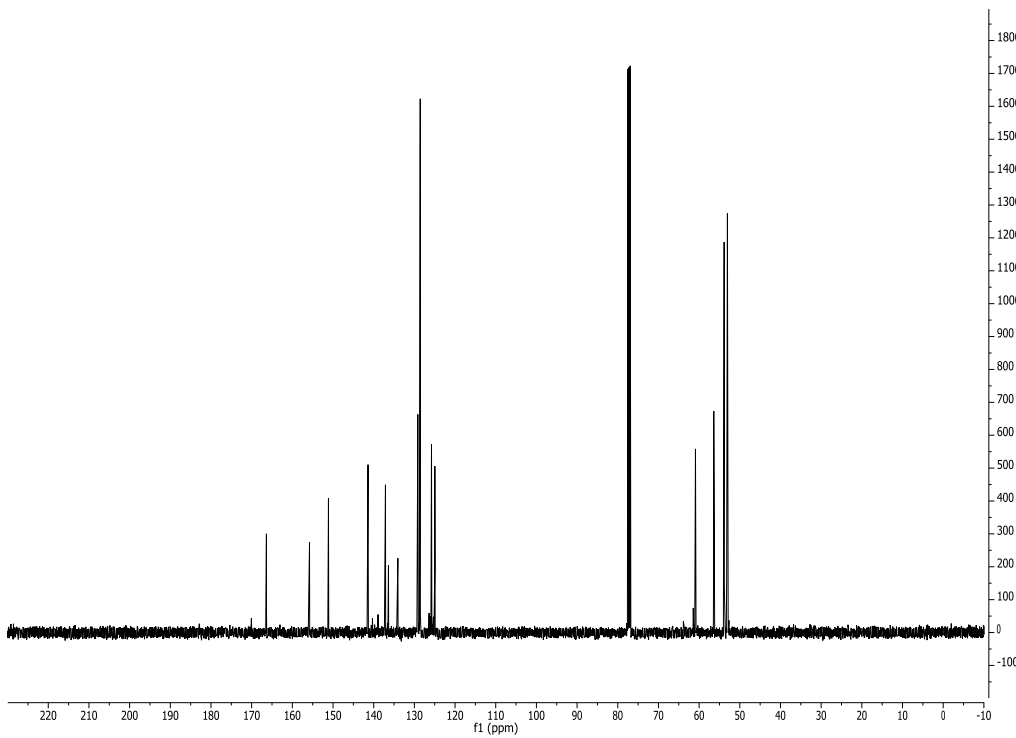
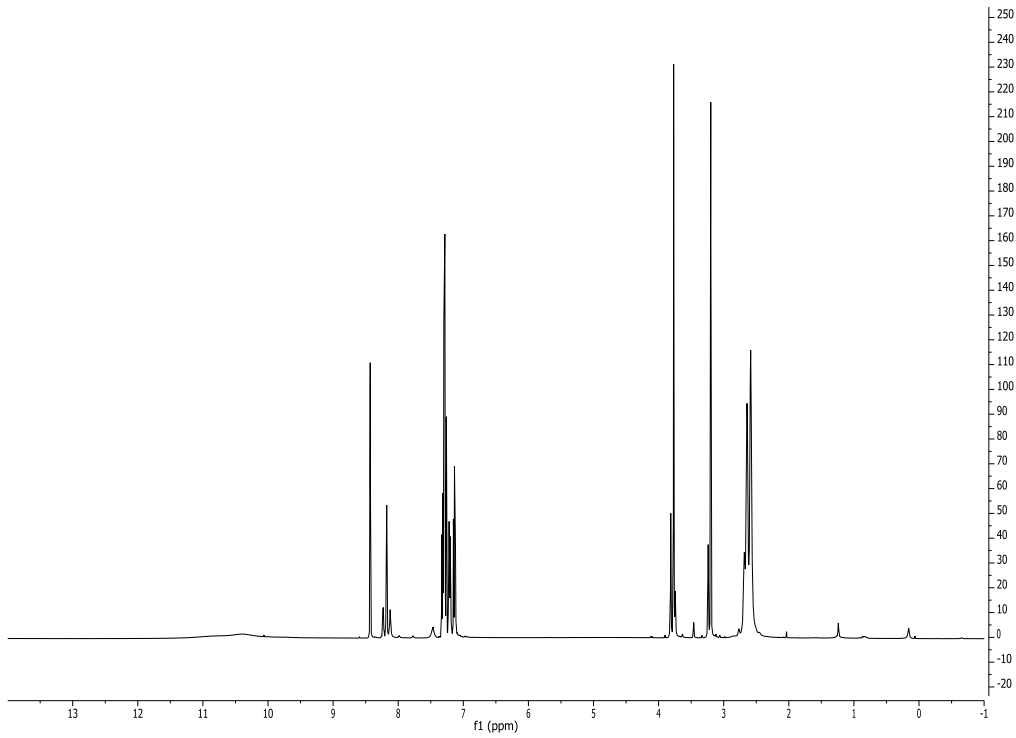
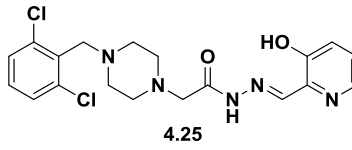


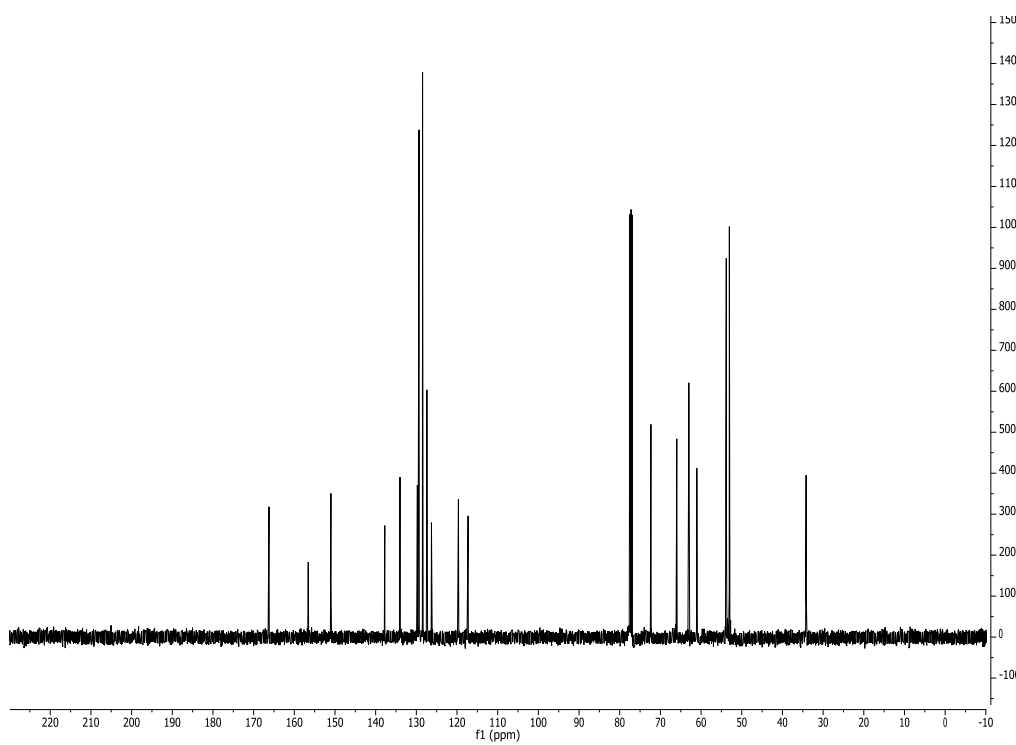
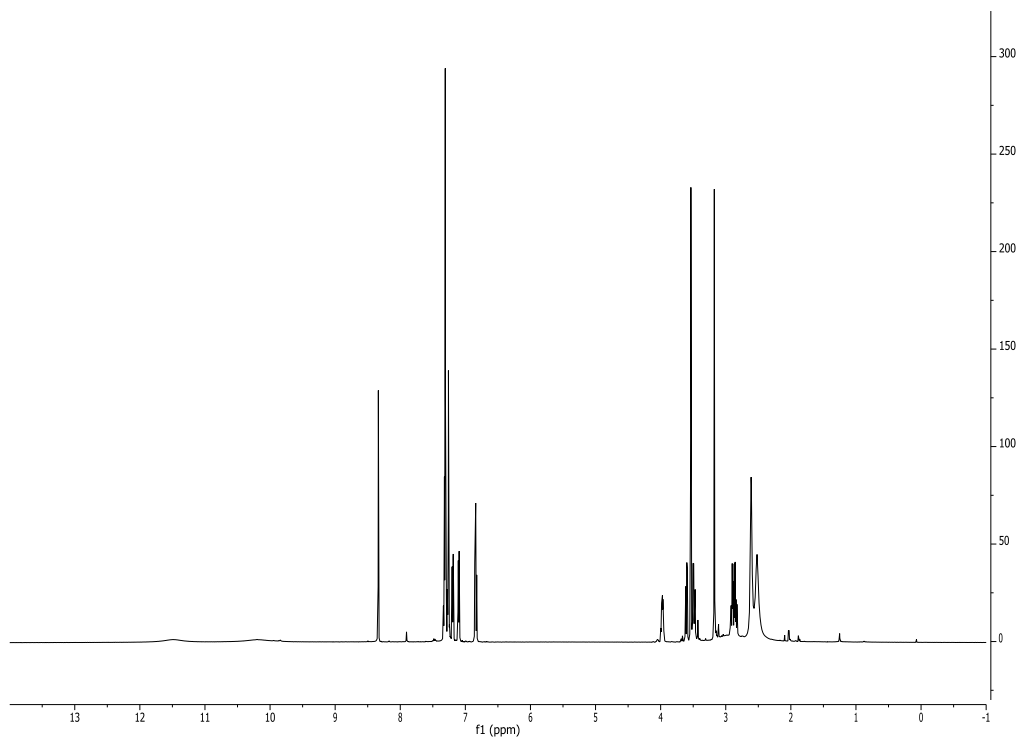
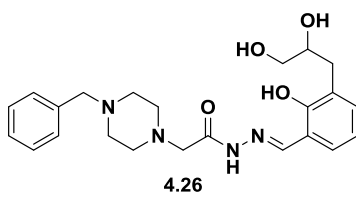


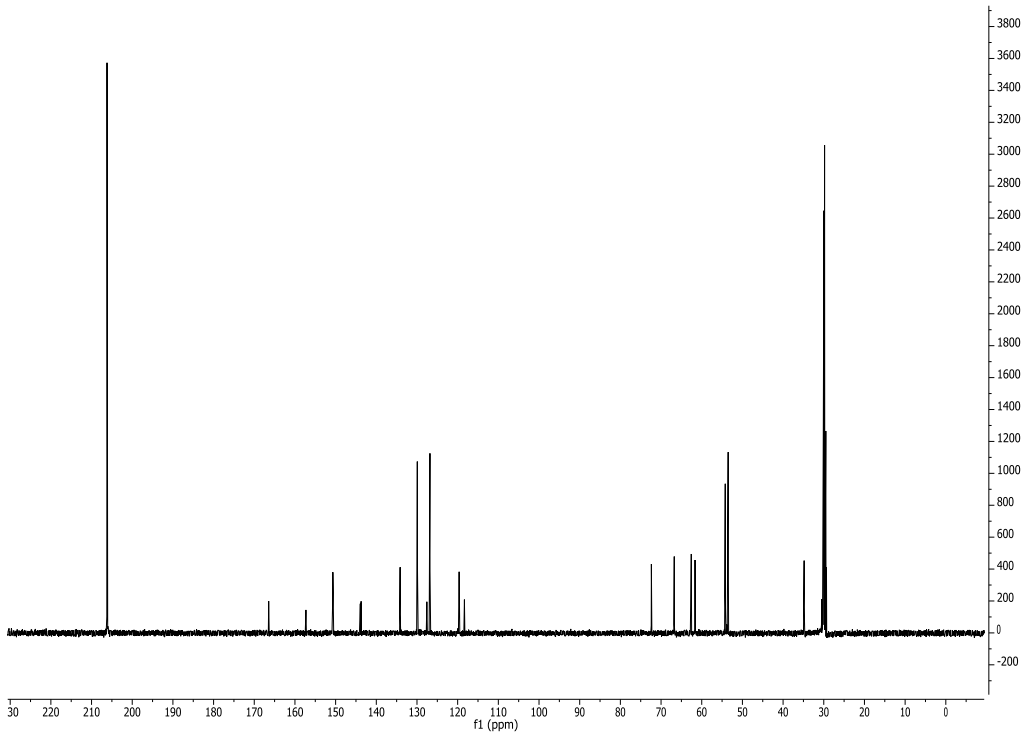
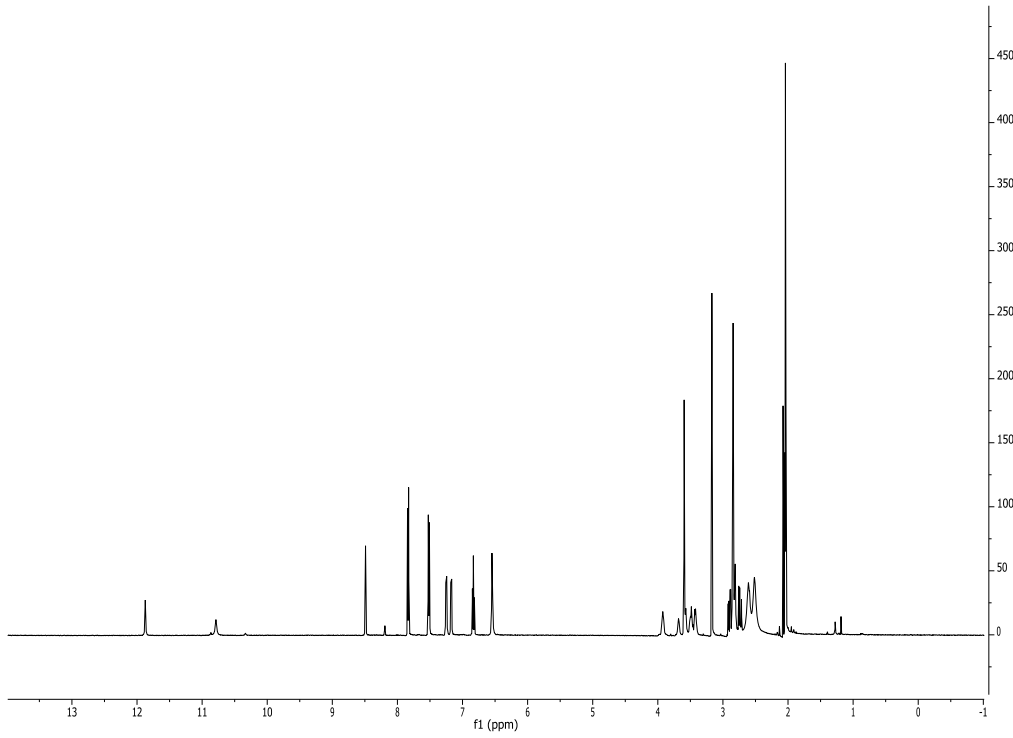
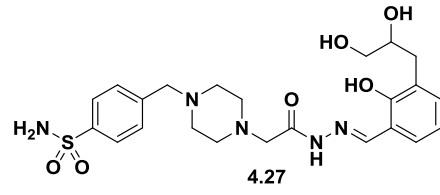


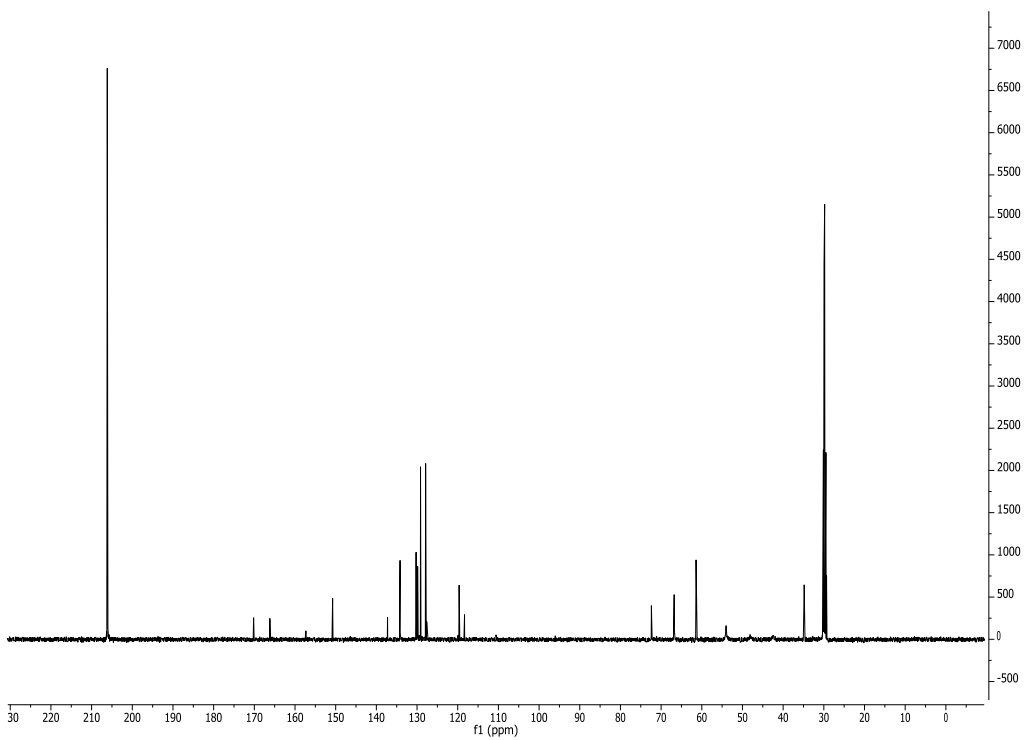
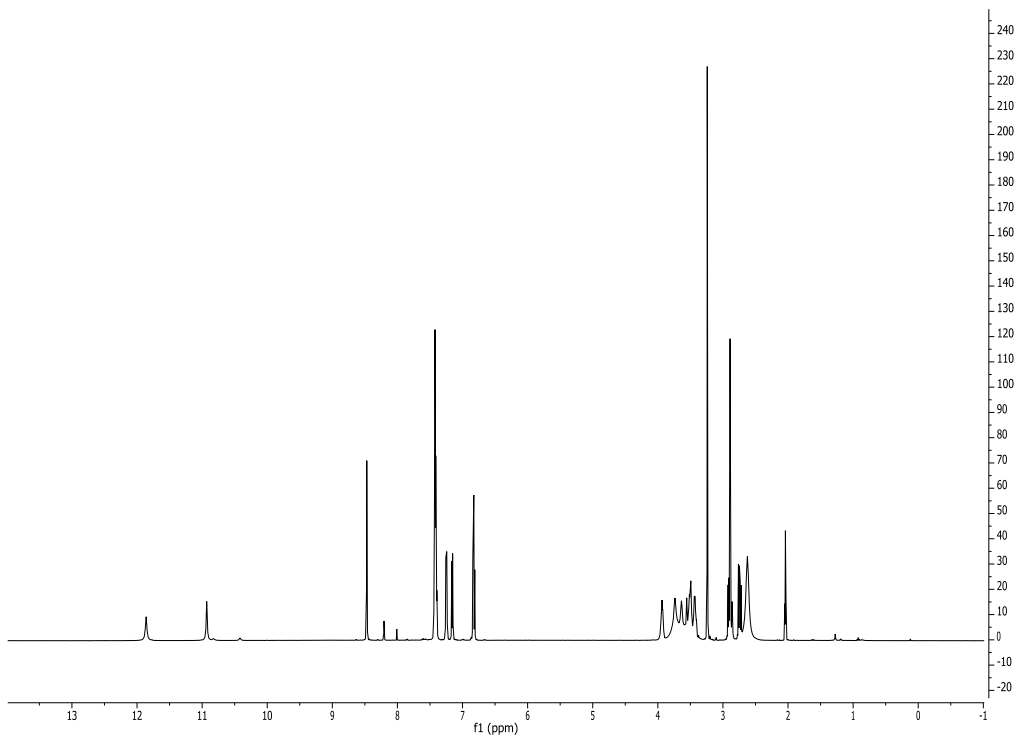
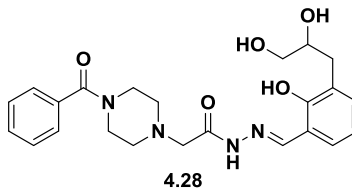


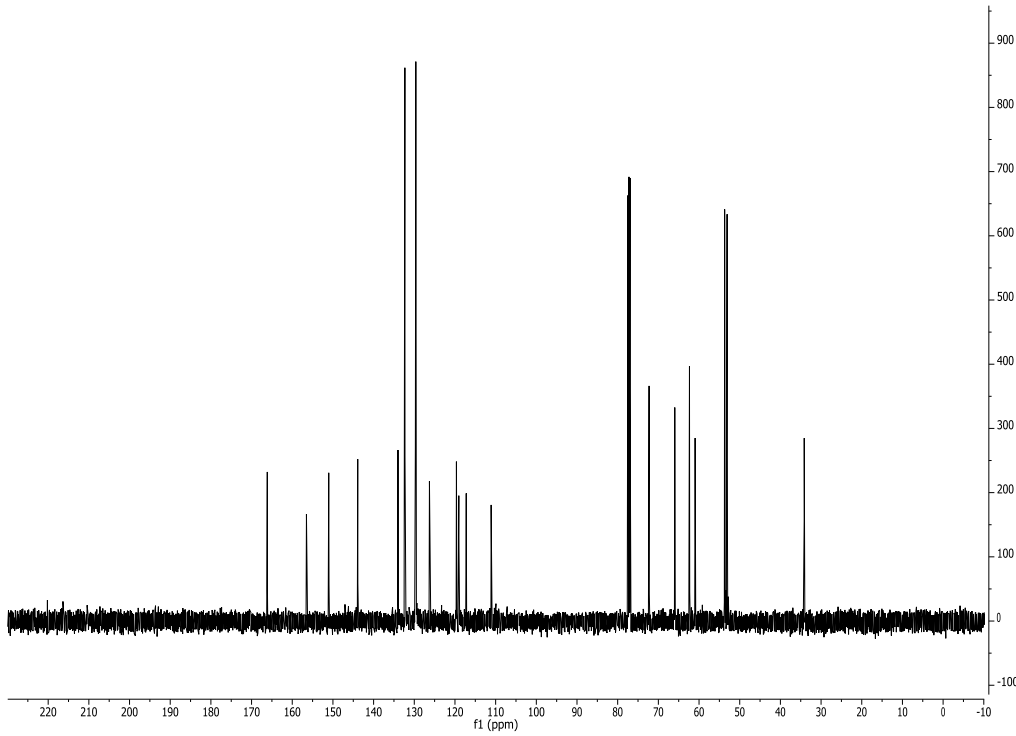
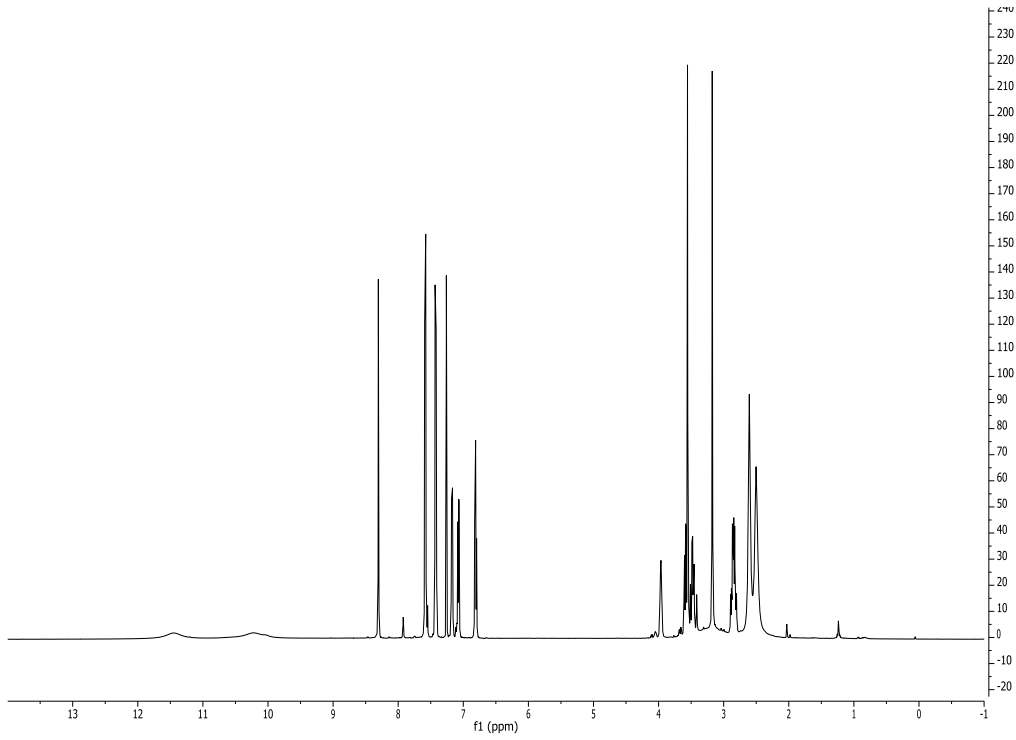
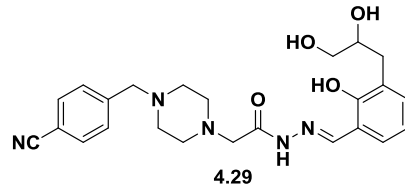


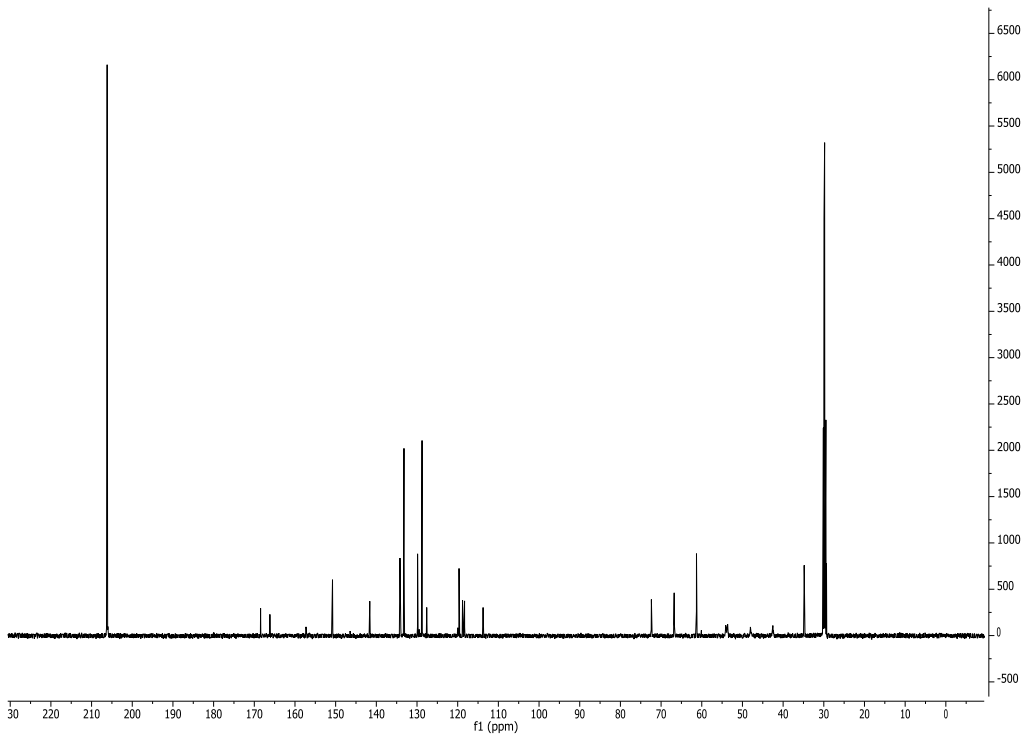
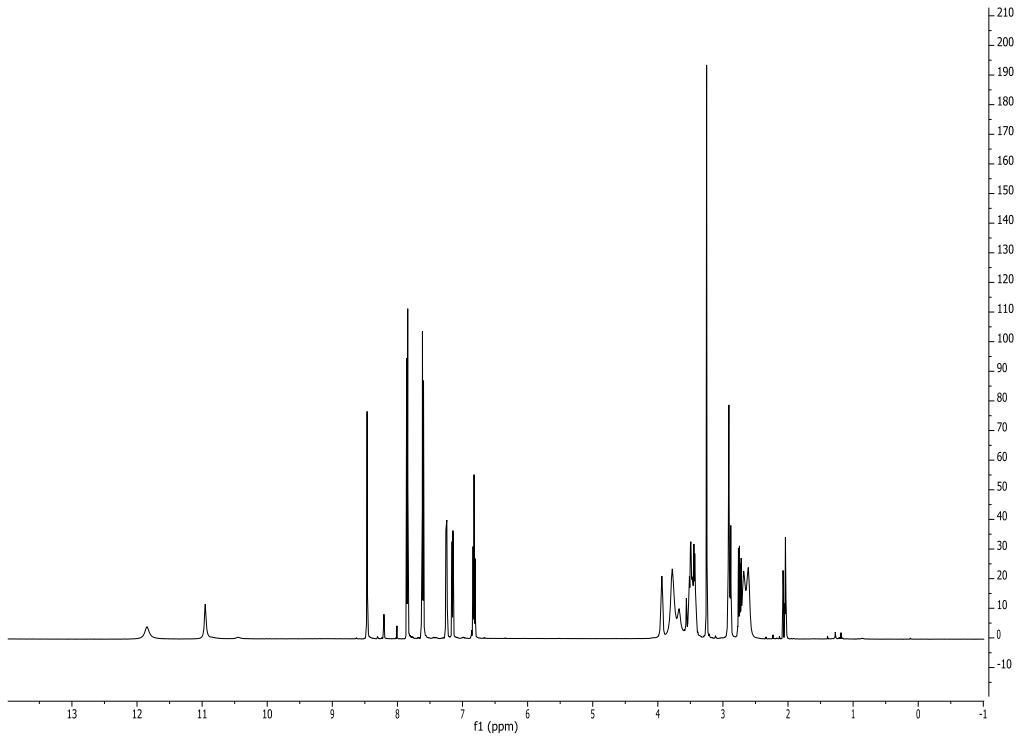
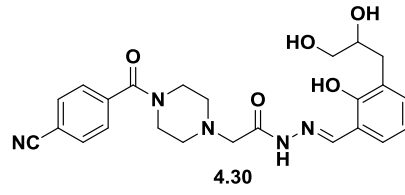


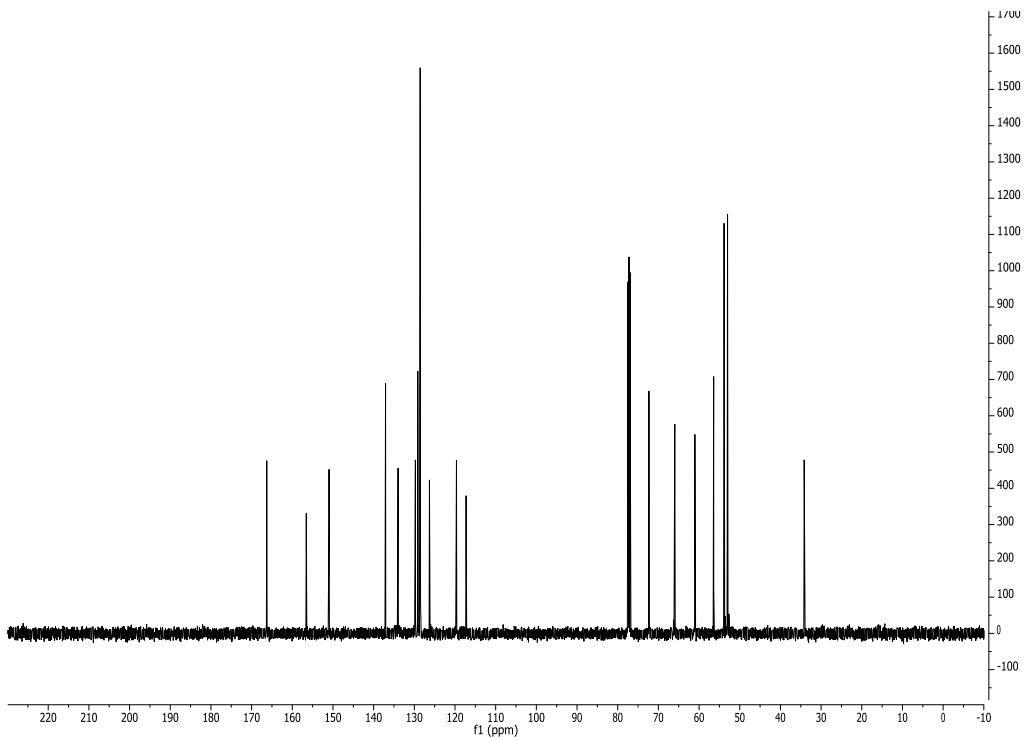
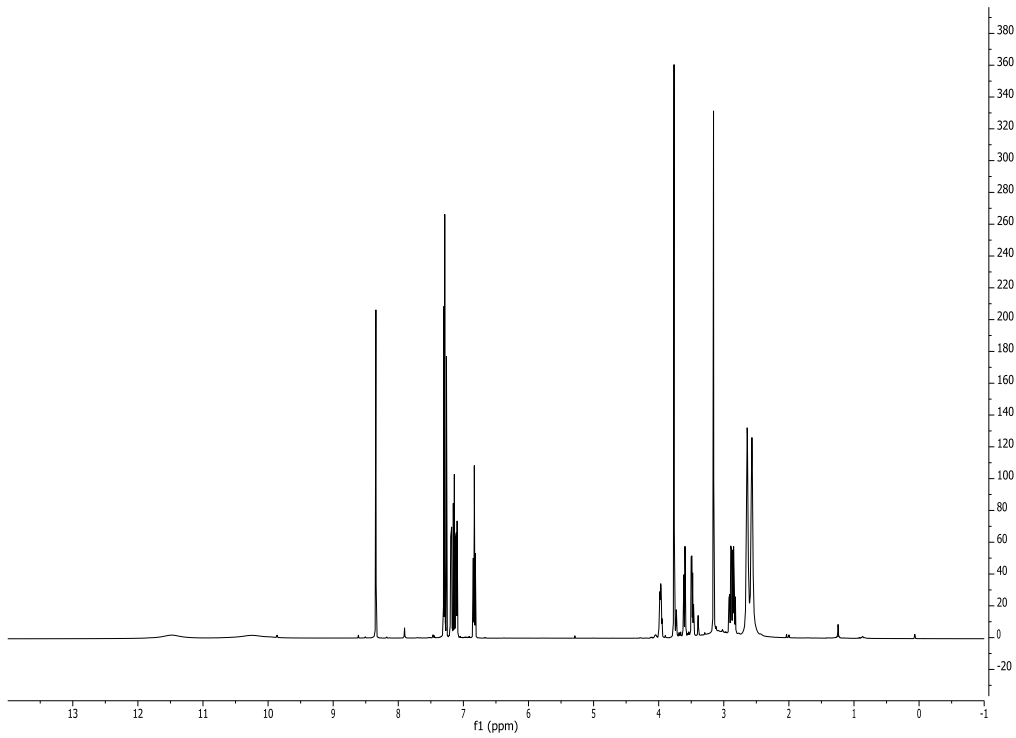
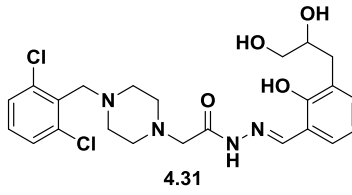












4.10. References

1. Roth, H. S.; Botham, R. C.; Schmid, S. C.; Fan, T. M.; Dirikolu, L.; Hergenrother, P. J. Removal of metabolic liabilities enables development of derivatives of Procaspase-Activating Compound 1 (PAC-1) with improved pharmacokinetics. *J. Med. Chem.* **2015**, *58*, 4046-4065.
2. Lucas, P. W.; Schmit, J. M.; Peterson, Q. P.; West, D. C.; Hsu, D. C.; Novotny, C. J.; Dirikolu, L.; Churchwell, M. I.; Doerge, D. R.; Garrett, L. D.; Hergenrother, P. J.; Fan, T. M. Pharmacokinetics and derivation of an anticancer dosing regimen for PAC-1, a preferential small molecule activator of procaspase-3, in healthy dogs. *Invest. New Drugs* **2011**, *29*, 901-911.
3. Peterson, Q. P.; Hsu, D. C.; Novotny, C. J.; West, D. C.; Kim, D.; Schmit, J. M.; Dirikolu, L.; Hergenrother, P. J.; Fan, T. M. Discovery and canine preclinical assessment of a nontoxic procaspase-3-activating compound. *Cancer Res.* **2010**, *70*, 7232-7241.
4. Ren, L.; Bi, K.; Gong, P.; Cheng, W.; Song, Z.; Fang, L.; Chen, X. Characterization of the in vivo and in vitro metabolic profile of PAC-1 using liquid chromatography–mass spectrometry. *J. Chromatogr. B* **2008**, *876*, 47-53.
5. Putt, K. S.; Chen, G. W.; Pearson, J. M.; Sandhorst, J. S.; Hoagland, M. S.; Kwon, J. T.; Hwang, S. K.; Jin, H.; Churchwell, M. I.; Cho, M. H.; Doerge, D. R.; Helferich, W. G.; Hergenrother, P. J. Small-molecule activation of procaspase-3 to caspase-3 as a personalized anticancer strategy. *Nat. Chem. Biol.* **2006**, *2*, 543-550.
6. Peterson, Q. P.; Hsu, D. C.; Goode, D. R.; Novotny, C. J.; Totten, R. K.; Hergenrother, P. J. Procaspase-3 activation as an anti-cancer strategy: structure-activity relationship of Procaspase-Activating Compound 1 (PAC-1) and its cellular co-localization with caspase-3. *J. Med. Chem.* **2009**, *52*, 5721-5731.
7. Peterson, Q. P.; Goode, D. R.; West, D. C.; Ramsey, K. N.; Lee, J. J. Y.; Hergenrother, P. J. PAC-1 activates procaspase-3 in vitro through relief of zinc-mediated inhibition. *J. Mol. Biol.* **2009**, *388*, 144-158.
8. Hsu, D. C.; Roth, H. S.; West, D. C.; Botham, R. C.; Novotny, C. J.; Schmid, S. C.; Hergenrother, P. J. Parallel synthesis and biological evaluation of 837 analogues of Procaspase-Activating Compound 1 (PAC-1). *ACS Comb. Sci.* **2012**, *14*, 44-50.
9. Astrand, O. A. H.; Aziz, G.; Ali, S. F.; Paulsen, R. E.; Hansen, T. V.; Rongved, P. Synthesis and initial in vitro biological evaluation of two new zinc-chelating compounds: comparison with TPEN and PAC-1. *Bioorg. Med. Chem.* **2013**, *21*, 5175-5181.
10. Zhai, X.; Huang, Q.; Jiang, N.; Wu, D.; Zhou, H. Y.; Gong, P. Discovery of hybrid dual N-acylhydrazone and diaryl urea derivatives as potent antitumor agents: design, synthesis and cytotoxicity evaluation. *Molecules* **2013**, *18*, 2904-2923.
11. Hao-ming, L.; Chun-ling, Y.; Xiao-ying, Z.; Ming-ming, Z.; Dan, J.; Jun-hai, X.; Xiao-hong, Y.; Song, L. Design, synthesis, and antitumor activity of a novel series of PAC-1 analogues. *Chem. Res. Chin. Univ.* **2013**, *29*, 906-910.
12. Ma, J.; Zhang, G.; Han, X.; Bao, G.; Wang, L.; Zhai, X.; Gong, P. Synthesis and biological evaluation of benzothiazole derivatives bearing the ortho-hydroxy-N-acylhydrazone moiety as potent antitumor agents. *Arch. Pharm. Chem. Life Sci.* **2014**, *347*, 936-949.
13. Wang, F. Y.; Wang, L. H.; Zhao, Y. F.; Li, Y.; Ping, G. F.; Xiao, S.; Chen, K.; Zhu, W. F.; Gong, P.; Yang, J. Y.; Wu, C. F. A novel small-molecule activator of procaspase-3 induces apoptosis in cancer cells and reduces tumor growth in human breast, liver and gallbladder cancer xenografts. *Mol. Oncol.* **2014**, *8*, 1640-1652.

14. Zhang, B.; Zhao, Y. F.; Zhai, X.; Fan, W. J.; Ren, J. L.; Wu, C. F.; Gong, P. Design, synthesis and antiproliferative activities of diaryl urea derivatives bearing N-acylhydrazone moiety. *Chin. Chem. Lett.* **2012**, *23*, 915-918.
15. Zhang, B.; Zhao, Y. F.; Zhai, X.; Wang, L. H.; Yang, J. Y.; Tan, Z. H.; Gong, P. Design, synthesis and anticancer activities of diaryl urea derivatives bearing N-acylhydrazone moiety. *Chem. Pharm. Bull.* **2012**, *60*, 1046-1054.
16. Wang, F.; Liu, Y.; Wang, L.; Yang, J.; Zhao, Y.; Wang, N.; Cao, Q.; Gong, P.; Wu, C. Targeting procaspase-3 with WF-208, a novel PAC-1 derivative, causes selective cancer cell apoptosis. *J. Cell. Mol. Med.* [Online early access]. DOI: 10.1111/jcmm.12566. Published Online: March 8, 2015.
17. Nassar, A. E. F.; Kamel, A. M.; Clarimont, C. Improving the decision-making process in the structural modification of drug candidates: enhancing metabolic stability. *Drug Discov. Today* **2004**, *9*, 1020-1028.
18. Fleming, F. F.; Yao, L.; Ravikumar, P. C.; Funk, L.; Shook, B. C. Nitrile-containing pharmaceuticals: efficacious roles of the nitrile pharmacophore. *J. Med. Chem.* **2010**, *53*, 7902-7917.
19. Mori, A.; Miyakawa, Y.; Ohashi, E.; Haga, T.; Maegawa, T.; Sajiki, H. Pd/C-catalyzed chemoselective hydrogenation in the presence of diphenylsulfide. *Org. Lett.* **2006**, *8*, 3279-3281.
20. Clark, D. E. Rapid calculation of polar molecular surface area and its application to the prediction of transport phenomena. 2. Prediction of blood-brain barrier penetration. *J. Pharm. Sci.* **1999**, *88*, 815-821.
21. West, D. C.; Qin, Y.; Peterson, Q. P.; Thomas, D. L.; Palchaudhuri, R.; Morrison, K. C.; Lucas, P. W.; Palmer, A. E.; Fan, T. M.; Hergenrother, P. J. Differential effects of procaspase-3 activating compounds in the induction of cancer cell death. *Mol. Pharmaceutics* **2012**, *9*, 1425-1434.
22. Soars, M. G.; Gelboin, H. V.; Krausz, K. W.; Riley, R. J. A comparison of relative abundance, activity factor and inhibitory monoclonal antibody approaches in the characterization of human CYP enzymology. *Br. J. Clin. Pharmacol.* **2003**, *55*, 175-181.
23. Huang, S.; Clark, R. J.; Zhu, L. Highly sensitive fluorescent probes for zinc ion based on triazolyl-containing tetradentate coordination motifs. *Org. Lett.* **2007**, *9*, 4999-5002.
24. Huang, Q.; Fu, Q.; Liu, Y.; Bai, J.; Wang, Q.; Liao, H.; Gong, P. Design, synthesis and anticancer activity of novel 6-(aminophenyl)-2,4-bismorpholino-1,3,5-triazine derivatives bearing arylmethylene hydrazine moiety. *Chem. Res. Chin. Univ.* **2014**, *30*, 257-265.
25. Patel, V.; Balakrishnan, K.; Keating, M. J.; Wierda, W. G.; Gandhi, V. Expression of executioner procaspases and their activation by a procaspase activating compound in chronic lymphocytic leukemia cells. *Blood* **2015**, *125*, 1126-1136.
26. Purser, S.; Moore, P. R.; Swallow, S.; Gouverneur, V. Fluorine in medicinal chemistry. *Chem. Soc. Rev.* **2008**, *37*, 320-330.
27. Park, B. K.; Kitteringham, N. R.; O'Neill, P. M. Metabolism of fluorine-containing drugs. *Annu. Rev. Pharmacol. Toxicol.* **2001**, *41*, 443-470.
28. Vichai, V.; Kirtikara, K. Sulforhodamine B colorimetric assay for cytotoxicity screening. *Nat. Protoc.* **2006**, *1*, 1112-1116.

Chapter 5. Investigation of Neurotoxicity Induced by PAC-1

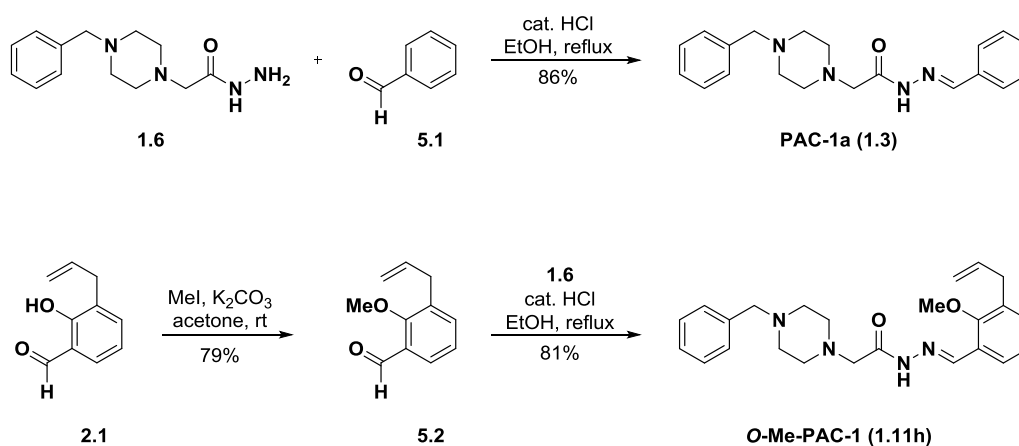
Cell culture evaluation was performed in collaboration with Jessie Peh. Initial animal experiments were performed by Dr. Quinn P. Peterson. The second set of animal experiments was performed by Prof. Timothy M. Fan and Rachel C. Botham.

5.1. PAC-1 neurotoxicity is most likely not mechanism-based

As discussed in Chapter 1, neurotoxicity was observed in early animal studies when **PAC-1** was dosed at high levels. Animals treated with **PAC-1** experienced reversible neuroexcitatory symptoms at doses as low as 20 mg/kg via i.v. injection, and symptoms increased in severity with increasing doses.¹ The biochemical basis of this toxicity was not well understood, but it was hypothesized that **PAC-1** crosses the blood-brain barrier (BBB) and chelates inhibitory zinc from NMDA receptors within the central nervous system (CNS);¹ structurally unrelated zinc chelators have been shown to elicit neurological responses similar to those observed upon treatment with **PAC-1**.^{2, 3} Initial attempts toward developing a non-neurotoxic **PAC-1** derivative involved the design of compounds that would not cross the BBB; these efforts produced **S-PAC-1**, as discussed in Chapter 1.¹ Less than 1% of the total dose of **S-PAC-1** administered to mice enters the brain,⁴ as the highly polar sulfonamide group prevents the compound from crossing the BBB.

While initial results with **S-PAC-1** were promising, recent studies have demonstrated the potential for **PAC-1** to be used to treat brain tumors,⁵ making a BBB-permeable **PAC-1** derivative desirable, especially if a non-neurotoxic derivative could be developed. One method discovered to attenuate the neurological symptoms of **PAC-1** was oral administration of compound.⁵ Both the peak plasma concentration and the area under the concentration-time curve decrease upon oral administration as compared to i.v. or i.p. injections, indicating decreases to both the maximum amount of compound in the brain as well as the total exposure; a slower uptake of compound into the bloodstream is also observed for oral administration as compared to i.v. or i.p. injections. However, the potential for adverse events still exists, and if the toxicity is not related to zinc chelation, it would be most desirable to have a BBB-permeable **PAC-1** derivative that is incapable of producing a neurological response. In order to understand determine whether the toxicity is mechanism-based, an experiment was designed in which mice

were treated with **PAC-1** or inactive derivatives **PAC-1a** (**1.3**), which lacks the allyl and hydroxyl groups of **PAC-1**, and the methyl ether of **PAC-1**, **O-Me-PAC-1** (**1.11h**). Upon treatment, mice were monitored for neurological symptoms. Synthetic routes toward the compounds are shown in Scheme 5.1. Condensation of hydrazide **1.6** with benzaldehyde (**5.1**) gave **PAC-1a**. Methylation of the phenol of **2.1** gave aldehyde **5.2**, and condensation of this aldehyde with hydrazide **1.6** gave **O-Me-PAC-1**.



Scheme 5.1. Synthesis of inactive derivatives of **PAC-1** used in initial neurotoxicity study.

PAC-1, **PAC-1a**, and **O-Me-PAC-1** were formulated at 10 mg/mL in 200 mg/mL aqueous 2-hydroxypropyl- β -cyclodextrin (HP β CD) and dosed at 180 mg/kg via i.p. injection, a dose at which **PAC-1** elicits a strong neuroexcitatory response. Mice treated with **PAC-1**, **PAC-1a**, and **O-Me-PAC-1** were indistinguishable between treatment groups; all mice experienced severe seizures from the treatment. Given that the derivatives that do not bind zinc lead to the same phenotype *in vivo*, it is likely that the toxicity observed with **PAC-1** is not mechanism-based, and that it is related to a different property of the molecule. Therefore, if the portion responsible for the toxicity can be determined, it may be possible to design a non-neurotoxic, BBB-permeable **PAC-1** derivative for the treatment of brain tumors.

The study described herein represents an attempt to further define the functional groups responsible for **PAC-1**-induced neurotoxicity. A series of compounds with minor modifications to **PAC-1** was designed and synthesized. The compounds were evaluated *in vitro* and in cell culture to confirm and expand upon previously determined structure-activity relationships. Finally, the neurological phenotypes induced by compounds were evaluated in mice.

5.2. Compound design and synthesis

In order to further determine the portion of the molecule responsible for neurotoxicity, a series of compounds was designed that contained minimal modifications to the **PAC-1** structure (Figure 5.1). The compounds were designed either with an intact *ortho*-hydroxy-*N*-acylhydrazone (Figure 5.1B) or with modifications to the *ortho*-hydroxy-*N*-acylhydrazone (Figure 5.1C). Compound modifications compared to **PAC-1** are highlighted in red; for reference, **PAC-1** is shown in Figure 5.1A. Modifications to portions other than the *ortho*-hydroxy-*N*-acylhydrazone include removal of the allyl group (**1.2**), reduction (**5.3**) or removal (**5.4**) of the phenyl group, removal of one (**5.5**) or both (**5.6**) of the methylene groups adjacent to the piperazine, and removal of the benzylpiperazine (**5.7**) or the piperazine (**5.8**). Modifications to the *ortho*-hydroxy-*N*-acylhydrazone include removal of the allyl and hydroxyl (**1.3**), methylation of the hydroxyl (**1.11h**), removal of the group entirely (**5.9**), removal (**1.17b**) or reduction (**1.19**) of the hydrazone, and changing the benzylidene to an isopropylidene (**5.10**). Previous studies of the structure-activity relationships (SAR)⁶ suggest that the compounds in Figure 5.1C should be inactive, while the structures in 5.1B should maintain activity, although some may be less potent than **PAC-1**.

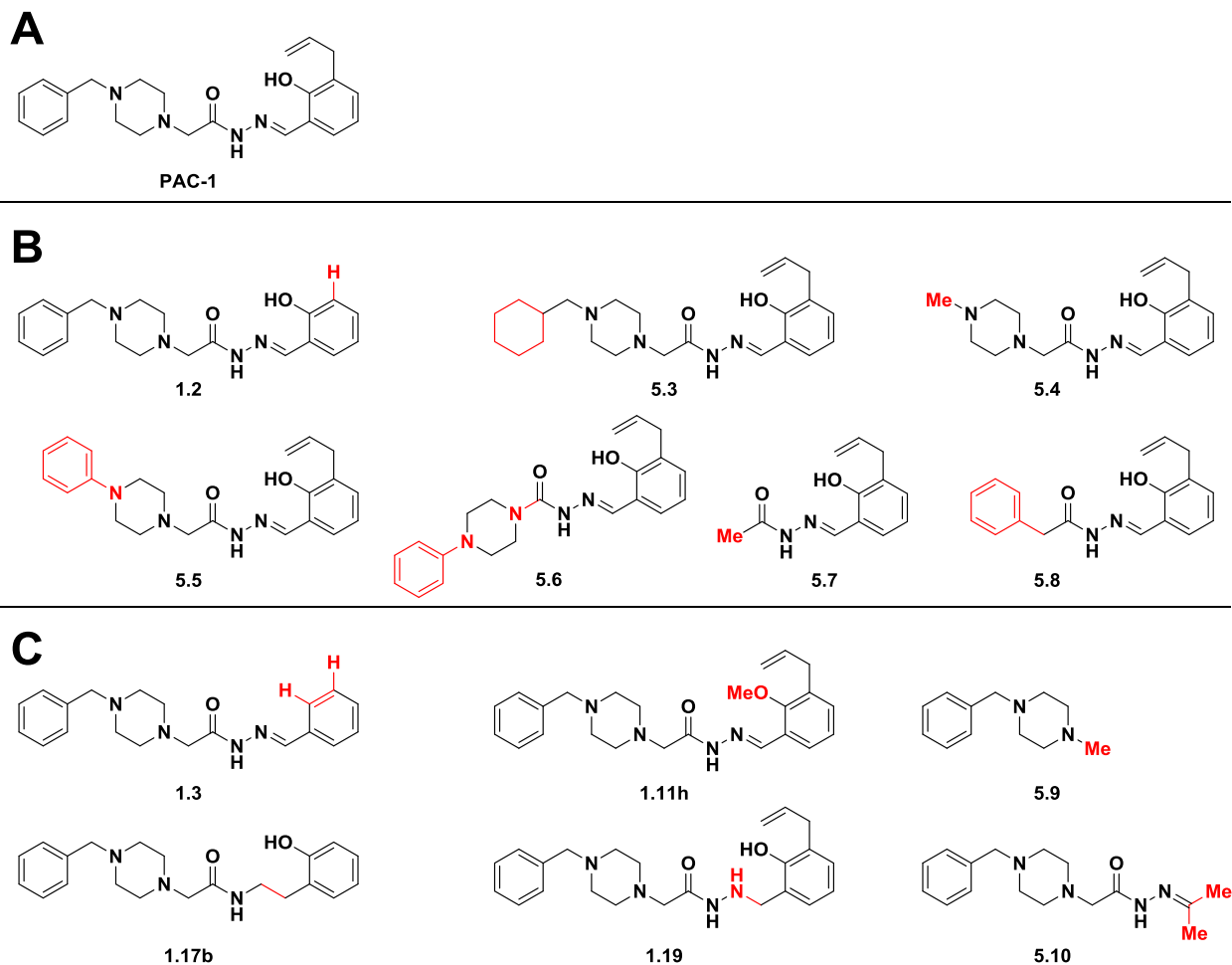
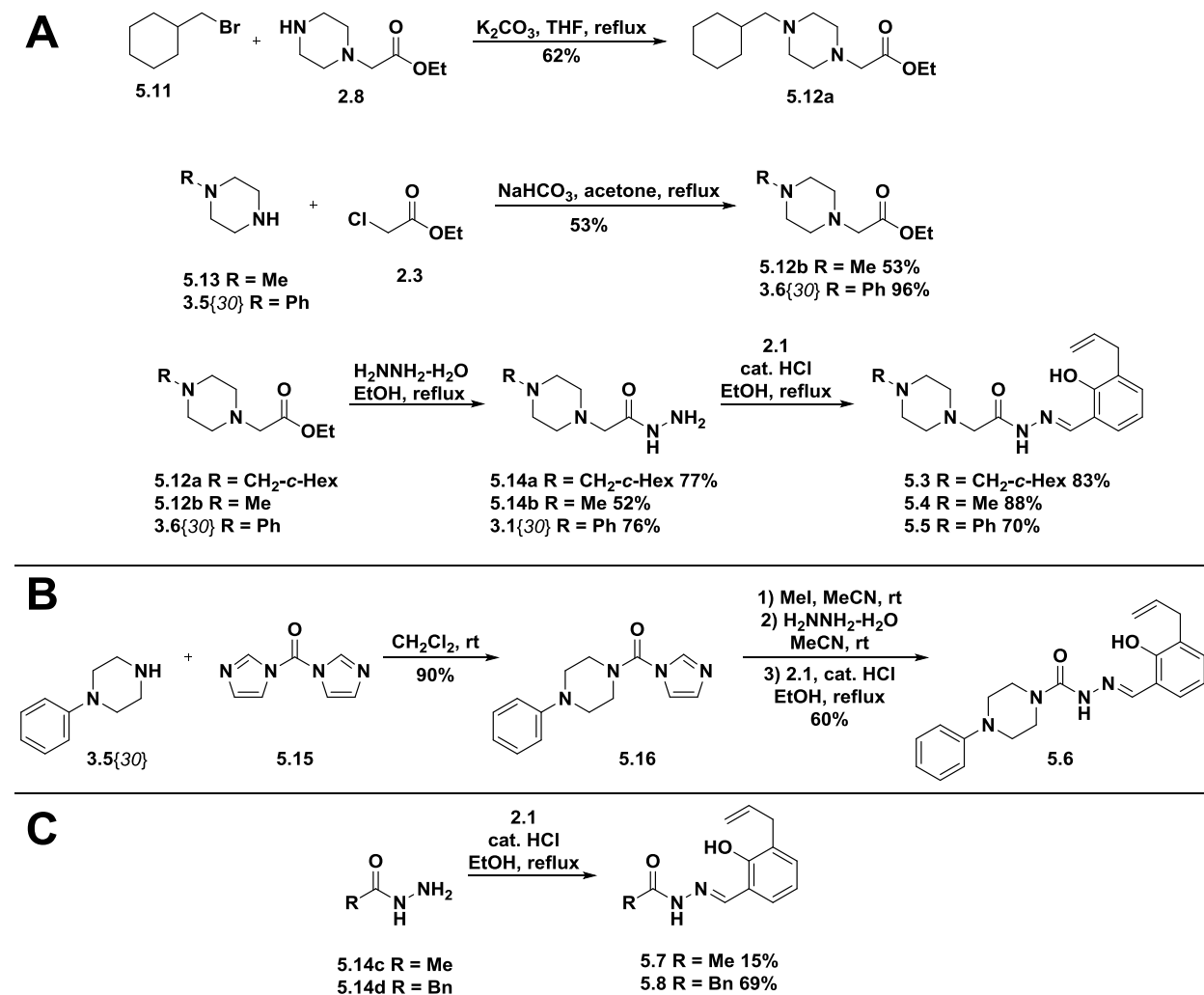


Figure 5.1. Structures of compounds used to evaluate neurotoxicity. **A.** PAC-1. **B.** PAC-1 derivatives with intact *ortho*-hydroxy-*N*-acylhydrazone. **C.** PAC-1 derivatives with modified *ortho*-hydroxy-*N*-acylhydrazone. Modifications to PAC-1 are highlighted in red.

Scheme 5.2 shows the synthetic routes toward compounds **5.3-5.8**, each of which involves condensation with 3-allylsalicylaldehyde (**2.1**) as the last step of the synthesis. Synthesis of **5.3** (Scheme 5.2A) involves alkylation of monosubstituted piperazine **2.8** with (bromomethyl)cyclohexane (**5.11**) to form **5.12a**. Similarly, formation of **5.4** and **5.5** require first reacting 1-methylpiperazine (**5.13**) and 1-phenylpiperazine (**3.5**{30}), respectively, with ethyl chloroacetate, to form **5.12b** and **3.6**{30}. Reaction of each of these three ethyl esters with hydrazine monohydrate gives hydrazides **5.14a**, **5.14b**, and **3.1**{30}. Condensation of each hydrazide with aldehyde **2.1** gives the desired PAC-1 derivatives **5.3-5.5**. Synthesis of semicarbazone **5.6** (Scheme 5.2B) begins with the reaction of **3.5**{30} with 1,1'-

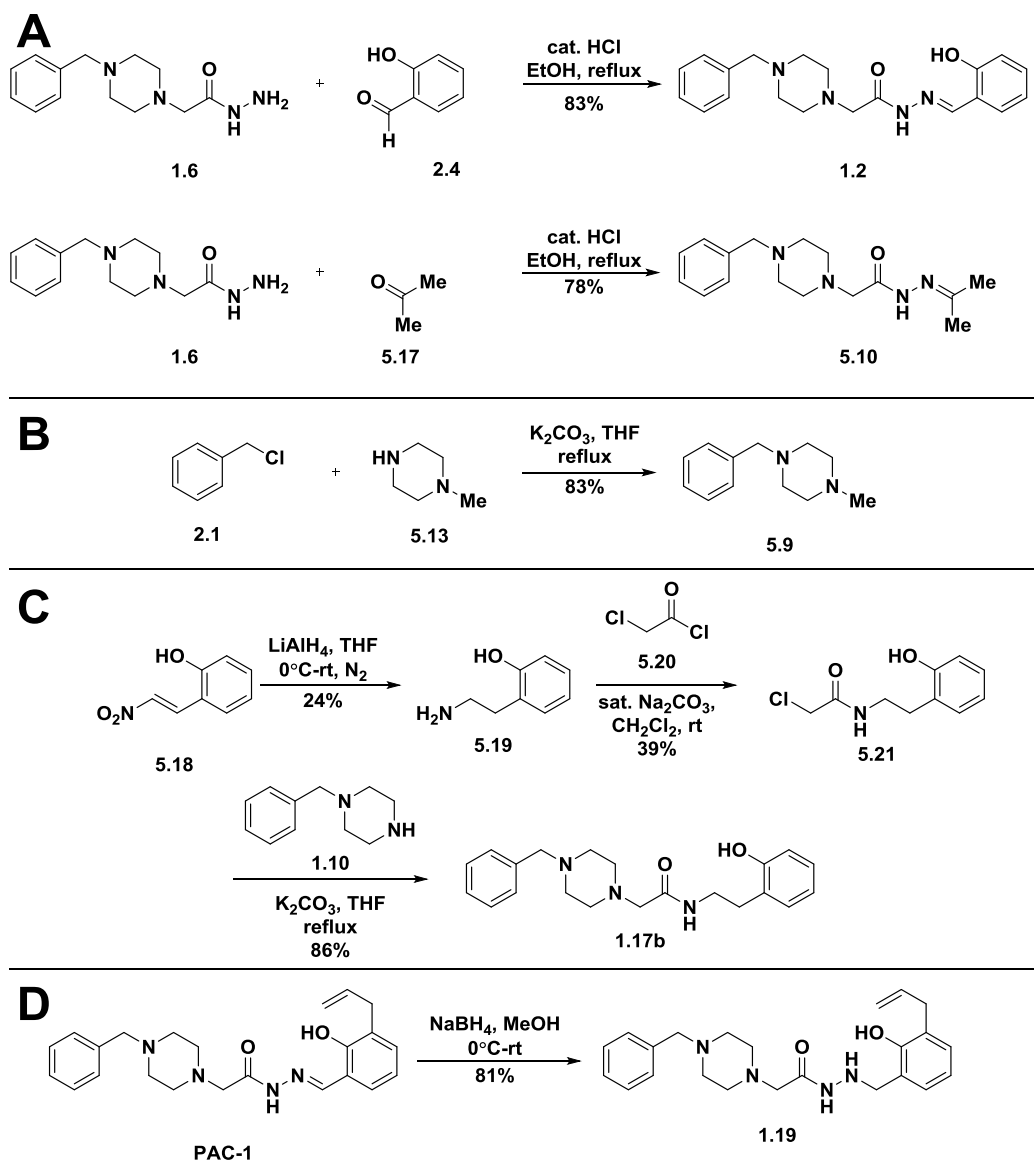
carbonyldiimidazole (**5.15**) to form urea **5.16**. This compound is then methylated, and reaction with hydrazine monohydrate gives the semicarbazide. Condensation of the crude material with **2.1** gives semicarbazone **5.6**. Compounds **5.7** and **5.8** (Scheme 5.2C) were synthesized by the condensation of **2.1** commercially available hydrazides **5.14c** and **5.14d**, respectively.



Scheme 5.2. Synthesis of A. **5.3-5.5**, B. **5.6**, and C. **5.7-5.8**.

Synthetic routes toward **1.2**, **5.8**, **5.9**, **1.17b**, and **1.19**, which do not require reaction with **2.1**, are shown in Scheme 5.3. Condensation of hydrazide **1.6** with salicylaldehyde (**2.4**) or acetone (**5.17**) gives **1.2** and **5.10**, respectively (Scheme 5.3A). Alkylation of **5.13** with benzyl chloride (**2.1**) gives compound **5.9** (Scheme 5.3B). Synthesis of **1.17b** (Scheme 5.3C) begins with the lithium aluminum hydride-mediated reduction of nitrostyrene **5.18** to form

phenethylamine **5.19**. Acylation of the amine with chloroacetyl chloride (**5.20**) under Schotten-Baumann conditions gives amide **5.21**, and substitution of the chloride with 1-benzylpiperazine (**1.10**) gives **1.17b**. Finally, reduction of PAC-1 with sodium borohydride gives hydrazide **1.19** (Scheme 5.3D).



Scheme 5.3. Synthesis of A. **1.2**, **5.8**, B. **5.9**, C. **1.17b**, and D. **1.19**

5.3. Evaluation of PAC-1 derivatives

5.3.1. Predicted blood-brain barrier permeability

Because the neurotoxicity induced by **PAC-1** is related to its ability to cross the BBB, it was important to design the compounds such that the BBB permeability would not differ greatly from that of **PAC-1**. This will be most important to determine whether any compounds are false negatives: reductions in neurotoxicity should be due to reduced interactions with the target that leads to the neuroexcitation, rather than inability to cross the BBB. As discussed in Chapter 3, BBB permeability is frequently represented as logBB, and predicted logBB was calculated using Equation 3.2 (reproduced below):⁷

$$\text{predicted logBB} = (-0.0148 \times \text{PSA}) + (0.152 \times \text{AlogP}) + 0.139 \quad (\text{Equation 3.2})^7$$

The PSA and AlogP values for **PAC-1** and the 13 derivatives were calculated using the Schrodinger software, and insertion of these values into Equation 3.2 gave the predicted logBB values (Table 5.1). **PAC-1** has a predicted logBB value of -0.37, which is very close to the experimentally determined value of -0.36.⁴ Most of the other derivatives have predicted logBB values between -0.17 and -0.61, which are close to the value of **PAC-1**. The only compound with a significantly different predicted logBB value (+0.32) is compound **5.9**. These predictions suggest that BBB permeability should not be a significant variable when evaluating the neurotoxicity of the compounds *in vivo*.

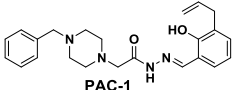
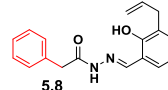
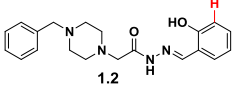
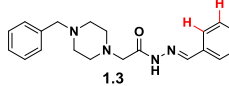
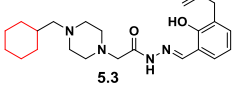
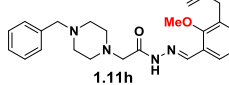
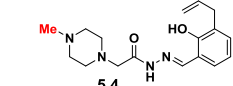
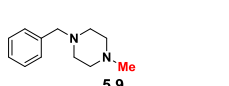
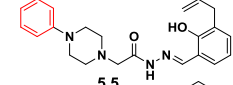
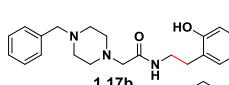
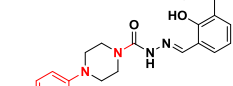
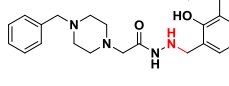
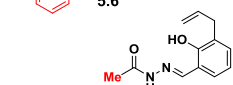
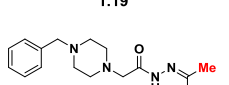
| | Predicted logBB | 72-hour IC ₅₀ (μM) | | Zn ²⁺ K _d (nM) | | Predicted logBB | 72-hour IC ₅₀ (μM) | | Zn ²⁺ K _d (nM) |
|--|-----------------|-------------------------------|------------|--------------------------------------|---|-----------------|-------------------------------|------------|--------------------------------------|
| | | D54 | U-937 | | | | D54 | U-937 | |
|  PAC-1 | -0.37 | 2.3 ± 0.4 | 4.2 ± 0.5 | 1.28 ± 0.03 | | | | | |
|  5.8 | -0.24 | 4.4 ± 1.0 | 6.6 ± 0.5* | N.D. | | | | | |
|  1.2 | -0.52 | 7.4 ± 0.5 | 12.4 ± 1.7 | 1.48 ± 0.06 |  1.3 | -0.18 | >100 | 64.9 ± 6.9 | >10 ⁶ |
|  5.3 | -0.28 | 1.5 ± 0.1 | 3.3 ± 0.2 | 8.39 ± 0.26 |  1.11h | -0.17 | 41.3 ± 10.9 | 53.6 ± 8.7 | >10 ⁶ |
|  5.4 | -0.61 | 5.4 ± 0.7 | 19.0 ± 1.8 | 1.56 ± 0.04 |  5.9 | +0.32 | >100 | >100 | >10 ⁶ |
|  5.5 | -0.35 | 7.8 ± 0.9 | >10 | N.D. |  1.17b | -0.30 | >100 | >100 | >10 ⁶ |
|  5.6 | -0.21 | 1.6 ± 0.2 | 3.3 ± 0.3 | 1.56 ± 0.07** |  1.19 | -0.44 | 53.1 ± 2.9 | 31.5 ± 1.5 | >10 ⁶ |
|  5.7 | -0.51 | 9.4 ± 0.1 | 8.4 ± 0.4 | 1.75 ± 0.09 |  5.10 | -0.46 | >100 | >100 | >10 ⁶ |

Table 5.1. Predicted BBB permeability,^a cytotoxicity,^b and zinc affinity^c of **PAC-1** derivatives.

(a) Calculated using Equation 3.2:

$$\text{predicted logBB} = (-0.0148 \times \text{PSA}) + (0.152 \times \text{ClogP}) + 0.139.$$

(b) Cells treated with compounds for 72 hours. Biomass quantified by sulforhodamine B assay.

IC₅₀ values shown are mean ± s.e.m. (n = 3, except *n = 2).

(c) Increasing amounts of Zn(OTf)₂ added to a buffered solution of EGTA (7.3 mM) and **PAC-1** derivative (100 μM, except **10 μM). K_d was determined by comparing fluorescence intensity (ex. 410 nm, em. 475 nm) and free zinc concentration. N.D. = not determined (due to insolubility).

5.3.2. Cell culture evaluation

With the 14 compounds in hand, the cytotoxicity to cancer cells in culture was evaluated. The compounds were evaluated in 72-hour experiments in D54 (human glioblastoma) cells, because the goal will be to use the compounds to treat brain tumors, as well as U-937 (human lymphoma) cells, because of the extensive use of this cell line in previous efforts with **PAC-1** and derivatives.^{1, 4, 6, 8-12} The results of these experiments are shown in Table 5.1. The potency is relatively consistent across the two cell lines. **PAC-1** is cytotoxic with IC₅₀ values in the single-

digit micromolar range. Removal of the allyl group (**1.2**) and most modifications to the benzylpiperazine (**5.4**, **5.5**, **5.7**, **5.8**) led to a slight decrease in potency. However, reduction of the phenyl (**5.3**) or removal of both methylene groups (**5.6**) gave compounds with equal or slightly improved potency. As expected, modification of the *ortho*-hydroxy-*N*-acylhydrazone led to a significant loss in potency, including several compounds that were not cytotoxic up to the highest concentration tested (100 μ M). Compounds **5.5** and **5.8** were insoluble above 10 μ M and were not evaluated in subsequent experiments.

The compounds were then evaluated further in D54 cells to determine the mode of cell death induced by the compounds. Cells were treated with compounds at 30 μ M for 24 hours, and cell death was assessed by Annexin V-FITC/propidium iodide staining (Figure 5.2). Treatment with DMSO alone induced minimal cell death, while all cytotoxic compounds induced cell death via apoptosis. **PAC-1** induced approximately 50% cell death under these conditions, while compounds **5.3** and **5.6** showed comparable potency. No derivative lacking the *ortho*-hydroxy-*N*-acylhydrazone induced greater than 25% cell death. Compound **5.7**, which lacks the benzylpiperazine, was minimally cytotoxic under these conditions, suggesting that this compound may require longer treatment times for induction of apoptosis.

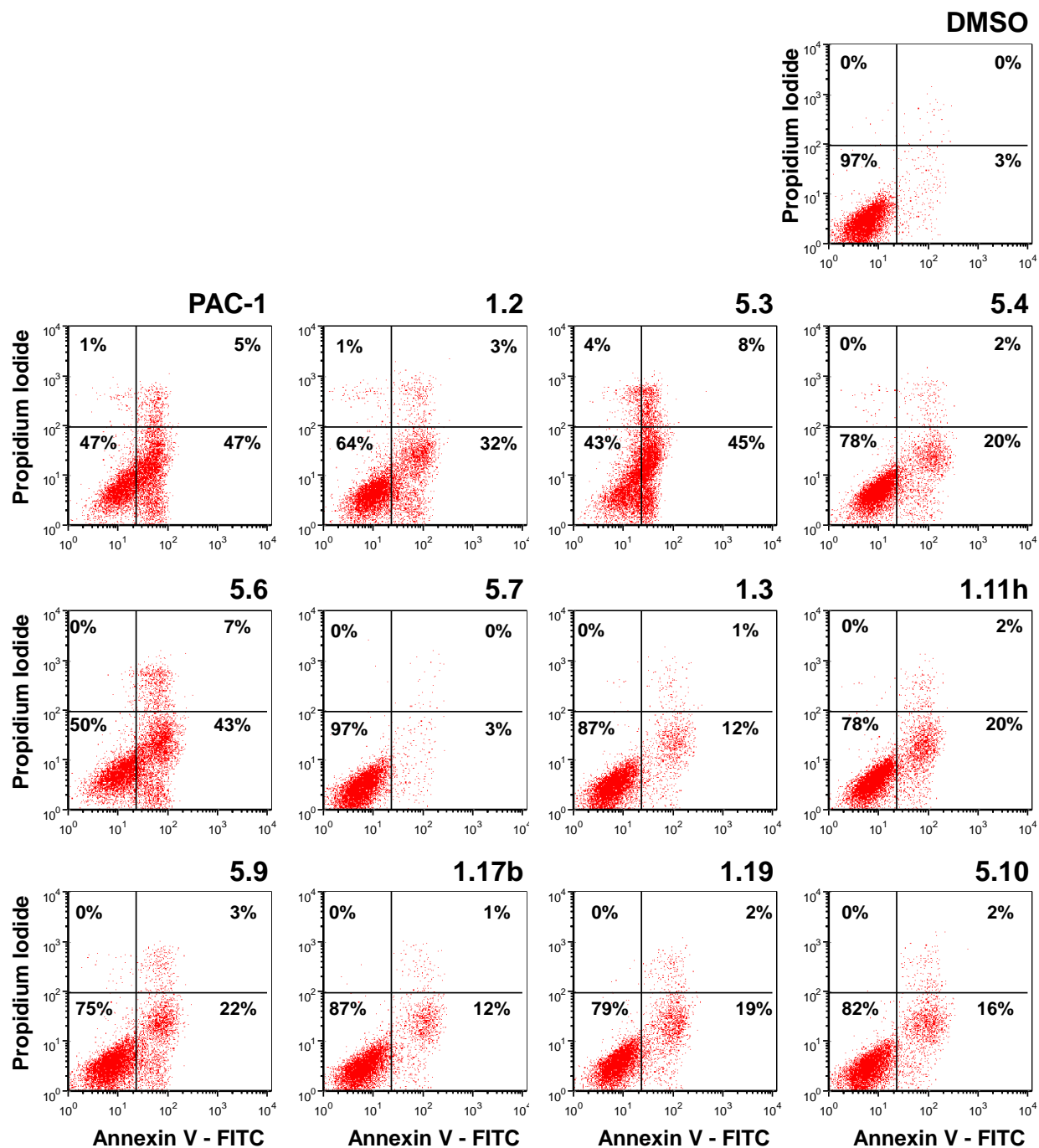


Figure 5.2. Annexin V-FITC/propidium iodide staining of D54 cells treated with compounds (30 μ M) for 24 hours. Data shown are representative of three independent experiments.

5.3.3. Zinc binding determination

In order to establish with certainty whether the observed neurotoxicity induced by **PAC-1** is due to zinc chelation, the ability of the new derivatives to bind zinc was evaluated (Table 5.1).

As with the compounds in Chapter 4, zinc binding was determined using an EGTA titration experiment.¹³ Varying concentrations of Zn(OTf)₂ were added to each well of a 96-well plate with a HEPES-buffered solution containing EGTA and **PAC-1** derivative (100 μM, except 10 μM for compound **5.6**), and the fluorescence of the complex was analyzed. **PAC-1**, **1.2**, **5.4**, **5.6**, and **5.7** all bound zinc with affinity in the 1-2 nM range. Each of these compounds contains the *ortho*-hydroxy-*N*-acylhydrazone, confirming the essential nature of this group for metal binding. Cyclohexyl-containing compound **5.3**, which also contains the *ortho*-hydroxy-*N*-acylhydrazone, bound zinc slightly more weakly, but still with low nanomolar affinity. Compounds **1.3**, **1.11h**, **5.9**, **1.17b**, **1.19**, and **5.10** all contain modifications to the *ortho*-hydroxy-*N*-acylhydrazone, and none of these compounds bound zinc at concentrations lower than 1 mM.

5.3.4. Summary of structure-activity relationships

The experiments described above confirmed previously determined SAR for **PAC-1**, summarized in Figure 5.3. As shown previously, the *ortho*-hydroxy-*N*-acylhydrazone is required for zinc binding and cell culture activity. The allyl group and benzylpiperazine both improve cell culture potency relative to derivatives that lack these groups: **PAC-1** is more potent than **1.2** ($p = 0.0008$ (D54); $p = 0.02$ (U-937)), which lacks the allyl group, as well as **5.4** ($p = 0.02$ (D54); $p = 0.007$ (U-937)) and **5.7** ($p = 0.005$ (D54); $p = 0.02$ (U-937)), which lack the phenyl and benzylpiperazine groups respectively (p -values calculated via two-tailed Student's *t*-test in Microsoft Excel). However, the allyl group is not required for zinc binding, as demonstrated by the comparable zinc binding constants for **PAC-1** and **1.2**. It is possible that the increased potency in cells may be due to the increased hydrophobicity of the allyl and benzyl groups; this trend was observed for the hydrophobic derivatives discussed in Chapter 3.¹⁰ The effect of the benzylpiperazine moiety on zinc binding is not clear; compounds **5.4** and **5.7**, which lack the benzyl and benzylpiperazine groups, respectively, each bind zinc with affinity comparable to that of **PAC-1**, but compound **5.3**, in which the phenyl group is reduced to a cyclohexyl group, has a slightly lower affinity for zinc. In total, these results suggest that if the neurotoxicity is not due to the presence of the *ortho*-hydroxy-*N*-acylhydrazone, it may be possible to design a derivative of **PAC-1** that is potent but not neurotoxic, thereby increasing the therapeutic window for anticancer efficacy.

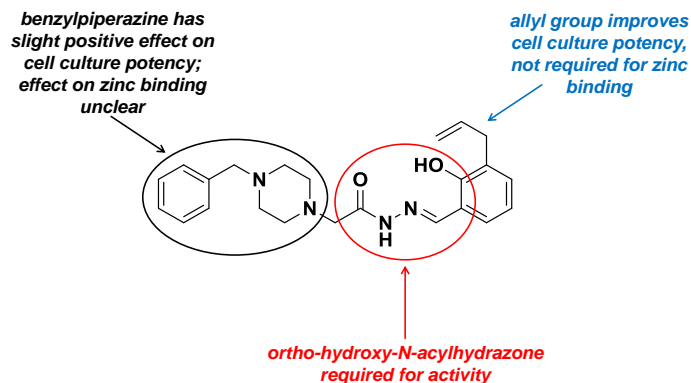


Figure 5.3. Summary of structure-activity relationships for **PAC-1**.

5.4. Evaluation of PAC-1 derivatives in mice

After evaluation of the compounds in cell culture and *in vitro*, the 12 **PAC-1** derivatives were evaluated *in vivo* to assess the induction of the neurologic phenotype. Compounds were formulated at 20 mM in a 200 mg/mL aqueous solution of hydroxypropyl- β -cyclodextrin (HP β CD), and mice were administered a dose of 150 μ mol/kg via i.v. injection (150 μ L injection). Three mice were included in each treatment group. Responses were graded on a scale of 0-4, with 0 indicating no effect, and 4 indicating the most significant reaction to the dose. **PAC-1** induces rapid and severe, but transient, neuroexcitation at this dose (grade 3), and the mice survive, while no adverse events are observed upon treatment with HP β CD alone (grade 0). HP β CD and **PAC-1** were used as controls, while the remaining compounds were randomized, and the identities of the compounds were not known to the experimenters during the experiment.

Table 5.2 shows the graded responses to compounds, along with a brief description of symptoms. Predicted logBB values, initially presented in Table 5.1, are reproduced in Table 5.2. All responses were initially apparent within the first minute of treatment, although symptoms slowly increased in intensity in response to some of the compounds. Responses were identical among the three mice for all treatment groups. Several compounds induced neurotoxicity to a greater extent than **PAC-1**, including methyl ether **1.11h** and reduced derivative **1.19**, while semicarbazone **5.6** induced neuroexcitation to the same extent as **PAC-1**. Cyclohexyl-containing compound **5.3** was more neurotoxic than **PAC-1**, and the dose was lethal to two of the three treated mice within 24 hours. Responses to compounds **1.2** (lacking the allyl group), **5.7** (lacking the benzylpiperazine), **1.17b** (changing the hydrazone to an ethylene linker), and **PAC-1a** (**1.3**, lacking the allyl and hydroxyl groups) were less severe than responses to **PAC-1**. Mice treated

with compounds **5.4** (lacking the phenyl group), **5.9** (lacking the *ortho*-hydroxy-*N*-acylhydrazone), and **5.10** (isopropylidene hydrazone) were asymptomatic following treatment.

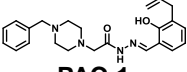
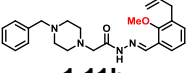
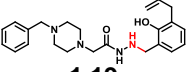
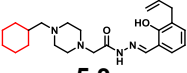
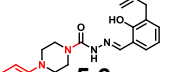
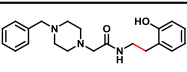
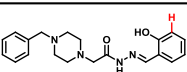
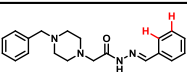
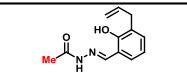
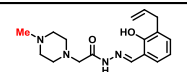
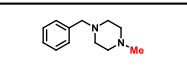
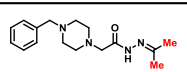
| compound | murine toxicity | Predicted logBB |
|--|---|-----------------|
| HPβCD | 0 No effect | N/A |
|  PAC-1 | 3 Seizure (mild at first, escalating), rapid breathing, hind limbs splayed | -0.37 |
|  1.11h | 4 Immediate seizure, rapid breathing (more severe than PAC-1) | -0.17 |
|  1.19 | 4 Immediate seizure, rapid breathing (more severe than PAC-1) | -0.44 |
|  5.3 | 4 Immediate seizure, rapid breathing (more severe than PAC-1); lethal to 2/3 mice | -0.28 |
|  5.6 | 3 Delayed onset of symptoms from PAC-1. Wobbly, rapid breathing, escalating from minor seizures to full seizures. | -0.21 |
|  1.17b | 2 Wobbly (still active and mobile), slightly sedative | -0.30 |
|  1.2 | 1 A little wobbly (still active and mobile) | -0.52 |
|  1.3 | 1 A little wobbly (still active and mobile) | -0.18 |
|  5.7 | 1 A little wobbly (still active and mobile) | -0.51 |
|  5.4 | 0 Asymptomatic | -0.61 |
|  5.9 | 0 Possibly a little hyper or a little wobbly, but highly asymptomatic | +0.32 |
|  5.10 | 0 Asymptomatic | -0.46 |

Table 5.2. Responses to treatment with **PAC-1** derivatives. Compounds were formulated at 20 mM in 200 mg/mL aqueous HP β CD and administered to C57BL/6 mice at 150 μ mol/kg via i.v. injection (150 μ L, n = 3 per compound). Responses are graded on a scale of 0 (no effect) to 4 (most severe toxicity). Predicted logBB values are also provided.

While few general trends were observed for structural features that induce neurotoxicity, this experiment appears to confirm previously determined results, in that neurotoxicity is most likely not related to zinc affinity. This is most evident for compounds **5.4**, which chelates zinc but is not neuroexcitatory, and **1.19**, which does not bind zinc but induced neurotoxicity more severe than that induced by **PAC-1**. It is possible that the improved tolerability of compound **5.4** as compared to **PAC-1** is due to decreased BBB permeability; further experiments are necessary to determine whether compound **5.4** is well tolerated because it does not enter the brain, or because it does not interact with the biological macromolecule(s) responsible for induction of neuroexcitation. Of note, these experiments do not eliminate the possibility that the *ortho*-hydroxy-*N*-acylhydrazone or a smaller fragment thereof is responsible for neuroexcitation; it is possible that this portion of the molecule interacts with a biological macromolecule in the brain, but it is unlikely that the mechanism of neurotoxicity involves binding of zinc by this motif.

Compound **5.6**, which showed favorable activity in cell culture and *in vitro*, may also be of interest. The predicted BBB permeability (predicted 38:62 brain:blood) is higher than that of **PAC-1** (experimentally 30:70 brain:blood), but the neurological response was comparable, and perhaps slightly lessened. It will be important to confirm that **5.6** is more BBB permeable than **PAC-1**. If a higher concentration of compound **5.6** is present in the brain than **PAC-1** after administration of equivalent doses, this may indicate the potential for improved efficacy in animal studies of brain tumors, as a higher dose would reach the site of the tumor, but neurological symptoms would not increase in severity. This may also be useful in the design of new derivatives that would be better tolerated.

5.5 Comparison of PAC-1 derivatives

In the preceding chapters, the design, synthesis, and evaluation of a wide variety of **PAC-1** derivatives have been discussed. Detailed experiments have been performed for many of these compounds in order to elucidate mechanism of action and possible *in vivo* anticancer efficacy. A comparison of favorable and unfavorable characteristics, as well as unknown aspects of the compounds that merit further study, is presented in Table 5.3.

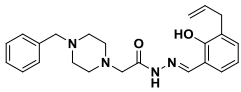
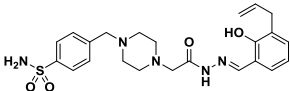
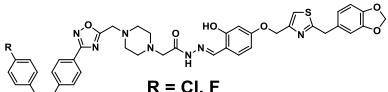
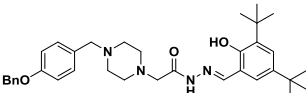
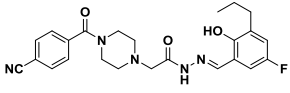
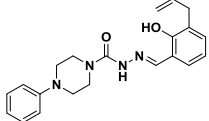
| Compound | Favorable Characteristics | Unfavorable/ Unknown Characteristics |
|---|---|--|
|  <p>PAC-1</p> | <ul style="list-style-type: none"> • Anticancer efficacy • BBB permeable | <ul style="list-style-type: none"> • Rapid clearance • Neurotoxicity at elevated doses |
|  <p>S-PAC-1</p> | <ul style="list-style-type: none"> • Well tolerated in mice and dogs • BBB impermeable • Potential for efficacy | <ul style="list-style-type: none"> • Rapid clearance • Efficacy may be lower than PAC-1 |
|  <p>WF-208/WF-210 R = Cl, F</p> | <ul style="list-style-type: none"> • Efficacy in cell culture and <i>in vivo</i> • Selectivity for cancer cell death in culture | <ul style="list-style-type: none"> • Large size • BBB permeability unknown • Pharmacokinetics unknown |
|  <p>B-PAC-1</p> | <ul style="list-style-type: none"> • Potency in cell culture • Selectivity for cancer cell death in culture • Favorable pharmacokinetics | <ul style="list-style-type: none"> • Expanded cancer type scope unknown • Anticancer efficacy <i>in vivo</i> unknown |
|  <p>4.62</p> | <ul style="list-style-type: none"> • Potency similar to PAC-1 • Favorable pharmacokinetics | <ul style="list-style-type: none"> • Expanded cancer type scope unknown • Anticancer efficacy <i>in vivo</i> unknown |
|  <p>5.6</p> | <ul style="list-style-type: none"> • Potency in cell culture and <i>in vitro</i> • Safety similar to PAC-1, but possible higher BBB permeability | <ul style="list-style-type: none"> • Neurotoxicity still exists • BBB permeability unknown • Anticancer efficacy <i>in vivo</i> unknown |

Table 5.3. Comparison of PAC-1 derivatives.

PAC-1 has been studied extensively; cell culture and *in vivo* anticancer efficacy have been promising,⁸ and the initial efficacy studies combined with the demonstrated BBB

permeability⁴ suggest the potential for the treatment of CNS cancers.⁵ However, rapid clearance from circulation in mice¹⁴ necessitates the administration of relatively large doses, and the observed neurotoxicity¹ may prove to be unacceptable at therapeutically relevant doses. Further, if the **PAC-1** mechanism of action proves to be unsuccessful in treating CNS tumors, and other cancer types are pursued, it is most likely that a cytotoxic agent entering the brain would lead to adverse side effects, in addition to the observed neuroexcitation, and a BBB-impermeable agent would be most favorable.

With the goal of identifying a BBB-impermeable **PAC-1** derivative, **S-PAC-1**, containing a highly polar sulfonamide group, was designed.¹ *In vivo* evaluation demonstrated that the sulfonamide successfully prevented entry into the brain,⁴ and the compound showed promise in a Phase 1 clinical trial in canine lymphoma patients.¹ However, **S-PAC-1** is also rapidly cleared from the body, which required a challenging continuous infusion strategy for administration to patients.¹ It is possible that oral administration may give favorable pharmacokinetics, although this has not been investigated. In addition, further experiments have demonstrated that **S-PAC-1** may show decreased efficacy *in vivo* as compared to **PAC-1**, and toxicity has been observed at doses necessary to elicit a therapeutic effect.

Gong, Wu, and coworkers identified **WF-208** and **WF-210** as highly potent **PAC-1** derivatives in cell culture across a wide variety of cell lines, and with considerably higher potency in cancer cells compared to non-cancerous cell lines. Extensive studies of **PAC-1** and these two derivatives demonstrated the necessity for procaspase-3 on the mechanism of action and showed that apoptosis occurs via a non-canonical pathway, with procaspase-3 activation prior to cleavage of initiator procaspases-8 or -9. Both compounds showed anticancer efficacy in various mouse xenograft models, and both were reported to be well tolerated by mice.^{15, 16} The initial studies demonstrate the promise for these two compounds as anticancer agents. However, the compounds are both much larger than typical small molecule drugs, with molecular weights of approximately 800, which may have detrimental effects on pharmacokinetics and bioavailability. Pharmacokinetic evaluation of these two compounds has not been reported, and it will be necessary to determine the pharmacokinetic profiles before further analysis is performed. **WF-210** demonstrated efficacy in two tumor models upon oral administration, so it is possible that the bioavailability will be acceptable, although the compound appears to show improved efficacy upon i.v. injection as compared to oral administration. If the size of these compounds

prevents them from advancing further, it will be useful to determine the structural features responsible for the improved activity, to determine if any portion of the molecules can be removed without a loss in potency. In addition, it is unknown whether these compounds are BBB permeable, but given the large compound sizes, it is unlikely that high concentrations of these compounds are present in the brains of treated animals.

Six highly potent **PAC-1** derivatives were identified from the library of 837 compounds discussed in Chapter 3,¹⁰ and **B-PAC-1** was selected for further evaluation.¹⁷ **B-PAC-1** was cytotoxic to primary isolates from leukemia patients in culture, and cytotoxicity was higher for cancer cells than healthy cells. Studies on the mechanism of action demonstrated the necessity for procaspase-3 and zinc, as well as the non-canonical apoptotic pathway that was observed for **PAC-1**, **WF-208**, and **WF-210**.¹⁷ Pharmacokinetic evaluation demonstrated the delayed clearance of **B-PAC-1** *in vivo*, although these results were highly unusual, and further evaluation may be necessary. The advancement of **B-PAC-1** has not faced significant obstacles, but further evaluation is necessary to determine the translational potential of the compound. **B-PAC-1** is potent in cells derived from white blood cancers, but it is not clear whether efficacy would be observed in cells derived from other tumor types. In addition, because *in vivo* toxicity is among the most significant challenges in working with **PAC-1**, it will be necessary to confirm that **B-PAC-1** can be administered safely at therapeutically relevant doses, and anticancer efficacy *in vivo* has yet to be demonstrated for **B-PAC-1**.

As discussed in Chapter 4, a set of compounds was designed to display improved pharmacokinetics. Four compounds were identified with extended elimination half-lives as compared to **PAC-1**, with compound **4.62** displaying the longest half-life in mice. All four compounds displayed comparable potency in cell culture and improved tolerability in mice. Initial studies of the mechanism of action demonstrated that compounds all chelate zinc and induce apoptosis in cancer cells.¹² However, as with **B-PAC-1**, further experiments are necessary to determine the translational potential for these derivatives. The compounds were only evaluated in cell lines derived from white blood cell cancers, and further evaluation in cells from diverse cancer types will be necessary to define the potential scope of these compounds as anticancer agents. In addition, the compounds have not yet shown anticancer efficacy *in vivo*.

Finally, a series of compounds was designed with the goal of understanding the neurotoxic phenotype observed in animals treated with **PAC-1**. Compound **5.6** was identified as

a potent derivative that may be more BBB permeable without increasing the degree of toxicity. However, the BBB permeability of the compound still remains unknown, and anticancer efficacy has not yet been demonstrated. In addition, the neurological symptoms are still present in response to treatment with compound **5.6**, and it is unclear whether this degree of toxicity can be tolerated at therapeutically relevant doses.

Initial results from the **PAC-1** derivatives discussed above have demonstrated therapeutic potential, although challenges exist for all of the compounds. To date, **PAC-1** is the most promising compound for CNS tumors, and therapeutically relevant doses can be administered safely. However, the rapid clearance and observed neurotoxicity may limit the clinical utility of the compound; the development of a non-neurotoxic, BBB-permeable **PAC-1** derivative would represent a significant advance. It is possible that compound **5.6** may have an improved safety profile, but the toxicity may still limit the utility of this compound. The most likely application for the other compounds discussed, including **S-PAC-1**, **WF-208**, **WF-210**, **B-PAC-1**, and **4.62**, would be tumors not present in the CNS. **S-PAC-1** was evaluated in canine lymphoma patients with promising initial results, although a narrow therapeutic window has limited further studies with the compound. **B-PAC-1** and **4.62** are cytotoxic to cells derived from white blood cell cancers in culture, but *in vivo* efficacy has not yet been demonstrated. **WF-208** and **WF-210** have demonstrated cytotoxicity in a wide variety of cancer cell lines in culture and have shown anticancer efficacy in several murine tumor models, although the large size of these compounds may limit their translational potential. Further evaluation of these and other agents will help to fully define the ability of procaspase activators to treat diverse cancers.

5.6. Summary and future directions

The flexible, modular synthesis of **PAC-1** has facilitated the construction of over 1000 **PAC-1** derivatives. Many of these compounds were produced in order to improve upon the potency, pharmacokinetics, and tolerability of **PAC-1**. In order to discover a more potent compound, a combinatorial library of 837 derivatives was synthesized.¹⁰ Through this effort, six highly potent compounds were identified, and one compound, **B-PAC-1**, is currently under evaluation in patient-derived leukemia samples by Gandhi and coworkers at MD Anderson Cancer Center.¹⁷ In order to improve pharmacokinetics, several derivatives were synthesized containing modifications designed to block oxidative metabolism, and four derivatives were

identified with extended serum half-lives as compared to **PAC-1**.¹² In order to better understand the neurotoxicity of **PAC-1**, a series of derivatives was synthesized containing small modifications or deletions, in order to identify functional groups responsible for induction of neuroexcitation. In addition, an improved process-scale synthesis of **PAC-1** was developed. The improvements to the synthesis were general, and if an improved derivative is identified, the lessons learned from the **PAC-1** synthesis should be applicable to most other derivatives as well.

The most significant challenge to be overcome for the translation of **PAC-1** remains the neuroexcitation observed at elevated doses. The tolerability is greatly improved for many compounds that do not enter the brain, such as **S-PAC-1**, but a BBB-permeable compound will be necessary for treatment of tumors of the CNS, as well as the many cancer types for which metastases to the brain are common. The experiments described herein provide preliminary evidence that the ability of **PAC-1** to bind zinc is most likely not responsible for the observed neurotoxicity *in vivo*. Further experiments will be necessary to confirm that reduction in neurotoxicity in response to certain compounds, such as compounds **5.4** and **5.10**, is not due to reduced BBB permeability. With a greater understanding of the mechanism of **PAC-1**-induced neurotoxicity, it may be possible to design a potent, safe, BBB-permeable **PAC-1** derivative, which would represent a significant advance in the development of procaspase-activating anticancer compounds.

5.7. Materials and Methods

5.7.1. Chemical Information

General All reactions requiring anhydrous conditions were conducted under a positive atmosphere of nitrogen or argon in oven-dried glassware. Standard syringe techniques were used for anhydrous addition of liquids. Unless otherwise noted, all starting materials, solvents, and reagents were acquired from commercial suppliers and used without further purification. Flash chromatography was performed using 230-400 mesh silica gel.

Compound Analysis All NMR experiments were recorded in CDCl₃ (Sigma or Cambridge), (CD₃)₂CO (Sigma or Cambridge), or (CD₃)₂SO (Sigma or Cambridge) on a Varian Unity 500 MHz spectrometer with residual undeuterated solvent as the internal reference for ¹H-NMR (CDCl₃ – 7.26 ppm; (CD₃)₂CO – 2.04 ppm; (CD₃)₂SO – 2.48 ppm) and ¹³C-NMR (CDCl₃ –

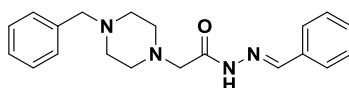
77.23 ppm; (CD₃)₂CO – 29.80 ppm; (CD₃)₂SO – 39.50 ppm). Chemical shift, δ (ppm); coupling constants, J (Hz); multiplicity (s = singlet, d = doublet, t = triplet, q = quartet, quint = quintet, sext = sextet, m = multiplet, br = broad); and integration are reported. High-resolution mass spectral data was recorded on a Micromass Q-ToF Ultima hybrid quadrupole/time-of-flight ESI mass spectrometer or a Micromass 70-VSE at the University of Illinois Mass Spectrometry Laboratory. Copies of NMR spectra for compounds not available in the literature are provided below.

General Procedure A: Alkylation of monoalkyl piperazines. A mixture of monoalkylated piperazine, alkyl halide, and base in acetone or THF was stirred at reflux overnight. The reaction mixture was filtered, and the solid was washed with acetone. The filtrate was concentrated and purified by silica gel column chromatography to yield pure dialkylated piperazine.

General Procedure B: Synthesis of hydrazides. A solution of the ester (1.0 equiv.) and hydrazine monohydrate (4.0 equiv.) in EtOH (0.5 M) was stirred at reflux overnight. The reaction mixture was cooled to room temperature and concentrated. The residue was partitioned between CH₂Cl₂ (20 mL)/1:1 brine:0.1 M KOH (20 mL). The layers were separated, and the aqueous layer was extracted with CH₂Cl₂ (2 x 20 mL). The combined organic layers were dried over MgSO₄, filtered, and concentrated to yield hydrazide, which was used without further purification.

General Procedure C: Synthesis of hydrazones. A solution of hydrazide (1.0 equiv.), aldehyde (1.0-2.0 equiv.), and 1.2 M HCl (0.070 equiv.) in EtOH (0.15 M) was stirred at reflux overnight. The reaction mixture was cooled to room temperature, concentrated, and purified by silica gel column chromatography to yield the hydrazone.

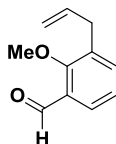
***N'*-benzylidene-2-(4-benzylpiperazin-1-yl)acetohydrazide (PAC-1a, 1.3)**



Synthesized according to General Procedure C: **1.6** (745 mg, 3.0 mmol, 1.0 equiv.), freshly distilled benzaldehyde (**5.1**, 0.31 mL, 3.0 mmol, 1.0 equiv.), 1.2 M HCl (0.18 mL, 0.21 mmol, 0.070 equiv.), EtOH (20 mL, 0.15 M). Purification by silica gel column chromatography (gradient, 0-20% MeOH/EtOAc) yielded **1.3** (868 mg, 85.9%) as an off-white solid. ¹H-NMR (500 MHz, CDCl₃) δ 10.08 (s, 1H), 8.20 (s, 1H), 7.77-7.74 (m, 2H), 7.41-7.38 (m, 3H), 7.34-7.29 (m, 4H), 7.29-7.24 (m, 1H), 3.55 (s, 2H), 3.19 (s, 2H), 2.63 (br s, 4H), 2.53 (br s, 4H). ¹³C-NMR

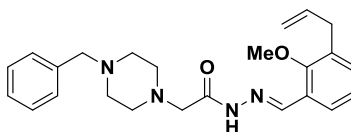
(125 MHz, CDCl₃) δ 166.5, 148.6, 138.0, 133.7, 130.7, 129.3, 128.8, 128.5, 127.9, 127.4, 63.1, 61.3, 53.9, 53.2. HRMS (ESI): 337.2014 (M+H)⁺; calcd. for C₂₀H₂₅N₄O: 337.2023.

3-allyl-2-methoxybenzaldehyde (**5.2**)



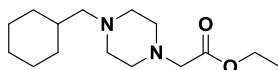
To a round-bottom flask were added **2.1** (487 mg, 3.0 mmol, 1.0 equiv.), K₂CO₃ (1.24 g, 9.0 mmol, 3.0 equiv.), and acetone (6 mL, 0.5 M). The mixture was stirred, and iodomethane (0.23 mL, 3.6 mmol, 1.2 equiv.) was added. The reaction mixture was stirred at rt overnight. The solid was filtered and washed with acetone, and the filtrate was concentrated. Purification by silica gel column chromatography (0-5% EtOAc/hexanes) yielded **5.3** (419 mg, 79.2%) as a pale yellow oil. ¹H-NMR (500 MHz, CDCl₃) δ 10.38 (s, 1H), 7.73 (dd, 1H, *J* = 2.0, 7.5 Hz), 7.47 (dd, 1H, *J* = 2.0, 7.5 Hz), 7.20 (t, 1H, *J* = 7.5 Hz), 5.98 (tdd, 1H, *J* = 6.5, 10.0, 16.5 Hz), 5.15-5.06 (m, 2H), 3.90 (s, 3H), 3.48 (d, 2H, *J* = 6.5 Hz). ¹³C-NMR (125 MHz, CDCl₃) δ 190.4, 161.6, 137.1, 136.6, 134.5, 129.6, 127.5, 124.8, 116.8, 64.5, 33.4. HRMS (ESI): 177.0919 (M+H)⁺; calcd. for C₁₁H₁₃O₂: 177.0916.

N'-(3-allyl-2-methoxybenzylidene)-2-(4-benzylpiperazin-1-yl)acetohydrazide (**1.11h**)



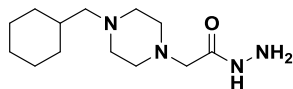
Synthesized according to General Procedure C: **1.6** (124 mg, 0.50 mmol, 1.0 equiv.), **5.2** (88 mg, 0.50 mmol, 1.0 equiv.), 1.2 M HCl (29 μ L, 0.035 mmol, 0.070 equiv.), EtOH (3 mL, 0.15 M). Purification by silica gel column chromatography (0-10% MeOH/EtOAc) yielded **1.11h** (165 mg, 81.0%) as an off-white solid. ¹H-NMR (500 MHz, CDCl₃) δ 10.12 (s, 1H), 8.44 (s, 1H), 7.95 (dd, 1H, *J* = 1.5, 8.0 Hz), 7.33-7.29 (m, 4H), 7.29-7.22 (m, 2H), 7.10 (t, 1H, *J* = 7.5 Hz), 5.98 (tdd, 1H, *J* = 6.5, 10.0, 16.5 Hz), 5.11-5.04 (m, 2H), 3.78 (s, 3H), 3.54 (s, 2H), 3.43 (d, 2H, *J* = 6.5 Hz), 3.19 (s, 2H), 2.63 (br s, 4H), 2.53 (br s, 4H). ¹³C-NMR (125 MHz, CDCl₃) δ 166.5, 157.8, 144.5, 138.0, 136.9, 133.3, 133.0, 129.2, 128.4, 127.3, 126.9, 125.8, 124.7, 116.3, 63.2, 63.0, 61.2, 53.8, 53.2, 33.7. HRMS (ESI): 403.2447 (M+H)⁺; calcd. for C₂₄H₃₁N₄O₂: 407.2442.

Ethyl 2-(4-(cyclohexylmethyl)piperazin-1-yl)acetate (**5.12a**)



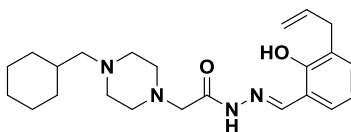
Synthesized according to General Procedure A: (bromomethyl)cyclohexane (**5.11**, 1.4 mL, 10.0 mmol, 1.0 equiv.), **2.8** (2.58 g, 15.0 mmol, 1.5 equiv.), K_2CO_3 (4.15 g, 30.0 mmol, 3.0 equiv.), acetone (20 mL, 0.5 M). The reaction mixture was stirred at reflux for four days. Purification by silica gel column chromatography (50-75% EtOAc/hexanes) gave **5.12a** (1.68 g, 62.5%) as a yellow oil. 1H -NMR (500 MHz, $CDCl_3$) δ 4.13 (q, 2H, $J = 7.0$ Hz), 3.14 (s, 2H), 2.53 (br s, 4H), 2.41 (br s, 4H), 2.07 (d, 2H, $J = 7.0$ Hz), 1.73-1.67 (m, 2H), 1.67-1.57 (m, 3H), 1.46-1.37 (m, 1H), 1.22 (t, 3H, $J = 7.0$ Hz), 1.18-1.05 (m, 3H), 0.84-0.76 (m, 2H). ^{13}C -NMR (125 MHz, $CDCl_3$) δ 170.4, 65.7, 60.6, 59.7, 53.5, 53.3, 35.1, 32.0, 26.9, 26.3, 14.4. HRMS (ESI): 269.2224 ($M+H$) $^+$; calcd. for $C_{15}H_{29}N_2O_2$: 269.2229.

2-(4-(cyclohexylmethyl)piperazin-1-yl)acetohydrazide (**5.14a**)



Synthesized according to General Procedure B: **5.12a** (1.68 g, 6.3 mmol, 1.0 equiv.), hydrazine monohydrate (1.3 mL, 25.2 mmol, 4.0 equiv.), EtOH (13 mL, 0.5 M). After extraction, **5.14a** (1.24 g, 77.4%) was isolated as a white solid, which was used without further purification. 1H -NMR (500 MHz, $CDCl_3$) δ 8.15 (br s, 1H), 3.83 (br s, 2H), 3.02 (s, 2H), 2.48 (br s, 4H), 2.35 (br s, 4H), 2.06 (d, 2H, $J = 7.5$ Hz), 1.73-1.57 (m, 5H), 1.45-1.37 (m, 1H), 1.22-1.06 (m, 3H), 0.85-0.75 (m, 2H). ^{13}C -NMR (125 MHz, $CDCl_3$) δ 170.7, 65.6, 60.8, 53.9, 53.8, 35.1, 32.0, 26.9, 26.2. HRMS (ESI): 255.2186 ($M+H$) $^+$; calcd. for $C_{13}H_{27}N_4O$: 255.2179

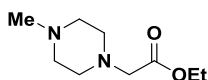
N'-(3-allyl-2-hydroxybenzylidene)-2-(4-(cyclohexylmethyl)piperazin-1-yl)acetohydrazide (**5.3**)



Synthesized according to General Procedure C: **5.14a** (127 mg, 0.50 mmol, 1.0 equiv.), **2.1** (81 mg, 0.50 mmol, 1.0 equiv.), 1.2 M HCl (29 μ L, 0.035 mmol, 0.070 equiv.), EtOH (3 mL, 0.15 M). Purification by silica gel column chromatography (gradient, 75-100% EtOAc/hexanes, then 5-10% MeOH/EtOAc) yielded **5.3** (165 mg, 82.8%) as a light yellow solid. 1H -NMR (500 MHz, $CDCl_3$) δ 11.12 (s, 1H), 10.13 (br s, 1H), 8.32 (s, 1H), 7.15 (d, 1H, $J = 7.0$ Hz), 7.04 (d, 1H, $J =$

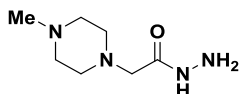
7.0 Hz), 6.81 (t, 1H, $J = 7.5$ Hz), 6.01 (tdd, 1H, $J = 6.5, 10.0, 16.5$ Hz), 5.09-5.01 (m, 2H), 3.43 (d, 2H, $J = 6.5$ Hz), 3.16 (s, 2H), 2.59 (br s, 1H), 2.44 (br s, 1H), 2.12 (d, 2H, $J = 7.5$ Hz), 1.77-1.60 (m, 5H), 1.49-1.40 (m, 1H), 1.26-1.08 (m, 3H), 0.89-0.78 (m, 2H). $^{13}\text{C-NMR}$ (125 MHz, CDCl_3) δ 166.1, 156.4, 151.0, 136.6, 132.3, 129.2, 128.2, 119.1, 117.0, 115.7, 65.6, 61.1, 53.8, 53.7, 35.1, 33.9, 31.9, 26.9, 26.2. HRMS (ESI): 399.2754 ($\text{M}+\text{H}$) $^+$; calcd. for $\text{C}_{23}\text{H}_{35}\text{N}_4\text{O}_2$: 399.2755.

Ethyl 2-(4-methylpiperazin-1-yl)acetate (**5.12b**)



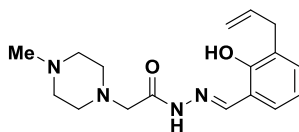
Synthesized according to general procedure A: 1-methylpiperazine (**5.13**, 1.1 mL, 10.0 mmol, 1.0 equiv.), ethyl chloroacetate (**2.3**, 1.6 mL, 15.0 mmol, 1.5 equiv.), NaHCO_3 (2.52 g, 30.0 mmol, 3.0 equiv.), acetone (20 mL, 0.5 M). The reaction mixture was stirred at reflux overnight. Purification by silica gel column chromatography (gradient, 0-20% MeOH/EtOAc) gave **5.12b** (993 mg, 53.4%) as a yellow oil. $^1\text{H-NMR}$ (500 MHz, CDCl_3) δ 4.05 (q, 2H, $J = 7.0$ Hz), 3.07 (s, 2H), 2.48 (br s, 4H), 2.37 (br s, 4H), 2.16 (s, 3H), 1.13 (t, 3H, $J = 7.0$ Hz). $^{13}\text{C-NMR}$ (125 MHz, CDCl_3) δ 171.1, 61.5, 60.4, 55.8, 53.9, 47.0, 15.2. HRMS (ESI): 187.1443 ($\text{M}+\text{H}$) $^+$; calcd. for $\text{C}_9\text{H}_{19}\text{N}_2\text{O}_2$: 187.1441.

2-(4-methylpiperazin-1-yl)acetohydrazide (**5.14b**)



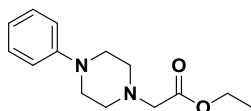
A solution of **5.12b** (990 mg, 5.3 mmol, 1.0 equiv.), hydrazine monohydrate (1.6 mL, 31.8 mmol, 6.0 equiv.), and EtOH (10 mL, 0.5 M) was stirred at reflux overnight. The reaction mixture was cooled to room temperature and concentrated. The residue was dissolved in CHCl_3 (20 mL), dried over MgSO_4 , filtered, concentrated, and dried under high vacuum to afford **5.14b** (471 mg, 51.5%) as a white solid, which was used without further purification. $^1\text{H-NMR}$ (500 MHz, CDCl_3) δ 8.10 (br s, 1H), 3.78 (br s, 2H), 2.90 (s, 2H), 2.38 (br s, 4H), 2.27 (br s, 4H), 2.11 (s, 3H). $^{13}\text{C-NMR}$ (125 MHz, CDCl_3) δ 170.2, 60.4, 54.9, 53.4, 45.9. HRMS (ESI): 173.1405 ($\text{M}+\text{H}$) $^+$; calcd. for $\text{C}_7\text{H}_{17}\text{N}_4\text{O}$: 173.1397.

***N'*-(3-allyl-2-hydroxybenzylidene)-2-(4-methylpiperazin-1-yl)acetohydrazide (5.4)**



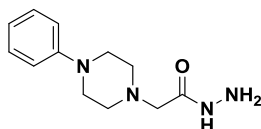
Synthesized according to General Procedure C: **5.14b** (172 mg, 1.0 mmol, 1.0 equiv.), **2.1** (162 mg, 1.0 mmol, 1.0 equiv.), 1.2 M HCl (58 μ L, 0.070 mmol, 0.070 equiv.), EtOH (7 mL, 0.15 M). Purification by silica gel column chromatography (gradient, 0-60% MeOH/EtOAc) yielded **5.4** (277 mg, 87.6%) as a light yellow solid. $^1\text{H-NMR}$ (500 MHz, CDCl_3) δ 11.33 (br s, 1H), 10.23 (br s, 1H), 8.18 (s, 1H), 7.05 (d, 1H, $J = 7.5$ Hz), 6.91 (d, 2H, $J = 7.0$ Hz), 6.69 (t, 1H, $J = 7.5$ Hz), 5.91 (tdd, 1H, $J = 6.5, 10.0, 16.5$ Hz), 5.03-4.91 (m, 2H), 3.32 (d, 2H, $J = 6.5$ Hz), 2.52 (br s, 4H), 2.38 (br s, 4H), 2.18 (s, 3H). $^{13}\text{C-NMR}$ (125 MHz, CDCl_3) δ 165.8, 156.0, 150.7, 136.3, 132.0, 129.0, 127.8, 118.9, 116.7, 115.5, 60.7, 54.8, 53.4, 45.8, 33.6. HRMS (ESI): 317.1981 ($\text{M}+\text{H}$) $^+$; calcd. for $\text{C}_{17}\text{H}_{25}\text{N}_4\text{O}_2$: 317.1972.

Ethyl 2-(4-phenylpiperazin-1-yl)acetate (3.6{30})



Synthesized according to general procedure A: 1-phenylpiperazine (**3.5{30}**, 1.62 g, 10.0 mmol, 1.0 equiv.), ethyl chloroacetate (**2.3**, 1.6 mL, 15.0 mmol, 1.5 equiv.), NaHCO_3 (2.52 g, 30.0 mmol, 3.0 equiv.), acetone (20 mL, 0.5 M). The reaction mixture was stirred at reflux overnight. Purification by silica gel column chromatography (25-50% EtOAc/hexanes) gave **3.6{30}** (2.38 g, 96.1%) as a yellow oil. $^1\text{H-NMR}$ (500 MHz, CDCl_3) δ 7.26 (dd, 2H, $J = 7.5, 9.0$ Hz), 6.93 (d, 2H, $J = 9.0$ Hz), 6.85 (t, 1H, $J = 7.5$ Hz), 4.20 (q, 2H, $J = 7.0$ Hz), 3.27 (s, 2H), 3.25 (t, 4H, $J = 5.0$ Hz), 2.74 (t, 2H, $J = 5.5$ Hz), 1.28 (t, 3H, $J = 7.0$ Hz). $^{13}\text{C-NMR}$ (125 MHz, CDCl_3) δ 170.3, 151.3, 129.2, 119.9, 116.2, 60.8, 59.6, 53.2, 49.1, 14.4. HRMS (ESI): 249.1605 ($\text{M}+\text{H}$) $^+$; calcd. for $\text{C}_{14}\text{H}_{21}\text{N}_2\text{O}_2$: 249.1598.

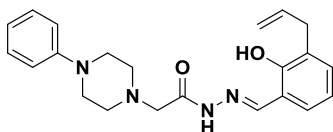
2-(4-phenylpiperazin-1-yl)acetohydrazide (3.1{30})



Synthesized according to General Procedure B: **3.6{30}** (2.38 g, 9.6 mmol, 1.0 equiv.), hydrazine monohydrate (1.9 mL, 38.4 mmol, 4.0 equiv.), EtOH (20 mL, 0.5 M). After extraction,

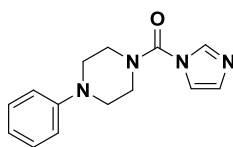
3.1{30} (1.72 g, 76.3%) was isolated as a white solid, which was used without further purification. ¹H-NMR (500 MHz, CDCl₃) δ 8.21 (br s, 1H), 7.28 (dd, 2H, *J* = 7.5, 8.5 Hz), 6.92 (d, 2H, *J* = 8.5 Hz), 6.88 (t, 1H, *J* = 7.5 Hz), 3.92 (br s, 2H), 3.19 (t, 4H, *J* = 5.0 Hz), 3.14 (s, 2H), 2.68 (t, 2H, *J* = 5.0 Hz). ¹³C-NMR (125 MHz, CDCl₃) δ 170.3, 151.0, 129.2, 120.1, 116.2, 60.7, 53.7, 49.3. HRMS (ESI): 235.1558 (M+H)⁺; calcd. for C₁₂H₁₉N₄O: 235.1553.

***N'*-(3-allyl-2-hydroxybenzylidene)-2-(4-phenylpiperazin-1-yl)acetohydrazide (5.5)**



Synthesized according to General Procedure C: **3.1{30}** (117 mg, 0.50 mmol, 1.0 equiv.), **2.1** (81 mg, 0.50 mmol, 1.0 equiv.), 1.2 M HCl (29 μL, 0.035 mmol, 0.070 equiv.), EtOH (3 mL, 0.15 M). Purification by silica gel column chromatography (gradient, 25-100% EtOAc/hexanes) yielded **5.5** (133 mg, 70.4%) as a yellow solid. ¹H-NMR (500 MHz, CDCl₃) δ 11.34 (s, 1H), 10.14 (br s, 1H), 8.34 (s, 1H), 7.30 (t, 2H, *J* = 7.5 Hz), 7.20 (d, 1H, *J* = 7.0 Hz), 7.06 (d, 1H, *J* = 7.0 Hz), 6.95 (d, 2H, *J* = 8.0 Hz), 6.91 (t, 1H, *J* = 7.0 Hz), 6.85 (t, 1H, *J* = 7.5 Hz), 6.04 (tdd, 1H, *J* = 6.5, 10.0, 17.0 Hz), 5.13-5.04 (m, 2H), 3.46 (d, 2H, *J* = 6.5 Hz), 3.31-3.23 (m, 6H), 2.76 (br s, 4H). ¹³C-NMR (125 MHz, CDCl₃) δ 165.8, 156.4, 151.3, 151.0, 136.6, 132.4, 129.3 (2 signals), 128.3, 120.2, 119.2, 116.9, 116.3, 115.8, 61.1, 53.8, 49.3, 34.0. HRMS (ESI): 379.2131 (M+H)⁺; calcd. for C₂₂H₂₇N₄O₂: 379.2129.

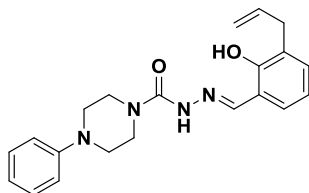
(1*H*-imidazol-1-yl)(4-phenylpiperazin-1-yl)methanone (5.16)



To a round-bottom flask were added 1-phenylpiperazine (**3.5{30}**), 406 mg, 2.5 mmol, 1.0 equiv.), CH₂Cl₂ (25 mL, 0.1 M), and 1,1'-carbonyldiimidazole (**5.15**, 454 mg, 2.8 mmol, 1.1 equiv.). The reaction mixture was stirred at room temperature overnight. The reaction mixture was diluted with H₂O (25 mL). The layers were separated, and the aqueous layer was extracted with CH₂Cl₂ (2 x 25 mL). The combined organic layers were washed with brine (25 mL), dried over MgSO₄, filtered, and concentrated. Purification by silica gel column chromatography (gradient, 50-100% EtOAc/hexanes, then 5% MeOH/EtOAc) yielded **5.16** (578 mg, 90.2%) as a white solid. ¹H-NMR (500 MHz, CDCl₃) δ 7.89 (s, 1H), 7.28 (t, 2H, *J* = 8.0 Hz), 7.22 (s, 1H),

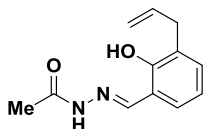
7.10 (s, 1H), 6.94-6.90 (m, 3H), 3.75 (t, 4H, $J = 5.0$ Hz), 3.22 (t, 4H, $J = 5.0$ Hz). ^{13}C -NMR (125 MHz, CDCl_3) δ 150.9, 150.6, 137.0, 130.0, 129.4, 121.1, 118.0, 116.9, 49.5, 46.4. HRMS (ESI): 257.1402 ($\text{M}+\text{H}$) $^+$; calcd. for $\text{C}_{14}\text{H}_{17}\text{N}_4\text{O}$: 257.1397.

***N'*-(3-allyl-2-hydroxybenzylidene)-4-phenylpiperazine-1-carbohydrazide (5.6)**



To a round-bottom flask were added **5.16** (570 mg, 2.2 mmol, 1.0 equiv.), MeCN (11 mL, 0.2 M), and iodomethane (0.55 mL, 8.8 mmol, 4.0 equiv.). The reaction mixture was stirred at rt overnight. The reaction mixture was then concentrated. The crude residue was resuspended in MeCN (5 mL, 0.5 M), and hydrazine monohydrate (1.1 mL, 22.0 mmol, 10.0 equiv.) was added. The reaction mixture was stirred at rt overnight. The reaction mixture was diluted with 1:1 brine:1M NaOH (20 mL) and extracted with CH_2Cl_2 (3 x 20 mL). The combined organic layers were dried over MgSO_4 , filtered, concentrated, and dried under high vacuum. The crude material was dissolved in EtOH (15 mL, 0.15 M), and **2.1** (357 mg, 2.2 mmol, 1.0 equiv.) was added. The reaction mixture was stirred at reflux overnight. The reaction mixture was cooled to rt and concentrated. Purification by silica gel column chromatography (25-50% EtOAc/hexanes) yielded **5.6** (479 mg, 59.8%) as a light brown solid. ^1H -NMR (500 MHz, CDCl_3) δ 11.58 (s, 1H), 9.79 (s, 1H), 8.26 (s, 1H), 7.22 (t, 2H, $J = 7.5$ Hz), 7.11 (d, 1H, $J = 7.5$ Hz), 7.01 (d, 1H, $J = 6.5$ Hz), 6.88 (t, 1H, $J = 7.5$ Hz), 6.79 (t, 1H, $J = 7.0$ Hz), 6.79 (d, 2H, $J = 8.0$ Hz), 5.96 (tdd, 1H, $J = 6.5, 10.0, 17.0$ Hz), 5.07-4.97 (m, 2H), 3.72 (s, 4H), 3.40 (d, 2H, $J = 6.5$ Hz), 3.15 (s, 4H). ^{13}C -NMR (125 MHz, CDCl_3) δ 155.9, 155.1, 150.9, 147.9, 136.6, 131.6, 129.3, 128.7, 128.1, 120.5, 119.2, 117.7, 116.6, 115.9, 49.3, 44.5, 33.9. HRMS (ESI): 365.1972 ($\text{M}+\text{H}$) $^+$; calcd. for $\text{C}_{21}\text{H}_{25}\text{N}_4\text{O}_2$: 365.1972.

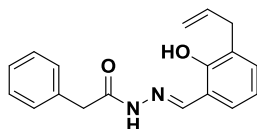
***N'*-(3-allyl-2-hydroxybenzylidene)acetohydrazide (5.7)**



Synthesized according to General Procedure C: acetohydrazide (**5.14c**, 146 mg, 2.0 mmol, 1.0 equiv.), **2.1** (324 mg, 2.0 mmol, 1.0 equiv.), 1.2 M HCl (0.12 mL, 0.14 mmol, 0.070 equiv.), EtOH (13 mL, 0.15 M). Purification by silica gel column chromatography (gradient, 25-75%

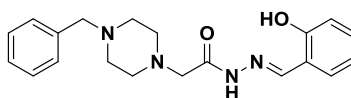
EtOAc/hexanes) yielded **5.7** (66 mg, 15.1%) as a white solid. $^1\text{H-NMR}$ (500 MHz, CDCl_3) δ 10.54 (s, 1H), 10.50 (br s, 1H), 8.01 (s, 1H), 7.20 (d, 1H, $J = 7.0$ Hz), 7.14 (dd, 1H, $J = 1.0, 7.5$ Hz), 6.89 (t, 1H, $J = 7.5$ Hz), 6.04 (tdd, 1H, $J = 6.5, 9.5, 16.0$ Hz), 5.12-5.05 (m, 2H), 3.46 (d, 2H, $J = 6.5$ Hz), 2.37 (s, 3H). $^{13}\text{C-NMR}$ (125 MHz, CDCl_3) δ 173.2, 155.7, 148.0, 136.5, 132.6, 129.6, 128.0, 119.8, 117.1, 116.0, 33.9, 20.8. HRMS (ESI): 219.1131 ($\text{M}+\text{H}$) $^+$; calcd. for $\text{C}_{12}\text{H}_{15}\text{N}_2\text{O}_2$: 219.1128.

***N'*-(3-allyl-2-hydroxybenzylidene)-2-phenylacetohydrazide (5.8)**



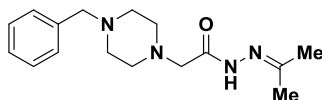
Synthesized according to General Procedure C: phenylacetohydrazide (**5.14d** 150 mg, 1.0 mmol, 1.0 equiv.), **2.1** (162 mg, 1.0 mmol, 1.0 equiv.), 1.2 M HCl (58 μL , 0.070 mmol, 0.070 equiv.), EtOH (7 mL, 0.15 M). Purification by silica gel column chromatography (25-50% EtOAc/hexanes) yielded **5.8** (203 mg, 68.9%) as a light brown solid. $^1\text{H-NMR}$ (500 MHz, $(\text{CD}_3)_2\text{SO}$) δ 11.97 (br s, 1H), 11.81 (s, 1H), 8.33 (s, 1H), 7.32-7.21 (m, 6H), 7.14 (d, 1H, $J = 7.0$ Hz), 6.85 (t, 1H, $J = 7.5$ Hz), 5.94 (tdd, 1H, $J = 6.5, 10.0, 17.0$ Hz), 5.06-4.97 (m, 2H), 3.57 (s, 2H), 3.33 (d, 2H, $J = 6.5$ Hz). $^{13}\text{C-NMR}$ (125 MHz, $(\text{CD}_3)_2\text{SO}$) δ 166.4, 155.4, 148.9, 136.5, 135.3, 131.5, 129.14, 129.09, 128.4, 127.0, 126.7, 119.0, 117.3, 115.7, 40.8, 33.3. HRMS (ESI): 295.1447 ($\text{M}+\text{H}$) $^+$; calcd. for $\text{C}_{18}\text{H}_{19}\text{N}_2\text{O}_2$: 295.1441.

2-(4-benzylpiperazin-1-yl)-*N'*-(2-hydroxybenzylidene)acetohydrazide (1.2)



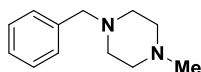
Synthesized according to General Procedure C: **1.6** (124 mg, 0.50 mmol, 1.0 equiv.), salicylaldehyde (**2.4**, 0.11 mL, 1.0 mmol, 2.0 equiv.), 1.2 M HCl (29 μL , 0.035 mmol, 0.070 equiv.), EtOH (3 mL, 0.15 M). Purification by silica gel column chromatography (gradient, 0-15% MeOH/EtOAc) yielded **1.2** (146 mg, 83.1%) as a white solid. $^1\text{H-NMR}$ (500 MHz, CDCl_3) δ 11.06 (br s, 1H), 10.13 (br s, 1H), 8.38 (s, 1H), 7.34-7.25 (m, 6H), 7.19 (d, 1H, $J = 7.5$ Hz), 6.98 (d, 2H, $J = 8.5$ Hz), 6.88 (t, 1H, $J = 7.5$ Hz), 6.85 (t, 1H, $J = 7.5$ Hz), 3.54 (s, 2H), 3.18 (s, 2H), 2.62 (br s, 4H), 2.53 (br s, 4H). $^{13}\text{C-NMR}$ (125 MHz, CDCl_3) δ 166.1, 158.6, 151.1, 137.8, 131.9, 131.0, 129.2, 128.4, 127.3, 119.4, 117.5, 117.2, 62.9, 61.0, 53.8, 53.0. HRMS (ESI): 353.1982 ($\text{M}+\text{H}$) $^+$; calcd. for $\text{C}_{20}\text{H}_{25}\text{N}_4\text{O}_2$: 353.1972.

2-(4-benzylpiperazin-1-yl)-N'-(propan-2-ylidene)acetohydrazide (**5.10**)



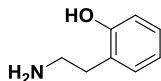
Synthesized according to General Procedure C, but at room temperature: **1.6** (248 mg, 1.0 mmol, 1.0 equiv.), acetone (**5.17**, 0.15 mL, 2.0 mmol, 2.0 equiv.), 1.2 M HCl (58 μ L, 0.070 mmol, 0.070 equiv.), EtOH (7 mL, 0.15 M). Purification by silica gel column chromatography (gradient, 0-20% MeOH/EtOAc) yielded **5.10** (224 mg, 77.7%) as a yellow oil. $^1\text{H-NMR}$ (500 MHz, CDCl_3) δ 9.86 (s, 1H), 7.23-7.19 (m, 4H), 7.18-7.13 (m, 1H), 3.42 (s, 2H), 3.06 (s, 2H), 2.51 (br s, 4H), 2.39 (br s, 2H), 2.01 (s, 3H), 1.80 (s, 3H). $^{13}\text{C-NMR}$ (125 MHz, CDCl_3) δ 165.6, 154.4, 137.7, 128.8, 128.1, 127.0, 62.6, 60.6, 53.3(2), 53.2(5), 25.2, 16.4. HRMS (ESI): 289.2028 ($\text{M}+\text{H}$) $^+$; calcd. for $\text{C}_{16}\text{H}_{25}\text{N}_4\text{O}$: 289.2023.

1-benzyl-4-methylpiperazine (**5.9**)



Synthesized according to General Procedure A: benzyl chloride (1.2 mL, 10.0 mmol, 1.0 equiv.), 1-methylpiperazine (1.7 mL, 15.0 mmol, 1.5 equiv.), K_2CO_3 (4.15 g, 30.0 mmol, 3.0 equiv.), THF (20 mL, 0.5 M). The reaction mixture was stirred at reflux overnight. Purification by silica gel column chromatography (gradient, 50-100% EtOAc/hexanes, then 10-20% MeOH/EtOAc) gave **5.9** (1.57 g, 82.8%) as a yellow oil. $^1\text{H-NMR}$ (500 MHz, CDCl_3) δ 7.34-7.28 (m, 4H), 7.26-7.22 (m, 1H), 3.51 (s, 2H), 2.46 (br s, 8H), 2.29 (s, 3H). $^{13}\text{C-NMR}$ (125 MHz, CDCl_3) δ 138.2, 129.2, 128.2, 127.0, 63.1, 55.2, 53.2, 46.1. HRMS (ESI): 191.1543 ($\text{M}+\text{H}$) $^+$; calcd. for $\text{C}_{12}\text{H}_{19}\text{N}_2$: 191.1543.

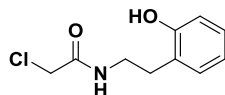
2-(2-aminoethyl)-phenol (**5.19**)



To an oven-dried round-bottom flask were added lithium aluminum hydride (569 mg, 15.0 mmol, 3.0 equiv.) and anhydrous THF (5 mL). The mixture was stirred at 0°C under N_2 , and a solution of 2-hydroxy- β -nitrostyrene (**5.18**, 826 mg, 5.0 mmol, 1.0 equiv.) in anhydrous THF (10 mL) was added dropwise via addition funnel. The reaction mixture was stirred at rt for 2h. The reaction mixture was cooled to 0°C and quenched by the dropwise addition of H_2O (20 mL). The solid was filtered and washed with THF. The filtrate was acidified with 1 M HCl (20 mL) and

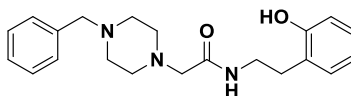
extracted with EtOAc (2 x 20 mL). The combined organic layers were extracted with 1 M HCl (2 x 20 mL). The combined aqueous layers were treated with L-tartaric acid (3.0 g, 20.0 mmol, 4.0 equiv.), basified with 28% aqueous NH₃ (20 mL), and extracted with CHCl₃ (3 x 20 mL). The combined organic layers from the CHCl₃ extraction were washed with brine (20 mL), dried over MgSO₄, filtered, and concentrated. Purification by silica gel column chromatography (gradient, 0-60% MeOH/EtOAc) yielded **5.19** (165 mg, 24.1%) as a light yellow solid. ¹H-NMR (500 MHz, CDCl₃) δ 7.13 (dt, 1H, *J* = 1.5, 7.5 Hz), 7.01 (dd, 1H, *J* = 1.5, 7.5 Hz), 6.91 (dd, 1H, *J* = 1.0, 8.0 Hz), 6.77 (dt, 1H, *J* = 1.5, 7.5 Hz), 5.25 (br s, 3H), 3.05 (t, 2H, *J* = 5.0 Hz), 2.78 (t, 2H, *J* = 5.0 Hz). ¹³C-NMR (125 MHz, CDCl₃) δ 156.9, 131.1, 128.3, 128.1, 119.3, 117.8, 42.4, 36.5.

2-chloro-*N*-(2-hydroxyphenethyl)acetamide (**5.21**)



To a round-bottom flask were added **5.19** (165 mg, 1.2 mmol, 1.0 equiv.), CH₂Cl₂ (2 mL), sat. Na₂CO₃ (2 mL), and chloroacetyl chloride (**5.20**, 0.16 mL, 2.4 mmol, 2.0 equiv.). The reaction mixture was stirred vigorously at rt overnight. The reaction mixture was diluted with 1 M HCl (10 mL) and extracted with CH₂Cl₂ (3 x 10 mL). The combined organic layers were washed with brine (10 mL), dried over MgSO₄, filtered, and concentrated. Purification by silica gel column chromatography (gradient, 10-40% EtOAc/hexanes) yielded **5.21** (100 mg, 39.1%) as a white solid. ¹H-NMR (500 MHz, (CD₃)₂CO) δ 8.50 (s, 1H), 7.67 (br s, 1H), 7.09 (d, 1H, *J* = 7.5 Hz), 7.04 (t, 1H, *J* = 7.5 Hz), 6.85 (d, 1H, *J* = 8.0 Hz), 6.75 (t, 1H, *J* = 7.5 Hz), 4.06 (s, 2H), 3.47 (q, 2H, *J* = 6.5 Hz), 2.84 (t, 2H, *J* = 7.0 Hz). ¹³C-NMR (125 MHz, (CD₃)₂CO) δ 166.9, 156.1, 131.3, 128.4, 126.2, 120.4, 115.9, 43.2, 40.8, 30.6. HRMS (ESI): 214.0629 (M+H)⁺; calcd. for C₁₀H₁₃NO₂: 214.0629.

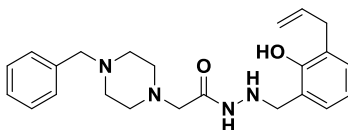
2-(4-benzylpiperazin-1-yl)-*N*-(2-hydroxyphenethyl)acetamide (**1.17b**)



Synthesized according to General Procedure A: **1.10** (166 mg, 0.94 mmol, 2.0 equiv.), **5.21** (100 mg, 0.47 mmol, 1.0 equiv.), K₂CO₃ (130 mg, 0.94 mmol, 2.0 equiv.), THF (2 mL, 0.25 M). Purification by silica gel column chromatography (gradient, 0-10% MeOH/EtOAc) gave **1.17b** (143 mg, 86.0%) as a white solid. ¹H-NMR (500 MHz, (CD₃)₂CO) δ 8.83 (br s, 1H), 7.51 (t, 1H, *J* = 5.5 Hz), 7.34-7.31 (m, 4H), 7.29-7.26 (m, 1H), 7.11-7.06 (m, 2H, *J* = 7.5 Hz), 6.84 (d, 1H, *J*

= 7.5 Hz), 6.79 (t, 1H, $J = 7.5$ Hz), 3.59 (q, 2H, $J = 7.0$ Hz), 3.53 (s, 2H), 3.01 (s, 2H), 2.89 (t, 2H, $J = 7.0$ Hz), 2.49 (br s, 4H), 2.44 (br s, 4H). ^{13}C -NMR (125 MHz, $(\text{CD}_3)_2\text{CO}$) δ 171.4, 155.4, 137.5, 130.7, 129.4, 128.4, 128.0, 127.3, 125.1, 119.7, 115.8, 62.9, 61.3, 53.3, 52.9, 39.2, 30.5. HRMS (ESI): 354.2173 ($\text{M}+\text{H}$) $^+$; calcd. for $\text{C}_{21}\text{H}_{28}\text{N}_3\text{O}_2$: 354.2176.

***N'*-(3-allyl-2-hydroxybenzyl)-2-(4-benzylpiperazin-1-yl)acetohydrazide (1.19)**



To a round-bottom flask were added **PAC-1** (196 mg, 0.50 mmol, 1.0 equiv.) and MeOH (2.5 mL, 0.2 M). The solution was stirred at 0°C, and NaBH_4 (95 mg, 2.5 mmol, 5.0 equiv.) was added. The reaction mixture was stirred while allowing to gradually warm to rt. After 22 hours, an additional portion of NaBH_4 (95 mg, 2.5 mmol, 5.0 equiv.) was added, and the solution was stirred at rt overnight. The reaction mixture was diluted with H_2O (10 mL) and extracted with EtOAc (3 x 10 mL). The combined organic layers were washed with brine (10 mL), dried over MgSO_4 , filtered, and concentrated to yield **1.19** (159 mg, 80.9%) as a light yellow solid. ^1H -NMR (500 MHz, CDCl_3) δ 9.31 (br s, 1H), 8.50 (d, 1H, $J = 4.5$ Hz), 7.34-7.25 (m, 5H), 7.10 (dd, 1H, $J = 2.0, 7.5$ Hz), 6.87 (dd, 1H, $J = 2.0, 7.5$ Hz), 6.75 (t, 1H, $J = 7.5$ Hz), 6.06 (tdd, 1H, $J = 6.5, 10.0, 16.5$ Hz), 5.14-5.07 (m, 2H), 5.04 (br s, 1H), 4.17 (s, 2H), 3.47-3.45 (m, 4H), 3.02 (s, 2H), 2.41 (br s, 4H), 2.32 (br s, 2H). ^{13}C -NMR (125 MHz, CDCl_3) δ 170.0, 154.7, 137.8, 137.1, 130.0, 129.2, 128.3, 128.0, 127.6, 127.2, 120.4, 119.6, 115.5, 62.9, 60.5, 54.3, 53.5, 52.9, 34.1. HRMS (ESI): 395.2428 ($\text{M}+\text{H}$) $^+$; calcd. for $\text{C}_{23}\text{H}_{31}\text{N}_4\text{O}_2$: 395.2442.

5.7.2. Biological Evaluation

Materials All reagents were obtained from Fisher unless otherwise indicated. All buffers were made with MilliQ purified water. Annexin V Binding Buffer contains 10 mM HEPES (pH 7.4), 140 mM NaCl, 2.5 mM CaCl_2 .

Cell Culture U-937 cells were obtained from the American Type Culture Collection. All cultures were maintained at low passage number in RPMI 1640 (U-937) or DMEM (D54) supplemented with 10% fetal bovine serum and 1% penicillin-streptomycin and grown at 37°C and 5% CO_2 .

72hr IC₅₀ Cell Death Assay – U-937 cells To each inner well of a 96-well plate was added 49 μL of RPMI 1640 complete growth media. To each inner well was added 1 μL of compound stock solutions in DMSO at nine concentrations such that the cells were treated with half-log concentrations between 0.01 μM and 100 μM compound. 50 μL of a suspension of cells at 300,000 cells/mL were plated into the wells, for a final density of 15,000 cells per well. Each concentration was tested in triplicate per plate. In each plate 3 wells received 1 μL of a positive death control and 3 wells received 1 μL DMSO as a live cell vehicle control. The outer wells were filled with sterile PBS pH 7.4 (200 μL), and the plates were then incubated at 37°C with 5% CO₂ for 72 hours. After the 72 hour incubation period, the plates were analyzed using a Sulforhodamine B assay.¹⁸ Specifically, to each well of the plate 25 μL of a 50% (w/v) solution of trichloroacetic acid in H₂O was added and the plates were incubated for 4 hours at 4°C. The plates were then washed gently with H₂O five times. The plates were allowed to air dry after which 100 μL of a 0.057% (w/v) Sulforhodamine B in a 1% (v/v) acetic acid solution was added to each well for 30 minutes at room temperature. The plates were gently washed 5 times with 1% (v/v) acetic acid and air dried. 200 μL of 10 mM Tris base (pH 10.4) was added to each well and the plates were placed on a shaker for thirty minutes. The level of SRB was quantified by absorbance at 510 nm on a SpectraMax Plus 384 Microplate Reader (Molecular Devices). The percent cell death was calculated and normalized to the positive control (100% cell death) and the negative control (0% cell death). The percent cell death was averaged for each compound concentration and plotted as a function of compound concentration. The data were fit to a logistical dose response curve using OriginPro 9.1, and the IC₅₀ value was calculated. The experiment was repeated three times and the average of the calculated IC₅₀ values was reported. The standard error of the mean (s.e.m.) was determined and reported for the triplicate experiments.

72hr IC₅₀ Cell Death Assay – D54 cells To each inner well of a 96-well plate was added 50 μL of a suspension of cells in DMEM complete growth media at 50,000 cells/mL, for a final density of 2500 cells/well. Outer wells were filled with sterile PBS pH 7.4 (200 μL). The plates were incubated at 37°C with 5% CO₂ for 2-3 hours to allow cells to adhere. Compound solutions were prepared in 2% DMSO/DMEM complete growth media at 2x final concentration, and solutions were added to the plates (1% DMSO final concentration). Cells were treated at nine

concentrations in half-log increments between 0.01 μM and 100 μM compound. Each concentration was tested in triplicate per plate. In each plate 3 wells received 1 μL of a positive death control and 3 wells received 1 μL DMSO as a live cell vehicle control. The plates were then incubated at 37°C with 5% CO_2 for 72 hours. After the 72 hour incubation period, the plates were analyzed using a Sulforhodamine B assay.¹⁸ Specifically, to each well of the plate 100 μL of a 10% (w/v) solution of trichloroacetic acid in H_2O was added and the plates were incubated for 4 hours at 4°C. The plates were then washed gently with H_2O five times. The plates were allowed to air dry after which 100 μL of a 0.057% (w/v) Sulforhodamine B in a 1% (v/v) acetic acid solution was added to each well for 30 minutes at room temperature. The plates were gently washed 5 times with 1% (v/v) acetic acid and air dried. 200 μL of 10 mM Tris base (pH 10.4) was added to each well and the plates were placed on a shaker for thirty minutes. The level of SRB was quantified by absorbance at 510 nm on a SpectraMax Plus 384 Microplate Reader (Molecular Devices). The percent cell death was calculated and normalized to the positive control (100% cell death) and the negative control (0% cell death). The percent cell death was averaged for each compound concentration and plotted as a function of compound concentration. The data were fit to a logistical dose response curve using OriginPro 9.1, and the IC_{50} value was calculated. The experiment was repeated three times and the average of the calculated IC_{50} values was reported. The standard error of the mean (s.e.m.) was determined and reported for the triplicate experiments.

Induction of Apoptosis by Hit Compounds To each well of a 12-well plate for compound treatment was added 1 mL of a suspension of D54 cells in DMEM complete growth media at 70,000 cells/mL. The cells were incubated at 37°C with 5% CO_2 for 2-3 hours to allow cells to adhere. To each well was then added 10 μL of 3 mM DMSO solutions to achieve a final compound concentration of 30 μM . 10 μL of DMSO was added to one well as a live cell vehicle control. Wells not containing compounds were filled with 1 mL sterile PBS pH 7.4. The cells were incubated at 37 °C with 5% CO_2 for 24 hours. The media was transferred to flow tubes. Sterile PBS pH 7.4 (0.5 mL) was then added to the wells to wash and transferred to flow tubes, and the remaining cells were harvested with trypsin (0.5 mL, 1-2 min) and transferred to flow tubes. The cells were centrifuged (1000 x g for 3 min) and resuspended in 450 μL Annexin V Binding Buffer containing 3 μL of FITC-conjugated Annexin V stain (Southern Biotech) and

0.25 μL of a 1 mg/mL solution of propidium iodide (Sigma) to a final concentration of 0.56 $\mu\text{g/mL}$. Samples were stored on ice until assessment. Cell populations were analyzed on a Becton Dickinson LSR II cell flow cytometer. 10,000 events per sample were recorded.

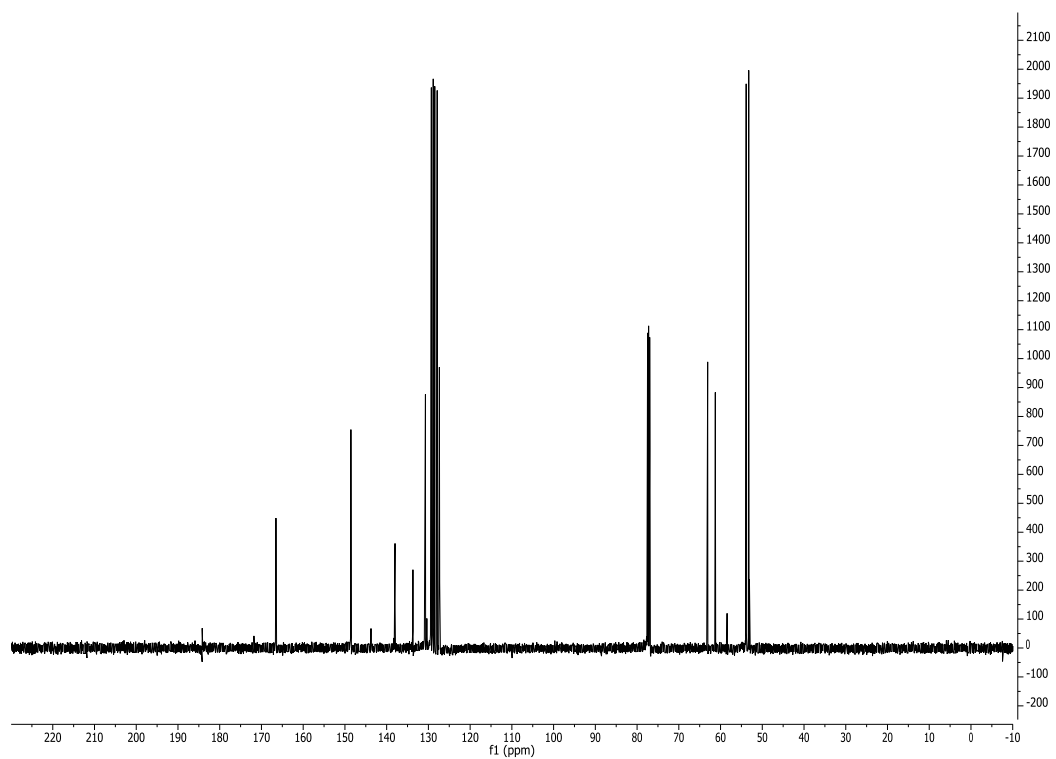
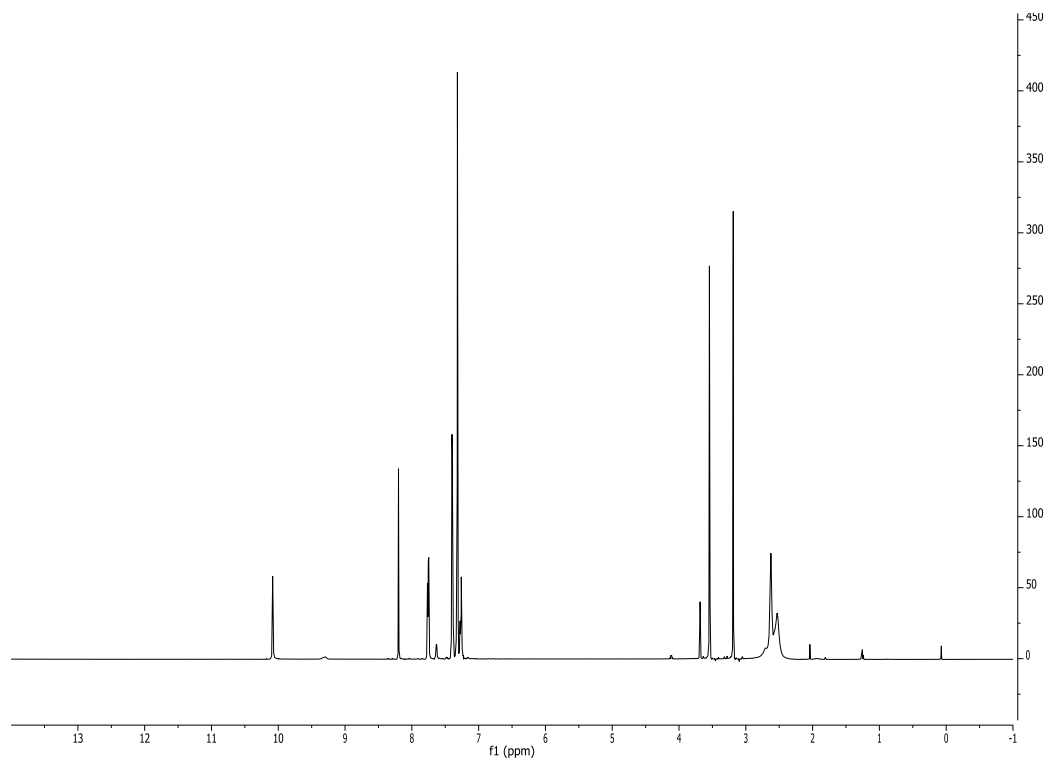
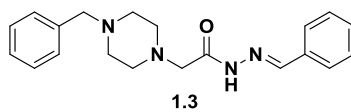
EGTA Fluorescence Titration Assay This titration assay is based on a published protocol.¹³ Buffer (50 mM HEPES, 100 mM KNO_3 , 8.1 mM EGTA, pH 7.2) and solutions of compounds (1 mM in DMSO) and $\text{Zn}(\text{OTf})_2$ (100 μM -1 M in H_2O) were prepared. The compound solutions were diluted ten-fold with buffer (final [compound] = 100 μM , final [EGTA] = 7.3 mM), and 198 μL of the resulting solution was added to each well of a 96-well plate. Each of 24 $\text{Zn}(\text{OTf})_2$ solutions was added to four wells in each plate. The wells were allowed to equilibrate for 5 minutes, and the plates were analyzed via a Molecular Devices SpectraMax M3 fluorescent plate reader (ex. 410 nm, em. 475 nm). Fluorescence intensity at 475 nm of each of four technical replicates was plotted against free Zn^{2+} concentration ($[\text{Zn}^{2+}]_F$), calculated using the MaxChelator program (maxchelator.stanford.edu). The data were analyzed using OriginPro 9.1 and fitted to a formation curve based on Equation 4.1:¹³

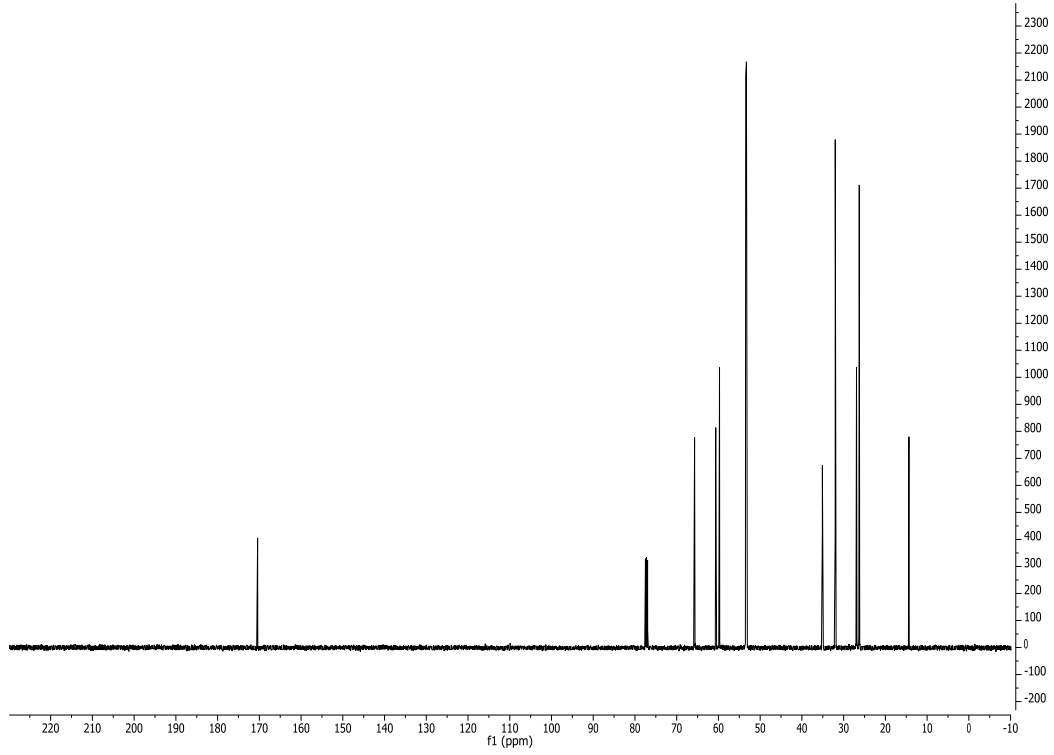
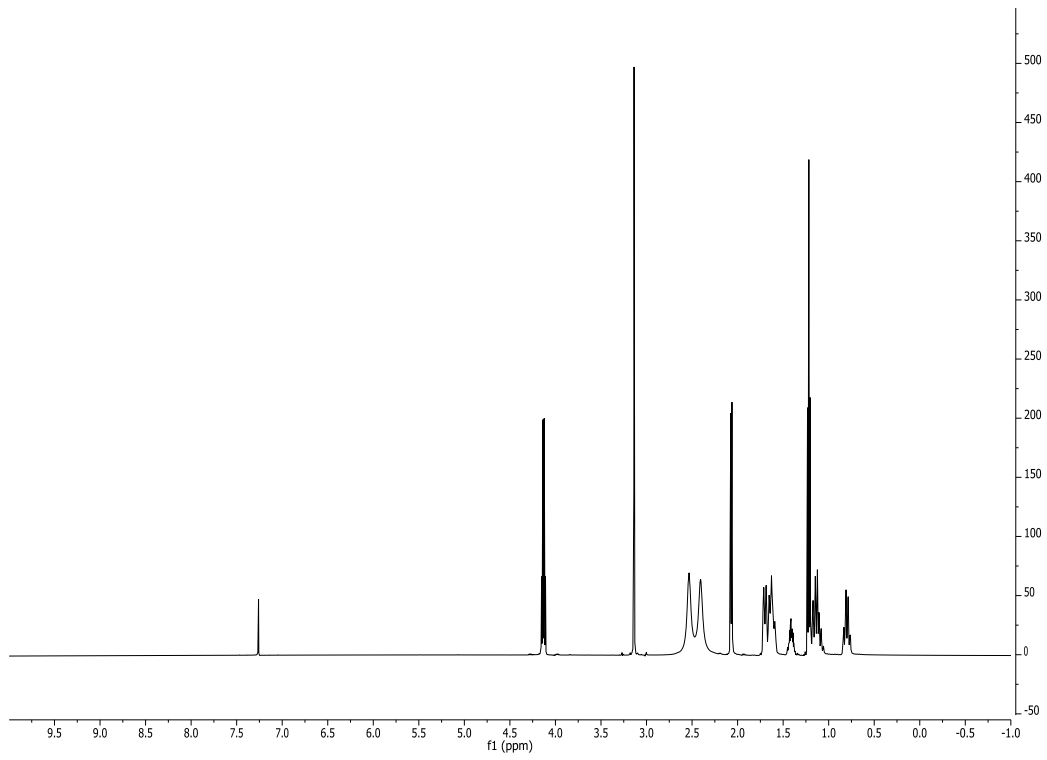
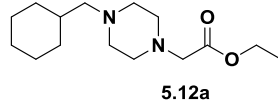
$$I = (I_{\min}K_d + I_{\max}[\text{Zn}^{2+}]_F)/(K_d + [\text{Zn}^{2+}]_F) \quad (\text{Equation 4.1})$$

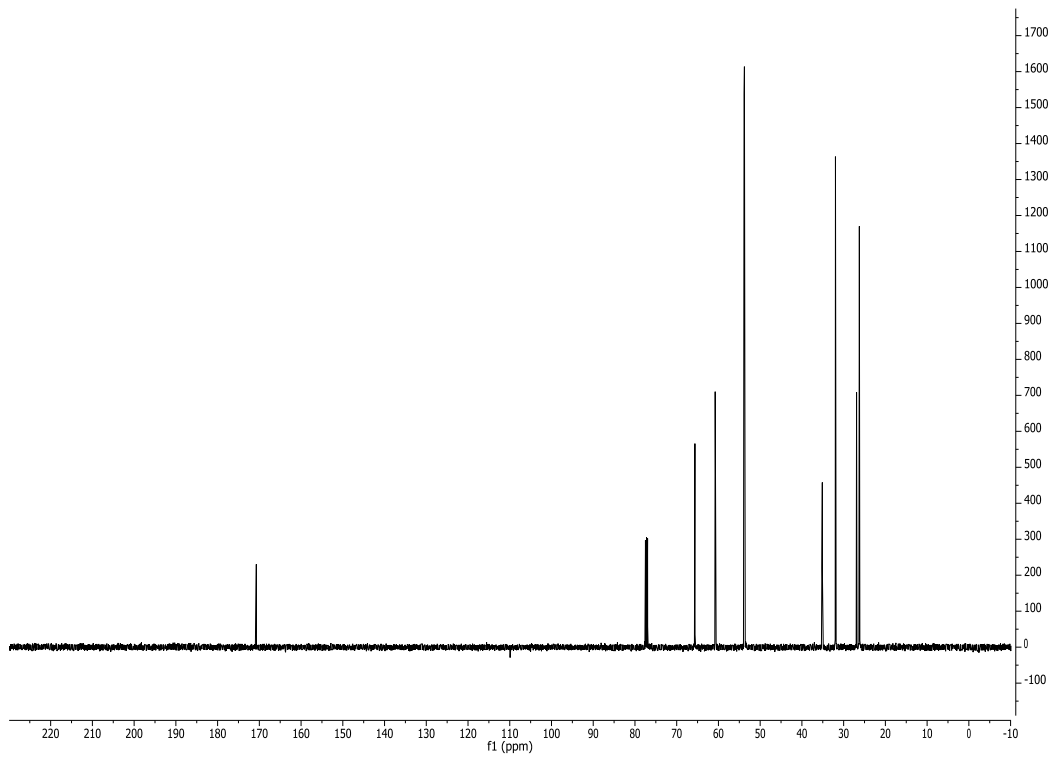
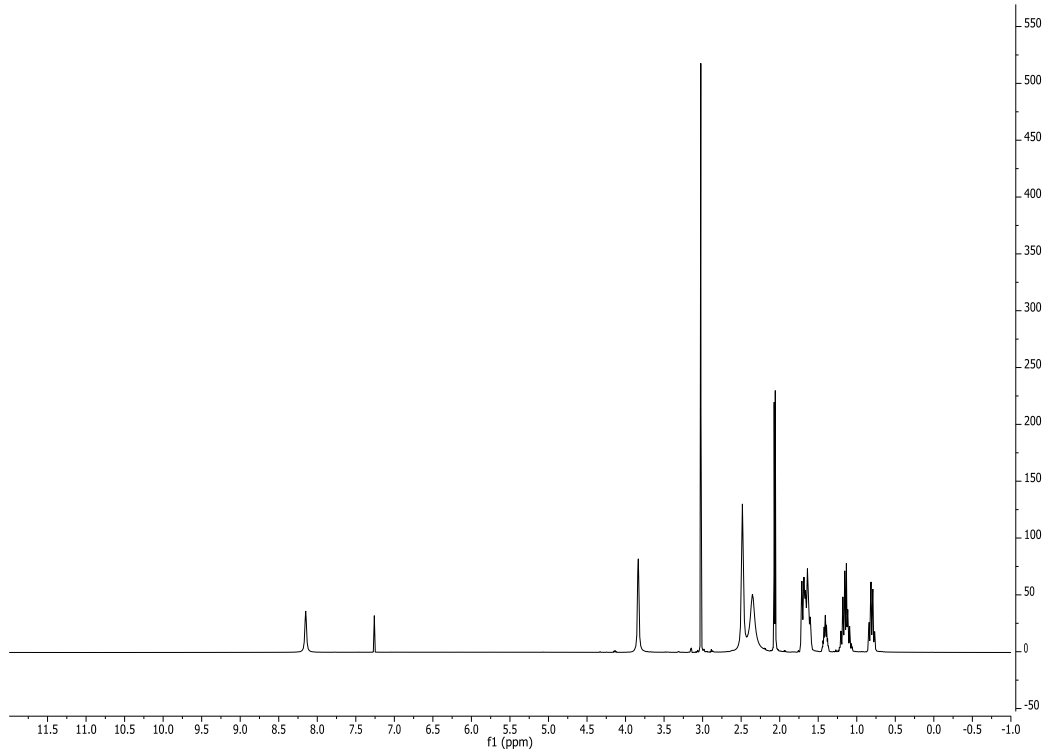
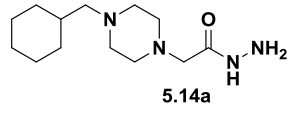
where I_{\min} and I_{\max} were defined as the fluorescence intensity of the free probe (**PAC-1** or derivative) and that of the Zn^{2+} -probe complex, respectively.

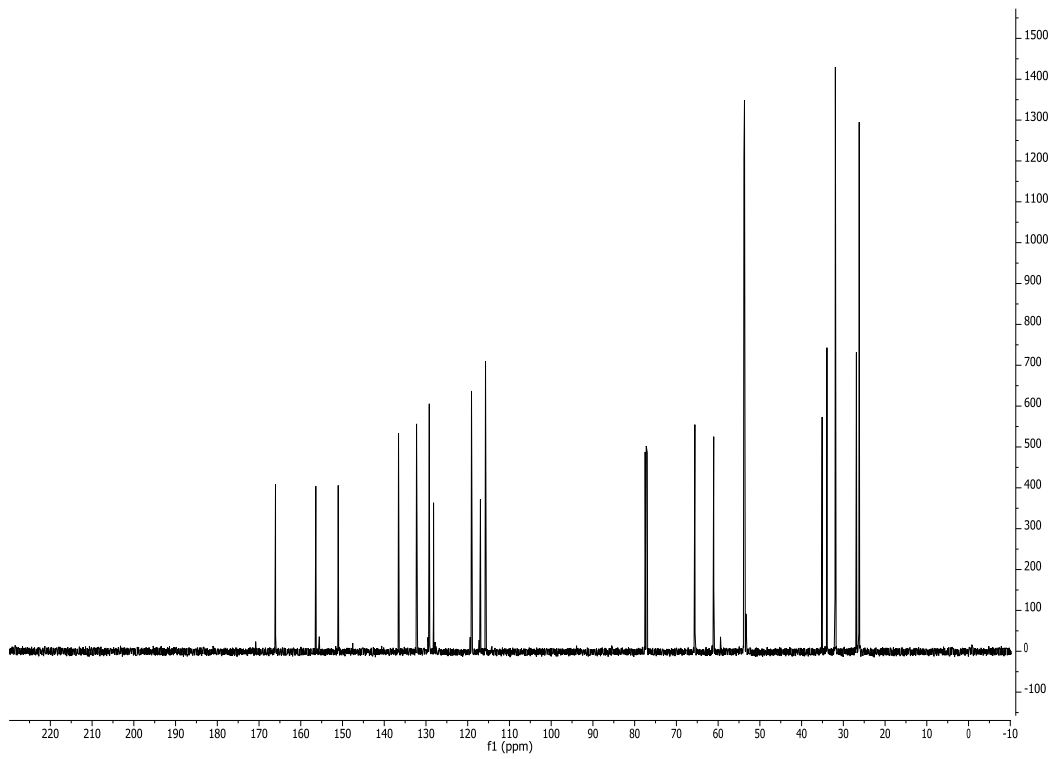
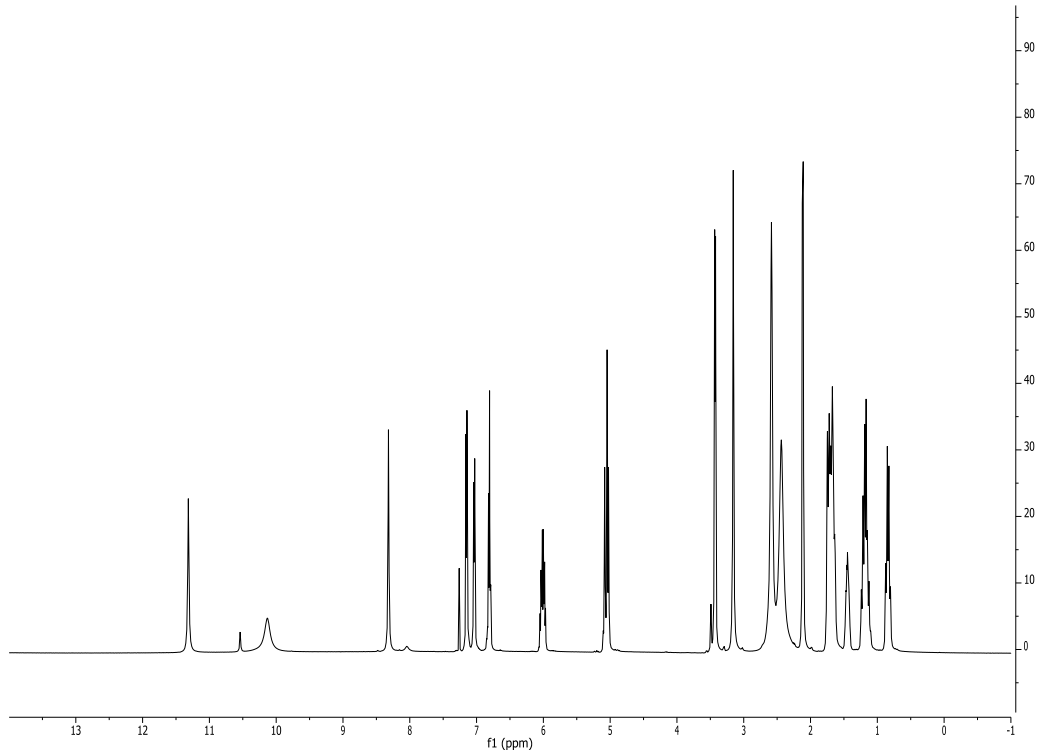
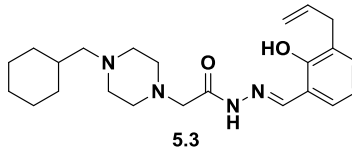
Evaluation of Compound Tolerability in vivo. All experimental procedures were reviewed and approved by the University of Illinois Institutional Animal Care and Use Committee. 8-10 week old C57BL/6 mice were used in all experiments (Charles River). Mice ($n = 3/\text{cohort}$) were evaluated for their ability to tolerate a single 150 $\mu\text{mol/kg}$ intravenous dosage of compounds, formulated at 20 mM in 200 mg/mL hydroxypropyl- β -cyclodextrin (HP β CD) at pH 5.5. Mice were treated, then videotaped for 30 seconds immediately upon return to their cages. Mice were observed for clinical signs continuously for 30 minutes and intermittently over the next 24 hours. Mice were further allowed 1 week to demonstrate delayed effects of treatment. The extent of initial response was graded from 0 (no effect) to 4 (most severe toxicity). Compounds that proved lethal were noted.

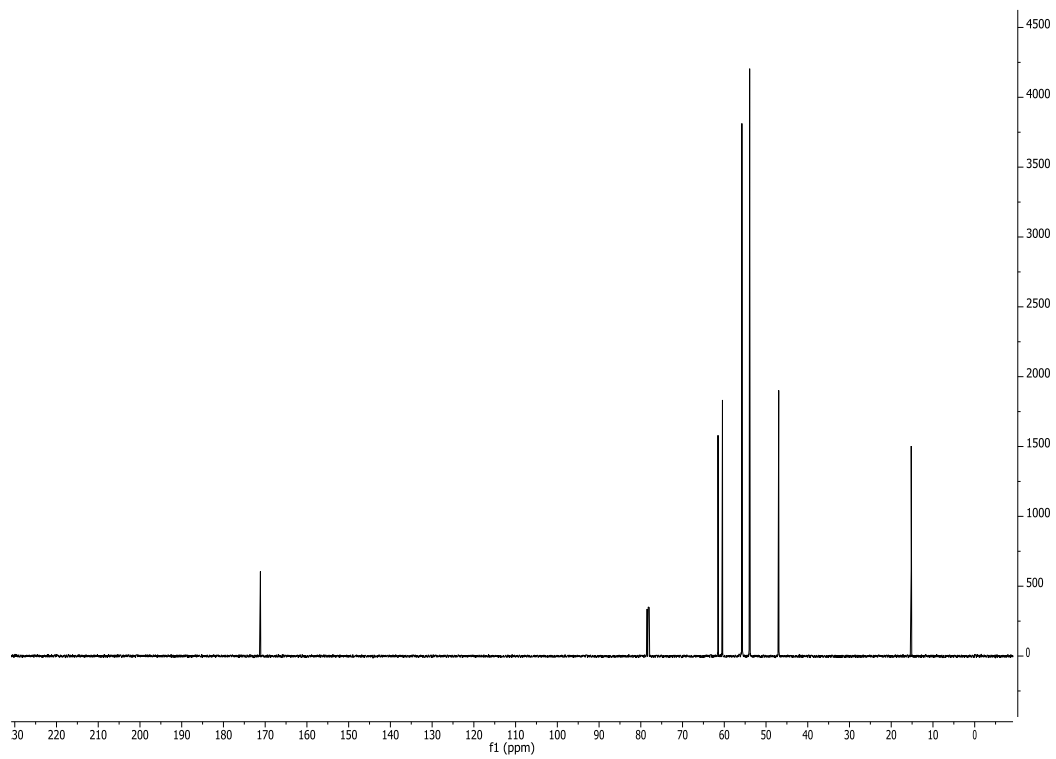
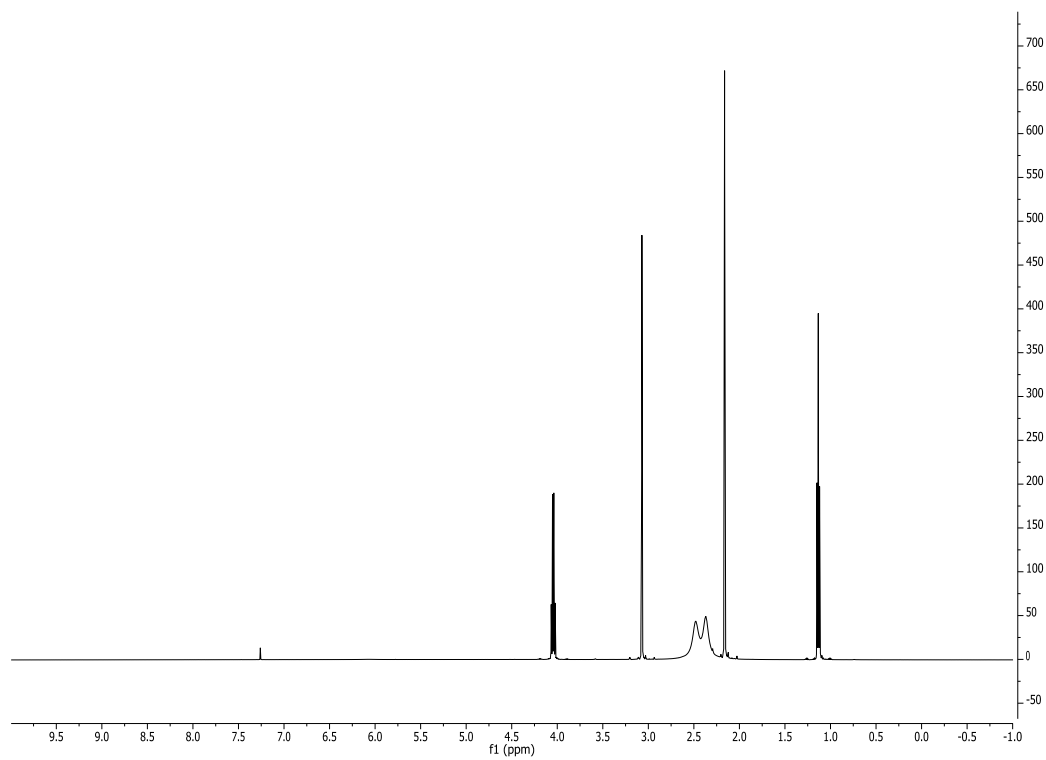
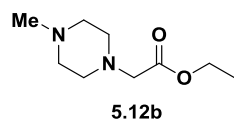
5.7.3. Spectra

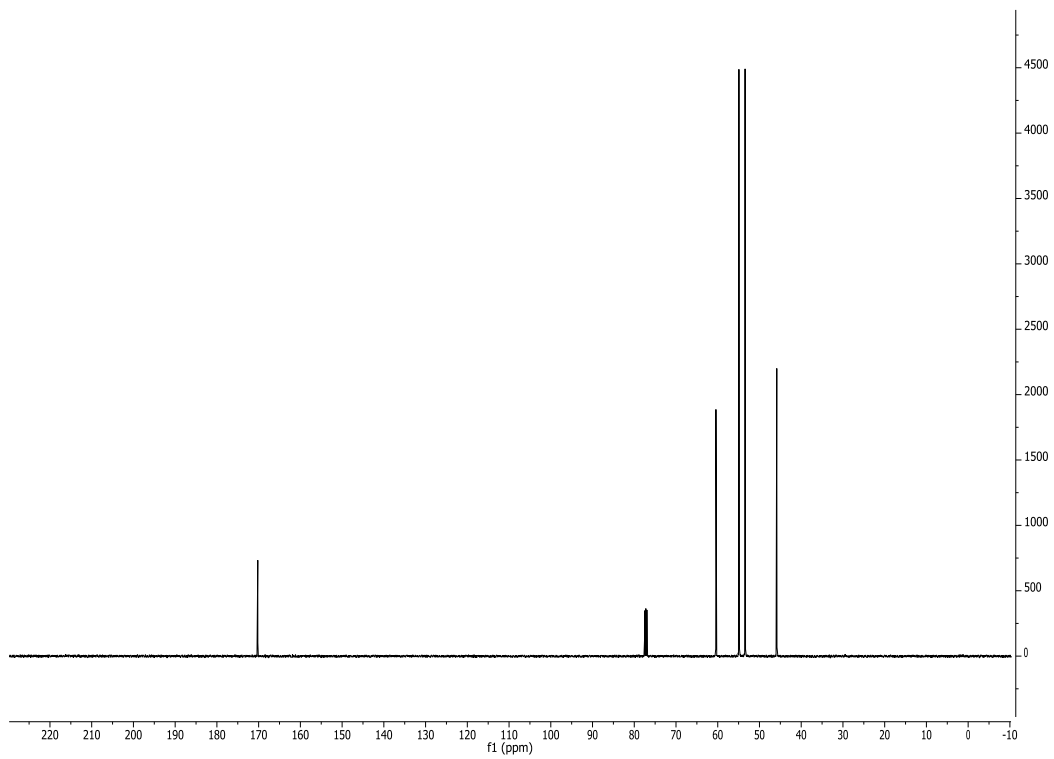
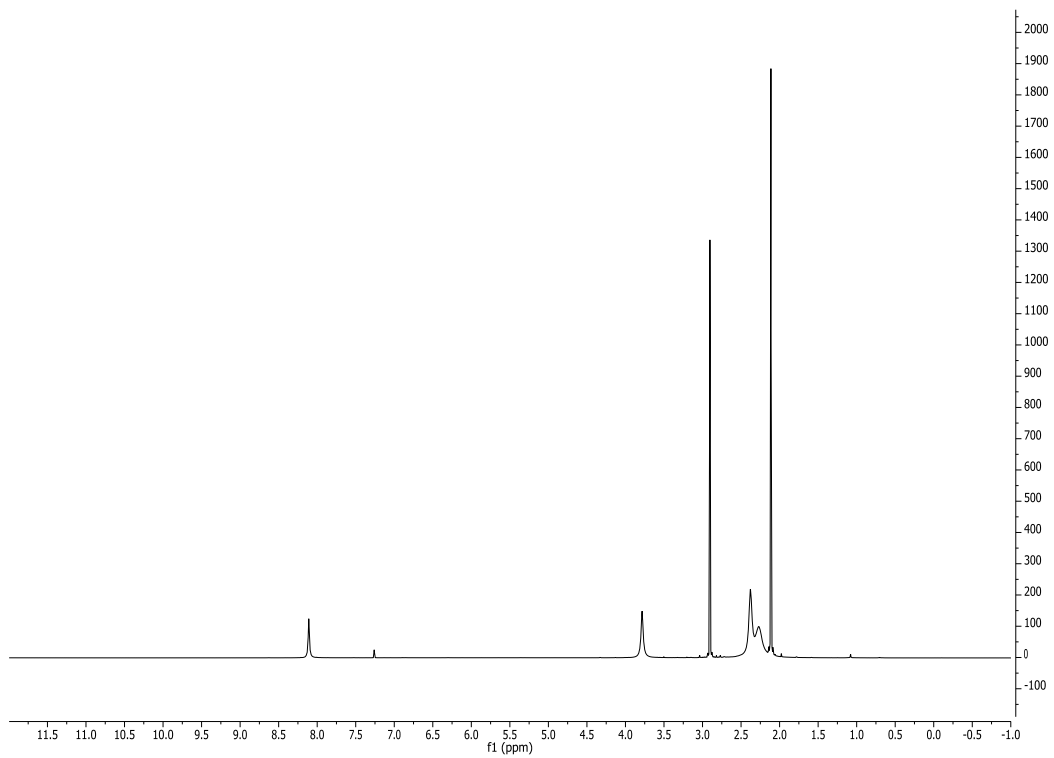
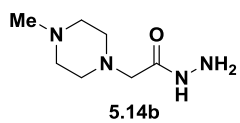


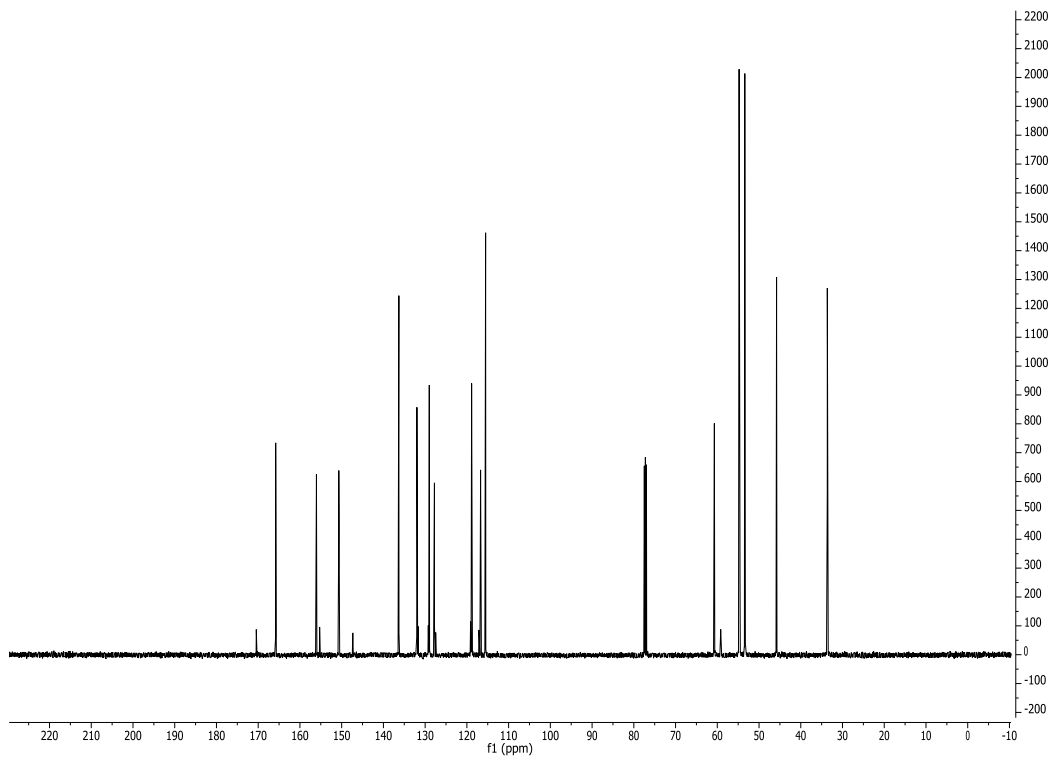
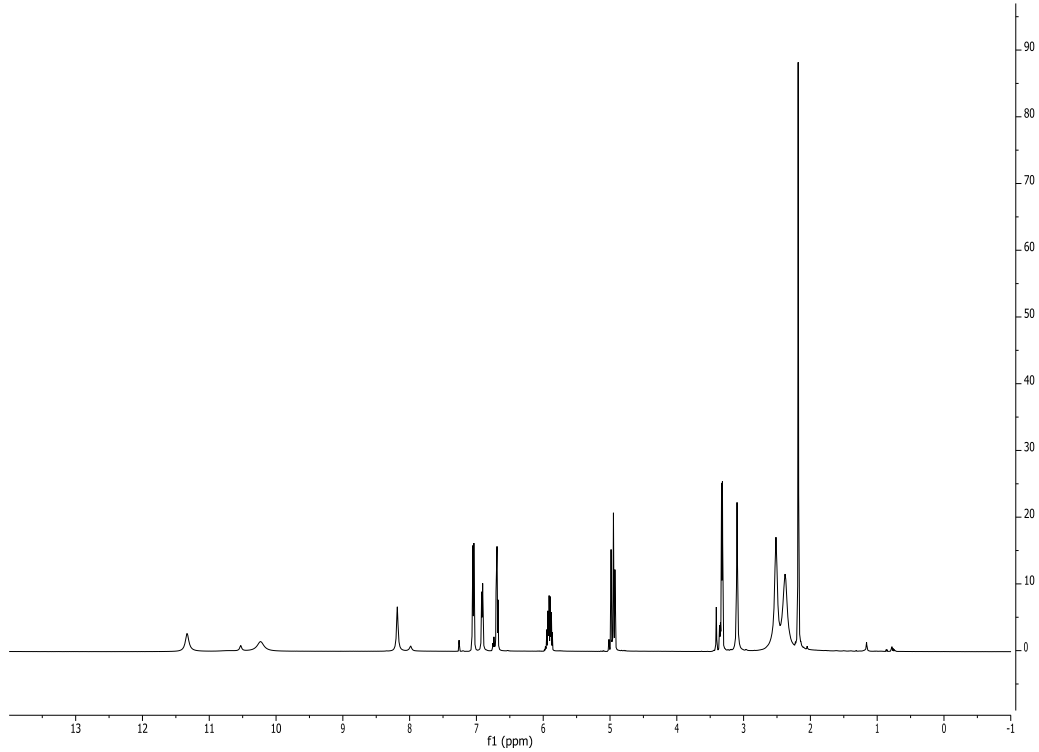
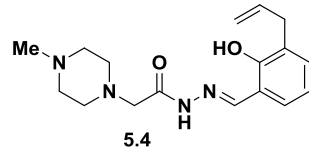


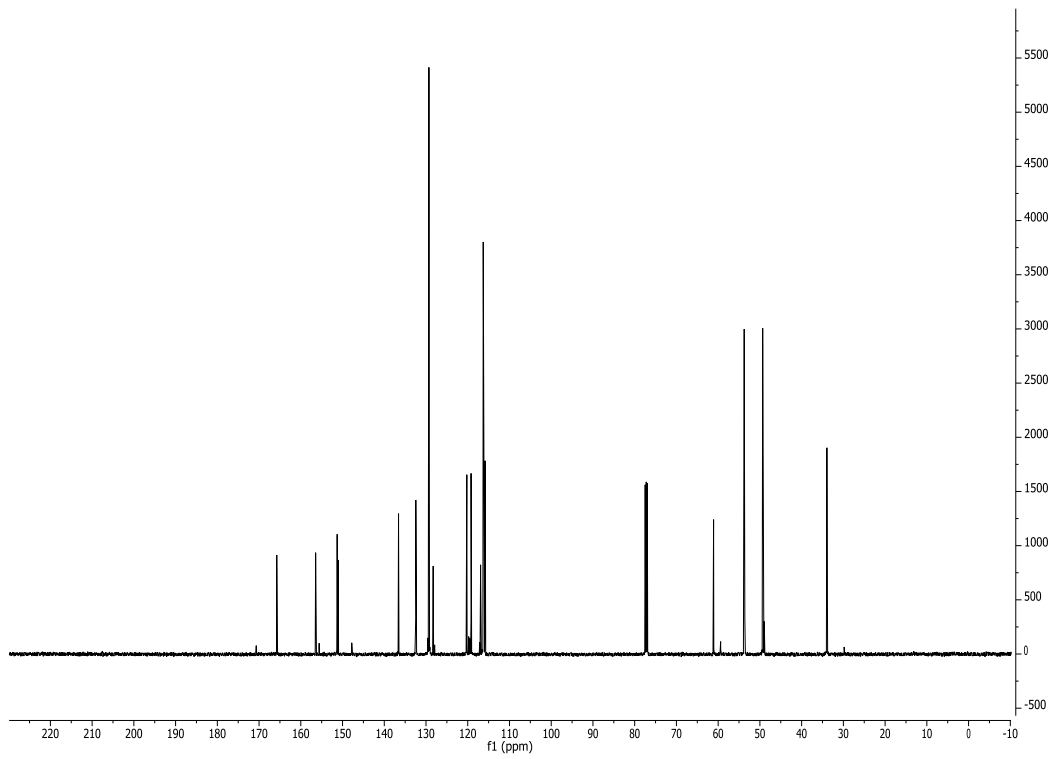
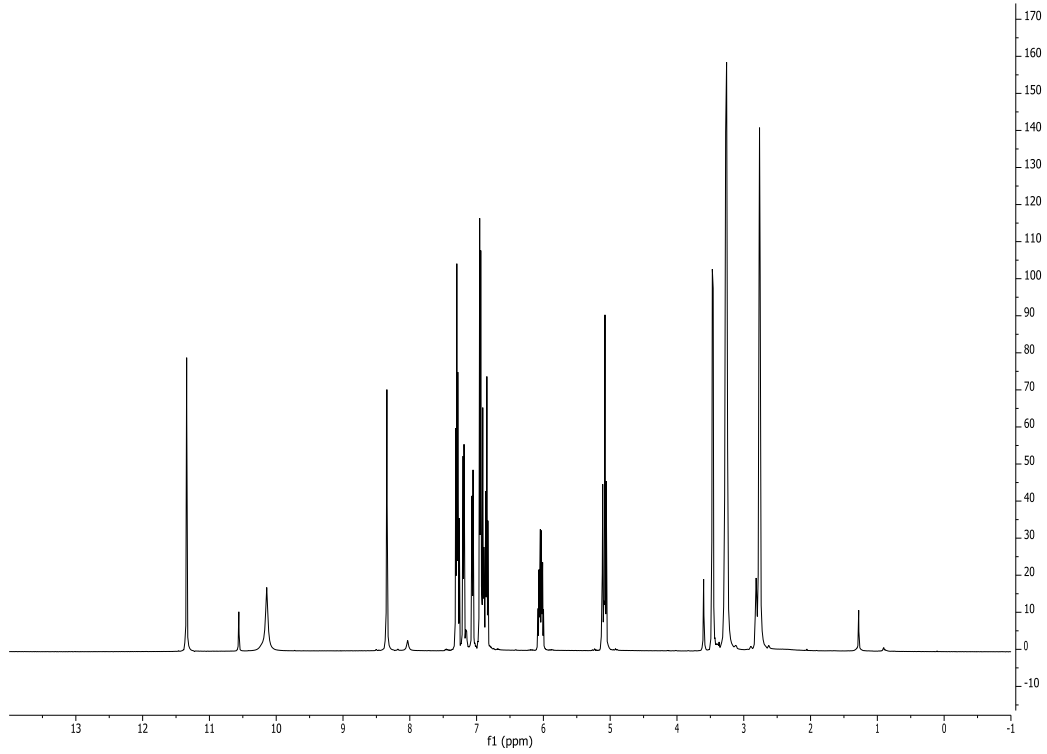
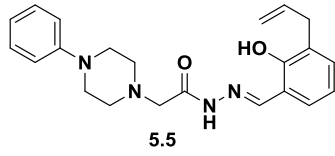


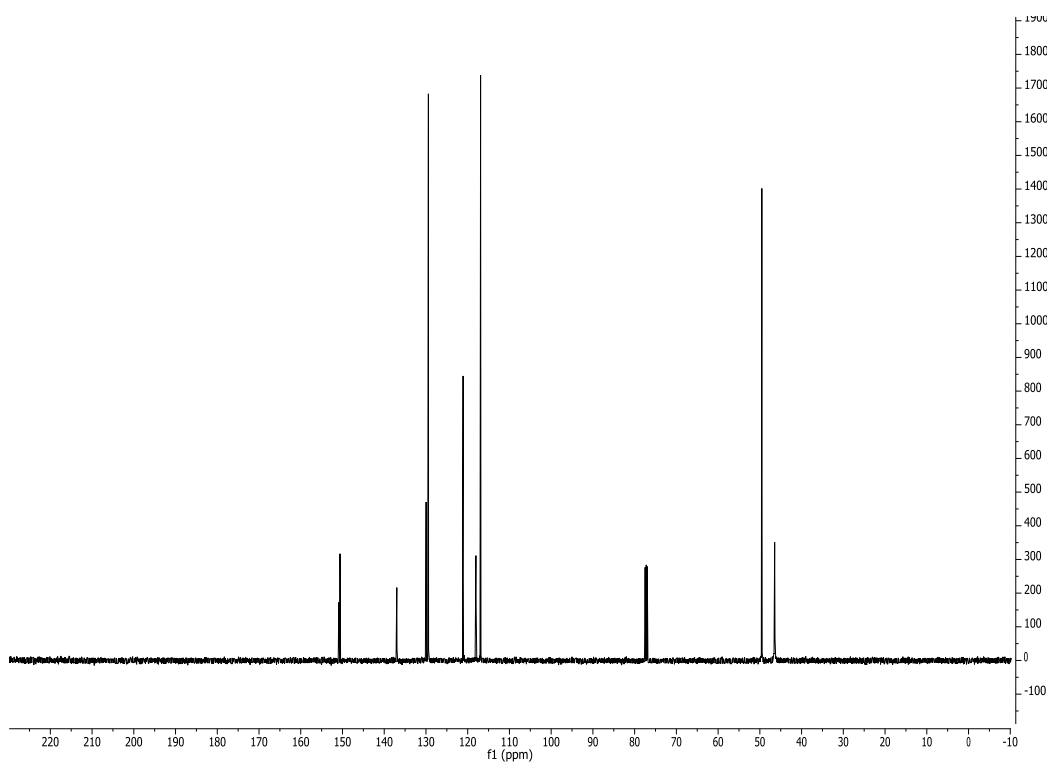
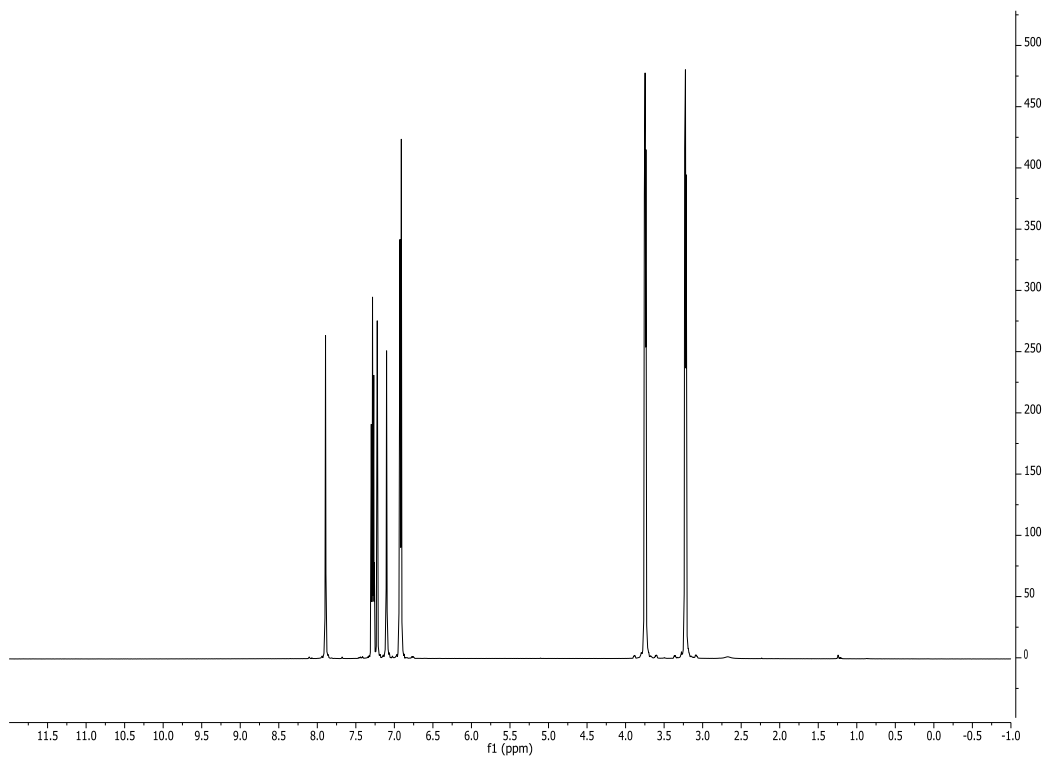
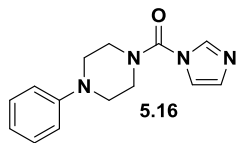


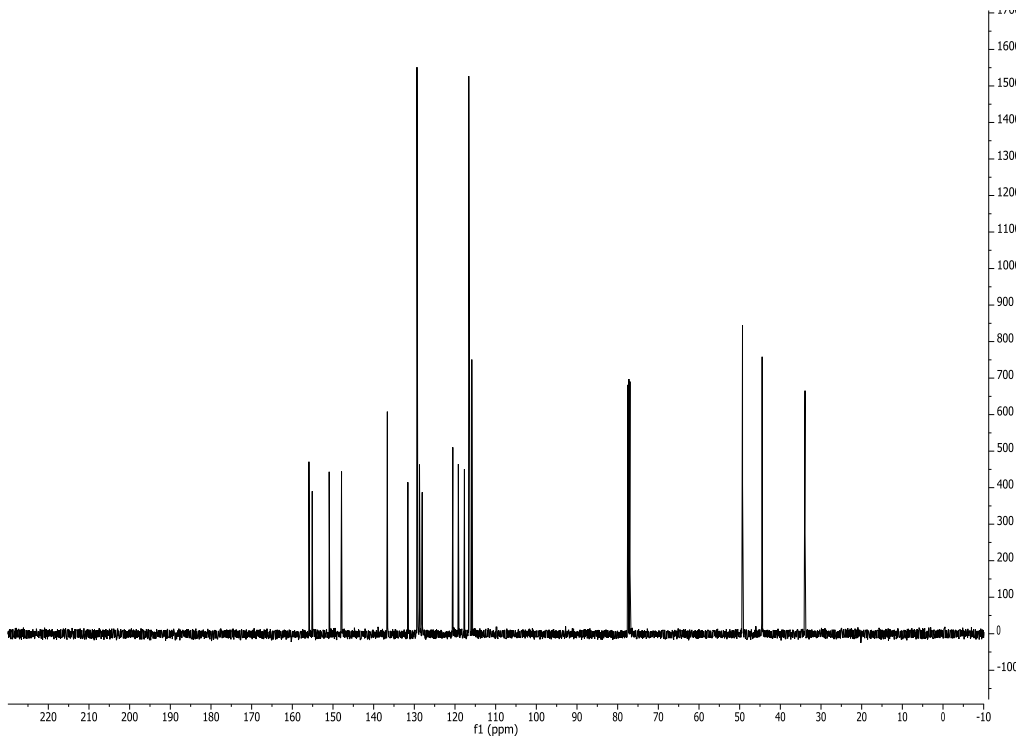
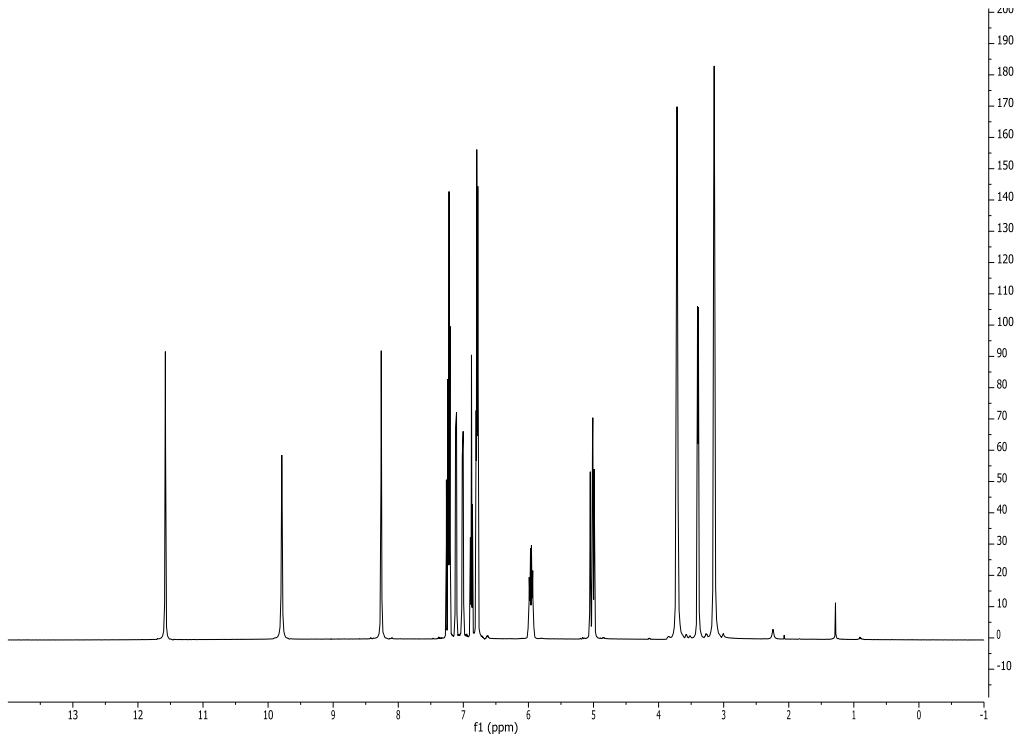
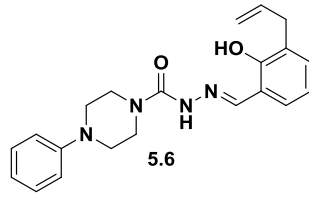


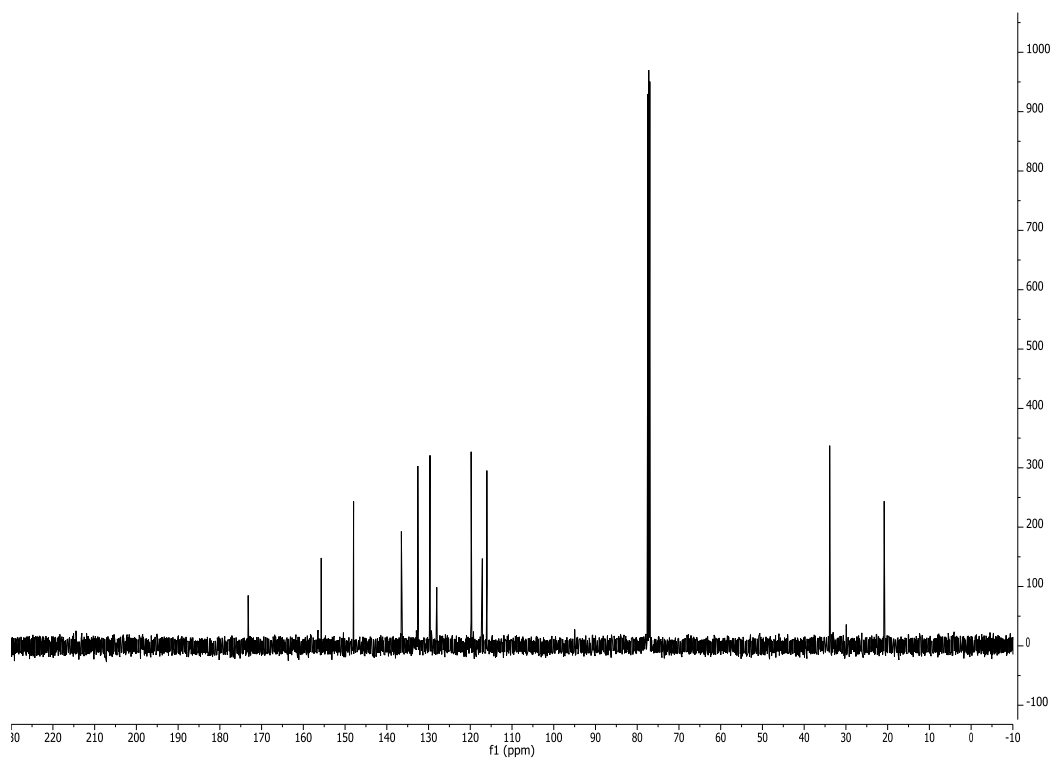
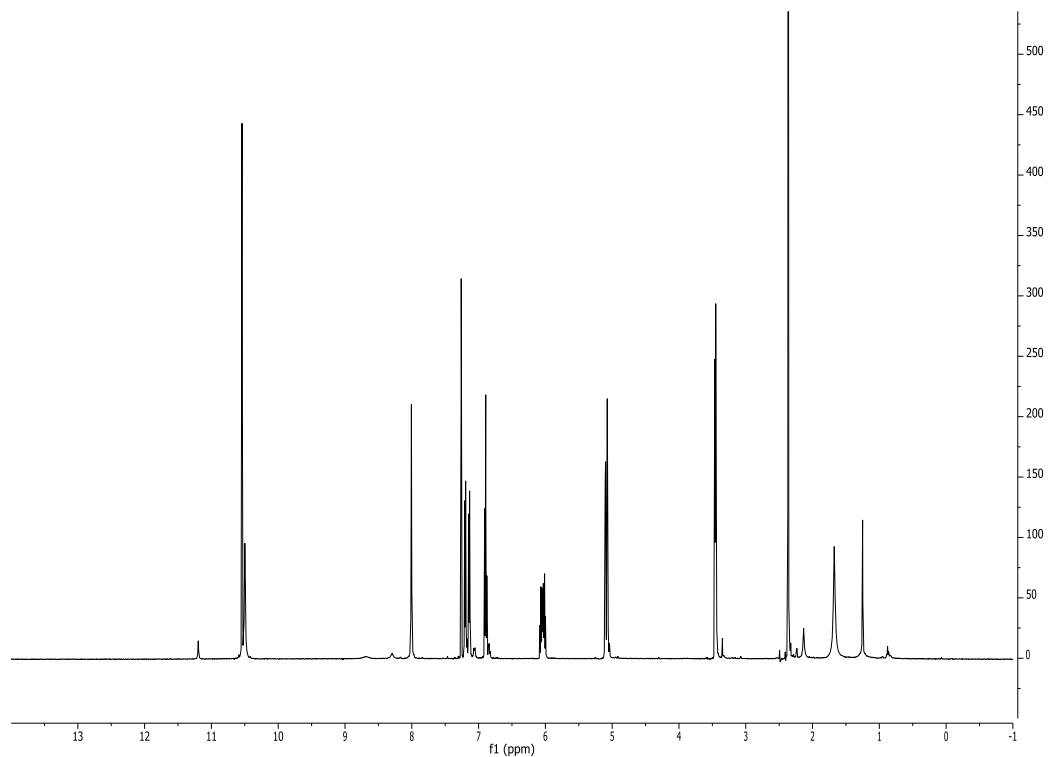
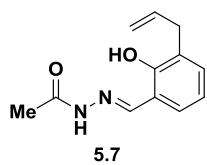


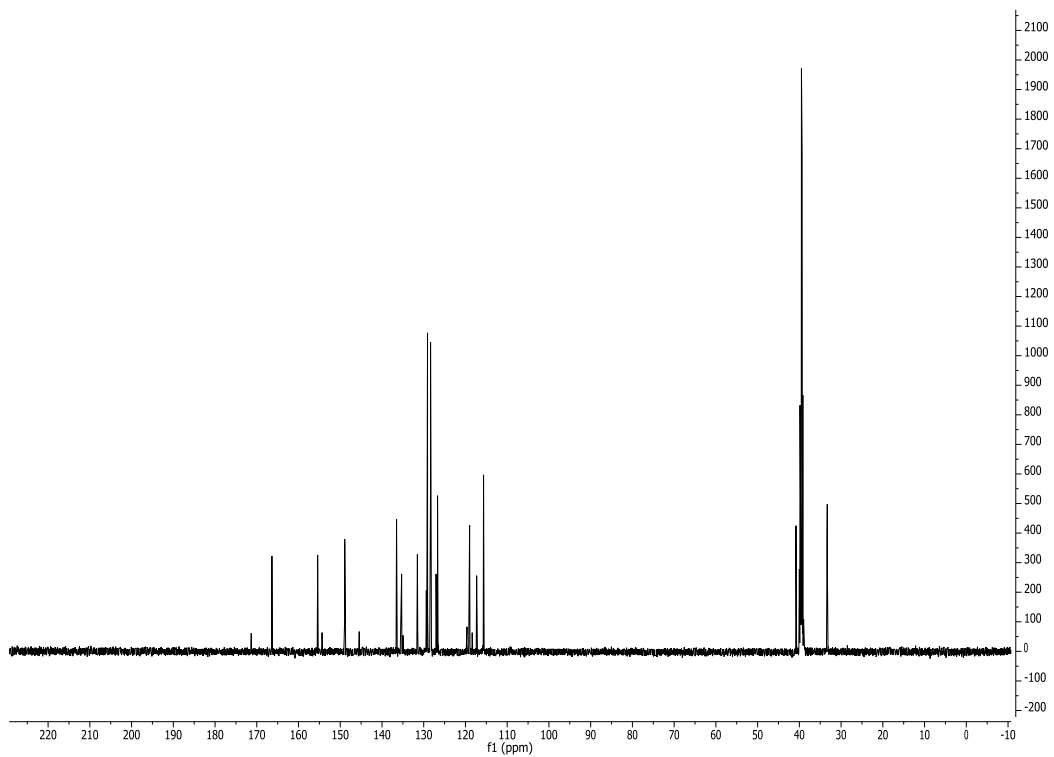
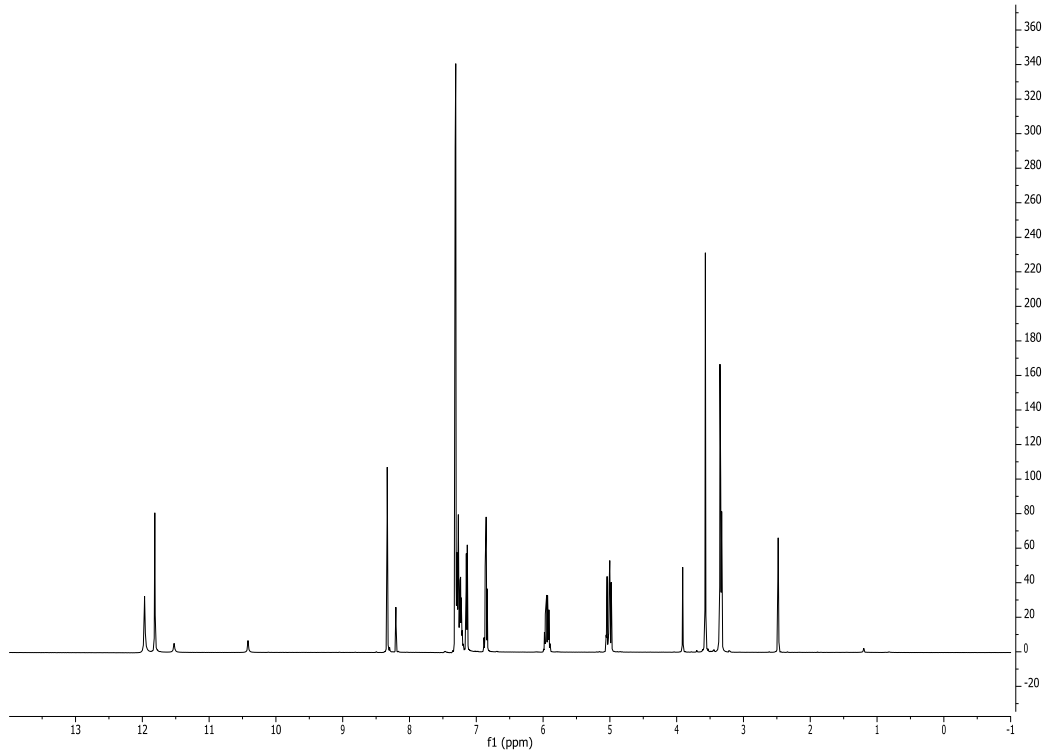
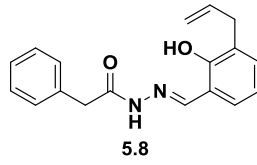


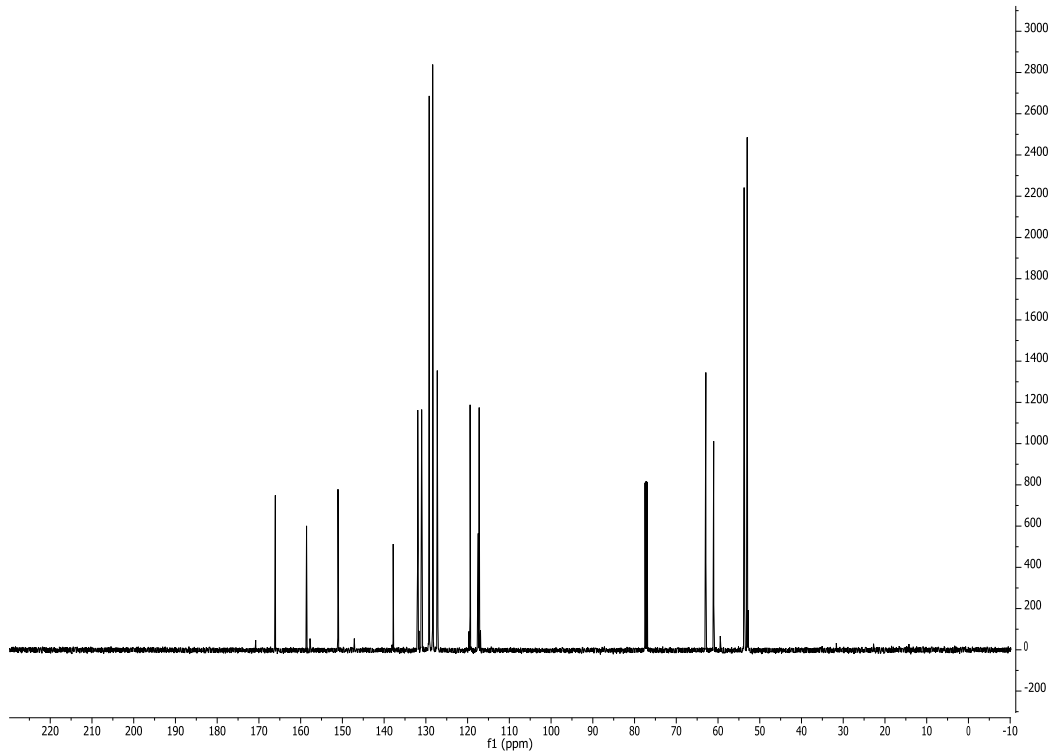
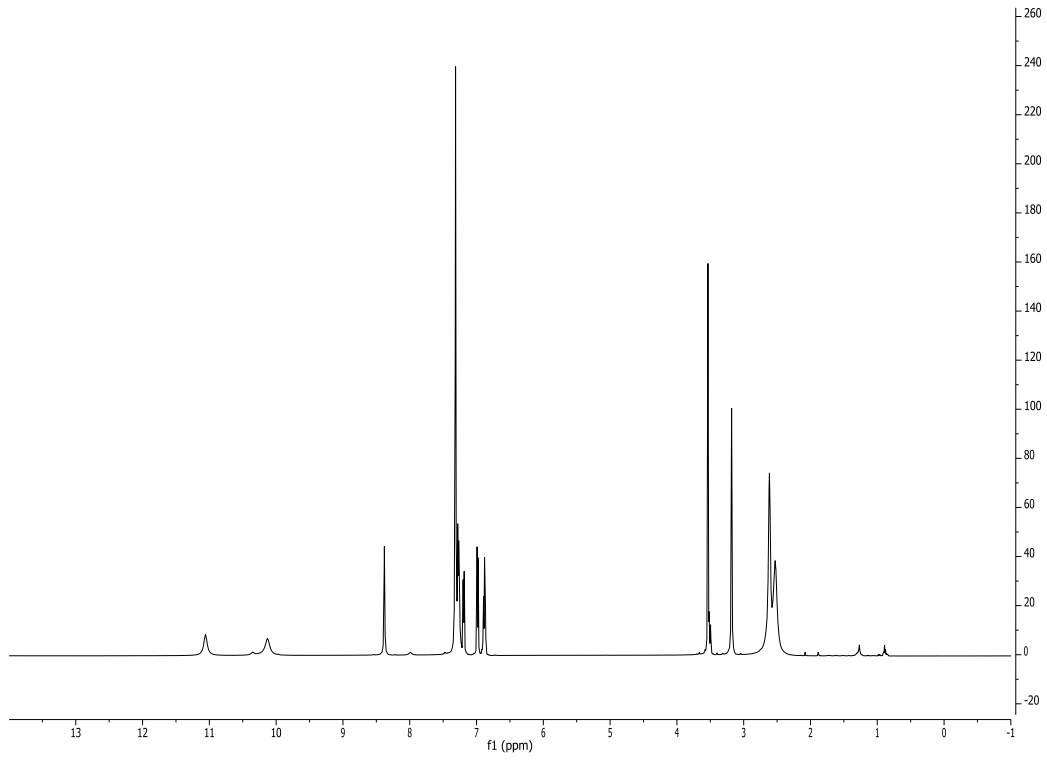
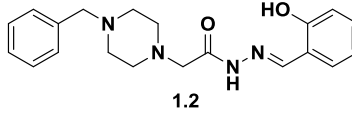


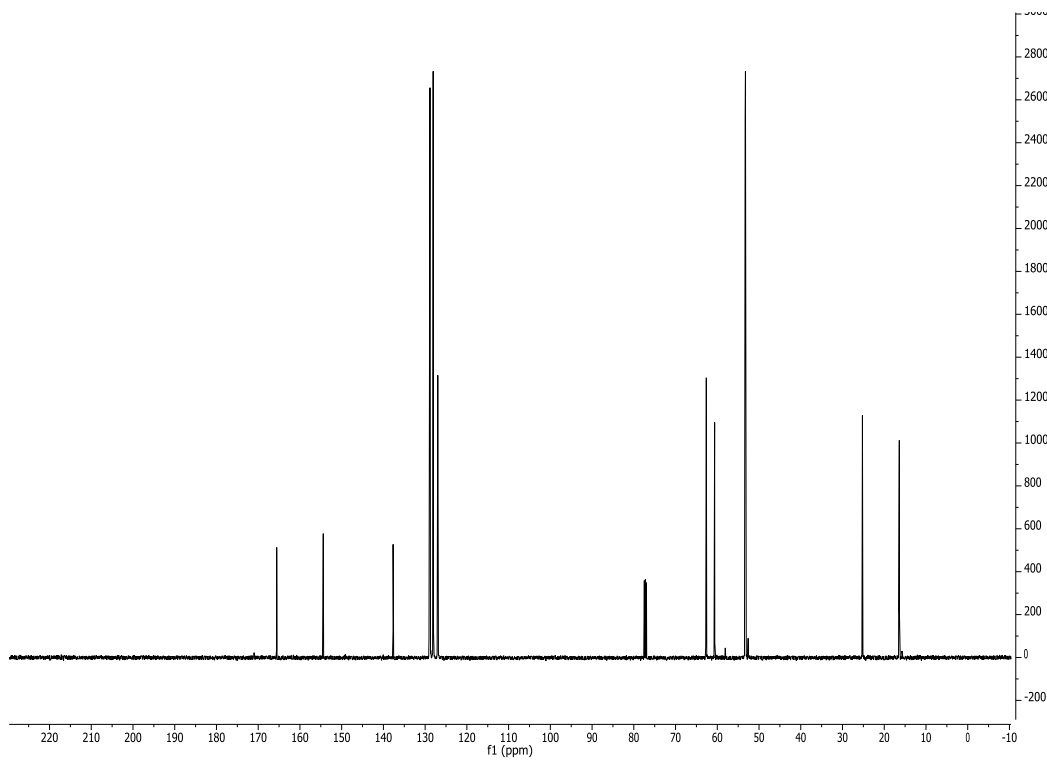
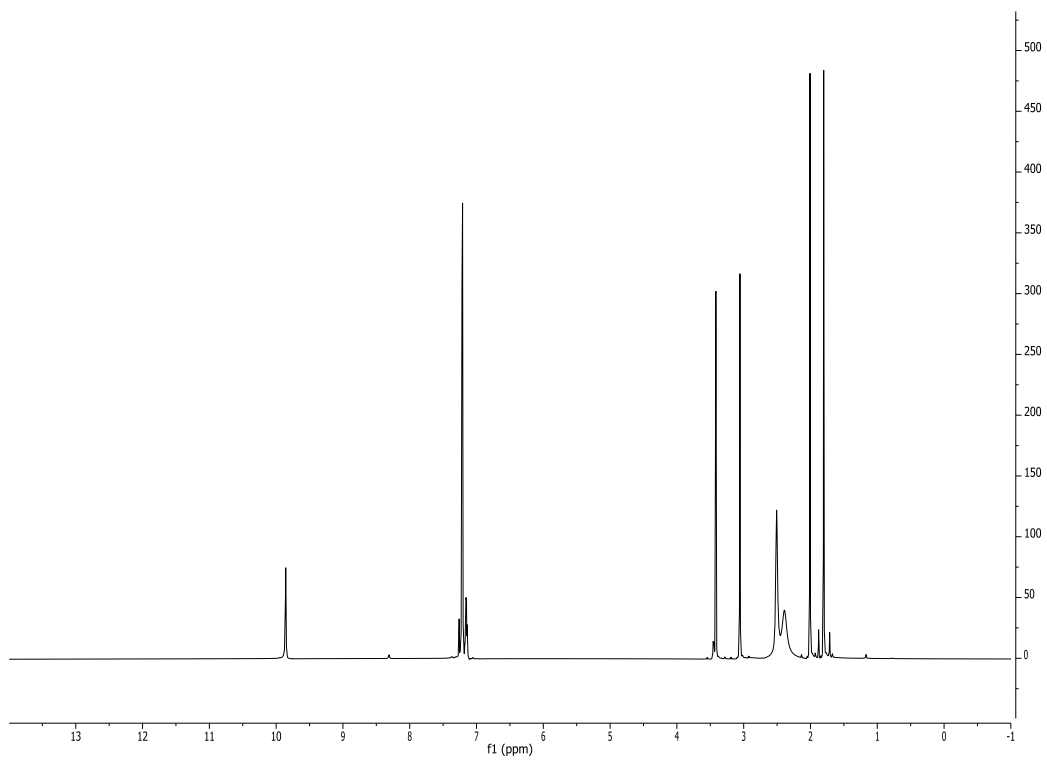
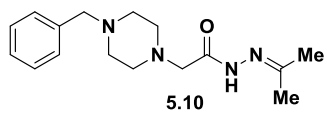


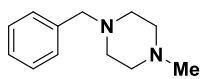




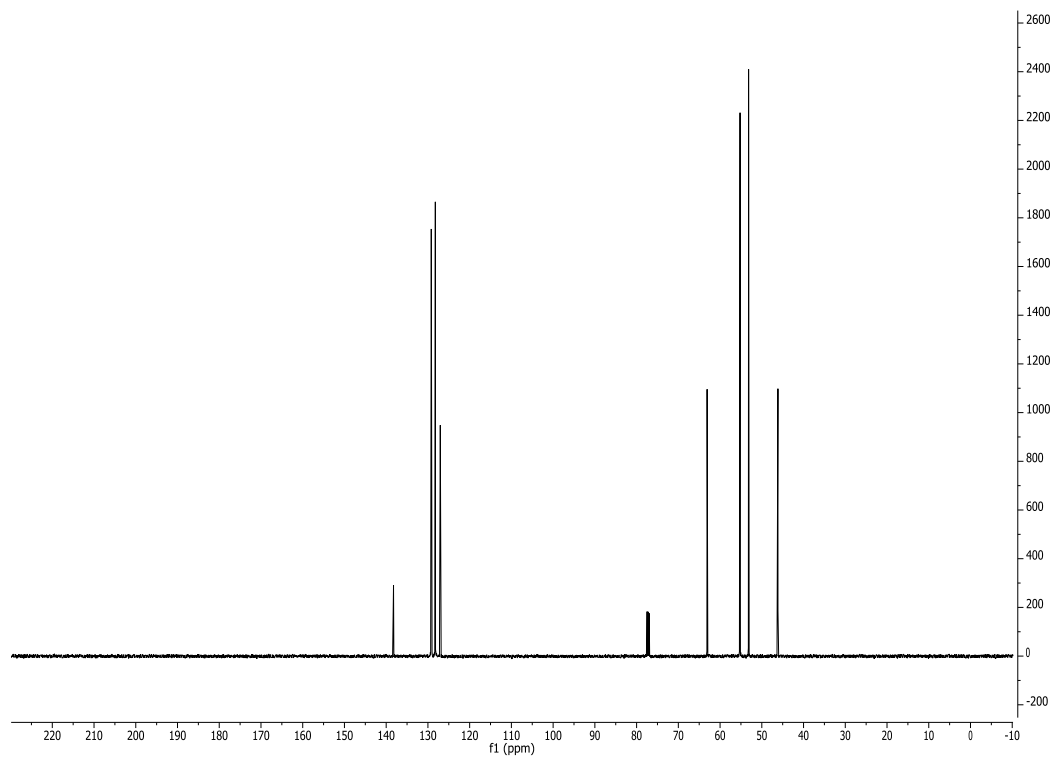
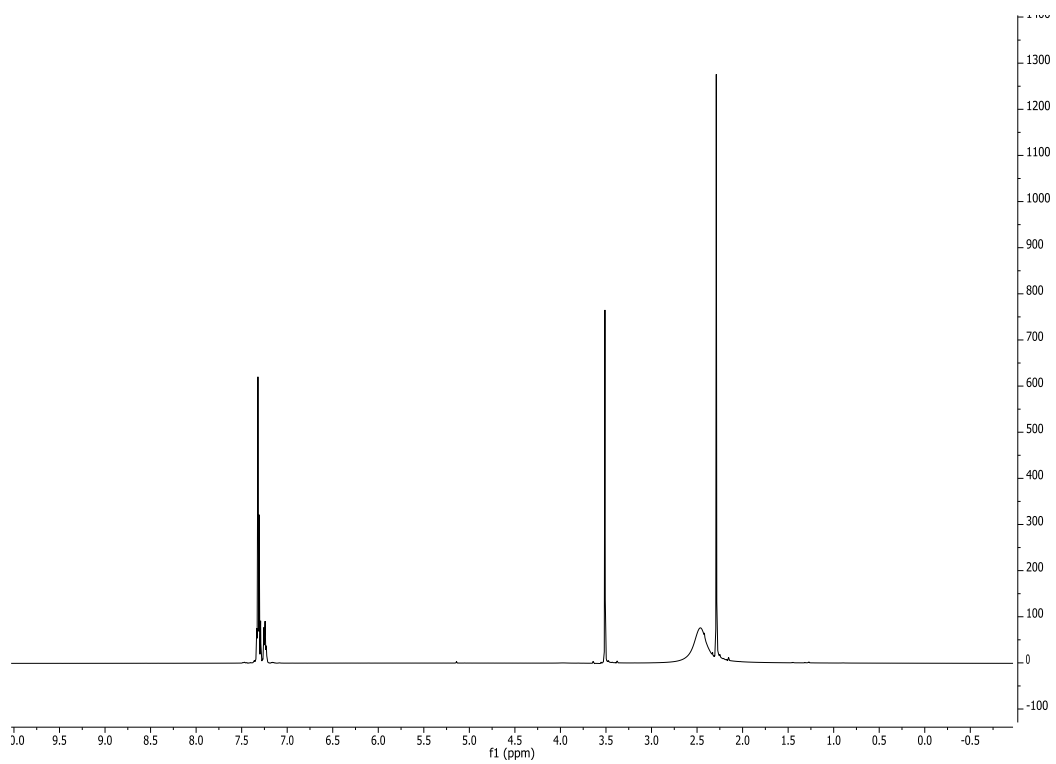








5.9



5.8. References

1. Peterson, Q. P.; Hsu, D. C.; Novotny, C. J.; West, D. C.; Kim, D.; Schmit, J. M.; Dirikolu, L.; Hergenrother, P. J.; Fan, T. M. Discovery and canine preclinical assessment of a nontoxic procaspase-3-activating compound. *Cancer Res.* **2010**, *70*, 7232-7241.
2. Dominguez, M. I.; Blasco-Ibanez, J. M.; Crespo, C.; Marques-Mari, A. I.; Martinez-Guijarro, F. J. Zinc chelation during non-lesioning overexcitation results in neuronal death in the mouse hippocampus. *Neuroscience* **2003**, *116*, 791-806.
3. Dominguez, M.-I.; Blasco-Ibanez, J.-M.; Crespo, C.; Nacher, J.; Marques-Mar, A.-I.; Martinez-Guijarro, F.-J. Neural Overexcitation and Implication of NMDA and AMPA Receptors in a Mouse Model of Temporal Lobe Epilepsy Implying Zinc Chelation. *Epilepsia* **2006**, *47*, 887-899.
4. West, D. C.; Qin, Y.; Peterson, Q. P.; Thomas, D. L.; Palchadhuri, R.; Morrison, K. C.; Lucas, P. W.; Palmer, A. E.; Fan, T. M.; Hergenrother, P. J. Differential effects of procaspase-3 activating compounds in the induction of cancer cell death. *Mol. Pharmaceutics* **2012**, *9*, 1425-1434.
5. Joshi, A. D.; Botham, R. C.; Roth, H. S.; Mangraviti, A.; Borodovsky, A.; Tyler, B.; Fan, T. M.; Hergenrother, P. J.; Riggins, G. J. A procaspase-3 activator synergizes with temozolomide to extend survival in intracranial models of glioma. **2015**, Unpublished Work.
6. Peterson, Q. P.; Hsu, D. C.; Goode, D. R.; Novotny, C. J.; Totten, R. K.; Hergenrother, P. J. Procaspase-3 activation as an anti-cancer strategy: structure-activity relationship of Procaspase-Activating Compound 1 (PAC-1) and its cellular co-localization with caspase-3. *J. Med. Chem.* **2009**, *52*, 5721-5731.
7. Clark, D. E. Rapid calculation of polar molecular surface area and its application to the prediction of transport phenomena. 2. Prediction of blood-brain barrier penetration. *J. Pharm. Sci.* **1999**, *88*, 815-821.
8. Putt, K. S.; Chen, G. W.; Pearson, J. M.; Sandhorst, J. S.; Hoagland, M. S.; Kwon, J. T.; Hwang, S. K.; Jin, H.; Churchwell, M. I.; Cho, M. H.; Doerge, D. R.; Helferich, W. G.; Hergenrother, P. J. Small-molecule activation of procaspase-3 to caspase-3 as a personalized anticancer strategy. *Nat. Chem. Biol.* **2006**, *2*, 543-550.
9. Peterson, Q. P.; Goode, D. R.; West, D. C.; Ramsey, K. N.; Lee, J. J. Y.; Hergenrother, P. J. PAC-1 activates procaspase-3 in vitro through relief of zinc-mediated inhibition. *J. Mol. Biol.* **2009**, *388*, 144-158.
10. Hsu, D. C.; Roth, H. S.; West, D. C.; Botham, R. C.; Novotny, C. J.; Schmid, S. C.; Hergenrother, P. J. Parallel synthesis and biological evaluation of 837 analogues of Procaspase-Activating Compound 1 (PAC-1). *ACS Comb. Sci.* **2012**, *14*, 44-50.
11. Botham, R. C.; Fan, T. M.; Im, I.; Borst, L. B.; Dirikolu, L.; Hergenrother, P. J. Dual small-molecule targeting of procaspase-3 dramatically enhances zymogen activation and anticancer activity. *J. Am. Chem. Soc.* **2014**, *136*, 1312-1319.
12. Roth, H. S.; Botham, R. C.; Schmid, S. C.; Fan, T. M.; Dirikolu, L.; Hergenrother, P. J. Removal of metabolic liabilities enables development of derivatives of Procaspase-Activating Compound 1 (PAC-1) with improved pharmacokinetics. *J. Med. Chem.* **2015**, *58*, 4046-4065.
13. Huang, S.; Clark, R. J.; Zhu, L. Highly sensitive fluorescent probes for zinc ion based on triazolyl-containing tetradentate coordination motifs. *Org. Lett.* **2007**, *9*, 4999-5002.
14. Lucas, P. W.; Schmit, J. M.; Peterson, Q. P.; West, D. C.; Hsu, D. C.; Novotny, C. J.; Dirikolu, L.; Churchwell, M. I.; Doerge, D. R.; Garrett, L. D.; Hergenrother, P. J.; Fan, T. M.

Pharmacokinetics and derivation of an anticancer dosing regimen for PAC-1, a preferential small molecule activator of procaspase-3, in healthy dogs. *Invest. New Drugs* **2011**, *29*, 901-911.

15. Wang, F. Y.; Wang, L. H.; Zhao, Y. F.; Li, Y.; Ping, G. F.; Xiao, S.; Chen, K.; Zhu, W. F.; Gong, P.; Yang, J. Y.; Wu, C. F. A novel small-molecule activator of procaspase-3 induces apoptosis in cancer cells and reduces tumor growth in human breast, liver and gallbladder cancer xenografts. *Mol. Oncol.* **2014**, *8*, 1640-1652.

16. Wang, F.; Liu, Y.; Wang, L.; Yang, J.; Zhao, Y.; Wang, N.; Cao, Q.; Gong, P.; Wu, C. Targeting procaspase-3 with WF-208, a novel PAC-1 derivative, causes selective cancer cell apoptosis. *J. Cell. Mol. Med.* [Online early access]. DOI: 10.1111/jcmm.12566. Published Online: March 8, 2015.

17. Patel, V.; Balakrishnan, K.; Keating, M. J.; Wierda, W. G.; Gandhi, V. Expression of executioner procaspases and their activation by a procaspase activating compound in chronic lymphocytic leukemia cells. *Blood* **2015**, *125*, 1126-1136.

18. Vichai, V.; Kirtikara, K. Sulforhodamine B colorimetric assay for cytotoxicity screening. *Nat. Protoc.* **2006**, *1*, 1112-1116.